



Greenwich Academic Literature Archive (GALA)
– the University of Greenwich open access repository
<http://gala.gre.ac.uk>

Citation:

[Armitage, Paul Edward Blake \(2011\) Development of the Platreef in the northern limb of the Bushveld Complex at Sandsloot, Mokopane District, South Africa. PhD thesis, University of Greenwich.](#)

Please note that the full text version provided on GALA is the final published version awarded by the university. "I certify that this work has not been accepted in substance for any degree, and is not concurrently being submitted for any degree other than that of (name of research degree) being studied at the University of Greenwich. I also declare that this work is the result of my own investigations except where otherwise identified by references and that I have not plagiarised the work of others".

Armitage, Paul Edward Blake (2011) Development of the Platreef in the northern limb of the Bushveld Complex at Sandsloot, Mokopane District, South Africa. ##thesis type##, ##institution##

Available at: <http://gala.gre.ac.uk/9079/>

Contact: gala@gre.ac.uk

**DEVELOPMENT OF THE PLATREEF IN THE NORTHERN
LIMB OF THE BUSHVELD COMPLEX AT SANDSLOOT,
MOKOPANE DISTRICT, SOUTH AFRICA**

By

PAUL EDWARD BLAKE ARMITAGE

[BA (Hons), BSc (Hons), MSc]

A thesis submitted in partial fulfilment of the requirements of the
University of Greenwich for the Degree of Doctor of Philosophy

October 2011




DECLARATION


I certify that this work has not been accepted in substance for any degree, and is not concurrently being submitted for any degree other than that of Doctor of Philosophy being studied at the University of Greenwich. I also declare that this work is the result of my own investigations except where otherwise identified by references and that I have not plagiarised the work of others.

Signed  Paul E. B. Armitage (Candidate)

.....

DOCTORAL SUPERVISORS

Signed  Prof. Stephen A. Leharne (1st Supervisor)

Signed  Dr. Iain McDonald (2nd Supervisor)

Date 14 OCT 2011

ACKNOWLEDGEMENTS

This thesis is the culmination of a long (rather too long?) academic career. Many people have inspired, encouraged and assisted me. They all deserve praise and will get it, either here in writing or in a pint glass. In the time I have spent intermittently writing this thesis, I have entered the very career that the PhD was intended to help me into. Whilst this and other commitments have distracted me from the thesis, there was no question of giving up despite some serious struggles.

First and foremost, my enormous gratitude goes to Iain McDonald. He has shown undeserved patience towards me in the production of this thesis, and I cannot thank him enough for sticking with the role of supervisor through the years and for encouraging me to write a couple of papers. It was Iain's recruitment of my services for a mapping job in South Africa, relating to platinum, which ultimately led to this study. In more recent times, my gratitude goes to Steve Leharne and Babur Chowdhry for their administrative supervision (and for their patience too).

I am very grateful to Alan Bye, Alfred Sarila, Theo Van Strijp and Eric McClean for their assistance in gaining access to the Sandsloot Mine and its facilities in the early days of the study. Others who must be mentioned for their part in supervision, discussion and technical assistance are Steve Edwards, Geoff Manby, Ian Slipper and Dave Wray (all formerly or currently at the University of Greenwich); and Jackie Skipper, Terry Williams, John Spratt and Anton Kearsley (all formerly or currently at the Natural History Museum). Thanks also to Dave Holwell, Grant Cawthorn, Judith Kinnaird, Paul Nex and Tony Naldrett for occasional discussions at a number of events. There are others who deserve a nod of appreciation.

This work is dedicated to my long suffering partner Kelly and our amazing daughter Freya – tomorrow I will be carrying three thick copies of the thesis in one arm for submission, and Freya in the other. I should be pretty well balanced.

Cliffe Woods, Rochester

13th October 2011

ABSTRACT

The Platreef is a Ni-Cu-PGE mineralised tabular body at the base of the Rustenburg Layered Suite in the northern limb of the Bushveld Complex. The reef lies unconformably on a footwall (floor) sequence of Transvaal Supergroup sedimentary rocks and Archaean granite/gneiss basement, and is overlain by a hangingwall (roof) of Main Zone gabbro-norites.

Structural relationships suggest that the Platreef was emplaced as a broadly horizontal sill-like sheet into the Transvaal Supergroup, but local variations in its thickness and path of intrusion were caused by pre-existing structures in the country rocks. As the Platreef cooled and was nearly crystallised, ductile deformation occurred, possibly as an episode in a longer event. Main Zone magma was emplaced above the deformed, nearly consolidated Platreef and eroded the uppermost portion, locally assimilating mineralised reef. The Main Zone magma also intruded into shear zones as thin dykes down through the Platreef and metasedimentary floor. Structural patterns around a prominent dome in the floor rocks suggest that regional deformation may still have been active when the earliest Main Zone layers were developing, but ceased by Upper Main Zone time.

Other studies of the Platreef beyond Sandsloot have shown that its earliest Ni-Cu-PGE mineralisation was orthomagmatic, largely preserved where the floor rocks are unreactive basement granite/gneiss. However, interaction between the Platreef magma and surrounding sedimentary rocks has produced different mineralogical associations and assemblages that were influenced by the local floor and roof rocks along the strike of the reef. At Sandsloot, the floor rocks are represented by reactive siliceous dolomites of the Malmani Subgroup. The Platreef magma caused contact metamorphism and metasomatism of the dolomites, releasing volatiles that entered the reef. These hydrothermal fluids stripped PGE from primary sulphides and redistributed the PGE within the reef and into the metasedimentary country rocks. In places, primary platinum group minerals were overprinted by lower-temperature species.

CONTENTS

1. INTRODUCTION.....	1
1.1 PRELUDE	1
1.2 THE PLATINUM GROUP ELEMENTS	1
1.2.1 <i>Physical and chemical properties</i>	1
1.2.2 <i>PGE distribution in the Earth</i>	3
1.2.3 <i>Aqueous geochemistry of the PGE</i>	3
1.2.4 <i>Uses of the PGE</i>	4
1.3 PLATINUM GROUP MINERALS	5
1.4 TYPES OF PGE DEPOSITS	7
1.4.1 <i>Physical environments for PGE deposits</i>	7
1.4.2 <i>Overview of PGE deposits in igneous rocks</i>	8
1.4.3 <i>Hydrothermal PGE deposits</i>	13
1.5 PURPOSE OF THE STUDY	13
1.5.1 <i>Problem statement</i>	13
1.5.2 <i>Aims and objectives</i>	15
2. THE BUSHVELD COMPLEX.....	16
2.1 INTRODUCTION TO THE BUSHVELD COMPLEX.....	16
2.2 STRUCTURE OF THE BUSHVELD COMPLEX	17
2.3 PALAEOTECTONIC SETTING	22
2.4 SOURCE OF BUSHVELD MAGMA	22
2.5 AGE OF THE BUSHVELD COMPLEX	27
3. THE NORTHERN LIMB.....	30
3.1 INTRODUCTION TO THE NORTHERN LIMB.....	30
3.2 STRUCTURE OF THE NORTHERN LIMB	30
3.3 DEVELOPMENT OF THE RLS IN THE NORTHERN LIMB	37
3.3.1 <i>Stratigraphy of the northern limb</i>	37
3.4 AGE OF THE NORTHERN LIMB	43
4. THE PLATREEF	45
4.1 INTRODUCTION	45
4.2 SETTING OF THE PLATREEF	45
4.2.1 <i>Sulphur isotope studies</i>	48
4.3 EXPLORATION AND RESEARCH ON THE PLATREEF.....	49
4.4 GEOLOGY OF THE PLATREEF AND ASSOCIATED UNITS.....	51
4.4.1 <i>Footwall lithologies</i>	52
4.4.2 <i>Hangingwall lithologies</i>	52

4.4.3	<i>Platreef lithologies</i>	53
4.5	EMPLACEMENT AND TIMING OF THE PLATREEF.....	58
4.6	MINERALISATION OF THE PLATREEF.....	59
4.7	EFFECTS OF CONTAMINATION AND HYDROTHERMAL ACTIVITY.....	60
4.7.1	<i>Contamination of the Platreef by country rocks</i>	60
4.7.2	<i>Hydrothermal modification</i>	62
5.	GEOLOGY OF THE PLATREEF AT SANDSLOOT	64
5.1	INTRODUCTION.....	64
5.1.1	<i>Field methods</i>	65
5.2	THE SANDSLOOT MINE.....	65
5.3	GENERAL STRATIGRAPHY AT SANDSLOOT.....	65
5.4	STRUCTURAL GEOLOGY AT SANDSLOOT.....	66
5.5	LITHOLOGICAL DESCRIPTIONS.....	74
5.5.1	<i>Hangingwall gabbro-norite</i>	74
5.5.2	<i>The Platreef</i>	75
5.5.3	<i>Footwall lithologies</i>	77
5.6	FACE MAP DESCRIPTIONS AND PETROGRAPHY.....	84
5.6.1	<i>Face 138/038 (N1)</i>	85
5.6.2	<i>Face 132/032 (S1)</i>	89
5.6.3	<i>Face 141/022 (N2)</i>	91
5.6.4	<i>Face 144/011 (N3)</i>	92
5.6.5	<i>Face 135/014 (SW1)</i>	95
5.6.6	<i>Face 138/014 (SW2)</i>	97
5.6.7	<i>Face 141/021 (SW3)</i>	99
5.7	DRILL CORES.....	101
5.7.1	<i>Core SSP242</i>	101
5.7.2	<i>Core SSP257</i>	104
5.7.3	<i>Core SSP258</i>	106
5.8	SUMMARY OF OBSERVATIONS.....	109
6.	MINERALOGY AND GEOCHEMISTRY OF THE PLATREEF AT SANDSLOOT	110
6.1	METHODOLOGY.....	110
6.2	BULK GEOCHEMICAL DATA.....	111
6.2.1	<i>Major element trends</i>	111
6.3	MINERAL CHEMISTRY.....	114
6.3.1	<i>Plagioclase compositions</i>	116
6.3.2	<i>Olivine compositions</i>	117
6.4	TRACE ELEMENT GEOCHEMISTRY.....	117
6.4.1	<i>Rare earth elements</i>	117
6.4.2	<i>Spidergrams</i>	121
6.5	BULK PGE GEOCHEMISTRY.....	126
6.5.1	<i>PGE mineralisation in the lowermost hangingwall</i>	127

6.5.2	<i>Comparison of PGE data with other Platreef sectors</i>	<i>130</i>
6.5.3	<i>Comparison of PGE data with Merensky Reef and UG2.....</i>	<i>130</i>
6.6	PLATINUM GROUP MINERALOGY	132
6.6.1	<i>PGM species.....</i>	<i>132</i>
6.6.2	<i>Grain size and morphology.....</i>	<i>133</i>
6.6.3	<i>PGM distribution.....</i>	<i>135</i>
6.7	SUMMARY	136
7.	DISCUSSION	138
7.1	EMPLACEMENT OF PLATREEF MAGMA	138
7.1.1	<i>Intrusive relations.....</i>	<i>138</i>
7.1.2	<i>Constraints on relative timing</i>	<i>140</i>
7.1.3	<i>Structural controls on Platreef emplacement</i>	<i>140</i>
7.1.4	<i>Controls on the shape of the Platreef.....</i>	<i>141</i>
7.2	INTERACTION OF PLATREEF MAGMA WITH COUNTRY ROCKS	147
7.2.1	<i>Contamination and source of sulphur.....</i>	<i>147</i>
7.2.2	<i>Metamorphism</i>	<i>150</i>
7.3	MECHANISMS OF PGE DISTRIBUTION.....	151
7.3.1	<i>Primary magmatic mineralisation.....</i>	<i>151</i>
7.3.2	<i>Hydrothermal redistribution of PGE.....</i>	<i>152</i>
8.	SUMMARY AND CONCLUSIONS.....	155
8.1	DEVELOPMENT OF THE PLATREEF AT SANDSLOOT.....	155
8.1.1	<i>Synopsis</i>	<i>156</i>
8.2	CONCLUSION.....	159
8.3	EPILOGUE.....	160
9.	REFERENCES.....	162

APPENDIX 1: Armitage *et al.* 2002: Platinum-group element mineralization in the Platreef and calc-silicate footwall at Sandsloot, Potgietersrus District, South Africa.

APPENDIX 2: Holwell *et al.* 2005: Observations on the relationship between the Platreef and its hangingwall.

APPENDIX 3: McDonald *et al.* 2005: Geochemistry and mineralogy of the Platreef and “Critical Zone” cumulates of the Northern limb of the Bushveld Complex, South Africa: implications for Bushveld stratigraphy and the development of PGE mineralization.

APPENDIX 4: Holwell *et al.* 2006: Platinum-group mineral assemblages in the Platreef at the South Central Pit, Sandsloot Mine, northern Bushveld Complex, South Africa.

APPENDIX 5: Armitage *et al.* 2007: A geological investigation of the Waterberg hydrothermal platinum deposit, Mookgophong, Limpopo Province, South Africa.

TABLES

<i>Table 1-1. Physical properties of the platinum-group elements (data from Johnson Matthey 2011a).....</i>	<i>2</i>
<i>Table 6-1. Concentrations of selected trace elements in reef, ORR and hybrid lithologies in faces SW1 and SW2. Data from McDonald et al. (2005a).....</i>	<i>113</i>
<i>Table 6-2. PGE and Au concentrations and ratios for Platreef, hangingwall, footwall and dyke lithologies (expanded after Armitage et al. 2002). PGE and Au data are reported in parts per billion. Additional data are also given for the Merensky Reef (SARM-7 preferred values from Steele et al. 1975) and the UG2 chromitite (McLaren & De Villiers 1982) for comparison.....</i>	<i>128</i>

FIGURES

Fig. 1-1. [Left column] Global supply of Pt, Pd and Rh by region and [right column] global demand for Pt, Pd and Rh by application in 2010 (pie charts from Johnson Matthey 2011b).	6
Fig. 1-2. Cartoon of conduits showing common geometries of structural traps in which sulphide liquid may accumulate (from Mungall 2005).	8
Fig. 1-3. Pt, Pd and Rh resources of major mining areas of the world (from Naldrett et al. 2008).	9
Fig. 1-4. Simplified model of a layered intrusion showing the types of PGE deposits and their likely location within the intrusion (from Naldrett 2005a).	10
Fig. 2-1. Simplified geological map of the Bushveld Complex (after Kinnaird et al. 2005).	17
Fig. 2-2. Aeromagnetic map of the Bushveld Complex with approximate town locations (modified after Kinnaird 2005b). High to low gravimetric signatures are purple (highest) through red, yellow, green, pale blue and dark blue (lowest). Note the lobate structure of the complex associated with east-west to ENE-WSW trending lineaments, especially the Thabazimbi-Murchison Lineament close to Mookgophong.	20
Fig. 2-3. Tectonic scenario for the evolution of the Kaapvaal Craton (after Silver et al. 2004). TML = Thabazimbi-Murchison Lineament; CL = Colesberg Lineament; TSZ = Triangle Shear Zone; PSZ = Palala Shear Zone; SR = Soutpansberg Rift.....	23
Fig. 2-4. Gravity map of the Bushveld Complex (after Cawthorn & Webb 2001). Solid outline delimits surface outcrop of mafic rocks.	25
Fig. 3-1. Simplified map of the outcrops and estimated areal extent of the layered suite of the northern lobe of the Bushveld Complex (from van der Merwe 2008).	31
Fig. 3-2. Geological map of the lower portion of the northern limb, showing the locations described in the text (from McDonald et al. 2005a).	33
Fig. 3-3. Traditional stratigraphic relationships between the eastern and western limbs and the northern limb of the Bushveld Complex (after White 1994; Cawthorn & Lee 1998).	38
Fig. 3-4. Geological map of the northern limb of the Bushveld Complex with farm boundaries (from Maier et al. 2008b, adapted from Ashwal et al. 2004).	40
Fig. 3-5. Stratigraphy of the northern limb south of Mokopane showing the major chromitite, magnetite and Ni-Cu-PGE deposits (from McDonald et al. 2005a, modified after Von Gruenewaldt et al. 1989).	41
Fig. 4-1. Simplified geological map of part of the northern limb, showing boundaries of farms referred to in the text (slightly modified from Kinnaird 2005b).	46
Fig. 4-2. Schematic longitudinal section through the Platreef along the entire strike length (from Kinnaird et al. 2005). Note that between Witrivier and Altona a significant strike length is not shown.	47
Fig. 5-1. Wireframe plan view of Sandsloot open pit in July 2000 showing locations of faces mapped and corresponding sample suites in this study. Solid lines represent major bench crests. Deepest area of the pit (south central area) is approximately 190 m below outer rim level. Stippled grey line is approximate trace of Platreef.	64

- Fig. 5-2. Map of the Sandsloot open pit mine (after Bye et al. 1999) showing its approximate outline shortly before this study. Important features of the map are the faults and the westward deflection of the Platreef in the south part of the pit. Note that ‘parapyroxenite’ is attributed to the Platreef, but is shown in this study to be a footwall lithology. ‘Chuniespoort Group carbonate’ is Malmani Dolomite at this location. 67
- Fig. 5-3. LandSat TM image of Sandsloot and neighbouring properties. Image acquired in 1992, before mining began at Sandsloot. Area corresponds to that in aeromagnetic image in Fig. 5-8. Note prominent WSW-pointing ‘dolomite tongue’ below left of centre, transgressed near its west tip by Sandsloot river where open pit mine is now located. Image is RGB 457 (red, green, blue; bands 4, 5 and 7) false colour composite, 30 m spatial resolution. 68
- Fig. 5-4. Approximately southward view perpendicular to south highwall from base of Sandsloot pit showing open, asymmetrical antiform defined by footwall bedding. Direction of view is along or subparallel to axis of antiform. Note location of face S1 in left foreground on east limb of antiform. 69
- Fig. 5-5. Approximately southeastward view from west rim of Sandsloot pit showing south limb of open, approximately ENE-WSW trending syncline defined by footwall bedding. Direction of view is oblique to fold axis. Location of mapped face S1 is indicated. 70
- Fig. 5-6. Approximately northeastward view from southwest part of Sandsloot pit showing hinge zone/axis and north limb of approx. E-W trending, very open syncline (‘Sandsloot Syncline’ in Friese 2004) rising into north pit in the distance. View is oblique to fold axis. 70
- Fig. 5-7. Schematic southeastward view of footwall structure as exposed in the Sandsloot south pit. Stippled lines represent bedding. 71
- Fig. 5-8. Local aeromagnetic image superimposed on aerial photograph of Sandsloot and adjacent properties (image and boundaries from Potgietersrus Platinums Ltd internal presentation). Note ‘dolomite tongue’ immediately south and southwest of Sandsloot pit; Main Zone layering abutting the tongue on farms Sandsloot and Knapdaar; and high aeromagnetic signature of Penge banded iron formation (purple zone at Tweefontein). 72
- Fig. 5-9. Southwestward oblique view of orebody in south pit at Sandsloot (red in vertical section). Pit faces are outlined in pale blue from data in early 2000, boreholes in dark blue. Longest axis (north-south) is approx. 1.7 km. 73
- Fig. 5-10. Margin of large hydrothermal vein (right of hammer) in floor rocks in south highwall of pit. Note brittle-ductile shear along vein margin, expressed as disharmonious folding of country rocks. Serpentinisation (dark layers) of calc-silicate hornfels highlights fold pattern. 74
- Fig. 5-11. Photomicrograph of fine-grained hangingwall gabbronorite (plane polarised light), consisting of cumulus plagioclase and intercumulus pyroxene. Accessory phases are phlogopite and opaques. Specimen N1-31. Field of view ~2 cm wide. 75
- Fig. 5-12. Photomicrograph of hangingwall gabbronorite with fresh cumulus plagioclase and intercumulus pyroxene. Specimen N1-31. Field of view approx. 4 mm wide. 75
- Fig. 5-13. Drill core of coarse-grained Platreef pyroxenite with minor plagioclase content (middle core) and medium- to coarse-grained Platreef pyroxenite with rare plagioclase (lower core). Note also red-brown phlogopite in centre left. 76

Fig. 5-14. Lenticular bodies and contiguous bands of diopsidite (grey) in folded footwall calc-silicate hornfels (milky/beige colour). Large camera bag for scale, with hinge of open synform visible above it.	78
Fig. 5-15. Hydrogrossular (red) in footwall clinopyroxenite (diopsidite).....	79
Fig. 5-16. Coarse-grained footwall clinopyroxenite consisting of diopside (grey) and assumed vesuvianite (greenish).	79
Fig. 5-17. Local variation between unaltered footwall diopsidite (grey) and serpentinised diopsidite (black), with sharp irregular boundaries.	79
Fig. 5-18. SEM images of metamorphic olivine at [left] incipient stage of alteration to serpentine (darkest pervasive veins) and magnetite (bright wispy bands); and [right] more advanced stage of alteration. Specimen N1-4.	80
Fig. 5-19. Footwall calc-silicate hornfels in drill core SSP242 at 321.95 m depth. Large grey/green crystals are diopside.....	81
Fig. 5-20. Ovoid body of pure, white wollastonite in footwall calc-silicate hornfels.	81
Fig. 5-21. Photomicrograph of meta olivine clinopyroxenite (plane polarised light) pervaded by network of serpentine microveins (dark material). Specimen PA-E142. Field of view ~2 cm wide.	81
Fig. 5-22. Dark serpentinite associated with intersections of joints/fractures in footwall. Note compositional variation in footwall layers and thin, bedding-parallel, dark serpentinite bands. Yellow field book (20 cm long) for scale.....	82
Fig. 5-23. Photograph of pegmatoidal mafic dyke. Note well developed, cumulus feldspar laths.	83
Fig. 5-24. Photomicrograph of pegmatoidal mafic dyke (crossed nicols) consisting of highly altered cumulus plagioclase (sericite and epidote from sericite) and orthopyroxene, in this case in eutectic intergrowth, with reaction rim around orthopyroxene. Specimen PA-N1-0. Field of view approx. 4 mm.....	83
Fig. 5-25. Highly pegmatoidal anorthosite-pyroxenite pocket in the Platreef near the major dyke shown in Fig. 5-23 above.	83
Fig. 5-26. Smaller pegmatoidal vein branching from the major pegmatoidal dyke in Fig. 5-23. Note large bowed pyroxene crystal right of centre.	83
Fig. 5-27. Geological map and composite photograph of face 132/038 (N1).	87
Fig. 5-28. Photomicrograph of Platreef gabbronorite (plane polarised light), consisting of euhedral to subhedral cumulus orthopyroxene and clinopyroxene in intercumulus plagioclase. Minor phases are red-brown phlogopite and opaques. Specimen N1-14. Field of view ~3 cm wide.	88
Fig. 5-29. Photomicrograph of Platreef gabbronorite (crossed nicols) showing interstitial twinned plagioclase in variable state of saussuritisation between euhedral to subhedral crystals of orthopyroxene and clinopyroxene. Specimen N1-26. Field of view approx. 4 mm wide.	88
Fig. 5-30. Dark serpentinite xenolith in very coarse Platreef gabbro in face N1, cut by a late quartz-feldspathic vein. Note possible igneous layering in gabbro in centre right part of photograph (detail in Fig. 5-31).	88
Fig. 5-31. Detail of apparent crude igneous layering in very coarse-grained Platreef gabbro in face N1.	88
Fig. 5-32. Detail of pegmatoidal gabbroic pod at base of Platreef in face N1. Pale portion is aplite.	88
Fig. 5-33. Detail of highly mineralised gabbro in pegmatoidal pod in face N1.....	88

<i>Fig. 5-34. Geological map and photograph of face 132/032 (sample suite PA-S1) consisting entirely of footwall lithologies with minor igneous ‘tubes’. Labels 32GP9 and 32GP10 are survey geopoints. Sampling locations and sample numbers are shown.....</i>	<i>90</i>
<i>Fig. 5-35. Geological map of face 141/022 (N2).....</i>	<i>91</i>
<i>Fig. 5-36. Geological map of face 144/011 (N3).....</i>	<i>93</i>
<i>Fig. 5-37. Detail of hangingwall contact zone in face N3 (from McDonald et al. 2005a).....</i>	<i>93</i>
<i>Fig. 5-38. Fine-grained Main Zone gabbro-norite intruded above mottled anorthosite in a dry river bed at Zwartfontein South, a short distance north of the Sandsloot pit, prior to commencement of the Zwartfontein open pit operation. Note wavy contact. The anorthosite overlies oxidised Platreef beneath sandy cover beyond the lower right margin of the photograph.....</i>	<i>94</i>
<i>Fig. 5-39. Composite photomicrograph showing the contact between fine-grained, hangingwall poikilitic leuconorite (upper half of photograph) and coarse-grained, mineralised Platreef feldspathic pyroxenite (lower half). Note the embayments made by hangingwall plagioclase in the cumulus Platreef orthopyroxenes (arrowed). Dark patches within the plagioclase are alteration (from Holwell et al. 2005).....</i>	<i>94</i>
<i>Fig. 5-40. Photograph and geological map of face 135/014 (SW1).....</i>	<i>96</i>
<i>Fig. 5-41. Photomicrograph of specimen SW1-43 (plane polarised light). Note dull green olivine around eroded orthopyroxene grains (grey).</i>	<i>96</i>
<i>Fig. 5-42. Photomicrograph of fresh, fractured olivine in orthopyroxene (crossed nicols). Specimen SW1-40.</i>	<i>96</i>
<i>Fig. 5-43. Olivine replacement texture in specimen SW1-40. Note embayments of olivine in orthopyroxene.....</i>	<i>97</i>
<i>Fig. 5-44. Geological map of face 138/014 (SW2).</i>	<i>98</i>
<i>Fig. 5-45. Photomicrograph of footwall-reef hybrid (plane polarised light). Note eroded pyroxenes (grey) and network of serpentine veins (dark). Specimen SW2-28.</i>	<i>99</i>
<i>Fig. 5-46. Photomicrograph of Platreef gabbro-norite consisting of disaggregated cumulus euhedral orthopyroxene and minor clinopyroxene, and subhedral ortho- and clinopyroxene aggregates with saussuritised intercumulus plagioclase. Minor phases are red-brown phlogopite and opaques. Specimen SW2-49.</i>	<i>99</i>
<i>Fig. 5-47. Photomicrograph of Platreef feldspathic pyroxenite consisting of aggregates of coarse, sub- to anhedral ortho- and clinopyroxene with minor interstitial plagioclase. Green mineral is chlorite. Specimen SW2-77.</i>	<i>99</i>
<i>Fig. 5-48. Composite photograph (shadow of drill rig in centre) and geological map of face 141/021 (SW3)....</i>	<i>100</i>
<i>Fig. 5-49. Geological log of drill core SSP242. Colours for the various lithologies are the same as for the face maps (see legend in Fig. 5-27).</i>	<i>103</i>
<i>Fig. 5-50. Geological log of drill core SSP257. Colours for the various lithologies are the same as for the face maps (see legend in Fig. 5-27).</i>	<i>105</i>
<i>Fig. 5-51. Geological log of drill core SSP258. Colours for the various lithologies are the same as for the face maps (see legend in Fig. 5-27).</i>	<i>107</i>
<i>Fig. 6-1. Major element concentrations (wt%) in samples collected along face N1, with schematic face map (red lines and text) to show sampling locations.....</i>	<i>113</i>

Fig. 6-2. Major elements concentrations (wt%) in samples collected along face SW1, with schematic face map (red lines and text) to show sampling locations.	114
Fig. 6-3. Major elements concentrations (wt%) in samples collected by Harris & Chaumba (2001) from bench 20 in the east-central part of the Sandsloot pit. Schematic face map (red lines and text) shows sampling locations.....	115
Fig. 6-4. Compositions of pyroxenes in Platreef gabbros (samples N1-26, SW2-49) and pyroxenites (SW2-77, SW1-40, SW1-43) at Sandsloot, from McDonald et al. (2005a). Shaded area shows the range of typical Merensky Reef pyroxenes (Buchanan et al. 1981).	116
Fig. 6-5. Chondrite-normalised REE plot for a selection of Platreef samples.	118
Fig. 6-6 (a-c). Chondrite-normalised REE plots for the Platreef and associated units at [a] Townlands (Manyeruke et al. 2005), [b] Overysel (Holwell & McDonald 2006) and [c] Sandsloot (this study and McDonald et al. 2005a). Overysel data is based on two drill cores. Figure modified from Holwell & McDonald (2006).....	118
Fig. 6-7. Chondrite-normalised REE plot for a selection of hangingwall and mafic dyke samples.	119
Fig. 6-8. Chondrite-normalised REE plot for footwall samples differentiated into main lithological types.	120
Fig. 6-9. Mantle-normalised concentrations of LILE and HFSE in a selection of reef samples in face N1. Trace element compositions of the model B1 basaltic andesite and B2/B3 tholeiitic basalt are given for comparison (data from Barnes & Maier 2002).	122
Fig. 6-10 (a-c). Mantle-normalised concentrations of LILE and HFSE in a selection of [a] reef (including olivine replaced reef), [b] hybrid and [c] footwall samples (calc-silicates, parapyroxenites, serpentinites) from face SW1 and SW2. Trace element composition of the model B1 basaltic andesite and B2/B3 tholeiitic basalt are given for comparison (B1 and B2/B3 data from Barnes & Maier 2002).	124
Fig. 6-11. Mantle-normalised concentrations of LILE and HFSE in a selection of hangingwall samples from faces N1, N3 and SW1.....	125
Fig. 6-12. Mantle-normalised concentrations of LILE and HFSE in mafic dyke samples from face N1.	126
Fig. 6-13. Chondrite-normalised PGE concentrations of hangingwall, dyke, Platreef and high-grade footwall samples.	129
Fig. 6-14. Mantle normalised metal patterns for the Merensky Reef, UG2 chromitite and Platreef (modified from Kinnaird 2005b).	131
Fig. 6-15. Pie charts showing proportions of different types of PGM in Platreef samples from Sandsloot [left] and in the Merensky Reef for comparison [right]. Platreef values are based on this study and Holwell et al. 2006, Merensky values from Anglo Research Centre.....	133
Fig. 6-16. [Left] SEM image of polyphase PGM grain with apparent matrix of isoferroplatinum and inclusions of rustenburgite and possible vincentite (with Sb, but no As or Te), occurring between large crystals of clinopyroxene and orthopyroxene in altered reef specimen SW2-49. [Right] Interpretation of PGM grain based on element mapping and spot analyses.....	134
Fig. 6-17. SEM images of composite PGM grain in an intersilicate setting in specimen SW1-32. Note cubic form of sperrylite.....	135
Fig. 8-1. Three-dimensional block model, viewed to southeast, for Platreef development at Sandsloot. (1) Deposition of Transvaal Supergroup ~2.7-2.2 Ga. (2) Two-phase compressive deformation of	

Transvaal Supergroup after 2.2 Ga, during or culminating with the Magondi Orogeny. (3) Intrusion of Platreef sheet with overall horizontal attitude, but thickness locally controlled by pre-existing structures. (4) Deformation of cooling Platreef and Transvaal Supergroup country rocks, possibly at late stage of Magondi Orogeny, with accentuation of previously formed structures. (5) Emplacement of Main Zone, eroding uppermost Platreef, and intrusion of associated pegmatoidal dykes into shear zones through Platreef and footwall. Continuing late-stage deformation affects lower Main Zone but ceases during Main Zone emplacement. (6) Subsidence of northern limb down to west, and erosion to present-day surface. 158

1. INTRODUCTION

1.1 *Prelude*

In the last decade or so, the unprecedented demand for platinum group elements (PGE) and the resultant surge in PGE prices has led to a worldwide boom in PGE exploration and mining. In recent years, new PGE mines have been opened and are being developed on the Merensky Reef and UG2 chromitite in the western and eastern limbs of the Bushveld Complex, and on the Platreef of the northern limb. In South Africa, which is the world's largest supplier of PGE, changes in mineral rights legislation has contributed to the boom. Several other igneous bodies in southern Africa have recently been or are being explored for PGE by a number of mining companies. Further, the historically high PGE prices have made PGE an increasingly significant and profitable by-product of some primary nickel mining operations.

The output of PGE mines in South Africa was reduced by a nationwide electricity shortage in 2008, raising fears of decreased PGE supply over the next 5 years and consequently lifting PGE prices higher still. In the latter part of 2008, however, the worldwide 'credit crunch' had a severe effect on the global economy. The resultant fall in demand for commodities such as PGE led to a sharp drop in commodity prices. Since then, prices have seen a rapid recovery, with an attendant appetite for investment, and the exploration boom for many commodities has resumed, fuelled largely by massive demand in rapidly developing, highly populated nations such as China and India. However, current fears over the excessive national deficits of major nations are now causing uncertainty and resultant volatility in the markets.

1.2 *The platinum group elements*

1.2.1 *Physical and chemical properties*

The platinum group elements (PGE) comprise a geochemically coherent group of siderophile to chalcophile metals that includes osmium (Os), iridium (Ir), ruthenium (Ru), rhodium (Rh), platinum (Pt) and palladium (Pd). They belong to the Group VIII transition elements together with Fe, Co and Ni, and are among the least abundant of all elements in the bulk Earth.

Based on their position within the Periodic Table, the PGE may be divided into two subgroups or triads: the 'heavy' Ir triad consisting of Os, Ir and Pt (atomic numbers 76, 77, 78

respectively), and the ‘light’ Pd triad consisting of Ru, Rh and Pd (atomic numbers 44, 45, 46 respectively). A more common subdivision on geochemical grounds separates the PGE into high temperature Ir-group PGE (IPGE) comprising Os, Ir and Ru; and the low temperature Pd-group PGE (PPGE), comprising Rh, Pt and Pd (e.g. Barnes *et al.* 1985; Tredoux *et al.* 1995). The PGE, together with gold and silver, are often called ‘precious metals’ or ‘noble metals’.

In chemical terms the PGE are highly siderophile, i.e. they tend to bond with metallic iron where it is present. The PGE form a diverse array of complete and partial solid solutions with each other, with Fe and Ni, and with elements such as Sn, Pb, Sb, and Bi (Berlincourt *et al.* 1981). The PGE dissolve slowly in concentrated acids but are virtually unreactive in diluted acids and alkalis. Pt and Pd are more reactive than the other PGE in concentrated acid, and dissolve readily in aqua regia. The PGE will all react with oxygen and halogens only at high temperatures to produce volatile PGE oxides and halide compounds. Perhaps the most important property of the PGE in the context of this study is that they dissolve in molten bases of the P block of the periodic table to form a wide range of sulphides, tellurides, arsenides, bismuthides, antimonides and selenides. These constitute many of the naturally occurring platinum group minerals (PGM), which will be outlined in a later section. Table 1-1 below shows some of the physical properties of the PGE.

Property	Ru	Rh	Pd	Os	Ir	Pt
Atomic number	44	45	46	76	77	78
Atomic weight	101.07	102.94	108.42	190.23	192.22	195.08
Density (g/cm ³)	12.45	12.41	12.02	22.61	22.65	21.45
Melting point (°C)	2310	1960	1554	3050	2443	1769
Boiling point (°C)	3900	3727	3140	5027	4130	3827
Resistivity at 0°C (μΩcm)	6.80	4.33	9.93	8.12	4.71	9.85
Hardness (annealed, VHN)	240	101	40	350	220	40
Atomic radius (cm ⁻⁸)	1.336	1.342	1.373	1.350	1.355	1.385
Oxidation state (common)	+3	+3	+2	+4	+3	+2
Oxidation state (highest)	+8	+6	+4	+8	+6	+6
Thermal conductivity (watts/m/°C)	105	150	76	87	148	73
Tensile strength (kg/mm ²)	165	71	17	-	112	14

Table 1-1. Physical properties of the platinum-group elements (data from Johnson Matthey 2011a).

1.2.2 PGE distribution in the Earth

It is believed that the siderophile nature of the PGE has resulted in their concentration in the Earth's core at an early stage of the planet's formation (e.g. Azbel *et al.* 1993; McDonough & Sun 1995; Righter 2003). Some studies suggest that siderophile elements are more abundant in the Earth's mantle than core-mantle partitioning models predict (Borisov *et al.* 1994). Moreover, highly siderophile elements occur in approximately chondritic relative abundances in the mantle. These two features have been used to support the 'late veneer hypothesis' in which highly siderophile elements were reintroduced into the mantle by intense meteoritic bombardment of the primitive Earth after core formation (Chou 1978; Morgan 1986; O'Neill 1991). However, this hypothesis may not be in agreement with more recently published PGE data that seem to show PGE fractionation and heterogeneity in the upper mantle that is inconsistent with any of the major chondrite groups (e.g. Pattou *et al.* 1996; Snow & Schmidt 1998).

Processes of partial melting of mantle, which contains intermediate amounts of PGE, followed by emplacement into the crust and the action of various magmatic and fluid processes may result in economic concentrations of the PGE. In terrestrial environments, PGE concentration ranges from sub-ppb (parts per billion) level in rocks of felsic and intermediate composition to generally 1-100 ppb in mafic and ultramafic rocks (e.g. Misra 2000; Crocket 1981, 2002; Barnes *et al.* 1985). Economic deposits typically contain 5-10 ppm (parts per million) PGE and involve concentration factors in the order of one thousand, similar to those for gold deposits. Whilst mafic and ultramafic rocks are the main exploration targets for PGE, it is not clear whether the essential silicate and accessory oxide minerals of these rocks are true collectors of PGE, or of specific PGE, in a magma (Crocket 2002); but there is evidence that PGE-rich inclusions may be present in the silicate phases (Keays & Campbell 1981; Barnes & Naldrett 1987). Rather, PGE are concentrated to much higher levels in sulphides and in rarer metallic alloys, tellurides, selenides, arsenides and sulpharsenides (Cabri 1992, 1994, 2002).

1.2.3 Aqueous geochemistry of the PGE

The PGE are mobile in aqueous fluids, and it is generally considered that Pt and Pd are more mobile than Rh, Ru, Os and Ir (Westland 1981; Wood 2002). Aqueous fluids can be magmatic, metamorphic or meteoric, and hydrothermal processes appear to have operated at some stage in the evolution of the majority of PGE deposits, but the importance of each of these processes in the concentration of PGE to economic levels is debated. The PGE can be transported as chloride complexes, in bisulphide solutions, as hydroxide complexes and as

organic ligand complexes (Wood 2002 and references therein). In some deposits, aqueous solutions may be the primary mechanism of PGE concentration. In the Waterberg Pt deposit, for example, Pt owes its presence exclusively to hydrothermal processes (Wagner 1929; McDonald *et al.* 1995; McDonald *et al.* 1999; Armitage *et al.* 2007).

1.2.4 Uses of the PGE

The outer electronic structure of the PGE gives them outstanding catalytic properties. They are highly resistant to wear and tarnish, making platinum particularly well suited to fine jewellery. Other distinctive properties include resistance to chemical attack, excellent high-temperature characteristics, and stable electrical properties. All of these properties have been exploited for industrial applications. Pure Pt, Pt alloys and Ir are used as crucible materials for the growth of single crystals, especially oxides. The chemical industry uses a significant amount of either Pt or a Pt-Rh alloy catalyst in the form of gauze to catalyse the partial oxidation of ammonia to yield nitric oxide, which is the raw material for fertilisers, explosives, and nitric acid. In recent years, a number of PGE have become important as catalysts in synthetic organic chemistry. Ru dioxide is used as coatings on dimensionally stable titanium anodes used in the production of chlorine and caustic soda. Pt-supported catalysts are used in the refining of crude oil, reforming, and other processes used in the production of high-octane gasoline and aromatic compounds for the petrochemical industry. Since 1979, the automotive industry has emerged as the principal consumer of PGE. Pd, Pt, and Rh have been used as oxidation catalysts in catalytic converters to treat automobile exhaust emissions (e.g. Huuhtanen *et al.* 2005). A wide range of PGE alloy compositions is used in low-voltage and low-energy contacts, thick- and thin-film circuits, thermocouples and furnace components, and electrodes.

Pt has the ability, in certain chemical forms, to inhibit the division of living cells, and the discovery of this property has led to the development of Pt-based anti-cancer drugs such as the intravenously administered Cisplatin, Carboplatin and Oxaliplatin (marketed under the trade name Eloxatin). Satraplatin, a new orally administered Pt anti-cancer drug, is undergoing clinical trials for treatment of prostate cancer. Pacemakers for heart disorders usually contain at least two Pt-Ir electrodes, and Pt electrodes are also found in pacemaker-like devices (e.g. internal cardioverter defibrillators). Many catheters contain Pt marker bands and guide wires, which are used to help the surgeon guide the device to the treatment site. The radio-opacity of Pt enables doctors to monitor the position of the catheter by X-ray during treatment.

Pt and principally Pd are the main PGE used in dental restorations. They are usually mixed with gold or silver as well as copper and zinc in varying ratios to produce alloys suitable for dental inlays, crowns and bridges. Small amounts of Ru or Ir are sometimes added. The most common application is in crowns, where the alloy forms the core onto which porcelain is bonded to build up an artificial tooth.

Fig. 1-1 illustrates the supply of Pt, Pd and Rh by region and the demand for the same metals by application in the year 2010. This was 1-2 years after the ‘credit crunch’ and notable changes in PGE supply and demand (and therefore prices) have come about since 2007, when world markets were at a high. In particular, there was a shortfall in Pt supply of 265,000 oz (troy ounces) in 2007, but demand fell by about 1 Moz (million troy ounces) in 2009, levelling into 2010, and was only just met by supply in 2009 and 2010. Pd demand fell only slightly between 2007 and 2009, but was still comfortably fulfilled despite a fall in supply of 1.145 Moz. In 2010, Pd demand rose by 1.26 Moz from 2009 while supply only rose by 115,000 oz. Rh was in slight undersupply in 2007 but in oversupply in 2009 due to a fall in demand of 260,000 oz. In 2010, Rh demand fell by 11,000 oz while supply fell by 32,000 oz but there was still an oversupply of 114,000 oz.

1.3 Platinum group minerals

Cabri (1976) published a glossary of 74 platinum group minerals (PGM) and mentioned the reported occurrence of 65 or more unnamed PGM awaiting further characterisation. Later, the same author reviewed the mineralogy, geology and recovery of the PGE (Cabri 1981), covering inorganic chemistry, phases and phase relations, geochemistry, sample preparation techniques, analytical methods, PGM, PGE deposits and the relationship of mineralogy to the recovery of PGE from ores. By 1997 there were 96 approved PGM, over 500 unidentified platinum group phases, and more than 20 non-platinum group minerals containing varying concentrations of one or more of the six PGE. Daltry & Wilson (1997) reviewed the published literature and evaluated approximately 1500 published chemical analyses of PGM that had been accepted by the International Mineralogical Association as discrete mineral species, and unidentified (unnamed or inadequately described) platinum group phases reported in the literature but not proven to be discrete minerals. The database revealed some chemically related trends concerning the PGE themselves and the essential non-PGE constituents. In an update of his 1981 work, Cabri (2002) lists 109 PGM, the majority of which are recognised by the Commission on New Minerals and Mineral Names, and characterises their general appearance, physical and optical properties, chemical analytical data, reported localities, occurrence and relationship to other species.

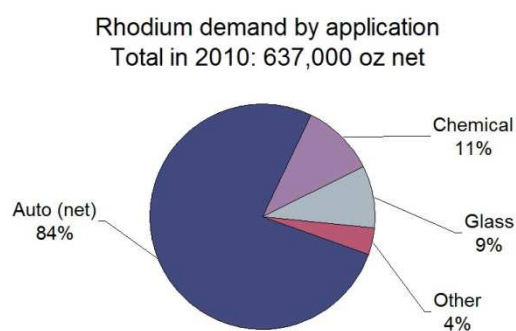
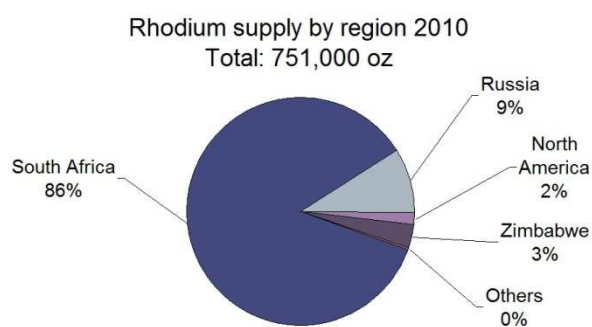
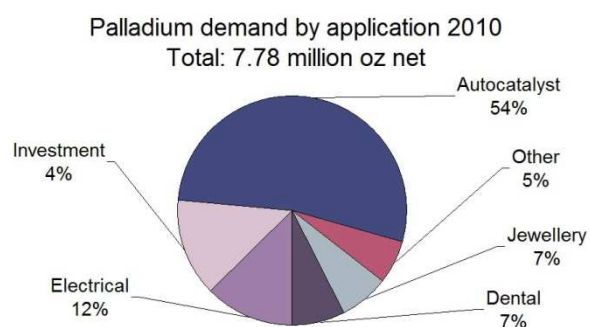
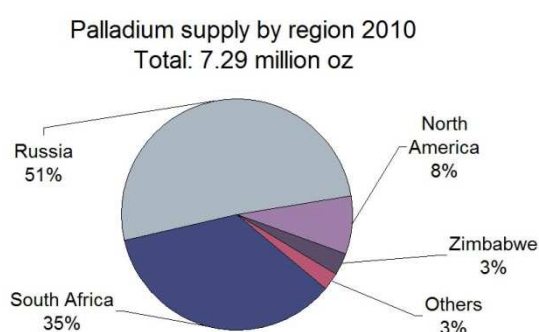
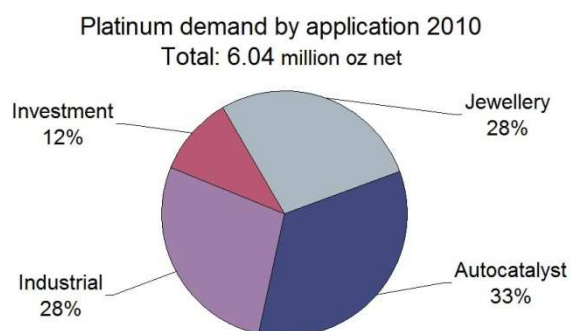
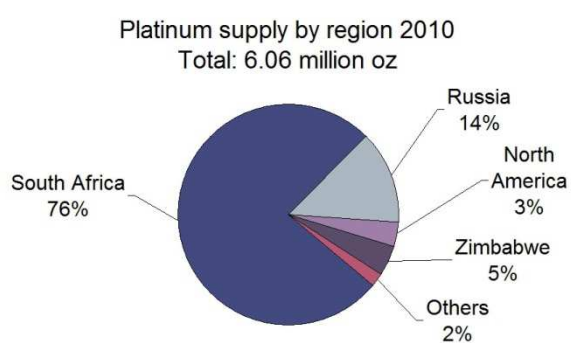


Fig. 1-1. [Left column] Global supply of Pt, Pd and Rh by region and [right column] global demand for Pt, Pd and Rh by application in 2010 (pie charts from Johnson Matthey 2011b).

1.4 Types of PGE deposits

Anomalous concentrations of PGE have been identified in geological environments ranging from high-temperature magmatic to low-temperature hydrothermal and sedimentary settings (e.g. Kucha 1982; MacDonald 1987; Lechler 1988; Naldrett *et al.* 1990; McDonald *et al.* 1995; Naldrett 2004; Armitage *et al.* 2007; Barkov *et al.* 2008). Significant concentrations, however, are almost exclusively found in the mafic-ultramafic portions of large tholeiitic intrusions of Late Archaean to Early Proterozoic age (Maier 2005). Few examples are older or younger, and the scarcity of relatively young PGE-rich intrusions might be explained by the Archaean Earth being hotter than during subsequent aeons (Richter 1988). As a result, the degree of partial mantle melting (and thus the MgO, Cr, Ni and PGE contents of the magmas) has decreased with time, reflected by the rarity of post-Archaean komatiites. The scarcity of PGE-enriched intrusions of Early Archaean age may be partly due to the poor preservation of Archaean terranes. Another possibility is that the Archaean crust was denser than younger crust, such that mantle derived magmas could have ascended faster without being stored in crustal magma chambers.

About 98% of the world's identified PGE resources occur in two types of deposits that are both intimately associated with Ni-Cu sulphides or chromitite (Misra 2000; Mungall *et al.* 2004; Naldrett 2004). These are: (a) stratiform or stratabound deposits in large layered complexes (e.g. the Bushveld Complex, Stillwater Complex of the USA, and Great Dyke of Zimbabwe), mined principally for PGE; and (b) massive Ni-Cu sulphide deposits mined primarily for Ni and Cu, but containing recoverable amounts of PGE as by-products, e.g. Sudbury intrusion of Canada, Noril'sk-Talnakh intrusion of Russia, Jinchuan intrusion of China, and Kambalda intrusion of western Australia.

1.4.1 Physical environments for PGE deposits

In order to form PGE deposits, magmas must initially be PGE-rich and a process must operate by which PGE-enriched phases become highly concentrated out of a large volume of magma into a smaller column of rock. The two principal collector phases are sulphide liquid and chromitite, and one of the optimal physical settings for collection of PGE is a conduit through which a large volume of magma passes (Mungall 2005). Sulphide melt may form due to assimilation of wall rocks at any point along the margins of the intrusion, but can be entrained in flowing magma or settle from crystal mushes, and will only accumulate to significant extents where changes in the conduit structure decelerate the flow regime and allow suspended droplets to be deposited (Maier *et al.* 2001). A great array of structural traps has been recognised within conduits: typical environments include embayments in the margins of

dykes or sills, hollows in the bases of ultramafic lava channels, sharp bends or sudden widenings of dykes or sills, magmatic breccias, or the entry points of dykes into larger magma chambers (Fig. 1-2).

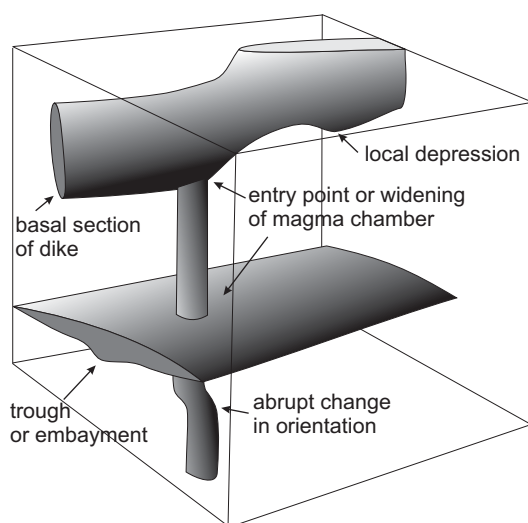


Fig. 1-2. Cartoon of conduits showing common geometries of structural traps in which sulphide liquid may accumulate (from Mungall 2005).

Conduits occur in many shapes and sizes, for example as dykes (the Great Dyke, Zimbabwe), sills (Noril'sk-Talnakh, Russia) and cylindrical bodies of ultramafic cumulates such as Alaskan-Uralian type complexes (Uktus, Russia). Large layered intrusions are essentially enormous sills (Bushveld Complex, South Africa, and Stillwater Complex, USA) and are the product of magma that flowed through and emerged from a conduit system. A key feature of a conduit system is that it typically contains excessive quantities of cumulus phases (which may include the collector phase itself), such that the bulk composition of the rocks preserved within the conduit differs markedly from the bulk composition of the original magma that passed through it. Conduits can therefore be recognised as bodies of ultramafic rock lacking complementary mafic or felsic fractionates. A secondary characteristic of conduits for basaltic magmas is the common presence of a thermal metamorphic aureole that is unusually wide in relation to the size of the intrusion. This results from the continuous passage of hot magma through the conduit, and therefore a continuous transmission of heat into the host rocks, as opposed to the heat that could be accomplished by injection and cooling of a single pulse of magma (Naldrett 2005a).

1.4.2 Overview of PGE deposits in igneous rocks

Layered igneous complexes account for about 90% of the world's PGE resources, with the Bushveld Complex alone providing about two thirds of the global PGE production. Of the individual PGE, the Bushveld Complex hosts 75% of the world's resources of Pt, 54% of Pd

and 82% of Rh (Naldrett 2004, 2008; Fig. 1-3). As of 1999, proven and probable Bushveld ore reserves totalled 204 Moz (million troy ounces) Pt and 116 Moz Pd to a depth of 2 km, while total reserves and resources amounted to 1140 Moz Pt, with 387 Moz outside South Africa. Assuming an increase in demand of 6% per year, this is sufficient for 50 years (Cawthorn 1999).

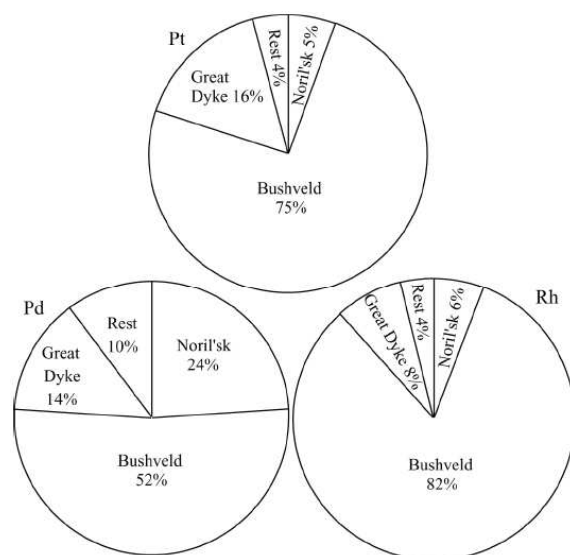


Fig. 1-3. Pt, Pd and Rh resources of major mining areas of the world (from Naldrett *et al.* 2008).

The initial step in PGE exploration is the identification of prospective igneous bodies, so it is logical to group known PGE deposits by their petrological association. The resulting classification can then be used as an aid to exploration. However, a single layered intrusion may contain several different styles of deposit. These styles or associations are outlined below, and their settings in and around a hypothetical layered intrusion is shown in Fig. 1-4. Note that no single intrusion is likely to contain all of the styles shown, and deposits with magmatic mineralisation are the main focus of this section.

1.4.2.1 T- and U-type magma mixing association

The largest PGE deposits occur in intrusions that are characterised by a high proportion of an early magma with a distinctive Al_2O_3 -poor and MgO-, Cr- and yet SiO_2 -rich (U-type) composition, followed in the same intrusion by one with a more typical tholeiitic composition (T-type) (e.g. Iljina 1994; Miller & Andersen 2002; Alapieti & Lahtinen 2002). Many of the PGE concentrations occur at levels in the intrusions at which trace element and isotopic signatures indicate variable degrees of mixing of these two magma types.

In the Bushveld Complex, the lowest stratiform concentration of PGE-enriched sulphides is that of the MG3 chromitite, followed by the UG1 and UG2 chromitites, the Pseudo Reef and finally the Merensky Reef. These horizons occur within the interval over

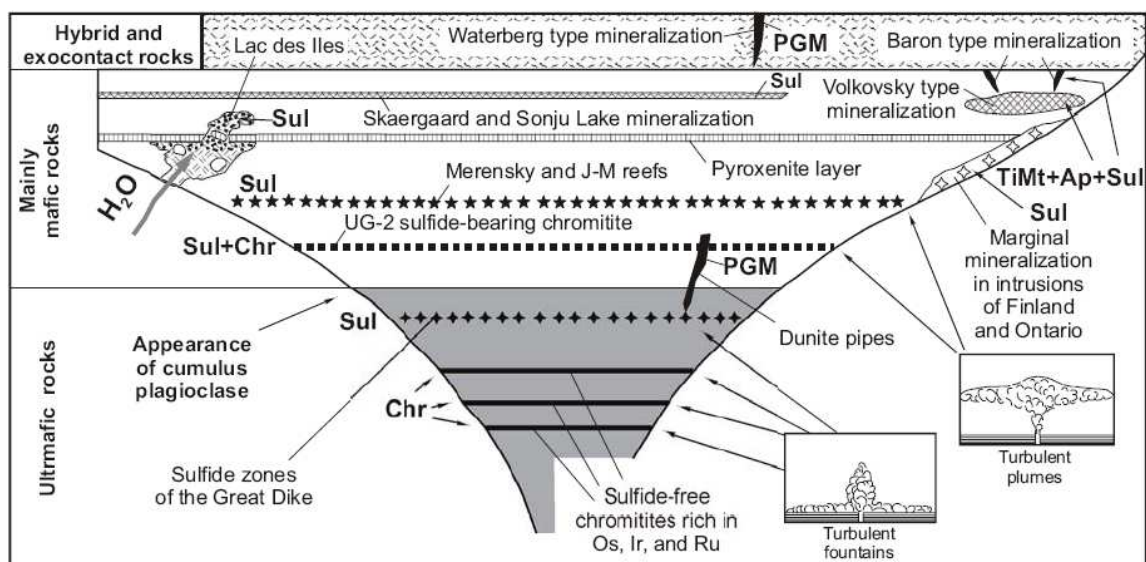


Fig. 1-4. Simplified model of a layered intrusion showing the types of PGE deposits and their likely location within the intrusion (from Naldrett 2005a).

which petrological, isotopic and geochemical data indicate the periodic introduction of new magma into the chamber, melted roof rocks in the case of the chromitites (Kinnaird 2004) and T-type magma in the case of the Merensky Reef. In the Stillwater Complex, the J-M Reef lies 400 m stratigraphically above the level at which T-type magma was first introduced, in a sequence of rocks characterised by frequent small influxes of such magma (e.g. Zientek 1983; Todd *et al.* 1982; Helz 1985). The principal PGE reefs in the Finnish intrusions (S-J Reef at Pennikat, S-K Reef at Portimo) lie at the base of the first cyclic unit in which T-type magma was first involved (Iljina 1994; Alapieti & Lahtinen 2002).

Much controversy surrounds the genesis of these ‘classic’ PGE reefs. Magma mixing leading to sulphide immiscibility in a high ‘*R* factor’ environment has long been favoured. The *R* factor is the mass ratio of source silicate magma to the sulphide liquid that extracts metals from it (Campbell & Naldrett 1979; Campbell *et al.* 1983). However, modelling of sulphur solubility has raised doubts as to whether sulphide immiscibility will ensue in this way (Cawthorn *et al.* 2002b; Li *et al.* 2001).

A consistent key feature of the ‘classic’ stratiform reefs is their occurrence in or close to orthocumulates that are associated with reversals in cryptic variation or modal cyclicity (in some cases also associated with magma quenching). This, along with the occurrence of these particular reefs close to levels at which the introduction of a second magma type has been documented, makes it difficult to rule out magma mixing as a major factor in their development.

In the Bushveld Complex and the Finnish intrusions, stratabound (but not stratiform) mineralisation occurs in marginal rocks (e.g. the Platreef of the Bushveld Complex, and

Kontijärvi and Ahmavara bodies of the Portimo Complex) which are equated with the introduction of T-type magma into an intrusion that previously had developed largely from U-type magma. Naldrett (2004) has proposed that upon injection of T-type magma, this mixed with U-type magma already in the intrusion and led to the precipitation of PGE-rich sulphide, some of which was swept out along the margins as the overall volume of the intrusion increased. Maier (2005) notes that the Platreef represents the only example of basal PGE mineralisation that is presently mined. However, as the present study will show, the Platreef was not originally a basal facies and is only marginal in its *present* setting.

1.4.2.2 T-type magma association

In some cases PGE deposits occur in intrusions that were produced by T-type magma with no evidence of an early U-type. Examples include the Keweenaw intrusions of the Lake Superior area, including the Sonju Lake intrusion within the Duluth Complex, and the Coldwell intrusion, the Cap Edvard Holm and Skærgaard intrusions of East Greenland, the Lac des Îles deposit in Canada, and the Stella reefs (Maier *et al.* 2003a) which are being evaluated by Platinum Australia.

Miller & Andersen (2002) call attention to the contrast between (i) PGE reefs such as the Platinova reef of the Skærgaard Intrusion, Greenland, and the PGE-enriched horizon in the Sonju Lake intrusion, Duluth Complex, and (ii) what they define as ‘classic’ reefs of the Merensky type. They point out that the former occur in the fractionated portions of intrusions that are the consequence of closed-system differentiation of T-type magma. They attribute PGE concentration to the accumulation of sulphur in the magma as a result of crystal fractionation, perhaps aided by periodic pressure release.

The Lac des Îles intrusion (e.g. Lavigne & Michaud 2001) contains a very different, discordant style of mineralisation associated with rocks of this association. PGE (principally Pd, with the Pd/Pt ratio about 10) occur in an igneous breccia and associated mafic rocks that resulted from the remelting of the gabbroic portion of a mafic/ultramafic layered complex.

1.4.2.3 Chromitite-hosted PGE

Most chromitite seams in layered intrusions are enriched in PGE relative to their silicate host lithologies. In the case of the Bushveld Complex, grades of the major seams range from 0.1 ppm to c. 6-7 ppm total PGE, but the <2 cm Merensky Reef chromitite stringers carry up to 50 ppm. The only major chromitite that is presently mined for its PGE content is the UG2. Four major models may be distinguished for PGE mineralisation in chromitites (Maier 2005) but all are contentious to some degree:

- (i) Concentration of PGE by magmatic sulphides, followed by (a) sulphide+chromite supersaturation triggered by contamination, or (b) sulphide supersaturation triggered by precipitation of chromite in response to contamination or other processes (e.g. Haughton *et al.* 1974; Naldrett & Von Gruenewaldt 1989).
- (ii) Concentration of some of the PGE, especially the IPGE and Rh, by means of solid solution in chromite (e.g. Capobianco *et al.* 1994; Peach & Mathez 1996; Righter *et al.* 2004). This model is supported by the positive correlation between the IPGE and Cr in some mafic-ultramafic intrusions.
- (iii) Localised reduction of silicate melt by crystallisation of chromite, causing nucleation and crystallisation of PGE alloys and their subsequent enclosure by the crystallising chromite (Mungall 2002; Finnigan & Brenan 2004; Finnigan *et al.* 2008).
- (iv) Crystallisation of chromitite stringers in response to flux melting of norite-pyroxenite by percolating fluid-rich intercumulus magma rising through the semi-consolidated cumulate pile. If the protocumulates contained small amounts of disseminated sulphides, it is conceivable that these were concentrated during flux melting to form the reef (Nicholson & Mathez 1991).

1.4.2.4 Dunite pipes

Discordant, olivine-rich, pipe-like bodies in the Upper Critical Zone of the Bushveld Complex contained up to 100 ppm Pt (now mined out). The best known of these are the Onverwacht, Driekop, Mooihoek and Maandagshoek pipes and have some of the highest PGE grades reported in the complex (up to 2050 ppm: Wagner 1929; McDonald *et al.* 1995). Their origin has been ascribed to the injection of late-stage magmatic fluids, although associated with metasomatism of the enclosing igneous rocks (Schiffries 1982; Stumpfl & Rucklidge 1982; Tegner *et al.* 1993). Scoon & Mitchell (2004), however, argue against the fluid model and suggest that the pipes formed by downward percolation of dense, evolved Fe-rich melt from within the Bushveld Complex that scavenged PGE from reef-style deposits higher in the succession. These melts are only fertile in localities where the earlier-formed magnesian dunite pipes have provided the necessary heat to selectively melt PGE-bearing phases from layered cumulates at higher levels.

1.4.2.5 Ural-Alaskan type

In some areas, PGE production has been almost exclusively derived from the valleys of rivers associated with distinctive calc-alkaline intrusions with alkaline affinities (shoshonitic) that are commonly referred to as the Ural-Alaskan type (e.g. Johan 2002). Examples include

intrusions of the Platinum Belt in the Ural mountains of Russia, where at both the Volkovsky deposit (Poltavets *et al.* 2006) and the Baronskoye prospect (Zaccarini *et al.* 2004) PGE are concentrated in zones rich in titaniferous magnetite, apatite and Cu sulphides (Potter 2002). The intrusions themselves are not economic, but are the source of the most important Pt placer deposits, e.g. the Soleviev Hills, Urals; Kondyor massif, Eastern Siberia; and the Seynav-Galmoznav massif, Koryakia, Russia.

1.4.2.6 Carbonatite-bearing alkaline association

PGE occur in placer deposits associated with carbonatite-bearing mafic/ultramafic intrusions that are clearly alkaline in composition. An example is the Early Triassic Guli intrusion in the northern part of the Siberian platform that is the source of Os-Ir placers (Malich 1999). The placers are not economic, but they are important because they constitute the only significant concentration of Os-Ir minerals in placers, and are exploited on a small scale by local prospectors (Naldrett 2005a).

1.4.3 Hydrothermal PGE deposits

Few cases have been documented where hydrothermal processes are the only or main factors responsible for the concentration of PGE. Many are localised remobilisations of originally magmatic PGE in shear zones or faults associated with mafic-ultramafic intrusions. However, there are instances where PGE have been hydrothermally leached from mafic-ultramafic source rocks at depth, then transported to and precipitated in a distal environment. The generation of the hydrothermal fluids and the causes of precipitation owe themselves to a variety of processes depending on the local setting. For example, at the Waterberg lodes in Rooiberg felsites near Mookgophong (formerly Naboomspruit), South Africa, hydrothermal PGE mineralisation with grades up to 990 ppm occurs in quartz-haematite-monazite veins (McDonald *et al.* 1995). The mineralisation is interpreted to have formed in response to neutralisation and/or reduction of highly oxidising fluids that may have leached PGE from underlying mafic-ultramafic rocks of Bushveld Complex (Armitage *et al.* 2007).

1.5 Purpose of the study

1.5.1 Problem statement

PGE mining and exploration in the eastern and western parts of the Bushveld Complex to date have produced sufficient data to bring the genetic understanding of the Merensky Reef and UG2 chromitite mineralisation to a mature stage, although some aspects of their genesis are

still debated, e.g. Kinloch & Peyerl (1990), Wilson *et al.* (1999) Barnes & Maier (2002), Smith *et al.* (2004), Wilson & Chunnett (2006) and Mitchell & Scoon (2007) for the Merensky Reef; and Eales (2000), Mathez & Mey (2005) and Mondal & Mathez (2007) for the UG2. In the northern limb, PGE are associated with the Platreef, but until recent years the lack of mining activity in this area has meant that the economic geology has received considerably less attention than the eastern and western lobes. For example, Kinnaird & McDonald (2005) noted that the seminal volume of *Mineral Deposits of South Africa*, published in 1986, contains papers on the tin (Pringle 1986) and chromium (Hulbert & Von Gruenewaldt 1986) deposits of the region, but nothing on the Ni-Cu-PGE deposits of the area. Prior to 2003, reviews of Bushveld PGE mineralisation that included a description of the Platreef (Lee 1996; Viljoen & Schürmann 1998; Barnes & Maier 2002) focused exclusively on the central portion of the Platreef outcrop, where historical mining and exploration had been concentrated, and relied primarily on earlier summaries (e.g. Buchanan 1988; White 1994).

The Platreef rests directly on the Palaeoproterozoic sediments and Archaean gneiss/granite basement that form the floor of the Bushveld complex. It is a contaminated, frequently xenolith-rich unit that is geologically more complex than any of the PGE reefs in the eastern and western lobes, but which is also thicker and carries sufficiently consistent grade to allow large-scale open pit mining along some sections of its strike (Viljoen & Schürmann 1998; Bye 2001; Kinnaird & Nex 2003). Anglo Platinum currently operate five open pit mines on or straddling the farms Sandsloot 236 KR, Vaalkop 819 LR, Zwartfontein 818 LR and Overysel 815 LR, and have plans for a further four (projects named Tweefontein North and Tweefontein Hill) to the south/southeast of Sandsloot. The potential for more high-tonnage and low-cost open pits in this sector has led other companies to explore on the Platreef adjacent to Anglo Platinum's licence area, and the northern lobe is currently one of the most active exploration centres on the Bushveld Complex.

The Platreef contains high grades of PGE and stands as a PGE deposit in its own right, unlike sulphide mineralisation in the contact zones of other layered complexes such as the Jimberlana intrusion (Keays & Campbell 1981), the Stillwater Complex (Page *et al.* 1985) and the Duluth Complex (Tyson *et al.* 1985; Miller & Ripley 1996; Ripley *et al.* 1999; Severson & Hauck 2005) where Ni and Cu are the primary metals and the PGE are by-products. However, the genesis of the Ni-Cu-PGE bearing Platreef is not fully understood, likewise its mineralisation and relationship to the main mafic layered sequence of the Bushveld Complex complex.

1.5.2 Aims and objectives

This study aims to identify and evaluate the geological processes that have operated in the development of the Platreef and its mineralisation at Sandsloot. The objectives are: (i) acquisition of first-order data by geological mapping and sampling of exposures in the Sandsloot open pit mine; (ii) petrographic and geochemical analyses of the collected samples; (iii) critical assessment of the mapping and analytical data in order to evaluate the nature and extent of the geological processes they reflect.

Chapter 2 contains a review of the Bushveld Complex. This is followed by a more detailed review of the northern limb of the complex in Chapter 3 and of the Platreef in Chapter 4. Chapter 5 presents geological descriptions based on first-order observation of the Platreef and associated units in the Sandsloot open pit mine during fieldwork in 2000 and 2001. Chapter 6 presents the mineralogy and geochemistry of lithologies sampled at Sandsloot. Chapter 7 discusses and synthesises the foregoing chapters, concluding with a model in Chapter 8 for the development of the Platreef at Sandsloot.

2. THE BUSHVELD COMPLEX

2.1 Introduction to the Bushveld Complex

The mafic component of the Bushveld Complex of South Africa is the largest igneous intrusion known on Earth and contains some of the most important magmatic ore deposits yet discovered. It hosts about 75% of the world's resources of PGE (Kendall 2006). The most widely accepted description of the complex is a concentric set of 7-8 km thick mafic and ultramafic cumulate units situated almost entirely within the bounds of the Transvaal Basin. The complex spans a distance of about 240 km × 300 km, and covers an area of approximately 65,000 km² (Tankard *et al.* 1982; Eales *et al.* 1993; Eales & Cawthorn 1996; Cawthorn 1999). The layered igneous rocks, known as the Rustenburg Layered Suite (RLS: South African Committee on Stratigraphy 1980) is divided into eastern and western lobes or limbs of roughly the same size, a southern lobe identified beneath cover rocks by gravity studies (Cawthorn *et al.* 2002b), and a smaller northern limb. Emplacement was concordant to the sedimentary layers in the western limb and discordant in the eastern and northern limbs (Button 1986; White 1994). The northern limb differs in several important aspects from the better known eastern and western limbs (e.g. van der Merwe 1976; Buchanan *et al.* 1981; McDonald *et al.* 2005a). The major platinum group element (PGE) deposits of the complex are the stratiform Merensky Reef and UG2 chromitite layer in the eastern and western limbs, and the stratabound, but not stratiform, Platreef in the northern limb.

The Bushveld Complex, in a looser sense than known today, was first named the *Bushveld Plutonic Series* (translated from French; Molengraaff 1898a, 1898b). Within a few years the term changed to *Bushveld Plutonic Complex* to denote the intricate relationships between the various intrusive components. However, it became apparent that the extensive flows of felsite in the province showed that both intrusive and volcanic rocks constituted the Bushveld cycle, so the term *Bushveld Igneous Complex* was introduced by Hatch & Corstorphine (1905) and came into general use. Other references to the complex include *Bushveld laccolite* (e.g. Palache 1922) and *Bushveld lopolith* (Daly 1928). Hall (1932) preferred the aforementioned term *Bushveld Igneous Complex*, as “no single word could do justice to the collection of sills, dykes, stocks, surface flows, etc.” This term persisted until the qualifying term ‘igneous’ became generally discontinued in modern usage. Fig. 2-1 shows the currently accepted constituents of the complex.

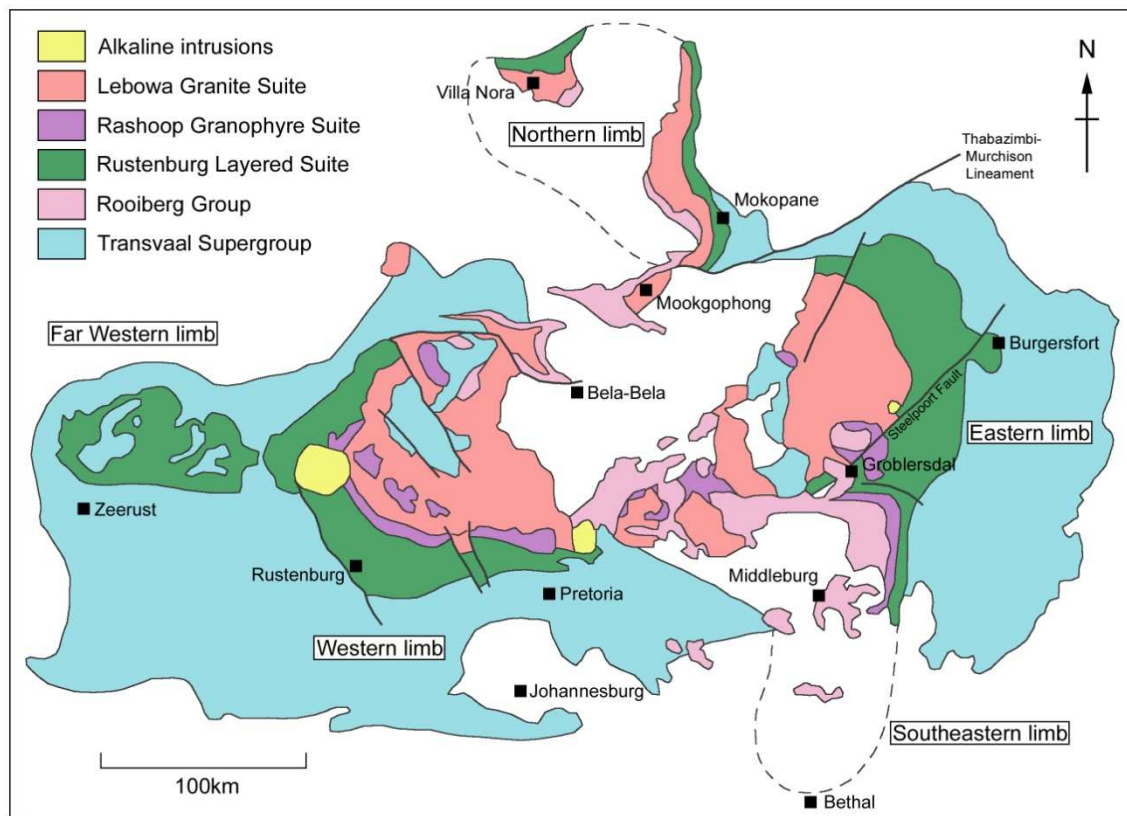


Fig. 2-1. Simplified geological map of the Bushveld Complex (after Kinnaird *et al.* 2005).

Although Fig. 2-1 includes alkaline intrusions and felsic intrusives and volcanics in the Bushveld Complex, much of the literature restricts the term to the mafic and ultramafic sequence of the Rustenburg Layered Suite (RLS). This practice is also adopted in the present study. Harmer & Armstrong (2000) have suggested that between 0.7 and 1.0 million km³ of mafic magma was produced within 1-3 Ma (Ma = *mega anna*: million years), which would require magma generation rates of between 0.3 and 1.0×10^6 km³ per Ma, respectively. If the estimates of magma volumes of 384×10^6 km³ for the Rustenburg Layered Suite (Cawthorn & Walraven 1998) and 200×10^6 km³ for the coeval Molopo Farms Complex (Reichardt 1994) are included, then a cumulative volume of magma in excess of 1 to 1.5×10^6 km³ was generated, which is comparable in volume to major flood basalt provinces such as the Deccan and North Atlantic Tertiary Provinces (Gibson & Stevens, 1998).

2.2 Structure of the Bushveld Complex

The shape, distribution and constituent parts of the Bushveld Complex remain controversial topics. While several studies describe these aspects of the complex, it is surprising that there have been relatively few attempts to associate the shape and distribution of the complex with the broad geological structure and tectonic history of the surrounding Kaapvaal Craton.

Rather, local structure and isolated ‘fragments’ of the floor or roof rocks have received more attention (e.g. Verwoerd 1963; De Waal 1970; Sharpe & Chadwick 1982; Rozendaal *et al.* 1986; Hartzer 1987; Uken & Watkeys 1997; Scoon 2002).

Older geophysical models of the Bushveld Complex include a single gigantic lopolith (e.g. Hall 1932) and dipping sheet models (e.g. Du Plessis & Kleywegt 1987; Meyer & De Beer 1987). Hall (1932) and Cousins (1959) included the Great Dyke, the Trompsburg Complex and other similar ‘detached’ intrusives in their definitions of the Bushveld Complex, but subsequent age determinations have revealed that these intrusions have very different ages and therefore cannot be related to the same event: Vredefort ultramafics (3.5-3.3 Ga: Tredoux *et al.* 1999), Great Dyke (2.575 Ga: Mukasa *et al.* 1998; Armstrong & Wilson 2000; Oberthür *et al.* 2002), Bushveld Complex (2.06-2.05 Ga: Kruger *et al.* 1986; Walraven *et al.* 1990) and Trompsburg Complex (1.9 Ga: Maier *et al.* 2003b).

Du Plessis & Walraven (1990) employed a five-fold geographical subdivision for the coeval parts of Bushveld Complex: (1) a far western or Nietverdiend compartment; (2) a western compartment; (3) the Villa Nora–Potgietersrust compartment; (4) the eastern compartment; and (5) the covered Bethal compartment in the south; and additionally the Molopo Farms Complex in Botswana. Excluding the Molopo Farms Complex, this is the subdivision used today (e.g. Cawthorn *et al.* 2002b), but the ‘compartments’ are usually called ‘limbs’ or ‘lobes’ and the Villa Nora-Potgietersrust compartment is known as the northern limb. It is the western, eastern and northern limbs that receive most attention as these areas of the complex host the majority of PGE deposits that are currently mined.

Based on mineral assemblages, the Bushveld Complex is divided vertically into a medium-grained Marginal Zone, an ultramafic Lower Zone, an ultramafic to mafic Critical Zone with prominent layering, a gabbro-noritic Main Zone, and a gabbroic to ferrodioritic Upper Zone. A complete succession occurs only in the northern sectors of the eastern and western limbs. In the eastern limb, for example, the full sequence is exposed north of Steelpoort, but to the south the Lower, Critical, and Main Zones successively abut against and terminate against the sedimentary floor rocks; a similar geometry is recorded in the northern limb and will be detailed in Chapter 3.

The stratigraphy and the positions of the PGE horizons in the eastern and western lobes of the complex are broadly the same (Lee 1996; Cawthorn & Lee 1998; Barnes & Maier 2002). This, together with geophysical evidence, led Cawthorn & Webb (2001) to infer that the eastern and western lobes have been connected throughout much of the evolution of the Bushveld Complex, that similar magmas were present in both lobes, and that mineralisation processes operated concurrently in both lobes to produce stratiform PGE deposits such as the

Merensky Reef and the UG2 chromitite. Kruger (1999, 2003) followed the conventional stratigraphy and considered the northern lobe to have been linked with the eastern and western lobes during Upper Critical Zone and Main Zone times: a mixed Main Zone and Upper Critical Zone magma flowed north across the chamber, overtopped the Thabazimbi-Murchison Lineament (locally manifested as the Zebediela and Ysterberg-Planknek Faults) and flowed into the northern lobe, generating the Platreef along the base. Webb *et al.* (2004) present gravity modelling in support of connectivity between the eastern and western lobes, envisaging a downwarp in the Moho beneath the Bushveld Complex to achieve isostatic balance. This interpretation supports the much earlier proposal of Hall (1932).

Von Gruenewaldt (1979) reviewed concepts of the Bushveld Complex and concluded that the broad locus of emplacement was at the intersection of several prominent structural directions in the Kaapvaal craton, with the present-day configuration of the complex controlled by a series of pre-Bushveld dome- and basin-like features that were generated by interfering NNW-SSE and ENE-WSW oriented anticlinal and synclinal warps. Du Plessis & Walraven (1990) highlighted the observation that the ENE-trending Thabazimbi-Murchison Lineament (TML: Fig. 2-1) controls the cratonic structural grain in its vicinity. In this regard it appears to have played an important role in determining pre-Bushveld structures, and thus the emplacement of the Bushveld Complex, as well as post-Bushveld deformation. The TML is seen as a crust-rupturing lineament which, together with related ENE-trending *en echelon* lineaments, exerts control on the major stratigraphic differences in the Bushveld Complex north and south of the TML. An aeromagnetic image of the complex (Fig. 2-2) clearly shows the lobate structure of the complex and the apparent control of major lineaments on the lobes.

In a palaeomagnetic study, Hattingh (1995) envisaged that the mafic rocks of the Bushveld Complex were emplaced and formed with the layering in a horizontal orientation and, after temperatures had dropped below Curie temperature of the carrier of the remnant magnetisation (580°C: Gough & van Niekerk 1959; Hattingh 1991), subsidence in the centre of the Bushveld Complex led to the present general inward dip directions of the pseudo-layering. It follows that where the igneous layering locally dips away from the centre of the complex, the dips are attributed to dome-like features that must postdate emplacement of the Bushveld Complex and cooling below 580°C.

A number of large domal structures occur in the high-grade metasedimentary rocks in the thermal aureole of the Bushveld Complex, and were already well known in early work on the north sector of the eastern limb (e.g. Kynaston 1906; Daly 1928; Hall 1932). The domes, which have spacings of 20-40 km and wavelengths of several km, have disturbed the footwall contact and penetrate the RLS to variable structural levels. Although the origin of the

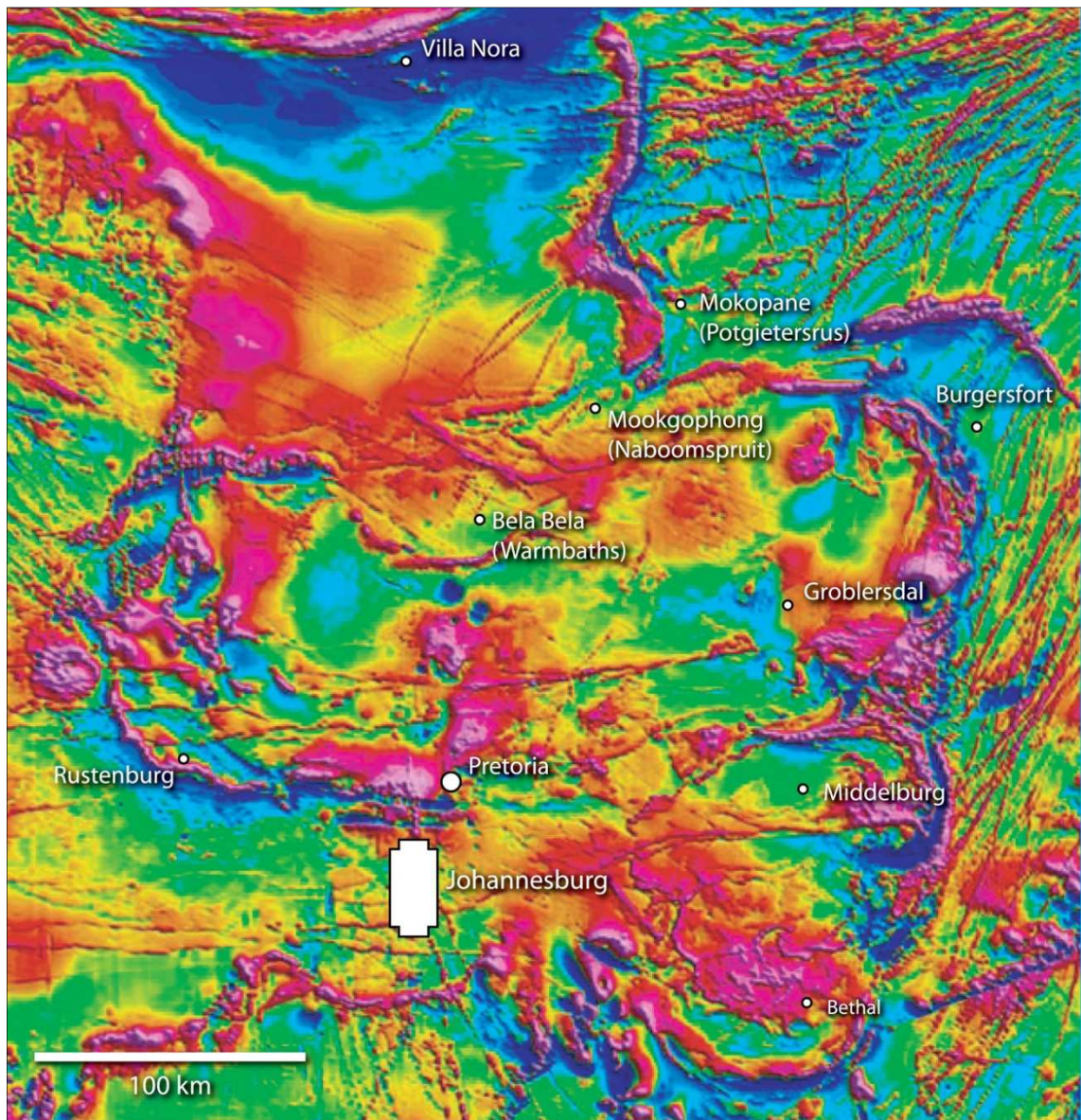


Fig. 2-2. Aeromagnetic map of the Bushveld Complex with approximate town locations (modified after Kinnaird 2005b). High to low gravimetric signatures are purple (highest) through red, yellow, green, pale blue and dark blue (lowest). Note the lobate structure of the complex associated with east-west to ENE-WSW trending lineaments, especially the Thabazimbi-Murchison Lineament close to Mookgophong.

structures has been debated, most authors suggest that they represent pre-RLS folds that were modified following emplacement of the mafic-ultramafic rocks (e.g. de Waal 1970; Sharpe & Chadwick 1982; du Plessis & Walraven 1990; Hartzer 1995; Bumby *et al.* 1998). Daly (1928) was perhaps the first worker to propose that deformation of country rock strata at the Bushveld margin was a response to the sinking of crust under the weight of the layered sequence, and Button (1978) first proposed that the structures are diapiric. Uken & Watkeys (1997) suggested that the lower parts of the RLS intruded as fingers and that the diapirs formed by magma loading and upward amplification of ductile floor rocks in the ‘interfinger’ areas. Marlow & van der Merwe (1977) describe the deformation of RLS rocks around an

antiform in the Malope area adjacent to the Wonderkop Fault, concluding that the antiform developed by folding that not only started well before intrusion of RLS, but continued until after emplacement of the Nebo Granite. Walraven (1974) presented a similar conclusion from an area southwest of the Crocodile River Dome. However, neither of the two latter studies suggests explicitly that the developing fold structures were accentuated by diapirism. Hunter (1975) considered that the Crocodile River and Moos River Domes reflect conditions of compressional deformation during subsidence of the Transvaal sedimentary basin, and proposed that deformation in the vicinity of the domes continued during crystallisation of the RLS, causing disruption of reefs and discrete layers. Hartzler (1995) suggested that the 'Crocodile River Fragment' could be interpreted as a dome rather than a fault block as previously believed. Scoon (2002) studied the occurrence of the Merensky Reef on the flanks of several domes in the Dwarsrand area. The domes are interpreted to have formed by diapirism triggered by gravitational loading and heating of the Transvaal Supergroup in response to intrusion of the Bushveld Complex. This interpretation is similar to that of Uken & Watkeys (1997) but with more pronounced diapirs in the Dwarsrand area. Here, a pattern is seen in the mafic and ultramafic rocks that is suggested to be the product of episodic intrusion and uplift by multiple magma replenishment, in which each of the many cycles that comprise the Critical and Main zones corresponds to a new magma pulse, with the oldest layers being dragged to higher structural levels in response to diapiric uplift. The geometric result is similar to a sedimentary offlap model, and uplift may be several km on the flanks of the larger domes. Scoon & Teigler (1994) had previously proposed a magma replenishment model for syn-Bushveld deformation in the western limb, and suggested that the western, eastern and northern limbs of the Bushveld Complex are subdivided into compartments that are structurally controlled and with a unique stratigraphy. In a slightly later study, Scoon & Teigler (1995) stated that the structural dislocation and lithostratigraphical changes associated with domes and basins in the Bushveld Complex are controlled by primary magmatic processes and that faulting is a subordinate effect, not the causal mechanism.

Another observation in Scoon's (2002) study is that the Upper Zone is transgressive in relation to the Critical and Main zones, and may have formed by an entirely new intrusive phase rather than the generally accepted model of differentiation within the Bushveld chamber (Wager & Brown 1968; Kruger *et al.* 1987). Similar transgressive relationships are reported in the western limb (Viljoen *et al.* 1986a, 1986b; Wilson *et al.* 1994).

2.3 Palaeotectonic setting

The Kaapvaal Craton, which hosts the Bushveld Complex, is an amalgamation of crustal blocks that were assembled at 3.7–2.7 Ga (De Wit *et al.* 1992). The assemblage can be divided into two periods: (1) at 3.7–3.1 Ga, continental lithosphere separated from the mantle by intraoceanic obduction and amalgamation followed by within-shield melting, granite formation and chemical differentiation of the upper lithosphere to create the Kaapvaal Craton; (2) Silver *et al.* (2004) interpreted mantle fabrics revealed by seismic anisotropy to conclude that an unknown orogeny prior to 2.9 Ga imparted a mantle fabric on the Zimbabwe craton (Fig. 2-3a). Then, around 2.9 Ga, the Pietersburg and Kimberley blocks collided with the Kaapvaal Shield, imparting an arc-like mantle fabric and forming the Thabazimbi-Murchison Lineament (TML in Fig. 2-3b). The Limpopo orogeny followed at 2.7–2.6 Ga, generating the Limpopo Belt between the Kaapvaal and Zimbabwe cratons, concomitant with intrusion of the Great Dyke and Ventersdoorp Supergroup (Fig. 2-3c). During the Magondi orogeny around 2.0 Ga, shear zones in the Limpopo Belt were reactivated and the Bushveld Complex was intruded along the TML (Fig. 2-3d). The final stage is the 1.9–1.8 Ga Kheis orogeny (Cornell *et al.* 1998), which generated the Soutpansberg rift (Fig. 2-3e).

A seismic study by James *et al.* (2001) showed that thick mantle roots are confined to the Archaean cratons, with no evidence for similar structures beneath the adjacent Proterozoic mobile belts. The Bushveld magmatic event affected a broad swathe of Kaapvaal cratonic mantle beneath and to the west of the exposed Bushveld Complex. The mantle beneath the extended Bushveld province is characterised by seismic velocities lower than those observed in regions of undisturbed cratonic mantle. The mantle beneath the Limpopo Belt exhibits a cratonic signature.

2.4 Source of Bushveld magma

The mechanism(s) leading to the emplacement of the Bushveld Complex is a contested topic. Mills Davies (1925) hypothesised “*an active molten rock magma of common or normal composition deep down in the Central Transvaal area and its gradual advance upwards through thousands of feet of strata until it emerged through devious ways through the quartzites and shales of the Pretoria Group and ... spread out like a colossal cake*”. Wagner (1929) characterises the complex as a lopolith and suggests intrusion into horizontal strata but does not propose a mechanism for intrusion. Hatton (1995) viewed the Bushveld Complex as the plutonic equivalent of a continental flood basalt province. On the basis of MgO and SiO₂ contents, he calculated that melting occurred at a depth of 18–40 km and argued that only a

buoyant mantle plume breaching the base of the crust could cause melting at these depths to provide the Bushveld magma. Cawthorn *et al.* (2002b), however, claimed that this geochemical basis for calculation of the melting depth is invalidated by the possible effects of

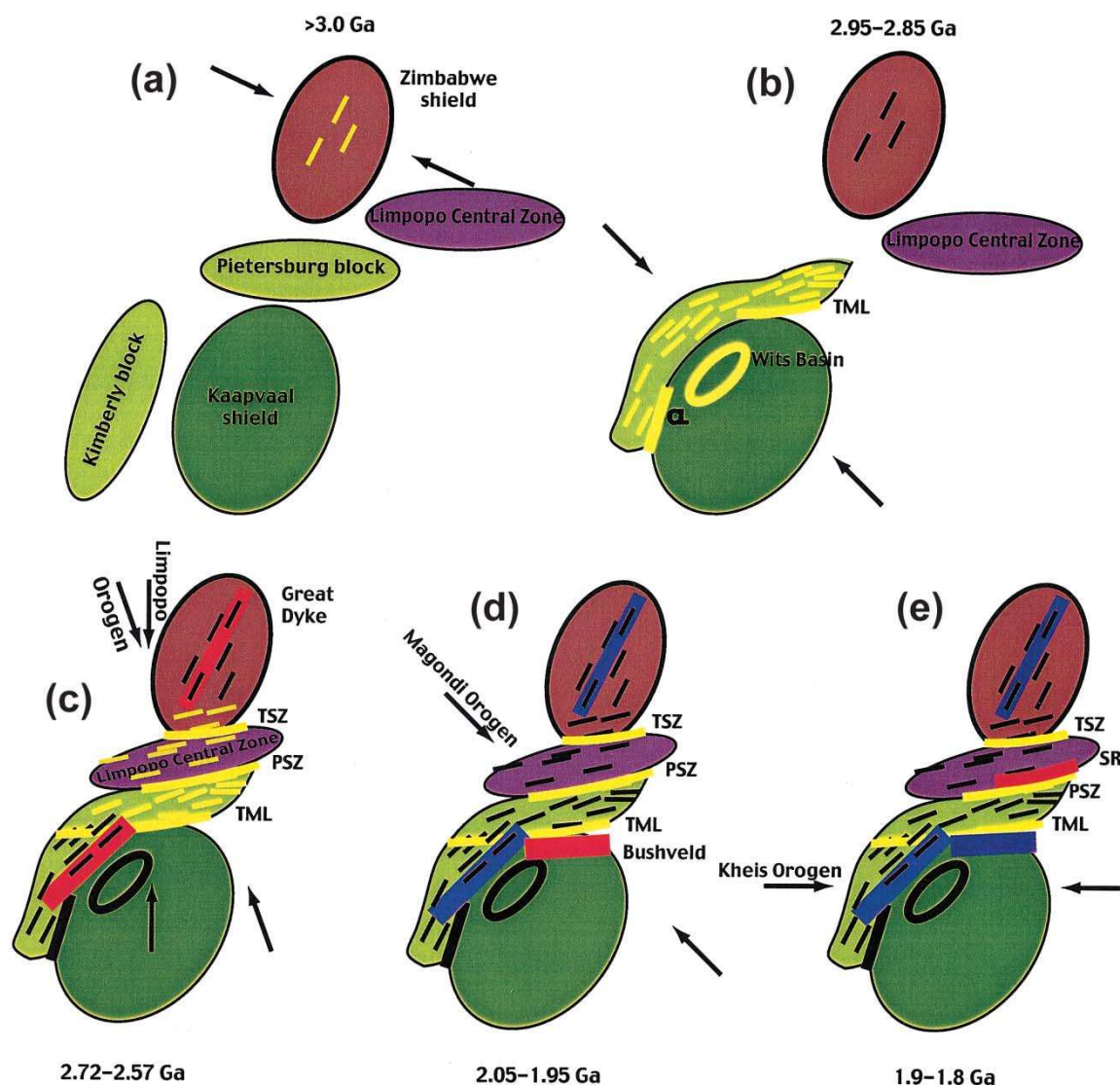


Fig. 2-3. Tectonic scenario for the evolution of the Kaapvaal Craton (after Silver *et al.* 2004). TML = Thabazimbi-Murchison Lineament; CL = Colesberg Lineament; TSZ = Triangle Shear Zone; PSZ = Palala Shear Zone; SR = Soutpansberg Rift.

fractionation and crustal contamination. These authors further note that kimberlites intruding the Bushveld Complex contain mantle xenoliths with an age of 3.0 Ga, much older than the Bushveld Complex, and argue that these xenoliths could not have been preserved if a plume had penetrated the mantle. They concluded that melting occurred at much greater depth in the asthenosphere, and magma rather than a plume penetrated the lithospheric upper mantle. In the Premier kimberlite in the eastern Kaapvaal shield, Carlson *et al.* (1999) determined Re/Os

ages around 2.0 Ga for xenoliths sourced from the upper lithosphere, and xenoliths with a deeper source have more typical Kaapvaal ages of around 3.0 Ga. The presence of the younger ages is explained by a resetting of the Re/Os system by a magmatic event, which for the younger xenoliths corresponds to the Bushveld Complex. Implicit in this argument is that if the Bushveld Complex was generated by a plume, the lower lithospheric mantle, where the older xenoliths are sourced, would also be 'reset'. Richardson & Shirey (2008) show that sulphide inclusions in ~2.0 Ga diamonds from the 1.2 Ga Premier and 0.5 Ga Venetia kimberlites, on opposite sides of the Bushveld Complex, have initial Os isotope ratios even more radiogenic than those of the Bushveld sulphide ore minerals. Sulphide Re-Os and silicate Sm-Nd and Rb-Sr isotope compositions indicate that continental mantle harzburgite and eclogite components, in addition to the original convecting mantle magma, most probably contributed to the genesis of both the diamonds and the Bushveld Complex. Coeval diamonds provide evidence that the main source of Bushveld PGE is the mantle rather than the crust.

Magma feeders to the Bushveld Complex have not been identified with certainty, though gravimetric studies have inferred several feeders (Kinloch 1982). Whilst it has been assumed that areas displaying positive Bouguer gravity anomalies represent pipe-like feeders (e.g. Sharpe *et al.* 1981), du Plessis & Kleywegt (1987) note that these anomalies in the eastern and western lobes coincide with the upper contact of the Upper Zone where the mafic rocks attain their greatest thickness, resulting in positive gravity anomalies that can only be ambiguously interpreted as feeders. Van der Merwe (1976) interprets a highly positive gravity anomaly in the northern limb just west of Mokopane (Potgietersrus in Fig. 2-4) as a feeder. This anomaly is the strongest in the Bushveld Complex and does not coincide with a particularly thick mafic package.

Further, van der Merwe (1976) found no gravimetric evidence of connectivity between the northern and eastern limbs. Rather, they are separated by a linear zone (the TML). Kruger (2005a) envisages that the Main Zone magma intruded through a feeder near Mokopane at the intersection of the TML and the Pietersburg Greenstone Belt. The magma first flowed north into the northern lobe (with the Lower Zone already in place) before flowing south to the main chamber to form the Merensky Reef at its base. The similarity in $^{87}\text{Sr}/^{86}\text{Sr}$ ratios is highlighted by Kruger (2005a) and this, along with other geological and mineralogical similarities, implies that the Platreef and Merensky Reef are consanguineous and virtually coeval. This is a long-held view that is now increasingly questioned (e.g. McDonald & Armitage 2003; McDonald *et al.* 2005a).

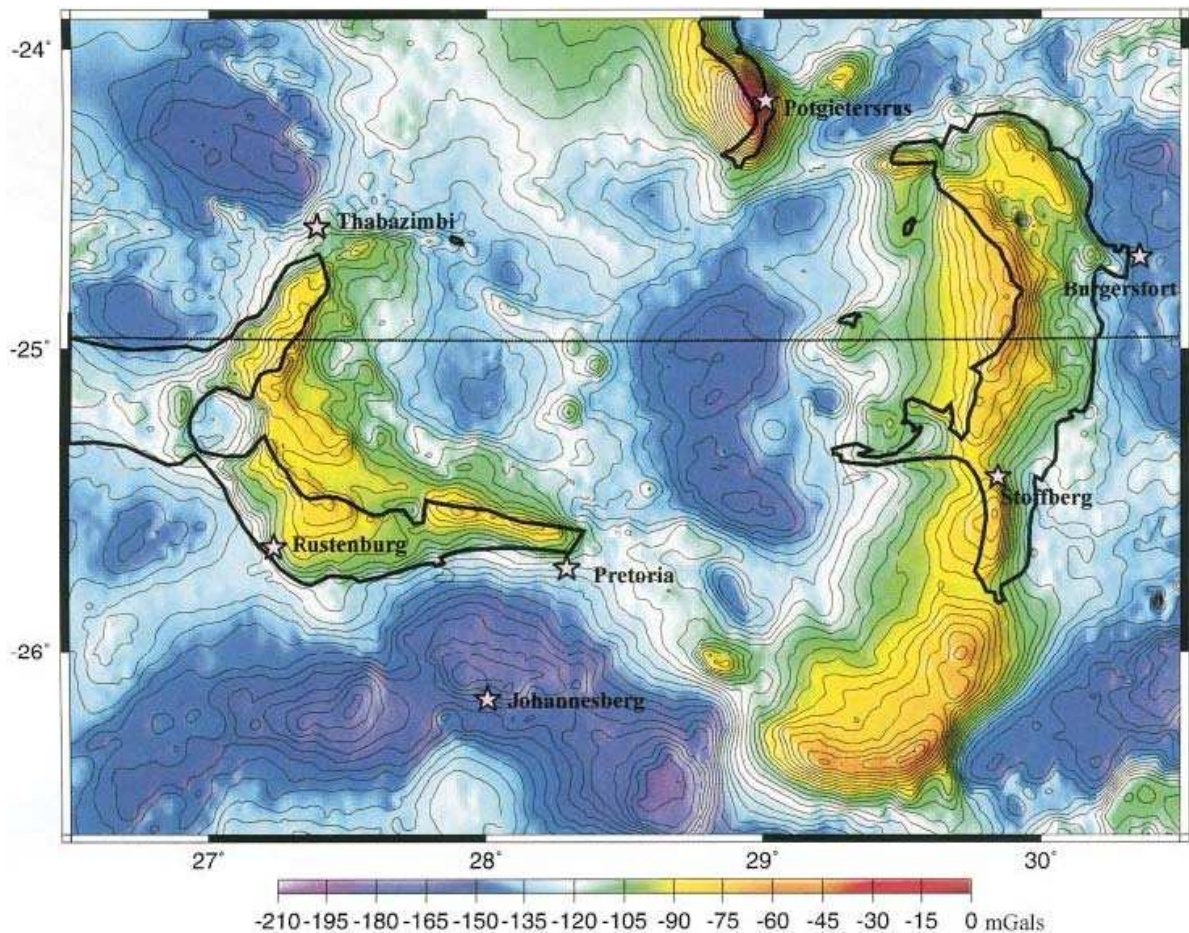


Fig. 2-4. Gravity map of the Bushveld Complex (after Cawthorn & Webb 2001). Solid outline delimits surface outcrop of mafic rocks.

Naldrett *et al.* (2008) propose a ‘pudding basin’ model for the marginal mineralisation of the Bushveld Complex. The authors note the absence of more differentiated cumulates and explain this by the expulsion of partially fractionated magma up and along the margins of the complex by the overpressure induced by a new influx. The analogy is the filling of the space between two nested pudding basins of similar size through a feeder at the base of the lower basin. In this regard, the complex is envisaged as a series of ‘pudding basins’, with one basin representing each lobe or limb and each basin displaying a different level of erosion. The eastern and western limbs are considered to be a single basin.

The role of tectonic features in the emplacement of the RLS is also debated. Sharpe & Lee (1986) concluded that faults played no part in the emplacement of the RLS. Du Plessis & Walraven (1990), however, examined and compared structural features within the Lebowa Granite Suite and RLS in various compartments of the Bushveld Complex and evaluated them in terms of relationships to major structural features of the Kaapvaal Craton: the TML; the Kgomodikae lineament (westward extension of the TML in Botswana); the Melinda, Abbotspoort, Rustenburg and Steelpoort faults; and the Barberton lineament in the south.

These authors conclude that a craton-scale *en echelon* set of ENE trending lineaments exercised extensive control on the emplacement of the complex and its subsequent deformation. Von Gruenewaldt *et al.* (1987) correlated the 2044 ± 24 Ma Molopo Farms Complex (Mapeo *et al.* 2004) with the Bushveld Complex and divided it into a mainly ultramafic northern facies and mafic-dominated southern facies. These facies are divided by the Kgomodikae lineament, an extension of the TML, which once again highlights the significance of this regional lineament.

Linear feeders represented by shear zones have been proposed as magma conduits (Cawthorn *et al.* 2002b; Friese 2004). The Steelpoort Fault is considered to be such a feeder (Cawthorn *et al.* 2002b), as there are differences in stratigraphic thicknesses in units of the Lower and Critical Zones across the fault (Hatton & von Gruenewaldt 1987), which Cawthorn *et al.* (2002b) consider to be a result of differential flow of magma northwards and southwards of the feeder. The same authors propose that other large faults separating compartments of the Bushveld Complex also acted as conduits.

The TML is a 500 km long, 25 km wide ENE-WSW striking deformation belt that has been reactivated as a fault (McCourt 1983; McCourt & Vearncombe 1987). Good & de Wit (1997) consider the TML to be a long-lived, repeatedly reactivated, craton-scale relay structure that has probably influenced the emplacement of the Bushveld Complex, since the northern lobe is significantly offset from the eastern and western lobes across the lineament. Implicit in their interpretation is that the Bushveld Complex intruded syntectonically with an episode of movement along the TML and that the northern lobe is connected with the eastern and western lobes. Friese (2004) also suggests that the Bushveld magma utilised the TML, the Palala Shear Zone and Barberton-Magaliesburg Lineament as conduits; and at a critical level in the crust the magmatic pressure equalled the lithostatic pressure, allowing the lateral spread of the sill-like intrusion of the Bushveld Complex. Kruger (2005a) relies heavily on the TML to explain emplacement of the different zones of the complex, notably Main Zone magma intruding first northwards to form the Platreef, then southwards to form the Merensky Reef. Note that this model implies the Platreef is a basal facies of the Main Zone, but this traditional view of the stratigraphy is increasingly contested (e.g. McDonald *et al.* 2005a). Nonetheless, the apparent control of crustal-scale lineaments on the lobate structure of the Bushveld Complex is very evident in an aeromagnetic image (Fig. 2-2).

The model of Silver *et al.* (2004) interprets the Bushveld Complex, Ventersdoorp Supergroup, Great Dyke, and Soutpansberg trough as collisional rifts. There is no plume mechanism in the model; instead, intrusion of the Bushveld Complex is controlled only by variations in lithospheric stress. Further, Silver *et al.* (2004) show the crust north of the TML

to be part of the Pietersburg Block, whereas the crust to the south belongs to the Kaapvaal Shield. These cratonic blocks were separate and had no common history prior to collision at 2.9 Ga. As the Bushveld Complex intruded on both sides of the TML, it is possible that the magmas on either side are derived from compositionally different sublithospheric mantle.

2.5 Age of the Bushveld Complex

Buick *et al.* (2001) sampled a large calc-silicate xenolith in the Upper Zone on the farm Avonduur 814 KS in the eastern limb of the complex. The xenolith preserves high-temperature ($\sim 1200^{\circ}\text{C}$), massive, vesuvianite-rich or wollastonite+clinopyroxenite rich mineral assemblages that were later metasomatised and completely retrogressed by hydrous, retrograde ($\sim 600\text{--}700^{\circ}\text{C}$) fluids. Non-pervasive hydrothermal alteration also affected the RLS itself over a temperature range of $700\text{--}400^{\circ}\text{C}$ (Schiffries & Rye 1990). Three possible explanations for retrogression are given: (1) hydrothermal circulation around the cooling RLS; (2) emplacement of slightly later Bushveld related granites; or (3) a younger event unassociated with Bushveld age magmatism. Stable isotope analyses by Schiffries & Rye (1990) had suggested that the retrograde fluids were derived from dehydration of the Transvaal Supergroup floor rocks during emplacement of the RLS. Buick *et al.* (2000) reached similar conclusions. U-Pb isotope data from newly grown titanite in the sampled xenolith yield an age of 2058.9 ± 0.8 Ma (Buick *et al.* 2001). The authors conclude that titanite very likely preserves the crystallisation age rather than the cooling age. Therefore, retrograde fluid infiltration within the xenolith most probably occurred at 2058.9 ± 0.8 Ma. This age is within error of a well constrained Bushveld emplacement age of 2060 ± 3 Ma (Kruger *et al.* 1986), also a less precise age of 2060 ± 27 Ma (Walraven *et al.* 1990) and is distinctly older than the emplacement of the Lebowa Granite Suite (2054 ± 2 Ma; Walraven & Hattingh 1993). The titanite crystallisation age therefore suggests that retrogression was due to hydrothermal circulation associated with the cooling RLS, not with slightly later Bushveld granites, and is a minimum age of emplacement of the RLS. This, along with the 2061 ± 2 Ma age of the Rooiberg Group roof rocks (Walraven 1997) would appear to tightly bracket the emplacement of the entire RLS of the eastern and western limbs of the Bushveld Complex to the interval 2059-2061 Ma.

However, a new precise U-Pb zircon age of 2054.4 ± 1.3 Ma has been determined for the Merensky Reef in the Rustenburg Section of the west limb (Scoates & Friedman 2008), and a U-Pb baddelyite age of 2057.7 ± 1.6 Ma for the Marginal Zone about 30 km directly west of Lydenburg (Olsson *et al.* 2010). The slightly older age for the Marginal Zone is

consistent with Bushveld stratigraphy. The former, younger age is interpreted as the crystallisation age of the Merensky Reef, while the same study attained a U-Pb rutile age of 2055.0 ± 3.9 ma, interpreted as the cooling age. The crystallisation and cooling ages are significantly younger than the crystallisation age determined by Buick *et al.* (2001). The younger age of 2054.5 ± 1.3 Ma for RLS crystallisation may be more reliable, because it is determined directly from the Merensky Reef and not interpreted through a xenolith in the RLS. Further, given the size of the Bushveld Complex and uncertainties about the intrusion sequence between the main lobes, crystallisation may not have occurred at the same time in widely different parts of the intrusion.

Dorland *et al.* (2006) present SHRIMP U-Pb zircon ages for quartz-porphry lavas in the Lower Swaershoek Formation (2054 ± 4 Ma) and correlative Rust de Winter Formation (2051 ± 8 Ma) in the Waterberg Group, stratigraphically close to the base of the formation. The Entabeni Granite is a post-tectonic granite that intrudes into the Limpopo Belt (Barton Jr *et al.* 1995) and its SHRIMP zircon age of 2021 ± 5 Ma constrains the maximum age of the unconformably overlying Soutpansberg Group. Therefore, at least part of the Waterberg Group is older than the Soutpansberg Group and was deposited immediately after intrusion of the Bushveld Complex, and may be tectonically related to it. Dolerite sills in the upper formation of the Waterberg Group have an age of ~ 1875 Ma (Hanson *et al.* 2004). Therefore, most of the Waterberg Group was deposited between ~ 2054 and ~ 1875 Ma, placing it within the time frame of the 2000 ± 50 Ma thermal metamorphic and non-penetrative shear deformation events in the Limpopo Belt. The deposition of the Waterberg Group and basin development could be coupled to tectonometamorphic events in the Limpopo Belt.

The Hekpoort Andesite within the sedimentary Pretoria Group has an Rb-Sr isochron age 2184 ± 76 Ma (Cornell *et al.* 1996). As the Pretoria Group is intruded by the Bushveld Complex, the Pretoria Group rocks above the extrusive Hekpoort Andesite must have been deposited before intrusion of the Bushveld Complex.

Other igneous complexes of Bushveld age occur within and on the margin of the Kaapvaal Craton. The Moshaneng Complex, occurring between the Bushveld Complex and Molopo Farms Complex, is a 35 km^2 oval-shaped pluton, with coarse- to medium-grained gabbros and diorites at the centre rimmed by granites and syenites that show evidence of mixing and mingling of co-existing mafic and felsic magmas. U-Pb zircon and titanite isotopic data indicate an emplacement age of 2054 ± 2 Ma (Mapeo *et al.* 2004), which is consistent with the age of Bushveld emplacement. The Okwa Basement Complex crops out at the northwestern edge of the Kaapvaal Craton, and all precise U-Pb zircon ages for all the major Palaeoproterozoic lithologies of the complex are indistinguishable at 2056 ± 2 Ma

(Mapeo *et al.* 2006; F. Corfu, pers. comm. 2007). This age can be broadly correlated with Palaeoproterozoic events in the Magondi belt at the northwestern margin of the Zimbabwe Craton and the Triangle Shear Zone in the Limpopo Belt (Fig. 2-3). However, the most precise correlation is with the Bushveld age, which is indistinguishable from that of the Okwa Basement Complex. This suggests a link between marginal and intra-cratonic Bushveld-age magmatism on the Kaapvaal Craton.

3. THE NORTHERN LIMB

3.1 *Introduction to the northern limb*

This chapter provides a review of previous studies on the northern limb of the Bushveld Complex, particularly its stratigraphy and age in relation to the main body of the Bushveld Complex.

The first thorough investigation of the structure of the northern limb, combining field mapping, analysis of drill cores and geophysics, was conducted by van der Merwe (1978), who called it the ‘Potgietersrus Compartment’ with an inferred triangular shape. The same author (1976, 1978) argued that the geophysical data suggest an overall shape which incorporates the following important elements: (i) a north-striking, trough-shaped body that widens northwards; (ii) a narrow feeder just west of Mokopane; (iii) a dyke-like southern sector but a wider, sill-like northern sector; (iv) no evidence of a broad linkage between the northern limb and the eastern limb; and (v) a dominant northwest-trending gravity feature northwest of Mokopane. In the northwestern Villa Nora area, the northern limb crops out again after disappearing beneath sedimentary cover further south. Here the limb dips to the south and southeast (Grobler & Whitfield 1970). Cawthorn & Lee (1998) and Cawthorn & Webb (2001) consider the northern limb and Villa Nora occurrence to be one compartment, formed by a postulated feeder west of Mokopane. This is supported by gravity data assessed by van der Merwe (1976, 1978).

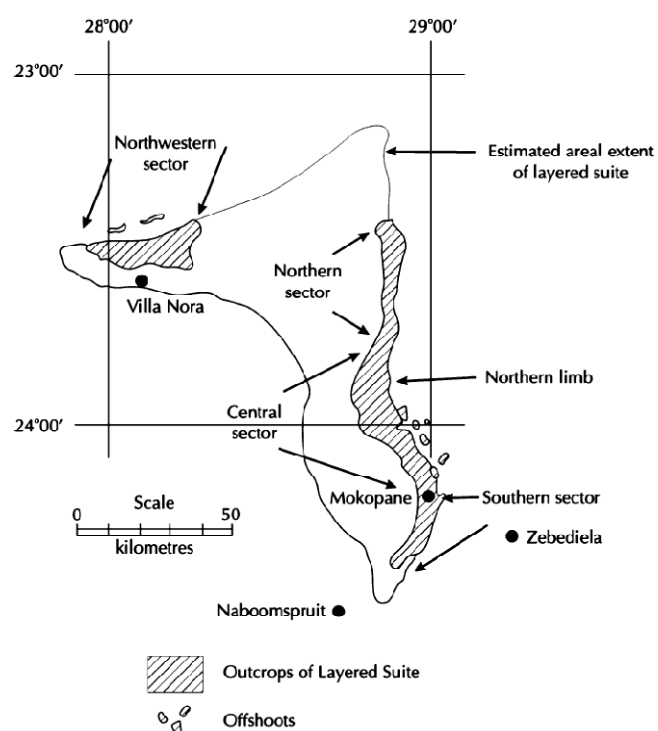
3.2 *Structure of the northern limb*

In plan view, the northern limb has roughly the shape of a right-angled triangle with Mokopane at the southern acute corner, Villa Nora in the northwestern acute corner and the northern 90° corner near Blouberg (Fig. 2-1). The outcrop of the northern limb is divided into three sectors (Fig. 3-1). The northern sector comprises primarily Upper Zone magnetite-bearing rocks, with a thin sliver of PGE-mineralised Main Zone gabbro-norite rocks at the base of the sequence (Harmer *et al.* 2004; McDonald *et al.* 2005b). The central sector displays the full sequence of mafic rocks with Lower Zone ultramafic offshoots near the base, while in the southern sector only the lower units of both the Upper Zone and Main Zone, upper units of the Critical Zone mafics and a body of Lower Zone are developed. In the south, the northern

limb is truncated by the Zebediela fault that brings the Karoo basalts into juxtaposition with the Rustenburg Layered Suite.

The gravity model suggests a maximum thickness of 10 km for the layered mafic rocks. Although other workers (e.g. Kruger 2005a) have suggested that the northern limb may extend much further to the west and have a more saucer-like shape, van der Merwe's (1976) model is corroborated by reports from deep drilling carried out by the Council for Geoscience (formerly the Geological Survey of South Africa) at Afguns: this locality is southwest of the northwesternmost Villa Nora exposure, and drilling intersected no basic or ultramafic rock of the Bushveld Complex (cited by van der Merwe 1978).

Fig. 3-1. Simplified map of the outcrops and estimated areal extent of the layered suite of the northern lobe of the Bushveld Complex (from van der Merwe 2008).



The northern limb outcrop indicates a total thickness of 4 km for the Critical, Main and Upper Zones. The 'hidden' Lower Zone in the northern limb is inferred to occupy the remaining 6 km suggested by the gravity data, most notably in the southern part of the limb on the farms Grasvally, Volspruit and Zoetveld where the Lower Zone crops out most extensively and is in contact with the other units of the mafic sequence. The Lower Zone also crops out as several recognised satellite bodies, or 'offshoots': the Uitloop I and II, Rietfontein, Bultongfontein I and II and Zwartfontein bodies (van der Merwe 1978; Fig. 3-1, Fig. 3-2). The satellite bodies occur as separate sheet-like bodies arranged in a semicircle centred on the position of the northern limb feeder inferred by gravity data west of Mokopane. Discordant relationships on Grasvally and Zwartfontein suggest a hiatus between the intrusion of the Lower Zone and the main coherent northern limb (Hulbert 1983; van der Merwe 1978; de Klerk 2005). Recent

exploration around the Grasvally area indicates that the Lower Zone is exposed here due to upfaulting along one or more prominent north-south trending faults (Hulbert 1983; Hulbert and Von Gruenewaldt 1986; Verbeek & Lomberg 2005).

The northern limb has an outcrop width of 15 km at its southern extent near Mokopane, but south of the town, between the farms Moordrift and Rooiport, the sequence is condensed to 4.5 km and the Main Zone is only a few hundred metres wide. From south to north, the eastern margin of the northern limb transgresses progressively lower units of the Transvaal Supergroup: the Magaliesberg quartzites and shales of the Pretoria Group, and the Penge Banded Iron Formation and Malmani Dolomite of the Chuniespoort Group. The Malmani Dolomite wedges out at Zwartfontein, north of Sandsloot, where the mafic rocks come into contact with Archaean gneiss/granite basement (Fig. 3-2).

The outcrop (and presumably the deeper structure) of the northern limb appears to be influenced by a number of structural features in the footwall rocks. In particular, the Malmani Dolomite protrudes into the layered sequence immediately south of the Sandsloot mine, and is expressed as an east-west trending antiformal 'tongue' about 3 km long and 1 km wide (Fig. 3-2). A strong, northwest trending gravity low in the area (Fig. 2-2) is considered to correspond to lighter underlying sedimentary rocks in a synformal part of the Transvaal Supergroup called the Eersteling Basin. The dolomite tongue is interpreted to be part of a tectonically positive area, the Uitloop platform (Button 1973), on the edge of the Transvaal Supergroup basin. Importantly, according to van der Merwe (1978) the Main Zone layering extends up to the tongue margin and is truncated against it without any noticeable change in strike, bending of igneous layering or any offset across the tongue. A map of geological relations around the tongue by the same author shows an uncertain path for the Platreef approaching the tongue from north and south: the reef is stippled to express its assumed occurrence approaching the tongue, but the stippling terminates near the base of the tongue with no observed occurrence of Platreef indicated around the structure. The tongue is therefore interpreted as a pre-Main Zone structure, and since van der Merwe (1976, 1978) considers the Platreef to be the base of the Main Zone, the structure implicitly predates the Platreef. This scenario is elaborated and discussed in later sections and chapters. Further, van der Merwe (1978) observed scattered occurrences of disseminated chromitite partly encircling the tongue, implying that the Platreef is 'draped' around the antiformal structure. These fragments may represent a disrupted Platreef facies, but the present author observed fragments of banded ironstone widely scattered around the south edge of the dolomite tongue, superficially resembling chromitite, and respectfully suggests that van der Merwe (1978) might have misidentified these.

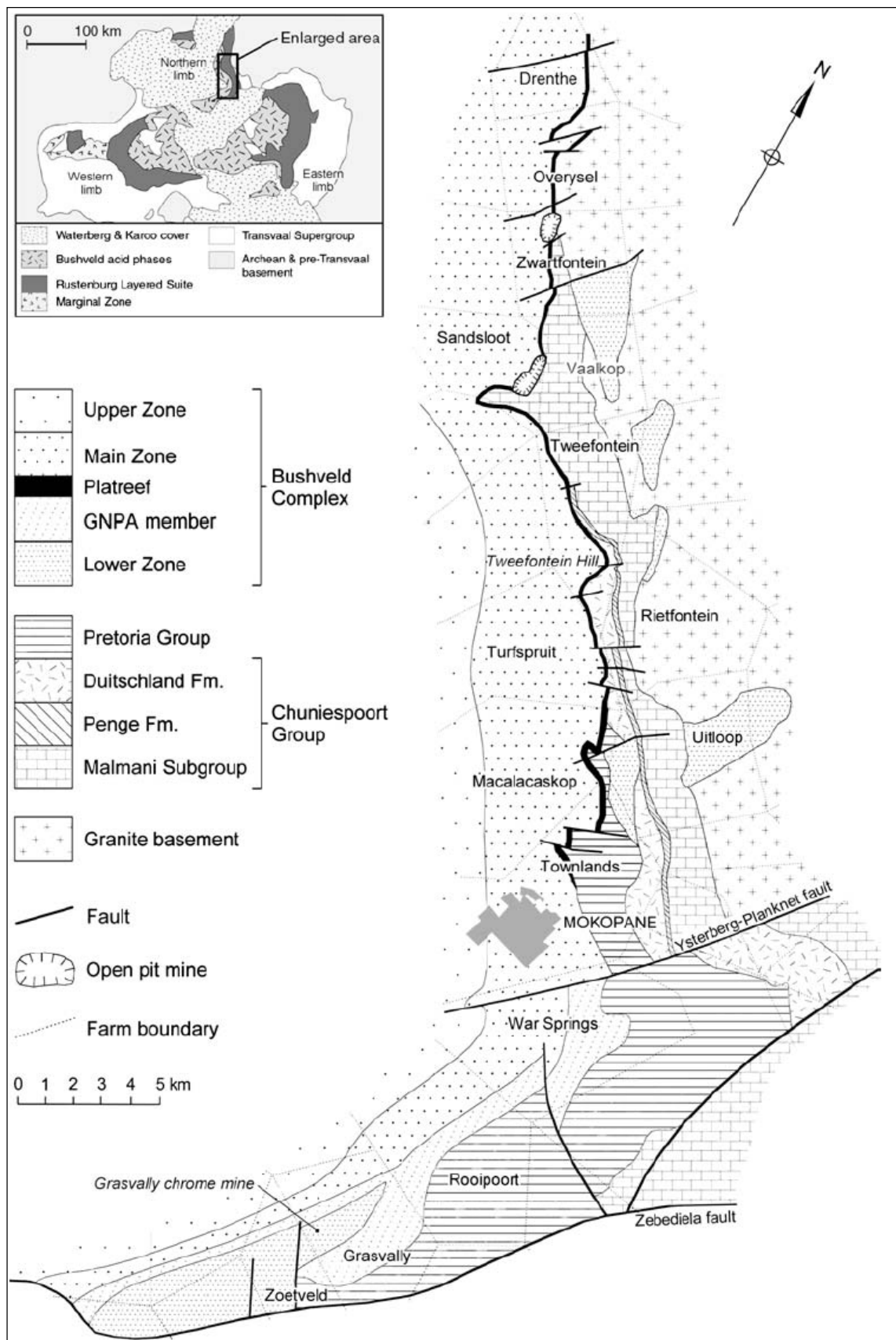


Fig. 3-2. Geological map of the lower portion of the northern limb, showing the locations described in the text (from McDonald *et al.* 2005a).

In contrast to the other limbs of the Bushveld Complex where the igneous layering is generally conformable and there are no gaps in crystallisation, the northern limb may have intruded in a more episodic fashion and transgressive relationships are more evident. For example, Hulbert (1983) and Hulbert & Von Greunewaldt (1985) have argued for a break between intrusion of the Lower Zone and younger cumulates. More recently, Holwell *et al.* (2005) and Holwell & Jordaan (2006) have documented a break in time, followed by deformation and magmatic erosion, between formation of the Platreef and the base of the Main Zone. Indications of this hiatus had already been observed in the present study and are described in Chapter 5.

The Upper Zone usually lies concordantly on the Main Zone, but northwards from the farm Malokongskop the Upper Zone cuts northeastwards across the whole layered sequence, and for more than 20 km of strike it lies directly on the Archaean granite basement. Another, less dramatic, transgression of the Upper Zone across the layered suite occurs further south on the farm Gezond. Van der Merwe (1978) notes that the transgression has different directions in two major, NE-trending synclines in the layered suite and floor rocks, and corresponds to a trough-like Upper Zone structure that truncates all underlying units.

Three sets of major faults affecting the northern limb were identified by Truter (1947), van Rooyen (1954) and de Villiers (1967): (i) N and NNW striking faults; (ii) NE-ENE striking faults; and (iii) NW trending faults. The NE-ENE trending faults appear to be very important structures as they divide the rock types and settings on the northern limb. The Lower Zone, except for the satellite bodies, is confined to an area south of the Ysterberg-Planknek Fault, and the Platreef (*sensu stricto*) and Platreef-analogue rocks are also separated by the same faults. Hulbert (1983) recognised four episodes of fault deformation in the following order: (i) an episode of N–S-trending reverse faulting; (ii) WNW-striking faults; (iii) NE-striking faults assumed to be post-Waterberg; (iv) post-Karoo faults best demonstrated by the almost E–W-striking Zebediela Fault. Northwards, most of the faults strike NE and have a normal displacement with a downthrow to the south (White 1994).

Friese (2004) carried out an exhaustive structural investigation of the northern limb including the Villa Nora occurrence, concluding with a tectonomagmatic model for the development of the Platreef. Disregarding the timing and geological/tectonic environment of Platreef intrusion, which will be discussed in a later section, Friese (2004) arrived at the following sets of structures in the northern limb, from oldest to youngest:

1. Shallow, NW dipping, SE verging thrusts and associated ENE trending, subhorizontal, low-amplitude regional folds with the Archaean basement, Transvaal Supergroup and Rustenburg Layered Suite.
2. NW to WNW trending, moderate to steeply dipping extensional faults within the Transvaal Supergroup and Bushveld Complex, formed by reactivation of the similarly oriented Neoarchaeal (~2.98-2.96 Ga) impactogenic (?) Pongola rift system developed in the underlying Archaean basement during the Murchison Orogeny.
3. ENE to NNE trending, steep to subvertical, mainly SE dipping, dextral strike slip shear zones with associated NE verging, layer-parallel thrusts. These are interpreted as lateral ramps and oblique/frontal ramps, respectively. This system developed in the Transvaal Supergroup by reactivation of the upper section of a Neoarchaeal (~2.78-2.64 Ga) sinistral strike slip system that developed in the underlying Archaean basement in response to sinistral transpressive tectonism during the Limpopo Orogeny. Note: Friese (2004) states that this system developed in the Bushveld Complex as well as the Transvaal Supergroup, but this is impossible as the 2.06 Ga Bushveld Complex did not exist at the time of the 2.7-2.6 Ga Limpopo Orogeny.
4. N-S striking, moderately west dipping extensional faults, typically undulating and with imbricate, normal dip slip and sinistral strike slip duplexes in their immediate hangingwall. These faults transgress the Archaean basement, Transvaal Supergroup and Rustenburg Layered Suite.
5. NW dipping, SE verging thrusts and associated ENE trending, subhorizontal, low amplitude regional folds of pre- to syn-Rustenburg Layered Suite age formed by mild SE directed stress within the northern Kaapvaal Craton at an early stage of the Ubendian (Magondi) Orogeny at ~2.1–2.058 Ga.
6. WNW to WSW trending extensional fractures and joints with minor displacement that cut all other structural discontinuities. These represent the youngest population of structures.

Except for the youngest group of structures, all populations of structures have undergone several phases of reactivation, such that the present magnitude and sense of displacement is an accumulative product of a kinematic history spanning more than 2 Ga.

A prominent tectonic feature of the northern Transvaal outlined in Chapter 2 is a ~500 km long, 25 km wide lineament striking ENE-WSW across the Kaapvaal Craton, called the Thabazimbi-Murchison Lineament (TML; du Plessis & Walraven 1990). The seismic signature of the TML suggests it is a deep lithosphere-mantle break within the Kaapvaal Craton and appears to form and/or influence: (1) the Palala Shear Zone marking the boundary to the north between the Archaean granite/greenstone terrain of the Kaapvaal Craton and the southern margin of the high grade terrain of the Limpopo Mobile Belt (Silver *et al.* 2004); (2) the southern margin of the Mesoproterozoic Waterberg Basin; and (3) probably also the emplacement of the Mesoproterozoic Bushveld Complex. The TML has a history of episodic tectonic activity spanning more than 2.5 Ga, and is characterised by a system of relay faults that were repeatedly reactivated with all senses of movement (extensional, lateral and reverse). Field data reveal a transition from a ductile dominated regime in the east to a brittle dominated regime in the west. This transition corresponds to a change in rheology from the granite basement upwards through the Proterozoic and Mesozoic sedimentary cover (Good & de Wit 1995, 1997; Good 1997). Karoo (Mesozoic) basalts and sediments of the Springbok Flats were deposited in half grabens formed by normal (extensional) reactivation of the formerly strike-slip Zebediela Fault (Fig. 3-2), which is part of the TML relay system. The TML is transgressed by a Mesozoic dyke swarm associated with the incipient dispersal of Gondwana.

Major deformation and fluid activity are recorded along the TML at 2.7 Ga and 2.0 Ga. The older event is correlated with the formation of the Ventersdorp Graben and associated volcanism in the Witwatersrand Basin further south, and major uplift of the Limpopo mobile belt. The younger event is associated with the Magondi orogeny and the intrusion of the Bushveld Complex, which resulted in massive fluid expulsion along the TML from the underlying and flanking Transvaal basin. Analysis of the brittle structures suggests a sinistral transpressive system around 2.0 Ga and later. Accommodation structures are evident, for example the positive flower structure defined by the Ysterberg Shear Zone together with the Uitkyk Shear Zone and associated splay shears (Good & de Wit 1997).

Variations in structural style with time along the TML are indicative of variable stress fields, possibly resulting from variable P-T conditions and strain partitioning along the zone throughout its long history. One curiosity, however, is that the TML does not appear to have responded to the dispersal of Gondwana even though the lineament was favourably oriented as a major extensional/transensional fault zone. A possible explanation is the absence of contemporaneous fluid activity within the TML and the Kaapvaal lithosphere (Good & de Wit 1997), possibly due to devolatilisation caused by emplacement of the Bushveld Complex.

The magnitude and direction of total accumulative displacement along the TML remains uncertain. The displacements of some sections are known, and in the case of the Ysterberg-Planknek Fault Zone is shown to be 8-10 km of dextral lateral movement and up to 10 km vertical displacement in the Archaean (de Wit *et al.* 1992). The significance of the TML in this study is that it defines a tectonic boundary between the northern limb and the eastern and western limbs of the Bushveld Complex, and therefore obscures the relationship of the Platreef to the rest of the complex, which is a topic of current debate. Furthermore, components of the TML compartmentalise the mafic rocks of the northern limb, particularly the Lower Zone and the Platreef and its analogues; and the Waterberg Pt deposit appears to be hosted by a fault in the TML system (Armitage *et al.* 2007).

3.3 Development of the RLS in the northern limb

The subdivision of the mafic and ultramafic lithologies of the Bushveld Complex into four principal zones (Lower, Critical, Main and Upper zones) is based on characteristic mineral assemblages, and has been applied to the entire complex. Whether all of these stratigraphic zones are present in the northern limb and whether they can be correlated directly with rocks in the eastern and western limbs are controversial questions, and will be addressed to a modest extent in this thesis.

3.3.1 Stratigraphy of the northern limb

The stratigraphy of the northern limb differs in a number of ways from the Rustenburg Layered Suite south of the TML. Fig. 3-3 summarises the traditional view of the stratigraphic relationship between the main units of the Bushveld Complex. Further, there is a stratigraphic break within the northern limb marked by the NE-SW striking Ysterberg-Planknek Fault: the Lower Zone seems to be developed continuously south of the fault at Mokopane, while to the north the Lower Zone only occurs as satellite bodies in the sedimentary country rocks (Fig. 3-4).

3.3.1.1 Lower Zone

Drilling by Rio Tinto Exploration Ltd in 1970, followed by more recent exploration by Pan Palladium during 2002-2004, intersected significant concentrations of Ni, Cu and platinum and palladium in harzburgites, dunites and pyroxenites of the Lower Zone in the southern sector of the northern limb. This is the only significant discovery of stratiform Ni-PGE mineralisation in the Lower Zone in the entire Bushveld Complex. Lower Zone lithologies are confined to two different geological settings. South of Mokopane – on the farms Grasvally,

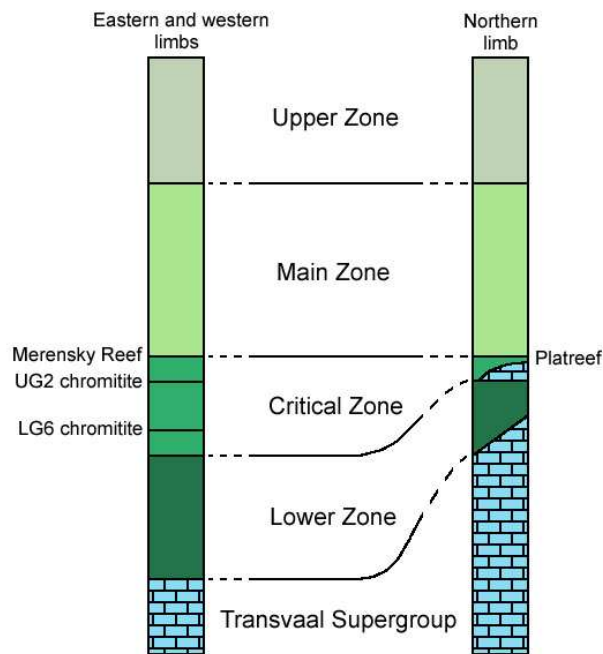


Fig. 3-3. Traditional stratigraphic relationships between the eastern and western limbs and the northern limb of the Bushveld Complex (after White 1994; Cawthorn & Lee 1998).

Volspruit and Zoetveld – a north trending block containing a sequence of pyroxenite and harzburgite with chromitite layers (Hulbert & Von Gruenewaldt 1986) forms a horst between younger cumulates correlated with the ‘Critical’ and Main Zones. Intensive faulting conceals the total succession, but a stratigraphic column more than 1600 m thick has been revealed by drilling (Hulbert 1983) and consists of at least 37 distinct cyclic units (Hulbert & Von Gruenewaldt 1985). The Lower Zone is divided into three subzones: (1) the Volspruit Subzone, in which pyroxenites predominate over harzburgite with chromitite; (2) the Drummondlea Subzone, containing harzburgite with chromitite layers; and (3) the Moorddrift Subzone, characterised by pyroxenite and harzburgite in approximately equal proportions (Fig. 3-5).

The Lower Zone also occurs as smaller, pyroxenite-dominated satellite bodies north of Mokopane. These bodies form sheet-like intrusions in the Archaean granite and in the Transvaal Supergroup sediments, with inferred thicknesses of 200-700 m, but poor exposure makes their dimensions somewhat uncertain (van der Merwe 1976, 1978). Compared to similar Lower Zone rocks elsewhere in the Bushveld Complex, these mafic rocks are characterised by higher Mg# values – i.e. $Mg/(Mg+Fe)$ – in olivine and orthopyroxene, contain chromitites with higher Cr_2O_3 (Hulbert 1983), and hosts a PGE-rich sulphide horizon (Hulbert & Von Gruenewaldt 1982). Van der Merwe (1976, 1998) considers these to be unique features of the northern limb that distinguish it from the rest of the Bushveld Complex. Willemse (1964, 1969) suggests that the northern limb Lower Zone occurrences are most probably representative of a postulated hidden level of the Lower Zone. Naldrett (2004) has

suggested that the sequences in the northern limb might represent a ‘Lower Lower Zone’, that is more primitive than the ‘Upper Lower Zone’ which is exposed throughout most of the Bushveld Complex.

Field relationships and the mineralogy of the Lower Zone satellite bodies and rocks ascribed to the ‘Critical’ Zone and the Main Zone suggest a hiatus between emplacement of the Lower Zone and the younger cumulates (van der Merwe 1978; Hulbert 1983; de Klerk 2005). However, the length of this break is poorly constrained and the wider question of whether Lower Zone-type magma was involved in later magmatic events such as the Platreef (e.g. McDonald *et al.* 2005a; McDonald & Holwell 2007; McDonald *et al.* 2009) remains open.

3.3.1.2 GNPA Member (‘Critical Zone’)

A 350 m thick sequence of rocks known as the Grasvally norite-pyroxenite-anorthosite (GNPA) member is developed over the Lower Zone and sedimentary rocks of the Pretoria Group south of Mokopane, on the farm Grasvally (Hulbert 1983; Hulbert & Von Gruenewaldt 1985, 1986) (‘Critical Zone’ in Fig. 3-4). The GNPA member consists of layered norites, gabbronorites and anorthosites along with a chromitite layer, and has been labelled the ‘Critical Zone’ of the northern limb (van der Merwe 1976, 1978; Hulbert 1983). Recent drilling into the GNPA member on the adjacent farm, Rooipoort, has shown that over strike lengths of 5-6 km it consists of a lower mafic unit dominated by pyroxenites and melanogabbros, with a chromitite layer, and an upper felsic unit dominated by gabbros and anorthosites. Both units contain Ni-Cu-PGE mineralisation associated with the chromitite layer, and a layer of pyroxenite-melanorite respectively. Surprisingly, there is also evidence on Rooipoort that the lower mafic unit and the upper felsic unit are often separated by a fine- to medium-grained gabbronorite unit that appears to be related to a younger sill of possible Main Zone affinity (de Klerk 2005).

The chromitite layer of the GNPA member has been called the ‘UG2-like chromitite’ by Hulbert (1983) and has been directly correlated with the UG2 chromitite in the Critical Zone of the central Bushveld Complex (e.g. van der Merwe 1998). However, while the Cr₂O₃ contents of the GNPA member and UG2 chromitites are similar, the PGE pattern determined by Von Gruenewaldt *et al.* (1989) for the GNPA chromitite does not closely resemble the UG2, and the northern limb chromites have higher TiO₂ and Al₂O₃ than normal UG2 (Hulbert 1983). The associated silicates in the northern limb are also consistently richer in Fe (McDonald *et al.* 2005a).

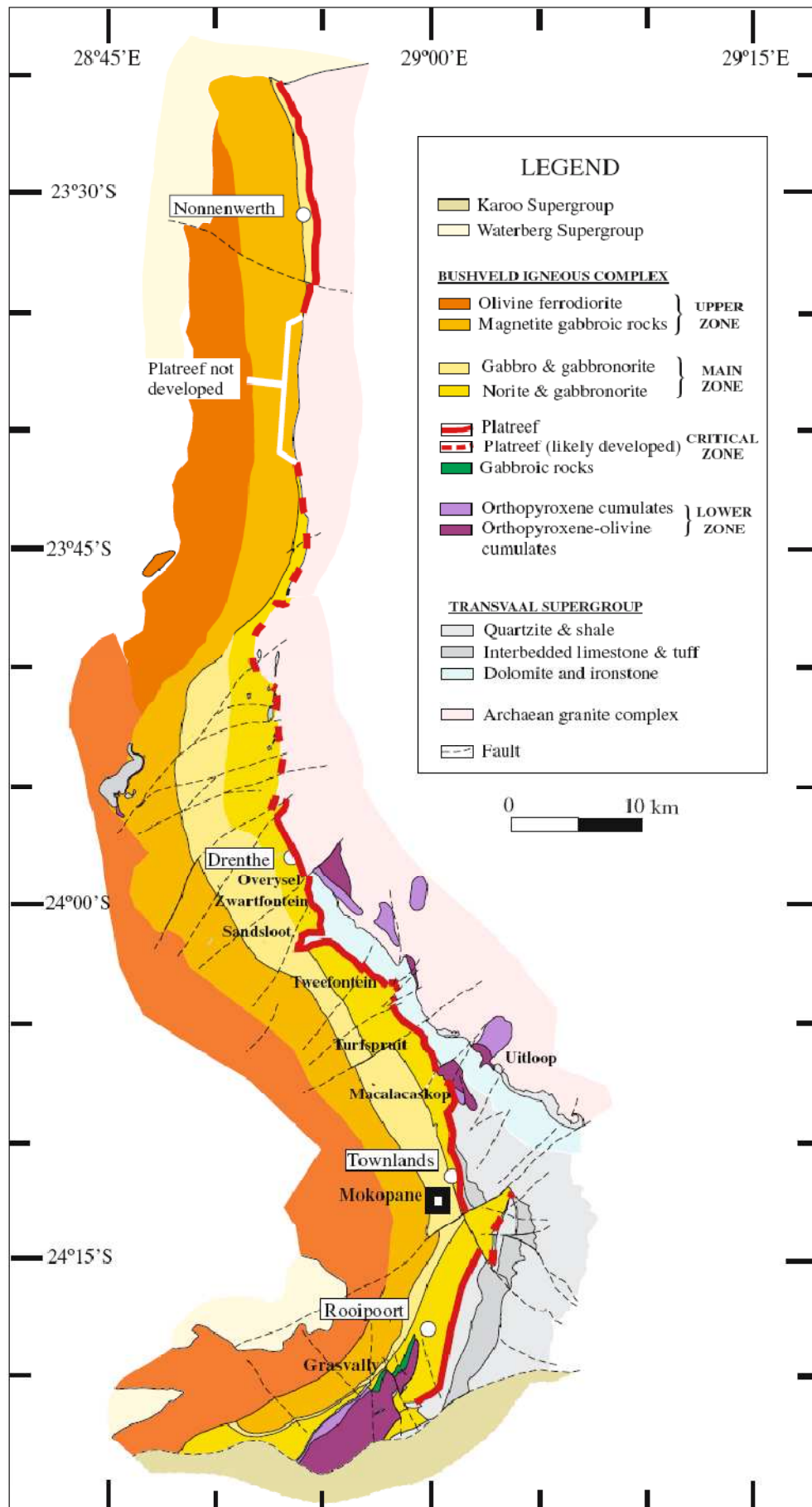


Fig. 3-4. Geological map of the northern limb of the Bushveld Complex with farm boundaries (from Maier *et al.* 2008b, adapted from Ashwal *et al.* 2004).

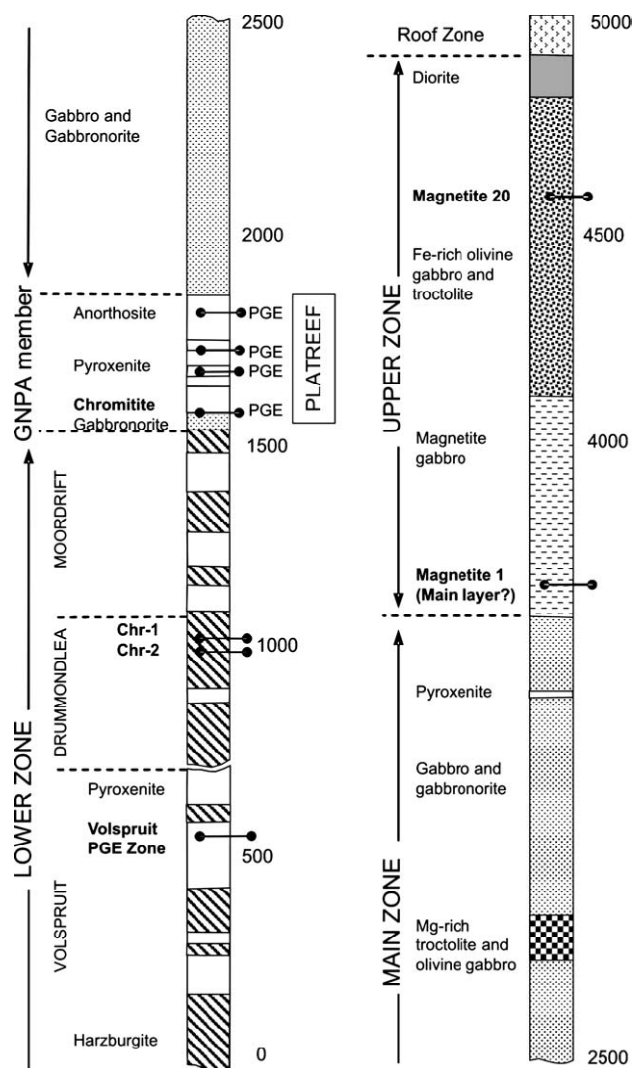


Fig. 3-5. Stratigraphy of the northern limb south of Mokopane showing the major chromitite, magnetite and Ni-Cu-PGE deposits (from McDonald *et al.* 2005a, modified after Von Gruenewaldt *et al.* 1989).

The abundance of xenoliths and the presence of PGE mineralisation in the upper part of the GNPA member have led some authors to suggest that the top of the GNPA member may correlate with the Platreef north of Mokopane (Von Gruenewaldt *et al.* 1989). Maier *et al.* (2008b) correlates the GNPA member with the Upper Critical Zone and suggests that, where the Upper Critical Zone abuts the margin of the Bushveld Complex, “*it can transform into contact-style mineralization resembling the Platreef*”. This postulated correlation remains unclear, as limited geochemical and mineralogical information is currently available for the GNPA rocks (Kinnaird & McDonald 2005). However, van der Merwe (2008) observes a lateral lithological transformation/variation of Merensky Reef/UG2 south of the Ysterberg-Planknek Fault into Platreef north of the fault, best demonstrated in borehole intersections either side of the fault. The same author supports this lateral transformation by drawing

attention to well documented lateral lithological variations in the western limb (Maier & Eales 1997). The cause of this variation is considered to be a combination of interaction in the chamber between the magma, its differentiates and the variable floor rocks, and floor structures. South of the Ysterberg-Planknek Fault, Bushveld mafics are concordant with relatively refractory quartzite of the Magaliesberg or Smelterskop Formations and ultramafic Lower Zone rocks. Less reactive conditions (Manyeruke *et al.* 2005) prevailed in this part of the chamber, causing the magma to differentiate into or develop a sequence similar to that in the eastern or western limbs of the complex where it is mainly concordant with the floor. North of the fault, the chamber cut across an uneven, protuberant floor comprising reactive dolomite, shale, and less reactive quartzite layers; here, the chamber is also closer to the postulated feeder (van der Merwe 2008). Conditions in such surroundings may trigger precipitation of sulphide and spinel layers (De Waal 1977; Manyeruke *et al.* 2005).

3.3.1.3 Main Zone

The Main Zone comprises a relatively monotonous, up to 2200 m thick succession of gabbros and gabbro-norites (van der Merwe 1976). Northwest of Mokopane, persistent marker horizons occur in the form of four prominent pyroxenites developed at around 300 m above the base of the Main Zone and a 100-200 m thick troctolite and olivine gabbro-norite is developed at 1100 m above the base. These markers are not known in the rest of the Bushveld Complex. Van der Merwe (1976) suggests that a pyroxenite horizon that occurs 2000 m above the base of the Main Zone corresponds to the well established Pyroxenite Marker in the eastern and western limbs. However, Harris *et al.* (2004) and Ashwal *et al.* (2004) discount this correlation, as the dominant pyroxene in the unit they have formally termed the 'Pyroxenite Horizon' is pigeonite (low-Ca clinopyroxene with augite exsolution lamellae) whereas in the Pyroxenite Marker it is low-Ca orthopyroxene. Further, the Pyroxenite Horizon appears to be absent south of Mokopane where the Main Zone is unusually thin and is not present in the stratigraphic compilations of Hulbert (1983) or Von Gruenewaldt *et al.* (1989).

Nex *et al.* (1998) have reviewed previous studies of Main Zone mineralogy and present a new subdivision into 5 zones (A to E), based on the variation in relative abundance of different pyroxenes. Although the study was conducted in the western limb of the Bushveld Complex, the five-fold subdivision can also be recognised in the lithologies of the eastern limb. Significantly, however, there was no attempt to apply this subdivision to the northern limb.

In contrast to the Main Zone of the eastern and western limbs, which are devoid of significant Ni-Cu-PGE mineralisation, the Main Zone in the northern limb is mineralised. The

most significant occurrence is in the far north of the limb, principally on the farms La Pucella 693LR, Altona 696LR, Kransplaats 422LR and Nonnenwerth 421LR; currently being developed as the Aurora Project by SA Metals Ltd (currently delisted, formerly Pan Palladium Ltd). This company has reported a resource estimate of 133 Mt containing 5.77 Moz 3E (Pt+Pd+Au) at a grade of 1.34 g/t for the Aurora area (Pan Palladium annual report 2006). The PGE are associated with sulphides in a number of zones but the sulphides are notably richer in Cu when compared to the Platreef. The Aurora mineralisation is hosted within gabbros and anorthosites thought to be part of the upper Main Zone (Harmer *et al.* 2004). The Main Zone is also mineralised south of the Planknek-Ysterberg Fault (Caledonia Mining Corporation 2005; de Klerk 2005; Maier *et al.* 2008a).

3.3.1.4 Upper Zone

Upper Zone rocks are scarcely exposed in the northern limb, and knowledge of the Upper Zone is acquired from boreholes. It is 1400 m thick and consists of a lower 500 m of mainly magnetite gabbro, anorthosites and olivine diorites, with a number of magnetite layers. One of these magnetite layers has been correlated with the Main Magnetite layer elsewhere in the Bushveld Complex on the basis of thickness and V₂O₅ content (van der Merwe 1976; Von Gruenewaldt *et al.* 1989). Sulphides are common in the lowermost part of the Upper Zone. The upper 900 m of the Upper Zone consists almost entirely of olivine-bearing cumulates exhibiting great variation in the proportions of cumulus olivine, pyroxene, magnetite, plagioclase and apatite, with some magnetite layers (Ashwal *et al.* 2004). The Upper Zone also crops out in the Villa Nora area, where the main lithologies are leuconorites, leucogabbros and anorthosites (Hattingh & Pauls 1994). Here, the lower parts of the Upper Zone are truncated by the Abbotspoort Fault. In terms of PGE, the Upper Zone is barren throughout (Barnes *et al.* 2004).

3.4 Age of the northern limb

As explained in Chapter 2, the age of the Bushveld Complex has been accepted by most workers as 2.06 Ga (Walraven *et al.* 1990) for all three or four limbs of the complex. Buick *et al.* (2001) confirmed this age with a more precise determination using U-Pb dating of titanites in calc-silicate xenoliths in the eastern limb. Further, the Merensky Reef has more recently been dated to 2054.4 ± 1.3 Ma (Scoates & Friedman 2008). Some recent studies, however, cast doubt on synchronicity between the northern limb and the eastern and western limbs (e.g. McDonald *et al.* 2005a) and this necessitates a re-evaluation of the Bushveld age, which may be more heterogeneous than previously thought.

There are currently only three successful attempts to date the northern limb, all of which indicate a slightly younger age for emplacement of the limb: (i) an Re-Os isotope study on Platreef sulphides from Turfpruit that gave an age of 2011 ± 50 Ma (Ruiz *et al.* 2004), virtually identical to (ii) an Re-Os age of 2011 ± 51 Ma on Platreef pyroxenites at Sandsloot (Reisberg *et al.* 2011) – these ages agree within the upper error with the accepted Bushveld age of 2060 Ma. Reisberg *et al.* (2006) had previously obtained a less constrained Re-Os age of 2011 ± 90 Ma for the Platreef at Sandsloot. Further, (iii) a new SHRIMP zircon age for the Platreef at 2056.2 ± 4.4 Ma (Yudovskaya *et al.* 2009) is indistinguishable from a 2053.7 ± 3.2 Ma zircon age for a granitic vein that cuts the Platreef and which may be derived from local melting of country rocks by the Platreef magma (Hutchinson *et al.* 2004; Kinnaird *et al.* 2005).

Thus, the Platreef appears to be synchronous with the Merensky Reef (2054.4 ± 1.3 Ma: Scoates & Friedman 2008). Even well constrained ages, however, carry error margins that are large in relation to the likely short-lived emplacement history of the Bushveld Complex. The phases of intrusion are therefore difficult to distinguish temporally.

4. THE PLATREEF

4.1 Introduction

This chapter provides a review of previous studies on the Platreef, including an account of its exploration history. The Platreef is the principal mineralised unit of the northern limb and contains significant Ni-Cu-PGE mineralisation along strike for >30 km (Fig. 4-1). The Pt+Pd content of the reef is estimated to be 16.3 Moz (Cawthorn 1999). With its high PGE tenor and thickness of up to 400 m, it is amenable to open pit mining (Bye 2001). Potgietersrus Platinums Ltd, a subsidiary of Anglo Platinum, now operates five open pit mines at Sandsloot, Zwartfontein South, Zwartfontein North and Overysel. Collectively these are known as Mogalakwena. The ore is milled at the new, fully operational North Concentrator and at the older South Concentrator. The Mogalakwena life-of-mine extends to well beyond 2060. The current life-of-mine plan consists of a mineral resource (exclusive of ore reserves) of 141.6 Moz 4E (Pt+Pd+Rh+Au) and an ore reserve of 55.3 Moz 4E. A further four open pit operations are planned: one in the southeastern corner of the Sandsloot property and three on Tweefontein. Several junior companies have joined the exploration bandwagon, making the northern limb one of the most intensively explored areas for PGE in the world.

4.2 Setting of the Platreef

The reason for treating the Platreef in a separate chapter is the lack of consensus on whether the Platreef is of Critical Zone affinity (e.g. White 1994) or Main Zone affinity (e.g. Kruger 2005a); whether it is the northern limb equivalent of the Merensky Reef (e.g. Wagner 1929; Kruger 2005a; Naldrett *et al.* 2008); or whether it represents an event unique to the northern limb (McDonald *et al.* 2005a). These questions warrant more review than would be practical in the outline of the Bushveld Complex in Chapter 2. The Platreef (*sensu stricto*) is defined by Kinnaird & McDonald (2005) as “*mafic units enriched in Ni-Cu-PGE that occur between the Archaean granite-gneiss basement or the Transvaal Supergroup and the gabbros/gabbro-norites of the Main Zone, north of the Planknek Fault*”. The Platreef can be traced for >30 km north of Mokopane, and along its path it transgresses progressively lower sedimentary units of the Transvaal Supergroup and eventually abuts against Archaean granite/gneiss basement (Fig. 4-1). The thickness of the Platreef varies from 400 m in the south to <50 m in the north. At the surface, the common strike is north to northwest and the

dip is moderate (40-45°) to the west, but becomes more gentle downdip. However, the overall geometry appears to have been controlled by irregular floor topography (Fig. 4-2). On the farms Macalacaskop and Turfspruit there are basement highs with thinned Platreef on the flanks and thick reef in the intervening basins. In the Macalacaskop basin, the Platreef is 400 m thick, dips 32° NE on the south side and 47° SW on the north side. In the Turfspruit basin, the reef is 250 m thick with 40° inward dips on both sides (Kinnaird *et al.* 2005). The nature of these basement highs is equivocal, possibly representing an undulating floor, antiforms or horst blocks.

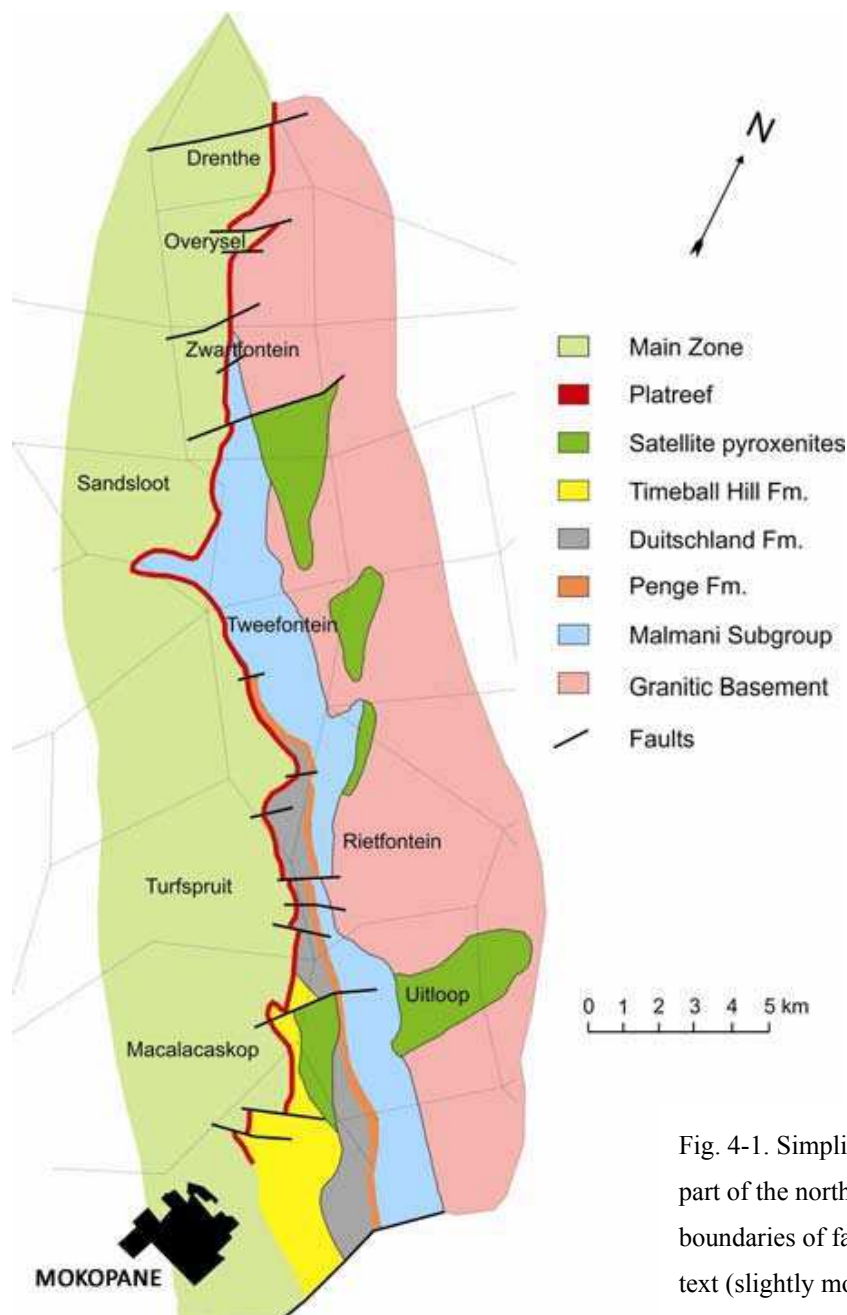


Fig. 4-1. Simplified geological map of part of the northern limb, showing boundaries of farms referred to in the text (slightly modified from Kinnaird 2005b).

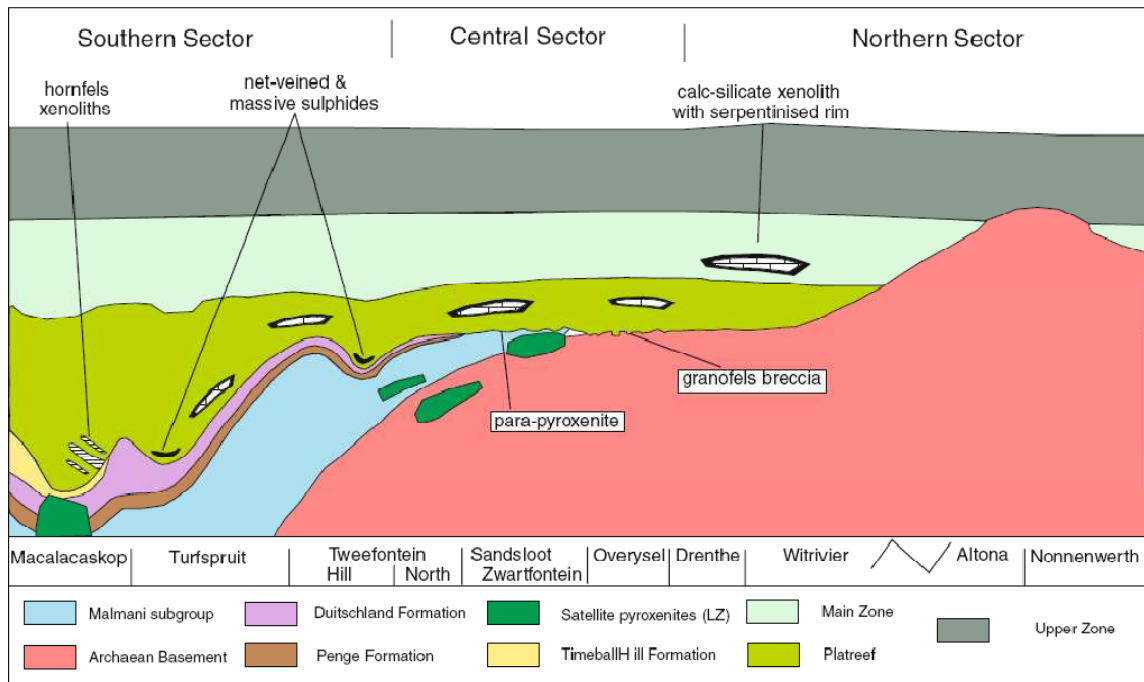


Fig. 4-2. Schematic longitudinal section through the Platreef along the entire strike length (from Kinnaird *et al.* 2005). Note that between Witrivier and Altona a significant strike length is not shown.

In plan view, a prominent ‘tongue’ of Malmani Dolomite protrudes into the Platreef and Main Zone south of Sandsloot, separating the Sandsloot open pit from Platreef exposures on Tweefontein. The tongue has a metamorphic aureole, with a maximum thickness of 200 m, consisting of an outer pegmatitic plagioclase-quartz-hornblende rock and an inner serpentinised dolomite (van der Merwe 1978). The formation of this structure relative to the Platreef and Main Zone will be addressed in more detail in Chapters 5 and 7.

On a broader scale, the strike of the Platreef changes abruptly in association with faults: a north-south striking, steeply dipping set predominates, with secondary ENE and ESE striking sets dipping 50-70° south. The faults are pre-Bushveld and locally control thickening and thinning of the layered sequence, especially in the south. Changes in strike of the Platreef are also noted in association with pre-Platreef synforms, and thick basal sulphide mineralisation occurs in this structural setting, such as at Tweefontein Hill (Nex 2005).

The unresolved questions of the age and origin of the Platreef have important implications for the long-assumed link between the Platreef and Merensky Reef. This link is fundamental in the prevailing view of the stratigraphy of the northern limb and its relationship to the rest of the Bushveld Complex, but some recent studies have cast doubt on the stratigraphic link between the Platreef and Merensky Reef (e.g. McDonald *et al.* 2005a; Holwell & Jordaan 2006). Pronost *et al.* (2008) argue that the similarity in initial Sr- and Nd-isotope composition between the Platreef and its immediate hangingwall norites and the

Merensky Reef suggests that the Platreef and Merensky Reef share a common origin, as originally suggested by Wagner (1929); and this would explain the similarity in initial Os-isotope ratios between the Platreef and the Merensky Reef reported by Reisberg *et al.* (2006).

Nex (2005) studied the structural setting of the Platreef on Tweefontein Hill, south of Sandsloot, noting a significant change in the strike of the Platreef and Transvaal Supergroup metasedimentary floor rocks. The study documents two pre-Bushveld ductile deformation events resulting in a major southwest plunging fold into which massive sulphides have been concentrated by gravitational settling.

4.2.1 Sulphur isotope studies

Peniston-Dorland *et al.* (2008) report sulphur (S) isotope measurements made on samples collected along two profiles through the Platreef into underlying metapelitic and metacarbonate footwall rocks, concluding that the Platreef magma was apparently S saturated prior to emplacement and, counterintuitively, lost S during the formation of the present Platreef ore horizon. In both profiles, igneous rocks far from the contact have low $\Delta^{33}\text{S}$ values (average $\Delta^{33}\text{S} = 0.15\text{‰}$), whereas metasedimentary rocks far from the contact have high $\Delta^{33}\text{S}$ values ($\Delta^{33}\text{S}$ up to 5.04‰) with a smoothly varying profile between the two end members. The midpoint in both isotope profiles is displaced into the footwall, but the same geometry is not present in the associated $\delta^{34}\text{S}$ values. The displacement of the $\Delta^{33}\text{S}$ front suggests fluid transport and advection of S into the country rocks; this was accompanied by back diffusion of the S isotope tracer into the Platreef. The multiple S isotope results suggest a different interpretation of Platreef mineralisation than that reached by consideration of $\delta^{34}\text{S}$ values alone. The $\Delta^{33}\text{S}$ measurements reflect a dominantly magmatic signature for S in the Platreef that is obscured in $\delta^{34}\text{S}$ measurements by late-stage disequilibrium and fractionation effects likely due to hydrothermal activity. This interpretation is consistent with the results of Harris & Chaumba's (2001) study using oxygen isotopes, which suggested a large degree of fluid-rock interaction in the Platreef, with a magmatic origin for the fluid. Although $\delta^{34}\text{S}$ analyses can decipher this signature when carefully linked to specific sulphide textures (e.g. Holwell *et al.* 2007), the chemically conservative nature of $\Delta^{33}\text{S}$ values removes the masking effect of secondary processes that are mass dependent and fractionate $\delta^{34}\text{S}$, but not $\Delta^{33}\text{S}$. Most intriguing, $\Delta^{33}\text{S}$ measurements preclude local footwall-derived S as a significant trigger for mineralisation in the Platreef. The $\Delta^{33}\text{S}$ profile indicates that contact enrichment of S in the Platreef is limited to distances <5 m from the contact and is best explained by minor amounts of back diffusion through fluids as S is transported away from a cooling and crystallising magma (Penniston-Dorland *et al.* 2008).

4.3 Exploration and research on the Platreef

Exploration in the Platreef area began with early mining operations for tin, starting with the discovery of the Zaaipplaats and Union tin fields in the period 1906-1908 (Kynaston & Mellor 1909; Pringle 1986). This was followed by the discovery of platinum in quartz veins near Mookgophong (formerly Naboomspruit) in 1923 (Wagner & Trevor 1923; McDonald *et al.* 1999; McDonald & Tredoux 2005; Armitage *et al.* 2007). In 1924, Andries Lombaard discovered platinum on Maandagshoek in the eastern Bushveld, and soon afterwards Hans Merensky announced that he had located a ‘platinum-bearing horizon’ in the Rustenburg (Wagner 1926) and Mokopane areas (Wagner 1929; White 1994). Early mapping revealed the general NNW-SSE strike and enormous lateral extent of the mafic rocks in the northern limb as well as broad similarities to the mafic sequences established in the rest of the Bushveld Complex (Hall 1908, 1926; Mellor & Hall 1910). After successfully tracing the Merensky Reef westwards to the Rustenburg area, the similarities in rock types outlined by Hall and Mellor led Hans Merensky and other prospectors back to the northern limb and to the discovery of the Platreef in 1925 (Mills Davies 1925). Merensky identified higher grade zones at the top of the pyroxenite sequence on Sandsloot, Vaalkop and Zwartfontein, and shafts were sunk on these properties. Platinum was also discovered in ‘crush zones’ in the Penge banded ironstone on Tweefontein Hill (Merensky 1925).

In recent years, prospecting activity on the Platreef has reached levels not seen since the 1925 ‘platinum rush’. The manner in which the Platreef formed was construed just a few months after the discovery of the reef – it was quickly recognised that the Bushveld magma had intruded into and transgressed the sedimentary Transvaal Supergroup, and that the mineralisation resulting from envelopment of the sedimentary rocks was a process that “*might reasonably be looked for*” (Mills Davies 1925).

By August 1925, the financiers Becker and Ohlthaver had amassed rights to an area of 130,000 acres covering many of the key farms where Platreef mineralisation would be discovered. This land package was used to register a new company, Potgietersrust Platinums Limited (PPL). Finally, Becker and Ohlthaver approached Wakkerstroom Oil Company in November 1925 and secured the farms Tweefontein and Rietfontein for PPL. By the end of the year, PPL had acquired nearly all key platinum properties in the Mokopane area, and were then taken over by Johannesburg Consolidated Investments (JCI) (Matier 2004).

About 9 months of systematic exploration ensued on Tweefontein, Sandsloot, Vaalkop and Zwartfontein, and in September 1926 PPL built a processing plant. By 1928, PPL had produced 22,500 ounces of platinum from underground workings (White 1994). However,

1925 had been a boom year and the platinum production rate in 1928 was less than the market had expected. Much of the early work on the deposits of the northern limb was summarised in Wagner's (1929) seminal volume 'The Platinum Deposits of South Africa'. In May 1930, PPL ceased production on reported recovery problems and due to a falling metal price with the onset of the Great Depression.

The next 38 years was a dormant period for the Platreef deposits. In 1969, JCI resumed drilling and shaft sinking, then conducted underground mining, which halted in 1971 because JCI were unable to follow the reef underground. However, interest in the platinum fields had developed among other companies, with drilling programmes undertaken by Chrome Corporation Limited, Rand Mines Limited, Rio Tinto Zinc PLC and Union Carbide Corporation. In March 1976, JCI's interest was rekindled when they started a further systematic drilling programme, which led to a feasibility study and an exploration shaft on Overysel in 1980 (White 1994).

Another few years of inactivity followed until 1986 when JCI resumed drilling and, following positive results, it was decided to sink several incline shafts on the farms Sandsloot and Tweefontein followed by trial mining to obtain a metallurgical bulk sample. In October 1990, a public report was issued by JCI stating that a new underground mine would be opened at Sandsloot with an initial open pit operation (White 1994).

In 1992 PPL (now fully owned by Anglo American) opened the Sandsloot mine. For almost the entire decade, this open pit operation was the only significant activity on the Platreef. The successful, low-cost, high-tonnage model prompted a dramatic revival in exploration activity for Ni-Cu-PGE deposits along the length of the northern limb, and many junior companies have purchased exploration licences for farms covering the strike of the Platreef adjacent to the area held by Anglo Platinum. The boom in exploration on the northern limb also prompted a new wave of research, much of which was conducted on Anglo American's property between the farms Tweefontein and Overysel, e.g. White (1994) and Viljoen & Schürmann (1998). The Sandsloot mine then became the focus of several studies that addressed Platreef contamination, mineralisation, structure, geochemistry, emplacement and mineralogy (respectively: Harris & Chaumba 2001; Armitage *et al.* 2002; Friese 2004; McDonald *et al.* 2005a; Holwell *et al.* 2005; Holwell *et al.* 2006).

In 2010, the Mogalakwena Mine (formerly PPL) produced 589,100 oz refined 4E (combined Pt+Pd+Rh+Au) with 8,500 t (dry metric tonnes) Ni and 5,600 t Cu. Mogalakwena Mine's proven and probable Platreef ore reserves, including primary ore stockpiles, were 609.3 Mt (million tonnes) at a grade of 2.82 g/t 4E, equating to contained metal of 55.3 Moz (1,628.6 t) 4E. Measured and indicated Platreef mineral resources were 970.3 Mt at 2.21 g/t

4E, equating to contained metal of 69.0 Moz (2,145.5 t) 4E. Inferred mineral resources were 1,200.1 Mt at 1.88 g/t 4E, equating to contained metal of 72.7 Moz (2,260.2 t) 4E. The applied 4E pay limit grade ('cut-off grade') is 1.7 g/t for Sandsloot and Zwartfontein South and 1.0 g/t for Mogalakwena North and Central (Anglo American 2010; estimates as of 31 December 2010).

The continuing exploration boom has been accompanied by an accelerating rate of academic publications. These publications now cover sections of the Platreef outside Anglo American's property. Drilling on the farms Turfspruit and Macalacaskop, currently owned by Ivanhoe Nickel & Platinum Ltd ('Ivanplats'), has enabled studies on geology, geochemistry, mineralogy, isotope characteristics and geometric profile (respectively: Kinnaird *et al.* 2005; Kinnaird 2005a; Hutchinson & Kinnaird 2005; Sharman-Harris *et al.* 2005; Kinnaird *et al.* 2010). The nature of the Platreef at the farm Piet Potgietersrus Town and Townlands (initially developed by Thabex Ltd and currently owned by Blackthorn Resources, formerly called AIM Resources) is described by Manyeruke *et al.* (2005).

Much of the recent research is based on Mogalakwena Mine's new open pit operations north of Sandsloot: magmatic relationships at Zwartfontein are documented by Holwell & Jordaan (2006), while Holwell & McDonald (2006) studied the petrology and geochemistry of the Platreef at Zwartfontein, and the same authors (Holwell & McDonald 2007) analysed the distribution of PGM at Overysel. Holwell *et al.* (2007) investigated variations in sulphur isotope signatures to study the origin of sulphur in different sectors of the Platreef. The most recent studies address the relationship between footwall composition, crustal contamination, and fluid-rock interaction in the Platreef at Overysel, Sandsloot, Turfspruit and Macalacaskop (Pronost *et al.* 2008); the source of Platreef mineralisation based on the geometry of sulphur isotope distribution in the Platreef and metasedimentary footwall rocks (Peniston-Dorland *et al.* 2008); an assessment of the potential involvement of an early magma staging chamber in the generation of the Platreef (McDonald *et al.* 2009); and the importance of semimetals in the partitioning behaviour of PGE in natural magmatic sulphide ore systems (Holwell & McDonald 2010). The themes of these studies will be incorporated in the discussion in Chapter 7.

4.4 Geology of the Platreef and associated units

Wagner (1929) published the first account of the Platreef, describing it in general terms as a basal package of pyroxenites, norites, serpentinites and xenoliths of floor rocks carrying PGE-Ni-Cu mineralisation that transgresses a variety of floor rocks and is overlain by gabbronorites ascribed to the Main Zone. On a more local scale, however, the Platreef is a

complex body of igneous and hybrid lithologies exhibiting along-strike variation that is caused, to a considerable extent, by the interaction between the Platreef magma and local floor rocks. The Platreef has a thickness of as little as 10 m in places at Sandsloot (Armitage *et al.* 2002) to as much as 400 m at Turfspruit (Kinnaird 2005a). Studies suggest that structures in the footwall have exerted some control on Platreef thickness and mineralisation (e.g. Friese 2004; Nex 2005). An overview of the Platreef follows, first with a description of the main footwall and hangingwall rocks (alternatively called floor and roof rocks), then a review of Platreef literature in geographical order starting at Townlands in the south, northwards through Macalacaskop, Turfspruit, Tweefontein, Sandsloot, Zwartfontein, Overysel and finally Drenthe (Fig. 4-1).

4.4.1 Footwall lithologies

A series of Palaeoproterozoic Transvaal Supergroup sedimentary rocks and Archaean basement comprise the footwall of the Platreef. Wagner (1929) describes the discordant relationship between the Platreef and floor rocks as an ‘igneous transgression’, in which the Platreef has intruded progressively older units northwards along its strike. From south to north, and therefore youngest to oldest, these units are: quartzites and shales of the Timeball Hill Formation; shales and diamictites of the Duitschland Formation; the Penge banded iron formation; and dolomite of the Malmani Subgroup that lies directly on Archaean basement granite and gneisses. At Sandsloot and Zwartfontein South, the dolomite has been thermally metamorphosed to what can broadly be labelled as calc-silicate hornfels with a wide variety of skarn assemblages.

As noted above, the interaction between the Platreef magma and the various floor rocks has resulted in a complex body including hybrid lithologies, e.g. serpentinised websterites identified by McDonald *et al.* (2005a). Clinopyroxenites with low whole-rock Cr and high CaO at Sandsloot and Zwartfontein South, normally found between the Platreef and footwall calc-silicates, are interpreted as metamorphic clinopyroxenites (Harris & Chaumba 2001) produced by thermal metamorphism and hydrothermal activity in the footwall contact zone. Wagner (1929) first used the term ‘parapyroxenite’ for these clinopyroxenites in recognition of footwall origin, and the name has been in local use ever since.

4.4.2 Hangingwall lithologies

Along the northern limb, the Platreef is overlain by a thick (up to 2000 m) package of gabbro, magnetite gabbro and diorite belonging to the Main and Upper Zones. At least in the present study area and its vicinity, the hangingwall is Main Zone and comprises medium-grained

norites and gabbro-norites containing cumulus plagioclase, cumulus and intercumulus orthopyroxene (En₆₄₋₇₀) and generally oikocrystic clinopyroxene. In the Sandsloot-Zwartfontein section, the base of the hangingwall is frequently observed as a thin fine-grained poikilitic leuconorite up to 30 cm thick, containing up to 90% cumulus plagioclase and oikocrystic pyroxenes. Occasional xenoliths of calc-silicate derived from metamorphosed dolomite similar to that observed in the footwall are present in the hangingwall (Gain & Mostert 1982; Kinnaird & Nex 2003; and this study), and pyroxenites with petrographic and geochemical characteristics similar to the Platreef are present within the hangingwall (McDonald *et al.* 2005a).

4.4.3 Platreef lithologies

The Platreef is recognised as a commonly feldspathic pyroxenite of cumulus orthopyroxene and intercumulus clinopyroxene and plagioclase, with accessory interstitial sulphides. Based on the results of trial mining by JCI at Overysel during the 1980s, White (1994) introduced a threefold subdivision of the Platreef, naming the three units A, B and C reef. The ‘A’ reef was defined as a pegmatoidal feldspathic pyroxenite at the base of the sequence, carrying sporadic base metal sulphide (BMS) mineralisation. The ‘B’ reef was the principal PGE carrier overlying the ‘A’ reef, comprised of coarse-grained feldspathic pyroxenite with 50-90% orthopyroxene, intercumulus plagioclase, common BMS and very sporadic chromitite. The ‘C’ reef was the top unit and consists of a PGE-poor, fine-grained poikilitic feldspathic pyroxenite with up to 70% clinopyroxene. This simplified tripartite division of the Platreef was based purely on mineralogical characterisation and was primarily used in mining terminology, but has become entrenched in the literature (e.g. Barton Jr *et al.* 1986; Lee 1996; Viljoen & Schürmann 1998; Cawthorn & Lee 1998; Barnes & Maier 2002; Cawthorn *et al.* 2002b). The unfortunate consequence of the uncritical acceptance of the A-B-C sequence is that it has been assumed to represent ‘typical’ Platreef. However, even before the A-B-C sequence was proposed, earlier investigations on Drenthe 788LR (Gain & Mostert 1982) and Overysel 815LR (Cawthorn *et al.* 1985) had already shown petrological and stratigraphic relationships that are incompatible with the A-B-C sequence, and further mismatches have been revealed in more recent studies (Kinnaird *et al.* 2005; McDonald *et al.* 2005a). Armitage *et al.* (2002) presented the initial findings of the present study and used the term ‘B-reef’, as it fitted the characterisation of White (1994), but also pointed out that rocks corresponding to ‘A’ and ‘C’ reef seemed to be absent in the sections they investigated at Sandsloot while other, previously uncharacterised reef lithologies were present. At Platreef workshops

convened in 2004 and 2005, the inappropriate nature of the A-B-C scheme was highlighted (e.g. Nex & Kinnaird 2004) and it is now falling out of use.

Townlands

Manyeruke *et al.* (2005) described a core through the Platreef at its southernmost outcrop on the farm Townlands. Here the Platreef overlies quartzites and shales of the Timeball Hill Formation. The reef is described as a 150 m thick package of three igneous units (Lower, Middle, Upper) separated by hornfels (metamorphosed shales), and each of the three units is interpreted as a distinct intrusive phase based on geochemical characteristics. The major silicate minerals of the Lower Platreef are subhedral or anhedral cumulus orthopyroxene (55-75 modal %), mostly anhedral (intercumulus) and, to a lesser extent, subhedral (cumulus) plagioclase (20-40 modal %) and interstitial clinopyroxene (0-10 modal %). Accessory minerals include olivine, quartz, magnetite, sulphides and secondary biotite, amphibole, sericite and epidote. Notably, there is a relatively high amount of quartz (up to 3 modal %) in some of the rocks. The Middle Platreef is predominantly composed of cumulus orthopyroxene (65-80%), interstitial and poikilitic clinopyroxene (10-15 modal %) and mostly interstitial plagioclase (10-25 modal %) with some apparently cumulus plagioclase laths. In addition, variable amounts of olivine (up to 20 modal %) may occur. Minor phases are biotite, sulphides, magnetite and amphibole. The Upper Platreef is predominantly composed of cumulus orthopyroxene (55-75 modal %), with subordinate intercumulus clinopyroxene (0-20 modal %) and intercumulus plagioclase (20-40 modal %). Olivine, quartz, biotite, magnetite, sulphide and amphibole are minor phases. The geochemical data reveal a reversed differentiation trend within the Platreef, with progressively more primitive rocks, enriched in Cr and MgO and depleted in incompatible trace elements, being found towards the top.

The available S isotopic data on the Platreef has been summarised by White (1994), who showed that the Platreef rocks have $\delta^{34}\text{S}$ between -3 to +9 ‰, indicating the presence of external (crustal) S. At Townlands, all the Platreef samples have positive $\delta^{34}\text{S}$ values. The highest values are found in the hornfels and calc-silicates of the floor rocks, which have broadly similar S-isotopic signatures. The Lower Platreef and Upper Platreef tend to have higher $\delta^{34}\text{S}$ than the Middle Platreef. There is also a tentative trend of an increase in the $\delta^{34}\text{S}$ values towards the base within the Middle and Lower Platreef, a phenomenon that could possibly be explained by enhanced assimilation of crustal sulphur towards the floor of each layer, perhaps by means of continued degassing of the floor rocks during crystallisation of the Platreef.

Notably, the Pt/Pd ratios of <1 in the Platreef at Townlands and in other sectors of the northern limb are much lower than in sulphides and rocks elsewhere in the Bushveld Complex (Pt/Pd 1.8–2.9, Maier & Barnes 1999).

Contrary to the study of Manyeruke *et al.* (2005), a reassessment of the core by Snowden Mining Consultants using a wider range of drilling data from Townlands (presumably including boreholes not studied by Manyeruke *et al.* 2005) showed the Platreef to be a pegmatoidal pyroxenite interfingered with pyroxenites, norites and melanorites with xenoliths of footwall sedimentary rocks (Snowden Mining 2004). There is no indication of intercalated sedimentary units in the reassessed core.

Macalacaskop and Turfspruit

At Macalacaskop and Turfspruit, the footwall rocks of the Platreef are hornfelses and dolomites of the Duitschland Formation. A few studies (Kinnaird *et al.* 2005; Kinnaird 2005a; Hutchinson & Kinnaird 2005; Sharman-Harris *et al.* 2005) have shown the Platreef here to be a much thicker sequence with a greater variety of lithologies than previously known in the Tweefontein-Overysel section. At Turfspruit the Platreef appears to be up to 800 m thick in drill core and some thick Lower Zone occurs around the same area, but not consistently. There also seems to be an unusual distribution of very thick Platreef and Lower Zone, in that the Lower Zone may occur as interlayers in the thick Platreef. However, the Mohlosane stream section exhibits an angular unconformity between the Lower Zone and assumed Platreef (J. Kinnaird, pers. comm. 2009). Thus, any Lower Zone interlayers in the Platreef are likely to be a result of the Platreef intruding the Lower Zone.

At both Macalacaskop and Turfspruit, feldspathic pyroxenite is again the main constituent of the Platreef, but it also contains norites, melanorites, serpentinites, gabbro-norites and micronorites. The micronorites are categorised as Marginal Zone. In a core from Turfspruit, Buchanan & Rouse (1984) describe 70 m of peridotite comprising the base of the succession. Serpentinised peridotites are noted here by Kinnaird *et al.* (2005) and Mothetha & Kinnaird (2005) and are classified as Lower Zone. These lithologies are only known in satellite bodies north of Mokopane, never as part of the Platreef package.

Tweefontein North and Tweefontein Hill

At Tweefontein Hill, north of Turfspruit, the floor rocks are aluminous argillaceous shales of the Duitschland Formation, and the Platreef is composed of feldspathic pyroxenites with xenoliths of ironstone and shale on the southern side (Wagner 1929). On the hill itself, the footwall is banded ironstone of the Penge Formation partially metamorphosed to magnetite-

bearing hornfels (White 1994). Nyama *et al.* (2005) describe the Platreef here as a 220 m thick package dominated by pyroxenites and norites with a basal micronorite. At Tweefontein North, Buchanan *et al.* (1981) note a basal pegmatoidal pyroxenite and a 6 m thick massive sulphide in one borehole. Pre-Bushveld sills and metamorphosed shales overlie the pegmatoidal pyroxenite, and these are overlain by 200 m of Platreef gabbros. Other workers also note the relatively thick section of Platreef on Tweefontein Hill and attribute this to a structural downwarp in which the inert footwall has allowed gravitational settling of a sulphide liquid, resulting in net-textured and massive sulphides (White 1994; Viljoen & Schürmann 1998; Nex 2005). White (1994) draws a likeness to the Merensky Reef on the basis that 80% of boreholes at Tweefontein contain chromitite layers. These are generally uncommon in the Platreef but do occur as discontinuous bands at Sandsloot, Zwartfontein and Overysel (Holwell & McDonald 2006).

Sandsloot

The opening of the Sandsloot open pit mine in 1992 offered the only subsurface exposures of the Platreef for more than a decade. A series of studies followed at Sandsloot, such that the Platreef is better characterised at Sandsloot than elsewhere (Bye & Bell 2001; Harris & Chaumba 2001; Armitage *et al.* 2002; Friese 2004; McDonald *et al.* 2005a; Holwell *et al.* 2005; Holwell *et al.* 2006). Here, the Platreef is a relatively thin package dominated by coarse-grained feldspathic pyroxenites with gabbros, peridotites, serpentinites and clinopyroxenites. The reef also contains xenoliths of metamorphic clinopyroxenites and calc-silicate hornfels derived from its immediate country rocks. These footwall lithologies are commonly serpentinitised and sporadically mineralised. The hangingwall to the reef consists of Main Zone gabbro-norites, commonly with a basal mottled anorthosite representing the reef-hangingwall contact that is described by Holwell *et al.* (2005). Detailed descriptions of the Platreef, footwall and hangingwall at Sandsloot will follow in Chapter 5.

New deep drilling at Sandsloot, specifically boreholes SS360 and SS361 (J. Kinnaird, pers. comm. 2009), has revealed a thick, PGE-mineralised feldspathic pyroxenite package underlying the dolomite footwall (Winch 2011). This is possibly another Platreef sheet, and the drill core indicates that a thick Lower Zone may also occur below it. The dolomite between the possible and known Platreef bodies also carries some PGE grade.

Zwartfontein

On the farm Zwartfontein, north of Sandsloot, the footwall changes from Malmani Dolomite to Archaean basement of granite and gneiss. At southern Zwartfontein, the footwall is similar

to that at Sandsloot but the Platreef is much thicker and considerably more serpentinised due to the alteration of entrained calc-silicate rafts (Holwell & Jordaan 2006). In Lonmin's Akanini Project area, which is west and downdip of the surface outcrop of the Platreef on Zwartfontein, drilling has intersected Platreef with a gneissic footwall: the reef is described as occasionally chromitiferous, coarse-grained feldspathic pyroxenite with calc-silicate xenoliths (Spies 2005).

Overysel

The footwall to the Platreef here is commonly called 'granofels' (tonalitic gneisses brecciated by granitic veins), and this gneissic package is intruded by the domal Utrecht granite. Cawthorn *et al.* (1985) describe the Platreef at Overysel as an up to 200 m thick unit with a thin basal medium-grained norite grading into a coarse pyroxenite. Two drill cores through the reef described by Holwell & McDonald (2006) contain feldspathic pyroxenite, serpentinised calc-silicate xenoliths, norite intrusions, chromitite xenoliths and a basal hybrid quartz-feldspathic pyroxenite. The latter is interpreted to have formed by invasion of a felsic melt derived from partial melting of the footwall. White (1994) noted the presence of occasionally thick, discontinuous chromitite bands in the reef. Viljoen & Schürmann (1998) observe large calc-silicate rafts (tens of metres in core) within the pyroxenitic reef but no gneissic or granitic material, even though the immediate footwall is tonalitic gneiss and granite. A possible explanation given by Cawthorn *et al.* (1985) is that the gneiss/granite fragments may have been completely assimilated, while the metamorphic olivine and pyroxene of the altered dolomite are refractory.

Drenthe

The northernmost sector of the Platreef described in the literature is on the farm Drenthe. Here the Platreef is described as a 250 m thick package with a 40–80 m basal feldspathic pyroxenite chilled at its base against footwall granites (Mostert 1982; Gain & Mostert 1982). This chill zone, however, is not reported in Cawthorn *et al.* (1985) and not observed by Holwell & McDonald (2006) at Overysel. The reef pyroxenites at Drenthe are overlain by 170 m of norites and melanorites containing many calc-silicate xenoliths, and the top of the reef is a 10–30 m thick feldspathic pyroxenite. The most recent study (Naldrett 2005b) reports intrusions of hangingwall gabbro-norites into the Platreef, similar to observations at Zwartfontein by Holwell & Jordaan (2006).

4.5 Emplacement and timing of the Platreef

Opinions on the temporal and stratigraphic aspects of Platreef emplacement are not only contentious but in some cases greatly at odds with each other. Some workers have correlated the Platreef with the Upper Critical Zone of the RLS, mainly on the basis of the 'Platinum Horizon' occurring with pyroxenitic rocks that are overlain by the Main Zone (e.g. Wagner 1929; White 1994). Hulbert (1983) and van der Merwe (1978) positioned the Platreef at the base of the Main Zone and equated the GNPA Member with Critical Zone. This interpretation is supported by Kruger (2005b), who proposes that the Platreef and Merensky Reef are coeval and were formed when the main pulse of Main Zone magma entered the complex from north of the TML and spread over the northern limb while collecting sulphur from the country rocks, then overtopped the TML and flooded the rest of the complex. This interpretation envisages the Platreef as a basal unit in the northern limb and the Merensky Reef as the base of the Main Zone in the rest of the complex, overlying the Upper Critical Zone.

Naldrett *et al.* (2008) suggest that the Platreef is the consequence of several surges of magma that were responsible for the different units within the main chamber of the Bushveld Complex, including the UG2 and Merensky Reef. These magmas were displaced and exited up the walls of the chamber in response to new influxes of magma entering the main chamber.

A study by Nell (1985) suggests that the metamorphic aureole in the Mokopane area was generated in two stages of thermal metamorphism caused by magma emplacement. The first event relates to emplacement of Lower Zone magma and is estimated to have attained 750°C at 1.5 kb pressure. The second event is suggested to have been caused by intrusion of the more voluminous gabbroic magmas of the Upper Critical, Main and Upper Zones, with equilibrium temperatures and pressures of about 900°C and 4–5 kb. Kruger (2005b) also presents a two-stage emplacement model based on Cr/MgO ratios. The model proposes that the Platreef is intermediate between Main Zone and Lower Zone, and formed when the initial Main Zone magmas assimilated Lower Zone rocks, citing the occurrence of chromitite schlieren in the Platreef as evidence. These studies imply a temporal hiatus between Lower Zone emplacement and the intrusion of the rest of the Bushveld Complex.

An alternative view of McDonald *et al.* (2005a) is that the Platreef and GNPA Member are not Critical Zone but a mixture of Lower Zone and Main Zone magmas that formed during one or more mixing events rather than by Main Zone assimilation of Lower Zone proposed by Kruger (2005b). While the magma mixing scenario would seem incompatible with van der Merwe's (1978) observation that the Lower Zone was fully consolidated and tilted before the intrusion of later magmas, this observation applies only to the satellite bodies of Lower Zone and not the continuous sequence south of Mokopane.

Friese (2004) and Friese & Chunnett (2004) advocated that the Platreef was emplaced as a syntectonic, boudinaged/duplexed, sheet-like intrusion along an east- to northeast-verging thrust zone that developed along the contact between the Main Zone and country rocks, at the same time as the Pyroxenite Marker in the rest of the complex, i.e. in post-lower Main Zone time. This view does not fit the direct evidence presented in Chapter 5 of the present study and the related study of Holwell & Jordaan (2006) that presents three-dimensional mapping of the Platreef-Main Zone contact at Zwartfontein. Further, these authors have not only shown that the Main Zone significantly post-dates the Platreef, but also that the Platreef was intruded, cooled and deformed *before* intrusion of the Main Zone.

4.6 Mineralisation of the Platreef

It was recognised at an early stage of exploration that Platreef PGE mineralisation is associated with BMS carried in the igneous pyroxenitic package and the immediate footwall metasedimentary rocks and Archaean gneisses (Wagner 1929). Mineralisation in the footwall, however, is highly variable in terms of extent and grade (White 1994; Armitage *et al.* 2002). Local, thin zones of mineralisation are also reported at the base of the hangingwall (Holwell *et al.* 2005; Kinnaird *et al.* 2005). The average Pt/Pd ratio along the length of the Platreef is around unity or slightly lower (Kinnaird & Nex 2003). An exception is Townlands, where the reef is relatively Pd-rich and the Pt/Pd ratio is about 0.5 (Manyeruke *et al.* 2005). Several authors have remarked on the fact that the contact-style (Platreef) mineralisation shows relatively low Pt/Pd ratios (Pt/Pd mostly <1) compared to the internal reefs and silicate rocks of the western and eastern Bushveld Complex (Pt/Pd >1). Maier *et al.* (2008b) suggest that the difference in Pt/Pd between the internal and the contact-style mineralisation can largely be assigned to two processes: (1) palladium (as well as S) may be mobilised in percolating late magmatic or hydrothermal melts and/or fluids, particularly if the sulphides are completely resorbed; and (2) in the contact-style environments, Pd could show enhanced partitioning into sulphide melt relative to Pt and Ir.

In the feldspathic pyroxenites of the Platreef, the BMS occur as interstitial blebs, and sulphide content is variable along strike but can be up to 30 modal % in some cores (Kinnaird 2004). The position of mineralisation within the Platreef is also variable, apparently being either top-, middle- or bottom-loaded (Viljoen & Schürmann 1998; Kinnaird *et al.* 2005), but there is no conclusive view of any mechanisms that might have controlled the distribution of mineralisation. At Turfspruit and Tweefontein Hill, net-textures and massive sulphides are common (White 1994; Nex 2005; Hutchinson & Kinnaird 2005), and here the abundance of sulphides is thought to be due to an upgrade of the original sulphur content of the magma by

assimilation of footwall sulphide (Sharman-Harris *et al.* 2005). At Tweefontein Hill, sulphides are believed to have accumulated in a structural downwarp by gravitational settling (Viljoen & Schürmann 1998; Nex 2005).

Gain & Mostert (1982) and Armitage *et al.* (2002) found that high grades of mineralisation are carried in altered (serpentinised) zones of the footwall and in serpentinised calc-silicate xenoliths in the reef. Whilst PGE are generally associated with BMS in the reef, decoupling of PGE from BMS has occurred in places (Gain & Mostert 1982; Hutchinson & Kinnaird 2005; Kinnaird 2005a; Holwell *et al.* 2006). The cause of this decoupling is probably late-stage hydrothermal redistribution of PGE and BMS resulting in, for example, serpentinites containing either high PGE grade and low BMS or vice versa (Armitage *et al.* 2002; Holwell *et al.* 2006).

Regarding PGM assemblages, the present study was the first to investigate PGM at Sandsloot in any detail, and up to the time when fieldwork for this study was carried out, only Kinloch (1982) provided any detail of PGM in other parts of the Platreef. In recent years, however, comprehensive PGM studies have been conducted at Turfspruit (Hutchinson & Kinnaird 2005; Hutchinson & McDonald 2008), Sandsloot (Holwell *et al.* 2006) and Overysel (Holwell & McDonald 2007). PGM throughout the reef are dominated by tellurides and sperrylite with locally common antimonides, sulphides and bismuthides, but it has become evident that footwall lithology exerts a direct control on mineralisation styles and particularly the presence of certain PGM types and their concentration (Viljoen & Schürmann 1998; Holwell & McDonald 2005; Holwell *et al.* 2006; Holwell *et al.* 2007).

4.7 Effects of contamination and hydrothermal activity

4.7.1 Contamination of the Platreef by country rocks

Many workers consider the mineralisation of the Platreef to have been extensively controlled by the interaction of the Platreef magma with the variety of country rocks it has discordantly intruded. Of specific interest is how these interactions affect the amount of sulphur in a magma and the sulphur-carrying capacity of the magma. Magmatic sulphur isotope signatures cluster around zero per mil. Assimilation of sedimentary rocks may be evident as the sulphur isotope ratio is driven away from zero to heavy or light values, depending on the nature of the contaminant.

Buchanan *et al.* (1981) examined the role of footwall contamination in the precipitation of sulphides in the Platreef at Tweefontein, where the Malmani Dolomite is overlain by the Penge banded iron formation and graphitic sediments. On the basis of isotope analyses for unmetamorphosed sedimentary rocks in the area, the authors conclude that the

sulphur-carrying capacity of the Platreef magma was boosted by the addition of iron from the Penge banded iron formation, by the addition of carbon (a reductant) in the form of organic graphite, and additional sulphur was supplied by dolomitic xenoliths with anhydrite layers. Gain & Mostert (1982) consider mineralisation of the Platreef at Drenthe to have been caused by devolatilisation of dolomite xenoliths that added CO₂, H₂O and sulphur to the magma, thus lowering the sulphur solubility of the magma and adding sulphur from an external source, resulting in the precipitation of an immiscible sulphide liquid. Buchanan & Rouse (1984) presented sulphur isotope data for metallic sulphides at Tweefontein and Turfspruit that also indicate a significant contribution from an isotopically heavy source of sulphur in the footwall, thought to be anhydrite in the Malmani Dolomite.

Barton Jr *et al.* (1986) compared the role of footwall contamination of the Platreef and hangingwall at locations where the immediate footwall consists of siliceous dolomite or granite/granitic gneiss. Vertical profiles for Rb and Sr isotope ratios through the Platreef overlying both types of footwall suggest contamination by a granitic component in both cases. The authors conclude that the dolomite footwall acted as a barrier that delayed contamination of the Platreef by the granitic basement below.

Cawthorn *et al.* (1985) investigated the interaction of floor rocks with the Platreef at Overysel. There the floor rocks consist of a suite of highly metamorphosed banded tonalitic gneisses with leucocratic veins. High ⁸⁷Sr/⁸⁶Sr, Rb/Zr and Ba/Zr ratios in the cumulate pyroxenites of the Platreef and the presence of relatively sodic plagioclase, phlogopite and quartz support substantial assimilation of siliceous material. It is argued that where the Platreef rests on dolomite and banded iron formation, e.g. at Sandsloot and Tweefontein, contamination cannot be explained by assimilation of the floor rocks, which have low ⁸⁷Sr/⁸⁶Sr ratios and low K₂O, Rb and SiO₂ contents. Isotope and trace element modelling suggests instead that the contaminant was a fluid rather than a partial melt. None of the Transvaal sedimentary rocks exhibit appropriate chemistry, but the geochemical signatures of the granitic basement suggest it is the source of the contaminant fluid.

On the basis of an oxygen isotope study in the Sandsloot area, Harris & Chaumba (2001) deduced that the Platreef magma has assimilated up to 18% dolomite. The devolatilisation of this volume of dolomite would have produced a considerable amount of CO₂, which could have increased *f*O₂ (oxygen fugacity), lowering the FeO content of the magma and thus the sulphur carrying capacity, inducing sulphur saturation as suggested by Buchanan *et al.* (1981).

More recently, other lithologies have been shown to be a source of sulphur to the Platreef. For example, Manyeruke *et al.* (2005) presented data that indicate a significant

addition of sulphur from Timeball Hill shales and quartzites. Also, Sharman-Harris *et al.* (2005) identified pyrite in the Duitschland shales as a significant source of sulphur at Rietfontein, Turfspruit and Macalacaskop.

While silicic and sulphurous contamination of the Platreef has been thought to trigger precipitation of immiscible sulphides, Barton Jr *et al.* (1986) conversely regarded contamination at Overysel to be later than sulphur saturation, while Lee (1996) further interpreted sulphide mineralisation to be a primary magmatic event, generated when pre-formed PGE-rich sulphides were introduced from a staging chamber and settled out along the base of the intrusion to form the proto-Platreef, with footwall contamination occurring later. Holwell *et al.* (2007) show that contamination of the Platreef by footwall sulphur appears to be a localised process that upgraded the sulphur content of the reef, but did not directly trigger sulphur saturation. Further, sulphate in the floor rocks, particularly in the Malmani Dolomite, is unlikely to have contributed significantly to early sulphide mineralisation, but is more likely to have been incorporated into later-stage hydrothermal fluids.

4.7.2 Hydrothermal modification

Studies on the Platreef have demonstrated that the PGE in the Platreef are originally magmatic but have been redistributed within the reef and also transported into the footwall. The likely medium is hydrothermal fluids generated by the interaction of the Platreef magma with the country rocks, and the volumes and types of hydrothermal fluids depend on the local country lithology. Variations in PGM mineralogy along the Platreef (Kinloch 1982; Viljoen & Schürmann 1998; Hutchinson & Kinnaird 2005; Holwell *et al.* 2006) correspond to transitions in the footwall lithologies. PGM mineralogy also varies in different Platreef lithologies (Armitage *et al.* 2002; Kinnaird *et al.* 2005; Holwell *et al.* 2006; Holwell & McDonald 2006) and this variation is interpreted to be a result of hydrothermal fluids generated by interaction between the Platreef magma and the different country rocks on all scales.

There are two known mechanisms that have distributed mineralisation in the footwall. One of these is hydrothermal and affects areas where the footwall consists of reactive sedimentary rocks such as the Malmani Dolomite at Sandsloot and Zwartfontein South. Footwall mineralisation is common at these localities (Armitage *et al.* 2002; Holwell *et al.* 2006; Holwell & Jordaan 2006). Where the footwall consists of more resilient hornfels further south, mineralisation is restricted to a narrower zone adjacent to the Platreef (Hutchinson & Kinnaird 2005). The second mechanism applies to areas where the footwall consists of Archaean gneiss/granite, e.g. at Overysel. Here the predominantly anhydrous nature of the footwall has permitted only minor release of fluids, and textural evidence suggests that

mineralisation was introduced into the gneiss via an interconnected melt network in the partially melted footwall rocks (Holwell & McDonald 2006).

5. GEOLOGY OF THE PLATREEF AT SANDSLOOT

5.1 Introduction

This chapter presents first-order data from fieldwork carried out during 2000-2001 in the Sandsloot open pit mine. The data includes descriptions of the general three-dimensional geological structure of the pit, six rock faces exposed by blasting shortly before or during fieldwork, and three drill cores that were available for logging at the time (Fig. 5-1). Some microphotographs and SEM images of sampled lithologies from the mapped rock faces are also presented to substantiate the first-order data.

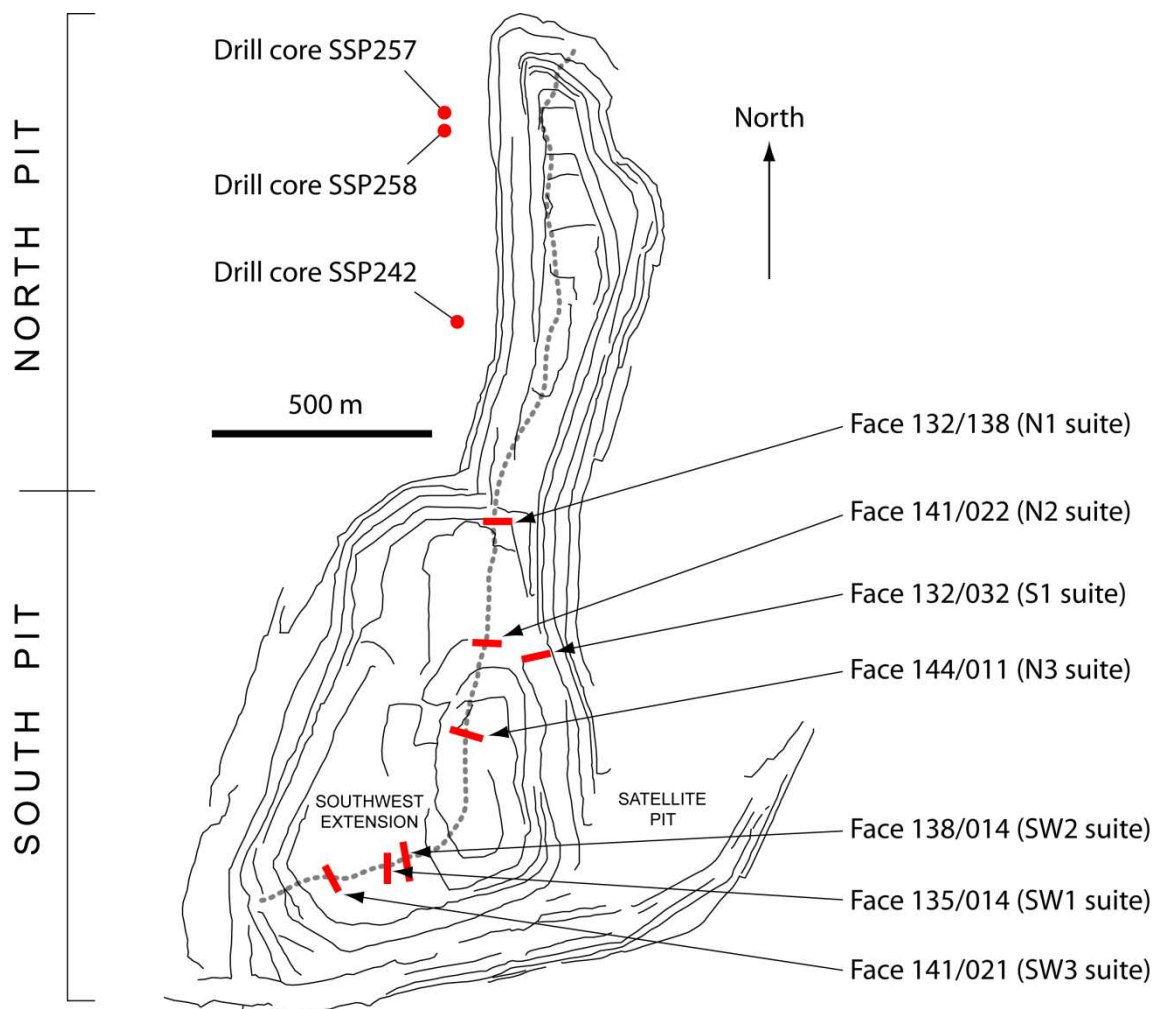


Fig. 5-1. Wireframe plan view of Sandsloot open pit in July 2000 showing locations of faces mapped and corresponding sample suites in this study. Solid lines represent major bench crests. Deepest area of the pit (south central area) is approximately 190 m below outer rim level. Stippled grey line is approximate trace of Platreef.

5.1.1 Field methods

The stepped benches of the Sandsloot pit have subvertical rock faces 10-15 m high, and those that exhibit complete sections across the Platreef were mapped at 1:100 scale. The mapped sections were delineated by spray-painting geopoints at the outer limits of the rock face, then the latitude, longitude and elevation were established by mine surveyors using a global positioning system. The lowermost approx. 3 m of the rock faces could be mapped with relative confidence, while much of the exposure above that height was often inaccessible and covered by thick dust, although this was periodically removed by hosing on some faces. About 200 rock specimens were collected from most of the major Platreef and metasedimentary footwall lithologies at 2-5 m intervals along each face, and at spot localities of special interest. Specimens selected for microscopy and geochemical analysis were cut into three parts: one part for preparation of polished thin sections and polished blocks, one part was powered in an agate tema mill for geochemical analysis, and one part was stored as spare material.

5.2 The Sandsloot mine

The Platreef orebody at Sandsloot is tabular, dips at approximately 45° and is sufficiently thick to allow the orebody to be excavated by open pit mining methods, which is considerably cheaper than conventional underground mining. The Sandsloot open pit is the largest open pit platinum mine in the world and has a final depth of 260 m. Waste stripping began in January 1992 and the first blast at the Sandsloot site took place on 12 February 1992, with the first production in 1994. At the time fieldwork was carried out for the present study, the Sandsloot pit was only a half of its final size. The shape of the pit at that time and the main lithological units, delineated by drilling and subsequent face mapping by mine geologists, is shown in Fig. 5-2. The Mogalakwena North, Central and South open pits and Zwartfontein South open pit mines are now in operation, and four other pits will be opened for mining along the outcrop of the Platreef south of the Sandsloot pit, extending the total open pit life to at least 100 years. Subsequent underground mining will add at least a further 200 years of operations to the Mogalakwena lease area (Bye 2001).

5.3 General stratigraphy at Sandsloot

The Platreef and associated lithological units at Sandsloot can be outlined by the stratigraphic column in Fig. 3-3. The Platreef itself is a mix of lithologies broadly described as gabbros and

pyroxenites in variable states of alteration, overlain by a hangingwall of norites and gabbro-norites belonging to the Main Zone. The footwall consists of siliceous Malmani Dolomite of the Transvaal Supergroup thermally metamorphosed to calc-silicate hornfelses and metasomatised to clinopyroxenites ('parapyroxenite' after Wagner 1929) that have undergone variable degrees of retrograde alteration.

While the metamorphic clinopyroxenites ('parapyroxenite') are thought to represent the highest grade of metamorphism within the footwall and are believed to occur between the Platreef and calc-silicate assemblages, observations in the present study do not support a persistent zone of clinopyroxenites immediately beneath the Platreef. Further, the lowermost section of the Platreef in places exhibits hybrid igneous and metamorphic features. These observations depart from the typical image of the Platreef and associated units. They will be illustrated in later sections with suggestions for possible controls on the pattern of their occurrence.

The hangingwall contact is a primary magmatic boundary locally marked by a chill zone at the base of the Main Zone and/or by erosion of primary and altered Platreef assemblages. In places the hangingwall contact is tectonic, juxtaposing the Platreef and hangingwall at unknown stratigraphic levels in each unit. In vertical pit faces that intersect the Platreef at a high angle, layering in the Main Zone appears to be parallel to the Platreef (this study and Holwell 2006). The footwall contact is consistently magmatic and discordant to footwall bedding, and is marked by an abrupt transition from Platreef rocks to footwall calc-silicates, or by a transition from Platreef rocks through hybrid lithologies to metamorphic clinopyroxenites or calc-silicate hornfelses of the footwall.

5.4 Structural geology at Sandsloot

Major structures are apparent in regional map view and in the south and east highwalls of the Sandsloot pit, allowing broad three-dimensional characterisation of the immediate area. The open pit is disturbed by three major northeast trending faults: the most prominent one in the southeast and two in the far north; also north trending faults exposed in the southwest (Fig. 5-2). The Sandsloot area has been intruded by late phase quartz-feldspathic veins, which are associated with most of the critical jointing system. These veins dip steeply and are laterally and vertically continuous over hundreds of metres (Bye *et al.* 1999). The most extensive structure is the 'dolomite tongue', previously mentioned in Chapter 3 and expressed as a west-pointing lobe of metadolomite attached to the main dolomitic floor rocks (Fig. 3-2; Fig. 5-3). The genesis of the tongue is equivocal and might be a diapir of the type proposed by Uken & Watkeys (1997), or a dome created by the interference of two fold phases (van der Merwe

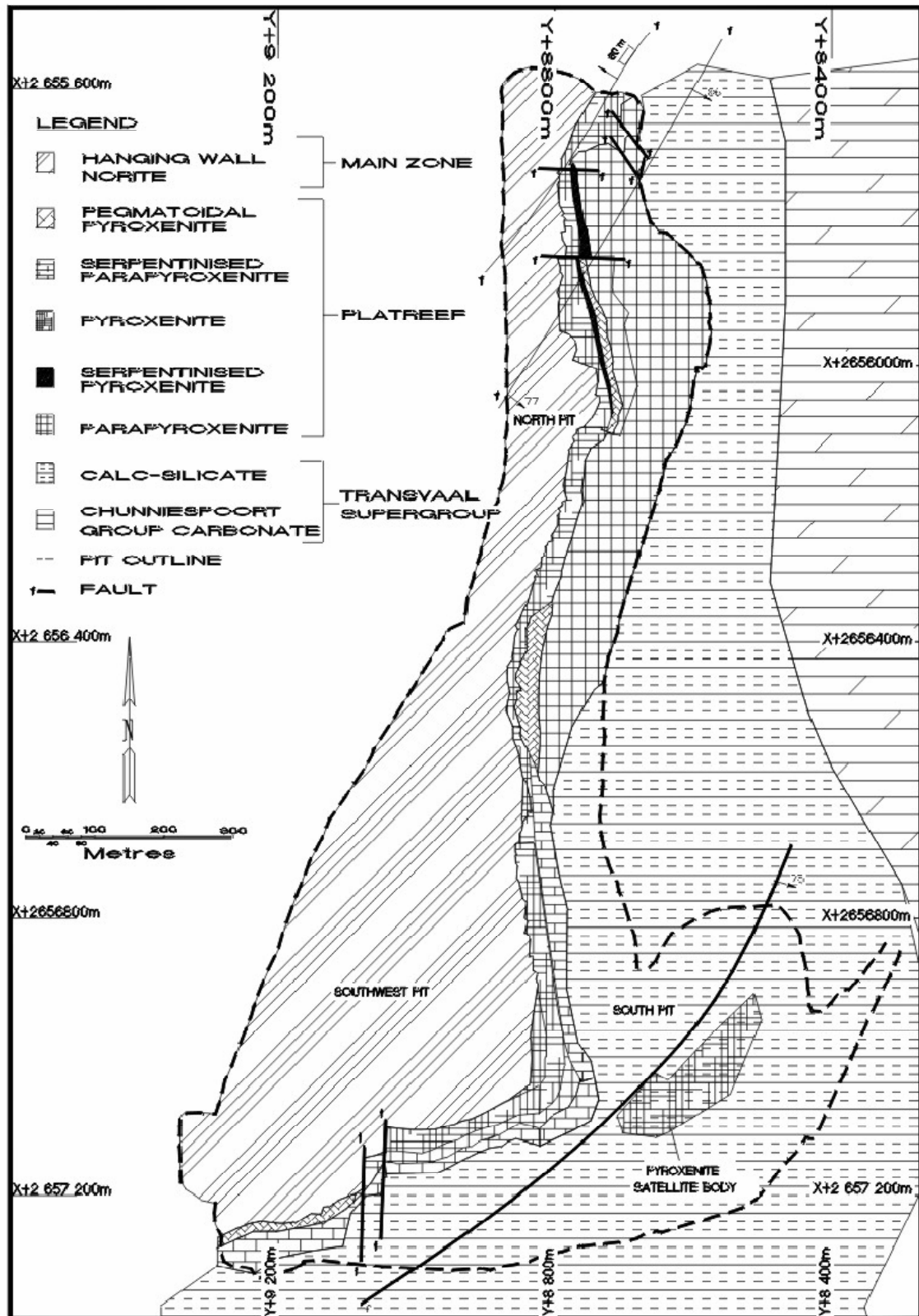


Fig. 5-2. Map of the Sandsloot open pit mine (after Bye *et al.* 1999) showing its approximate outline shortly before this study. Important features of the map are the faults and the westward deflection of the Platreef in the south part of the pit. Note that 'parapyroxenite' is attributed to the Platreef, but is shown in this study to be a footwall lithology. 'Chuniespoort Group carbonate' is Malmani Dolomite at this location.

1978; Nell 1985; Friese 2004). The structure has a prominent ENE-WSW axis in outcrop, but it also has an approximately north-south axis, photographed in Fig. 5-4 from the north limb of the structure. The east wall of the pit (Fig. 5-5, Fig. 5-6) displays a more open syncline with an approximately ENE-WSW axis, and the south limb of the syncline rises towards the tongue structure in the south wall. The resultant three-dimensional structure, as expressed by the

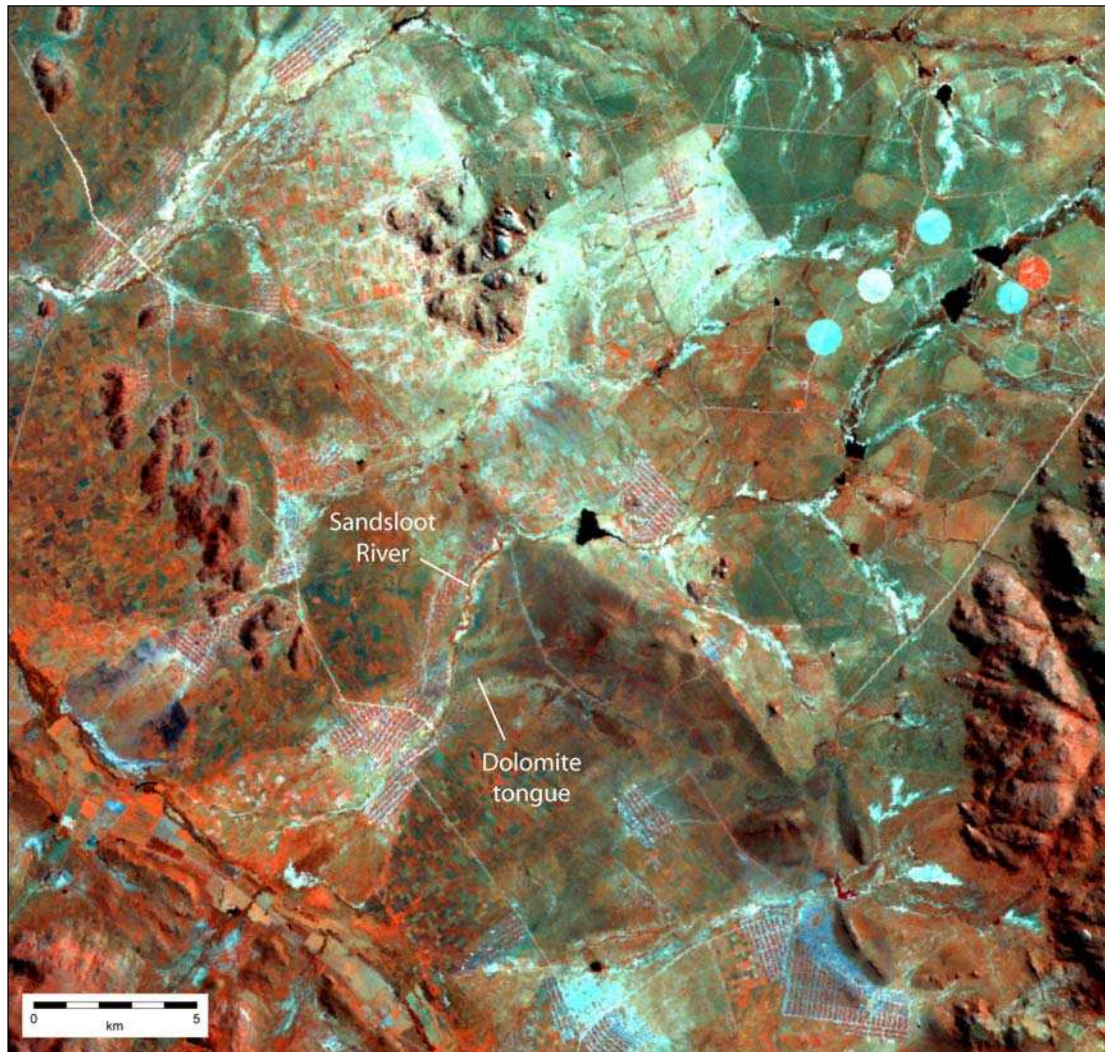


Fig. 5-3. LandSat TM image of Sandsloot and neighbouring properties. Image acquired in 1992, before mining began at Sandsloot. Area corresponds to that in aeromagnetic image in Fig. 5-8. Note prominent WSW-pointing ‘dolomite tongue’ below left of centre, transgressed near its west tip by Sandsloot river where open pit mine is now located. Image is RGB 457 (red, green, blue; bands 4, 5 and 7) false colour composite, 30 m spatial resolution.

metaedimentary footwall rocks, is illustrated in Fig. 5-7. Regional geological maps (e.g. van der Merwe 1976, 1978; Friese 2004) show a series of these open folds in the Transvaal Supergroup adjacent to the mafic rocks of the northern limb, with the tongue closely associated with a pattern of regional folds. Further, the asymmetry of the structure in E-W

section (Fig. 5-4) is suggestive of a tectonic as opposed to diapiric dome and will be discussed further in Chapter 7. The geometry of the structure expresses the interference of approximately N-S and ENE-WSW axes (e.g. Fig. 3-4, Fig. 4-1 and Fig. 5-8).



Fig. 5-4. Approximately southward view perpendicular to south highwall from base of Sandsloot pit showing open, asymmetrical antiform defined by footwall bedding. Direction of view is along or subparallel to axis of antiform. Note location of face S1 in left foreground on east limb of antiform.

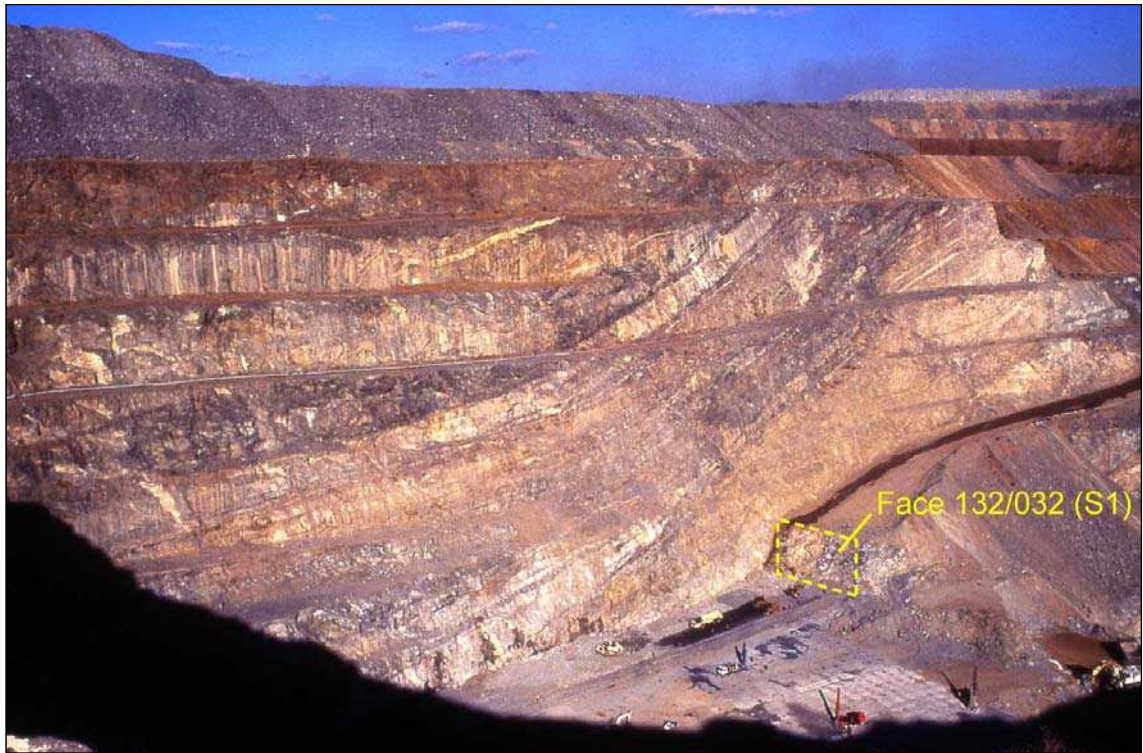


Fig. 5-5. Approximately southeastward view from west rim of Sandsloot pit showing south limb of open, approximately ENE-WSW trending syncline defined by footwall bedding. Direction of view is oblique to fold axis. Location of mapped face S1 is indicated.



Fig. 5-6. Approximately northeastward view from southwest part of Sandsloot pit showing hinge zone/axis and north limb of approx. E-W trending, very open syncline ('Sandsloot Syncline' in Friese 2004) rising into north pit in the distance. View is oblique to fold axis.

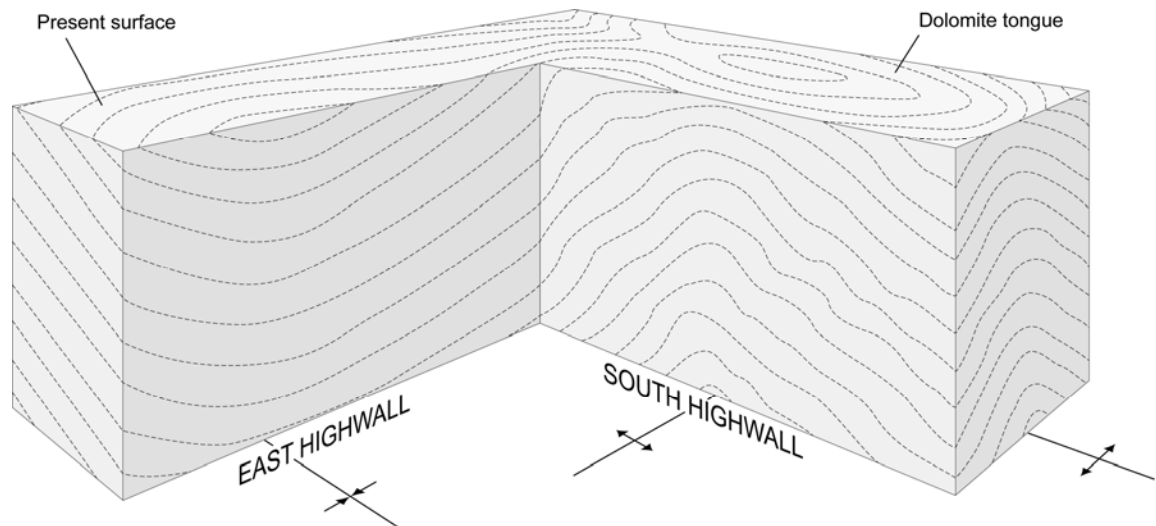


Fig. 5-7. Schematic southeastward view of footwall structure as exposed in the Sandsloot south pit. Stippled lines represent bedding.

A local aeromagnetic image (Fig. 5-8) shows that the lowermost (easternmost) Main Zone layering is deflected stratigraphically upwards (westwards) at the margins of the dolomite tongue. However, the degree of deflection decreases up-sequence (westwards) towards the tip of the tongue, where no deflection is apparent. Curiously, van der Merwe (1978) states that Main Zone layering is not deflected by the Sandsloot tongue but is only interrupted by it, even though his own map shows the same slight deflection of Main Zone layering as the aeromagnetic image in Fig. 5-8 and is possibly interpreted from that image or from an earlier version of it. The significance of the dolomite tongue will be discussed further in Chapter 7. The local aeromagnetic image also shows a curious magnetic high just east of the Sandsloot pit. There is no obvious geological control on this anomaly as the area is covered by the mine infrastructure, and since it has not been possible to ascertain when the image was acquired, the anomaly could be due to the numerous steel-framed buildings.

Most of the west highwall, especially the upper part of the wall in the south pit and the entire wall in the north pit, consists of highly jointed hangingwall gabbro-norite in which no other major structures are visible. The joints are a geotechnical hazard and have caused troublesome slip failure (Bye 2001).

The shape of the orebody, consisting mostly of the Platreef, has been delineated by fire assays of drill cores and is illustrated in Fig. 5-9. The structural pattern here equates to that photographed in Fig. 5-5 and Fig. 5-6. Further, the strike of the reef swings from N-S to NE-SW in the south to southwest part of the pit, where the northern flank of the 'dolomite tongue' occurs. On some geological maps of the northern limb (e.g. Fig. 4-1) the Platreef is

shown to wrap around the ‘tip’ of the tongue to Tweefontein on the south side of Sandsloot. On other maps, the Platreef is shown to ‘onlap’ against the tongue and does not wrap around it (e.g. Fig. 3-4). Vertical drilling through the tongue did not encounter Platreef (R. Montjoie, pers. comm.), supporting the surface observation that the structure is attached to the floor rocks. Note also that the major fault in the satellite pit shown in Fig. 5-2 isolates a body of mineralised pyroxenite (lower right of Fig. 5-2 and top left of Fig. 5-9), which Ashwal *et al.* (2004) ascribed to gabbroic rocks of the Critical Zone. Alternatively, it could be part of a ‘Lower Platreef’ body (Winch 2011).

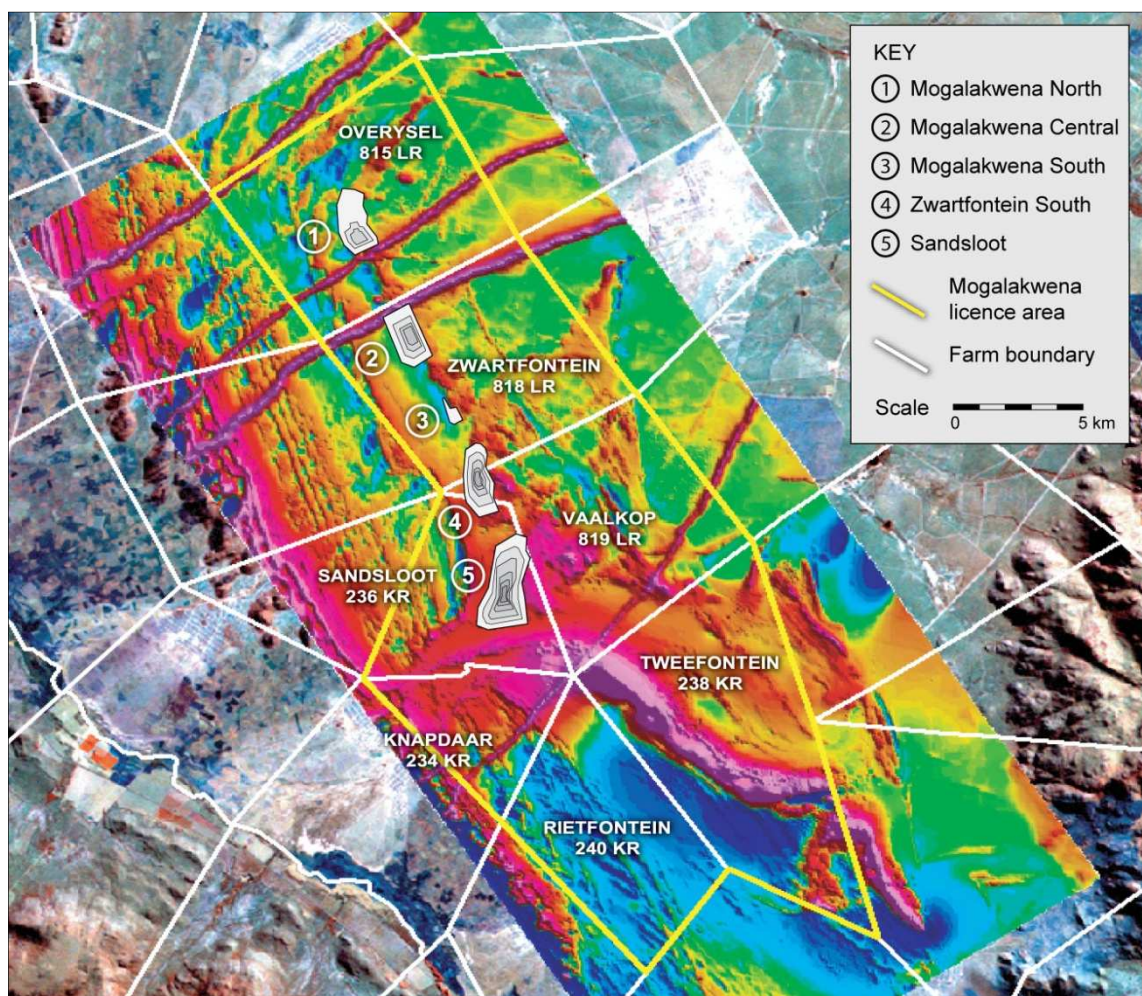


Fig. 5-8. Local aeromagnetic image superimposed on aerial photograph of Sandsloot and adjacent properties (image and boundaries from Potgietersrus Platinums Ltd internal presentation). Note ‘dolomite tongue’ immediately south and southwest of Sandsloot pit; Main Zone layering abutting the tongue on farms Sandsloot and Knapdaar; and high aeromagnetic signature of Penge banded iron formation (purple zone at Tweefontein).

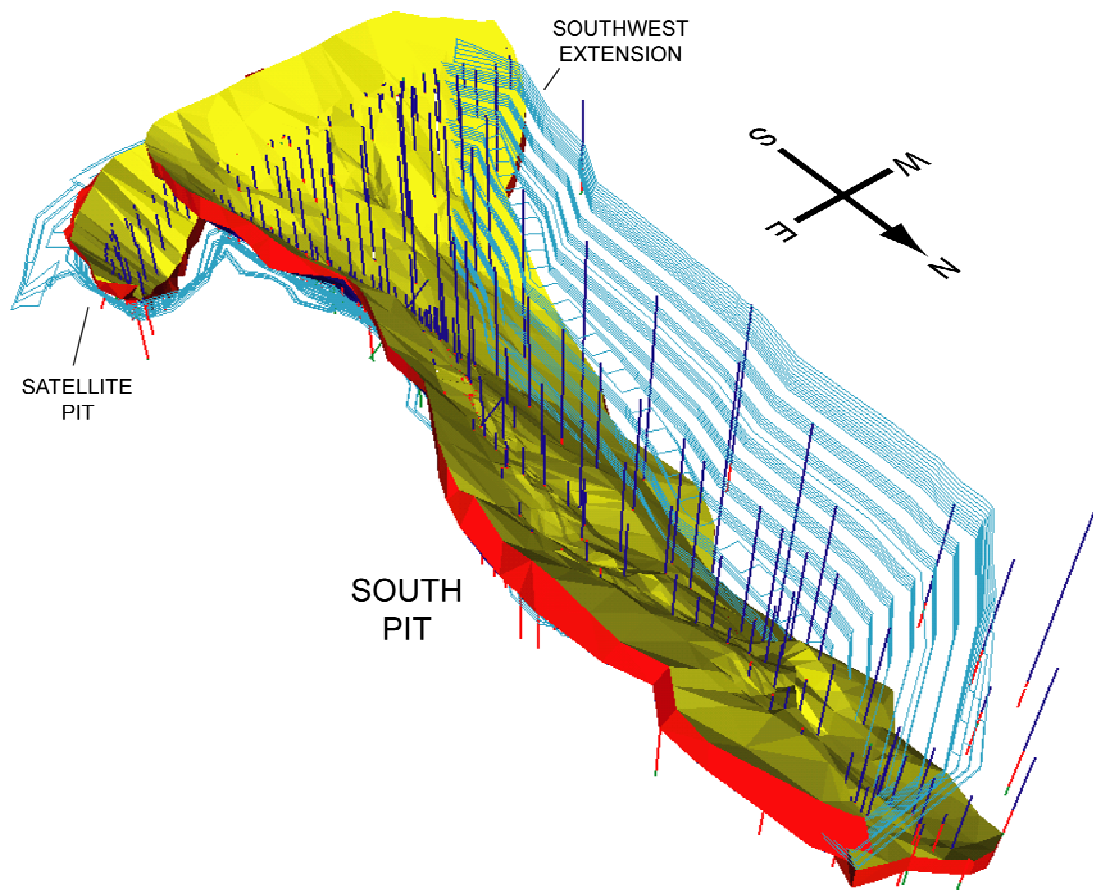


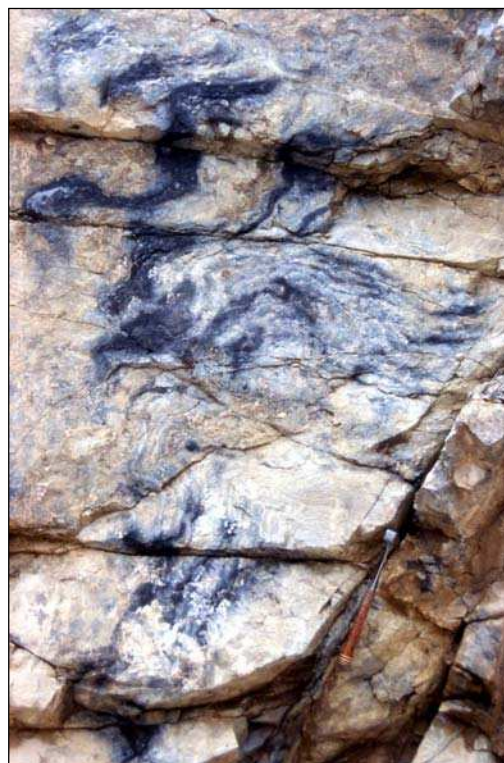
Fig. 5-9. Southwestward oblique view of orebody in south pit at Sandsloot (red in vertical section). Pit faces are outlined in pale blue from data in early 2000, boreholes in dark blue. Longest axis (north-south) is approx. 1.7 km.

Assays of drill chips from boreholes drilled in grid pattern for blasting are used to compile grade plans for recovery of ore after blasting. The grade plans confirm the shape illustrated in Fig. 5-9 and corroborate the position of the Platreef in the vertical face maps in this chapter.

Two approximately north-south striking, moderately to steeply east-dipping, large (>2 m wide) hydrothermal quartz-feldspathic veins cross the Sandsloot pit. They are observed in the footwall in the south wall of pit and in some exposures in the central area of the south pit, and they cut the hangingwall in the north wall. In addition to coarse-grained quartz and feldspar, calcite and fibrous white chrysotile aggregates occur as later, lower-temperature phases. Locally, calcite occurs as spectacular pyramidal crystals in large vugs. Minor brittle-ductile shear structures occur at the margins of the largest vein (the only one that could be closely observed), but do not occur within the vein itself. This suggests either that an earlier shear zone was the locus of hydrothermal precipitation concurrent with vein dilation, or that the competence contrast between the vein and country rocks has generated high contact strains during deformation and shearing was focused along the contacts. In either case, incompetent rocks adjacent to the vein, such as the footwall calc-silicate hornfelses, have

deformed plastically (Fig. 5-10). The veins may correspond to the N-S striking faults shown in Fig. 5-2. The relationship of this shearing to the Platreef and hangingwall could not be established.

Fig. 5-10. Margin of large hydrothermal vein (right of hammer) in floor rocks in south highwall of pit. Note brittle-ductile shear along vein margin, expressed as disharmonious folding of country rocks. Serpentinisation (dark layers) of calc-silicate hornfels highlights fold pattern.



5.5 Lithological descriptions

5.5.1 Hangingwall gabbronorite

The hangingwall of the Platreef consists of fairly homogeneous gabbronorites thought to be representative of the Main Zone elsewhere in the Bushveld Complex. An abrupt change in the pyroxene composition from bronzite (En_{72-78} : ferriferous enstatite) in the Platreef to inverted pigeonite (En_{64-67} : low-Ca clinopyroxene with augite exsolution lamellae) in the hangingwall has been cited as evidence that the hangingwall gabbronorites formed from a separate magma (Gain & Mostert 1982) prior to this work. Some sections of the hangingwall contact show an essentially planar, macroscopically sharp, magmatic boundary. Wagner (1929) reported veins of hangingwall gabbronorite cutting the Platreef in exploration trenches opened up in the 1920s. Details of the hangingwall contact observed in the present study will be given in the face map descriptions later in this chapter.

The most common variety of hangingwall gabbronorite is a medium to coarse-grained, isotropic assemblage of approximately 50 modal % plagioclase, 35% orthopyroxene and 15% clinopyroxene. Its appearance is transitional between leuco- and melanocratic. The modal

content of pyroxene can be as high as 75% in the darkest melanorites and as low as 30% in the palest leuconorites. Accessory phases, such as phlogopite, oxides and sulphides, account for up to 5 modal %. The pyroxenes are dark grey to dark grey-green and have an anhedral to ragged habit, occasionally forming large aggregates (Fig. 5-11). Plagioclase occurs as randomly oriented twinned laths and, in contrast to the Platreef, generally constitutes the cumulus phase (Fig. 5-12). Xenoliths of calc-silicate hornfels that are similar to the footwall to the Platreef occur sporadically in the hangingwall, as observed in one of the three drill cores described later. Calc-silicate xenoliths are also known from studies of other sections of the Platreef (Kinnaird *et al.* 2005).



Fig. 5-11. Photomicrograph of fine-grained hangingwall gabbro-norite (plane polarised light), consisting of cumulus plagioclase and intercumulus pyroxene. Accessory phases are phlogopite and opaques. Specimen N1-31. Field of view ~2 cm wide.

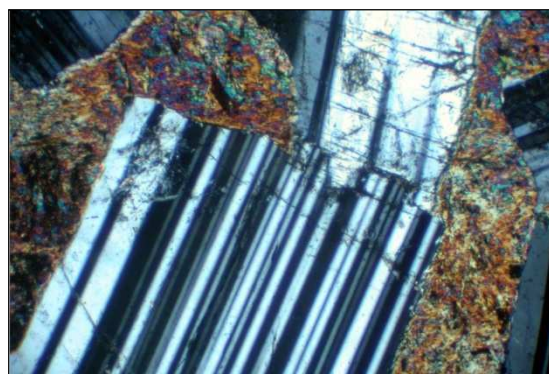


Fig. 5-12. Photomicrograph of hangingwall gabbro-norite with fresh cumulus plagioclase and intercumulus pyroxene. Specimen N1-31. Field of view approx. 4 mm wide.

5.5.2 The Platreef

The Platreef at Sandsloot consists of pyroxenites and gabbros in various states of alteration, with the degree of alteration apparently dependent on primary mineralogy. Saussuritisation of plagioclase is common in the gabbros, while pyroxenites display considerable serpentinisation and replacement textures. No evidence was found for a consistent spatial and temporal relationship between the pyroxenites and gabbros. The thickness of the Platreef varies from a few metres in the centre of the pit (in faces N1, N2 and N3: Fig. 5-1) to 30-55 m at several localities in the southwest parts of the pit (faces SW1 and SW2). The contact to the footwall lithologies is irregular, and variably altered footwall xenoliths up to several metres long occur sporadically in the reef. A chill zone was not found at the footwall contact of the Platreef or around xenoliths within the reef. In most mapped faces, the hangingwall contact was a

macroscopically sharp break between coarse Platreef pyroxenites and hangingwall gabbronorites.

5.5.2.1 Pyroxenites

Pyroxenites dominate the Platreef in the southwest part of the pit. They are commonly coarse-grained, dark grey-green assemblages of anhedral to subhedral orthopyroxene (60-90 modal %) with a subordinate content of intercumulus clinopyroxene (10-40 %) (Fig. 5-13).

Postcumulus plagioclase occurs locally in small pods and constitutes up to 15 modal %.

Accessory phases include small booklets of red-brown phlogopite and finely disseminated BMS identified by reflected light microscopy and microprobe analysis (pyrrhotite, pentlandite, chalcopyrite, bornite, pyrite and minor galena-clausthalite). Minor oxides present are magnetite, ilmenite, perovskite, chromian spinel (picotite) and chromite.

Extensive zones within the pyroxenites have undergone high degrees of alteration to serpentine and talc. In these zones the pyroxenes have a more rounded, ragged habit and are pervaded by networks of serpentine microveins, suggesting widespread infiltration of hydrothermal fluids. The inter- and intragranular serpentine is black, giving the altered rocks a distinctly darker colour than the unaltered pyroxenites.



Fig. 5-13. Drill core of coarse-grained Platreef pyroxenite with minor plagioclase content (middle core) and medium- to coarse-grained Platreef pyroxenite with rare plagioclase (lower core). Note also red-brown phlogopite in centre left.

5.5.2.2 Gabbros (feldspathic pyroxenites)

Platreef gabbros have coarse-grained to pegmatoidal textures. Dark green orthopyroxene occurs as a sub- to euhedral cumulus phase (40-70 modal %) with dark clinopyroxene (up to 10%) in a colourless postcumulate mass of plagioclase (30-50%). Most plagioclase has a cloudy appearance due to saussuritisation, whereas pyroxene appears to have evaded alteration in most of the observed gabbros. Quartz is a minor phase (<1%), while other accessory and minor phases are the same as those in the reef pyroxenites. However, interstitial sulphides are larger and more sporadic, rather than finely disseminated throughout the rock body as they are in the pyroxenites. Coarse gabbros occur at different stratigraphic positions in the reef, apparently as large irregular pods or contiguous bodies, and seem to dominate the northern and central parts of the south pit. This is typified by face N1, where the reef consists almost exclusively of gabbro, although it should be noted that a shear zone has possibly removed a significant part of the upper reef here.

In terms of mineralisation, the reef pyroxenites and feldspathic pyroxenites are rich in pyrrhotite (Fe_7S_8), pentlandite $(\text{Fe,Ni})_9\text{S}_8$, chalcopyrite (CuFeS_2) and minor secondary pyrite (FeS_2) and bornite (Cu_5FeS_4). These are unevenly distributed and occur within the interstitial phases in the reef pyroxenites and gabbros. The intergrowth of sulphides with plagioclase and alteration amphiboles (e.g. actinolite), epidote and micas means the sulphide crystals have a ragged morphology rather than occurring as euhedral crystal aggregates with sharp linear contacts to surrounding silicates as they do in, for example, the Merensky Reef (Li *et al.* 2004; Holwell *et al.* 2006). Sausseritised plagioclase is characterised by small sulphide blebs rimming the interstitial area. Surrounding pyroxenes only occasionally contain sulphides, and in such cases the sulphide blebs occur along cleavage planes.

5.5.3 Footwall lithologies

5.5.3.1 Clinopyroxenites (diopsidites)

A characteristically pale grey, coarse-grained, granoblastic, diopsidic pyroxenite normally occurs between the Platreef and layered calc-silicate hornfels. These clinopyroxenites are also seen as elongate lenses and contiguous bands concordantly interlayered with calc-silicate hornfels (Fig. 5-14), and the boundaries between these two lithologies are usually transitional over a few millimetres to centimetres.

In mining terminology the grey clinopyroxenites are known as ‘parapyroxenite’, following the term originally used by Wagner (1929), who evidently regarded the diopside-rich footwall lithologies as highly metamorphosed dolomites. In the present study they will be

referred to as diopsidites in order to avoid any confusion with igneous lithologies. Geochemical analyses have shown that the diopsidites have a non-igneous genesis: the diopsidites contain little Cr, whereas the ‘normal’ reef pyroxenites and gabbros have Cr contents of thousands of ppm. Serpentine with relict cores of metamorphic olivine is common in the diopsidites and the varieties that are rich in olivine also contain little Ni, whereas igneous olivine with the same Mg/Fe ratio contains thousand of ppm Ni. Some diopsidites do contain Ni but also have high Cu contents because sulphides are present as well as olivine and the Ni is contained in the sulphides (Harris & Chaumba 2001). These trace-element characteristics suggest that both diopside and olivine are derived by high-grade metamorphism/metasomatism of the siliceous footwall dolomites, corroborating Wagner’s (1929) original interpretation. Further support for a metamorphic origin is the presence of grossular-andradite (Fig. 5-15) and vesuvianite (Fig. 5-16). Similar lithologies in the metamorphic aureole of the northern limb of the Bushveld Complex are considered to reflect extreme metasomatism (Buick *et al.* 2000). At Sandsloot, the paragenesis of the diopsidites has involved such a thorough textural transformation that no primary layering is preserved. The mineralogy of the diopsidite bodies also appears to correspond to at least one of the 11 assemblage groups identified by Nell (1985) in calcareous rocks of the Bushveld metamorphic aureole in the Mokopane area. At Sandsloot, serpentinisation is common in irregular zones (Fig. 5-17).



Fig. 5-14. Lenticular bodies and contiguous bands of diopsidite (grey) in folded footwall calc-silicate hornfels (milky/beige colour). Large camera bag for scale, with hinge of open synform visible above it.



Fig. 5-15. Hydrogrossular (red) in footwall clinopyroxenite (diopsidite).



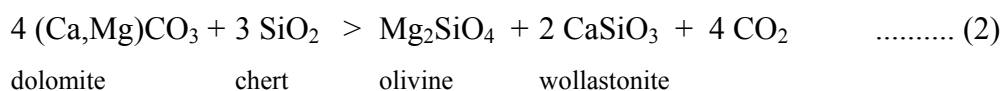
Fig. 5-16. Coarse-grained footwall clinopyroxenite consisting of diopside (grey) and assumed vesuvianite (greenish).



Fig. 5-17. Local variation between unaltered footwall diopsidite (grey) and serpentinised diopsidite (black), with sharp irregular boundaries.

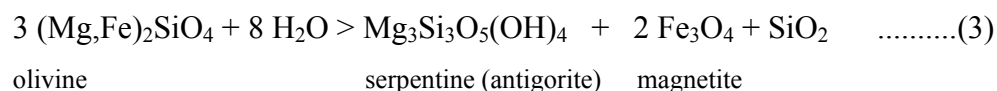
5.5.3.2 Calc-silicate hornfels and serpentinites

The calc-silicate hornfels and serpentinite footwall lithologies can be crudely described as skarns and contain minerals that reflect a very wide range of prograde and retrograde metamorphic reactions (Fig. 5-19 to Fig. 5-21). The original sedimentary layering is clearly preserved, with a bedding thickness of 5-60 cm. Relatively unaltered footwall hornfels have a mottled beige and pale green colour. Several small ovoid bodies and thin bands of pure wollastonite were observed (Fig. 5-20), interpreted as the high-grade metamorphic product of chert nodules and bands in the carbonate protolith:



Bands and nodules of dominantly red chert are common in the Malmani Dolomite beyond the thermal metamorphic aureole (personal observation).

Where alteration is evident, it is expressed by retrograde serpentinisation of prograde metamorphic phases such as forsterite by the following reaction:



The magnetite from this reaction is seen in serpentine microveins in and around relict olivine (Fig. 5-18).

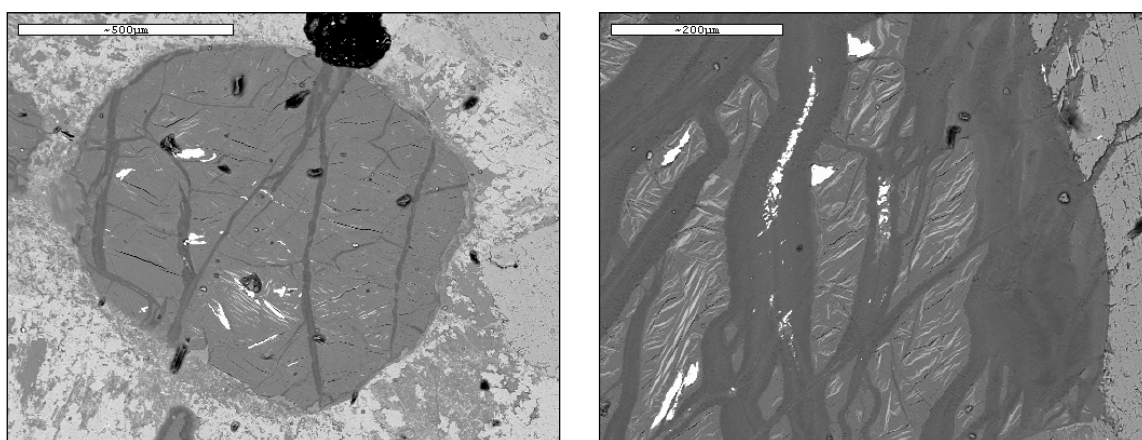


Fig. 5-18. SEM images of metamorphic olivine at [left] incipient stage of alteration to serpentine (darkest pervasive veins) and magnetite (bright wispy bands); and [right] more advanced stage of alteration. Specimen N1-4.

The colour of the footwall at any locality is usually an indication of the extent of serpentinisation, such that the darkest (practically black) zones represent extreme alteration to virtually pure serpentinite. These zones tend to comprise irregular bodies varying in size from a few decimetres to tens of metres and are often elongate parallel to the footwall layering. However, serpentinite often occurs in the intersection of joints/fractures that would offer a natural pathway for fluids. Less extensive serpentinisation in the hornfelses follows the original bedding, such that darker layers are visibly continuous. The varying degrees of alteration between layers are thought to reflect primary variations in mineralogical composition. Several thin, highly continuous, very friable layers of a serpentine-rich lithology occur with a strong sulphurous odour. These may originally have been beds of anhydrite, which is known from unmetamorphosed parts of the Malmani Dolomite, but macroscopic evidence for original anhydrite is lacking at Sandsloot.

Like the Platreef, the footwall rocks contain common sulphides such as pyrrhotite-troilite (Fe_{1-x}S – FeS), pentlandite ($\text{Fe,Ni}_9\text{S}_8$), chalcopyrite (CuFeS_2) and bornite (Cu_5FeS_4), but less common sulphides occur in the footwall that have not yet been identified in the Platreef. These are sphalerite (ZnS), bravoite (Fe,Ni,CoS_2), godlevskite (Ni_7S_6), millerite (NiS) and hydrous valeriite: $(\text{CuFeS}_2)_{1.5}(\text{Mg,Al})(\text{OH})_2$. An unidentified Fe-Zn-Mn-S phase (ferroan sphalerite?) is frequently encountered in footwall serpentinites, and stibnite (Sb_2S_3) and molybdenite (MoS_2) are found as rare phases in the hornfelses and serpentinites. Magnetite is the only oxide found in the footwall. Other rare phases include altaite (PbTe), plumboanbarite or hokutolite $(\text{Ba,Pb})\text{SO}_4$ as well as halogen-bearing phases such as bismoclite (BiOCl) and unidentified Fe-F-bearing and Pb-Cl-bearing phases.



Fig. 5-19. Footwall calc-silicate hornfels in drill core SSP242 at 321.95 m depth. Large grey/green crystals are diopside.



Fig. 5-20. Ovoid body of pure, white wollastonite in footwall calc-silicate hornfels.

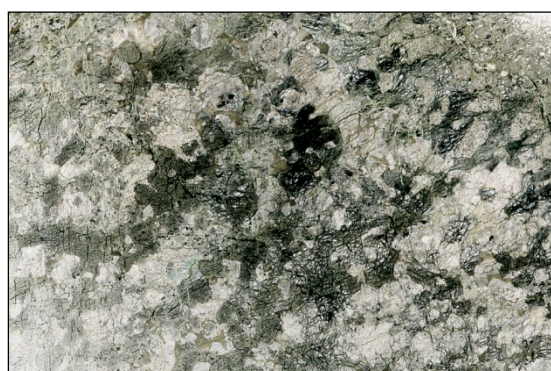


Fig. 5-21. Photomicrograph of meta olivine clinopyroxenite (plane polarised light) pervaded by network of serpentine microveins (dark material). Specimen PA-E142. Field of view ~2 cm wide.



Fig. 5-22. Dark serpentinite associated with intersections of joints/fractures in footwall. Note compositional variation in footwall layers and thin, bedding-parallel, dark serpentinite bands. Yellow field book (20 cm long) for scale.

5.5.3.3 Pegmatoidal mafic dykes

In the east-central part of the pit, a 4-5 m thick pegmatoidal dyke intrudes almost vertically through the footwall, but its relationship to the Platreef could not be seen. Several smaller dykes and veins branch from this dyke into the Platreef (suggesting the main body of the dyke also cuts the reef) and are seen as small pods on the rock face. Locally the texture is extremely pegmatitic, with pyroxene crystals up to 30 cm long in blasted-out boulders near the main exposure of the dyke. Small dykes and veins of similar composition were observed in some drill cores from various locations around the mine. The dyke has no chilled margins against the footwall serpentinitised clinopyroxenites and Platreef. Its relationship to the hangingwall is not known, but the pegmatoid is notably lacking in the hangingwall in drill cores. There are, however, similar pegmatoidal dykes emating from the Main Zone (hangingwall) at Zwartfontein, mapped by Holwell & Jordaan (2006).

Two consistently characteristic features of the main dyke and its branching veins are their pegmatoidal texture and cumulus plagioclase laths with intercumulate graphite-grey to black pyroxene (Fig. 5-23), although locally the two phases display eutectic intergrowth. In the most pegmatoidal zones, pyroxene and assumed plagioclase were eutectic but the plagioclase is thoroughly altered to a microscopically fibrous epidote (Fig. 5-24) that is pale

green in hand specimen. In places, the branching veins are extremely feldspar-rich and sub- to euhedral pyroxene crystals in tooth-like or radial patterns grow inwards from the margins of the veins (Fig. 5-25). Within the dyke and some of the associated veins, bowed pyroxene crystals (Fig. 5-26) and fragments of pyroxene evidently broken away from the dyke margins suggest some form of directed stress, possibly the result of flow of melt or crystal mush, as there are no expressions of tectonic stress. Phlogopite occurs as an accessory phase, comprising large ‘booklets’. Sulphides are notably rarer than in the Platreef but large, interstitial blebs of pyrrhotite and pentlandite occur sporadically. Ilmenite and perovskite represent minor oxide phases, sometimes containing chlorapatite ($\text{Ca}_5(\text{PO}_4)_3\text{Cl}$) and baddelyite (ZrO_2). Narrow veins of similar composition and appearance to this major dyke are observed in the footwall lithologies along the east highwall of the pit.



Fig. 5-23. Photograph of pegmatoidal mafic dyke. Note well developed, cumulus feldspar laths.

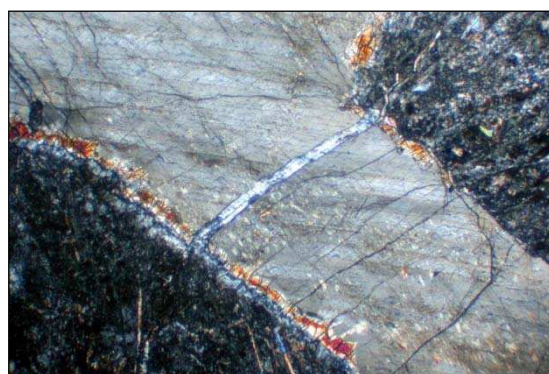


Fig. 5-24. Photomicrograph of pegmatoidal mafic dyke (crossed nicols) consisting of highly altered cumulus plagioclase (sericite and epidote from sericite) and orthopyroxene, in this case in eutectic intergrowth, with reaction rim around orthopyroxene. Specimen PA-N1-0. Field of view approx. 4 mm.



Fig. 5-25. Highly pegmatoidal anorthosite-pyroxenite pocket in the Platreef near the major dyke shown in Fig. 5-23 above.



Fig. 5-26. Smaller pegmatoidal vein branching from the major pegmatoidal dyke in Fig. 5-23. Note large bowed pyroxene crystal right of centre.

5.6 Face map descriptions and petrography

Fig. 5-1 shows a plan of the Sandsloot open pit as of July 2000 and indicates the locations of all rock faces mapped for the present study. Composite photographs and accompanying maps of the individual faces are given in this section. Sampling points and numbers for all of the specimens collected for petrography and/or geochemical analysis are indicated on each map. Fig. 5-1 also shows the locations of three boreholes in the Sandsloot north pit, and graphic logs of the drill core are presented and described in a later section.

In each face number, for example 138/038, the bench number is identified by the first three digits of the first number. The greater the number, the deeper the bench, and because the Platreef dips west or northwest, the reef occurs at increasing depth progressing westwards. The second set of digits in the face numbers represents a horizontal zone in the respective bench plan. This is the mining terminology. For simplicity, however, each face is given an abbreviated code; e.g. N1, SW3, indicating location in the north and southwest parts of the south pit respectively. These codes are used to prefix sample numbers, in which the number denotes distance in metres along the face; e.g. sample PA-N1-24 is from 24 m along face N1 (the author's initials PA are a fixed identifier).

Six face maps that show the relationships between footwall, Platreef and hangingwall lithologies are presented in this section (N1, N2, N3, SW1, SW2, SW3), and structural detail of another face in partly mineralised footwall rocks (S1) is also described. An additional long face (E1) that joins faces N1 and S1 was also mapped and sampled, but it is exclusively footwall. Therefore it is not described here, but samples and photographs from the face are used for illustration.

- Face 132/038 (N1 – Fig. 5-27) – a 32 m long, south facing exposure in the northwest corner of the south pit, displaying a virtually cross-strike section through the Platreef, where the reef has its general north-south strike and moderate dip to the west.
- Face 132/032 (S1 – Fig. 5-34) – a 35 m long, north facing exposure in the east part of the south pit exhibiting structures in locally platiniferous footwall lithologies. No hangingwall or Platreef is exposed here.
- Face 141/022 (N2 – Fig. 5-35) – a 35 m long, south facing exposure in the south pit displaying an approximately 10 m thick section of reef with contacts to the hangingwall and footwall. Again the reef strikes roughly north-south and dips to the west.
- Face 144/011 (N3 – Fig. 5-37) – a 60 m long, south facing exposure in the central part of the pit showing the hangingwall contact zone but no footwall.

- Face (SW1 – Fig. 5-40) – a 50 m long, east-facing exposure in the ‘southwest extension’ of the pit with a full section through footwall, Platreef and hangingwall. The reef has an approximately SW-NE strike and NW dip and displays significant compositional variation.
- Face 138/014 (SW2 – Fig. 5-44) – another east-facing exposure, 85 m long, a short distance east of SW1 and geologically similar in many ways, but exhibits a thicker reef section and different internal variation.
- Face 141/021 (SW3 – Fig. 5-48) – a 40 m long, NE-facing exposure further west/southwest of SW1/SW2 and, although it is a simpler package, it displays important variation within the reef.

The locations of the mapped pit faces describe an arc (Fig. 5-1), with faces N1-N2-N3 lying along the regional strike of the Platreef, but between the N series of faces and faces SW1-SW2-SW3, the strike of the reef swings abruptly westwards (cf. Fig. 5-2). This is where the reef turns towards the ‘tip’ of the dolomite tongue along the north limb of the approximately ENE-WSW trending domal structure.

5.6.1 Face 138/038 (N1)

In face 138/038 (specimen suite N1: Fig. 5-27), the Platreef has a thickness of 12-15 m and is dominated by coarse-grained, pyroxene rich gabbro-gabbro-norite that grades locally into pyroxenite and websterite. Cumulus orthopyroxene is ubiquitous and is accompanied by cumulus or intercumulus clinopyroxene, and intercumulus plagioclase that may occur as large oikocrysts. BMS and PGM are generally restricted to interstitial sites between the cumulate pyroxenes (Fig. 5-28, Fig. 5-29). Chromite, ilmenite, rutile, armalcolite, perovskite, phlogopite and zircon are present as accessories (Armitage *et al.* 2002; McDonald *et al.* 2005a). The reef contains ragged xenoliths of dark serpentinite, which is assumed to be highly altered footwall calc-silicate hornfels (Fig. 5-30). Relict sedimentary lamination is clearly visible in the largest xenolith, and the shape of the smaller xenolith closer to the hangingwall seems to reflect bedding.

A pegmatoidal zone of aplitic gabbro and fragmented pyroxenite (Fig. 5-32, Fig. 5-33) occurs along the footwall contact where the reef thickens but is absent from thinner reef lower down the face. The shape of this feature gives it some morphological similarity to ‘potholes’ in, for example, the Merensky Reef.

The contact to the hangingwall is tectonic in this rock face, comprising a serpentinitised brittle-ductile shear zone up to 20 cm thick. It is considered very unlikely that the shear zone

has exploited the original hangingwall contact, as an original magmatic hangingwall contact is exposed in other rock faces nearby (N2 and N3). Thus, it is likely that the top of the reef is truncated in face N1. The hangingwall is a medium- to coarse-grained norite with cumulus plagioclase and intercumulus pyroxene.

A distinct pegmatoidal mafic dyke dominates the eastern end of the face and was described in section 5.5.3.3. It intrudes the footwall, and smaller offshoots are observed in the gabbroid rocks of the Platreef. The relationship of the dyke to the Platreef and hangingwall could not be observed above face N1.

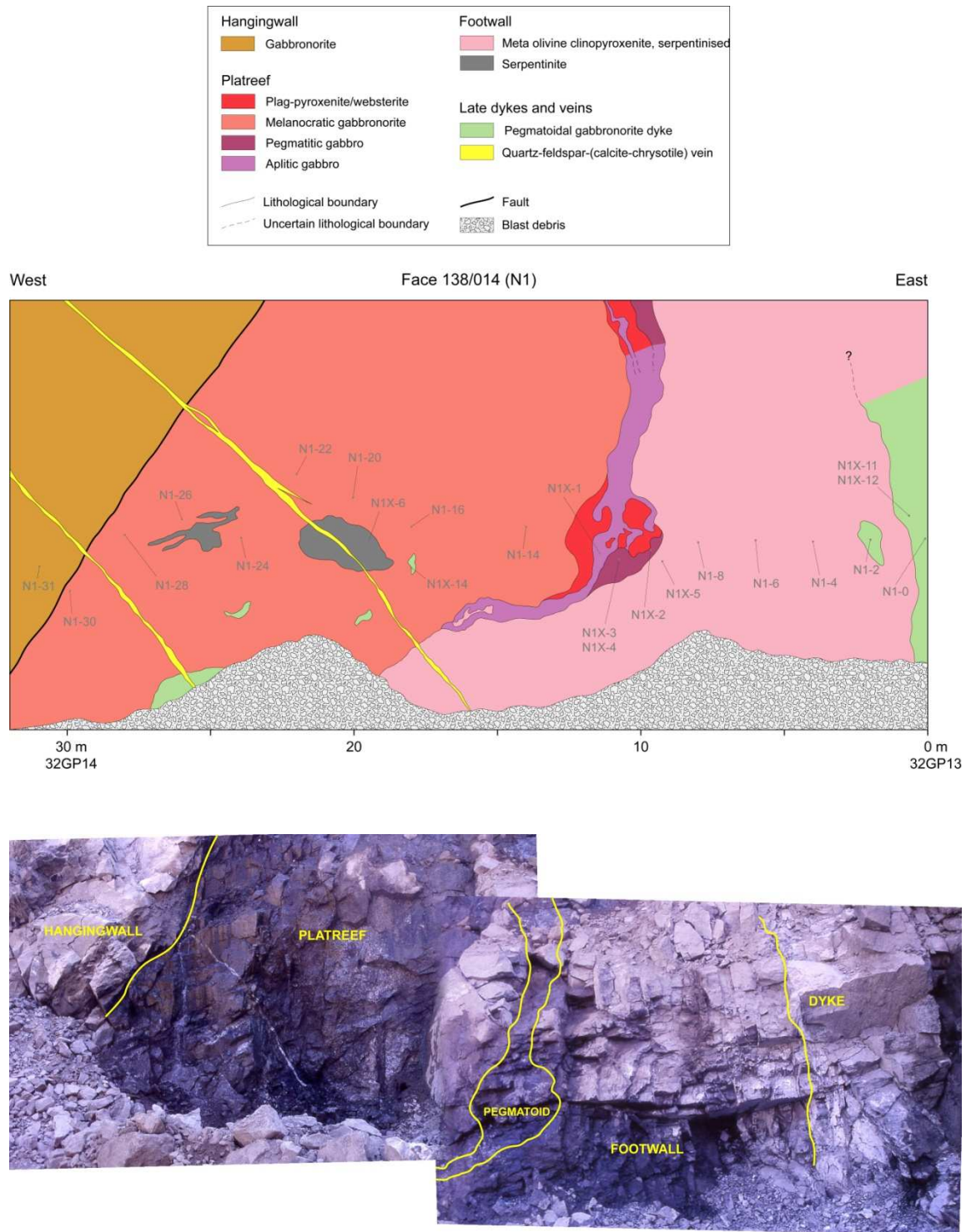


Fig. 5-27. Geological map and composite photograph of face 132/038 (N1).

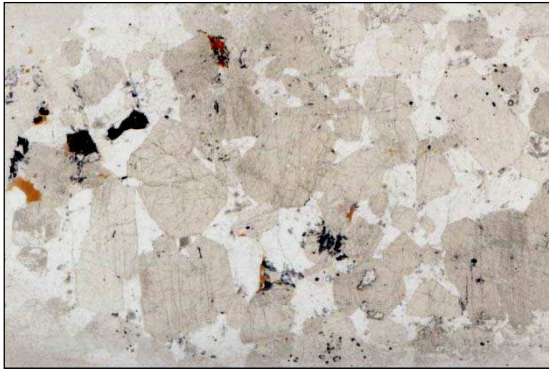


Fig. 5-28. Photomicrograph of Platreef gabbronorite (plane polarised light), consisting of euhedral to subhedral cumulus orthopyroxene and clinopyroxene in intercumulus plagioclase. Minor phases are red-brown phlogopite and opaques. Specimen N1-14. Field of view ~3 cm wide.

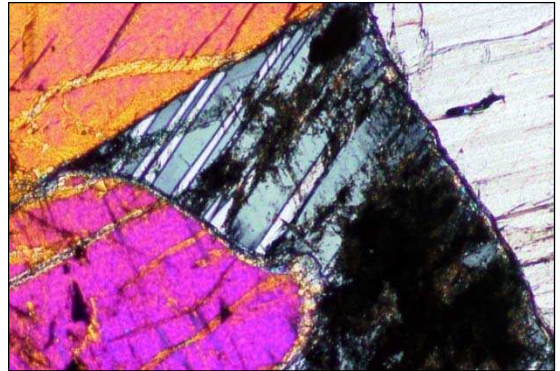


Fig. 5-29. Photomicrograph of Platreef gabbronorite (crossed nicols) showing interstitial twinned plagioclase in variable state of saussuritisation between euhedral to subhedral crystals of orthopyroxene and clinopyroxene. Specimen N1-26. Field of view approx. 4 mm wide.

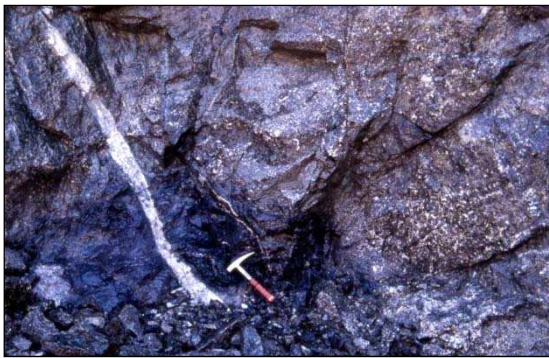


Fig. 5-30. Dark serpentinite xenolith in very coarse Platreef gabbro in face N1, cut by a late quartz-feldspathic vein. Note possible igneous layering in gabbro in centre right part of photograph (detail in Fig. 5-31).



Fig. 5-31. Detail of apparent crude igneous layering in very coarse-grained Platreef gabbro in face N1.



Fig. 5-32. Detail of pegmatoidal gabbroic pod at base of Platreef in face N1. Pale portion is aplite.



Fig. 5-33. Detail of highly mineralised gabbro in pegmatoidal pod in face N1.

5.6.2 Face 132/032 (S1)

Face 132/032 (specimen suite S1, S2 and S3: Fig. 5-34) is a headwall from which a ramp was constructed for mine traffic soon after the face was mapped. It is a short, north facing exposure entirely within the footwall on the east side of the south pit (Fig. 5-1). Although the face displays no Platreef and may be several to tens of metres below the base of the reef, it was mapped in order to illustrate a system of shear zones that deform the footwall at this location. Samples were also collected for fire assay.

The face shows interlayered calc-silicate hornfelses, diopsidites and meta olivine clinopyroxenites, with minor igneous tubes (assumed offshoots from related concealed dykes). Lithological variation appears to broadly follow bedding but with notable exceptions, and while the face map illustrates only the major variations, composition varies on a much smaller scale. Up to ~3 m from ground level, the face could be mapped with confidence. At higher levels, visual extrapolation was necessary in order to complete the structural picture, though some higher parts were accessible by climbing.

The mapped structures are west- to southwest-verging shear zones that initiated along bedding planes but have broken upwards (ramped), forming an incipient duplex. The shear zones are characterised by dark, similarly oriented serpentine fibres and by slickenlines and slickensteps in quartz, calcite and fibrolite. While the slip structures display a variety of orientations, the majority are aligned with the westward vergence of the shear zones. As the shear structures overprint prograde metamorphic assemblages, they are late syn- to post-metamorphic in relation to hornfelsing of the metadolomite footwall. If the structures are extrapolated southwards, they are located on the east limb of the large anticline in the south wall of the pit (Fig. 5-4), and may then be part of a shear system that generated major N-S trending folds; or perhaps they represent ‘out of the syncline’ accommodation structures in the hinge of a syncline that pairs with the anticline seen in the south highwall. East of face S1, bedding can be seen to dip approximately southwest, supporting the existence of a syncline.

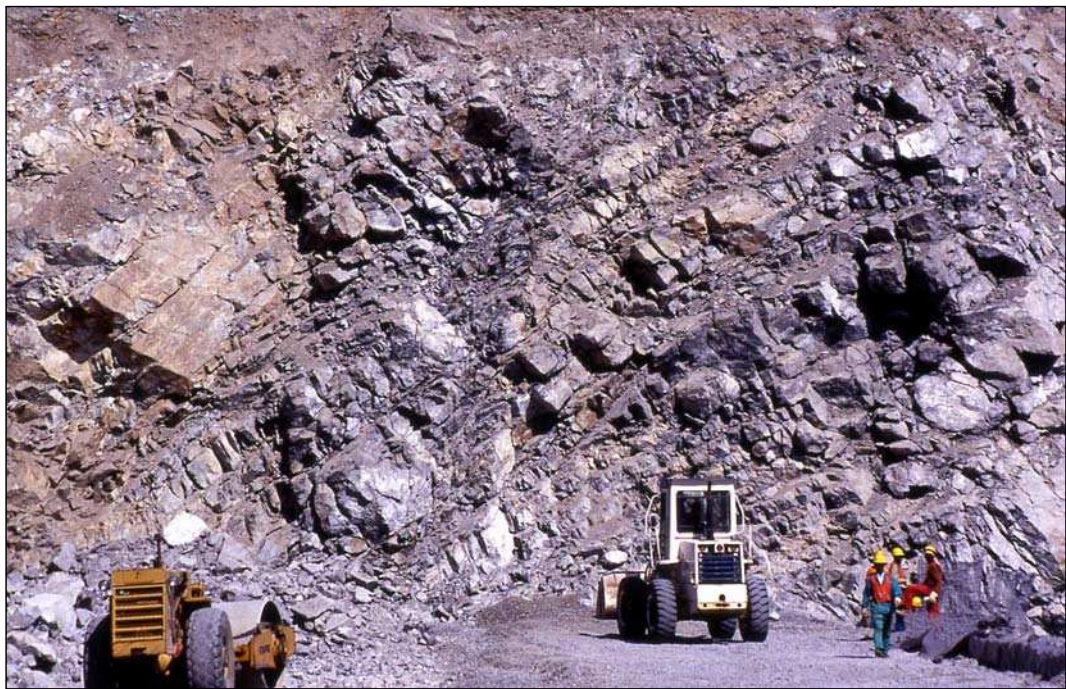
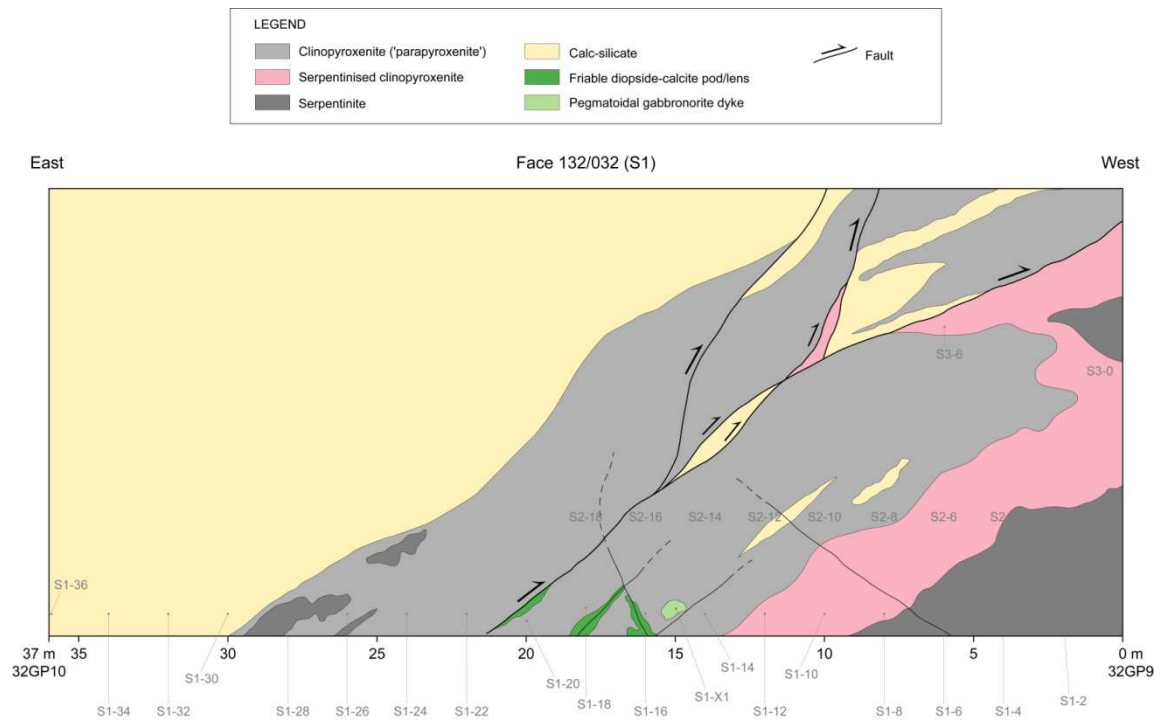


Fig. 5-34. Geological map and photograph of face 132/032 (sample suite PA-S1) consisting entirely of footwall lithologies with minor igneous 'tubes'. Labels 32GP9 and 32GP10 are survey geopoints. Sampling locations and sample numbers are shown.

5.6.3 Face 141/022 (N2)

This south facing exposure towards the northeast corner of the south pit shows an unbroken sequence through the hangingwall, Platreef and footwall. The hangingwall is an unremarkable, medium-grained gabbro norite with a sharp magmatic contact to the underlying Platreef package, but could only be observed clearly in the lowermost part of the face because it was generally covered by much loose debris.

The upper section of the reef from about 2 to 5 m along the face is a dark, coarse pyroxenite with some visible plagioclase but no visible sulphides. The upper zone of pyroxenite and the sharp magmatic hangingwall contact distinguish this face from face N1, where the hangingwall gabbro norite is in tectonic contact with coarse feldspathic pyroxenites. It is possible, but not provable, that the shear zone in face N1 has eliminated part of the reef that differs from the exposed feldspathic pyroxenites.

The lower section of the reef from about 5 m to the footwall contact at 14 m is a coarse gabbroid rock similar to that in face N1, and is increasingly feldspathic, pegmatoidal and sulphide-rich towards the footwall contact. Despite this tendency towards a pegmatoidal texture, however, there is no distinct pegmatoidal pocket/pod at the base of the reef as there is in face N1.

From the footwall contact at 14 m to at least 36 m, meta olivine clinopyroxenite occurs with little lithological variation but with abundant small patches of sulphides.

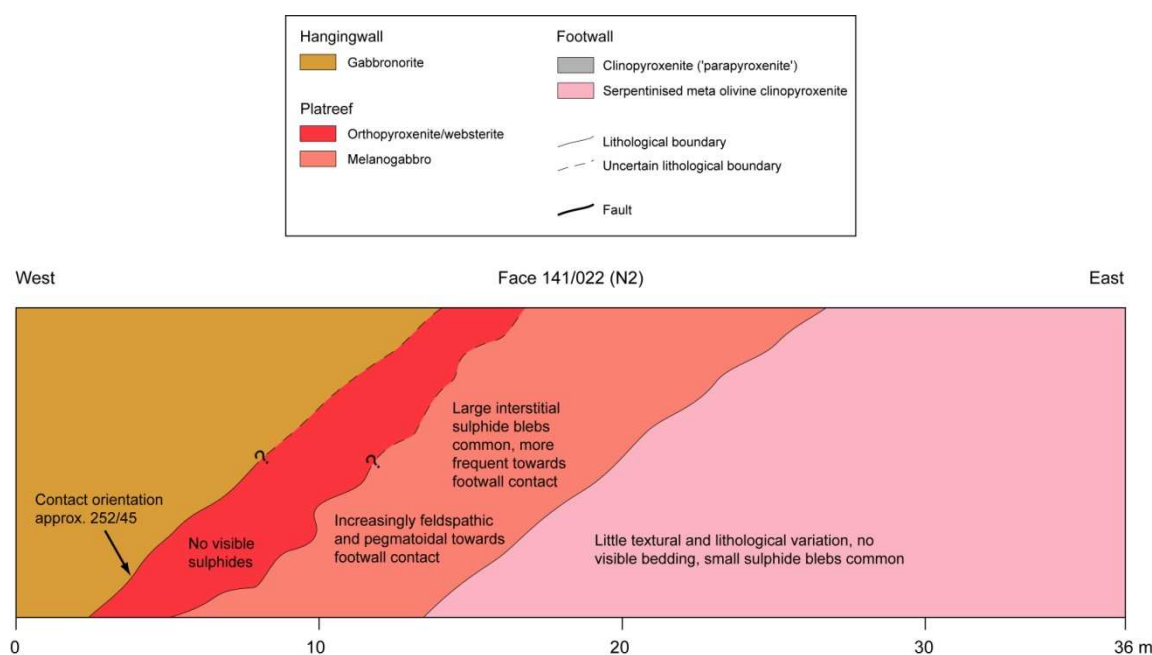


Fig. 5-35. Geological map of face 141/022 (N2).

5.6.4 Face 144/011 (N3)

The Platreef in face N3 (Fig. 5-36) is ~21 m thick and the upper 10 m is very similar to the gabbroic reef in face N1 (Fig. 5-27) and face N2 (Fig. 5-35), except with a 2-3 m thick zone of altered reef towards the top of the section. Again in similarity to face N2, a 12 m thick section of mainly meta olivine clinopyroxenite with abundant sulphides occurs beneath the reef, but with some relatively unaltered diopsidite. At around 29 m along the face there is a transition to the common layered calc-silicate hornfelses and diopsidites, which become increasingly serpentinised beyond about 40 m. The calc-silicate hornfelses and diopsidite zones reflect footwall bedding, which appears to have a relatively low angle to the reef-footwall contact here.

The hangingwall contact is well displayed and, rather than being a tectonic boundary as in face N1 or a single sharp magmatic contact as in face N2, is instead a planar magmatic contact zone defined by a 10-15 cm thick leuconorite with cumulus plagioclase and orthopyroxene oikocrysts (initially termed ‘mottled anorthosite’ in the field), overlain by a 5 cm thick layer of fine-grained gabbro-norite. The leuconorite and gabbro-norite specimens are numbered N3X-4B and N3X-4A, respectively, in Table 1 in Appendix 3. A similar relationship was observed north of Sandsloot in the dry river bed at Zwartfontein (Fig. 5-38), which is now an operational pit. A further observation in face N3 is that a slightly irregular zone of serpentinised pyroxenite near the top of the Platreef appears to be truncated by the hangingwall.

Holwell *et al.* (2005) provide crucial microscopic evidence of the nature of the contact between hangingwall poikilitic leuconorite and coarse-grained, mineralised Platreef pyroxenite of a sample taken from the northern part of the Sandsloot pit (Fig. 5-39). The cumulus orthopyroxene crystals at the top of the Platreef are visibly eroded and resorbed by cumulus plagioclase of the fine-grained poikilitic leuconorite. The leuconorite does not permeate the pyroxenite, and the embayments made by the small plagioclase crystals into the pyroxenes strongly suggest that the Platreef was completely or nearly completely solidified before intrusion of the hangingwall magma.

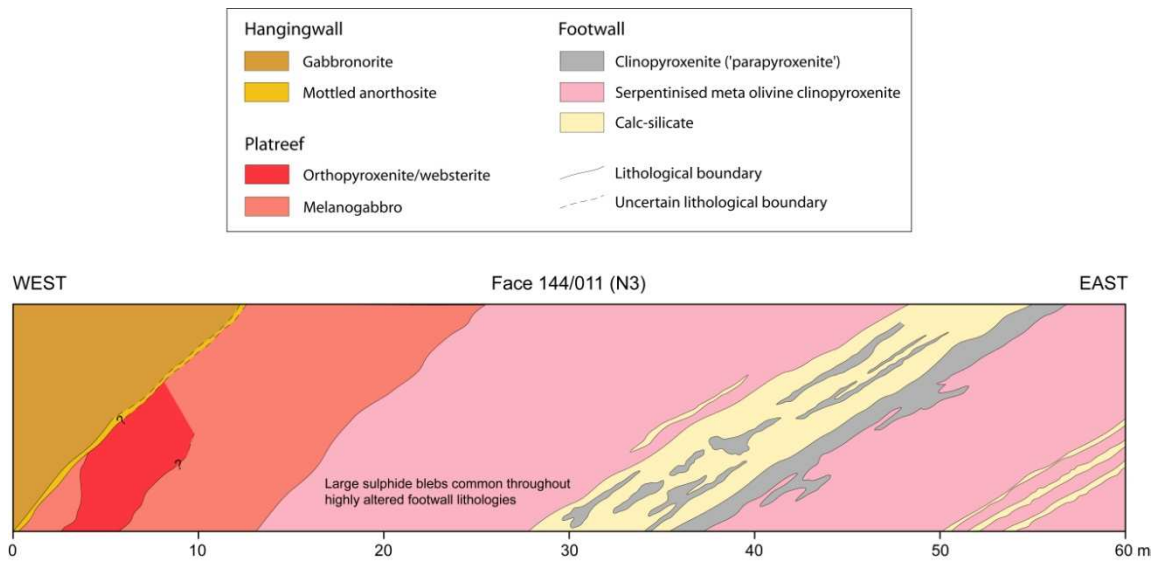


Fig. 5-36. Geological map of face 144/011 (N3).

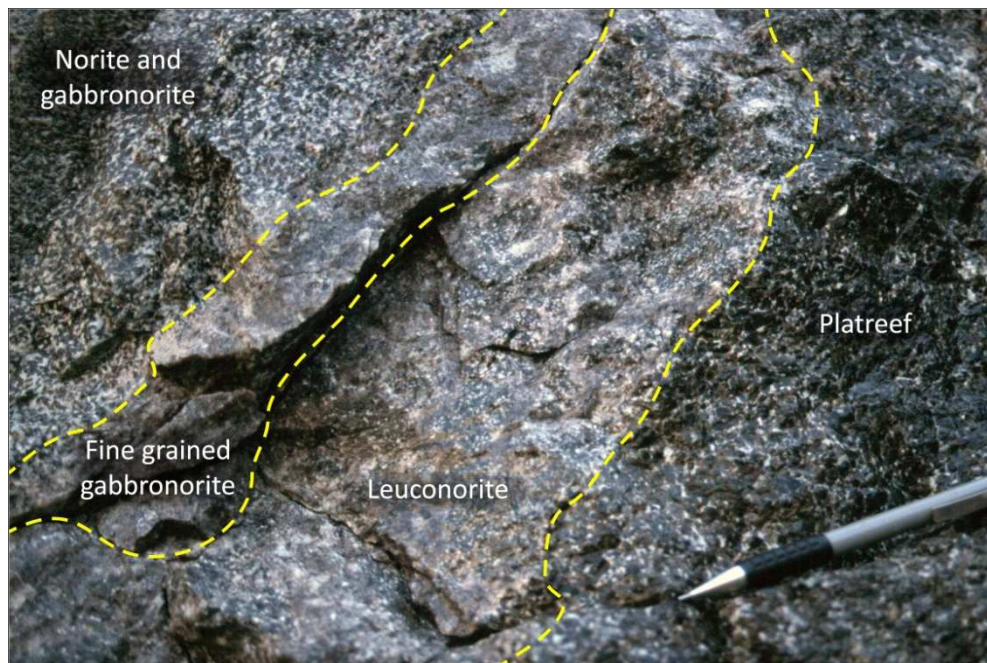


Fig. 5-37. Detail of hangingwall contact zone in face N3 (from McDonald *et al.* 2005a).



Fig. 5-38. Fine-grained Main Zone gabbro-norite intruded above mottled anorthosite in a dry river bed at Zwartfontein South, a short distance north of the Sandsloot pit, prior to commencement of the Zwartfontein open pit operation. Note wavy contact. The anorthosite overlies oxidised Platreef beneath sandy cover beyond the lower right margin of the photograph.

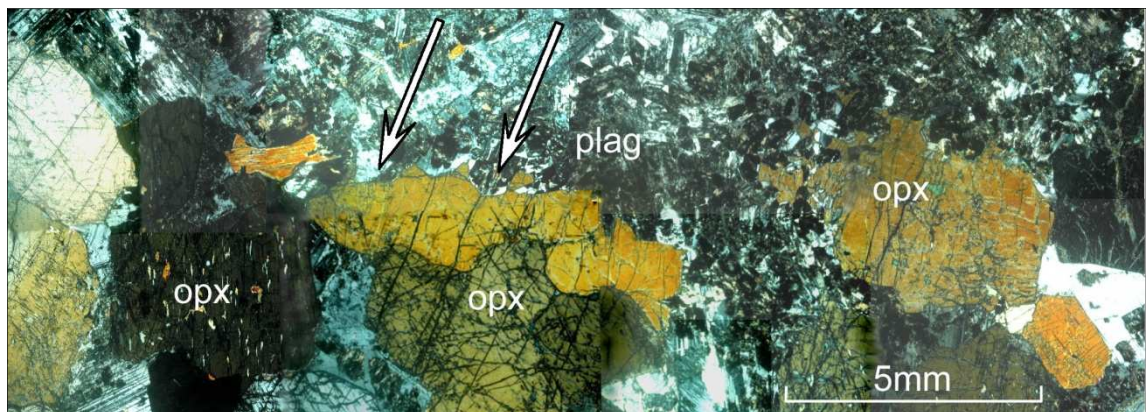


Fig. 5-39. Composite photomicrograph showing the contact between fine-grained, hangingwall poikilitic leuconorite (upper half of photograph) and coarse-grained, mineralised Platreef feldspathic pyroxenite (lower half). Note the embayments made by hangingwall plagioclase in the cumulus Platreef orthopyroxenes (arrowed). Dark patches within the plagioclase are alteration (from Holwell *et al.* 2005).

5.6.5 Face 135/014 (SW1)

In the southwest part of the pit, the Platreef shows important mineralogical and textural differences to the reef exposed to the north. In face SW1 (Fig. 5-40), Fe-rich olivine is widespread and occurs as a late-stage mineral (Fig. 5-41 to Fig. 5-43). It replaces orthopyroxene through many metres of the reef. Plagioclase may also be replaced by Fe-rich clinopyroxene, resulting in the development of Fe-rich wehrlites, olivine lherzolites and harzburgites, and an overall darkening of the rock conspicuous in the photograph of the face (Fig. 5-40). The Fe-rich zone also appears highly fractured after blasting. These rock types have been noted to the south where the Platreef rests on banded ironstone (Buchanan *et al.* 1981; Buchanan & Rouse 1984) but have not been described elsewhere. The Fe enrichment and reaction textures observed here are similar to those found in Fe-rich pipes and pegmatoids elsewhere in the Bushveld Complex (Schiffries 1982; Viljoen & Scoon 1985) and may have been produced from reaction between reef pyroxenites and gabbros and a late-stage Fe-rich melt or fluid. This type of Fe-rich ultramafic reef will be referred to as ‘olivine replaced reef’ (ORR – after McDonald *et al.* 2005a; Holwell *et al.* 2006). Perhaps more importantly, these feldspar-poor ultramafic zones are invariably truncated by hangingwall lithologies that contain fresh plagioclase. Thus, the Fe replacement event is restricted to the Platreef and never happened in the hangingwall. This is a vital constraint on the relative timing of the Platreef and Main Zone.

At this location, however, the reef does not overlie banded ironstone and since the hangingwall truncates the Fe replacement zone, the cause of Fe enrichment can only be speculated. One reasonable possibility is that the Penge banded iron formation, which underlies the reef south of Sandsloot, continued above the Platreef at Sandsloot when the reef was emplaced but before the Main Zone intruded above it and eliminated the sedimentary roof rocks. This scenario assumes that the original roof rocks of the Platreef were the continuation of the Transvaal Supergroup known from the present footwall.

Face SW1 also shows a serpentinitised mixed rock comprising relict metamorphic clinopyroxenite (with or without olivine) and pyroxenites and websterites with igneous textures forming the base of the Platreef. This type of rock will be referred to as ‘footwall-reef hybrid’ (after McDonald *et al.* 2005a). The primary Platreef is extensively replaced and mixtures of orthopyroxenites, websterites, gabbro-norites and wehrlites are common. The rocks become more pegmatoidal and olivine-rich upwards, grading into Fe-rich olivine lherzolite close to the hangingwall contact. For at least a few metres above the contact, the hangingwall is fine-grained gabbro-norite with cumulus plagioclase (specimen PA-SW1-47).

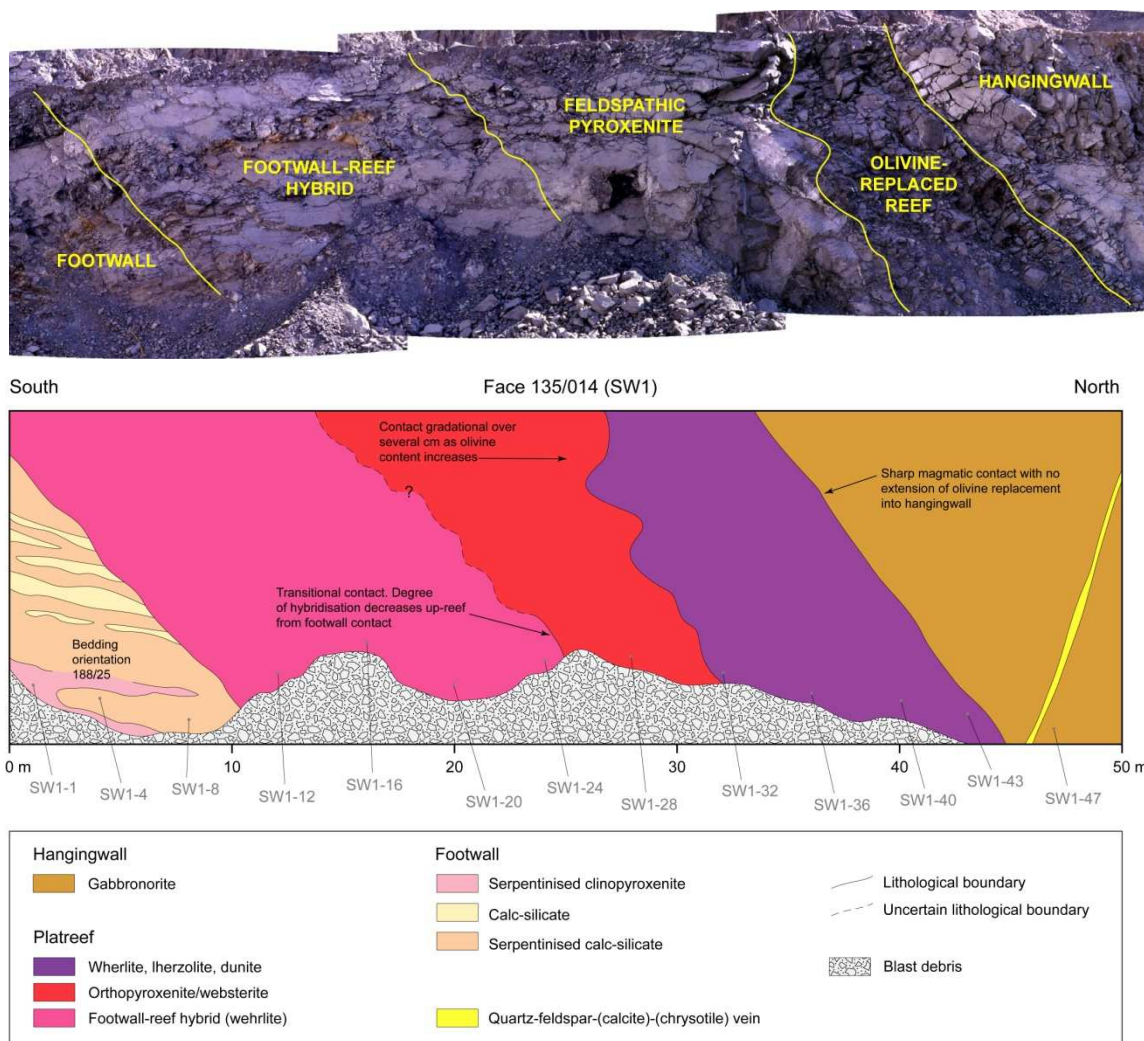


Fig. 5-40. Photograph and geological map of face 135/014 (SW1).



Fig. 5-41. Photomicrograph of specimen SW1-43 (plane polarised light). Note dull green olivine around eroded orthopyroxene grains (grey).

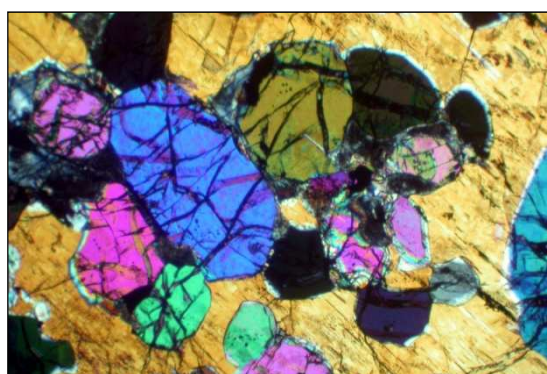


Fig. 5-42. Photomicrograph of fresh, fractured olivine in orthopyroxene (crossed nicols). Specimen SW1-40.

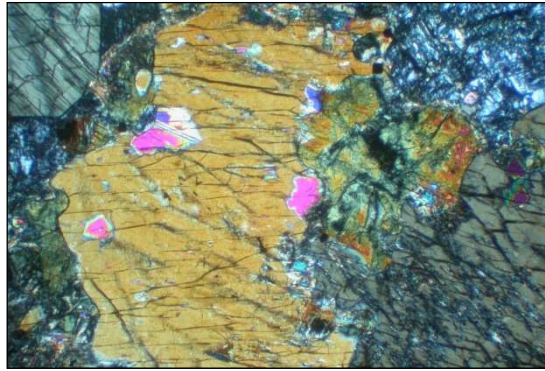


Fig. 5-43. Olivine replacement texture in specimen SW1-40. Note embayments of olivine in orthopyroxene.

5.6.6 Face 138/014 (SW2)

Face SW2 (Fig. 5-44) also exhibits Platreef cutting the footwall bedding at a high angle and is similar in some respects to face SW1 (Fig. 5-40), probably due to their proximity. Olivine in the footwall is extensively serpentinised and these rocks contain an intricate fracture network filled with magnetite and ilmenite. A thick zone of serpentinised hybrid rocks (Fig. 5-45) is present at the base of the reef, and wehrlite occurs close to the hybrid rocks. This merges upwards into gabbronorite (Fig. 5-46) and pyroxenite (Fig. 5-47) that become very Fe-rich close to the hangingwall, but with little obvious development of olivine.

A 15 cm wide, dark xenolith of websterite (specimen PA-SW2-83) that carries high levels of Cr and some PGE grade occurs a few metres above the contact in the hangingwall gabbronorite. This is interpreted as a xenolith of Platreef (Holwell *et al.* 2005) and the whole-rock and cumulus orthopyroxene compositions (En_{78}) are consistent with the Platreef (McDonald *et al.* 2005a).

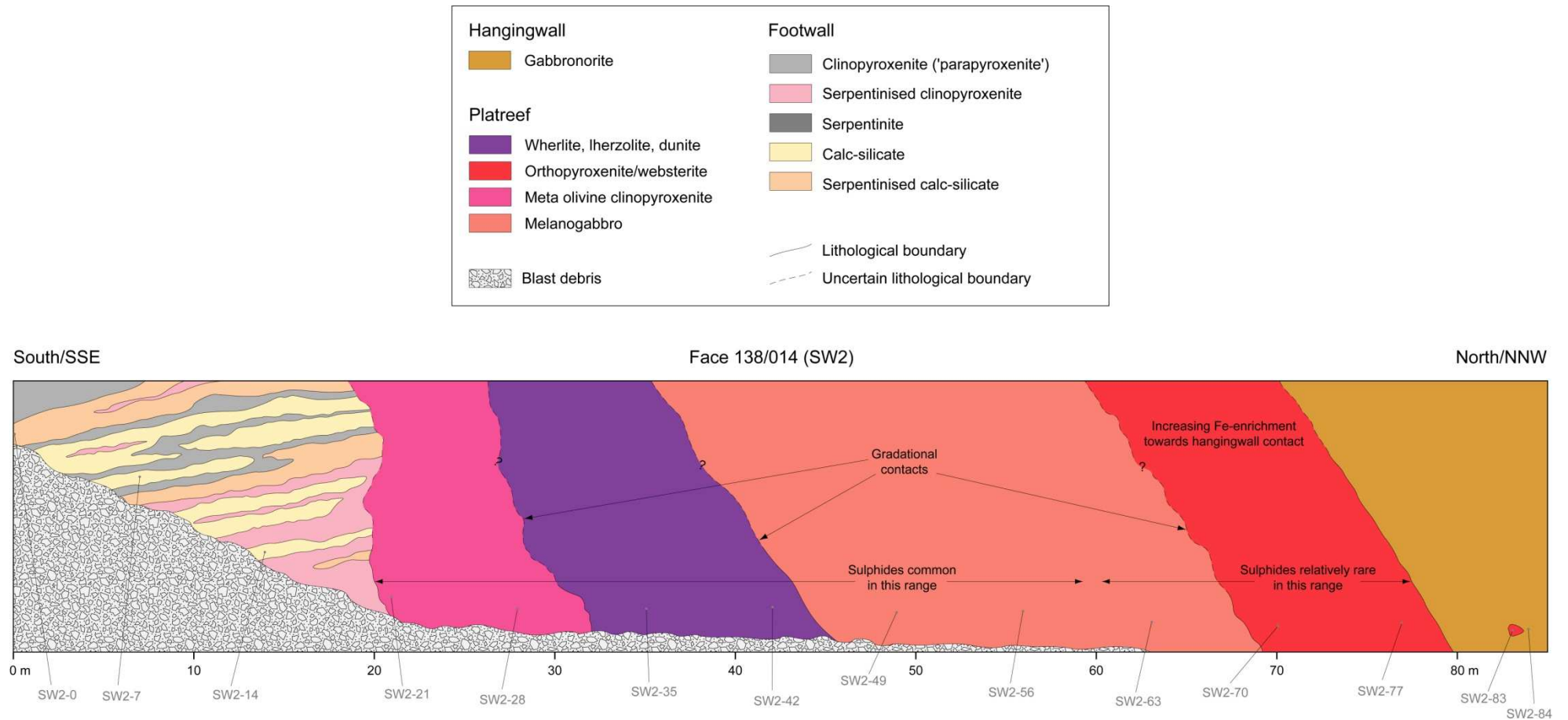


Fig. 5-44. Geological map of face 138/014 (SW2).



Fig. 5-45. Photomicrograph of footwall-reef hybrid (plane polarised light). Note eroded pyroxenes (grey) and network of serpentine veins (dark). Specimen SW2-28.

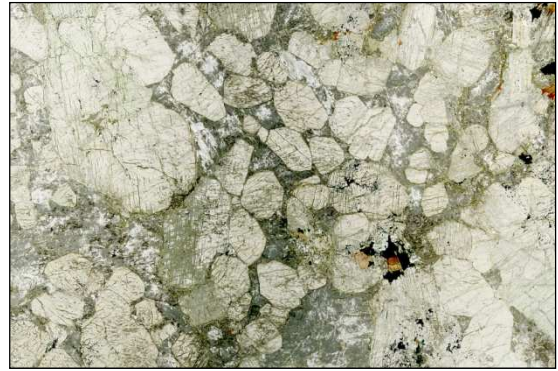


Fig. 5-46. Photomicrograph of Platreef gabbro-norite consisting of disaggregated cumulus euhedral orthopyroxene and minor clinopyroxene, and subhedral ortho- and clinopyroxene aggregates with saussuritised intercumulus plagioclase. Minor phases are red-brown phlogopite and opaques. Specimen SW2-49.



Fig. 5-47. Photomicrograph of Platreef feldspathic pyroxenite consisting of aggregates of coarse, sub- to anhedral ortho- and clinopyroxene with minor interstitial plagioclase. Green mineral is chlorite. Specimen SW2-77.

5.6.7 Face 141/021 (SW3)

Face SW3 (Fig. 5-48) exhibits a relatively simple sequence of lithologies but with some important features. The clean appearance and unbroken verticality of the face reflects a general lack of alteration. The footwall-reef contact is highly unconformable and is a primary igneous boundary showing no sign of tectonic disturbance. A distinct interlayering of pale calc-silicate hornfels and grey diopsidites characterises the footwall immediately beneath the Platreef, with a thick band of coarse-grained granoblastic calcite (marble). The continuity of these layers up to the igneous contact is evidence that metamorphic clinopyroxenites do not always occur adjacent to the lowermost reef. Further, the lack of tectonism in the footwall, in similarity to other mapped faces but much clearer in face SW3, is at variance with the conclusion of Friese (2004) that the Platreef intruded along a thrust zone.

The lowermost part of the Platreef is approximately 20 m thick and consists of footwall-reef hybrid, indicating some interaction with the footwall despite the sharp contact. The hybrid rock is overlain by a main body of websterite with a transition to a thin zone of melanocratic gabbronorite. The shape of the constituent reef lithologies is uncertain, as transitions could only be seen in the lower ~3 m of the face.

The hangingwall contact is a sharp magmatic boundary, and although it is difficult to see the relative chronology of reef and hangingwall at the contact, the hangingwall gabbronorite is clearly in a fresher condition and is therefore likely to be the younger magma. A brittle fault displaces the contact with an apparent 3 m downthrow in face view.

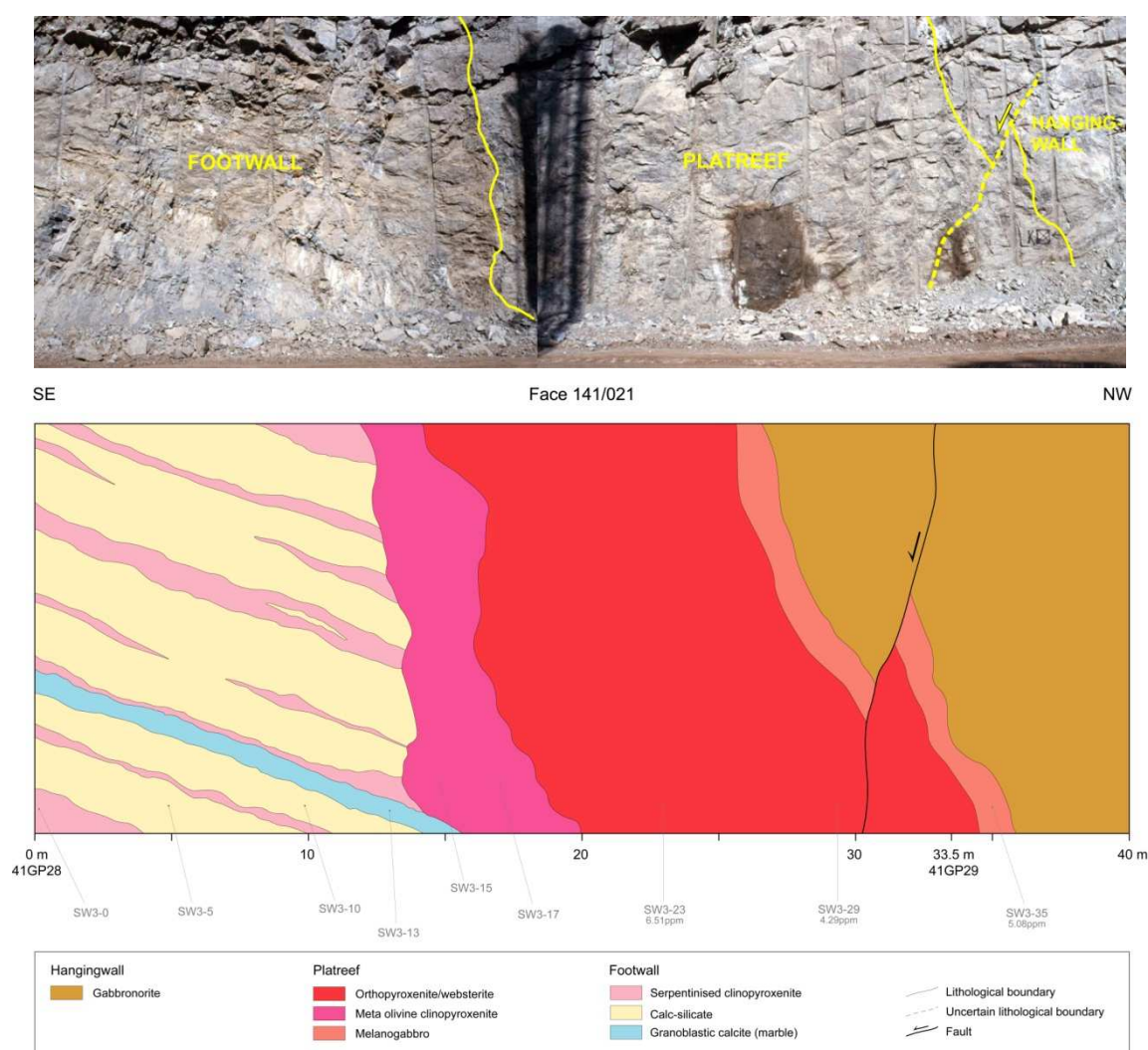


Fig. 5-48. Composite photograph (shadow of drill rig in centre) and geological map of face 141/021 (SW3).

5.7 Drill cores

Three drill cores were available for logging during fieldwork at Sandsloot. The drilling locations in the northwest part of Sandsloot pit are shown in Fig. 5-1. The three cores are illustrated in Fig. 5-49, Fig. 5-50 and Fig. 5-51 and are described in turn. Each core is a vertical section through the hangingwall, Platreef and footwall, and show features that were also encountered in the mapped pit faces described earlier, supporting the observations made there. Despite the extremely limited view across a drill core, one advantage of cores is that they display very fresh rock and far longer, continuous sections through hangingwall and footwall than can be observed in rock faces. The cores are described from ‘end of hole’ to top, i.e. stratigraphically upwards. The top of each core log is an arbitrary depth in the hangingwall above which no significant features were observed. The angles of lithological contacts in the graphical logs are not real, but only serve to illustrate that the main units dip moderately relative to the vertical boreholes. Thicknesses given in the description are therefore apparent thicknesses, such that real unit thicknesses normal to stratification are significantly smaller. Differences in dips between the magmatic and metasedimentary units are not necessarily real and are only intended to illustrate the discordant intrusion of the Platreef above the footwall.

5.7.1 Core SSP242

In core SSP242 (Fig. 5-49), a typical interlayering of footwall calc-silicate hornfelses and diopsidites occurs in variably serpentinised varieties from 343 m (end of hole) to 302 m depth. There is a sharp magmatic contact above the uppermost diopsidite to a coarse gabbro of cumulus pyroxene with intercumulus milky white plagioclase and large interstitial sulphide blebs. This unit is approximately 2 m thick and overlain by a thin band of coarse melanogabbro. These magmatic lithologies are interpreted as Platreef. The melanogabbro has a sharp contact to a pale mottled anorthosite approximately 1 m thick in section, which in turn has a sharp magmatic contact to a medium-grained gabbro-norite. This is macroscopically unmineralised, exhibits modal layering and downward fining. The mottled anorthosite is interpreted as a chill zone at the margin of an intrusion above the Platreef, and the gabbro-norite as ‘normal’ hangingwall.

The gabbro-norite continues to 287.5 m, where it is truncated by a thin quartz-feldspathic vein. Above the vein is a thin (2 m) succession of coarse mineralised gabbro similar to that at 302–300 m, topped by a thin band of coarse, mineralised pyroxenite and melanogabbro again similar to that described at about 299.5 m. The upper contact of the melanogabbro is a thin transition to a band of serpentinised pyroxenite above which is a sharp

contact to fresh-looking gabbro-norite very similar to that described at 297–287.5 m. Holwell & Jordaan (2006) mapped irregularly shaped, intrusive, fine-grained melagabbro-norites towards the base of the hangingwall at Zwartfontein, and very occasionally these penetrate the Platreef and may contain minor PGE and BMS mineralisation. Returning to core SSP242 at Sandsloot, the sequence above 275.5 m depth is interpreted as hangingwall juxtaposed against an upper section of Platreef by a fault that has been filled by hydrothermal felsite. This upper section of Platreef has a magmatic contact to hangingwall gabbro-norite, with the conspicuous absence of the mottled anorthosite that occurs deeper in the core. The possibility that the band of serpentinised pyroxenite may represent a minor shear zone was considered, but the hangingwall gabbro-norite above it lacks tectonic fabric. The two possibilities for this upper reef-hangingwall contact are: (i) a chill zone did not develop; or (ii) the hangingwall magma has eroded a previously developed chill zone of mottled anorthosite and now rests directly on Platreef (cf. Holwell *et al.* 2005; Holwell & Jordaan 2006).

A final and important observation in core SSP242 is that a 4–5 m section of a xenolith of calc-silicate hornfels occurs in the hangingwall gabbro-norite at a much higher level than illustrated in Fig. 5-49. This has two possible explanations: (i) the hangingwall (Main Zone) magma was locally in direct contact with the Malmani Dolomite, perhaps at greater depth, due to local absence of the Platreef or due to total erosion of the Platreef by the Main Zone; or (ii) the roof rocks of the Platreef were the same as the floor rocks in pre-Main Zone time. The latter scenario is the most likely, as there is no evidence from Sandsloot or elsewhere of total erosion of the Platreef by the Main Zone.

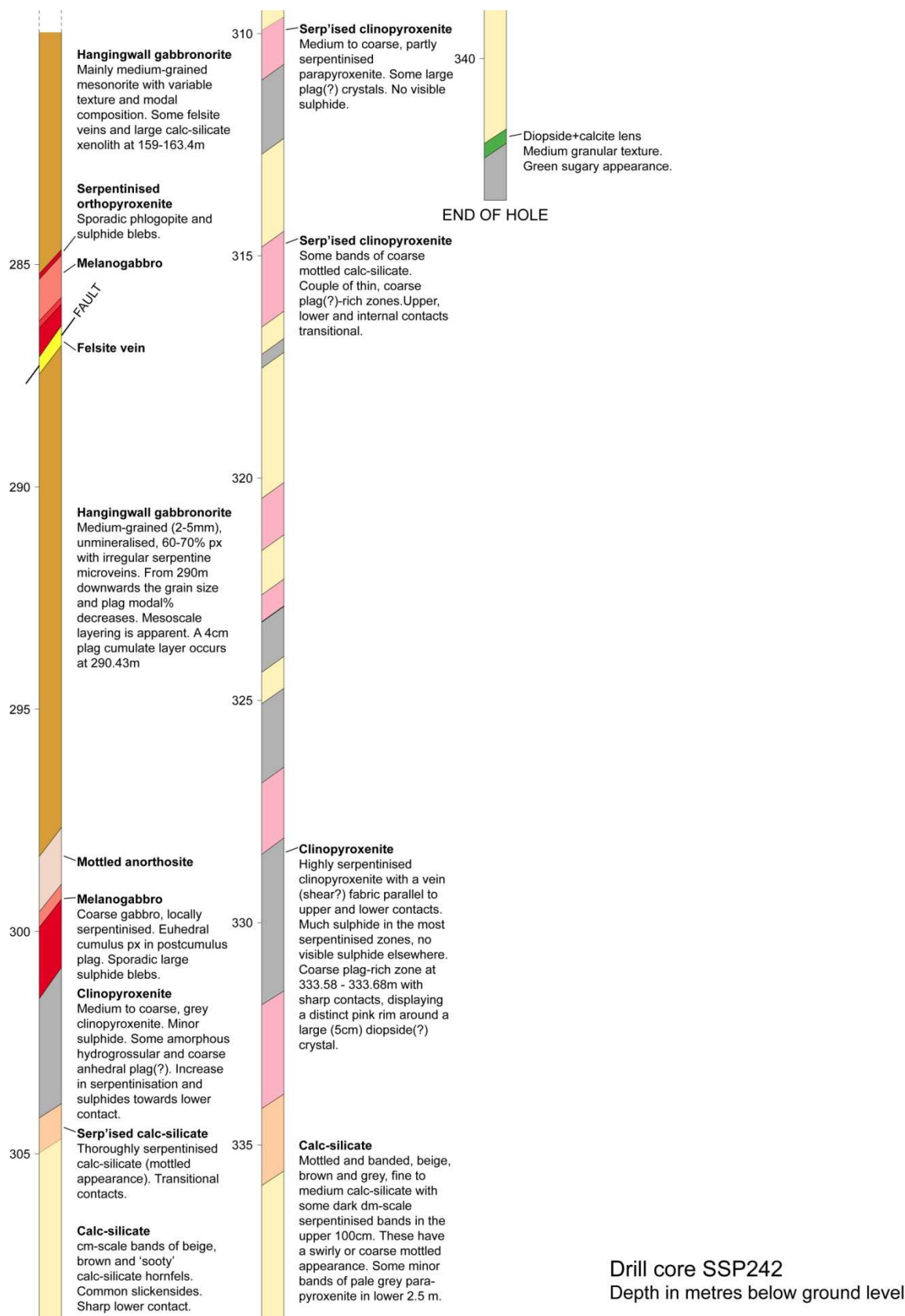


Fig. 5-49. Geological log of drill core SSP242. Colours for the various lithologies are the same as for the face maps (see legend in Fig. 5-27).

5.7.2 Core SSP257

Drill core SSP257 is illustrated in Fig. 5-50. From 373 m (end of hole) to 259 m, footwall clinopyroxenite and serpentinised clinopyroxenites occur, with relatively minor units of variably serpentinised calc-silicate hornfelses and lesser volumes of almost pure serpentinites. From the sharp upper contact at 259 m is a 19 m thick succession of mineralised melanogabbros, pyroxenites and serpentinised pyroxenites all interpreted as Platreef. A 2 m thick felsite vein interrupts the upper pyroxenite unit. There is no evidence to suggest this is an infilled fault zone, especially as the pyroxenite country rock exhibits no brittle or ductile shear fabric. At 240 m, immediately above the Platreef, is a homogenous leuconorite with a sharp lower contact, interpreted as hangingwall. Although distinctly paler than the hangingwall gabbro-norite seen in core SSP242, it is not an obvious chill zone of mottled anorthosite.

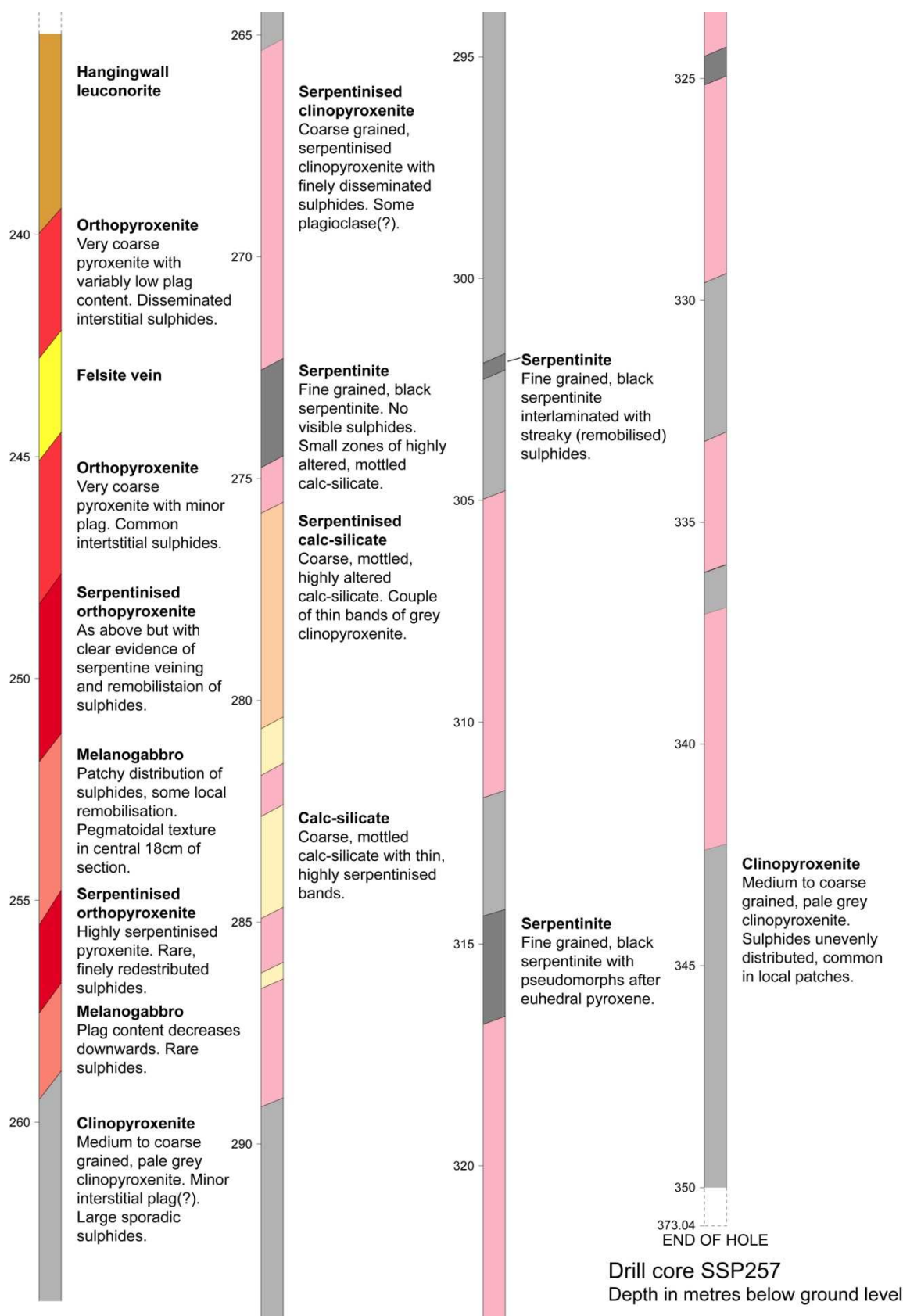


Fig. 5-50. Geological log of drill core SSP257. Colours for the various lithologies are the same as for the face maps (see legend in Fig. 5-27).

5.7.3 Core SSP258

Although core SSP258 and core SSP257 are only 100 m apart (Fig. 5-1), they display some significant differences. In core SSP258 (Fig. 5-51) from 375 m (end of hole) to 342 m depth, the broad characteristic of the footwall is a transition from calc-silicate hornfels through serpentinised clinopyroxenite to relatively unaltered clinopyroxenite beneath the Platreef. A sharp magmatic contact marks the boundary to a dark, mineralised, serpentinised pyroxenite that continues about 25 m in the core to 317.5 m, and is succeeded by a 5 m thick section of coarse, mineralised gabbro. The gabbro is interrupted by a band of noritic pegmatite that may be a dyke or offshoot of a larger dyke, as the appearance of the pegmatite is similar to that of the dyke in the far right of face N1 (Fig. 5-27). Other, likely related pegmatite bands occur at various depths in this core.

The mineralised gabbro is followed by another thin zone of serpentinised pyroxenite (2 m), then by 3 m of serpentinised clinopyroxenite in upper contact with mineralised gabbro (2 m). These pyroxenites and gabbros are interpreted as Platreef. There is no evidence of tectonic contacts to the intervening clinopyroxenite, which is therefore interpreted as a metasomatised footwall xenolith.

A steep felsite vein terminates the magmatic succession at 305 m and marks an abrupt transition to a thick section (27 m) of serpentinised clinopyroxenite and relatively unaltered clinopyroxenite that are part of the footwall. The felsite vein is interpreted as a fault that has juxtaposed the footwall against a relatively high level of the Platreef. The footwall succession continues to 278 m where it is terminated by an apparent pegmatitic dyke. This does not resemble pegmatoidal variants of the reef and is again interpreted as a relatively late dyke akin to that in face N1. Above the dyke, and intruded by it, is a 10 m thick section of mineralised Platreef pyroxenite with a sharp, upper magmatic contact to hangingwall mesonorite.

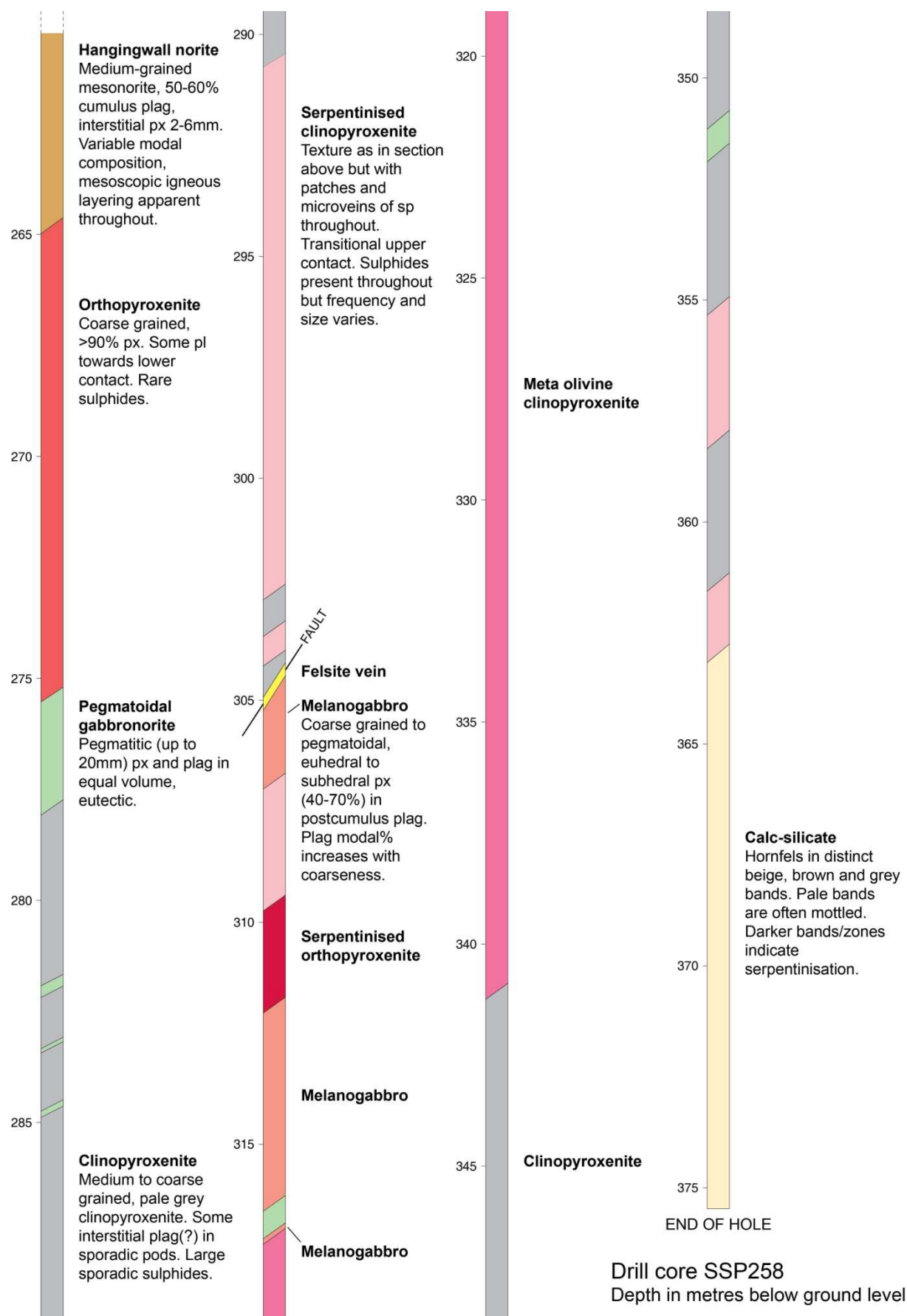


Fig. 5-51. Geological log of drill core SSP258. Colours for the various lithologies are the same as for the face maps (see legend in Fig. 5-27).

The three individual cores are no more remarkable than the face maps, but when considered together they reveal several significant features. Starting in the footwall, bands of clinopyroxenites occur at considerable distance from the base of the reef, and are separated from it by up to tens of metres of granular calc-silicate hornfels. It is believed that the clinopyroxenites represent the highest grade of footwall metamorphism (e.g. Buick *et al.* 2000), indicative of thorough metasomatism and recrystallisation of siliceous dolomite to coarse diopsidites that preserve no textural sign of their sedimentary origin. The highest grade of metamorphism would be expected immediately below the Platreef, as commonly represented in illustrations of ‘typical’ Platreef stratigraphy. However, the occurrence of thick bands and roughly lenticular bodies of clinopyroxenites at various distances from the reef (e.g. Fig. 5-14) strongly suggests there are other controls on footwall metamorphism and metasomatism. These may be primary mineralogy, variations in degree of dolomitisation, variations in fluid content between beds, or a combination of these factors. The lenticular bodies are not tectonic as there are no discontinuities bordering them. Further, the angle of unconformity between footwall bedding and the footwall-reef contact does not appear to have affected the degree of metasomatism in beds abutting the contact (e.g. Fig. 5-48).

Faults are responsible for the major differences between cores SSP257 and SSP258, which are from two locations in close proximity. The presence of faults in the cores disguises the true thickness of the Platreef. Core SSP257, however, appears to represent a fairly ‘normal’ untectonised stratigraphy. Core SSP258 has by far the thickest section of (serpentinised) pyroxenite, and as serpentinisation has rendered the rock very friable in places, it is very difficult to distinguish possible faults in the strongly serpentinised rock. The thickness of this unit in core is compatible with the volume of serpentinised pyroxenite encountered in pit faces shown in Fig. 5-40, Fig. 5-44 and Fig. 5-48. Thus, in either case, faulting may not have affected the unit thickness.

The coarse gabbros of the Platreef nearly always have a fresh appearance suggestive of only slight alteration, in stark contrast to the pyroxenites, which are usually strongly serpentinised. Two possible explanations are considered: (i) the gabbros represent a relatively late intrusive phase of the Platreef, emplaced after alteration of the earlier pyroxenites; or (ii) the postcumulus plagioclase that envelopes the cumulate pyroxene crystals has acted as a barrier to fluids that would otherwise alter the pyroxenes – it is also notable that the plagioclase is often saussuritised. Further, the gabbros are coarser than the pyroxenites, offering fewer crystal boundaries as pathways for infiltrating fluids.

5.8 Summary of observations

There are five major conclusions to be drawn from the face mapping, drill core logging and petrography:

1. The Platreef was emplaced before the hangingwall and a considerable gap in time separates them, as the Platreef had evidently cooled below solidus prior to its erosion by the hangingwall.
2. The original thickness of the Platreef (pre-Main Zone) is unknown but probably not much thicker than its present expression, as the Platreef is not totally eroded by the Main Zone at any locality at Sandsloot or, as far as other studies show, in other sections of the reef.
3. Despite some lateral similarity, e.g. between faces N3 and SW3 in the same pit bench, the Platreef shows significant compositional variation in three dimensions. The variation is a primary igneous heterogeneity as well as a result of alteration processes. However, there is no evidence of relative chronology of the igneous phases within the reef, e.g. magmatic contacts between gabbroid and pyroxenitic lithologies.
4. The general shape and thickness of the Platreef mapped in available rock faces, and possibly the thickness of the orebody, is structurally controlled by a pre-existing ~ENE-WSW fold phase and a ~N-S fold phase, but structures do not appear to be responsible for the lateral and vertical variation in the composition of the reef.
5. Fe replacement of pyroxenitic Platreef occurs in the southwest extension of the pit, indicating that that ironstone may have constituted the roof rocks of the Platreef at this location.

6. MINERALOGY AND GEOCHEMISTRY OF THE PLATREEF AT SANDSLOOT

This chapter presents data for bulk geochemistry comprising major element, trace element and PGE concentrations for a wide range of reef, hangingwall, footwall and dyke lithologies. The purpose is to elucidate patterns and anomalies to verify the first and second order observations presented in Chapter 5, providing more evidence for the interpretation of the various lithologies and their relationships. In addition, the results of mineral analyses and studies of PGM are also discussed. These geochemical and mineralogical data further serve to highlight similarities and differences between the Platreef at Sandsloot, other sectors of the Platreef and other major PGE deposits of the Bushveld Complex.

6.1 Methodology

Bulk analysis for major element and trace elements was carried out at Cardiff University using a JY Horiba Ultima 2 inductively coupled plasma optical emission spectrometer (ICP-OES) and Thermo X7 series inductively coupled plasma mass spectrometer (ICP-MS). Samples were first ignited at 900°C to determine loss on ignition and then fused with Li metaborate on a Claisse Fluxy automated fusion system to produce a melt that could be dissolved in 2% HNO₃ for analysis. Full details of the standard ICP analysis procedures and the instrumental parameters are given in McDonald & Viljoen (2006). The geochemical data for Platreef, hangingwall and footwall samples in the present study are presented in McDonald *et al.* (2005a) in Appendix 3.

Detailed mineralogical examination and analysis of polished thin sections and blocks were performed at the University of Greenwich with a JEOL JSM-5310LV scanning electron microscope (SEM) and energy dispersive spectrometer with the aid of the Oxford Instruments ISIS 300 software suite. Further work on the same suite of samples was carried out at Cardiff University using a Cambridge Instruments LEO S360 SEM coupled to an Oxford Instruments INCA energy dispersive X-ray analysis system. Additional analyses were also conducted at the Natural History Museum, London, using a JEOL 5900LV (SEM) with attached Oxford Instruments EDX INCA system.

6.2 Bulk geochemical data

This section describes the bulk geochemical data of a range of reef, hangingwall, footwall and mafic dyke lithologies that characterise ‘typical’ reef. It also presents data for the ‘olivine replaced reef’ (ORR) and the ‘reef-footwall hybrid’ rocks that were identified petrographically in Chapter 5.

6.2.1 Major element trends

Fig. 6-1 and Fig. 6-2 show major element weight% for samples collected from faces N1 and SW1. These are given as face profiles for compatibility with the geological face maps in Chapter 5 (Fig. 5-27, Fig. 5-40). Faces N1 and SW1 were selected because they contain lithologies typical of the northern part of the central pit and of the southwest extension of the pit, respectively. As described in Chapter 5, the number and variety of reef lithologies is greater in the southwest and most of the variants occur in face SW1.

The major element profile of face N1 can be broadly divided into 5 sections, each reflecting the main lithological unit as follows: (1) mafic dyke at 2 m along the face; (2) footwall at 4 m; (3) pegmatoidal pod at 10-12 m; (4) Platreef gabbro between 22 and 30 m; and (5) hangingwall at 31 m. SiO₂ contents are in the region of 49-51 wt% for all lithologies except the footwall. MgO, Fe₂O₃, Al₂O₃ and CaO contents are fairly consistent in the Platreef gabbro from 22 to 30 m along the face and reflect the homogeneous appearance of the reef in face N1. The sample from the base of the reef at 11.5 m is low in MgO, possibly due to its proximity to the low-MgO pegmatoidal pod below. The proportions of these elements in the hangingwall and mafic dyke, however, are markedly different: both lithologies have far lower MgO and Fe₂O₃ relative to the reef, and a far higher Al₂O₃ content, reflecting the observed increase in plagioclase and decrease in modal pyroxene. While the difference is most prominent in the hangingwall, the fairly similar major element geochemistry observed between the dyke and hangingwall suggests a possible connection between the two rock types and this will be examined in more detail below. Note that there was no visible junction between the dyke and hangingwall on the bench above face N1 (thickly covered by blast debris). Although the dyke is highly pegmatitic and has no visible resemblance to the hangingwall, it does have a textural similarity in that plagioclase is generally the cumulus phase.

In the major element profile of face SW1 (Fig. 6-2), footwall rocks are not included because geochemical analyses began within the reef at 20 m along the face. As with face N1, there is a marked transition between reef and hangingwall, with low MgO and Fe₂O₃ contents in the hangingwall relative to the reef, and a higher Al₂O₃ content. Within the reef, major

element contents vary considerably and in different ways between samples: MgO shows a slight increase towards the top of the reef while Al₂O₃ exhibits a parallel and more subtle decrease that corresponds with an observed decrease in modal plagioclase. However, this trend is reversed at 43 m. The Fe₂O₃ content is consistent at ~14 wt% in samples collected at 20, 24, 28 and 36 m, then increases dramatically to a maximum of 22 wt% in the uppermost 7 metres of the reef. There is also a relatively high Fe₂O₃ anomaly at 32 m. This Fe₂O₃ enrichment near the top of the reef may be due to the presence of the Penge banded iron formation above the reef before emplacement of the Main Zone, as suggested in Chapter 5, or due to the presence of a xenolith of the iron formation.

The CaO content decreases dramatically from 20 to 32 m, which is the zone where petrographic work suggests that footwall-hybrid rocks are developed. Thereafter the CaO content attains values of 5-7 wt%, which are typical of the normal Platreef in face N1, and in the hangingwall there is a marked increase in CaO that corresponds to the observed increase in plagioclase content. A slight increase that reverses the trend at 36 m coincides with a decrease in Fe₂O₃. The petrography of SW1 samples, however, suggests the rock at 36 m is similar to that at 40 and 43 m, i.e. olivine-replaced reef. The CaO and Fe₂O₃ anomaly might therefore reflect minor local contamination by an assimilated country-rock carbonate xenolith, i.e. CaO enrichment at the expense of Fe₂O₃.

The convincingly high CaO content at 20 and 24 m, at the expense of MgO, is consistent with the petrography of samples from these localities that suggests a footwall-reef hybrid lithology. The high CaO content is likely a result of the physical mixing of footwall dolomite with the reef magma. Consistent differences are also seen in other elements (Table 6-1): Cr concentrations are 2406–3065 ppm in reef rocks and ORR but markedly lower (600–800 ppm) in the hybrids. Cobalt concentrations show a more subtle difference, ranging between 53 and 137 ppm in the reef and footwall, but the lower half of the range generally characterises the hybrid rocks, and the footwall in faces SW1/SW2 has lower Co concentrations than the hybrids. Manganese shows similar concentrations in ORR and hybrids but significantly higher concentrations in the footwall. Titanium again shows broadly similar concentrations in ORR and hybrids (possibly slightly higher in ORR as one specimen stands out at 0.62 wt%) but great variability in the footwall, not only in faces SW1/SW2 but in all sampled faces. Thus, Cr and Co concentrations appear to reflect the mixing of footwall with the reef, while Mn and Ti seem inconclusive. However, ORR and hybrid samples in faces SW1/SW2 have higher Mn and Ti concentrations than ‘normal’ Platreef in face N1, and at least in the case of Mn it is possible that some Mn in altered reef in faces SW1/SW2 derives from the country rocks.

		Reef lithologies	Olivine replaced reef	Hybrid lithologies
Cr	ppm	2406–3065	1568–3104	602–835
V	ppm	126–133	127–261	76–333
Hf	ppm	0.26–0.55	0.35–1.22	0.32–1.70
Co	ppm	113–123	85–137	53–93
Mn	wt%	0.22–0.29	0.32–0.38	0.29–0.40
Ti	wt%	0.14–0.20	0.18–0.37	0.15–0.62

Table 6-1. Concentrations of selected trace elements in reef, ORR and hybrid lithologies in faces SW1 and SW2. Data from McDonald *et al.* (2005a).

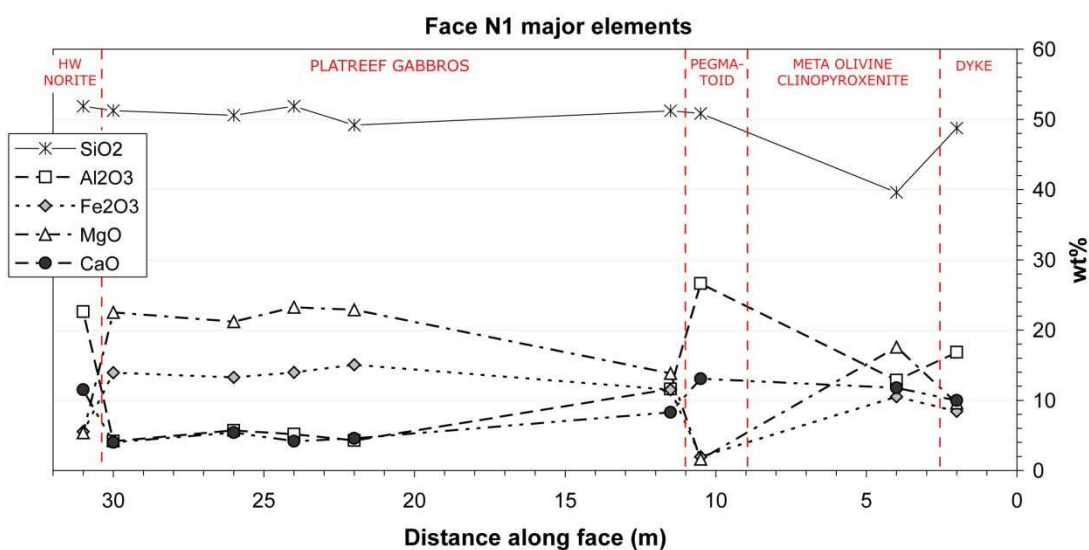


Fig. 6-1. Major element concentrations (wt%) in samples collected along face N1, with schematic face map (red lines and text) to show sampling locations.

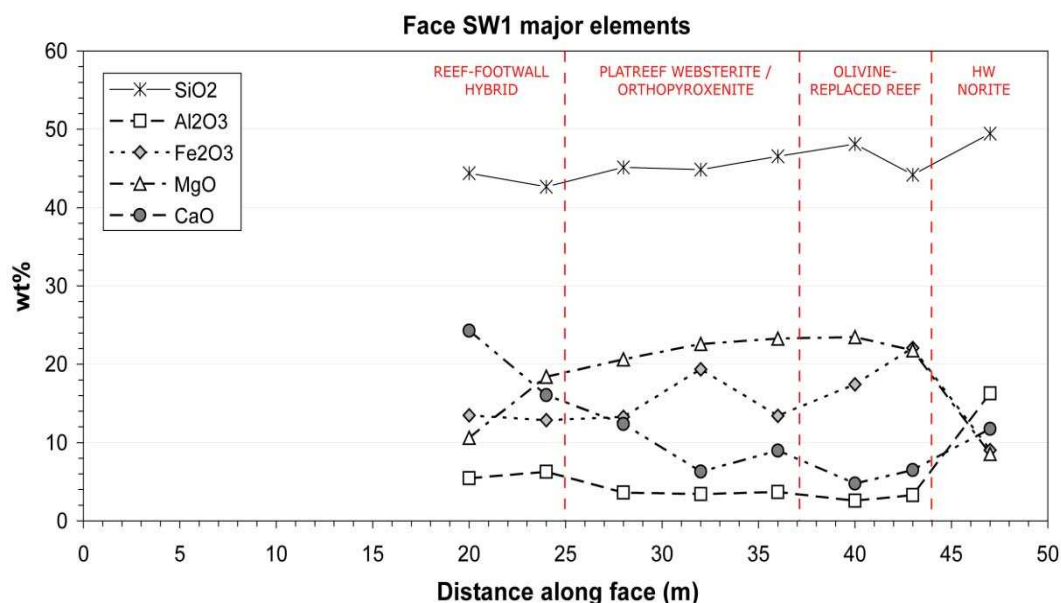


Fig. 6-2. Major elements concentrations (wt%) in samples collected along face SW1, with schematic face map (red lines and text) to show sampling locations.

Harris & Chaumba (2001) carried out a similar geochemical profiling study at Sandsloot. Although their work focussed on the significance of oxygen isotopes ($\delta^{18}\text{O}$ values) for crustal contamination and fluid-rock interaction, they also present major element data for a suite of samples collected across a 64 m long face (Fig. 6-3) on bench 20 in the east-central part of the Sandsloot south pit in 1995. This probably represented the lowermost available exposures at the time, 12-15 benches above the faces mapped in the present study. Those authors also recognised abrupt changes in composition across the hangingwall contact; particularly lower FeO and MgO but higher CaO in the hangingwall relative to the Platreef pyroxenites, which is consistent with higher plagioclase and lower orthopyroxene content in the hangingwall. For the parapyroxenites (metamorphic footwall clinopyroxenites), their study demonstrated an increase in CaO and decrease in MgO and Cr with increasing distance from the reef-footwall contact. This is consistent with the chemistry of the rocks either side of the parapyroxenites.

6.3 Mineral chemistry

Data for mineral analyses of orthopyroxene, clinopyroxene, plagioclase and olivine obtained during this work are provided in McDonald *et al.* (2005a; see Appendix 3).

Pyroxene is the most common mineral in the Platreef and can be readily compared between localities along the strike of the reef beyond Sandsloot. However, the Platreef pyroxene compositions are complicated by the presence of a reactive footwall that is rich in

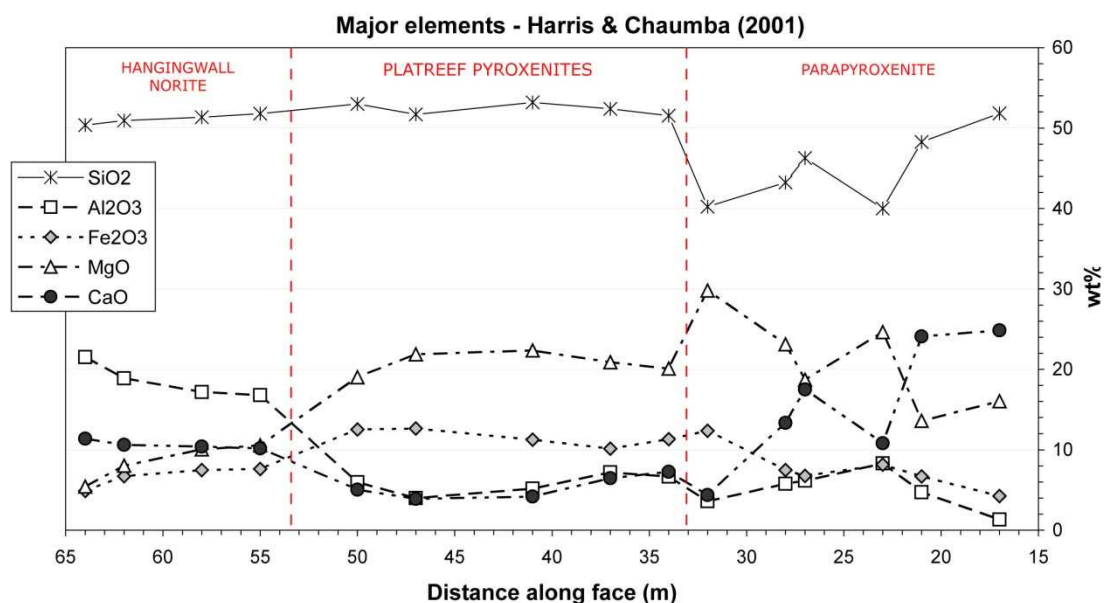


Fig. 6-3. Major elements concentrations (wt%) in samples collected by Harris & Chaumba (2001) from bench 20 in the east-central part of the Sandsloot pit. Schematic face map (red lines and text) shows sampling locations.

both Ca and Mg. The original roof rocks were probably identical to the footwall, as demonstrated in Chapter 5. The data for Sandsloot show a range of orthopyroxene compositions with a main population between $Mg\#_{76-80}$ in samples of primary reef gabbro and pyroxenite, but with sub-populations of $Mg\#_{81-83}$ and $Mg\#_{64-74}$ (Fig. 6-4). Harris & Chaumba (2001) acquired similar results for pyroxenes in Platreef pyroxenites and norites in a higher bench in the Sandsloot mine. The high $Mg\#$ population in the present study represents one gabbro sample (N1-26) associated with ragged serpentinite xenoliths (Fig. 5-27, Fig. 5-30) and another gabbro (SW2-49) that has been partially altered to an assemblage of tremolite, actinolite, chlorite and sericite. Analyses from these two specimens are presented as ‘contaminated reef’ (N1-26) and ‘altered reef’ (SW2-49). In both specimens, the Ca content of clinopyroxenes is higher than expected for igneous pyroxenes (Wo_{45-48} ; Fig. 6-4) and the pyroxene compositions of these specimens seem to be affected by local enrichment in Ca and Mg.

The low $Mg\#$ population in the dataset (Fig. 6-4) represents specimens of ORR collected near the top of the reef in faces SW1 and SW2. Orthopyroxene is commonly replaced by Fe-rich olivine, strongly suggesting that the Fe-rich pyroxene composition is not primary but related to a late-stage influx of Fe-rich fluid (as suggested by McDonald *et al.* 2005a) or contamination of the reef by Fe-rich country rocks that formed the roof to the

Platreef, in a manner similar to that found further south on the farm Tweefontein where ironstones form the floor rocks (Buchanan & Rouse 1984).

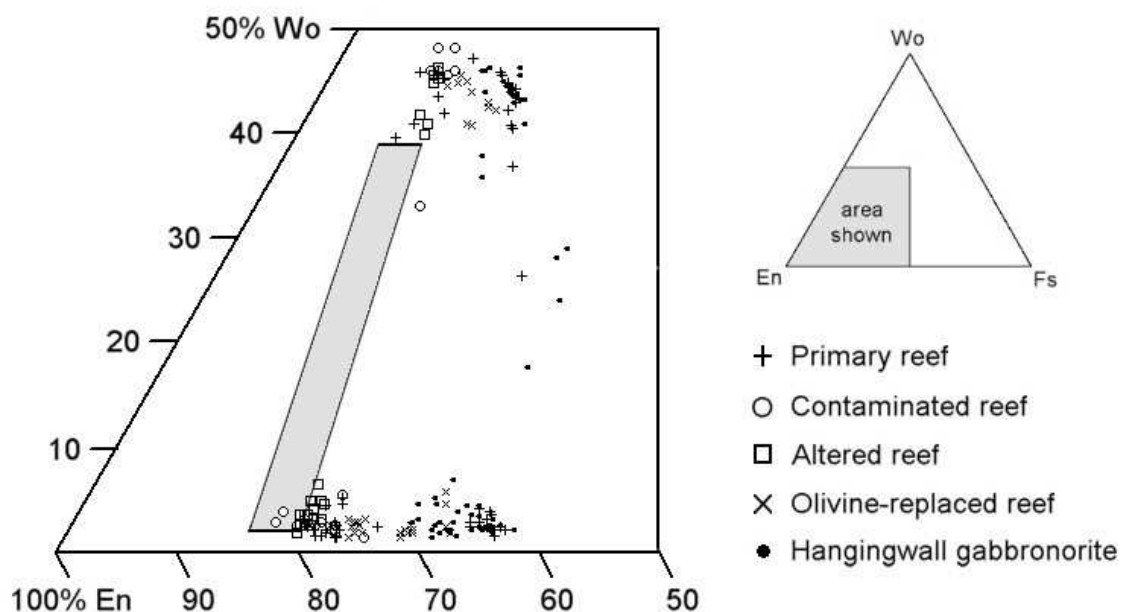


Fig. 6-4. Compositions of pyroxenes in Platreef gabbros (samples N1-26, SW2-49) and pyroxenites (SW2-77, SW1-40, SW1-43) at Sandsloot, from McDonald *et al.* (2005a). Shaded area shows the range of typical Merensky Reef pyroxenes (Buchanan *et al.* 1981).

6.3.1 Plagioclase compositions

Plagioclase grains were analysed in 3 reef gabbro samples and 1 hangingwall sample from face N1, 2 replaced reef samples from face SW1 and a single reef gabbro sample from face SW2. The main population has compositions of An_{60-83} , representing typical intercumulus plagioclase in the reef and hangingwall samples. There are no subpopulations within this range. A small population at An_{92-98} represents radial calcic rims between the interstitial plagioclase and cumulus pyroxene grains.

The An_{63-84} range for plagioclase in this study overlaps with ranges for both the GNPA member south of Mokopane (Hulbert 1983) and the Upper Critical Zone in the rest of the complex. However, the Platreef range extends beyond the lower part of the Upper Critical Zone range and above the range observed in the GNPA member. Thus, plagioclase of less anorthitic composition is present in the Platreef at Sandsloot despite the presence of a carbonate footwall. A possible explanation is that Platreef plagioclase is the postcumulus phase, and much Ca had already been incorporated into the early crystallised cumulus pyroxenes.

6.3.2 Olivine compositions

Buchanan *et al.* (1981) analysed apparently igneous olivine (Fo₇₅₋₇₆) on the farm Tweefontein and Manyeruke *et al.* (2005) reported magmatic Mg-rich olivine (Fo₇₉₋₈₀) in the Platreef at Townlands, but primary (magmatic) olivine has not been observed in any reef, hangingwall or dyke samples at Sandsloot. Whilst no comparison of primary olivine is possible, high-Mg metamorphic olivine (Fo₈₂₋₈₅) occurs in the footwall at Sandsloot (Harris & Chaumba 2001; McDonald *et al.* 2005a) and secondary Fe-rich olivine (Fo₆₀₋₇₁) that has grown at the expense of orthopyroxene occurs at the top of the reef in faces SW1, SW2 and SW3.

6.4 Trace element geochemistry

6.4.1 Rare earth elements

Fig. 6-5 shows chondrite-normalised rare earth element (REE) plots for 14 reef samples from 3 different faces (N1, SW1 and SW2). Samples DH-P and DH-G are grab samples of reef collected from the bench above face N1 and are not shown on the face map. The chondrite normalised REE patterns for the reef gabbros and pyroxenites show moderate LREE enrichment with a tendency for U-shaped patterns in the most REE-poor samples, and a slight but consistent negative Eu anomaly. Sample N1-30 shows the lowest REE concentrations for all elements except La, perhaps due to the proximity of this sample to the serpentinised shear zone that juxtaposes the reef and hangingwall, where REE were possibly removed by fluids in the shear zone. Similarly, sample SW1-20 stands out above the general pattern and the higher concentration of REE here may be a reflection of the hybrid character of the lithology, in which footwall material has mixed with the reef but was not fully assimilated.

In general, the data from the three different faces at Sandsloot define a relatively restricted set of normalised patterns, similar to those found at Overysel (Holwell & McDonald 2006) and to the LREE enrichment and stronger REE fractionation observed in the Upper Platreef at Townlands by Manyeruke *et al.* (2005) – see Fig. 6-6(a).

Some important observations by Harris & Chaumba (2001) that the present study corroborates are: (1) the sudden change in texture and mineralogical and chemical composition across the hangingwall contact; (2) the much coarser grain size of the Platreef relative to the hangingwall; (3) a greater degree of visible alteration seen in the Platreef; and (4) a lack of dolomitic xenoliths in the hangingwall. All of these observations support a separate magma for the hangingwall and intrusion of the Platreef prior to emplacement of the hangingwall. Further, field and microscopic textural evidence proves the hangingwall magma intruded after the Platreef had cooled below solidus (Chapter 5, sections 5.6.4 and 5.7.1).

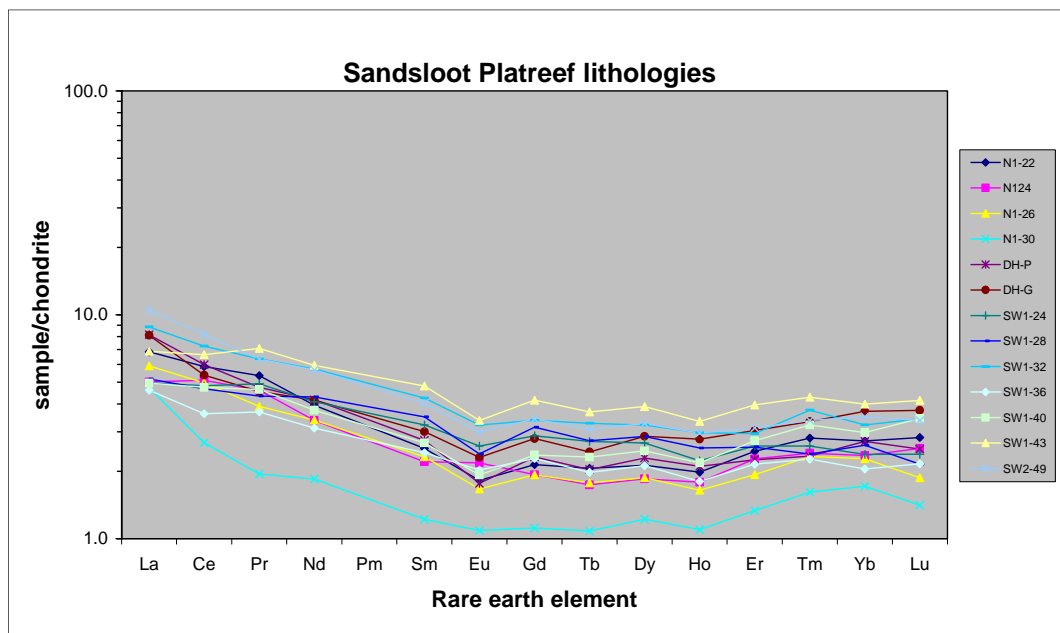


Fig. 6-5. Chondrite-normalised REE plot for a selection of Platreef samples.

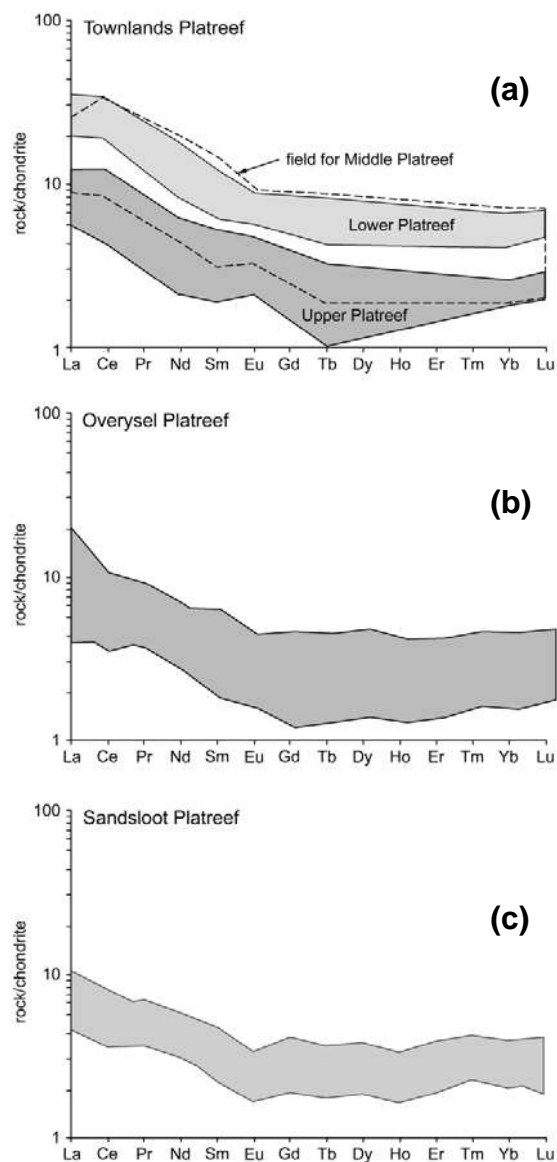


Fig. 6-6 (a-c). Chondrite-normalised REE plots for the Platreef and associated units at [a] Townlands (Manyeruke *et al.* 2005), [b] Overysel (Holwell & McDonald 2006) and [c] Sandsloot (this study and McDonald *et al.* 2005a). Overysel data is based on two drill cores. Figure modified from Holwell & McDonald (2006).

Fig. 6-7 is a chondrite-normalised REE plot for 6 hangingwall samples from 4 different faces (N1, N3, SW1 and SW2) and 3 dyke samples from face N1 (the E1-227 sample is from the northernmost extent of face E1 and is part of the dyke that occurs at the easternmost extent of adjoining face N1; Fig. 5-27). Again there is a generally flat pattern but with a marked positive Eu anomaly in contrast to the slight negative anomaly observed in the reef gabbros and pyroxenites. Two samples deviate from the general pattern. SW2-83 shares the general trend but shows a minor negative Eu anomaly. In Chapter 5, this was identified as a websterite reef xenolith that occurs a few metres above the hangingwall contact (Fig. 5-44), and its reef-like REE signature appears to be preserved. Sample N3X-4B, a leuconorite, has a consistently steeper REE curve (higher La/Lu_N ratio), with progressively lower HREE concentrations relative to LREE. The positive Eu anomaly, however, is the highest of all hangingwall samples, reflecting the high modal plagioclase content. Overlying the leuconorite in turn is a thinner band of fine-grained gabbro-norite (sample N3X-4A) that has a typical hangingwall REE signature. Above that is ‘normal’ hangingwall gabbro-norite (Fig. 5-37).

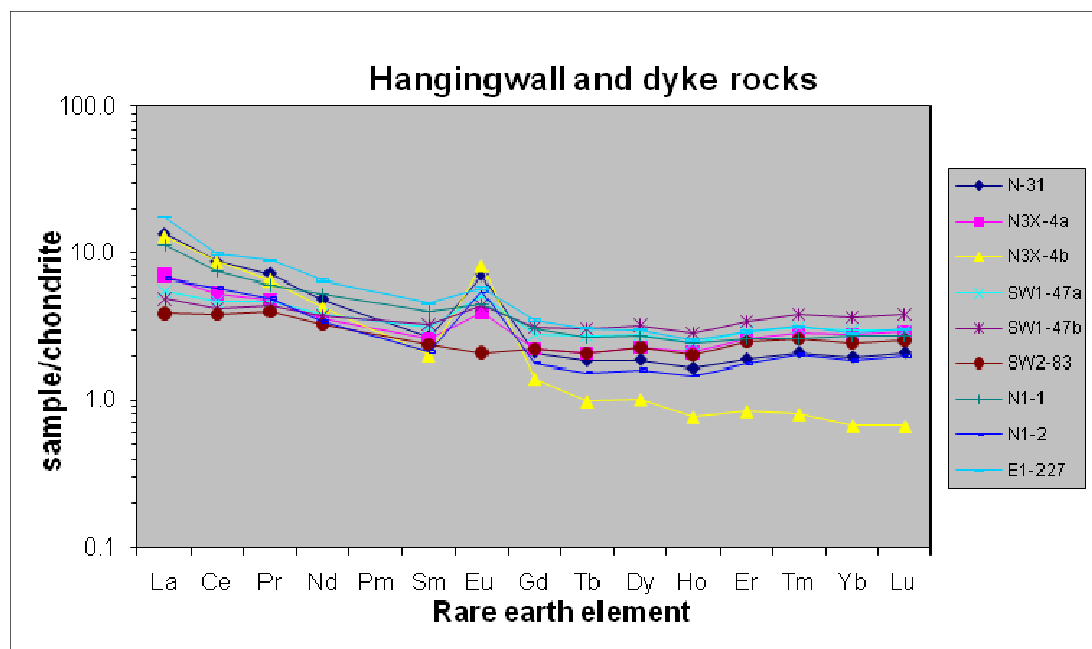


Fig. 6-7. Chondrite-normalised REE plot for a selection of hangingwall and mafic dyke samples.

Fig. 6-8 is a chondrite-normalised REE plot for 25 footwall samples from 4 different faces (N1, E1, S1, SW1). Faces N1 and E1, however, join at 90° such that the highest sample numbers in the long E1 face are close to face N1. A grab sample (P1) from a surface locality east of the satellite pit is also included. This is from a thin, discordant body of virtually pure, friable graphite that was exposed during surface stripping by a mechanical excavator. Similar

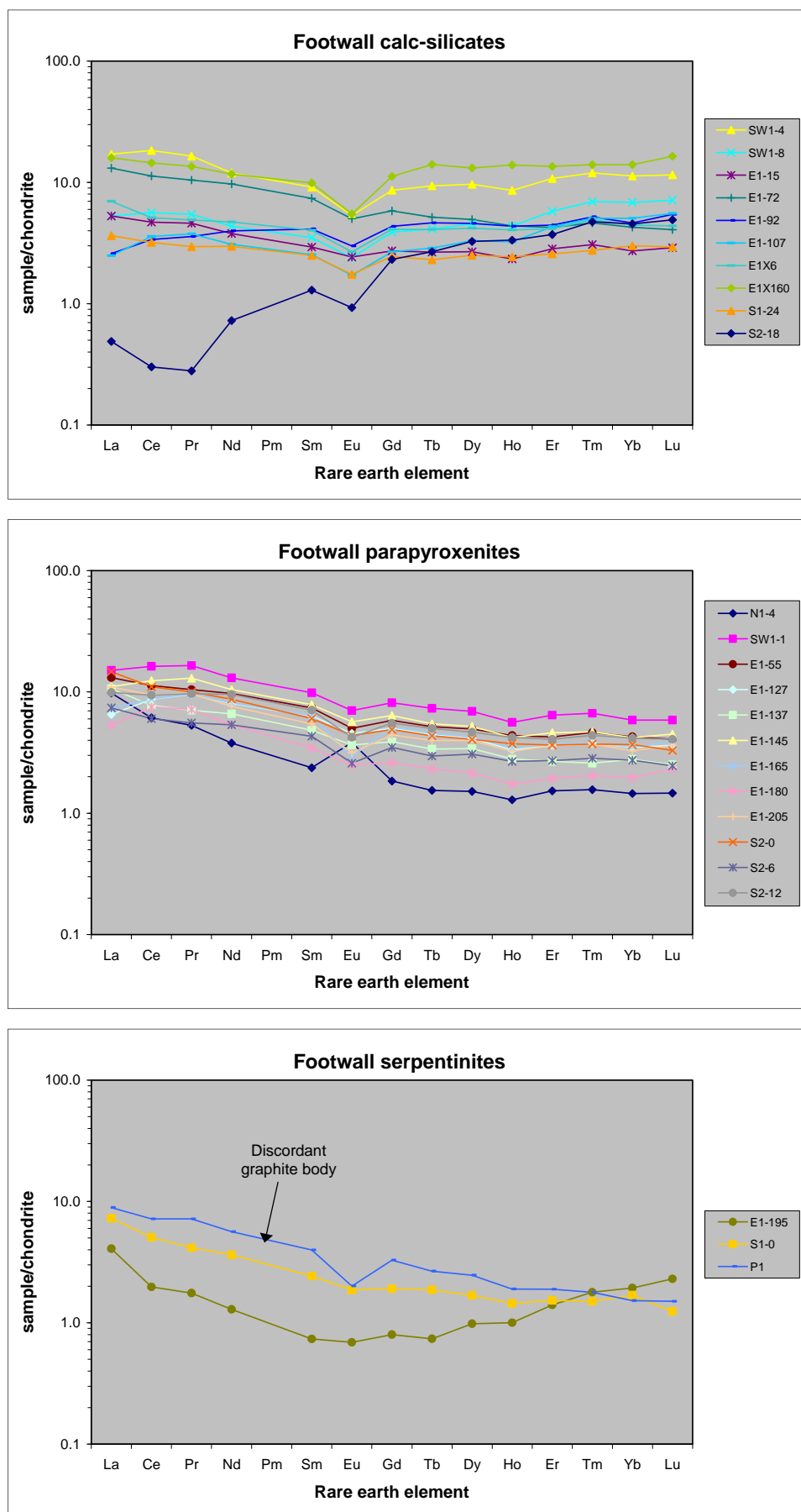


Fig. 6-8. Chondrite-normalised REE plot for footwall samples differentiated into main lithological types.

bodies were not observed in any exposures in the south pit. Its extent and relationship to the footwall is unknown but is likely a product of extreme devolatilisation and reduction of the original carbonate rock. It does, however, have a steeper and more negatively sloping REE curve than most other footwall lithologies.

The footwall rocks have a characteristic and in some cases quite pronounced negative Eu anomaly ($\text{Eu}/\text{Eu}^* 0.48\text{-}0.80$), and show a range of LREE:HREE fractionation. La/Lu_N in the footwall varies between 0.09 and 5.89, but most samples fall within the range 1.2-4.0, which overlaps with the narrow range (1.3-3.3) observed in the reef rocks.

Specimens E1-195 and S2-18 exhibit more prominent anomalous curves. E195 is unremarkable at the extremes of the REE range, although with lower concentrations than most other footwall specimens, but is progressively depleted from the extremes towards Eu. S2-18 is highly depleted in LREE and shows slight enrichment in HREE towards Lu. There is no obvious control on these patterns.

6.4.2 Spidergrams

This section presents and interprets primary mantle-normalised spider diagrams displaying the concentrations of REE, large ion lithophile elements (LILE) and high field strength elements (HFSE) in bulk samples of Platreef, hangingwall and mafic dyke. Two series of reef rocks are presented separately, one for the gabbro-norite-dominant N1 face (Fig. 6-9) and one for the pyroxenite-dominant SW1 and mixed SW2 faces (Fig. 6-10). Data for hangingwall samples from the same rock faces are given on a single separate graph (Fig. 6-11) as the hangingwall samples are macro- or microscopically very similar, in contrast to Platreef samples. Three samples were analysed from the mafic dyke in face N1 (Fig. 6-12): two from opposite margins of the dyke (specimens E227 and N1-2) and one from the middle of the dyke (N1-0).

Based on the composition of the marginal RLS rocks, it is generally proposed that they formed from two magma types: high-Mg basaltic andesite and tholeiitic basalt. The high-Mg basaltic andesite will be referred to as the B1 (Bushveld 1) magma and the tholeiitic basalt as the B2/B3 magma after Harmer & Sharpe (1985). In terms of major elements, the B1 magma could produce the Lower Zone and Lower Critical Zone cumulates, while the B2/B3 magma could produce the Main Zone cumulates (e.g. Harmer & Sharpe 1985). Primary mantle melt is expected to have smooth mantle normalised trace element patterns, but the shape of the patterns for the marginal RLS rocks suggest that they are not primary partial melts. The mantle normalised trace element pattern for the model B1 magma shows a strong enrichment

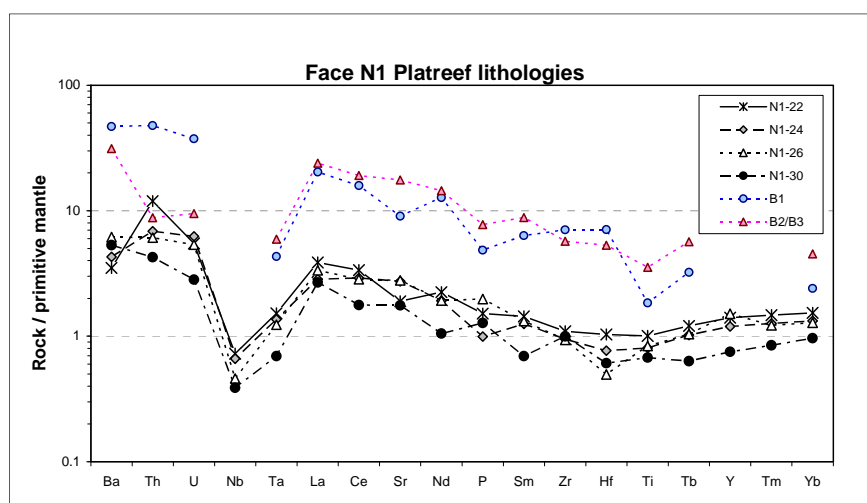


Fig. 6-9. Mantle-normalised concentrations of LILE and HFSE in a selection of reef samples in face N1. Trace element compositions of the model B1 basaltic andesite and B2/B3 tholeiitic basalt are given for comparison (data from Barnes & Maier 2002).

in Cs, Rb, Ba, Th and K (large ion lithophile elements: LILE). In contrast, the B2/B3 magma shows far less enrichment in LILE, although Ba is enriched and, consequently, the B2/B3 pattern has a positive Ba anomaly. Both magma types have large negative Ta, Nb, P and Ti HFSE anomalies. The shape of the B1 spidergram is similar to that of the upper crust, while the shape of the B2/B3 spidergram is similar to that of the lower crust. Thus, the trace elements suggest that the RLS magmas have undergone crustal contamination. Studies using various isotope systems confirm this: e.g. Sr isotope ratios, ϵNd values (Maier *et al.* 2000), and Pb isotope compositions (Harmer *et al.* 1995).

The most striking feature of the spidergram for face N1 (Fig. 6-9) is the strongly negative Nb-Ta anomaly for all specimens. This Nb-Ta anomaly characterises all Bushveld magmas (e.g. Barnes & Maier 2002). It can also be seen, for example, in the Rooiberg felsites (Fig. 12 in Appendix 5) and is a feature of arc-derived magmas. Further, it is common in lower crustal gneisses and granulites. In the Bushveld Complex, the Nb-Ta anomaly is thought to reflect large scale contamination of the parent magma by upper crustal material in a master magma chamber in the crust or at some level below the main intrusion (e.g. Hatton & Schweitzer 1995).

In terms of variation between specimens, N1-26 has a negative Rb anomaly, with a negative Hf anomaly nearly as pronounced as Nb. Adjacent specimens N1-22 and N1-24 display no anomalous patterns in terms of Rb, Zr or Hf and have very similar patterns overall. In sample N1-30, however, the concentrations of Rb to K and Hf to Yb are notably lower than in other specimens, but with small positive anomalies for La, Sr, P and Zr. This variation may

be due to processes associated with the adjacent serpentinised shear zone that defines the hangingwall contact in face N1, involving removal of most REE by the fluids responsible for serpentinisation.

Fig. 6-10 presents data for a range of Platreef, ORR, and hybrid lithologies in faces SW1 and SW2 in the southwest part of the pit. SW2-83 is a Platreef websterite xenolith in the hangingwall (Fig. 5-44) and its spidergram is similar to other reef samples in faces SW1/SW2, indicating that the entrainment of this reef fragment into the hangingwall magma has not affected its trace element signature. The ORR samples (Fig. 6-10b) have similar patterns to the reef samples, though SW2-35 is an oddity with no Nb-Ta anomaly; in fact it exhibits a slight positive Ta anomaly. The general similarity to 'pure' reef samples, however, implies that Fe enrichment of ORR was a process that did not involve major changes in trace element composition.

In contrast, the hybrid specimens (Fig. 6-10b) differ in several respects from the reef samples. Specimen SW1-20 stands out with strongly negative Ba, K, Sr and P anomalies but is enriched from Sm to Yb relative to the reef. Specimen SW1-24 is relatively enriched in Rb and K and shares pronounced K, Sr and P anomalies with SW1-20. The negative Sr anomaly is likely due to footwall influence, while the positive Sr and Nb-Ta anomalies in SW1-28 have no ready explanation. The unsystematic differences between the hybrid samples probably reflect incorporation of variable volumes of heterogeneous footwall material into the reef magma. Some differences are consistent with the settings of the specimens: SW1-20 was collected within the lower portion of the reef that was petrographically characterised as 'reef-footwall hybrid' (Fig. 5-40) and greater footwall content or contamination explains the overall variation in the spidergram; SW1-24 is also hybrid but represents the stratigraphically higher transition between lesser hybrid and 'purer' reef rocks, so a much smaller footwall influence is apparent.

Comparing 'normal' reef in face N1 to ORR in faces SW1/SW2, two differences are revealed: a near-flat Tb to Yb pattern and a negative P anomaly in faces SW1/SW2. The La-Hf pattern may be somewhat flatter in faces SW1/SW2 as well; at least Sm-Zr-Hf defines a flatter pattern with higher concentrations than in face N1, which has a concave pattern with a low at Hf. Notably, specimen SW2-35 lacks a Nb-Ta anomaly for no apparent reason.

Comparing the data for faces N1 and SW1/SW2, the SW1 series of reef specimens is characterised by a negative Ti anomaly which, like Nb-Ta depletion, is a sign of crustal contamination that is common in Bushveld magmas. The exception in the southwest area is specimen SW1-40, where the Ti anomaly is small and barely discernible relative to the Hf-Ti-Tb trend. More significantly, however, the Ti anomaly is not seen at all in any of the Platreef

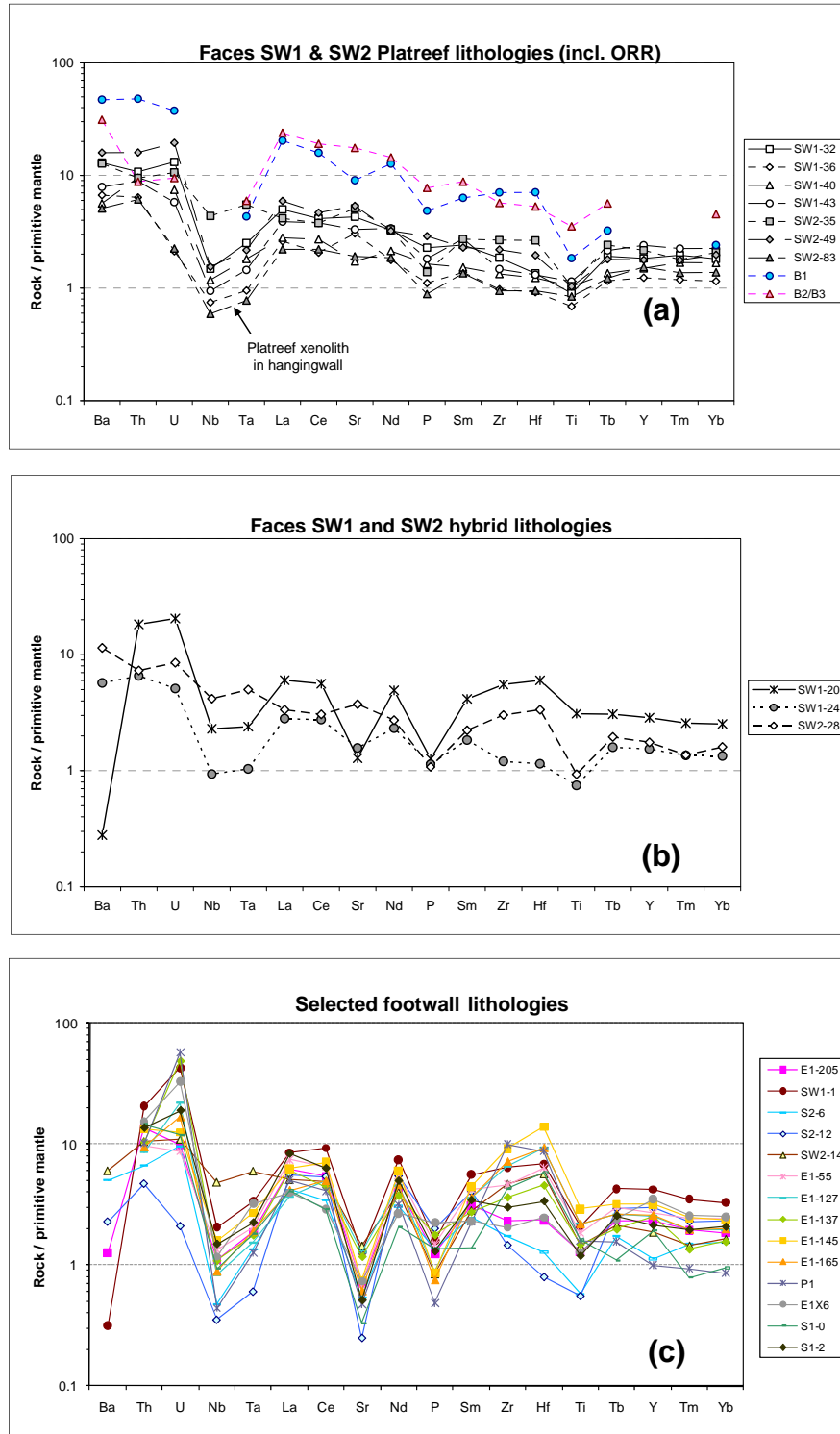


Fig. 6-10 (a-c). Mantle-normalised concentrations of LILE and HFSE in a selection of [a] reef (including olivine replaced reef), [b] hybrid and [c] footwall samples (calc-silicates, parapyroxenites, serpentinites) from face SW1 and SW2. Trace element composition of the model B1 basaltic andesite and B2/B3 tholeiitic basalt are given for comparison (B1 and B2/B3 data from Barnes & Maier 2002).

samples in face N1. This has no obvious explanation but is possibly some kind of Main Zone effect, as no Ti anomaly is seen in the hangingwall rocks (Fig. 6-11). However, it is questionable whether emplacement of the Main Zone would affect the composition of the underlying cooled reef below the very uppermost zone.

The spidergram for hangingwall samples (Fig. 6-11) from three different rock faces (N1, N3 and SW1 faces) are more consistent than Platreef samples. Hangingwall specimens show a generally steeper gradient, and within the range there is far greater variation relative to the Platreef. Notable differences are the enrichment in Rb, K, La and Sr and the more negative Nb-Ta anomalies. There is a less pronounced P depletion and Sm enrichment, and the general Zr to Yb pattern trends upward from Hf to Y, then flattens out. The Zr to Yb pattern is flatter in the Platreef, except for the negative Ti anomaly in the southwest faces.

Specimen N3X-4B has the steepest overall gradient with slight enrichment in LILE and a more marked depletion in HFSE, reflecting the REE pattern of the same specimen (Fig. 6-7).

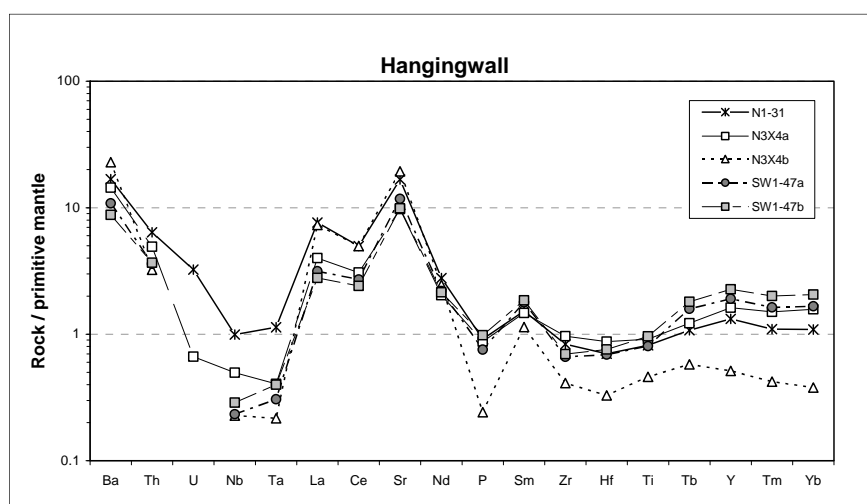


Fig. 6-11. Mantle-normalised concentrations of LILE and HFSE in a selection of hangingwall samples from faces N1, N3 and SW1.

The spidergram for the mafic dyke at the east end of face N1 (Fig. 6-12) is again distinct from the Platreef rocks and, to a far lesser extent, the hangingwall. The Ba to K pattern for the dyke is similar to the hangingwall but more enriched in these elements. Sr enrichment is equal to the hangingwall, and then from Nd to Yb there is slight variation between the specimens: E1-227 exhibits a gentle negative slope while N1-0 and N1-2 appear to have a minor positive Zr and Hf anomaly, with a minor negative Ti anomaly in N1-0.

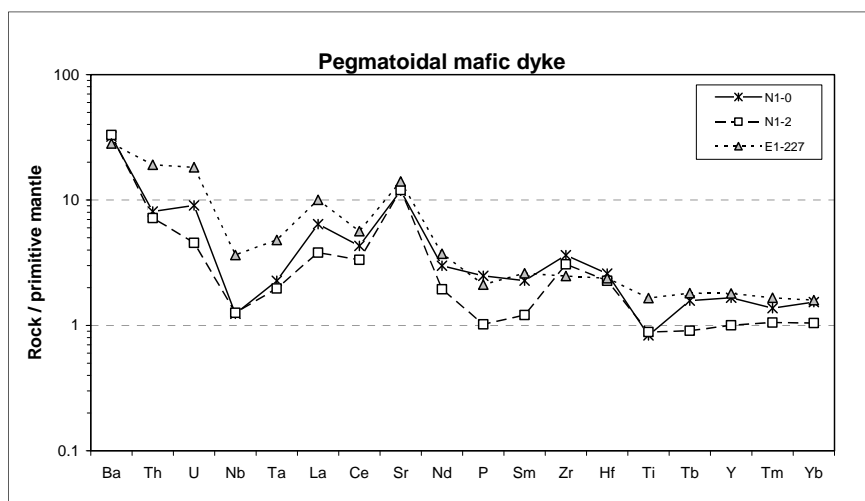


Fig. 6-12. Mantle-normalised concentrations of LILE and HFSE in mafic dyke samples from face N1.

6.5 Bulk PGE geochemistry

This section describes the bulk PGE geochemistry of a wide range of reef, footwall and hangingwall rocks, with evidence of high grade zones in non-reef units, and presents PGE ratios and normalised patterns for comparison with the Merensky Reef and UG2.

Bulk analysis for PGE and Au was carried out on a selection of samples using NiS fire assay collection followed by inductively coupled plasma mass spectrometry (ICP-MS) at the University of Greenwich. Details of the methodology and instrumentation have been given by Huber *et al.* (2001). The precision was determined by repeat analysis of a sub-suite of high and low grade specimens, and was 10-15% at PGE concentrations <5 ppb and 5-10% at PGE concentrations between 10 and 1000 ppb, but became worse again in specimens with PGE concentrations >1000 ppb due to the nugget effect – in these specimens the precision was 10-25%. Accuracy was determined by repeat analysis of the standard WPR-1. Solutions prepared from PGE-rich specimens were diluted by an additional factor of 50 to give comparable concentrations with the range of calibration standards.

PGE and Au concentrations and metal ratios in the Platreef and footwall lithologies are given in Table 6-2 and compared to those of other Bushveld PGE reefs. Chondrite-normalised patterns for PGE-rich samples are shown in Fig. 6-13. Although the reef pyroxenites and gabbros are consistently mineralised, there is considerable variation in PGE concentration within the reef. The mineralisation extends for a significant distance below the reef into the footwall. Some footwall lithologies are essentially barren, but certain zones and layers within the calc-silicate hornfels and serpentinites contain Rh+Pt+Pd+Au concentrations approaching those of the reef. The minor pegmatitic pods within the aplite body that separates

the footwall and reef in face N1 (Fig. 5-27) have high PGE concentrations, while the aplite itself is relatively poor in PGE. The pegmatoidal mafic dyke that cross-cuts the footwall contains very low PGE concentrations (<100 ppb Rh+Pt+Pd+Au): this is further support for a hangingwall origin, in addition to plagioclase being the cumulus phase, and an REE signature similar to the hangingwall.

6.5.1 PGE mineralisation in the lowermost hangingwall

PGE mineralisation is present within basal zones of the hangingwall where it overlies mineralised Platreef pyroxenite, and the primary PGM assemblage in these hangingwall zones is locally altered to one dominated by Pt/Pd germanides (Holwell *et al.* 2005, 2006). Evidence in Chapter 5 shows the hangingwall contact to be a magmatic unconformity and, as the hangingwall gabbro norites do not appear to be PGE-depleted (consistently 10-15 ppb), this suggests that PGE and S were scavenged or assimilated from the Platreef by the intruding hangingwall magma, producing zones of orthomagmatic PGE mineralisation in topographic depressions at the base of the crystallising hangingwall. It is notable that hangingwall mineralisation is absent where the hangingwall rests on the uppermost, thin, fine-grained, barren feldspathic pyroxenite of the reef, indicating that barren reef had to be breached by the hangingwall magma in order for it to scavenge PGE from the coarse-grained, mineralised feldspathic pyroxenite beneath.

The broader three-dimensional shape of the contact is uncertain due to the limited lateral exposure in the pit faces. The contact is likely to be either: (1) an irregular, undulatory surface with or without pothole-like structures, where PGE were scavenged from the reef and recrystallised *in-situ* in depressions; or (2) the contact may be a planar surface that cuts an undulatory contact between the barren fine-grained and mineralised coarse-grained reef pyroxenites, such that PGE now reside in the mottled anorthosite immediately above the breached, coarse-grained reef pyroxenite (Holwell *et al.* 2005). The first of these possibilities has some tentative field evidence; e.g. the small depression below the hangingwall contact in Fig. 5-48. The second possibility is illustrated by a similar relationship in Fig. 5-35, where an apparently planar hangingwall contact cuts an undulatory contact between reef pyroxenite/websterite and melanogabbro. Greater detail of the hangingwall contact here is shown in Fig. 5-37.

SAMPLE	LITHOLOGY	Ir	Ru	Rh	Pt	Pd	Au	Ru/Ir	Rh/Ir	Pt/Ir	Pd/Ir	Pt/Pd	Au/Ir
SW1-28	P'reef px'ite/websterite	61.5	226.0	207.3	3053	2378	398.5	3.7	3.4	49.6	38.6	1.3	6.5
SW1-32	P'reef px'ite/websterite	66.7	253.1	211.7	2125	2622	185.2	3.8	3.4	49.6	38.6	1.3	6.5
SW1-43	Platreef pyroxenites	117	503	540	6580	6460	1180	4.3	4.6	56.2	55.2	1.0	10.1
SW2-49	Platreef melanogabbro	119.9	393.0	273.0	4228	2857	313.2	3.3	2.3	35.3	23.8	1.5	2.6
SW2-83	Platreef websterite	2.3	5.0	4.7	175.6	106.7	25.3	2.2	2.0	76.0	46.2	1.6	11.0
N1-26	Platreef gabbro norite	34.4	109	137	4730	2440	880	3.2	4.0	137.5	70.9	1.9	25.6
N1-30	Platreef gabbro norite	85.8	385.9	302.4	3786	4082	472.9	4.5	3.5	44.1	47.6	0.9	5.5
DH-P	Platreef gabbro norite	51.1	200.7	194.6	864	1088	100.1	3.9	3.8	16.9	21.3	0.8	2.0
DH-G	Platreef gabbro norite	72.8	298.0	252.8	3052	2950	615.4	4.1	3.5	41.9	40.6	1.0	8.5
N1X-1	Gabbroic aplite	0.1	8.4	2.4	88.1	154	54	84.0	24.0	881	1540	0.6	540
N1X-3	Gabbroic pegmatite	58	103	55	1490	1570	220	1.8	0.9	25.7	27.1	0.9	3.8
N1-31	Hangingwall norite	0.16	0.22	0.00	3.62	2.67	5.83	1.4	0.0	22.6	16.7	1.4	36.4
N3X-4a	Basal h'wall gabbro norite	24.32	124.35	99.5	921.9	1014	19.84	5.1	4.1	37.9	41.7	0.9	0.8
N3X-4b	Basal h'wall anorthosite	1.15	8.2	0	24.43	28.1	4.42	7.1	0.0	21.2	24.4	0.9	3.8
SW1-47a	Hangingwall norite	2.29	7.84	8.65	166.1	170.5	20.28	3.4	3.8	72.5	74.5	1.0	8.9
SW1-47b	H'wall gabbro norite	1.03	2.36	2.24	45.8	48.4	10.81	2.3	2.2	44.5	47.1	0.9	10.5
N1-0	Pegm. mafic dyke	0.2	2.33	1.7	25.1	15.1	10.5	11.7	8.5	125.5	75.5	1.7	52.5
N1-0/2	Pegm. mafic dyke	0.1	0.31	0.51	2.2	0.8	0.9	3.1	5.1	22.0	8.0	2.8	9.0
S1-0	Serpentinite	7.4	30.3	36.0	341	629	40.9	4.1	4.9	46.0	84.8	0.5	5.5
S2-6	Diopsidite	0.1	9.1	6.2	30.1	10.9	7.7	91.0	62.0	301.0	109.0	2.8	77.0
S2-18	Calc-silicate hornfels	0.1	4.2	1.9	7.6	2.7	5.7	42.0	19.0	76.0	27.0	2.8	57.0
S2-12	Serp'ised clinopx'ite	0.8	6.3	2.8	55	100	35.2	7.9	3.5	68.8	125.0	0.6	44.0
S3-0	Serpentinite	0.1	0.73	0.25	10.8	109	69	7.3	2.5	108	1090	0.1	690
SW1-1	Serp'ised clinopx'ite	103.9	436.4	400.8	6755	7817	733.2	4.2	3.9	65.0	75.2	0.9	7.1
E1-55	Calc-silicate hornfels	27.9	66.2	100.3	1048	1064	40.8	2.4	3.6	37.6	38.2	1.0	1.5
E1-117	Diopsidite	7.4	31.8	55.6	698	1410	374	4.3	7.5	94.3	190.5	0.5	50.5
E1-165	Diopsidite	0.4	1.5	0.7	23.1	19.0	4.0	4.2	1.8	64.0	52.8	1.2	11.0
E1X-5	Serp'ised Ca-sil. hornfels	40.1	124	201	2590	3060	380	3.1	5.0	64.6	76.3	0.8	9.5
E1X-6	Serp'ised Ca-sil. hornfels	14.1	59.1	75.5	1060	1250	220	4.2	5.4	75.2	88.7	0.8	15.6
SARM-7	Merensky Reef	74	430	240	3740	1530	310	5.8	3.2	50.5	20.7	2.4	4.2
UG2	UG2 chromitite	60	106	600	3200	1960	50	1.8	10.0	53.3	32.7	1.6	0.8

Table 6-2. PGE and Au concentrations and ratios for Platreef, hangingwall, footwall and dyke lithologies (expanded after Armitage *et al.* 2002). PGE and Au data are reported in parts per billion. Additional data are also given for the Merensky Reef (SARM-7 preferred values from Steele *et al.* 1975) and the UG2 chromitite (McLaren & De Villiers 1982) for comparison.

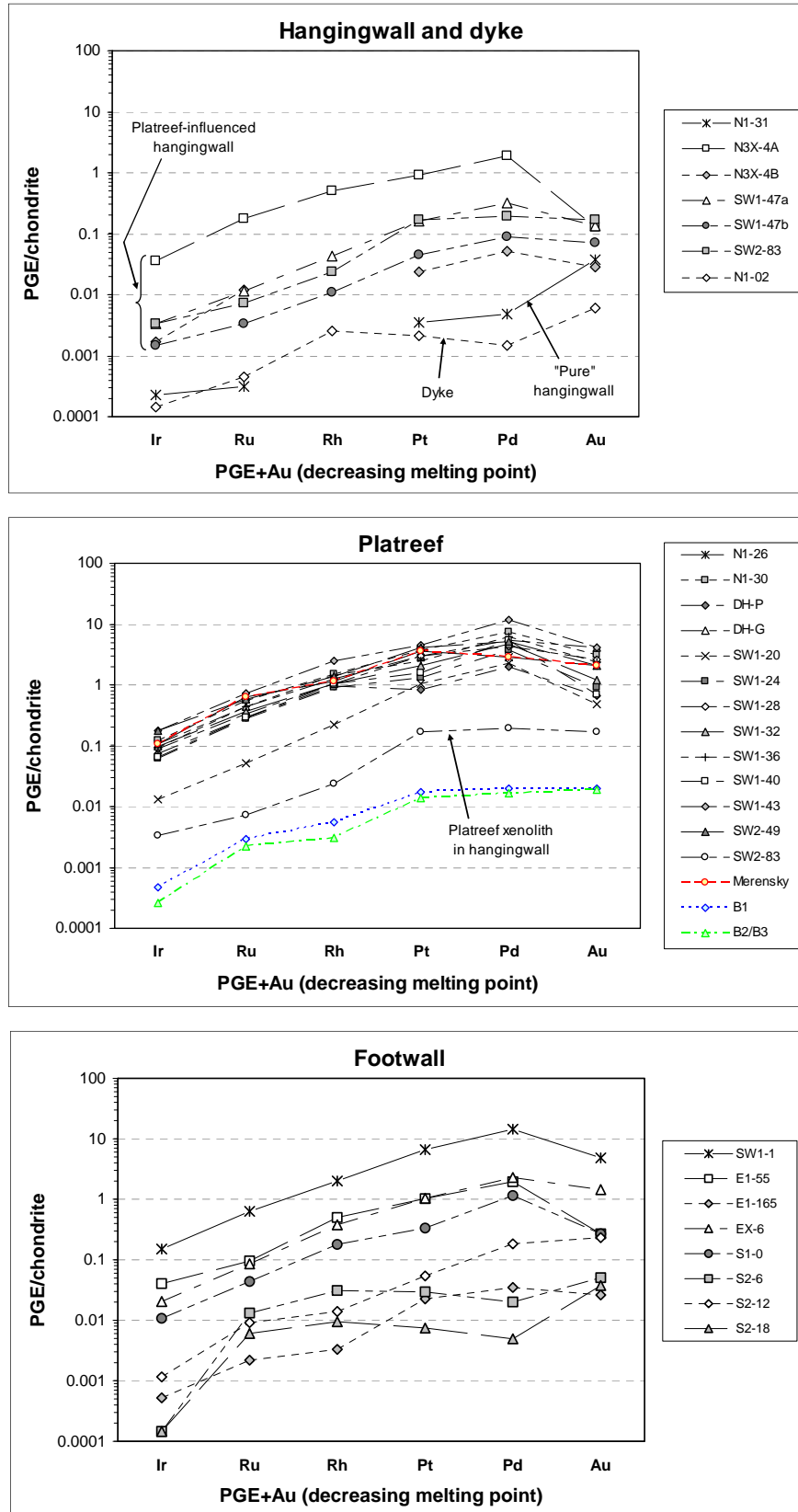


Fig. 6-13. Chondrite-normalised PGE concentrations of hangingwall, dyke, Platereef and high-grade footwall samples.

6.5.2 Comparison of PGE data with other Platreef sectors

Along the length of the Platreef, previously quoted Pt/Pd ratios vary widely from 0.3 (Manyeruke & Maier 2004) through 0.5 to 2 at the Turfspruit and Macalacaskop properties (Hutchinson *et al.* 2004; Kinnaird 2005a), 0.8–1.0 at Sandsloot (Vermaak 1995; this study) to 0.7–0.8 at Overysel (Holwell & McDonald 2006) with an average of 0.93 for several hundred analyses from both Drenthe in the north and Turfspruit/Macalacaskop in the south (Kinnaird *et al.* 2005). Earlier work indicated that there is a systematic variation in the Pt/Pd ratio from north to south (Lee 1996). However, data from both the southern and northern sectors indicates a similar overall ratio of 0.93 (Kinnaird 2005a), although there is as much variation in Pt/Pd ratios within one core as between areas (0.1–3.3 from >250 samples in one hole from the southern sector). Further, at Sandsloot, there is as much variation in the Pt/Pd ratio across one face as there is between faces and between different parts of the pit, even within identical rock (e.g. 0.8–1.9 in coarse gabbro in face N1; Fig. 5-27). In contrast, in the far south on Townlands, the Pt/Pd ratio is lower than elsewhere at 0.6 (Manyeruke *et al.* 2005). A further complexity is shown by geochemical and lithological work in the southern Platreef, indicating that it resulted from several pulses of magma, each of which is characterised by a package of rocks with distinctive geochemical characteristics and Pt/Pd ratios, with differing sulphide textures and proportions (Kinnaird 2005a).

6.5.3 Comparison of PGE data with Merensky Reef and UG2

Comparison of the PGE ratios of the Platreef and its PGE-rich footwall lithologies with the Merensky Reef and UG2 chromitite reveals some interesting features. The Platreef and footwall are richer in Pt, Pd and Au relative to Ir than the Merensky or UG2 reefs, producing more fractionated PGE patterns (Armitage *et al.* 2002; Fig. 6-14). Pt/Pd and Pt/Au ratios in the Platreef and mineralised footwall are lower than in the Merensky or UG2 reefs. PGE-rich footwall samples and pegmatoidal aplites have generally lower Pt/Pd than reef gabbro or pyroxenite (1.0 or greater). This would appear to indicate some fractionation of Pd over Pt into late-stage fluids in the reef and footwall – a feature noted by Wagner (1929) and Ainsworth (1998) – due to the greater relative mobility of Pd compared to Pt and the other PGE (e.g. Wood 2002). Greater amounts of Pd during remobilisation of PGE into the footwall would imply that the original Pt/Pd ratio of the reef was unity or lower. Rh/Ir in the Platreef is comparable to that of the Merensky Reef, but lower than the UG2.

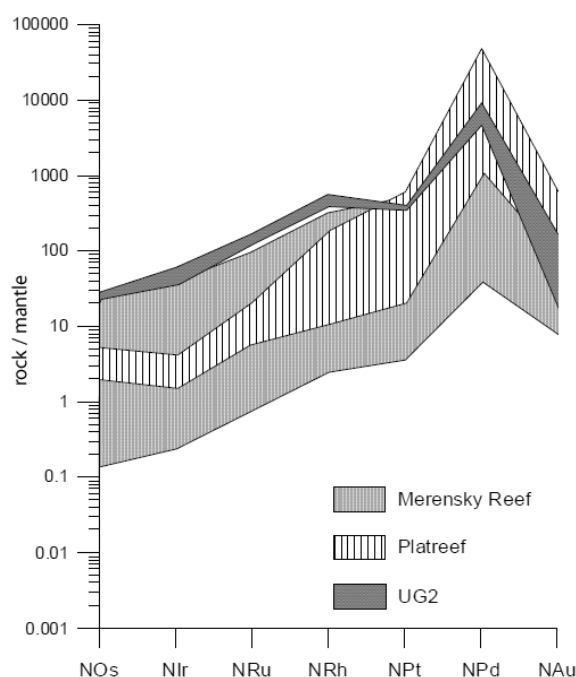


Fig. 6-14. Mantle normalised metal patterns for the Merensky Reef, UG2 chromitite and Platreef (modified from Kinnaird 2005b).

Nonetheless, the Platreef gabbros and pyroxenites and PGE-rich footwall lithologies show a remarkably close similarity in terms of PGE ratios and normalised patterns and define a restricted area on chondrite normalised plots. This has been substantiated by the follow-up study of Holwell *et al.* (2006) for the northern portion of the Sandsloot open pit. The aplitic pod and some of the low-grade footwall samples (e.g. S3-0 and S2-12) exhibit dramatic enrichments in Pt, Pd or Au, but the relative distribution of various PGE between PGE-rich reef and footwall is very consistent and seems to be more than mere coincidence. This type of footwall mineralisation is a general feature of the Platreef and it is present across the Sandsloot pit. An important finding is that the elevated Pt/Ir and Pd/Ir ratios found in the footwall at Overysel by Holwell & McDonald (2006) are not widely observed at Sandsloot. There is some enrichment of Pt and Pd over Ir in one diopsidite (E1-117) but other mineralised footwall hornfels and diopsidites produce patterns that are essentially sub-parallel with the normal reef.

Perhaps the most striking difference between the PGE deposits of the northern limb and the rest of the Bushveld Complex is to be found in their noble metal budgets: a feature first noted by Wagner (1929). The bulk Merensky PGE data compiled by Kinnaird *et al.* (2002) and Cawthorn *et al.* (2002a) show variation in the Pt/Pd ratio between different mining areas, in the range 1.8–2.9. This highlights the fact that Upper Critical Zone cumulates in general through the eastern and western Bushveld are systematically richer in Pt than Pd, i.e. Pt/Pd is >2.0 (with isolated values up to 24), for most of the sequence. The reasons for this striking Pt enrichment are not well understood but it seems to be a fundamental compositional feature of the magma(s) that fed the Upper Critical Zone.

PGE ratios for the Platreef at Sandsloot are lower than those found in the Upper Critical Zone elsewhere in the Bushveld Complex. The Platreef also shows greater fractionation of low temperature PGE (Pt and Pd) from high temperature PGE (Ir) than the UG2 and the Merensky Reef in the eastern and western lobes. The Platreef at Sandsloot and across the northern limb – e.g. Kinnaird (2005a), Holwell & McDonald (2006), Manyeruke *et al.* (2005) – shows Pt/Pd ratios lower than the Upper Critical Zone, where Pt/Pd ratios consistently exceed those in the northern lobe until well above the level of the Bastard Reef. Whatever the reason for the striking Pt enrichment in the eastern and western lobes during formation of the Upper Critical Zone, it is not repeated in the Platreef.

6.6 Platinum group mineralogy

6.6.1 PGM species

Prior to the beginning of this study, very little data had been published on the PGM assemblages of the Platreef. Only Schneiderhöhn (1929) and Mostert (1982) provided brief references to the most common PGM. Kinloch (1982) presented a summary of exploration borehole data from Zwartfontein and Overysel, and proposed a connection between regional variations in PGM and the degree of contamination and assimilation of the different footwall lithologies. Later, Viljoen & Schürmann (1998) calculated that the overall abundances of PGM in the Platreef were 30% Pt/Pd tellurides, 26% alloys, 21% PGE arsenides and 19% sulphides. However, these authors also emphasised the variations in PGM assemblages across the farms along the strike of the Platreef that had been explored by Anglo Platinum up to the early 1990s. They identified the most abundant PGM, from north to south, as: tellurides on Drenthe, sulphides and tellurides on Overysel, alloys and tellurides on Zwartfontein and Sandsloot, sulphides on Tweefontein North, and tellurides at Tweefontein Hill. Subsequently, Hutchinson & Kinnaird (2005) showed the Platreef on Macalacaskop and Turfspruit to be rich in Pd bismuthides, tellurides and antimonides.

In a preliminary characterisation of PGE mineralisation and PGM assemblages at Sandsloot (Armitage *et al.* 2002), 54 occurrences of individual PGM grains were identified in different reef and footwall lithologies. This was a forerunner to a more detailed study by Holwell *et al.* (2006) using a new set of thin sections from the same samples analysed in Armitage *et al.* (2002), as well as other samples collected from rock faces described in Chapter 5. More than 1000 individual PGM grains were identified. Platinum group mineralisation was found to occur throughout the Platreef, in footwall xenoliths in the reef, in the footwall and occasionally at the base of the hangingwall (Holwell *et al.* 2005; Holwell *et*

al. 2006). PGE grades vary within the reef and vary more erratically in the footwall. While overall grade in the footwall is lower than the reef, some serpentinised zones carry very high grades (section 6.5).

One of the most important findings of the studies by Armitage *et al.* (2002) and Holwell *et al.* (2006) is that there seems to be an almost total lack of PGE sulphides in the Platreef at Sandsloot. Even in the 1008 PGM grains analysed by Holwell *et al.* (2006) only a single grain of PGE sulphide (laurite: RuS₂) was found, and that was not in the reef but in basal mineralisation in the hangingwall gabbro-norite. The lack of PGE sulphides stands in stark contrast to the Merensky Reef (Fig. 6-15), UG2 chromitite and other sections of the Platreef, namely Overysel (Kinloch 1982; Holwell & McDonald 2007) and Drenthe (Gain & Mostert 1982), where PGE sulphides are common and occur as cooperite (PtS), braggite [(Pt,Pd)S], laurite and other rarer minerals. At Sandsloot, the only identified PGM containing any sulphur are a few instances of the sulpharsenide hollingworthite-platarsite-irarsite series (this study and Holwell *et al.* 2006).

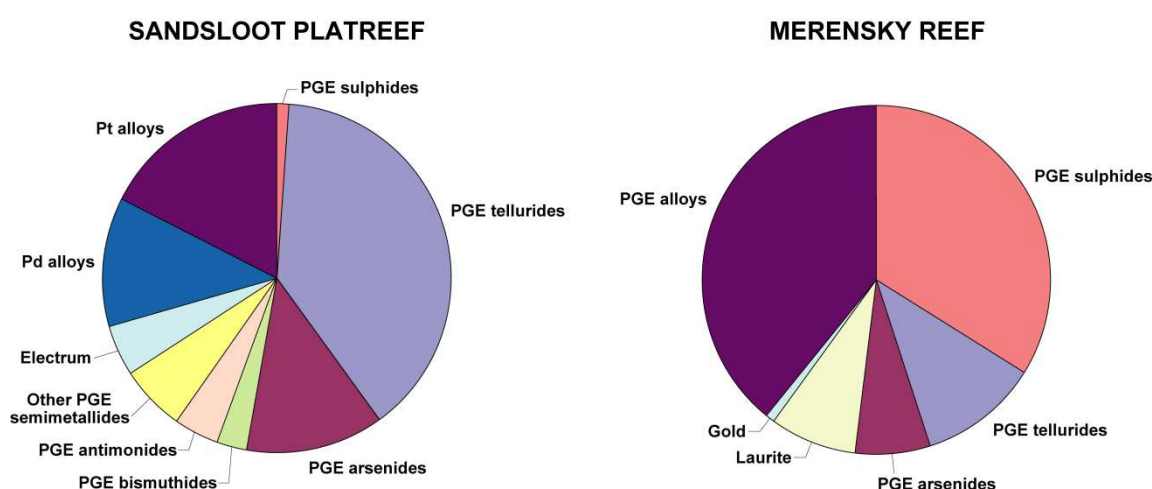


Fig. 6-15. Pie charts showing proportions of different types of PGM in Platreef samples from Sandsloot [left] and in the Merensky Reef for comparison [right]. Platreef values are based on this study and Holwell *et al.* 2006, Merensky values from Anglo Research Centre.

6.6.2 Grain size and morphology

In this study, the sizes of the great majority of PGM in the Platreef and footwall were found to be very small, nearly all <10 µm and mostly <5 µm. A few exceptions are in the size range 20–60 µm and these tend to occur in the coarsest igneous rocks. Similarly, analysis of grain size and morphology by Holwell *et al.* (2006) showed that in most rock types, ~80% of PGM

grains were $<10\ \mu\text{m}$ in longest dimension, except in the pegmatitic reef rocks, which had a higher average grain size with 50% of grains reported as $>5\ \mu\text{m}$ (presumably implying that a large portion of that 50% is $>10\ \mu\text{m}$). The lowest average grain sizes, where $>70\%$ of grains are $<5\ \mu\text{m}$, were found in the footwall calc-silicates, reef clinopyroxenites and hangingwall gabbro-norite. No grains $>100\ \mu\text{m}$ were found.

PGM morphology was found to vary according to phase and textural association. Where surrounded by sulphides, PGM grains and especially electrum occur as rounded blebs. Where surrounded by silicates, PGM grains are anhedral to euhedral (e.g. Fig. 6-16). Moncheite (PtTe_2) is commonly found as laths, Pt_2Fe as cubic crystals (e.g. Fig. 6-17), and sperrylite (PtAs_2) as tetrahedra (Holwell *et al.* 2006). A feature of the PGM assemblages revealed by the extensive dataset of Holwell *et al.* (2006) and not fully appreciated in the earlier study by Armitage *et al.* (2002) is that most PGM occur as single-phase grains. The earlier of these studies had suggested that compositionally zoned or polyphase PGM grains were common (e.g. Fig. 6-16), especially in some samples of olivine-replaced reef, but the wider study of Holwell *et al.* (2006) revealed the low frequency of these grains in the total PGM population.

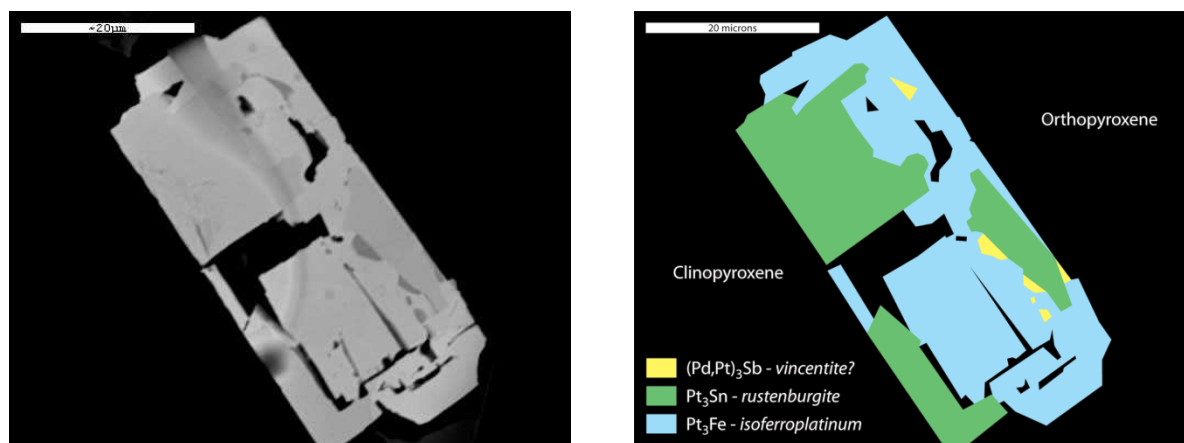


Fig. 6-16. [Left] SEM image of polyphase PGM grain with apparent matrix of isoferroplatinum and inclusions of rustenburgite and possible vincentite (with Sb, but no As or Te), occurring between large crystals of clinopyroxene and orthopyroxene in altered reef specimen SW2-49. [Right] Interpretation of PGM grain based on element mapping and spot analyses.

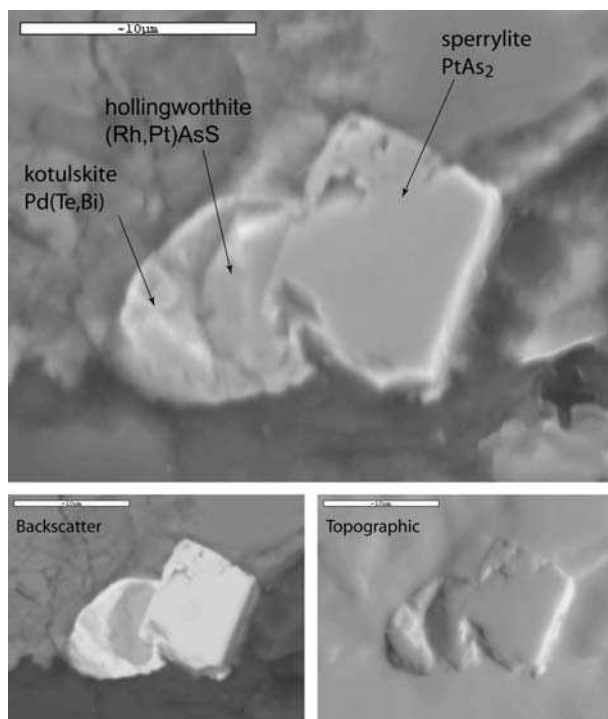


Fig. 6-17. SEM images of composite PGM grain in an intersilicate setting in specimen SW1-32. Note cubic form of sperrylite.

6.6.3 PGM distribution

The various host lithologies in the Platreef at Sandsloot contain their own characteristic PGM assemblages that reflect the processes controlling redistribution of the PGE through the reef and into the footwall during the evolution of the Platreef. The Platreef at Sandsloot is certainly richer in alloys and poorer in sulphides than at Overysel and Drenthe (Gain & Mostert 1982; Viljoen & Schürmann 1998; Holwell & McDonald 2007) where the footwall is Archaean granite/gneiss basement. This would suggest that greater volatile activity affected the Platreef where it intruded the dolomites than where it intruded the granites and gneisses, which is manifested in distinctively different PGM assemblages.

The pyroxenites and pegmatites of the igneous reef at Sandsloot contain a typical PGM assemblage dominated by Pt and Pd tellurides, electrum and some arsenides. Their presence in the interstitial regions, in close association with BMS, indicates a spatial relationship with the sulphides. The difference in PGM species between the igneous reef and mineralised metamorphic footwall units is striking. The dominance of tellurides, alloys and electrum with a total absence of antimony in the igneous reef is reversed in the footwall, where arsenides, bismuthides and antimonides dominate. The abundance of PGM containing semimetals such as As and Sb in the footwall lithologies suggests that significant volatile activity was involved in the redistribution of PGE into the footwall. The almost total absence of antimonides in the igneous reef is analogous to normal Merensky Reef, where PGE

antimonides are very rare (Kinloch 1982), while antimonides are common in areas where fluid activity has been prevalent.

Partial serpentinisation of footwall olivine has desulphurised BMS to form magnetite, a feature also seen in the Merensky Reef and UG2 (Li *et al.* 2004). In its early stages, the serpentinisation process appears to form a telluride-dominant PGM assemblage (often Pb-bearing) largely similar to that found in the olivine-replaced reef at Sandsloot. If there is a link between the two assemblages, it may be that the Fe-rich fluids that altered the reef originated from serpentinisation of the footwall (Holwell *et al.* 2005). An alternative put forward in the present study is that Fe enrichment is due to the presence of the Penge banded iron formation above the reef in pre-Main Zone time, which introduced Fe-rich fluids into the upper portion of the reef.

The PGM assemblage at the base of the hangingwall is of particular interest. Until the study of Holwell *et al.* (2005) the hangingwall was not thought to contain any PGE mineralisation, except around calc-silicate rafts (Kinnaird *et al.*, 2005). Holwell *et al.* (2005) conclude that the Platreef was almost completely crystallised when the hangingwall gabbro-norites were intruded. The PGE found in the basal portion of the hangingwall may be derived from sulphides and other low melting point components assimilated from the Platreef into the magma that formed the hangingwall gabbro-norites, forming an unusual ‘primary’ assemblage of PGM (e.g. thallides) including PGE sulphides and alloys. This assemblage formed as a result of the *in situ* cooling and fractional crystallisation of a PGE-rich sulphide liquid at the base of the hangingwall that is distinct from and postdates the main episode of mineralisation in the Platreef.

6.7 Summary

In face N1 in the northeast corner of the south pit (Fig. 5-27), the Platreef shows least evidence of replacement and is therefore considered to be the ‘freshest’ example of reef gabbro. There is a gradual increase in Fe₂O₃ towards the top of the reef where a serpentinised shear zone marks the boundary to the hangingwall. The plagioclase-rich hangingwall rocks and the discordant gabbro-norite dyke in face N1 carry a consistently positive Eu anomaly (Eu/Eu* > 1.0), while the opposite generally applies to the reef and footwall.

In face SW1 in the southwest part of the pit, Fe enrichment of the reef is dramatic and Fe replaced reef is also enriched in Ti, Mn, Hf and Nb, locally also in U and Th, relative to ‘primary’ reef. The source of Fe is uncertain but might have been a late-stage Fe-rich melt or fluid, or it may have been derived from contamination of the magma by banded ironstone of the Penge formation in the pre-Main Zone roof rocks.

The overall chemistry of dykes intruded into the footwall below the reef is distinct from the reef, and the LILE pattern of the dyke samples is similar to that of the hangingwall (Fig. 6-11). If the possibility is entertained that the dyke may originate from hangingwall magma, a direct parallel can be drawn with convincing observations at Overysel, where 3D mapping has shown hangingwall dykes penetrating the reef and footwall via previously formed shear zones (Holwell & Jordaan 2006). Additionally, some major element concentrations in the dyke, particularly Mn, are directly similar to the hangingwall, and are generally half the Platreef values and a quarter of Mn in the footwall (Appendix 3).

Relative to the model B1 basaltic andesite (Barnes & Maier 2002), Platreef lithologies in faces SW1 and SW2 show a similar spidergram pattern but are relatively depleted across the element range. In face N1, Platreef spidergrams follow the same general pattern as in faces SW1 and SW2 but lack the negative Ti anomaly seen in the model B1 basaltic andesite.

Footwall-reef hybrid rocks carry concentrations of Si, Mg, Ca, Fe, Co and Cr that are intermediate between reef and footwall concentrations. Nonetheless, Cr concentration is a useful indicator for primary reef, hybrid zones and footwall where lithological relations are ambiguous.

Previous studies on PGM mineralogy of the Platreef have identified sulphides, tellurides and arsenides as the dominant PGM, but in detail there appears to be significant variations as a function of the country rock intruded by the Platreef. The present study has shown that PGE sulphides are absent or extremely rare (e.g. hollingworthite in Fig. 6-17) in all parts of the reef at Sandsloot. Furthermore, different reef and footwall lithologies are characterised by different PGM assemblages, and the various rock types associated with the Platreef exercise a local control on the development of particular groups of PGM; e.g. Pt-Pd tellurides in the igneous reef, but arsenides, bismuthides and antimonides in the footwall.

The Platreef at Sandsloot has higher Pt/Pd and Pt/Au ratios than those of the Upper Critical Zone and the Merensky and UG2 reefs, but has higher Pt/Ir, Pd/Ir and Au/Ir ratios. Rh/Ir in the Platreef is comparable to that of the Merensky Reef, but lower than the UG2 chromitite.

7. DISCUSSION

This chapter aims to bring together the lines of evidence from the foregoing chapters to synthesise a model for the development of the Platreef at Sandsloot. The findings will be reviewed in light of the initial aims of the study presented in Chapter 1. Many aspects of the character of the Platreef at Sandsloot were poorly known before the present study began in 2000. This work, together with related studies, has shown the entire Platreef to have a more complex history than was previously appreciated. Deformation, magmatism, contamination by country rocks, and hydrothermal activity arising from thermal metamorphism of the country rocks have all contributed to the present-day character of the Platreef and its footwall.

7.1 *Emplacement of Platreef magma*

7.1.1 Intrusive relations

At present there is no proven magma feeder(s) to the northern limb. Point feeders have been proposed by some workers (van der Merwe 1976; Kinloch 1982; Kruger 2005a), while Friese (2004) and Kinnaird *et al.* (2005) have favoured the Steelpoort Fault and TML as linear feeders. On the basis of available data, the most likely location for a point feeder is the very high gravity anomaly located west of Mokopane and adjacent to the Ysterberg-Planknek Fault, which is part of the TML relay system.

The TML segregates the northern limb from the rest of the complex. A number of differences are apparent in the Bushveld stratigraphy north and south of the TML (Ashwal *et al.* 2004; McDonald *et al.* 2005a). Further, the crust and lithospheric mantle under the northern limb, known as the Pietersberg Block (Silver *et al.* 2004) is different to the crust and mantle below the Bushveld Complex south of the TML. There are similarities between the limbs that are summarised by Ashwal *et al.* (2004), but any attempt to apply the stratigraphy of the eastern and western limbs to the northern limb is perilous because it may lead to an uncritically assumed connection between the limbs, in the same way that the ‘A-B-C’ reef scheme for one Platreef locality was uncritically extrapolated to other sectors of the Platreef but was shown by this study and other work to be quite different.

An important first-order observation in this study has shown that the Main Zone gabbronorites intruded after the Platreef, and more detailed macro- and microscopic evidence presented by Holwell *et al.* (2005) and Holwell & Jordaan (2006) have shown that the Platreef

and Main Zone are temporally quite separate units with sufficient time for intrusion and deformation of the Platreef before intrusion of the Main Zone. Thus, the Platreef is not a basal facies of the Main Zone as was previously believed (e.g. van der Merwe 1976; Kruger 2005a) but represents an older intrusive phase. This relationship is pivotal when considering the source of PGE to the Platreef. Holwell & McDonald (2007) and McDonald *et al.* (2009) observe that the Platreef contains quantities of Ni, Cu and PGE concentrated from a larger volume of magma than represented by the Platreef itself: specifically, the PGE tenors of Platreef sulphides are very high and comparable to Merensky Reef. Cawthorn *et al.* (2002b) concluded that if the PGE were concentrated from above, it required many thousands of metres of overlying magma. In the eastern and western limbs, the Main Zone has been considered by some workers to be the source of PGE to the Merensky Reef (Page *et al.* 1982; Maier *et al.* 1996) and the Main Zone seems to be appropriately depleted in PGE (Maier & Barnes 1999). In the northern limb, however, the Main Zone gabbro-norites intruded after cooling and deformation of the Platreef and therefore could not have supplied Ni, Cu and PGE to the reef.

The findings of the present study also cast doubt on the assumption that intrusion of the RLS took place primarily along the junction between the Transvaal Group and the Rooiberg Group (e.g. Cheney & Twist 1991; Kruger 2005a) in the case of the northern limb. This is demonstrably not the case. Xenoliths of possible Rooiberg Group have not been reported anywhere in the Platreef. As Main Zone emplacement in the northern limb is now proven to be post-Platreef, the Platreef probably intruded entirely within Transvaal Supergroup sedimentary rocks or on the boundary between the Transvaal Supergroup and the basement granitic gneiss, such that these country rocks formed the roof as well as the floor to the reef (Holwell & Jordaan 2006). This would explain the presence of metadolomitic xenoliths in the Main Zone at Sandsloot (observed in drill core in this study) and further north beyond Zwartfontein, where the footwall is Archaean granite/gneiss basement and not Malmani Dolomite (e.g. van der Merwe 1978). PGE-mineralised calc-silicate xenoliths are reported in the Main Zone at Drenthe (Kinnaird *et al.* 2005), several km north of Zwartfontein where the Malmani Dolomite pinches out against Archaean basement. If the Platreef intruded along the contact between Archaean basement and Malmani Dolomite north of Zwartfontein, it is likely that the dolomitic roof rocks were mineralised in a similar way to the floor rocks at Sandsloot. The later Main Zone then intruded the mineralised metadolomite and preserved some of it as xenoliths.

7.1.2 Constraints on relative timing

The present work and a related study (Holwell *et al.* 2005) represent the most direct and detailed observations to date of the relationship between the Platreef and its hangingwall, and describe previously unrecognised features of the Platreef-hangingwall contact. Four complementary arguments are made for intrusion of Main Zone magma after emplacement of the Platreef: (1) cross-cutting relationships; (2) chilling and erosion at the base of the hangingwall; (3) PGE mineralisation in the hangingwall; and (4) source of calc-silicate xenoliths. This evidence was detailed in Chapter 5 and clearly shows that the Main Zone is post-Platreef. These observations have been confirmed in a wider study of the Platreef-hangingwall contact along strike in drill core by Weise *et al.* (2008). Therefore, a thrust zone could not have developed along the contact between the Main Zone and Transvaal Supergroup or between the Main Zone and Archaean basement, as envisaged by Friese (2004), because the country rocks were never in direct, full contact with the eastern margin of the Main Zone in the northern limb. Whilst in theory it would still be possible for a discordant thrust zone to have developed in the Transvaal Supergroup and be exploited by the intruding Platreef magma, the present study found no evidence of thrust-related fabrics associated with an east-verging thrust in the footwall, and Holwell & Jordaan (2006) report no such evidence from detailed pit mapping at Zwartfontein.

7.1.3 Structural controls on Platreef emplacement

The ‘four-leaf clover’ lobe-like shape of the Bushveld Complex is conspicuous and has been suggested to reflect the operation of different magmatic feeders and/or a conical fracture pattern caused by the Bushveld magma chamber. Alternatively, and perhaps more likely, the shape reflects the control of major lineaments such as the TML and related WSW-ENE crustal lineaments on the shape of the lobes/limbs, with magma entering the limbs at different crustal levels on either side of the lineaments. This does not necessarily imply that a single magma feeder supplied the entire complex, but does suggest an association between feeders and deep crustal-scale shear zones.

As discussed in the previous section, the present work has disproved emplacement of the Platreef along a thrust between the Main Zone and Transvaal Supergroup. Nonetheless, intrusion of the Platreef along some form of discontinuity in the country rocks still requires some consideration:

Friese (2004) presents annotated images from locations in the Sandsloot pit showing features interpreted as thrust-generated structures in the footwall immediately beneath the reef. The present study, however, found significantly sheared and duplexed footwall rocks at

just one locality (Fig. 5-34), and the orientation and vergence of the structures there are incompatible with the orientation of the Platreef. In fact, the orientations of the reef and shear structures are almost perpendicular to one another, and this geometry does not suggest a conjugate relationship. Even if a conjugate pattern were apparent, the Platreef is unlikely to have intruded exclusively into only one of the two sets of conjugate structures if magma emplacement was guided by those structures. At all other mapped and observed locations, bedding in the footwall meets the base of the Platreef at a discordant contact and sometimes at a high angle (see face maps in Chapter 5). Further, there are no observed pervasive thrust-related fabrics in the footwall that either cut the bedding or are roughly parallel to and adjacent to the Platreef, which would be the case if the reef intruded along a thrust zone. There are lenses of diopsidites in the footwall (described in Chapter 5), but these were shown to have primary mineralogical and/or metamorphic/metasomatic controls, as the lenticular diopsidites have margins that grade uninterrupted into the surrounding calc-silicate hornfels and are not bounded by tectonic discontinuities. Friese (2004) misinterprets these lenticular diopsidite zones as tectonic lenses after Armitage *et al.* (2002). It is also possible that Friese (2004) relied heavily on a pit exposure where footwall structures fortuitously have a similar vergence to the up-dip direction of the Platreef.

The development of a thrust zone within the Transvaal Supergroup in pre-Main Zone time cannot be entirely refuted, but it would mean that the Platreef completely obliterated the thrust fabrics. This seems unlikely, as no tectonic fabrics were found in the footwall even where the Platreef is thinnest. Further, Friese (2004) interprets the dolomite tongue as a pre-Bushveld structure, yet it seems highly improbable from a structural standpoint that the postulated thrust could have veered *around* this very prominent structure and was later exploited and filled by the Platreef. Another reason to doubt the thrust hypothesis is that the tongue is still intact and firmly attached to the sedimentary floor, as seen in the south highwall of the Sandsloot pit. In a thrust-tectonic setting, the tongue would probably have been detached from its floor.

7.1.4 Controls on the shape of the Platreef

The presence of the thick Main Zone, which is proven to have been emplaced *after* the Platreef and eroded it, means the original shape and thickness of the Platreef is not known. Only the basal contact of the reef is preserved, although the development of the olivine replaced reef facies may represent part of an upper contact zone. The most likely proto-Platreef geometry was a sheet a little thicker than the present Platreef, intruded above part of the Malmani Dolomite and below roof rocks that were likely to be the same sedimentary

sequence as the footwall. Tentative support is found in the southwest Sandsloot pit where Fe enrichment of the uppermost Platreef may have been sourced in overlying banded iron formation (continuation of the Penge Formation south of the pit on the northern flank of the dolomitic dome) prior to Main Zone emplacement. For the sake of discussion, the term 'Platreef sheet' will be used for the reef in pre-Main Zone time, as the Platreef is clearly a discordant body, whereas a sill implies parallelism to bedding or lithological contacts. Only north of Zwartfontein does it seem that the Platreef may have intruded along the basal contact of the Transvaal Supergroup with the basement Hout River gneisses and granites, e.g. at Drenthe.

The thickness of the Platreef sheet in pre-Main Zone time probably varied to some degree, controlled by pre-Bushveld country-rock structures that are preserved beneath the present footwall contact (e.g. Kinnaird *et al.* 2005). The final, present thickness is also controlled by Main Zone emplacement, as it appears the Main Zone has eroded more of the Platreef above structural highs than in the intervening lows and has 'levelled' the upper contact of the Platreef to some degree (illustrated schematically in Fig. 4-2). The degree of erosion is unknown but probably limited, considering that the reef has acted as a barrier to the Main Zone along its entire strike length (but not to the Upper Zone) and has not been totally assimilated by the Main Zone at any location; also considering that PGM which were 'cannibalised' from the Platreef (Holwell *et al.* 2005) have only been found locally in the lowermost 1-3 m of the Main Zone.

More importantly, the observation of a magmatic hangingwall contact in several pit faces and smaller exposures demonstrates that a magmatic boundary is the norm, with discordant shear zones locally juxtaposing hangingwall and Platreef lithologies, as in Fig. 5-27. Highly significant detail of the magmatic contact is presented in Holwell *et al.* (2005), who describe a specimen collected at the contact between fine-grained poikilitic leuconorite of the hangingwall and coarse-grained mineralised feldspathic pyroxenite of the Platreef in the northern part of the Sandsloot pit. The fact that the hangingwall rock is shown to erode the Platreef without permeating into it inherently requires a significant time break after emplacement of the Platreef, allowing the rock to cool sufficiently for it to behave in this manner. Holwell *et al.* (2005) found that in many of the mapped rock faces (additional to those in the present study), a planar magmatic contact occurs with poikilitic leuconorite or gabbronorite directly overlying the reef pyroxenites. A minority of faces display a sheared contact where the uppermost reef pyroxenites are sheared and subsequently altered to serpentine, sericite or carbonate. The overlying hangingwall rocks, however, show no evidence of shearing or alteration.

Another important finding of Holwell *et al.* (2005) is that PGE mineralisation occurs locally in the hangingwall, but specifically where the hangingwall overlies coarse-grained mineralised reef, and in these places the PGE grade in the lowermost hangingwall is sometimes comparable to that in the reef. Where the hangingwall overlies fine-grained, barren pyroxenite, there is no PGE mineralisation in the immediate hangingwall. This is a consistent relationship in the Sandsloot-Overysel sector. The mineralised zones in the hangingwall are typically in the lowermost 1 m and rarely more than 3 m. One example is an assemblage of Pd-bearing pentlandite, Pt-Fe alloy-BMS intergrowths and laurite. These are characteristic of an orthomagmatic PGM association (Kinloch & Peyerl 1990) and have not been observed in the Platreef pyroxenites (Armitage *et al.* 2002; Holwell *et al.* 2006; Hutchinson *et al.* 2004; Holwell & McDonald 2007; Hutchinson & McDonald 2008). Therefore the presence of mineralisation in the hangingwall appears to be very localised and highly constrained by the nature of the reef on which the hangingwall rests. Naldrett *et al.* (2008) observe high PGE tenors and Pt/Pd ratios in the upper portions of the reef in some boreholes at Sandsloot that they suggest is a primary feature. The sporadic occurrence of this high-grade zone may be related to its partial removal by the later Main Zone intrusion.

7.1.4.1 The dolomite tongue

The dolomite tongue is a critical structure at Sandsloot and is indicative of the relationships between the footwall, Platreef, Main Zone, and crustal or diapiric tectonism associated with the Platreef and/or Main Zone. The tongue is a contentious feature, as it is readily likened to structures in other parts of the Bushveld Complex that were formed by gravity inversion of country rocks (diapirs) during Lower Zone to Upper Zone emplacement. However, the Sandsloot tongue does not have the appearance of a fully developed diapir. Rather, there are strong indications that the tongue was largely a pre-Platreef structure but may have continued to form at a very late stage of Platreef emplacement or after emplacement:

- (1) An apparent attenuation of the Platreef around the tongue and the occurrence of scattered disseminated chromitite bands were noted by van der Merwe (1978). At face value, this suggests that the tongue may have been forming at a very late stage of Platreef emplacement or after emplacement. However, the present author found no surface exposure of the Platreef around the tongue just south of the pit (an area largely covered by mine dumps), although the area is strewn with small fragments of banded ironstone belonging to the Penge Formation that crops out a little further south at Tweefontein. It is possible that van der Merwe (1978) has misidentified the ironstone fragments for Platreef

chromitite. In any case, *widespread* fragments of (mistaken?) chromitite on the surface are unlikely to represent *rare* chromitite schlieren in the reef at Sandsloot mentioned by Holwell *et al.* (2006) and no chromitite bands/schlieren were observed in the mapped faces in the present study. Nonetheless, the major implication of the attenuation of the reef around the tongue (van der Merwe 1978) is that the tongue is unlikely to be a diapiric structure, as the original Platreef sheet may not have been much thicker than the present amplitude of the tongue. Therefore, the Platreef probably did not constitute a sufficient volume of magma to induce gravity inversion of the footwall.

A further implication is that the tongue could not have formed by diapirism prior to Platreef emplacement, as there was no other large igneous body that could have caused gravity inversion in the area at the time. The Lower Zone is only represented by relatively small satellite bodies in the study area and the dolomite tongue occurs west of and above the Zwartfontein Lower Zone satellite body. Although gravity data suggest a large volume of dense rocks and a more extensive development of the Lower Zone beyond the satellite intrusions, there is certainly not the 8 km thick sheet of Lower Zone rocks found in the eastern Bushveld Complex. Even with a thicker Lower Zone than is apparent at the surface in the study area, diapirism could not occur *above* the Lower Zone where the dolomite tongue occurs.

A more plausible explanation for the tongue is that it formed by N-S and ENE-SSW compressional fold interference prior to intrusion of the Bushveld Complex, and at least one of these folding events may have remained active during Platreef emplacement.

- (2) The Platreef has a fresh appearance in the southwest extension of the Sandsloot pit (e.g. Fig. 5-48), and preserves igneous textures despite minor deformation and some alteration. If the tongue was entirely a late syn- or post-Platreef structure, much more deformation would be expected in the southwest pit where the reef would be highly flexed by the developing tongue. The marked westward deflection of the reef here seems to be an emplacement feature controlled by the shape of the dolomite tongue, not caused by folding of the reef.
- (3) Van der Merwe (1978) observes that Main Zone layering is not deflected by the Sandsloot tongue but is only interrupted by it, strongly suggesting that the Main Zone was emplaced after the tongue formed and the layering onlaps against the existing structure. On the one hand, this is consistent with the argument above for a compressional tectonic origin for the tongue, and is also consistent with the proven *post*-Platreef emplacement of

the Main Zone. On the other hand, the Main Zone may represent a sufficiently large volume of magma to have caused diapirism of the footwall, leading to upwarping of igneous layering in a similar manner to that seen in large domal structures in the eastern and western limbs, e.g. in the Dwarsrand area. A tentative explanation of the apparent lack of syn-Main Zone diapirism (at least at Sandsloot) is that the dolomite tongue was ‘locked’ by the already cooled Platreef. Further, the Platreef may have provided a competent barrier to passive footwall tectonism along the entire northern limb during Main Zone emplacement, and this would explain the general lack of large domes penetrating the southern sector of the limb that is floored by the Transvaal Supergroup. In the northern sector, the gneisses that comprise the floor are even less likely to deform by diapirism. In other parts of the Bushveld Complex, diapirism appears to have been a continuous process beginning with Lower Zone emplacement and without a sufficient time break, such as the Platreef-Main Zone hiatus, to allow ‘locking’ of the underlying country rock structure by an earlier-formed igneous sheet. However, there are contradictory reports in studies of metasedimentary domes. For example, Gerya *et al.* (2004) consider the Schwerin fold in the eastern limb to be a syn-Bushveld diapir that penetrates the RLS, but Cawthorn (pers. comm. 2002) observed the Lower Zone pyroxenites above the Schwerin fold and found them to be undeformed.

- (4) It could be argued that the earliest layers in the Main Zone have been flattened by the later layers, thus bending the terminations of the early layers where they abutted and dragged against the dolomite tongue. Alternatively, the tongue was slightly accentuated by diapirism as a result of the overlying Main Zone magma, and upwarped the lowermost layers of the Main Zone as they developed. Minor diapirism of the dolomite tongue is conceivable if the Platreef did not entirely envelope the tongue. In either scenario, however, the tongue is implicitly a pre-Main Zone structure, which again is consistent with a compressional tectonic cause.

The corollary of the above relationships between the Platreef, Main Zone and dolomite tongue is that the tongue represents an interference of two orogenic fold phases, not a diapir, and that at least one of the two phases was in operation during Platreef intrusion, probably at a late stage but prior to total consolidation. This accounts for the attenuation of layers/bands within the reef and possibly some of the pre-Main Zone deformation observed in the reef (Holwell *et al.* 2005; Holwell & Jordaan 2006). Further support for this hypothesis is to be found in the geometry of the tongue: It clearly has an approximately ENE-WSW axis that renders a west-

pointing tip at the surface, but the fold geometry along this axis is unknown because there are no pit-face exposures *across* the axis. For the sake of argument, the ENE-WSW component is assumed to be a more or less upright open fold. When viewed along its approximately N-S axis in the south highwall of the Sandsloot pit, the tongue is asymmetrical with distinct eastward vergence (a steeper east limb but not overturned; Fig. 5-4, Fig. 5-7). A hypothetical diapir rising into Platreef magma would be affected by syn- to post-magmatic subsidence of the later Bushveld intrusions and consequent tilting of the layered rocks towards the centre of the limb, or towards the feeder, as documented by palaeomagnetic studies (Hattingh 1995). However, subsidence of the northern limb involving tilting to the west or southwest (seen in the overall dip of the Platreef and in Main Zone layering) cannot explain the slight *eastward* vergence of the dolomite tongue. In fact, the asymmetry of the tongue observed in the south highwall of the Sandsloot pit is exactly opposite to the tilt that would occur if a diapir was rotated by subsidence towards the west. The diapir would have a steeper or overturned west limb when viewed in E-W section such as the south highwall, whereas the opposite is the case.

An alternative explanation considered for the east-verging fold phase is a forcing mechanism caused by the subsiding northern limb as the volume of magma accumulated and cooled. This could have been caused by an outward thrusting of the Transvaal Supergroup at the margin of the Bushveld Complex such that radially verging structures were formed, as observed around other parts of the complex (P. Nex and J. Kinnaird, pers. comm. 2009). Similar structures are illustrated in Fig. 2a of Barnes & Maier (2002) but the cause appears to be the rising mantle plume beneath the Transvaal Supergroup. Neither of these mechanisms, however, explains why the emplacement shape of the Platreef appears to be affected by the dolomite tongue while the Main Zone does not.

Whilst an interference fold is the favoured interpretation for the Sandsloot tongue in this thesis, it does not discount a diapiric origin for large dome-like structures in other parts of the Bushveld Complex. A number of interpretations propose that some pre-Bushveld floor rock folds were accentuated by diapirism, but this cannot be the case at Sandsloot if, as stated by van der Merwe (1976), the lowermost Main Zone layering is undeflected along the tongue margin. Contrarily, in the local aeromagnetic image (Fig. 5-8), and as illustrated but curiously not considered by van der Merwe (1978), the lowermost Main Zone layering *is* upwarped against the base of the dolomite tongue and the degree of warping decreases towards the western tip of the tongue. This suggests that deformation ended in Upper Main Zone time. The contradictory nature of some findings of studies on Transvaal Group domes near the margin of the Bushveld Complex suggests that these structures may have formed at different

times and/or by different processes. In terms of diapirism, the major difference between the northern limb and the eastern and western limbs is that emplacement of the RLS south of the TML appears to have been a continuous process and therefore conducive to diapirism, whereas in the northern limb the Main Zone was probably the first igneous body capable of inducing significant diapirs, but was prevented from doing so by the previously emplaced Platreef sheet.

In summary, there are differing views in the literature regarding the genesis and timing of folds/domes in Bushveld country rocks, and a diapiric origin for the dolomite tongue at Sandsloot is too easily assumed. Some of the domal structures are interpreted as diapirs, others as compressional tectonic features possibly accentuated by diapirism. Regardless of their genesis, some of the structures appear to deform the entire RLS, even the Upper Zone, whereas others compartmentalise the mafic units, with magmatic zones or reefs being present on one flank of a fold/dome and absent on the other. These discrepancies suggest that there is no common genetic mechanism for all of the domes that occur at or near the margin of the RLS at the present surface. Rather, their development depends on their setting, in which the timing and thickness of major magma pulses played a strongly influential role. In light of this study, the relative timing and distribution of the RLS magmas north and south of the TML appear to be important factors. In the northern limb, the Lower Zone occurs only as isolated bodies separated from the rest of the RLS, except in the southern sector where it occurs directly below the GNPA member and occasional screens of Transvaal Supergroup country rocks (Maier *et al.* 2008b). Further, it has been shown that the Platreef intruded considerably earlier than the Main Zone. Thus, the development of the RLS in the northern limb was more episodic, involving spatially and temporally separate units, while south of the TML the development of the RLS was spatially continuous and temporally more continuous than in the northern limb. Further, the northern limb is characterised by pre-Bushveld deformation that generated structures such as the dolomite tongue at Sandsloot. This and related large-scale folds controlled the thickness of the Platreef.

7.2 Interaction of Platreef magma with country rocks

7.2.1 Contamination and source of sulphur

Whilst a study of oxygen isotopes at Sandsloot has shown that up to 18% dolomite has been assimilated by the Platreef (Harris & Chaumba 2001), a more recent study using bulk geochemistry reached a similar estimate but concluded that contamination by the country rocks had not affected the early formed magmatic sulphides, since their isotope signature was

indistinguishable from mantle sulphur (Holwell *et al.* 2007). This is supported by Peniston-Dorland *et al.* (2008), who concluded that the Platreef magma was apparently saturated in sulphur prior to emplacement (and, counterintuitively, lost sulphur during the formation of the present Platreef ore horizon). Conversely, at Turfpruit where the country rocks are shales of the Duitschland Formation, the early formed sulphides do indicate a strong contribution from country-rock sulphur (Sharman-Harris *et al.* 2005). At Sandsloot there is evidence of country rock sulphur only in late-stage calcite quartz veins that cut the reef and hangingwall; and it is suggested that the Main Zone magma set up a hydrothermal system large enough to dissolve sulphate and form sulphides in the late veins (Holwell *et al.* 2007).

An explanation for the different sulphur isotope signatures in early sulphides at Turfspruit and Sandsloot is the sulphur association in the footwall: at Turfspruit, sulphur is largely present as sulphide (in pyrite), which will be assimilated by a magma at magmatic temperatures; whereas at Sandsloot, footwall sulphur is present as sulphate (in anhydrite), which will not be assimilated by a magma at magmatic temperatures but may interact with magmatic sulphide by hydrothermal leaching (Ripley & Li 2003). The result, which is manifested in the sulphur isotopes of magmatic and fluid-affected lithologies of the Platreef, is that sulphur exchange is controlled by assimilation at an early stage of magma emplacement where the country rocks contain sulphide, while sulphur exchange is controlled by later-stage fluid activity where the country rocks contain sulphate (Holwell *et al.* 2007).

Buchanan *et al.* (1981), Buchanan & Rouse (1984) and Sharman-Harris *et al.* (2005) suggest that sulphur addition due to contamination by country rocks triggered sulphur saturation and collection of PGE in the Platreef. Holwell *et al.* (2007) and Hutchinson & McDonald (2008), however, argue that contamination is a localised process and serves primarily to upgrade the sulphur content of the Platreef on a local scale. The latter authors further argue that, along the Platreef as a whole, sulphur saturation is likely to have taken place prior to Platreef emplacement, such that the ore-forming process occurred before Platreef emplacement. Contamination of the reef during its emplacement only modified the earlier-formed ore. Processes such as silicic contamination or an increase in fO_2 (oxygen fugacity) might have triggered sulphur saturation in the Platreef magma during emplacement, but only on a local scale.

A synchronous but separate effect of local country-rock contamination is the variable lithological expression of the Platreef along its strike. At Sandsloot, the metamorphism, assimilation or alteration (generally serpentinisation) of country rocks have been instrumental in the paragenesis of the olivine-replaced reef and serpentinised pyroxenites described in Chapter 5. Similar peridotites and serpentinised pyroxenites are also observed at Zwartfontein

South (Holwell & McDonald 2007). Further north at Overysel, Holwell & McDonald (2006) describe a network of felsic melt in the gneissic footwall that allowed downward percolation of sulphides. This melt probably also migrated upwards and invaded the lower portions of the Platreef as the sulphides migrated downwards, and is manifested as interstitial quartz and quartz-feldspathic veinlets in the basal portions of the reef. Cawthorn *et al.* (1985), however, claimed that the source of contamination of the Platreef at Overysel could not be the highly metamorphosed floor of banded tonalitic gneisses with leucotonalitic veins or the sedimentary floor rocks to the south. Instead, those authors argue that a partial melt or fluid phase derived from a granite that intrudes the floor rocks is shown to be the most likely contaminant. A subsequent study by Barton Jr *et al.* (1986) presented vertical profiles for Rb and Sr isotope ratios calculated to 2.05 Ga through the Platreef and overlying Main Zone for a range of different floor rocks, and found that the ratios depend on the type of floor rock. On a granite floor, it is suggested that the range of $^{87}\text{Sr}/^{86}\text{Sr}$ ratios is due to contamination by a melt derived from the granite. On a dolomitic floor, the initial $^{87}\text{Sr}/^{86}\text{Sr}$ ratios are lower, but high Rb contents again suggest addition of a granitic component, and the extent of contamination is curiously least at the base. In the lowermost Main Zone gabbro-norites, pyroxene has a much lower initial ratio than its whole rock, indicating that the main cumulus phase crystallised before contamination and the granitic liquid from the floor rocks reacted with the interstitial basic magma to produce the contaminated intercumulus phases. This contamination is more likely to have arisen from assimilation of country rocks that formed the roof of the original Platreef sheet (banded ironstones or shales above the dolomite) and would be manifested in the intercumulus liquid rather than in early cumulus pyroxene. Further, the PGE grade of the Platreef is incompatible with the formation of an immiscible sulphide liquid from an interstitial liquid. It is an earlier formed phase, and therefore the separation of sulphide liquid may predate the main siliceous contamination process. At Turfspruit, however, Hutchinson & Kinnaird (2005) and Hutchinson & McDonald (2008) document the erosion of sulphides and redistribution of PGM by later stage quartz-feldspathic veins: some of these contain organic fluid inclusions and other phases suggestive of a footwall-derived melt. This mechanism does not appear to have operated in the Sandsloot-Overysel sector.

An important aspect of the discordant emplacement of the Platreef through the Transvaal Supergroup is the likelihood that, before Main Zone emplacement, the Penge banded iron formation continued above the Platreef from its present path below the reef south of Sandsloot. This is a potential source of Fe for the Fe-enriched zone at the top of face SW2 (Fig. 5-44), called ‘olivine replaced reef’ in this study. This may be viewed as the mirror image (upper contact) of Fe enrichment at Tweefontein where the Platreef rests on an

ironstone footwall (Buchanan & Rouse 1984). Alternatively, the source of Fe may have been a large country-rock xenolith, with the olivine-replaced reef developed as a halo around the xenolith. The xenolith itself is presumably assimilated by the Main Zone or floated in partial preservation elsewhere in the Main Zone.

7.2.2 Metamorphism

Nell (1985) documented two metamorphic events in the Transvaal floor rocks of the northern limb, where the estimated P/T conditions of metamorphism were ~1.5 kb and up to 750°C for the first phase, interpreted as the Lower Zone intrusion, and 4-5 kb and 850-900°C for the second phase, interpreted as the intrusion of magma that derived the Critical Zone, Main Zone and Upper Zone. Sharpe & Hulbert (1985) came to similar conclusions on P/T conditions for the eastern Bushveld, using similar mineral assemblages. However, more recent work by Waters & Lovegrove (2002) and Johnson *et al.* (2003) on P/T conditions in the eastern Bushveld suggest much lower pressures of 2–3 kb. The hiatus interpreted by Nell (1985) remains controversial and may represent a different time break than the pause between the Lower Zone and the combined Critical/Main/Upper Zones. If there is a significant time gap between the Platreef and the Main Zone, as initially recognised by this study and confirmed by Holwell *et al.* (2005), then Nell's (1985) hiatus might represent the time break between the earlier Lower Zone/Platreef and the later Main/Upper Zones. This interpretation presupposes that the Platreef-Main Zone hiatus was longer-lasting than the Lower Zone-Platreef hiatus. The latter is expressed by discordant contacts in the southern sector of the northern limb, indicating a significant time break that might explain Nell's (1985) metamorphic hiatus.

At Sandsloot, the most extensive and influential cause of metamorphism would have been the intrusion of the Lower Zone bodies and particularly the Platreef magma, as they came into direct contact with the sedimentary rocks. During the later emplacement of the Main Zone, the sedimentary sequence below the Platreef was shielded by the Platreef to a considerable degree. This 'barrier effect' probably varied according to the local thickness of the reef. The sheer volume of the Main Zone magma may still have caused some thermal metamorphism by conduction of heat through the Platreef and via injection of dykes and sills that penetrate the Platreef and intrude the floor (e.g. in face N1 at Sandsloot – see Fig. 5-27; and Holwell & Jordaan 2006). The metamorphic history is complicated, however, by the presence of 'gabbroic' bodies east of the Sandsloot pit that Ashwal *et al.* (2004) attribute to the Critical Zone, but their origin remains unclear. They could conceivably be pyroxenites related to the 'lower Platreef' mineralised package discovered below a 'regional raft' of dolomite by recent drilling (Winch 2011). A large Lower Zone body also occurs a little

further east. The intrusion of these igneous bodies before the Platreef may have had an early thermal metamorphic effect on the Malmani Dolomite in the Sandsloot area, and could explain the exclusive presence of calc-silicate hornfels between the Platreef and Lower Zone east of Sandsloot pit (van der Merwe 1978, p. 153). In the dolomite tongue and to the south, where no igneous bodies occur east of the Platreef, only a thin aureole of calc-silicate hornfels abuts the Platreef and quickly grades eastwards into dolomite.

7.3 Mechanisms of PGE distribution

7.3.1 Primary magmatic mineralisation

In a number of disseminated PGE sulphide deposits, the association of PGM with sulphides and the presence of PGM within sulphides is a strong indication of a magmatic genesis. Well known examples are the Merensky Reef (e.g. Prichard *et al.* 2004; Godel *et al.* 2007) and the Great Dyke (e.g. Prendergast & Wilson 1989; Oberthür *et al.* 2003). Whilst relatively low-temperature PGM such as tellurides and bismuthotellurides are also present in these orthomagmatic deposits, they commonly occur on the rims of sulphide blebs and are likely to have speciated by cooling and fractionation from a magmatic sulphide deposit.

The most primary (i.e. unmodified) assemblages in the Platreef are believed to occur where the common feldspathic pyroxenites of the reef overlie an unreactive, anhydrous floor such as the gneiss/granite basement rocks at north of Zwartfontein (Holwell & McDonald 2006; Holwell *et al.* 2007). At this location, there has been a very limited degree of contamination and hydrothermal activity affecting the Platreef and its mineralisation. This style of the primary mineralisation, which is largely preserved at Overysel, is characterised by Holwell & McDonald (2006), who found a strongly sympathetic relationship between the PGE and Ni, Cu and S, and concluded that the PGE and some semi-metals such as Te and Bi were collected by immiscible sulphide droplets; therefore the Platreef at Overysel can be considered in genetic terms to be an orthomagmatic sulphide deposit similar to the examples cited above (Holwell & McDonald 2007). Further, in a study of the source of Platreef sulphides, Holwell *et al.* (2007) found that the sulphur isotope signature of the earliest formed (and least modified) sulphides in uncontaminated Platreef is consistent with a mantle source. Sulphide inclusions in chromite are also strong evidence for an early sulphide liquid (e.g. Holwell *et al.* 2011). At Sandsloot, where the footwall is reactive siliceous dolomite, the sulphide association of PGM is all but totally absent due to pervasive decoupling of PGE from sulphides by fluids (Armitage *et al.* 2002; Holwell *et al.* 2005), and original PGM associations in different Platreef sectors (e.g. Overysel, Sandsloot and Turfspruit) are

influenced to different degrees by the effects of contamination (Holwell & McDonald 2006; Holwell & McDonald 2007). There is an emerging consensus that, in order to develop the high PGE tenors observed by Holwell & McDonald (2007) and Holwell *et al.* (2011), Platreef sulphides may have derived from a staging chamber. Nadrett *et al.* (2008) have recently developed a staging chamber model coupled with magma escape up the chamber walls for the development of the UG2 and the Merensky Reef. They believe this may be applicable to the Platreef as well. Alternatively, the association between the high grade Platreef sector and an apparently PGE-depleted Lower Zone intrusion nearby at Zwartfontein is believed to be significant in the local staging chamber models developed by McDonald & Holwell (2007) and McDonald *et al.* (2009). Lower Zone cumulates in the northern limb pre-date the Platreef, and some parts of the Lower Zone are depleted in Ni and Cu relative to similar rocks elsewhere in the Bushveld Complex, suggesting they may have interacted with sulphides in a sub-chamber or conduit. The scenario envisaged by McDonald & Holwell (2007) is that Lower Zone magma conduits may have stored PGE-rich sulphides that were later supplied to the Platreef.

7.3.2 Hydrothermal redistribution of PGE

The mineralisation style at Sandsloot contrasts with that found at Overysel to the north and with Turfspruit and Townlands much further to the south. The present study and Holwell *et al.* (2006) have shown that fluid activity has exercised a considerable influence on the distribution and mineralogy of PGE at Sandsloot, a feature that is minimal at Overysel except within xenolithic material. This is likely to be related to a fundamental footwall control, with the dolomites at Sandsloot and Zwartfontein releasing large volumes of fluids from both floor and roof during assimilation, metamorphism and subsequent serpentinisation, whereas the gneissic footwall at Overysel produced a felsic partial melt and very few volatiles. The mechanism of distribution of PGE into the footwall differs with footwall lithology. At Overysel, the redistribution of PGE into the footwall appears to be via a downwardly migrating sulphide liquid, with little fluid influence (Holwell & McDonald 2006) whereas at Sandsloot, fluid activity is largely responsible for the transportation of PGE into the calc-silicate footwall and has resulted in some decoupling of PGE from sulphides (Armitage *et al.* 2002; Holwell *et al.* 2006). Further south, on the farms Tweefontein and Turfspruit, where the footwall is comprised of Penge Formation ironstones and hornfelsed shales of the Duitschland Formation, PGE have not been significantly transported into the footwall (Hutchinson & Kinnaird 2005; Nex 2005; Hutchinson & McDonald 2008). The large crystals of sperrylite that are developed in the footwall on Tweefontein Hill (e.g. Wagner 1929) represent PGE that

have been remobilised during post-Platreef faulting (Nex 2005; Nex *et al.* 2008). Instead, at Tweefontein and Turfspruit, significant amounts of PGE are associated with sulphide-rich zones perched above competent, refractory footwall or above rafts of cordierite-spinel hornfels (Kinnaird 2005a; Sharman-Harris *et al.* 2005). While it is clear that many of these high-grade contact metamorphic rocks have not developed a partial melt network comparable to that found at Overysel, melting and devolatilisation of sedimentary rafts have released volatiles (notably S, Sb and As) into the Platreef magma that have influenced its mineralogy (Hutchinson & Kinnaird 2005).

Another study of melt generation and fluid flow in the thermal aureole of the Bushveld Complex was conducted by Harris *et al.* (2003). The study focuses on granite sheets emplaced into the migmatite zone of the eastern contact aureole of the Bushveld Complex, resulting from “*fluid-enhanced, incongruent biotite melting*” of the underlying Silverton Formation shales during prograde metamorphism. These authors interpreted rounded/resorbed quartz grains in contact with feldspar in the granite sheets to reflect quartz-melt relationships. The findings are consistent with the earlier study by Cawthorn *et al.* (1985), which concluded (specifically to Overysel) that a partial melt or fluid phase from footwall granites contaminated the Platreef. Barton Jr *et al.* (1986) reached a similar conclusion.

The presence of significant PGE grades in the footwall at Sandsloot requires that PGE were transported from the Platreef by fluids originating in the footwall or in the magma as it assimilated country rock fragments. The reef itself is a mafic-ultramafic package that would not have carried significant volumes of volatiles capable of transporting PGE directly into the footwall, and there was no other mafic body capable of doing so in the vicinity at the time of Platreef intrusion. Buick *et al.* (2000) present petrological, stable isotope and geochronological data to constrain the extent, source and timing of fluid flow in calcareous country rocks and xenoliths associated with the emplacement of the Bushveld Complex. Calc-silicate xenoliths in the RLS preserve high-temperature ($\sim 1200^{\circ}\text{C}$), anhydrous mineral assemblages that were later metasomatised by hydrous, retrograde ($\sim 600\text{--}700^{\circ}\text{C}$) fluids. Metasomatism was achieved by fluid flow derived from devolatilisation of interlayered metapelites up-temperature towards the intrusion. A similar mechanism is envisaged in the present study for the footwall at Sandsloot, but for siliceous carbonates rather than pelites. Heating of the footwall siliceous dolomites released high-temperature fluids which, possibly accompanied by metamorphic fluids and fluids released during serpentinisation of the Platreef, caused post-cumulus alteration of the reef. The same fluids also decoupled PGE from sulphides, redistributing them within the reef and into the country rocks. In this scenario, fluid movement is envisaged as circulatory, with fluids migrating up-temperature from the heated

footwall into the reef, where they were rapidly reheated and expelled downwards into the floor rocks as well as upwards (but down-temperature) into the roof rocks, thus mineralising the former roof. The recent finding of a series of 'lower Platreef' sheets below the mined reef would add complexity to the circulation of fluids, as they may have been progressively boiled, transported and reboiled. The actual pathways of the fluid system would have been determined by the sequence in which the 'main Platreef' and 'lower Platreef' were emplaced, but the sequence is unknown and can only be established by future work.

8. SUMMARY AND CONCLUSIONS

8.1 Development of the Platreef at Sandsloot

The following geometrical and geological relationships that were documented and discussed in the foregoing chapters form the basis of the tectonic and magmatic model presented later in this chapter:

- (1) The strike of Main Zone layering parallels the general strike of the Platreef, as seen in map view and aeromagnetic images. The dip of the layering also parallels the Platreef in vertical mine faces. As layering formed horizontally by definition, it follows that the Platreef was a more or less horizontal, sill-like body when it intruded. However, local variation in the thickness/shape of the reef was controlled by pre-existing or actively forming structures, and thickened to occupy synformal basins.
- (2) As the footwall contact is unconformable, with different angles of unconformity in all observed rock faces, the Transvaal Supergroup must have been deformed prior to intrusion of the Platreef.
- (3) The Platreef follows the shape of the dolomite tongue, at least near the ‘neck’ of the tongue where it connects to the main body of the country rocks. It was not possible to see on the surface whether the reef wraps around the entire tongue. Some maps show that it does, others do not, and no first-order evidence is presented in the literature for either case.
- (4) The local aeromagnetic image shows that the lowermost Main Zone layering is upwarped against both sides of the tongue, but to a decreasing degree up-sequence, i.e. towards the tip of the tongue.
- (5) Although ages for the Lower Zone and Platreef are not known, it is unlikely they are much older than the main body of the northern limb and not greatly younger or older than the central Bushveld Complex. Currently available age determinations (section 2.5) indicate a short period of intrusion for the complex, yet it is evident that some phases are more affected by deformation than others (particularly the Platreef versus the Main Zone, but also the Lower Zone versus the Platreef). This suggests, in combination with point 4 above, that regional deformation was still in progress during intrusion of the Platreef, though at a waning stage, and ceased in Upper Main Zone time in the northern limb.

Notably, the Rooiberg felsites are folded in the vicinity of the Thabazimbi-Murchison Lineament (e.g. Armitage *et al.* 2007), indicating that a tectonic event affected the area after 2.06 Ga (age of the Rooiberg Group, which is the earliest expression of Bushveld magmatism). Documented events are the Magondi orogeny at ~2.0 Ga and the Kheis orogeny at ~1.9-1.8 Ga. The former of these may have been a syn-Bushveld event that affected the Lower Zone, Platreef and Lower Main Zone.

8.1.1 Synopsis

In pre-Bushveld time, the Transvaal Supergroup was folded, with interference of N-S and ENE-WSW fold phases producing domes that are most prominently expressed by the dolomite tongue at Sandsloot, as well as more regional features such as the Eersteling Basin. As the upper formations of the ~2.7–2.2 Ga Transvaal Supergroup are affected by the folding, it is assumed to have commenced after 2.2 Ga but before emplacement of the Bushveld Complex. This possibly attributes folding to the Magondi Orogeny. Bushveld magma likely rose through reactivated crustal-scale shear zones, developing feeders such as the one postulated at a location west of Mokopane where an unusually high gravity anomaly occurs. Although the Platreef transgresses the regional bedding of the Transvaal Supergroup, the overall geometry of the reef suggests it was largely controlled by country-rock fold structures during intrusion. This relationship is also seen in southern sectors of the Platreef where the reef is shown to be thinner above footwall structural highs and thicker in structural lows; i.e. the Platreef magma has filled the synformal zones of the pre-existing folds (Kinnaird *et al.* 2005).

The Platreef intruded in at least two magma pulses at Sandsloot, as the reef represents too small a volume of magma to attain such a high concentration of PGE and the overlying Main Zone cannot be the source of PGE to the reef because the Main Zone was emplaced *after* the reef had cooled below solidus. Rather, PGE were initially associated with sulphides derived from the same magma(s) that formed the Merensky Reef and which injected up and out along the intrusion walls as the chamber expanded. Alternatively, the sulphides may have formed in pre-Platreef staging chambers where they were upgraded by repeated interactions with batches of Lower Zone magma before being expelled as a crystal-liquid-sulfide mush by an early injection of Main zone magma, prior to the formation of the bulk of the Main Zone (McDonald & Holwell 2011).

Post-cumulus alteration of the Platreef occurred due to high-temperature fluids released from the country rocks by heating of the footwall sedimentary rocks, and possibly due to metamorphic fluids and fluids released during serpentinisation. In a circulatory system

of boiling and re-boiling fluids as they migrated from the floor rocks into the Platreef and out again, PGE were decoupled from sulphides and redistributed within the reef and in its floor and roof rocks.

Following intrusion and during interaction with the country rocks, the Platreef cooled to a considerable degree, certainly below solidus, and was moderately sheared by tectonism that was at a waning stage during Platreef intrusion and earliest Main Zone emplacement. This tectonic event was responsible for the final shape of the dolomite tongue, causing upwarping of Main Zone layering at the root of the tongue. The cooled Platreef was followed by emplacement of the Main Zone, which eroded and assimilated the uppermost section of the reef, particularly above structural highs, and in places intruded through the reef as dykes via earlier formed shear zones that are not found in the Main Zone. Where the Main Zone completely eroded an uppermost, fine-grained, barren section of the Platreef, it assimilated a sufficient volume of the underlying mineralised reef to melt and cannibalise the Platreef sulphides and produce a locally sulphide-rich basal Main Zone (Holwell *et al.* 2005; Holwell *et al.* 2006). The Main Zone entrained calc-silicate xenoliths from the roof of the Platreef that had been mineralised by fluid infiltration resulting from the earlier Platreef intrusion. A possible additional means of mineralised country-rock entrainment in the Main Zone is that the Main Zone magma breached the Platreef above structural highs, or entrained refractory xenoliths from where the Platreef itself was assimilated.

The above sequence of events in the development of the Platreef and associated units is illustrated in Fig. 8-1 below.

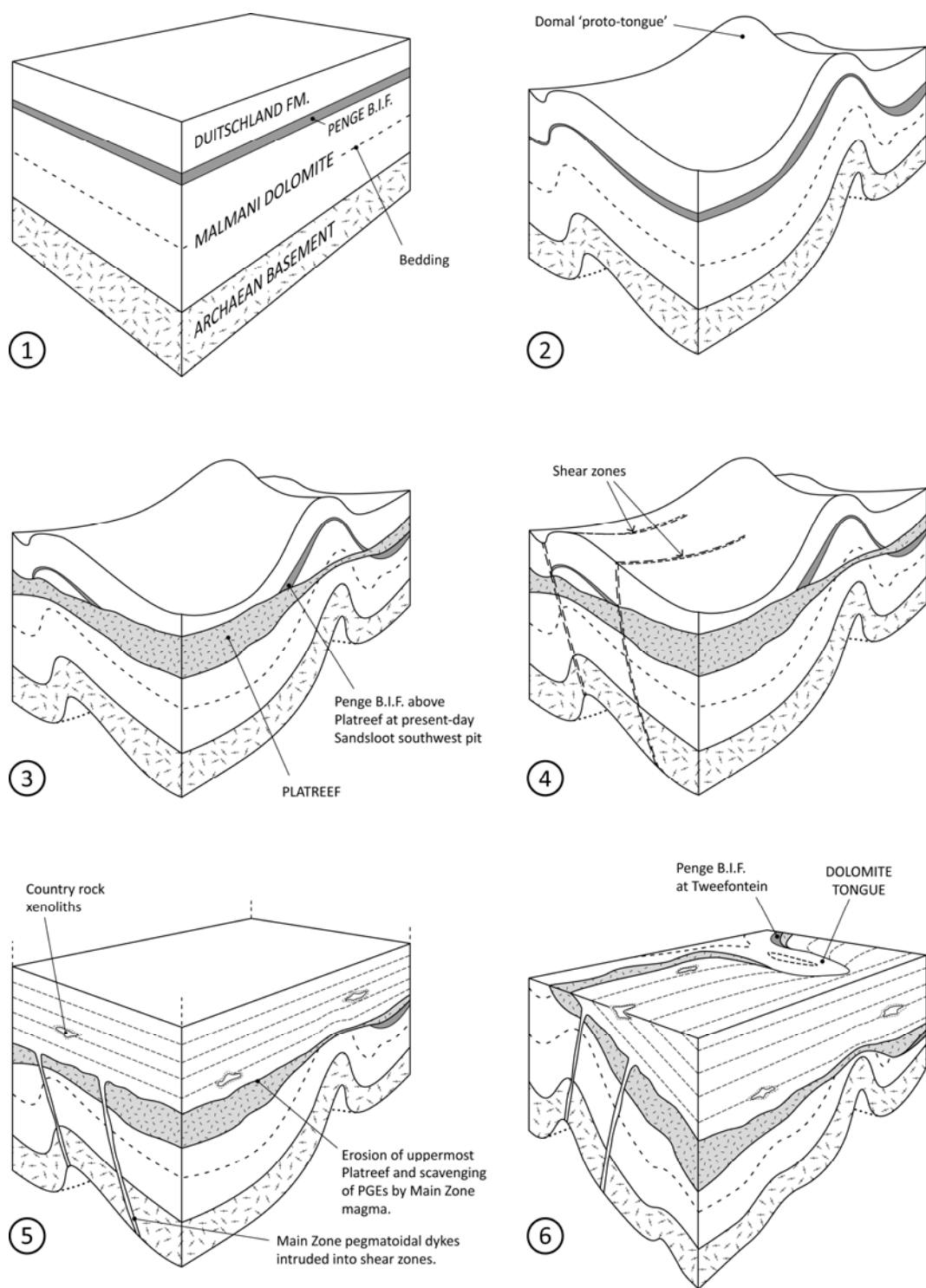


Fig. 8-1. Three-dimensional block model, viewed to southeast, for Platreef development at Sandsloot. (1) Deposition of Transvaal Supergroup ~2.7-2.2 Ga. (2) Two-phase compressive deformation of Transvaal Supergroup after 2.2 Ga, during or culminating with the Magondi Orogeny. (3) Intrusion of Platreef sheet with overall horizontal attitude, but thickness locally controlled by pre-existing structures. (4) Deformation of cooling Plateef and Transvaal Supergroup country rocks, possibly at late stage of Magondi Orogeny, with accentuation of previously formed structures. (5) Emplacement of Main Zone, eroding uppermost Platreef, and intrusion of associated pegmatoidal dykes into shear zones through Platreef and footwall. Continuing late-stage deformation affects lower Main Zone but ceases during Main Zone emplacement. (6) Subsidence of northern limb down to west, and erosion to present-day surface.

8.2 Conclusion

The mass of PGE in the Platreef is incompatible with the volume of the reef, and while contamination may have altered the chemistry and upgraded the sulphur budget of the reef, it cannot have provided the PGE required by the mass balance. Therefore, the PGE must have been concentrated from a large volume of magma elsewhere. Holwell *et al.* (2007) invoke a deep staging chamber as the locus of the PGE concentration process in which sulphur droplets in a sulphur-saturated magma scavenged PGE from the magma that passed over them. This is a feasible scenario that is supported by evidence from the present study. In particular, it has been proven that the Main Zone cannot have provided PGE to the Platreef as the Main Zone was emplaced after the Platreef had cooled below solidus. While the Main Zone formed the Merensky Reef at its base in the central complex, it is now known that there was a significant hiatus between the intrusion of the Platreef and Main Zone in the northern limb. The question of the relative timing of the Platreef and Merensky Reef remains open, as does the question of their genetic relationship.

This thesis has shown that while the Platreef shows similarities to contact-type deposits that acquire sulphur and other elements by assimilation of country rocks (e.g. Peck *et al.* 2000), the ‘proto-Platreef’ at Sandsloot and possibly Zwartfontein cannot have maintained its contact-type state for long, as fluids would have been quickly boiled out of the country rocks (particularly the sedimentary footwall) and then thermally circulated in the reef, where they were rapidly reboiled and expelled back into the country rocks, decoupling and redistributing PGE in their path. By this process, significant PGE grades are found in the footwall at Sandsloot and perhaps at Zwartfontein. Footwall sulphides are present in the orthogneissic footwall at Overysel, but they formed by downward migration of sulphides from the reef into a low density melt network in the footwall. In contrast, at Turfspuit there is no footwall mineralisation because the hornfels was too impermeable (Hutchinson & McDonald 2008). For clarity it has been necessary to restrict the use of the term ‘Platreef’ to that defined by Kinnaid & McDonald (2005), while the *orebody* is the total volume of grade-bearing rocks in the Platreef, footwall and to a lesser extent the hangingwall.

The present study has also provided macroscale observations on the nature of the hangingwall contact that led Holwell *et al.* (2005) and Holwell & Jordaan (2006) to gather clear evidence for post-Platreef intrusion of the Main Zone and a significant time break between these two igneous units. This invalidates the model of Friese (2004) that the Main Zone was pre-Platreef.

Structural considerations favour a compressional fold interference origin for the ‘dolomite tongue’, rather than gravity inversion (diapir), with the consequent admonition that

structures with dome-like surface expressions should not be automatically categorised as Bushveld magma-induced diapirs. Some structures may have formed before or during an early stage of Bushveld intrusion, and therefore imparted a local control on the emplacement of Bushveld magmas and possibly on the concentration of PGE by gravitational settling in synformal zones where, for example, the Platreef is thickest.

Removing the Main Zone as the source of PGE to the Platreef requires that the metals were sourced elsewhere. This study favours the model of McDonald & Holwell (2007) and McDonald *et al.* (2009), which suggests the magmas that formed the (pre-Platreef) Lower Zone may have been the source of PGE, and highlights important first-order differences between Lower Zone intrusions in the northern limb compared to the rest of the Bushveld Complex, notably a strong depletion of chalcophile elements (Ni, Cu and PGE) in the Lower Zone intrusion at Zwartfontein. Nonetheless, the possibility of a genetic link with the Merensky Reef (Naldrett *et al.* 2008, 2009; Reisberg *et al.* 2011) remains open.

8.3 Epilogue

Despite several years of focussed research on the Platreef, many questions remain. How can we prove or disprove a common magma for the Platreef and Merensky Reef? Why are all the northern limb deposits rich in palladium compared to other Bushveld PGE reefs? Is the Platreef a mineralisation event or a contact mineralisation style?

One of the advantages of this thesis is that it is largely based on first-order observation and mapping of rock faces in an open pit. Many studies in sectors of the Platreef that have not yet been mined have had to rely on boreholes, and while these provide excellent information in one dimension, much interpolation is required and geological relationships can often only be made by inference. The importance of grasping opportunities to map new exposures is borne out in Holwell & Jordaan (2006), who present a complete three-dimensional block illustrating relations between the Platreef, hangingwall and footwall, based entirely on first-order observations of vertical rock faces and the base of the Zwartfontein mine. Their study added detail and conclusive evidence to some of the findings developed by the author from his field observations.

A further important lesson is that detailed mapping should be not be blinkered by preconceived models. It is understandable that mine geologists are bound by company policies and standards, and their chief responsibility in the case of the Platreef is to demarcate the hangingwall, Platreef and footwall. However, a detailed academic study must objectively describe what is present in exposures, whether or not the observations agree with other schemes. For example, this study quickly recognised that the Platreef at Sandsloot does not

comply with the established A-B-C mining terminology, and also characterised previously unreported features that have changed the view of the genetic and temporal setting of the Platreef in the Bushveld Complex. Future studies that incorporate a significant component of mapping are strongly encouraged in new areas of the Platreef as they are opened up to mining, and will surely lead to an even more detailed insight into this remarkable PGE deposit.

9. REFERENCES

- ALAPIETI T.T. & LAHTINEN J.J. (2002). Platinum-group element mineralization in layered intrusions of northern Finland and the Kola Peninsula, Russia. *In*: Cabri L.J. (ed.), The geology, geochemistry, mineralogy and mineral beneficiation of platinum-group elements. *CIMMP*, **54**, 507-546.
- ANGLO AMERICAN (2010). Fact Book. [Online] Available at:
<http://www.angloamerican.com/media/fact_book/~media/Files/A/Anglo-American-Plc/siteware/docs/platinum_10.pdf> [Accessed 29 April 2011]
- ARMITAGE P.E.B., McDONALD I., EDWARDS S.J. & MANBY G.M. (2002). Platinum-group element mineralization in the Platreef and calc-silicate footwall at Sandsloot, Potgietersrus District, South Africa. *Appl. Earth Sci. (Trans. Inst. Min. Metall. B)*, **111**, B36-45.
- ARMITAGE P., McDONALD I., & TREDOUX M. (2007). A geological investigation of the Waterberg hydrothermal platinum deposit, Mookgophong, Limpopo Province, South Africa. *Appl. Earth Sci. (Trans. Inst. Min. Metall. B)*, **116**, B113-129.
- ARMSTRONG R. & WILSON A.H. (2000). A SHRIMP U–Pb study of zircons from the layered sequence of the Great Dyke, Zimbabwe, and a granitoid dyke. *Earth Planet Sci. Lett.*, **180**, 1-12.
- ASHWAL L.D., WEBB S.J. & KNOPER M.W. (2004). Magmatic stratigraphy in the Bushveld Northern Lobe: continuous geophysical and mineralogical data from the 2950 m Bellevue drillcore. *S. Afr. J. Geol.*, **108**, 199-232.
- AZBEL I. YA., TOLSTIKHIN I. N., KRAMERS D., PECHERNIKOVA V. & VITYAZEVA A. V. (1993). Core growth and siderophile element depletion of the mantle during homogeneous Earth accretion. *Geochim. Cosmochim. Acta*, **57**, 2889-2898.
- BARKOV A.Y., MARTIN R.F., LEBARGE W. & FEDORTCHOUK Y. (2008). Grains of Pt-Fe alloy and inclusions in a Pt-Fe alloy from Florence Creek, Yukon, Canada: evidence for mobility of Os in a Na–H₂O–Cl-rich fluid. *Can. Mineral.* **46**, 343-360.
- BARNES S-J. & MAIER W.D. (2002). Platinum-group element distributions in the Rustenburg Layered Suite of the Bushveld Complex, South Africa. *In*: Cabri L.J. (ed.), The geology, geochemistry, mineralogy and mineral beneficiation of platinum-group elements. *CIMMP*, **54**, 553-580.
- BARNES S-J., MAIER W.D., ASHWAL L.D. (2004). Platinum-group element distribution in the Main Zone and Upper Zone of the Bushveld Complex, South Africa. *Chem. Geol.*, **208**, 293-317

- BARNES S-J. & NALDRETT A. J. (1987). Fractionation of the platinum group elements and gold in some komatiites of the Abitibi greenstone belt, northern Ontario. *Econ. Geol.*, **82**, 165-183.
- BARNES S-J., NALDRETT A.J. & GORTON M. P. (1985). The origin of the fractionation of platinum-group elements in terrestrial magmas. *Chem. Geol.*, **53**, 303-323.
- BARTON JR. J.M. CAWTHORN R.G. & WHITE J. (1986). The role of contamination in the evolution of the Platreef of the Bushveld Complex. *Econ. Geol.*, **81**, 1096-1104.
- BARTON J.M., DOIG R & SMITH C.B. (1995). Age, origin and tectonic significance of the Entabeni Granite, northern Transvaal, South Africa. *S. Afr. J. Geol.*, **98**, 326-330.
- BERLINCOURT L.E., HUMMELL H.H. & SKINNER B.J. (1981). Phases and phase relations of the platinum-group elements. In: *Cabri L.J. (ed.), Platinum-Group Elements: Mineralogy, Geology, Recovery. Can. Inst. Mining Metall., Spec. Vol.*, **23**, 19-45.
- BORISOV A., PALME H. & SPETTEL B. (1994). Solubility of palladium in silicate melts: Implications for core formation in the Earth. *Geochim. Cosmochim. Acta*, **58**, 705-716.
- BUCHANAN D.L. (1988). Platinum-group element exploration. Elsevier: Amsterdam, 185 pp.
- BUCHANAN D.L., NOLAN J., SUDDABY P., ROUSE J.E., VILJOEN M.J. & DAVENPORT J.W.J. (1981). The genesis of sulphide mineralisation in a portion of the Potgietersrus Limb of the Bushveld Complex. *Econ. Geol.*, **76**, 568-579.
- BUCHANAN D.L. & ROUSE, J.E. (1984). Role of contamination in the precipitation of sulphides in the Platreef of the Bushveld Complex. In: Buchanan D.L. & Jones M.J. (eds.), *Sulphide deposits in mafic and ultramafic rocks*, London, IMM, 141-146.
- BUICK L.S., GIBSON R.L., CARTWRIGHT L, MAAS, R., WALLMACH, T. & UKEN, R. (2000). Fluid flow in metacarbonates associated with emplacement of the Bushveld Complex, South Africa. *J. Geochem. Explor.*, **69-70**, 391-396.
- BUICK I.S., MAAS R. & GIBSON R. (2001). Precise U-Pb titanite age constraints on the emplacement of the Bushveld Complex, South Africa. *J. Geol. Soc. Lond.*, **158**, 3-6.
- BUMBY A.J., ERIKSSON, P.G. & VAN DER MERWE, R. (1998). Compressive deformation in the floor rocks to the Bushveld Complex (South Africa). evidence from the Rustenburg Fault Zone. *J. Afr. Earth Sci.*, **27**, 307-330.
- BUTTON A. (1973). The stratigraphic history of the Malmani Dolomite in the eastern and north-eastern Transvaal. *Trans. Geol. Soc. S. Afr.*, **76**, 229-247.

- BUTTON A. (1978). Diapiric structures in the Bushveld, northeastern Transvaal. Econ. Geol. Res. Unit., Univ. Witwatersrand, Inf. Circ., **96**, 13 pp.
- BUTTON A. (1986). The Transvaal sub-basin of the Transvaal Sequence. *In*: Anhaeusser C.R. & Maske S. (eds.) 1986. Mineral Deposits of Southern Africa, *Geol. Soc. S. Afr.*, Johannesburg, 811-817.
- BYE A.R. (2001). Mining the Platreef. *Appl. Earth Sci. (Trans. Inst. Min. Metall. B)*, **110**, B209-210.
- BYE A.R. & BELL F.G. (2001). Stability and slope design at Sandsloot open pit, South Africa. *Int. J. Rock Mech. Min.*, **38**, 449-466.
- BYE A. R. BELL F. G. & JERMY C. A. (1999): Slope optimization and review of the geotechnical conditions at Sandsloot Open Pit, Potgietersrus Platinum Mine, South Africa. *Proceedings of the 9th ISRM Conference*, Paris, France, **1**, 77-79.
- CABRI L.J. (1976). Glossary of platinum-group minerals: *Econ. Geol.*, **71**, 1476-1480.
- CABRI L.J. (1981). Analyses of minerals containing platinum-group elements. *In*: Cabri L.J. (ed.), Platinum group elements – Mineralogy, geology, recovery. *Can. Inst. Mining Metall., Spec. Vol.*, **23**, 151-173.
- CABRI L.J. (1992). The distribution of trace precious metals in minerals and mineral products. *Mineral. Mag.*, **56**, 289-308.
- CABRI L.J. (1994). Current status of determination of mineralogical balances for platinum-group element-bearing ores. *Appl. Earth Sci. (Trans. Inst. Min. Metall. B)*, **103**, B3-B9.
- CABRI L.J. (2002). The platinum-group minerals. *In*: Cabri L.J. (ed.), The geology, geochemistry, mineralogy and mineral beneficiation of platinum-group elements. CIMMP, Spec. Vol., **54**, 13-129.
- CAMPBELL I.H. & NALDRETT A.J. (1979). The influence of silicate:sulfide ratios on the geochemistry of magmatic sulfides. *Econ. Geol.*, **74**, 1503-1505.
- CAMPBELL, I.H., NALDRETT, A.J. & BARNES, S-J. (1983). A model for the origin of platinum-rich sulfide horizons in the Bushveld and Stillwater Complexes. *J. Petrol.*, **24**, 133-165.
- CAPOBIANCO C.J., HERVIG R.L. & DRAKE M.J. 1994. Experiments on crystal/liquid partitioning of Ru, Rh and Pd for magnetite and hematite solid solutions crystallized from silicate melt. *Chem. Geol.*, **113**, 23-43.
- CARLSON R.W., PEARSON D.G., BOYD S.B., SHIREY S.B., IRVINE G., MENZIES A.H. & GURNEY J.J. (1999). Re-Os systematics of lithospheric peridotites: implications for lithosphere formation and preservation. *In*: Gurney

- J.J., Gurney J.L., Pascoe M.D. & Richardson S.H. (eds.), *Proceedings of the 7th International Kimberlite Conference*. Red Roof Design, Cape Town, South Africa, 99-108.
- CAWTHORN R.G. (1999). The platinum and palladium resources of the Bushveld Complex. *S. Afr. J. Sci.*, **95**, 481-489.
- CAWTHORN R.G., BARTON JR. J.M. & VILJOEN M.J. (1985). Interaction of floor rocks with the Platreef on Overysel, Potgietersrus, Northern Transvaal. *Econ. Geol.*, **80**, 988-1006.
- CAWTHORN R.G. & LEE C. (1998). Field excursion guide to the Bushveld Complex, 8th International Platinum Symposium, Geological Survey of South Africa, South Africa, 113 pp.
- CAWTHORN R.G., LEE C.A., SCHOUWSTRA R.P., & MELLOWSHIP P. (2002b). Relationship between PGE and PGM in the Bushveld Complex. *Can. Mineral.*, **40**, 311-328.
- CAWTHORN R.G., MERKLE R.K.W. & VILJOEN M.J. (2002a). Platinum-group elements in the Bushveld Complex. *In: Cabri L.J. (ed.), The geology, geochemistry, mineralogy and mineral beneficiation of platinum-group elements. CIMMP, Spec. Vol. 54*, 389-430.
- CAWTHORN R.G. & WALRAVEN F. (1998) Emplacement and crystallization time for the Bushveld Complex. *J. Petrol.*, **39**, 1669-1687.
- CAWTHORN R.G. & WEBB S.J. (2001). Connectivity between the western and eastern limbs of the Bushveld Complex. *Tectonophysics*, **330**, 195-209.
- CHENEY E. S. & TWIST D. (1991). The conformable emplacement of the Bushveld mafic rocks along a regional unconformity in the Transvaal succession of South Africa. *Prec. Res.*, **52**, 115-132.
- CHOU C-L. (1978). Fractionation of siderophile elements in the earth's upper mantle. *P. Lunar Planet. Sci. C.*, **IX**, 219-230.
- CORNELL D.H., ARMSTRONG R.A. & WALRAVEN F. (1998). Geochronology of the Proterozoic Hartley Basalt Formation, South Africa: constraints on the Kheis tectogenesis and the Kaapvaal Craton's earliest Wilson Cycle. *J. Afr. Earth Sci.*, **26**, 5-27.
- CORNELL D.H., SCHÜTTE S.S., EGLINGTON B.L. (1996). The Ongeluk basaltic andesite formation in Griqualand West, South Africa: submarine alteration in a 2222 Ma Proterozoic sea. *Prec. Res.*, **79**, 101-123.
- COUSINS C. A. (1959). The structure of the mafic portion of the Bushveld Igneous Complex. *Trans. Geol. Soc. S. Afr.*, **62**, 174-189.

- CROCKET J.H. (1981). Geochemistry of the platinum group elements. *In* Cabri L.J. (ed.), *Platinum-Group Elements: Mineralogy, Geology, Recovery. Can. Inst. Mining Metall., Spec. Vol., 23*, 47-64.
- CROCKET J.H. (2002). Platinum-group element geochemistry of mafic and ultramafic rocks. *In* Cabri L.J. (ed.), *The Geology, Geochemistry, Mineralogy and Mineral Beneficiation of Platinum-Group Elements. Can. Inst. Mining Metall., Spec. Vol., 54*, 177-210.
- DALTRY V.D.C. & WILSON A.H. (1997). Review of platinum-group mineralogy: compositions and elemental associations of the PG-minerals and unidentified PGE-phases. *Mineral. Petrol.*, **60**, 185-229.
- DALY R.A. (1928). Bushveld Igneous Complex of the Transvaal. *Geol. Soc. Am. Bull.*, **39**, 703-68.
- DE KLERK L. (2005). Bushveld stratigraphy on Rooipoort, Potgietersrus Limb. Platinum Symposium 2005. Eersteling Gold Mining Company, Johannesburg.
- DE VILLIERS J.S. (1967). The geology of the area south of Potgietersrus, with special reference to the chromite deposits. Ph.D. thesis, University of the Witwatersrand, 124 pp.
- DE WAAL S.A. (1970). Interference folding of Bushveld Igneous Complex age in the Transvaal Sequence north of Marble Hall. *In*: Visser D.J.L. & von Gruenewaldt G. (eds.), *Symposium on the Bushveld and Other Layered Intrusives. Geol. Soc. S. Afr., Spec. Publ., 1*, 283-298.
- DE WAAL S.A. (1977). Carbon dioxide and water from metamorphic reactions as agents for sulphide and spinel precipitation in mafic magmas. *Trans. Geol. Soc. S. Afr.*, **80**, 193-196.
- DE WIT M.J., ROERING C., ARMSTRONG R.A., TREDoux M., DE RONDE C.E.J., HART R.J., GREEN R., PEBERDY E. & HART R.A. (1992). Formation of an Archaean continent. *Nature*, **357**, 553-562.
- DORLAND H.C., BEUKES N.J., GUTZMER J., EVANS D.A.D. & ARMSTRONG R.A. (2006). Precise SHRIMP U-Pb zircon age constraints on the lower Waterberg and Soutpansberg Groups, South Africa. *S. Afr. J. Geol.*, **109**, 139-156.
- DU PLESSIS A. & KLEYWEGT R.J. (1987). A dipping sheet model for the mafic lobes of the Bushveld Complex. *S. Afr. J. Geol.*, **90**, 1-6.
- DU PLESSIS C.P. & WALRAVEN F. (1990). The tectonic setting of the Bushveld Complex in southern Africa, Part 1: Structural deformation and distribution. *Tectonophysics*, **179**, 305-319.
- EALES H. V. (2000). Implications of the chromium budget of the Western Limb of the Bushveld Complex. *S. Afr. J. Geol.*, **103**, 141-150.

- EALLES H.V., BOTHA W.J., HATTINGH P.J., DE KLERK W.J., MAIER W.D. & ODGERS A.T.R. (1993). The mafic rocks of the Bushveld complex: a review of emplacement and crystallization history, and mineralization, in the light of recent data. *J. Afr. Earth Sci.*, **16**, 121-142.
- EALLES H.V. & CAWTHORN R.G. (1996). The Bushveld Complex. *In*: Cawthorn R.G. (ed.), Layered Intrusions, Elsevier Science, 181-230.
- FINNIGAN C.S. & BRENAN J.M. (2004). Experimental evidence for the co-precipitation of PGE alloys and chromite as a result of local melt reduction during chromite crystallization. *Geoscience Africa*, Johannesburg, Abstr. 201.
- FINNIGAN C.D., BRENAN J.M., MUNGALL J.E. & McDONOUGH W. F. (2008). Experiments and Models Bearing on the Role of Chromite as a Collector of Platinum Group Minerals by Local Reduction. *J. Petrol.*, **49**, 1647-1665.
- FRIESE, A.E.W. (2004). Geology and tectono-magmatic evolution of the PPL concession area, Villa Nora-Potgietersrus Limb, Bushveld Complex. Geological Visitor Guide, Potgietersrus Platinums Limited, 57 pp.
- FRIESE A.E.W. & CHUNNETT G.K. (2004). Tectono-magmatic development of the northern limb of the Bushveld Igneous Complex, with special reference to the mining area of Potgietersrus Platinums Limited. *Geoscience Africa*, Abstract Volume, July 2004, University of the Witwatersrand, Johannesburg, South Africa, 209-210.
- GAIN S.B. & MOSTERT A.B. (1982). The geological setting of the platinoid and base metal sulphide mineralization in the Platreef of the Bushveld Complex in Drenthe, north of Potgietersrus. *Econ. Geol.*, **77**, 1395-1404.
- GERYA T.V., UKEN R., REINHARDT J., WATKEYS M.K., MARESCHE W.V. & CLARKE B.M. (2004). 'Cold' diapirs triggered by intrusion of the Bushveld Complex: Insight from two-dimensional numerical modelling. *In*: Whitney D.L, Teyssier C. & Siddoway C.S., Gneiss domes in orogeny. Boulder, Colorado, *Geol. S. Am. S.*, **380**, 117-127.
- GIBSON R. L. & STEVENS G. (1998). Regional metamorphism due to anorogenic intracratonic magmatism. *In*: Treloar P.J. & O'Brien P. (eds.), What drives metamorphism and metamorphic reactions? *J. Geol. Soc. London*, **138**, 115-129.
- GOOD N.E. (1997). Tectonic evolution and structural controls on the fluid flow along the Thabazimbi–Murchison Lineament, Northern Transvaal, South Africa. PhD thesis, University of Cape Town, RSA.
- GOOD, N.E. & DE WIT M.J. (1995). Fluid liberation and expulsion from the Transvaal Basin/Archean basement during emplacement and subsidence of the Bushveld Complex: Implications for fluid/rock ratios in the Thabazimbi–Murchison Lineament. *In*: GeoCongress '95 (Rand Afrikaans University, S. Africa.): Extended Abstracts, **1, 2**, 718-719.

- GOOD N. & DE WIT M. (1997). The Thabazimbi-Murchison Lineament of the Kaapvaal Craton, South Africa: 2700 Ma of episodic deformation. *J. Geol. Soc. Lond.*, **154**, 93-97.
- GOUGH D.I. & VAN NIEKERK C.B. (1959). A study of the palaeomagnetism of the Bushveld Complex. *Phil. Mag.*, **14**, 126-134.
- GROBLER N.J. & WHITFIELD G.G. (1970). The olivine-apatite magnetites and related rocks in the Villa Nora occurrence of the Bushveld Igneous Complex. *GSSA, Spec. Publ.*, **1**, 1161-1177.
- HALL A.L. (1908). Note on contemporaneous igneous rocks in the Pretoria Series of the Lydenburg and Rustenburg districts. *Trans. Geol. Soc. S. Afr.*, **11**, 47-54.
- HALL A.L. (1932). The Bushveld Igneous Complex of the Central Transvaal. *Geol. Surv. Union S.A. Mem.*, **28**, 560 pp.
- HARMER R.E., & ARMSTRONG R.A. (2000). Duration of Bushveld Complex (sensu lato) magmatism: constraints from new SHRIMP zircon chronology. Workshop on the Bushveld Complex, Gethane Lodge, Burgersfort, 18-21 November 2000, abstracts and programme.
- HARMER R.E., AURET J.M. & EGLINGTON B.M. (1995). Lead isotope variations within the Bushveld Complex, Southern Africa; a reconnaissance study. *J. Afr. Earth Sci.*, **21**, 595-606.
- HARMER R.E., PILLAY N. & DAVIS P.G. (2004). The Aurora project - Main Zone hosted PGE-base metal mineralization at the northern outcrop limit of the Bushveld northern limb, north of Mokopane. Platreef Workshop field guide, Geoscience Africa, Mokopane 16-19 July 2004, University of the Witwatersrand.
- HARMER R.E. & SHARPE M.R. (1985). Field relations and strontium isotope systematic of the marginal rocks of the eastern Bushveld Complex. *Econ. Geol.*, **80**, 813-837.
- HARRIS C. & CHAUMBA J.B. (2001). Crustal contamination and fluid-rock interaction during the formation of the Platreef, Northern Limb of the Bushveld Complex, South Africa. *J. Petrol.*, **42**, 1321-1347.
- HARRIS N.B.W., MCMILLAN A., HOLNESS M.B., UKEN R., WATKEYS M., ROGERS N. & FALICK A. (2003). Melt generation and fluid flow in the thermal aureole of the Bushveld complex. *J. Petrol.*, **44**, 1031-1054.
- HARRIS C., PRONOST J.M., ASHWAL L.D. & CAWTHORN R.G. (2004). Oxygen and hydrogen isotope stratigraphy of the Rustenburg Layered Suite, Bushveld Complex. Constraints on crustal contamination. *J. Petrol.*, **46**, p 579-601.
- HARTZER F.J. (1987). Die geologie van die krokodilrivier fragment, Transvaal. Unpublished MSc thesis, Rand Afrikaans University, 201 pp.

- HARTZER F.J. (1995). Transvaal Supergroup inliers: Geology, tectonic development and relationship with the Bushveld Complex, South Africa. *J. Afr. Earth Sci.*, **21**, 521-547.
- HATCH F.H. & CORSTORPHINE G.S. (1905). The Geology of South Africa. Macmillan, London, 348 pp.
- HATTINGH P. J. (1991). The magnetic susceptibility of the mafic rocks of the Bushveld Complex. *S. Afr. J. Geol.*, **94**, 132-136.
- HATTINGH P.J. (1995). Palaeomagnetic constraints on the emplacement of the Bushveld Complex. *J. Afr. Earth. Sci.*, **21**, 549-551.
- HATTINGH P.J. & PAULS N.D. (1994). New palaeomagnetic results from the northern Bushveld Complex of South Africa. *Prec. Res.*, **69**, 229-240.
- HATTON C.J. (1995). Mantle plume origin for the Bushveld and Ventersdorp provinces. *J. Afr. Earth. Sci.*, **21**, 571-577.
- HATTON C.J. & SCHWEITZER J.K. (1995). Evidence for synchronous extrusive and intrusive Bushveld magmatism. *J. Afr. Earth Sci.*, **21**, 579-594.
- HATTON C.J. & VON GRUENEWALDT. G. (1987). The geological setting and the petrogenesis of the Bushveld chomitite layers. *In*: Stowe C.W. (ed.), Evolution of the chromium orefields, Van Nostrand Reinhold, New York, 109-143.
- HAUGHTON D.R., ROEDER P.L. & SKINNER B.J. 1974. Solubility of Sulfur in Mafic Magmas. *Econ. Geol.* **69**, 451-467.
- HELZ R.T. (1985). Composition of fine-grained mafic rocks from sills and dikes associated with the Stillwater Complex, Montana. *In*: Montana Bur. Mines Geol. Spec. Publ., **92**, 97-117.
- HOLWELL D.A. (2006). The roles of magmatism, contamination and hydrothermal processes in the development of Platreef mineralization, Bushveld Complex, South Africa. Unpublished PhD thesis, Cardiff University, 208 pp + appendices.
- HOLWELL D.A., ARMITAGE P.E.B. & McDONALD I. (2005). Observations on the relationship between the Platreef and its hangingwall. *Appl. Earth Sci. (Trans. Inst. Min. Metall. B)*, **114**, B199-207.
- HOLWELL D.A., BOYCE A.J & McDONALD I. (2007). Sulfur isotope variations within the Platreef: genetic implications for the origin of sulfide mineralization. *Econ. Geol.*, **102**, 1091-1110.

- HOLWELL D.A. & JORDAAN A. (2006). Three-dimensional mapping of the Platreef at the Zwartfontein South mine: implications for the timing of magmatic events in the northern limb of the Bushveld Complex, South Africa. *Appl. Earth Sci. (Trans. Inst. Min. Metall. B)*, **115**, 41-48.
- HOLWELL D.A. & McDONALD I. (2005). Variations in platinum group element mineralization within the Platreef, northern Bushveld Complex, South Africa. *In*: Törmänen T.O. & Alapieti T.T. (eds.), 10th International Platinum Symposium, University of Oulu, Extended Abstracts, 110-113.
- HOLWELL D.A. & McDONALD I. (2006). Petrology, geochemistry and the mechanisms determining the distribution of platinum-group element and base metal sulfide mineralization in the Platreef at Overysel, northern Bushveld Complex, South Africa. *Miner. Deposita*, **41**, 575-598.
- HOLWELL D.A. & McDONALD I. (2007). Distribution of platinum-group elements in the Platreef at Overysel, northern Bushveld Complex: a combined PGM and LA-ICP-MS study. *Contrib. Mineral. Petr.*, **154**, 171-190.
- HOLWELL D.A. & McDONALD I. (2010). Review of the Behaviour of Platinum Group Elements within Natural Magmatic Sulfide Ore Systems. *Platinum Metals Review*, 54, 26-36. [Online] Available at: <<http://www.platinummetalsreview.com/dynamic/article/view/54-1-26-36>> [Accessed 29 April 2011]
- HOLWELL D.A., McDONALD I. & ARMITAGE P.E.B. (2004). Platinum-group mineral assemblages in the Platreef at Sandsloot mine, Limpopo Province, South Africa. *Geoscience Africa 2004, Abstract Volume*, July 2004. University of the Witwatersrand, Johannesburg, South Africa, 282-283.
- HOLWELL D.A., McDONALD I. & ARMITAGE P.E.B. (2006). Platinum-group mineral assemblages in the Platreef at the South Central Pit, Sandsloot Mine, northern Bushveld Complex, South Africa. *Miner. Mag.*, **70**, 83-101.
- HOLWELL D.A., McDONALD I. & BUTLER I.B. (2011). Precious metal enrichment in the Platreef, Bushveld Complex, South Africa: evidence from homogenized magmatic sulfide melt inclusions. *Contrib. Mineral. Petr.*, **161**, 1011-1026.
- HUBER H., KOEBERL C., McDONALD I. & REIMOLD W.U. (2001). Geochemistry and petrology of Witwatersrand and Dwyka diamictites from South Africa: Search for an extraterrestrial component. *Geochim. Cosmochim. Acta*, **65**, 2007-2016.
- HULBERT L.J. (1983). A petrographical investigation of the Rustenburg Layered Suite and associated mineralization south of Potgietersrus. Unpublished DSc dissertation, University of Pretoria, 511 pp.
- HULBERT L.J. & VON GRUENEWALDT G. (1982). Nickel, copper and platinum mineralisation in the Lower Zone of the Bushveld Complex, south of Potgietersrus. *Econ. Geol.*, **77**, 1296-1306.
- HULBERT L. J., VON GRUENEWALDT G. (1985). Textural and compositional features of chromite in the Lower and Critical Zones of the Bushveld Complex. *Econ. Geol.*, **80**, 872-895.

- HULBERT L.J. & VON GRUENEWALDT G. (1986). The structure of the upper and lower chromitite layers on the farms Grasvally and Zoetveld, south of Potgietersrus. *In*: Anhausser C.R. & Maske, S. (eds.), *Mineral Deposits of Southern Africa*. Volume 2, Geological Society of Southern Africa, Johannesburg, 1237-1249.
- HUNTER D.R. (1975). The regional geological setting of the Bushveld Complex (an adjunct to the provisional tectonic map of the Bushveld Complex). Information Circular, Economic Geology Research Unit, University of the Witwatersrand, Johannesburg, 18 pp.
- HUTCHINSON D. & KINNAIRD J.A. (2005). Complex multi-stage genesis for the Ni-Cu-PGE mineralisation in the southern region of the Platreef, Bushveld Complex, South Africa. *Appl. Earth Sci. (Trans. Inst. Min. Metall. B)*, **114**, B208-224.
- HUTCHINSON D., KINNAIRD J.A. & SCHÜRMANN L.W. (2004). Complex, multi-stage mineralization history in the southern sector of the Platreef, Bushveld Complex, RSA. *Geoscience Africa 2004, Abstract Volume*, July 2004. University of the Witwatersrand, Johannesburg, South Africa, 293-294.
- HUTCHINSON D. & McDONALD I. (2008). Laser ablation ICP-MS study of platinum-group elements in sulphides from the Platreef at Turfspuit, northern limb of the Bushveld Complex, South Africa. *Miner. Deposita*, **43**, 695-711.
- ILJINA, M. (1994). The Portimo Layered Igneous Complex, with emphasis on diverse sulphide and platinum-group element deposits. *Acta Universitatis Ouluensis, Series A. Scientiae Rerum Naturalium*, **258**, 1-158.
- JAMES D.E., FOUCH M.J., VANDECAR J.C, VAN DER LEE S. & KAAPVAAL SEISMIC GROUP (2001). Tectospheric structure beneath southern Africa. *Geophys. Res. Lett.*, **28**, 2485-2488.
- JOHAN Z. (2002). Alaskan-type complexes and their platinum-group element mineralization. *In*: Cabri L.J. (ed.), *The Geology, Geochemistry, Mineralogy and Mineral Beneficiation of Platinum-Group Elements. CIMMP, Spec. Vol.*, **54**, 669-719.
- JOHNSON MATTHEY (2011a). The PGM database. [Online] Available at: <http://www.platinummetalsreview.com/jmpgm/index.jsp> [Accessed 12 October 2011].
- JOHNSON MATTHEY (2011b). Platinum Today. [Online] Available at: <http://www.platinum.matthey.com/publications/market-data-charts> [Accessed 10 October 2011].
- JOHNSON T.E., GIBSON R.L., BROWN M., BUICK I.S. & CARTWRIGHT I. (2003). Partial melting of metapelitic rocks beneath the Bushveld Complex, South Africa. *J. Petrol.*, **44**, 789-813.
- KEAYS R. R. & CAMPBELL I. H. (1981). Precious metals in the Jimberlana Intrusion, Western Australia: implications for genesis of platiniferous ores in layered intrusions. *Econ. Geol.*, **76**, 1118-1141.

- KENDALL T. (2006). Platinum 2006. Johnson Matthey, Royston, UK, 52 pp.
- KINLOCH E.D. (1982). Regional trends in the platinum-group mineralogy of the Critical Zone of the Bushveld Complex, South Africa. *Econ. Geol.*, **77**, 1328-1347.
- KINLOCH E.D. & PEYERL W. (1990). Platinum-group minerals in various rock types of the Merensky Reef: genetic implications. *Econ. Geol.*, **85**, 537-555.
- KINNAIRD J.A. (2004). What are the questions we need to ask about the Platreef? Platreef Workshop field guide, Mokopane 16-19 July, 2004, Geoscience Africa, University of the Witwatersrand.
- KINNAIRD J.A. (2005a). Geochemical evidence of multiphase emplacement in the southern Platreef. *Appl. Earth Sci. (Trans. Inst. Min. Metall. B)*, **114**, B225-242.
- KINNAIRD J.A. (2005b). The Bushveld Large Igneous Province. [Online] Available at: <<http://www.largeigneousprovinces.org/sites/default/files/BushveldLIP.pdf>> [Accessed 11 October 2011].
- KINNAIRD J.A., HUTCHINSON D., SCHÜRMANN L., NEX P.A.M. & DE LANGE R. (2005). Petrology and mineralization of the southern Platreef: northern limb of the Bushveld Complex, South Africa. *Miner. Deposita*, **40**, 576-597.
- KINNAIRD J.A. & McDONALD I. (2005). An introduction to the mineralisation in the northern limb of the Bushveld Complex. *Appl. Earth Sci. (Trans. Inst. Min. Metall. B)*, **114**, B194-198.
- KINNAIRD J.A. & NEX P.A.M. (2003). Mechanisms of marginal mineralization in the Bushveld Complex. *Appl. Earth Sci. (Trans. Inst. Min. Metall. B)*, **112**, B206-208.
- KINNAIRD J.A., YUDOVSKAYA M., NICHOLL S., NALDRETT A.J., NEX P.A. (2010). Along-strike and down-dip variations in multiphase sills of the Platreef, Bushveld Complex. In: Jugo P.J., Leshner C.M. & Mungall J.E. (eds.), 11th International Platinum Symposium, 21-24 June 2010, Sudbury, Ontario, Canada. Ontario Geological Survey, Miscellaneous Release–Data 269, extended abstracts.
- KRUGER F.J. (1999). The Bushveld Complex unconformity related ore deposits: an isotopic perspective. In: Stanley C.J. *et al.* (eds.), Mineral Deposits: Processes to Processing. Balkema, Rotterdam, 737-738.
- KRUGER F.J. (2003). Filling the Bushveld Complex magma chamber: intrachamber magma dynamics and the generation of giant chromitite and PGE deposits [abs.]. The Geological Society's 2003 Fermor Flagship Meeting – World Class Mineral Deposits and Earth Evolution, Cardiff, 18-21 August 2003. *Appl. Earth. Sci. (Trans. Inst. Min. Metall. B)*, **112**, B208-B209.

- KRUGER F.J. (2005a). Filling the Bushveld Complex magma chamber: lateral expansion, floor interaction, magmatic unconformities and giant chromitite and PGE deposits. *Miner. Deposita*, **40**, 451-472.
- KRUGER F.J. (2005b). Thoughts on the Platreef – a Critical Zone or Main Zone phenomenon? 2nd Platreef Workshop, Abstract Volume, Geol. Soc. S. Afr.
- KRUGER F.J., CAWTHORN R.G., MEYER P.S. & WALSH K.L. (1986). Sr-isotopic, chemical and mineralogical variations across the pyroxenites marker and in the Upper Zone of the western Bushveld Complex. *In: Geocongress '86*, Johannesburg: Geological Society of South Africa, 609-612.
- KRUGER F.J., CAWTHORN R.G., WALSH K.L. (1987). Strontium isotopic evidence against magma addition in the Upper Zone of the Bushveld Complex. *Earth Planet Sci. Lett.*, **84**, 51-58.
- KUCHA H. (1982). Platinum metals in the Zechstein copper deposits, Poland. *Econ. Geol.*, **77**, 1578-1591.
- KYNASTON H. (1906). On Certain Rocks Associated with the Norites and Granites of the Central Transvaal. *Trans. Geol. Soc. S. Afr.*, **8**, 56-62.
- KYNASTON H. & MELLOR E.T. (1909). The geology of the Waterberg tin-fields. GSSA, Memoir **4**, 124 pp.
- LAVIGNE M.J. & MICHAUD M.J. (2002). Geology of North American Palladium Ltd's Roby Zone deposit, Lac des Îles. *Explor. Min. Geol.*, **10**, 1-17.
- LECHLER P.J. (1988). Platinum-group-element exploration in Nevada. *Explore*, **63**, 10-12.
- LEE C.A. (1996). A review of mineralization in the Bushveld Complex and some other layered mafic intrusions. *In: Cawthorn R.G. (ed.), Layered Intrusions*, Elsevier Science, 103-146.
- LI C., MAIER W.D. & DE WAAL S.A. (2001). The role of magma mixing in the genesis of PGE mineralization in the Bushveld Complex: thermodynamic calculations and new interpretations. *Econ. Geol.*, **96**, 653-662.
- LI C., RIPLEY E.M., MERINO E. & MAIER W.D. (2004). Replacement of base metal sulphides by actinolite, epidote, calcite and magnetite in the UG2 and Merensky Reef of the Bushveld Complex, South Africa. *Econ. Geol.*, **99**, 173-184.
- MACDONALD A.J. (1987). Ore deposit models #12. The platinum-group element deposits: classification and genesis. *Geosci. Can.*, **14**, 155-166.
- MAIER, W.D. (2005). Platinum-group element (PGE) deposits and occurrences: mineralization styles, genetic concepts, and exploration criteria. *J. Afr. Earth Sci.*, **41**, 165-191.

- MAIER W.D, ARNDT N.T., & CURL E. (2000). Progressive crustal contamination of the Bushveld Complex: Evidence from Nd isotopic analyses of the cumulus rocks. *Contrib. Mineral. Petrol.*, **140**, 328-343.
- MAIER W.D. & BARNES S.J. (1999). Platinum-group elements in silicate rocks of the Lower, Critical and Main Zones at union section, western Bushveld Complex. *J. Petrol.*, **40**, 1647-1671.
- MAIER W., BARNES S.J., GARTZ V. & ANDREWS G. (2003a). Pt-Pd reefs in magnetitites of the Stella layered intrusion, South Africa; a world of new exploration opportunities for platinum group elements. *Geology*, **31**, 885-888.
- MAIER W.D., BARNES S.-J. & SAVARD D. (2008a): 'PGE reefs in the main zone of the northern limb of the Bushveld on the farm Moordrift', Proc. 3rd Platreef Workshop, Mokopane, South Africa, 2008, Geological Society of South Africa.
- MAIER W.D., BARNES, S.-J. TEIGLER B., DE KLERK W.J., MITCHELL A.A. (1996). Cu/Pd and Cu/Pt of silicate rocks in the Bushveld Complex: implications for platinum-group element exploration. *Econ. Geol.*, **91**, 1151-1159.
- MAIER, W.D., BARNES, S.-J. & VAN DER MERWE, M.J. (2001). Platinum-group elements in the Pyroxenite Marker, Bushveld Complex: implications for formation of the Main Zone. *S. Afr. J. Geol.*, **104**, 301-308.
- MAIER W.D., DE KLERK L., BLAINE J., MANYERUKE T., BARNES S.-J., STEVENS M.V.A. & MAVROGENES J.A. (2008b). Petrogenesis of contact-style PGE mineralization in the northern lobe of the Bushveld Complex: comparison of data from the farms Rooipoort, Townlands, Drenthe and Nonnenwerth. *Miner. Deposita*, **43**, 255-280.
- MAIER W.D. & EALES H.V. (1997). Correlation within the UG 2–Merensky Reef interval of the western Bushveld Complex, based on geochemical, mineralogical and petrological data. Bulletin 120, Council for Geoscience, Geological Survey of South Africa, Pretoria, 56 pp and appendices.
- MAIER W. D., PELTONEN O., GRANTHAM G. & MANTTARI I. (2003b). A new 1.9 Ga age for the Trompsburg intrusion, South Africa. *Earth Plan. Sci. Lett.*, **212**, 351-360.
- MALICH K.N. (1999). Platinum-Group Elements in Clinopyroxenite-Dunite Massifs of Eastern Siberia (Geochemistry, Mineralogy, and Genesis). VSEGEI Press, St. Petersburg, Russia, 293 pp.
- MANYERUKE T.D. & MAIER W.D. (2004). The petrography and geochemistry of the Platreef on the farm Townlands, near Potgietersrus, northern Bushveld Complex. Geoscience Africa 2004 conference, University of the Witwatersrand, Johannesburg, South Africa, Abstracts, 411–412.

- MANYERUKE T.D., MAIER W.D. & BARNES S.-J. (2005). Major and trace element geochemistry of the Platreef on the farm Townlands, northern Bushveld Complex. *S. Afr. J. Geol.*, **108**, 381-396.
- MAPEO R.B.M., KAMPUZNU A.B., RAMOKATE L.V., CORFU F. & KEY R.M. (2004). Bushveld-age magmatism in southeastern Botswana: evidence from U-Pb zircon and titanite geochronology of the Moshaneng Complex. *S. Afr. J. Geol.*, **107**, 219-232.
- MAPEO, R.B.M., RAMOKATE L.V., CORFU F., DAVIS D.W. & KAMPUNZUA A.B. (2006). The Okwa basement complex, western Botswana: U-Pb zircon geochronology and implications for Eburnean processes in southern Africa. *J. Afr. Earth Sci.*, **46**, 253-262.
- MARLOW A.G. & VAN DER MERWE M.J. (1977). The geology and the potential economic significance of the Malope area, north-eastern Bushveld Complex. *Trans. Geol. Soc. S. Afr.*, **80**, 117-123.
- MATIER K.W.J. (2004). History of exploration on the Platreef from 1925 to today. Geoscience Africa 2004, Abstract Volume, July 2004, University of the Witwatersrand, Johannesburg, South Africa, p. 427.
- MCCOURT S. 1983. Archean lithologies of the Koedoesrand area, northern Transvaal. *Geol. Soc. S. Afr. Spec. Publ.*, **8**, 113-119.
- MCCOURT S. & VEARNCOMBE J. (1987). Shear zones bounding the Central Zone of the Limpopo Mobile Belt, southern Africa. *J. Struct. Geol.*, **9**, 127-137.
- MCDONALD I. & ARMITAGE P.E.B. (2003). The Platreef of the Northern Bushveld, South Africa – is it equivalent to the Merensky Reef? *Appl. Earth Sci. (Trans. Inst. Min. Metall. B)*, **112**, B212-213.
- MCDONALD I. & HOLWELL D.A. (2007). Did lower zone magma conduits store PGE-rich sulphides that were later supplied to the Platreef? *S. Afr. J. Geol.*, **110**, 611-616.
- MCDONALD I. & HOLWELL D.A. (2011). Geology of the northern Bushveld Complex and the setting and genesis of the Platreef Ni-Cu-PGE deposit. *Rev. Econ. Geol.*, **17**, in press.
- MCDONALD I., HOLWELL D.A. & ARMITAGE P.E.B. (2005a). Geochemistry and mineralogy of the Platreef and “Critical Zone” cumulates of the Northern limb of the Bushveld Complex, South Africa: implications for Bushveld stratigraphy and the development of PGE mineralization. *Miner. Deposita*, **40**, 526-549.
- MCDONALD I., HOLWELL D.A. & ARMITAGE P.E.B. (2005b). Stratigraphy and platinum-group element mineralization in the northern lobe of the Bushveld Complex, South Africa. In Törmänen T.O. & Alapieti T.T. (eds.), 10th International Platinum Symposium, University of Oulu, Ext. Abstracts, 193-196.
- MCDONALD I., HOLWELL D.A. & WESLEY B. (2009). Assessing the potential involvement of an early magma staging chamber in the generation of the Platreef Ni-Cu-PGE deposit in the northern limb of the Bushveld

- Complex: a pilot study of the Lower Zone Complex at Zwartfontein. *Appl. Earth Sci. (Trans. Inst. Min. Metall. B)*, **118**, 5-20.
- MCDONALD I., OHNENSTETTER D., ROWE J. P., TREDoux M., PATTRICK R. A. D. & VAUGHAN D. J. (1999). Platinum precipitation in the Waterberg deposit, Naboomspruit, South Africa. *S. Afr. J. Geol.*, **102**, 184–191.
- MCDONALD I., VAUGHAN D.J. & TREDoux M. (1995). Platinum mineralization in quartz veins near Naboomspruit, central Transvaal. *S. Afr. J. Geol.*, **98**, 168-175.
- MCDONALD I. & VILJOEN, K.S. (2006). Platinum-group element geochemistry of mantle eclogites: a reconnaissance study of xenoliths from the Orapa kimberlite, Botswana. *Appl. Earth Sci. (Trans. Inst. Min. Metall. B)*, **115**, 81-93.
- MCDONOUGH W. F. & SUN S.-S. (1995). The composition of the Earth. *Chem. Geol.*, **120**, 223-253.
- MCLAREN C.H. & DE VILLIERS J.P.R. (1982). The platinum-group chemistry and mineralogy of the UG-2 chromitite layer of the Bushveld Complex. *Econ. Geol.*, **77**, 1348-1366.
- MELLOR E.T. & HALL A.L. (1910). Explanation of Sheet No. 7 (Potgietersrus). *Geol. Surv. Union S.A.*
- MERENSKY H. (1925). Report on the platinum occurrence on the properties of Potgietersrust Platinums, Limited. Report to Shareholders, London and Rhodesia Mining and Land Company Ltd, Johannesburg, South Africa, 6 pp.
- MEYER R. & DE BEER H. (1987). Structure of the Bushveld Complex from resistivity measurements. *Nature*, **325**, 610-612.
- MILLER, J.D. & ANDERSEN, J.C.O. (2002). Attributes of Skærgaard-type PGE deposits [abs]. *In*: Boudreau, A. (ed.), 9th International Platinum Symposium, Billings Montana, Duke University, 305-308.
- MILLER JR. J.D. & RIPLEY E.M. (1996). Layered intrusions of the Duluth Complex, Minnesota, USA. *In*: Cawthorn R.G. (ed.), Layered Intrusions, Elsevier Science, 257-301.
- MILLS DAVIES J.E. (1925). The geology of the Transvaal platinum deposits. *S. Afr. Min. Eng.*, **36**, 63-66.
- MISRA K.C. (2000). Understanding mineral deposits. Kluwer Academic Publishers, Dordrecht, 845 p.
- MITCHELL A.A. & SCOON R.N. (2007). The Merensky Reef at Winnaarshoek, Eastern Bushveld Complex: A Primary Magmatic Hypothesis Based on a Wide Reef Facies. *Econ. Geol.*, **102**, 971-1009.
- MOLENGRAAFF G.A.F. (1898a). Geological sketch of the Waterberg district. Geological Survey of the Transvaal. Annual Report, 18-26.

- MOLENGRAAFF G.A.F. (1898b). Report of the State Geologist of the South African Republic for the year 1897. *Trans. Geol. Soc. S. Afr.*, **4**, 119-147.
- MONDAL S.K. & MATHEZ E.A. (2007). Origin of the UG2 chromitite layer, Bushveld Complex. *J. Petrol.*, **48**, 495-510.
- MORGAN J.W. (1986). Ultramafic xenoliths: Clues to Earth's late accretionary history. *J. Geophys. Res.*, **91**, 12375-12387.
- MOSTERT A.B. (1982). The mineralogy, petrology and sulfide mineralization of the Platreef north-west of Potgietersrus, Transvaal, Republic of South Africa. *GSSA Bulletin*, **72**, 48 pp.
- MOTHETHA M.V. & KINNAIRD J.A. (2005). Mineral chemistry for the southern sector of the Platreef. 2nd Platreef Workshop, Abstract Volume, GSSA.
- MUKASA S.B., WILSON A.H. & CARLSON R.W. (1998). A multielement geochronologic study of the great dyke, Zimbabwe: significance of the robust and reset ages. *Earth Plan. Sci. Lett.*, **164**, 353-369.
- MUNGALL J.E. (2002). A model for co-precipitation of platinum-group minerals with chromite from silicate melts. 9th International Platinum Symposium, Abstract with Program, 21-25 July 2002, Billings, Montana, 321-324.
- MUNGALL J.E. (2005). Magmatic geochemistry of the platinum-group elements. *In* Mungall J.E. (ed.), *Exploration for Platinum-Group Element Deposits*. Mineralogical Association of Canada Short Course Series, **35**, Ottawa, 512 pp.
- MUNGALL J.E., AMES, D.A. & HANLEY, J.J. (2004). Geochemical evidence from the Sudbury structure for crustal redistribution by large bolide impacts. *Nature*, **429**, 546-548
- NALDRETT A.J. (2004). *Magmatic Sulfide Deposits: Geology, Geochemistry and Exploration*. Springer Verlag, Heidelberg, 728 pp.
- NALDRETT A.J. (2005a). An overview of PGE Deposits in Igneous Rocks. *In*: *Platinum-group elements – from genesis to beneficiation and environmental impact*. 10th International Platinum Symposium, University of Oulu, Extended Abstracts, 9-15.
- NALDRETT A.J. (2005b). The Platreef: death at Drenthe; resurrection at Aurora. 2nd Platreef Workshop, Mokopane, Abstract Volume, GSSA.
- NALDRETT A. J., BRÜGMANN G. E. & CAN. WILSON A. H. (1990). Models for the concentration of PGE in layered intrusions. *Can. Mineral.*, **28**, 389-408.

- NALDRETT A., KINNAIRD J., WILSON A. & CHUNNET G. (2008). Concentration of PGE in the Earth's crust with special reference to the Bushveld Complex. *Earth Science Frontiers*, **15**, 264-297.
- NALDRETT A.J. & VON GRUENEWALDT G. (1989). Association of platinum-group elements with chromitite in layered intrusions and ophiolite complexes. *Econ. Geol.*, **84**, 180-187.
- NELL J. (1985). The Bushveld metamorphic aureole in the Potgietersrus Area: evidence for a two-stage metamorphic event. *Econ. Geol.*, **80**, 1129-1152.
- NEX P.A.M. (2005). The structural setting of mineralisation on Tweefontein Hill, northern limb of the Bushveld Complex, South Africa. *Appl. Earth Sci. (Trans. Inst. Min. Metall. B)*, **114**, B243-291.
- NEX P.A.M. & KINNAIRD J.A. (2004). The Platreef: It's not as simple as A, B, C. Geoscience Africa 2004 conference, University of the Witwatersrand, Johannesburg, South Africa, Abstracts, 494-495.
- NEX P.A.M., KINNAIRD J.A., INGLE L.J., VAN DER VYVER B.A. & CAWTHORN R.G. (1998). A new stratigraphy for the main Zone of the Bushveld Complex, in the Rustenburg area. *S. Afr. J. Geol.*, **101**, 215-223.
- NEX P.A.M., NICHOL S. & IXER R.A. (2008). Geological evidence for hydrothermal and supergene PGE mineralization in the footwall to the Platreef from Tweefontein Hill, South Africa. 3rd Platreef Workshop, Mokopane, South Africa, 11-13 July 2008, Abstracts.
- NICHOLSON D.M. & MATHEZ E.A. (1991). Petrogenesis of the Merensky Reef in the Rustenburg section of the Bushveld Complex. *Contrib. Mineral. Petrol.*, **107**, 293-309.
- NYAMA N., NEX P.A.M. & YAO Y. (2005). Preliminary petrological studies of the Platreef on Tweefontein Hill, Bushveld Igneous Complex, South Africa. In: Törmänen T.O. & Alapieti T.T. (eds.), 10th International Platinum Symposium, University of Oulu, Ext. Abstracts, 505-508.
- O'NEILL H. ST. C. (1991). The origin of the moon and the early history of the earth – A chemical model. Part 2: The Earth. *Geochim. Cosmochim. Acta*, **55**, 1159-1172.
- OBERTHÜR T., DAVIS D.W., BLENKINSOP T.G., HÖHNDORF A. (2002). Precise U–Pb mineral ages, Rb–Sr and Sm–Nd systematics for the Great Dyke, Zimbabwe—constraints on late Archean events in the Zimbabwe Craton and Limpopo Belt. *Prec. Res.*, **113**, 293-305.
- OBERTHÜR T., WEISER T.W., GAST L. & KOJONEN K. (2003). Geochemistry and mineralogy of platinum-group elements at Hartley Platinum Mine, Zimbabwe. *Miner. Deposita*, **38**, 312-326.

- PAGE N.J., VON GRUENEWALDT G., HAFFTY J. & ARUSCAVAGE P.J. (1982). Comparisons of platinum, palladium and rhodium distributions in some layered intrusions with specific relation to the late differentiates (Upper Zone) of the Bushveld Complex, South Africa. *Econ. Geol.*, **77**, 1405-1418.
- PAGE N.J., ZIENTEK M.L., CZAMANSKE K. & FOOSE M.P. (1985). Sulfide mineralization in the Stillwater Complex and underlying rocks. Montana Bur. Mines Geol. Spec. Publ., **92**, 93-96.
- PALACHE, C. (1922). Some problems on mineral genesis in South Africa. *Am. Mineral.*, **7**, 37-45.
- PATTOU L., LORAND J. P. & GROS M. (1996). Non-chondritic platinum group element ratios in the Earth's mantle. *Nature*, **379**, 712-715.
- PEACH C. L. & MATHEZ E. A. (1996). Constraints on the formation of platinum group element deposits in igneous rocks. *Econ. Geol.*, **91**, 439-450.
- PENISTON-DORLAND S.C., WING B.A., NEX P.A., KINNAIRD J.A., FARQUHAR J., BROWN M., SHARMAN E.R. (2008). Multiple sulfur isotopes reveal a magmatic origin for the Platreef platinum group element deposit, Bushveld Complex, South Africa. *Geology*, **36**, 979-982.
- POLTAVETS Y.A., SAZONOV V. N., POLTAVETS Z. I. AND NECHKIN G. S. (2006). Distribution of noble metals in ore mineral assemblages of the Volkovsky gabbroic pluton, central Urals. *Geochem. Int.*, **44**, 143-163.
- POTTER M. (2002). Palladium soil geochemistry, Baronskoye Pd-Au Prospect, Sverdlovsk Oblast, Russia. *Appl. Earth Sci. (Trans. Inst. Min. Metall.B)*, **111**, 58-64.
- PRENDERGAST M.D. & WILSON A.H. 1989. The Great Dyke of Zimbabwe – II, Mineralization and mineral deposits. In Prendergast M.D. & Jones J. (eds.), Magmatic sulphides – The Zimbabwe volume, London, The Institution of Mining and Metallurgy, 21-42.
- PRICHARD H.M., BARNES S.-J., MAIER W.D. & FISHER P.C. (2004). Variations in the nature of the platinum-group minerals in a cross-section through the Merensky Reef at Impala Platinum: implications for the mode of formation of the reef. *Can. Mineral.*, **42**, 423-437.
- PRINGLE I.C. (1986). The Zwartkloof fluorite deposits, Warmbad District. In: Anhaeusser C.R. & Maske, S. (eds). Mineral Deposits of Southern Africa, Vol II. Geological Society of South Africa, Johannesburg, 1343-1349.
- REISBERG L.C., TREDoux M. & HARRIS C. (2006). Re-Os systematics of the Platreef (Sandsloot mine) of the northern limb of the Bushveld Complex. *Geochim. Cosmochim. Acta Supplement*, **70**, A526-A526.

- REISBERG L., TREDoux M., HARRIS H., COFTIER A. & CHAUMBA J. (2011). Re and Os distribution and Os isotope composition of the Platreef at the Sandsloot–Mogolakwena mine, Bushveld complex, South Africa. *Chem. Geol.*, **281**, 352-363.
- RICHARDSON S.H. & SHIREY S.B. (2008). Continental mantle signature of Bushveld magmas and coeval diamonds. *Nature*, **453**, 910-913.
- RICHTER F.M. (1988). A major change in the thermal state of the Earth at the Archean-Proterozoic boundary: Consequences for the nature and preservation of continental lithosphere. *J. Petrol.*, **29**, 39-52.
- RIGHTER K. (2003). Mantle-silicate partitioning of siderophile elements and core formation in the early Earth. *Annu. Rev. Earth Pl. Sc.*, **32**, 135-174.
- RIGHTER K., CAMPBELL A.J., HUMAYUN M. & HERVIG R.L. (2004). Partitioning of Ru, Rh, Pd, Re, Ir, and Au between Cr-bearing spinel, olivine, pyroxene and silicate melt. *Geochim. Cosmochim. Acta*, **68**, 867-880.
- RIPLEY E.M. & LI C. (2003). S isotope exchange and metal enrichment in the formation of magmatic Cu-Ni-(PGE) deposits. *Econ. Geol.*, **98**, 635-641.
- RIPLEY E.M., PARK Y.R., LI C. & NALDRETT A.J. (1999). Sulfur and oxygen isotopic evidence of country rock contamination in the Voisey's Bay Ni–Cu–Co deposit, Labrador, Canada. *Lithos*, **47**, 53-68.
- ROZENDAAL A, TOROS M.S. & ANDERSON J.R. (1986). The Rooiberg tin-deposits, West-central Transvaal. In: Anhaeusser C. R. & Maske S. (eds.), Mineral Deposits of Southern Africa, **2**, Geological Society of South Africa, 1307-1328.
- RUIZ J., BARRA F., ASHWAL L.D. & LEGRANGE M. (2004). Re-Os systematics on sulfides of the Platreef, Bushveld Complex, South Africa. Geoscience Africa 2004, Abstract Volume, July 2004, University of the Witwatersrand, Johannesburg, South Africa, p. 564.
- SCHIFFRIES C.M. (1982). The petrogenesis of a platiniferous dunite pipe in the Bushveld Complex: infiltration metasomatism by a chloride solution. *Econ. Geol.*, **77**, 1439-1453.
- SCHIFFRIES C.M. & RYE D.M. (1990). Stable isotopic systematics of 547 the Bushveld Complex: II. constraints on hydrothermal processes in layered intrusions. *Am. J. Sci.*, **290**, 209-245.
- SCHNEIDERHÖHN H. (1929). The mineragraphy, spectrography and genesis of the platinum-bearing nickel-pyrrhotite ores of the Bushveld Complex. In Wagner P.A.: The platinum deposits and mines of South Africa, Oliver and Boyd, Edinburgh, 206-246.
- SCOATES J.S. & FRIEDMAN R.M. (2008). Precise age of the platiniferous Merensky Reef, Bushveld Complex, South Africa, but the U-Pb zircon chemical abrasion ID-TIMS technique. *Econ. Geol.*, **103**, 465-471.

- SCOON R.N. (2002). A new occurrence of Merensky Reef on the flanks of the Zaaikloof Dome, Northeastern Bushveld Complex: relationship between diapirism and magma replenishment. *Econ. Geol.*, **97**, 1037-1049.
- SCOON R.N. & MITCHELL A.A. (2004). The platiniferous dunite pipes in the eastern limb of the Bushveld Complex: Review and comparison with unmineralized discordant ultramafic bodies. *S. Afr. J. Geol.*, **107**, 505-520.
- SCOON R.N. & TEIGLER B. (1994). Platinum-group element mineralisation in the Critical Zone of the Western Bushveld Complex: I. Sulfide poor chromitites below the UG2. *Econ. Geol.*, **89**, 1094-1121.
- SCOON R.N. & TEIGLER B. (1995). A new LG-6 chromite reserve at Eerste Geluk in the boundary zone between the central, and southern sectors of the eastern Bushveld Complex. *Econ. Geol.*, **90**, 969-982.
- SEVERSEN M.J. & HAUCK S.A. (2003). Platinum group elements (PGEs) and platinum group minerals (PGMs) in the Duluth Complex. Technical Report NRRI/TR-2003/37, Natural Resources Research Unit, University of Minnesota, Duluth, 296 pp.
- SHARMAN-HARRIS E., KINNAIRD J.A., HARRIS C., HORSTMANN U.E. & WING B. (2005). A new look at sulphide mineralisation of the northern limb, Bushveld Complex: a stable isotope study. *Appl. Earth Sci. (Trans. Inst. Min. Metall. B)*, **114**, 252-263.
- SHARPE M.R., BAHAT D. & VON GRUENEWALDT G. (1981). The concentric elliptical structure of feeder sites to the Bushveld Complex and possible economic implications. *Trans. Geol. Soc. S. Afr.*, **84**, 239-244.
- SHARPE M.R. & CHADWICK B. (1982). The geometry of floor folds and xenoliths in the eastern compartment of the Bushveld Complex. *Trans. Geol. Soc. S. Afr.*, **85**, 29-42.
- SHARPE M.R. & HULBERT L.J. (1985). Ultramafic sills beneath the eastern Bushveld Complex: mobilized suspensions of early Lower zone cumulates in a parental magma with boninitic affinities. *Econ. Geol.*, **80**, 849-871.
- SHARPE M.R. & LEE CA. (1986). The structural setting of the Bushveld Complex – an assessment aided by LANDSAT imagery. In: Anhaeuser C.R. & Maske S. (eds.), Mineral Deposits of Southern Africa. Vols. I and II. Geological Society of South Africa, pp. 1031-1038.
- SILVER P.G., FOUCH M.J., GAO S.S., SCHMITZ M. & KAAPVAAL SEISMIC GROUP (2004). Seismic anisotropy, mantle fabric, and the magmatic evolution of Precambrian southern Africa. *S. Afr. J. Geol.*, **107**, 45-58.
- SMITH D.S., BASSON I.J., REID D.L. (2004). Normal Reef sub-facies of the Merensky Reef at Northam Platinum Mine, Zwartklip Facies, Western Bushveld Complex, South Africa. *Can. Mineral.*, **42**, 243-260.

- SNOW J. E. & SCHMIDT G. (1998). Constraints on Earth accretion deduced from noble metals in the ocean mantle. *Nature*, **391**, 166-169.
- SNOWDEN MINING (2004). Independent valuation of the Mokopane Platreef project, Republic of South Africa. Report prepared for AIM Resources, 19 February 2004, 21 pp.
- SOUTH AFRICAN COMMITTEE ON STRATIGRAPHY (SACS), 1980. Stratigraphy of South Africa. Part 1 (Comp. L.E. Kent). Lithostratigraphy of the Republic of South Africa, South West Africa/Namibia, and the Republics of Botswana, Transkei and Venda. *Handb. Geol. Surv. S. Afr.*, **8**, 690 pp.
- SPIES L. (2005). The Akanani Platinum Project. 2nd Platreef Workshop, Abstract Volume, GSSA.
- STUMPFL E.F. & RUCKLIDGE J.C. (1982). The platiniferous dunite pipes of the Eastern Bushveld. *Econ.Geol.*, **77**, 1419-1431.
- TANKARD A.J., JACKSON M.P.A., ERIKSSON K.A., HOBDAV D.K., HUNTER D.R. & MINTER W.E.L. (1982). Crustal Evolution of Southern Africa. Springer-Verlag, New York, 523 pp.
- TEGNER C., WILSON J.R. & BROOKS C.K. (1993). Intraplutonic Quench Zones in the Kap Edvard Holm Layered Gabbro Complex, East Greenland. *J. Petrol.*, **34**, 681-710.
- TODD S.G., KEITH D.W., LEROY L.W., SCHISSEL D.J., MANN E.L. & IRVINE T.N. (1982). The J-M platinum-palladium Reef of the Stillwater Complex, Montana. I. Stratigraphy and petrology. *Econ. Geol.*, **77**, 1454-1480.
- TREDOUX M., HART R. J., CARLSON R.W., AND SHIREY S. B. (1999). Ultramafic rocks at the center of the Vredefort structure: further evidence for the crust on edge model. *Geology*, **27**, 923-926.
- TREDOUX M., LINDSAY N.M., DAVIES G. & McDONALD I. (1995). The fractionation of platinum-group elements in magmatic systems, with the suggestion of a novel causal mechanism. *S. Afr. J. Geol.*, **98**, 157-167.
- TRUTER F.C. (1947) A remarkable transcurrent fault near Potgietersrust, Transvaal. *Trans. Geol. Soc. S Afr.*, **50**, 1-15.
- TYSON R.M., BONNICHSEN B. & SHIRLEY D.H. (1985). Precious metals associated with sulphide mineralization in the Ely-Hoyt district, Duluth Complex, Minnesota [abs.]. *Can. Mineral.*, **23**, p. 331.
- UKEN R. & WATKEYS M. K. (1997). Diapirism initiated by the Bushveld Complex, South Africa. *Geology*, **25**, 723-726.
- VAN DER MERWE M.J. (1976). The Layered Sequence of the Potgietersrus Limb of the Bushveld Complex. *Econ. Geol.*, **71**, 1337-1351.

- VAN DER MERWE M.J. (1978). The geology of the basic and ultramafic rocks of the Potgietersrus Limb of the Bushveld Complex. Unpublished PhD thesis, University of the Witwatersrand, 176 pp.
- VAN DER MERWE M.J. (1998). Platiniferous horizons of the Potgietersrus lobe of the Bushveld Complex. *In: 8th international platinum symposium. S. Afr. Inst. Min. Metall. Symposium Series*, **S18**, 407-409.
- VAN DER MERWE M.J. (2008). The geology and structure of the Rustenburg Layered Suite in the Potgietersrus/Mokopane area of the Bushveld Complex, South Africa. *Miner. Deposita*, **43**, 405-419.
- VAN ROOYEN D.P. (1954). Die geologie van 'n gedeelte van gebied 7 (Potgietersrus). *Report Geol. Survey S. Afr.*, Pretoria, 116 pp.
- VERBEEK J. & LOMBERG J. (2005). Rooipoort PGE, Mokopane, Limpopo province, South Africa. Qualified persons report by RSG Global for Caledonia Mining Corporation, 96 pp.
- VERWOERD W.J. (1963). Die geologiese struktuur van die Krokodilrivierfragment. *Trans. Geol. Soc. S. Afr.*, **66**, 49-74.
- VILJOEN M. J., DE KLERK W. J., COETZER P. M., HATCH N. P., KINLOCH E., PEYERL W. (1986b). The Union Section of Rustenburg Platinum Mines, with reference to the Merensky Reef. *In: Anhaeusser C. R. & Maske S. (eds.), Mineral Deposits of Southern Africa*, 2, Geological Society of South Africa, 1061-1090.
- VILJOEN M.J. & SCHÜRMANN L.W. (1998). Platinum group metals. *In: Wilson M.G.C. & Anhaeusser C.R. (eds.), The mineral resources of Southern Africa*, Council for Geoscience, 532-568.
- VILJOEN M.J. & SCOON R.N. (1985). The distribution and main geologic features of discordant bodies of iron-rich ultramafic pegmatite in the Bushveld Complex. *Econ. Geol.*, **80**, 1109-1128.
- VILJOEN M. J., THERON J., UNDERWOOD B., WALTERS B. M., WEAVER J., PEYERL W. (1986a). The Union Section of Rustenburg Platinum Mines, with reference to the Merensky Reef. *In: Anhaeusser C. R. & Maske S. (eds.), Mineral Deposits of Southern Africa* 2, Geological Society of South Africa, 1041-1060.
- VON GRUENEWALDT G. (1979). A review of some recent concepts of the Bushveld Complex, with particular reference to sulphide mineralisation. *Can. Mineral.*, **17**, 233-256.
- Von Gruenewaldt, G., Behr, S. & Wilhelm, H.J., (1987). Some preliminary investigations of the Molopo Farms Complex, Botswana, and its Ni-Cu sulfide mineralisation. *Inst. Geol. Res. Bushveld Complex*, Univ. Pretoria, S. Afr., Res. Rep., **64**, 23 pp.
- VON GRUENEWALDT G., HULBERT L.J. & NALDRETT A.J. (1989). Contrasting platinum-group element concentration patterns in cumulates of the Bushveld Complex. *Miner. Deposita*, **24**, 219-229.

- WAGER L.R. & BROWN G.M. (1968). Layered Igneous Rocks. Oliver and Boyd, Edinburgh, 588 pp.
- WAGNER, P.A. (1926). The preliminary report on the platinum deposits in the southeastern portion of the Rustenburg district, *Transvaal. Mem. Geol.Surv.S Afr.*, **24**, 37 pp.
- WAGNER, P.A. (1929). The platinum deposits and mines of South Africa. Oliver and Boyd, Edinburgh, 326 pp.
- WAGNER P.A. & TREVOR T.G. (1923). Platinum in the Waterberg district – a description of the recently discovered Transvaal deposits. *South African Journal of Industries*, **VI**, no. 12, December 1923.
- WALRAVEN F. (1974). Tectonism during emplacement of the Bushveld Complex and the resulting fold structures. *Trans. Geol. Soc. S. Afr.*, **77**, 323-328.
- WALRAVEN F. (1997). Geochronology of the Rooiberg Group, Transvaal Supergroup, South Africa. Economic Geology Research Unit Information Circular, University of the Witwatersrand, Johannesburg 316, 21pp.
- WALRAVEN F., ARMSTRONG R.A. & KRUGER F.J. (1990). A chronostratigraphic framework for the north-central Kaapvaal Craton, the Bushveld Complex and Vredefort structure. *Tectonophysics*, **171**, 23-48.
- WALRAVEN F. & HATTINGH E. (1993). Geochronology of the Nebo Granite, Bushveld Complex. *S. Afr. J. Geol.*, **96**, 31-41.
- WEBB S.J., NGUURI T., CAWTHORN R.G. & JAMES, D. (2004). Gravity modelling of Bushveld Complex connectivity supported by southern African seismic experiment result. *S. Afr. J. Geol.*, **107**, 207-218.
- WEISE S., YUDOVSKAYA M. & KINNAIRD J. (2008). Geological observations on the Main Zone – Platreef contact on the farms Tweefontein, Vaalkop, Zwartfontein and Overysel. Abstract, 3rd Platreef Workshop, Mokopane, South Africa, 11-13 July 2008.
- WESTLAND A.D. (1981). Inorganic chemistry of the platinum-group elements. In: Cabri, L.J. (ed.), Platinum-group elements: mineralogy, geology, recovery. *Can. Inst. Mining Metall., Spec. Vol.*, **23**, 5-18.
- WHITE J.A. (1994). The Potgietersrus Prospect – geology and exploration history: XVth CMMI Congress, Johannesburg, SAIMM, **3**, 173-181.
- WILLEMSE J. (1964). A brief outline of the geology of the Bushveld Igneous Complex. In: Houghton S.H. (ed.), The geology of some ore deposits in Southern Africa 11. Geological Society of South Africa, Johannesburg, 91-128.
- WILLEMSE J. (1969). The geology of the Bushveld Igneous Complex, the largest repository of magmatic ore deposits in the world. *Econ. Geol. Monograph*, **4**, 1-22.

- WILSON J.R., CAWTHORN R.G., KRUGER F.J. & GRUNDTVIG S. (1994). Intrusive origin for the unconformable upper zone in the Northern Gap, Western Bushveld Complex. *S. Afr. J. Geol.*, **97**, 462-472
- WILSON A. & CHUNNETT G. (2006) Trace element and platinum group element distributions and the genesis of the Merensky Reef, western Bushveld Complex. *S. Afr. J. Petrol.*, **47**, 2369-2403.
- WILSON A.H., LEE C. & BROWN R.T. (1999). Geochemistry of the Merensky Reef, Rustenburg section, Bushveld Complex: controls on the silicate framework and distribution of trace metals. *Miner. Deposita*, **34**, 657-672.
- WINCH J. (2011), The importance of drilling too deep: A Platreef perspective. Abstract, 4th Platreef Workshop, Mokopane, South Africa, 14–16 January 2011.
- WOOD S.A. (2002). The aqueous geochemistry of the platinum-group elements with applications to ore deposits. *In: Cabri L.J. (ed.), The geology, geochemistry, mineralogy and mineral beneficiation of platinum-group elements. CIMMP, Spec. Vol.*, **54**, 211-249.
- YUDOVSKAYA M., KINNAIRD J., NALDRETT A., RODIONOV N., ANTONOV A. & KAPITONOV I. (2009). Zircon as an indicator of changing conditions at chromite crystallisation (Bushveld Complex). Abstract, Geoanalysis 2009 conference, 6-11 September 2009, Kwazulu-Natal, South Africa.
- ZACCARINI F., ANIKINA E., PUSHKAREV E., RUSIN I. & GARUTI G. (2004). Palladium and gold minerals from the Baronskoe-Kluevsky ore deposit (Volkovky complex, Central Urals, Russia). *Miner. Petrol.*, **82**, 137-156.
- ZIENTEK, M.L. (1983). Petrogenesis of the Basal zone of the Stillwater Complex, Montana. Unpublished Ph.D. thesis, Stanford University, Stanford, California.

APPENDIX 1

Full reference:

ARMITAGE P.E.B., McDONALD I., EDWARDS S.J. & MANBY G.M. (2002). Platinum-group element mineralization in the Platreef and calc-silicate footwall at Sandsloot, Potgietersrus District, South Africa. *Appl. Earth Sci. (Trans. Inst. Min. Metall. B)*, **111**, B36-45.

Platinum-group element mineralization in the Platreef and calc-silicate footwall at Sandsloot, Potgietersrus District, South Africa

P. E. B. Armitage, I. McDonald, S. J. Edwards and G. M. Manby

Synopsis

The Platreef is a platinum-group element (PGE) deposit in the form of a mafic-ultramafic, tabular body at the base of the northern (Potgietersrus) limb of the 2050 m.y. Bushveld Igneous Complex. The reef transgresses sedimentary floor rocks (footwall) of the 2600–2200 m.y. Transvaal Supergroup and the Archaean granite basement. The roof rocks (hanging-wall) of the reef are PGE-free Main Zone gabbro-norites of the Rustenburg Layered Suite. At the Sandsloot open-pit mine the Platreef consists of coarse to pegmatoidal pyroxenites and gabbros with accessory phlogopite, base-metal sulphides and oxides. Thermal metamorphism of siliceous dolomites that form the footwall has produced clinopyroxenites and calc-silicate hornfelses with a variety of skarn assemblages. These were subjected to later hydrothermal alteration and serpentinization that also affected parts of the Platreef.

The link between sulphides and PGE in the Platreef has led previous authors to consider the mineralization as an orthomagmatic sulphide deposit, where sulphide separation collected PGE from a large volume of melt. In the reef and footwall, however, the development of extensive alteration zones with high concentrations of PGE- and semi-metal (Te, Sb, Se, Bi and Ge)-bearing platinum-group minerals that are typical of many low-temperature PGE deposits suggests syn- to post-magmatic crystallization or redistribution of PGE by hydrothermal fluids. The results obtained to date in a new study suggest that the Platreef at Sandsloot is a complex PGE deposit that has been subject to a number of different processes during its development.

The northern (Potgietersrus) limb of the 2050-m.y. Bushveld Igneous Complex of South Africa (BIC, see Fig. 1) has a north-striking, slightly sinuous outcrop over a length of 110 km and a maximum width of 15 km. The Platreef comprises the basal eastern margin of the northern Bushveld limb (Fig. 1) and is variable in thickness along strike, attaining a maximum thickness of 250 m. Wagner²⁸ provided the first descriptions of the Platreef during platinum-mining operations in the 1920s. These early operations soon ceased, but exploration was resumed in 1967 by the Johannesburg Consolidated Investment Company. Since Wagner's²⁸ early

reports there have been few detailed geological studies of the Platreef. Most of the literature^{27,4,13,22,6,9,3,5} has been based on surface mapping, drill core and geophysical data obtained at various localities along the reef before the Sandsloot open-pit was commissioned. A new isotopic study of the Platreef based on samples collected from the open-pit has recently been published by Harris and Chaumba.¹⁴

The initial results of fieldwork carried out in 2000–2001 at the Sandsloot open-pit mine, which is operated by Potgietersrus Platinums, Ltd., a subsidiary of Anglo Platinum, are presented here. The research is based on data from the central, south and southwest parts of the pit (Fig. 2), where new, deeper exposures of the Platreef and previously unrecognized three-dimensional features have been mapped, and is aimed at increasing our understanding of how PGE acquired their present distribution at Sandsloot. The estimated reserves at the Sandsloot mine in 1998 were 23500000 t ore at an average Pt+Pd+Rh+Au grade of 5.73 g/t, with further reserves of 150 000 000 t ore at a comparable grade located along strike to the north and south.¹⁰ It is worth noting that the term 'Platreef' has sometimes been applied to the total ore zone that embraces the igneous reef and the platiniferous parts of its metasedimentary footwall (e.g. Buchanan *et al.*⁴). In the present study the term 'Platreef' or simply 'reef' is used only for the platiniferous igneous body.

Regional overview

From south to north the mafic rocks of the northern Bushveld limb transgress progressively lower units of the 2600–2200 m.y. sedimentary Transvaal Supergroup (Fig. 1). These units are the Magaliesberg quartzites and shales of the Pretoria Group and the Penge Banded Iron Formation and Malmani Dolomite of the Chuniespoort Group. The Malmani Dolomite wedges out north of the Sandsloot mine, where the Platreef comes into direct contact with Archaean granite basement. Main Zone gabbro-norites of the Rustenburg Layered Suite constitute the roof rocks (hanging-wall) of the Platreef along its entire strike length. The Platreef appears to continue south of Potgietersrus and may become part of the normal Bushveld stratigraphic sequence rather than a marginal facies. To the south of Potgietersrus the Zebediela Fault juxtaposes the Platreef against the Phanerozoic Karoo sedimentary sequence (Fig. 1). In the north the Platreef is covered by 1800-m.y. Waterberg volcano-sedimentary rocks. A gravity high just west of Potgietersrus is thought to represent the throat or feeder of the northern limb, and differentiation indices suggest at least four major influxes of fresh, undifferentiated magma.¹⁰

North of Sandsloot the Platreef has been divided into three main units: (1) a PGE-poor, upper feldspathic pyroxenite ('C-reef') in contact with the hanging-wall of Main Zone gabbro-norites; (2) a medium- to coarse-grained pyroxenite ('B-reef'); and (3) a lower, generally coarse-grained felds-

Paper presented at '21st Century Pt–Pd deposits: current and future potential', a session arranged as part of the Mineral Deposits Studies Group (MDSG) 2002 annual meeting by the MDSG, the British Geological Survey and the Institution of Mining and Metallurgy and held at the University of Southampton, England, on 3 January, 2002. Paper published in *Trans. Instn Min. Metall. (Sect. B: Appl. earth sci.)*, **111/Proc. Australas. Inst. Min. Metall.**, **307**, January–April 2002. © The Institution of Mining and Metallurgy 2002.

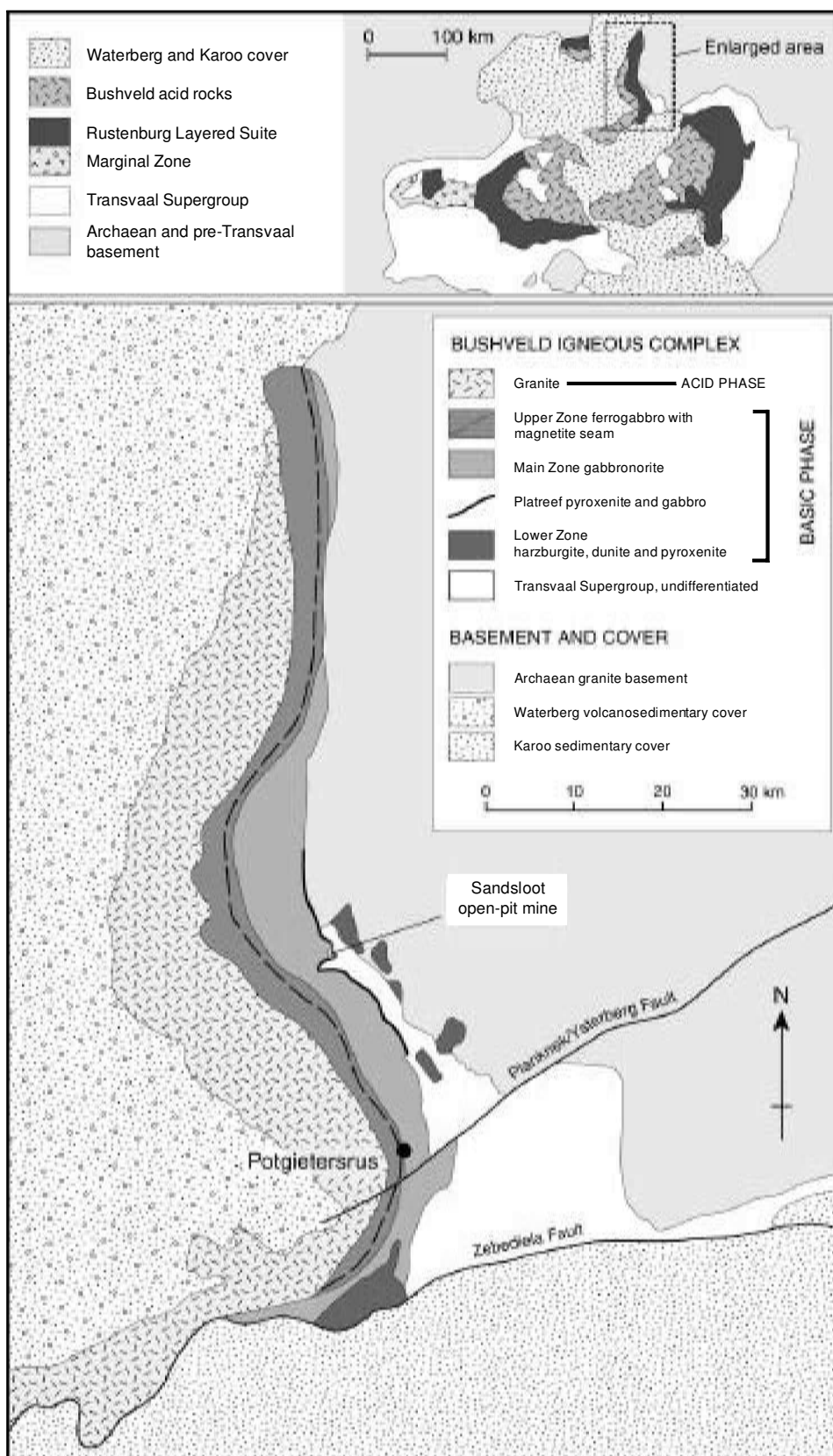


Fig. 1 (Top) Simplified map of Bushveld Igneous Complex emphasizing Rustenburg Layered Suite (mafic phase) and showing location of enlarged map of northern Bushveld limb. (Main map) Simplified geological map of northern Bushveld limb showing location of Sandsloot open-pit north of Potgietersrus

pathic pyroxenite ('A-reef') in contact with a dolomitic or granitic footwall.⁴ The thickness of the reef units varies along strike, and the B- and A-reefs are major economic targets.¹⁰ In the present study only B-reef pyroxenites and gabbros have been identified with certainty at Sandsloot.

Structure

Three linear geological features may have controlled the emplacement of the northern Bushveld limb.²⁷ These are the northeast-striking Eersteling Basin, the northwest-trending,

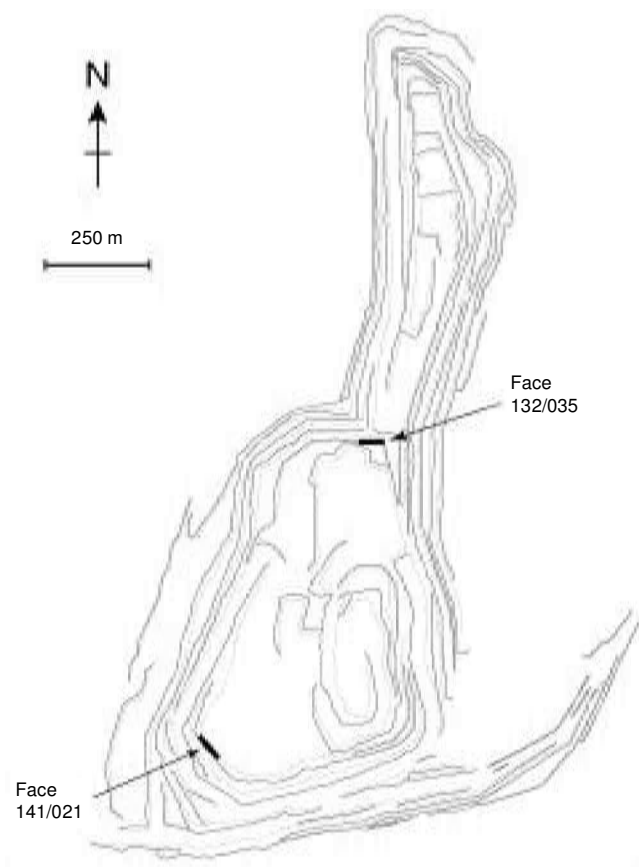


Fig. 2 Wireframe plan view of Sandsloot open-pit mine in July, 2000, showing approximate locations of geological face maps in Figs. 3 and 4. Solid black outlines bench tops, stippled grey lines bench feet. Deepest part of pit (southern central area) is approximately 190 m

2900-m.y. Usushwana basic dyke complex and a north-south chain of igneous bodies from the Great Dyke in Zimbabwe to the Trompsburg Complex in the south. The intersection of these three features just west of Potgietersrus coincides with the interpreted feeder of the northern Bushveld limb. Regionally, north-south- and WSW-ESE-trending fold structures have been identified.²⁷ The sinuous trace of the northern Bushveld limb appears to reflect a megascopic WSW-ENE-trending fold in the Transvaal Supergroup. More locally, a characteristic feature of the Sandsloot area is the 'dolomite tongue' at the south end of the Sandsloot pit (Fig. 1), which is

a shallowly plunging antiform or possibly a dome. The Platreef appears to be concordant with the 'dolomite tongue', i.e. enveloped around it, suggesting late- or post-tectonic intrusion of the reef. Pre-existing fold structures have been proposed to explain the presence of 'footwall domes' in the eastern Bushveld lobe²⁶ that compartmentalized the Lower Zone and Critical Zone magmas in that area. Compartmentalization of Lower Zone rocks around Potgietersrus may reflect similar pre-existing structures on the northern Bushveld limb that controlled the intrusion of the Platreef magma.

It is argued on the basis of geothermobarometry that the metamorphic aureole in the Potgietersrus area was generated in two stages.²³ The first event was related to emplacement of Lower Zone magma and is estimated to have attained 750°C at 1.5 kbar pressure. The second records the intrusion of the more voluminous gabbroic magmas of the Upper Critical, Main and Upper Zones, with equilibrium temperatures and pressures of about 900°C and 4–5 kbar. The higher pressure of the second event has been interpreted to reflect an elevated deviatoric stress component that generated a large fold in the floor rocks of the BIC.

Methods

The down-stepping benches of the Sandsloot open-pit have sub-vertical rock faces approximately 15 m high, and parts of faces that expose complete sections across the Platreef were mapped at 1 : 100 scale (Fig. 2). The mapped sections were delimited by spray-painting geopoints on the faces, whose latitude, longitude and elevation were established by the mine surveyors using global positioning. About 200 samples were collected from most of the major reef and footwall lithologies at 2–5-m intervals along each rock face and at spot localities of particular interest—for example, in areas of abrupt lithological variation. Samples selected for microscopy and geochemical analysis were then cut into three parts. One part was for preparation of thin sections and polished blocks, another part was powdered in an agate tema mill and the remaining part was stored as spare material. Thin sections and blocks were examined under microscopes in transmitted and reflected light. Detailed mineralogical examination and analysis were performed at the University of Greenwich with a JEOL JSM-5310LV scanning-electron microscope and energy-dispersive spectrometer with the aid of Oxford Instruments' ISIS 300 software suite.

Bulk analysis for PGE and Au was carried out on a selected group of samples using NiS fire-assay collection followed by inductively coupled plasma-mass spectrometry at the

Table 1 PGE and Au concentrations, ppb, and ratios for Platreef lithologies. For comparison, data are also given for the Merensky Reef (SARM-7 preferred values from Steele and co-workers²⁵) and the UG2 chromitite²⁰

Sample	Lithology	Ir	Ru	Rh	Pt	Pd	Au	Ru/Ir	Rh/Ir	Pt/Ir	Pd/Ir	Pt/PdAu/Ir	
PA-SW43	B-reef pyroxenite	117	503	540	6580	6460	1180	4.3	4.6	56.2	55.2	1.0	10.1
PA-N26	B-reef gabbro	34.4	109	137	4730	2440	880	3.2	4.0	137.5	70.9	1.9	25.6
PA-NX1	Gabbroic aplite	0.1	8.4	2.4	88.1	154	54	84.0	24.0	881.0	1540.0	0.6	540.0
PA-NX3	Gabbroic pegmatite	58	103	55	1490	1570	220	1.8	0.9	25.7	27.1	0.9	3.8
PA-E117	Clinopyroxenite	7.4	31.8	55.6	698	1410	374	4.3	7.5	94.3	190.5	0.5	50.5
PA-S2-6	Clinopyroxenite	0.1	9.1	6.2	30.1	10.9	7.7	91.0	62.0	301.0	109.0	2.8	77.0
PA-S2-18	Calc-silicate hornfels	0.1	4.2	1.9	7.6	2.7	5.7	42.0	19.0	76.0	27.0	2.8	57.0
PA-S2-12	Serpentinized clinopyroxenite	0.8	6.3	2.8	55	100	35.2	7.9	3.5	68.8	125.0	0.6	44.0
PA-S3-0	Serpentinite	0.1	0.73	0.25	10.8	109	69	7.3	2.5	108.0	1090.0	0.1	690.0
PA-EX5	Serpentinized Ca-silicate hornfels	40.1	124	201	2590	3060	380	3.1	5.0	64.6	76.3	0.8	9.5
PA-EX6	Serpentinized Ca-silicate hornfels	14.1	59.1	75.5	1060	1250	220	4.2	5.4	75.2	88.7	0.8	15.6
PA-N0	Pegmatoidal mafic dyke	0.2	2.33	1.7	25.1	15.1	10.5	11.7	8.5	125.5	75.5	1.7	52.5
PA-N0/2	Pegmatoidal mafic dyke	0.1	0.31	0.51	2.2	0.8	0.9	3.1	5.1	22.0	8.0	2.8	9.0
SARM-7	Merensky Reef	74	430	240	3740	1530	310	5.8	3.2	50.5	20.7	2.4	4.2
UG-2	UG2 chromitite	60	106	600	3200	1960	50	1.8	10.0	53.3	32.7	1.6	0.8

University of Greenwich. Details of the methodology and instrumentation have been given by Huber *et al.*¹⁵ The precision was determined by repeat analyses of a sub-suite of high- and low-grade samples.¹⁹ The precision was 10–15% at PGE concentrations <5 ppb and 5–10% at concentrations between 10 and 1000 ppb, but became worse again in samples with PGE concentrations >1000 ppb owing to the nugget effect; in these samples it was 10–25%. Accuracy was determined by repeat analysis of the standard WPR-1. Solutions prepared from PGE-rich samples were diluted by an additional factor of 50 to give comparable concentrations with the range of calibration standards. The PGE and Au data are reported in Table 1.

Platreef and associated units at Sandsloot

Two face maps that show the typical relationships of hanging-wall, reef and footwall lithologies are presented in Figs. 3 and 4 and brief field descriptions of the major lithologies are given below. The first map is a northeast-facing exposure on bench 41 in the southwest part of the Sandsloot mine. It exhibits a cross-strike section through the Platreef where the reef has an approximately southwest–northeast strike and a moderate to steep dip to the northwest. The second face map is a south-facing exposure on bench 32 in the central part of the pit. Again, it displays a cross-strike section through the Platreef, and here the reef displays its typical, approximately north–south strike and moderate dip to the west. The difference in the strike of the reef between the two rock faces is due to the emplacement of the reef around the antiformal ‘dolomite tongue’.

Hanging-wall gabbronorite

The hanging-wall of the Platreef consists of fairly homogeneous gabbronorite representative of the Main Zone elsewhere in the BIC. An abrupt change in pyroxene composition between the Platreef (bronzite) and hanging-wall

(inverted pigeonite) has been cited as evidence that the hanging-wall formed from a separate magma.¹³ Some exposures of the hanging-wall contact at Sandsloot show an essentially planar magmatic boundary (e.g. Fig. 4). Wagner²⁸ reported veins of hanging-wall gabbronorite cutting the Platreef in 1920s exploration trenches at Sandsloot, but in the sections studied by the present authors it is not clear whether the Platreef or hanging-wall gabbronorite was the younger magma. In other exposures the contact is tectonized, exhibiting a heavily serpentinized, brittle–ductile shear zone up to 20 cm thick (e.g. Fig. 3).

The most common variety of hanging-wall gabbronorite is a medium- to coarse-grained, isotropic assemblage of 50 modal% plagioclase, 35% orthopyroxene and 15% clinopyroxene. Its appearance is transitional between leuco- and melanocratic. The modal content of pyroxene can be as high as 75% in the darkest melanorites and as low as 30% in the palest leuconorites. Accessory phases, such as phlogopite, oxides and sulphides, account for up to 5% of the modal mineralogy. The pyroxenes are dark grey to dark grey-green and have a subhedral to ragged habit, sometimes forming large aggregates. Plagioclase occurs as randomly orientated laths. Xenoliths of calc-silicate hornfels that constitute the bulk of the footwall to the Platreef occur sporadically in the hanging-wall gabbronorites.

The Platreef

The Platreef at Sandsloot consists of pyroxenites and gabbros, mostly in a virtually unaltered state but in places showing considerable serpentinization. No conclusive evidence has yet been found for the spatial and temporal relationship of the pyroxenites and gabbros. The thickness of the Platreef varies from a few metres to about 30 m at several localities in the central and southwest parts of the Sandsloot pit. The contact with the footwall lithologies is irregular, and variably altered footwall xenoliths up to several metres in diameter occur sporadically in the reef. Chilled margins have

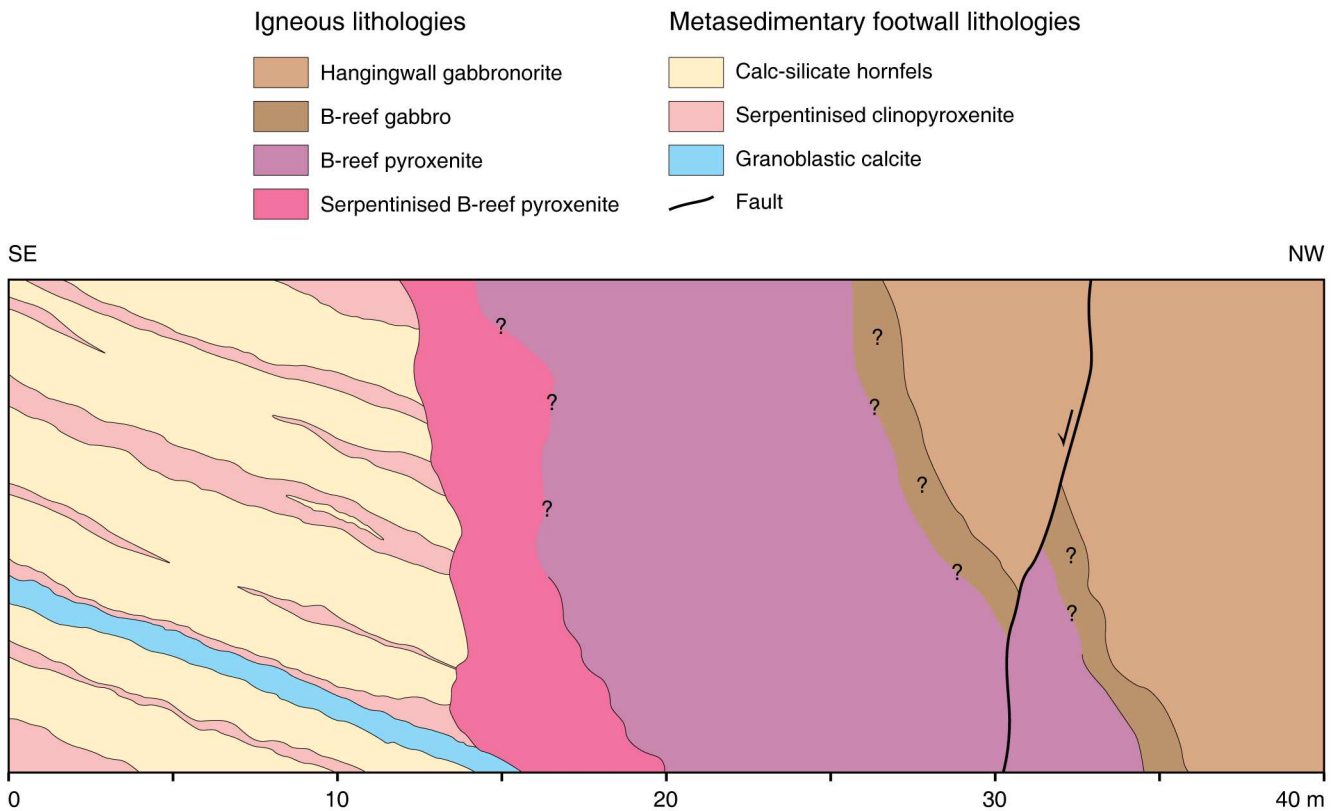


Fig. 3 Geological map of face 141/021 in central part of Sandsloot pit

not been found in the Platreef at the footwall contact, hanging-wall contact or around xenoliths. In face 132/038 (Fig. 3) a dyke-like body of aplitic gabbro with pegmatitic pods stands between the Platreef gabbro and the coarse, serpentized clinopyroxenite of the footwall. The composition of the partly pegmatitic aplite body appears to be the same as that of the Platreef gabbro and may represent an elongate pod of residual Platreef melt.

Pyroxenites

B-reef pyroxenites dominate the Platreef in the southwest part of the Sandsloot pit. They are commonly coarse-grained, dark grey-green assemblages of anhedral to subhedral orthopyroxene (60–90 modal%) with a subordinate content of intercumulus clinopyroxene (10–40%). Postcumulus plagioclase occurs locally in small pods and constitutes up to 15% of the modal mineralogy. Accessory phases are small booklets of phlogopite and finely disseminated base-metal sulphides (pyrrhotite, pentlandite, chalcopyrite, bornite, pyrite and minor galena–clausthalite); minor oxides present are magnetite, ilmenite, perovskite, chromian spinel (picotite) and chromite.

Large zones within the pyroxenites have undergone varying degrees of alteration to serpentine and talc. In such zones the pyroxenes have a more rounded, ragged habit and are shot through by networks of serpentine microveins, suggesting widespread infiltration of hydrothermal fluids. The inter- and intragranular serpentine is black, giving the altered rock a distinctly darker colour than its unaltered counterpart.

Gabbros

Platreef gabbros have coarse-grained to pegmatoidal textures. Dark green orthopyroxene occurs as a sub- to euhedral cumulus phase (40–70 modal%) with dark clinopyroxene (up to 10%) in a colourless postcumulate mass of plagioclase (30–50%). Plagioclase is locally saussuritized, whereas pyrox-

ene appears to have evaded alteration in most of the observed B-reef gabbros. Quartz is a minor phase. Other accessory and minor phases are the same as those found in the Platreef pyroxenites. However, interstitial base-metal sulphides are larger and more sporadic, rather than finely disseminated throughout the rock body as they are in the pyroxenites. Coarse gabbros occur at different stratigraphic positions in the Platreef (as large irregular pods or contiguous bodies?) and seem to dominate the central part of the pit. This is typified by face 132/038 (Fig. 3), where the reef consists almost exclusively of gabbro.

Footwall lithologies

Clinopyroxenites

A characteristically pale grey, granoblastic, diopsidic clinopyroxenite normally occurs between the Platreef and layered calc-silicate hornfels, but the shapes of the clinopyroxenite bodies are irregular. Clinopyroxenites are also seen as elongated lenses and semi-continuous bands concordantly interlayered with calc-silicate hornfels (e.g. Fig. 3), and the boundaries between these two lithologies are usually transitional over centimetre-scale distances.

The Sandsloot mine geologists refer to the clinopyroxenite bodies as ‘parapyroxenite’, probably following the term originally used by Wagner,²⁸ who evidently regarded the diopside-rich footwall lithologies as highly metamorphosed dolomites. Recent geochemical work has shown that the clinopyroxenites have a non-igneous genesis.¹⁴ The clinopyroxenites contain little Cr, whereas the ‘normal’ reef pyroxenites and gabbros have Cr contents of thousands of parts per million. Serpentine with relict cores of olivine is common and the clinopyroxenites rich in olivine also contain little Ni, whereas igneous olivine with the same Mg/Fe ratio contains thousands of parts per million Ni. Some clinopyroxenites do contain Ni, but also have high Cu contents because

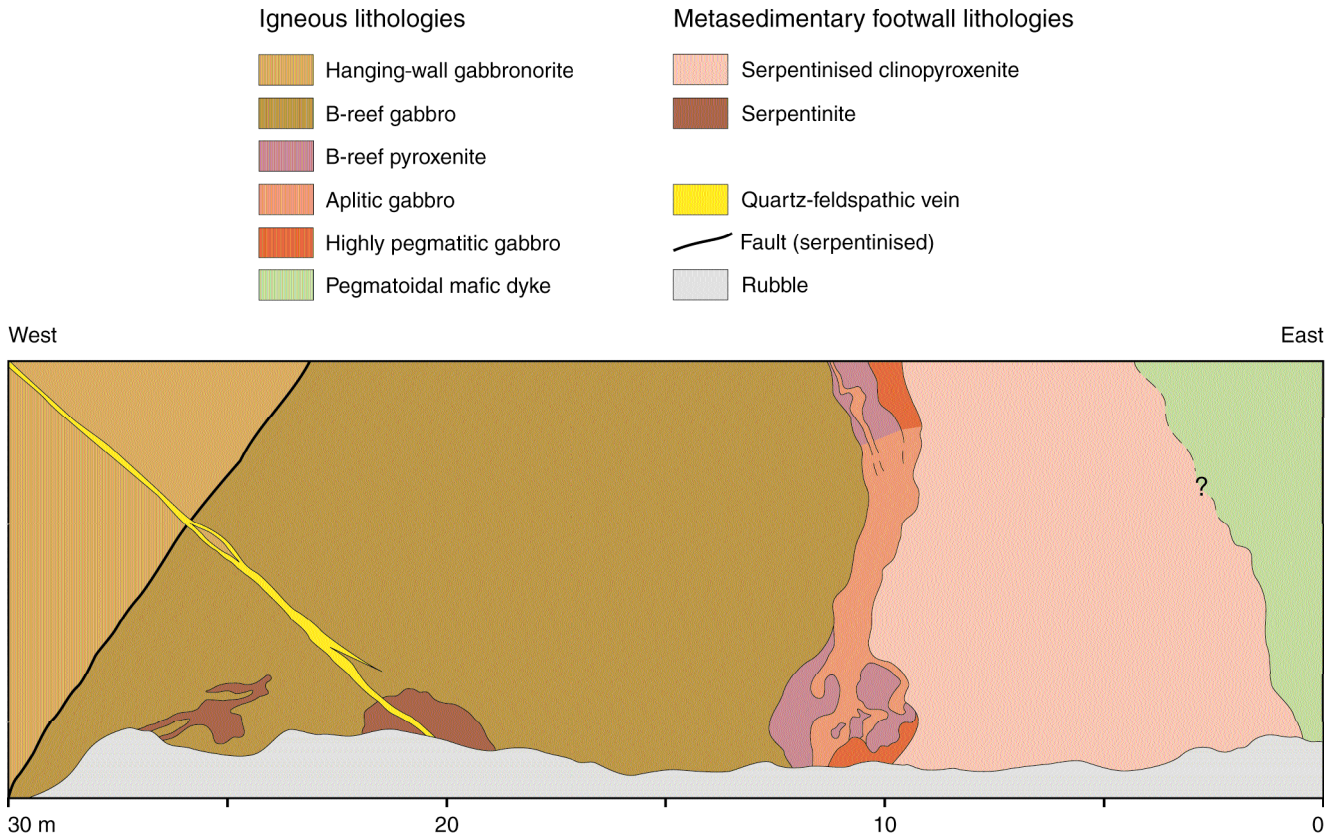


Fig. 4 Geological map of face 132/038 in southwest part of Sandsloot pit

sulphides are present as well as olivine and the Ni is contained in the sulphides. These trace-element characteristics suggest that both clinopyroxene and olivine are derived by high-grade metamorphism/metasomatism of the siliceous footwall dolomites. The paragenesis of the clinopyroxenites has involved such a thorough textural transformation that no primary layering is preserved. Further support for a metamorphic origin comes from the presence of grossular-andradite and idocrase (vesuvianite). Similar lithologies in the metamorphic aureole of the northern BIC limb are considered to reflect extreme metasomatism.⁷ The mineralogy of the clinopyroxenite bodies also appears to correspond to at least one of the 11 assemblage groups in calcareous rocks of the Bushveld metamorphic aureole in the Potgietersrus area identified by Nell.²³

Calc-silicate hornfels and serpentinites

The calc-silicate hornfels and serpentinite footwall lithologies can be crudely described as skarns and they contain minerals that reflect a wide range of prograde and retrograde metamorphic reactions. The original sedimentary layering is clearly preserved, with a bedding thickness of 5–60 cm. Relatively unaltered footwall hornfels have a mottled beige and pale green colour. Only minor parts of the footwall are untouched by retrograde hydrothermal alteration. This alteration is mostly characterized by serpentinization of prograde metamorphic phases, such as forsterite. The colour of the footwall at any locality is usually an indication of the extent of serpentinization, such that the darkest (virtually black) zones represent extreme alteration to virtually pure serpentinite. These zones tend to take the shape of irregular bodies varying in size from a few decimetres to tens of metres and are often elongate parallel to the footwall layering. The boundaries of serpentinized zones are usually transitional, yet surprisingly sharp in a few places. Less extensive serpentinization in the hornfels follows the original bedding, such that darker altered layers are visibly continuous. The varying degrees of alteration between layers are thought to reflect primary compositional variations.

Like the Platreef, the footwall rocks contain common base-metal sulphides, such as pyrrhotite-troilite ($\text{Fe}_7\text{S}_8\text{--FeS}$), pentlandite ($\text{Fe}_3\text{Ni}_9\text{S}_8$), chalcopyrite (CuFeS_2) and bornite (Cu_5FeS_4), but less common base-metal sulphides occur in the footwall that have not yet been identified in the reef. These are sphalerite (ZnS), bravoite (Fe,Ni,CoS_2), godlevskite (Ni_7S_6), millerite (NiS) and hydrous valeriite ($(\text{CuFeS}_2)_{1.5}(\text{Mg,Al})(\text{OH})_2$). An unidentified Fe–Zn–Mn–S phase is frequently encountered in serpentinites (highly altered calc-silicate hornfels), and stibnite (Sb_2S_3) and molybdenite (MoS_2) are rare sulphides in the hornfels and serpentinites. Magnetite is the only oxide found so far in the footwall. Other rare phases include altaite (PbTe), plumboanbarite or hokutolite (Ba,PbSO_4), as well as halogen-bearing phases, such as bismoclite (BiOCl), and unidentified Fe–Nd–F-bearing and Pb–Cl-bearing species.

Pegmatoidal mafic dykes

In the east-central part of the Sandsloot pit a 4–5 m thick, pegmatoidal mafic dyke intrudes almost vertically through the footwall (Fig. 3). Several smaller dykes and veins branch from the large dyke into the Platreef (these occur just below the base of the face map in Fig. 3). Locally the texture is extremely pegmatitic and pyroxene crystals up to 30 cm long have been found in blasted-out boulders near the main exposure of this dyke. Its relationship to the hanging-wall is not known. Small dykes and veins of similar composition are observed in some drill cores from various locations at the mine. Like the Platreef, the dyke has no chilled margins. Two

consistently characteristic features of the dyke and its branching veins are their pegmatoidal texture and green cumulus feldspar laths with intercumulate grey to black pyroxene, although locally the two phases display eutectic intergrowth. Sub- to euhedral pyroxene crystals in tooth-like or radial arrangements occur along the dyke margins. Within the dyke and larger veins signs of flow are observed in the form of bowed pyroxene crystals and fragments of pyroxene evidently broken away from the dyke margins and entrained in the central flow. Phlogopite is an accessory phase, comprising large booklets. Base-metal sulphides are notably rarer than in the Platreef, but large, interstitial blebs of pyrrhotite and pentlandite occur sporadically. Ilmenite and perovskite represent minor oxide phases, sometimes containing chlorapatite ($\text{Ca}_5(\text{PO}_4)_3\text{Cl}$) and baddeleyite (ZrO_2). Veins of similar composition and appearance to this major dyke are observed in the footwall lithologies along the east highwall of the Sandsloot mine, but the feldspar in these instances is often colourless to milky white.

Late hydrothermal veins

Planar, hydrothermal quartz-feldspathic veins cut all lithologies and their boundaries. Two large veins (>1 m) cross the Sandsloot pit, striking approximately north–south with a moderate to steep dip to the east. In addition to coarse-grained quartz and feldspar, calcite and fibrous white chrysotile aggregates occur in the veins as later, lower-temperature phases. Minor brittle–ductile shear structures occur at the margins of the largest vein, but do not occur within the vein itself. This suggests either that an earlier shear zone may have been the favoured locus of this hydrothermal channel or that the competence contrast between the vein and country rock has generated high contact strains during deformation and given rise to the shearing along the contacts.

PGE concentrations in the reef and footwall

PGE and Au concentrations and metal ratios in the Platreef and footwall lithologies are given in Table 1 and compared with those of other Bushveld PGE reefs. Chondrite-normalized patterns for PGE-rich samples are shown in Fig. 5. Although the B-reef pyroxenites and gabbros are consistently mineralized, there is considerable variation in PGE

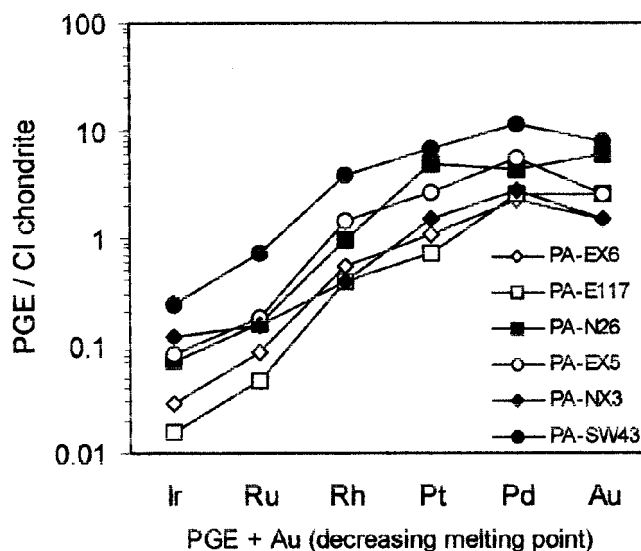


Fig. 5 Chondrite-normalized plot of PGE-rich reef and footwall lithologies. CI chondrite values from Jochum.¹⁶ Filled symbols, Platreef B-reef samples; open symbols, footwall samples

concentration within the reef. The mineralization extends for a significant distance below the reef into the footwall. Some footwall lithologies are essentially barren, but certain zones of clinopyroxenite and some highly serpentinized zones and layers within the calc-silicate hornfels contain Rh+Pt+Pd+Au concentrations approaching those in the B-reef. The minor pegmatitic pods within the aplite dyke that separates the footwall and B-reef in face 132/038 (Fig. 3) have high PGE concentrations, while the aplite itself is relatively poor in PGE. The pegmatoidal mafic dyke that crosscuts the footwall and B-reef contains very low PGE concentrations (<100 ppb Rh+Pt+Pd+Au).

Comparison of the PGE ratios of the PGE-rich Platreef and footwall lithologies with the Merensky Reef and UG-2 chromitite reveals some interesting features. The B-reef and footwall are richer in Pt, Pd and Au relative to Ir than the Merensky or UG-2 reefs, producing more fractionated PGE patterns. Pt/Pd and Pt/Au ratios in the Platreef and footwall are lower than those in the Merensky or UG-2 reefs, indicating that the Platreef is richer in Pd and Au relative to Pt than the Merensky or UG-2 reefs. PGE-rich footwall samples and pegmatoidal aplites have lower Pt/Pd (consistently <1.0) than B-reef gabbro or pyroxenite (1.0 or greater). This would appear to indicate some fractionation of Pd over Pt into late-stage fluids in the reef and footwall—a feature noted by Wagner²⁸ and Ainsworth.¹ Rh/Ir in the Platreef is comparable with that of the Merensky Reef, but lower than the UG-2.

Nonetheless, the B-reef and the PGE-rich footwall lithologies show a remarkably close similarity in terms of PGE ratios and normalized patterns (Fig. 5). The aplitic dyke and some of the low-grade footwall samples (e.g. PA-S3-0 and PA-S2-12) exhibit dramatic enrichments in Pt, Pd or Au, but the relative distribution of various PGE between PGE-rich reef and footwall is very consistent and seems to be more than mere coincidence. This type of footwall mineralization is a general feature of the Platreef and it is present across the Sandsloot pit as well as along strike at Tweefontein Hill to the south and at Zwartfontein to the north.²⁸ Any comprehensive genetic model for the Platreef must take it into account.

Platinum-group mineralogy

Initial SEM studies of four polished blocks from the Platreef—three from the footwall and one from a pegmatoidal mafic dyke—have revealed 54 individual occurrences of platinum-group minerals (PGM), ten occurrences of electrum (Au,Ag) and a single instance of stromeyerite (AgCuS). The last is the only precious-metal sulphide found to date. The great majority of the PGM in the Platreef and footwall are of very small grain size—nearly all <10 µm and most <5 µm; a few exceptions are in the size range 20–60 µm. Each PGM grain was analysed and grouped according to type and textural/mineralogical association. The PGM identified are classed as: (1) high-temperature alloys, e.g. Pt–Fe and Pt–Sn alloys; (2) high-temperature semi-metallides, e.g. (Pt,Pd) arsenides and antimonarsenides; (3) lower-temperature semi-metallides, e.g. Pd antimonides and (Pd,Pt) tellurides and bismuthotellurides; and (4) lower-temperature alloys, e.g. Pt–Pd–Ge–Pb, Pd–Au and Au–Ag alloys (Table 2).

The textural/mineralogical associations of the PGM are: (1) in base-metal sulphides; (2) on the rims of base-metal sulphides; (3) in oxides; (4) in primary silicates; and (5) in alteration silicates. Table 3 shows the types of PGM found in the Platreef, footwall and pegmatoidal mafic dyke. Table 4 gives a more detailed grouping of the PGM showing their textural/mineralogical associations. Unlike the Merensky Reef, in which PGE occur mostly as PGE alloys and sulphides and where laurite (RuS₂) is usually present even in the most alloy-

Table 2 Names, chemical formulae and relative equilibration temperatures for PGM and Au–Ag minerals analysed (total, 65; 16 high-temperature and 49 low-temperature)

Name	Formula	Instances	Relative equilibration temperature
Isoferroplatinum	Pt ₃ Fe	4	High
Mertieite II	Pd ₈ (Sb,As) ₃	2	High
Rustenburgite	(Pt,Pd) ₃ Sn	2	High
Sperrylite	PtAs ₂	4	High
Fengluanite	Pd ₃ Sb	1	Low
Kotulskite	PdTeBi	2	Low
Michenerite	(Pd,Pt)BiTe	3	Low
Moncheite	Pt(Te,Bi) ₂	1	Low
Vincenite	(Pd,Pt) ₃ Sb	1	Low
Zvyagintsevite	Pd ₃ Pb	3	Low
Palladian gold	(Au,Pd)	4	Low
Electrum	(Ag,Au)	10	Low
Stromeyerite	AgCuS	1	Low
Unnamed	Pt(As,Sb) ₂	2	High
Unnamed	(Pd,Pt) ₂ Ge	1	Low
Unnamed	(Pb,Ag)Te	1	Low
Unnamed	(Pd,Pt)Sb	1	Low
Unnamed	PdSb	7	Low
Unconstrained	Pt–Pd–As	1	High?
Unconstrained	Pt–As–Sb	1	Low
Unconstrained	Pt–Sn	1	High?
Unconstrained	Pd–Sb–As	2	Low
Unconstrained	Pd–Sb–Se	1	Low
Unconstrained	Ag–Te	1	Low
Unconstrained	Pd–Pt–Sb–Bi	1	Low
Unconstrained	Pd–Sb	2	Low
Composite, undifferentiated	Pd–Pt–Te–As–Sn	1	Low
Composite, undifferentiated	Pd–Pt–Te–Bi–As–Sn	1	Low
Composite, undifferentiated	Pd–Pt–Te–Bi	1	Low
Composite, undifferentiated	Pd–As–Sb–Se	1	Low
Composite, undifferentiated	Pd–Pt–Pb–Te–Sb	1	Low

Table 3 PGM types found in eight polished blocks from Platreef, footwall and pegmatoidal dyke samples

	High- <i>T</i> alloys	High- <i>T</i> semi-metallides	Low- <i>T</i> alloys	Low- <i>T</i> semi-metallides	Low- <i>T</i> sulphides
Platreef	6	1	12	10	0
Footwall	1	7	6	19	1
Mafic dyke	0	1	0	1	0

dominated assemblages, the Platreef at Sandsloot is virtually free of PGE sulphides. The authors’ preliminary data show that the Platreef and footwall host a wide variety of PGM associated with primary silicates, metamorphic silicates, alteration silicates, primary and remobilized sulphides, and oxides. More significantly, the present work demonstrates the abundance of lower-temperature PGM in the form of (Pd,Pt) tellurides and bismuthotellurides and low-temperature alloys, such as palladian gold (Au,Pd) and electrum (Au,Ag) (Table 2).

The data show a slight dominance of high-temperature PGM over low-temperature PGM in the reef samples, but a more convincing majority of low-temperature PGM in footwall samples. The types of low-temperature PGM and their associations with surrounding silicates and sulphides are similar in the reef and footwall, supporting a common mode of

Table 4 PGM types and their textural/mineralogical associations found in eight polished blocks from Platreef, footwall and pegmatoidal dyke samples

	High- T Pt-Pd alloys and semi-metallides					Lower- T Pt-Pd alloys and semi-metallides				
	In sulphide	On sulphide rim	In oxide	In primary silicate	In altered silicate	In sulphide	On sulphide rim	In oxide	In primary silicate	In altered silicate
Platreef	0	4	0	3	0	7	7	0	6	2
Footwall	0	3	2	2	1	5	1	0	7	13
Dyke	0	1	0	0	0	0	0	0	1	0

speciation. To date, the only deviation of possible significance among low-temperature PGM is that an unnamed Pd antimonide (PdSb) is predominant in a footwall serpentinite (sample PA-S3-0).

The PGM distribution in the Platreef is very different from that of almost all of the varieties of Merensky Reef described by Kinloch and Peyerl,¹⁸ with the exception of some pothole reef and reef that has been affected by late-stage dunite pegmatoids. The association of Pt-Fe alloys in pegmatoids and in the core of a pothole with a zone of telluride-rich mineralization on the rim of the pothole have both been attributed to the effects of fluids.^{17,18} Given the strong evidence for fluid activity in the Platreef and the footwall, it is likely that fluids have influenced the development of PGM in the Platreef in a similar manner to volatile-rich portions of the Merensky Reef.

Discussion

Previous investigations of the Platreef have shown that it exhibits differences in mineralogy, textures, thickness and PGE distribution along strike. These differences appear to reflect, in part, interactions with different floor rocks.^{28,10} Studies of the Platreef should proceed, therefore, with some form of broad-scale lithological (facies?) division, of which the mineralization at Sandsloot is viewed as one facies. Generalizations about the entire Platreef based on the observations at Sandsloot should, therefore, be viewed with caution until more data become available from new mining developments. Kinloch¹⁷ recognized similar large-scale facies variation within the Merensky Reef, which led to new thinking on the processes operating in that deposit. Given the extensive strike lengths involved in both the Merensky Reef and Platreef, it would be surprising if similar lateral variations were not apparent in the latter as well. In the view of the present authors, the true complexity of the Platreef is only just being appreciated.

Wagner²⁸ recognized the division between the pyroxenite reef and the underlying footwall assemblages and ascribed the formation of these units to magmatic and metamorphic/metasomatic processes, respectively. Many subsequent authors^{13,6,3,5,21,24} have emphasized contamination of the Platreef magma by the footwall. The impression given by many of these studies is that the PGE mineralization in the Platreef is the result of purely orthomagmatic sulphide segregation from a system with a high *r* factor⁸ and that the PGE in the reef are strongly associated with base-metal sulphides. Variable Fe/Mg ratios and PGE concentrations within the Platreef have even been ascribed to the introduction of multiple pulses of magma with different PGE budgets.¹ In none of these studies have the presence of significant PGE concentrations in the footwall and its implications for the development of the mineralization been considered.

The authors feel that one of the most significant results to come out of the present study so far is the complete absence of PGE sulphides—particularly laurite (RuS₂)—and the abundance of alloys and semi-metallides in the Platreef. This

trend acquires greater significance when comparison is made with other Bushveld PGE reefs^{17,20,18} and PGE-bearing sulphide deposits in other mafic intrusions, such as the Great Dyke¹¹ and the Munni Munni Complex,² where PGE sulphides constitute anywhere between 10% and 60% of the PGM assemblage. The PGM assemblage in the Platreef at Sandsloot is quite different from that in any of these deposits.

Another significant result to emerge from this study is the recognition of PGE signatures in the footwall broadly similar to those found in the igneous Platreef. This is not what would be expected if the PGE-rich footwall zones formed simply as a result of remobilization of the most mobile PGE (Pt and Pd) and Au from a pre-existing, PGE-rich magmatic sulphide layer (represented by the B-reef). Rather, it suggests that the final PGE distribution in both the B-reef and the PGE-rich footwall was influenced or controlled by similar processes. In accord with Wagner's study,²⁸ no evidence for a gravity-driven percolation of sulphide into the footwall has been found in the present work. Furthermore, models invoking assimilation and contamination of footwall rocks to produce the PGE-rich zones fail to explain why the footwall PGE mineralization is concentrated in zones that have seen the greatest fluid activity.

Table 3 clearly shows that the footwall contains a greater proportion of lower-temperature PGE antimonides, tellurides and alloys than the Platreef, in line with the obvious temperature gradient across the footwall contact. However, the same low-temperature species occur in the same associations in both units, indicating that *P-T-X* conditions in the Platreef and footwall were broadly similar during the crystallization of these PGM.

The evidence for 'resets' in MgO and Fe/Mg ratios and variation in PGE concentrations within the Platreef presented by Ainsworth¹ also merits further consideration. The reports of distinctive PGE-rich zones or shoots (over distances of more than 10 m) within the B-reef and the enrichment in Pd at the base of the B-reef reported by Ainsworth¹ are confirmed by observations of the present authors. Variations in PGE concentrations over these distances are difficult to reconcile with sulphide immiscibility and collection of sulphide droplets from an overlying magma unless there were multiple pulses of magma (and sulphide) or a single generation of sulphides (and associated PGE) was somehow redistributed. The low Fe/Mg ratios and MgO resets cited by Ainsworth¹ as evidence for multiple magmas actually correlate with the presence of serpentine and talc and reflect fluid replacement or the presence of highly altered olivine-bearing dolomite xenoliths, not primary magmatic variability. It is maintained here that the metre-scale variability in PGE concentration, coupled with the absence of any PGE sulphides and the abundance of low-temperature PGM, cannot be linked to any orthomagmatic model and is best explained by the action of fluids.

The observations outlined above lead to the view that the final distribution of PGE at Sandsloot was controlled by the action of fluids. These played the dominant role in mobilizing

and homogenizing PGE within the Platreef and carrying them into the footwall, where they formed irregular zones and regular layers containing high PGE concentrations. The PGM assemblage crystallized under hydrothermal conditions in a fluid envelope that affected both the reef and footwall, but the means by which the PGE were initially concentrated is less obvious. On the basis of stable isotope data Harris and Chaumba¹⁴ concluded that the Platreef fluid was a mixture of predominantly magmatic water with a minor component derived from the footwall. It is not yet possible to say whether this fluid activity introduced PGE into the Platreef from deeper cumulates or residual melt during fluid migration along the intrusion margin under a pressure and temperature gradient, or whether it simply disrupted and redistributed the metals from magmatic sulphides that had already scavenged PGE. At this stage both possibilities must remain open. What is clear is that the Platreef at Sandsloot can no longer be considered as a purely or predominantly orthomagmatic PGE deposit. The extent of PGE remobilization is poorly constrained, and attempts to model the PGE distribution in the Platreef using *r* factor calculations or sulphide fractionation models are likely to be invalid.

Although the role of fluids within the B-reef and footwall has been emphasized above, it is important to recognize that not all fluid-rich rocks associated with the Platreef contained PGE. The crosscutting pegmatoidal mafic dyke in face 132/038 in the central part of the pit (Fig. 3) is almost barren. PGE mineralization appears to have been restricted to the B-reef pyroxenites and their associated fluid envelope, but later intrusions or crosscutting pegmatoids carried little or no PGE.

Following Wagner's²⁸ original subdivision of the deposit, it could be argued that the Platreef and associated footwall at Sandsloot show features associated with skarn deposits.¹¹ The envelope of footwall PGE mineralization hosted within the metamorphosed carbonates could certainly be considered an 'exoskarn'. The case for the Platreef proper being an 'endoskarn' in the strictest sense is more difficult to establish. PGE(Ni,Cu) skarns have not been recognized as a skarn deposit type in themselves before this study. This work and Wagner's²⁸ early accounts have shown the widespread nature of the footwall mineralization and the presence of very high PGE concentrations in the serpentinized skarn assemblages. In the view of the present authors this style of PGE mineralization is consistent with a 'Pd-Pt-Au skarn'.

Conclusions

The Platreef is shown to be a complex PGE deposit that was subjected to different processes over the course of its development. At Sandsloot the B-reef facies of the Platreef is the principal orebody, but extensive PGE mineralization is also present in the metamorphic clinopyroxenites, calc-silicate hornfels and serpentinites that constitute the footwall of the intrusion. Mapping has revealed details of the relationships between the B-reef, the footwall lithologies and later intrusions. This highlights the need for preliminary mapping to provide a thorough understanding of the complexity of the structural and lithological relations before samples are collected. The Platreef is not a simple package of rocks, so sampling traverses across the reef or sampling of boreholes for geochemical studies need to be preceded by detailed mapping or logging on a metre scale or smaller.

There is widespread evidence for fluid activity in both the B-reef and the footwall. The PGM assemblages in both units are virtually free of sulphide species and are dominated by PGM that are rich in low-temperature metals and semi-metals found to be associated with fluid-rich conditions in

other areas of the Bushveld Complex. Orthomagmatic processes (e.g. sulphide collection) may have played a role in the initial development of the deposit, but these cannot be seen as the sole influence. The final distribution of the PGE in the reef and footwall was strongly influenced by fluid activity, and at this stage the Platreef should not be pigeonholed as an orthomagmatic deposit.

Acknowledgement

The management of Anglo Platinum is thanked for allowing Paul Armitage to carry out fieldwork at the Sandsloot mine and for giving permission for publication of this work. The staff of the Sandsloot geology department and assay/XRD laboratory provided valuable logistical and analytical assistance in the project. The authors are grateful to Ian Slipper for his assistance with SEM studies at the University of Greenwich and to C. Ballhaus and E. Mathez for reviewing the manuscript.

References

1. Ainsworth C. S. How many magma injections did it take to bring PGE enrichment to the Platreef in the Sandsloot area? In *8th International platinum symposium* (Johannesburg: South African Institute of Mining and Metallurgy, 1998), 3–5. *Symp. Series* 18
2. Barnes S. J. *et al.* Platinum-group element mineralization in the Munni Munni Complex, Western Australia. *Contrib. Mineral. Petrol.*, **42**, 1990, 141–62.
3. Barton J. M., Cawthorn R. G. and White J. The role of contamination in the evolution of the Platreef of the Bushveld Complex. *Econ. Geol.*, **81**, 1986, 1096–104.
4. Buchanan D. L. *et al.* The genesis of sulfide mineralization in a portion of the Potgietersrus limb of the Bushveld Complex. *Econ. Geol.*, **76**, 1981, 568–79.
5. Buchanan D. L. *Platinum-group element exploration* (Amsterdam: Elsevier, 1988), 185 p.
6. Buchanan D. L. and Rouse J. E. Role of contamination in the precipitation of sulphides in the Platreef of the Bushveld Complex. In Buchanan D. L. and Jones M. J. eds *Sulphide deposits in mafic and ultramafic rocks* (London: IMM, 1984), 141–6.
7. Buick I. S. *et al.* Fluid flow in metacarbonates associated with emplacement of the Bushveld Complex, South Africa. *J. geochem. Explor.*, **69–70**, 2000, 391–5.
8. Campbell I. H., Naldrett A. J. and Barnes S. J. A model for the origin of platinum-rich sulfide horizons in the Bushveld and Stillwater complexes. *J. Petrology*, **24**, 1983, 133–65.
9. Cawthorn R. G., Barton J. M. and Viljoen M. J. Interaction of floor rocks with the Platreef on Overysel, Potgietersrus, northern Transvaal. *Econ. Geol.*, **80**, 1985, 988–1006.
10. Cawthorn R. G. and Lee C. *Bushveld Complex excursion field guide, 8th International platinum symposium* (Johannesburg: Geological Society of South Africa, 1998).
11. Coghill B. M. and Wilson A. H. Platinum-group minerals in the Selukwe subchamber, Great Dyke, Zimbabwe: implications for PGE collection mechanisms and formational redistribution. *Mineralog. Mag.*, **57**, 1993, 613–33.
12. Einaudi M. T. and Burt D. M. Introduction—terminology, classification and composition of skarn deposits. *Econ. Geol.*, **77**, 1982, 745–54.
13. Gain S. B. and Mostert A. B. The geological setting of the platinoid and base metal sulfide mineralization in the Platreef of the Bushveld Complex in Drenthe, north of Potgietersrus. *Econ. Geol.*, **77**, 1982, 1395–404.
14. Harris C. and Chaumba J. B. Crustal contamination and fluid-rock interaction during the formation of the Platreef, northern limb of the Bushveld Complex, S. Afr. *J. Petrol.*, **42**, 2001, 1321–47.
15. Huber H. *et al.* Geochemistry and petrology of Witwatersrand and Dwyka diamictites from South Africa: search for an extraterrestrial component. *Geochim. cosmochim. Acta*, **65**, 2001, 2007–16.
16. Jochum K. Rhodium and other platinum-group elements in carbonaceous chondrites. *Geochim. cosmochim. Acta*, **60**, 1996, 3353–6.
17. Kinloch E. D. Regional trends in the platinum-group mineralogy of the Critical Zone of the Bushveld Complex, South Africa. *Econ. Geol.*, **77**, 1982, 1328–47.
18. Kinloch E. D. and Peyerl W. Platinum-group minerals in various rock types of the Merensky Reef: genetic implications. *Econ. Geol.*, **85**, 1990, 537–55.

19. McDonald I. The need for a common framework for collection and interpretation of data in platinum-group element geochemistry. *Geostand. Newslett.*, **22**, 1998, 85–91.
20. McLaren C. H. and De Villiers J. P. R. The platinum-group chemistry and mineralogy of the UG-2 chromitite layer of the Bushveld Complex. *Econ. Geol.*, **77**, 1982, 1548–66.
21. Misra K. C. *Understanding mineral deposits* (Dordrecht: Kluwer, 2000), 845 p (see especially 327–9).
22. Mostert A. B. The mineralogy, petrology and sulphide mineralization of the Plat Reef northwest of Potgietersrus, Transvaal, Republic of South Africa. *S. Afr. geol. Surv. Bull.*, **72**, 1982, 48 p.
23. Nell J. The Bushveld metamorphic aureole in the Potgietersrus area: evidence for a two-stage metamorphic event. *Econ. Geol.*, **80**, 1985, 1129–52.
24. Peck D. C. *et al.* Controls on the formation of contact-type platinum-group element mineralization in East Bull Lake intrusion. *Econ. Geol.*, **96**, 2001, 559–81.
25. Steele T. W., Levin J. and Copelowitz I. The preparation and certification of a precious metal ore. *Rep. Nat. Inst. Metall.* 1696, (Randburg: Council for Mineral Technology, 1975), 50 p.
26. Uken R. and Watkeys M. K. Diapirism initiated by the Bushveld Complex, South Africa. *Geology*, **25**, 723–6.
27. Van der Merwe M. J. The layered sequence of the Potgietersrus Limb of the Bushveld Complex. *Econ. Geol.*, **71**, 1976, 1337–51.
28. Wagner P. A. *The platinum mines and deposits of South Africa* (Edinburgh: Oliver & Boyd, 1929), 326 p.

Authors

Paul Armitage graduated with a B.A.(Hons) in Scandinavian and Icelandic studies from University College London in 1993 and subsequently gained cand.mag. (B.Sc.) and cand.scient. (M.Phil.) degrees in geology from the University of Tromsø, Norway. His main area of study was the structural development and metamorphism of Precambrian terrains in northern Norway, partly in collaboration with the Norwegian Geological Survey. He is now a Ph.D. student at the University of Greenwich, England.

Address: Department of Earth and Environmental Sciences, University of Greenwich at Medway, Chatham ME4 4TB.

Iain McDonald obtained a B.Sc. degree in chemistry and geology from Glasgow University, Scotland, in 1989 and a Ph.D. from the University of Cape Town, South Africa, in 1993. Following post-doctoral work on sulphide-poor PGE mineralization at Manchester University, England, he became a lecturer in geochemistry at the University of Greenwich. He is currently manager of the ICP laboratories at the Department of Earth Sciences, University of Cardiff, Wales.

Stephen Edwards graduated with a B.Sc.(Hons) in geochemistry from Queen Mary College, University of London, in 1985 and gained a Ph.D. from the Memorial University of Newfoundland, Canada, in 1991. At present he is a senior lecturer at the Department of Earth and Environmental Sciences, University of Greenwich.

Geoff Manby received a B.Sc.(Hons) from the University of Leicester, England, in 1973 and a Ph.D. from the University of Cambridge in 1978. He is currently a reader in the Department of Earth and Environmental Sciences, University of Greenwich.

APPENDIX 2

Full reference:

HOLWELL D.A., ARMITAGE P.E.B. & McDONALD I. (2005). Observations on the relationship between the Platreef and its hangingwall. *Appl. Earth Sci. (Trans. Inst. Min. Metall. B)*, **114**, B199-207.

Observations on the relationship between the Platreef and its hangingwall

D. A. Holwell, P. E. B. Armitage and I. McDonald

Observations on the nature of the contact between the Platreef and its hangingwall have revealed that not only were the hangingwall gabbonorites intruded after the Platreef igneous rocks and the development of platinum group element (PGE) mineralisation, but that there appears to have been a significant time-break separating the two intrusive events. The hangingwall gabbonorites truncate several features present within the Platreef pyroxenites but not in the hangingwall, such as shear zones and reef which has undergone alteration by Fe-rich fluids, implying that these features were formed prior to intrusion of the gabbonorites. A fine-grained leuconorite at the base of the hangingwall exhibits textures showing erosion of Platreef orthopyroxene by fine-grained cumulus plagioclase, suggesting intrusion of a hot magma over cooled Platreef. Xenoliths of reef pyroxenite are also found in the hangingwall. PGE mineralisation is present within basal zones of the hangingwall where the hangingwall overlies mineralised Platreef pyroxenite. We interpret the contact as a magmatic unconformity and, as the gabbonorites do not appear to be PGE-depleted, suggest that PGEs and S were scavenged or assimilated from the reef by the intruding magma, producing zones of orthomagmatic PGE mineralisation in topographic

depressions at the base of the crystallising hangingwall. The presence of calc-silicate xenoliths in the hangingwall gabbonorites can be explained by footwall anticlines or diapirism which the relatively thin Platreef had not overtopped, allowing footwall dolomite to be exposed to the main influx of hangingwall magma. The identification of a time-break between Platreef and hangingwall intrusion, and the most likely source of basal hangingwall PGE mineralisation being the underlying Platreef, shows that the magma that formed the gabbonorites could not have been the source of PGE for the Platreef as previously thought.

David Holwell (HolwellDA@Cardiff.ac.uk) and Iain McDonald (for correspondence – iain@earth.cf.ac.uk) are in the School of Earth, Ocean and Planetary Sciences, Cardiff University, Main Building, Park Place, Cardiff CF10 3YE, UK; Paul Armitage is at the University of Greenwich, London, UK

© 2005 Institute of Materials, Minerals and Mining and Australasian Institute of Mining and Metallurgy. Published by Maney on behalf of the Institutes. Manuscript received 28 June 2005; accepted in final form 7 October 2005.

Keywords: Platreef, hangingwall, PGE mineralisation

INTRODUCTION

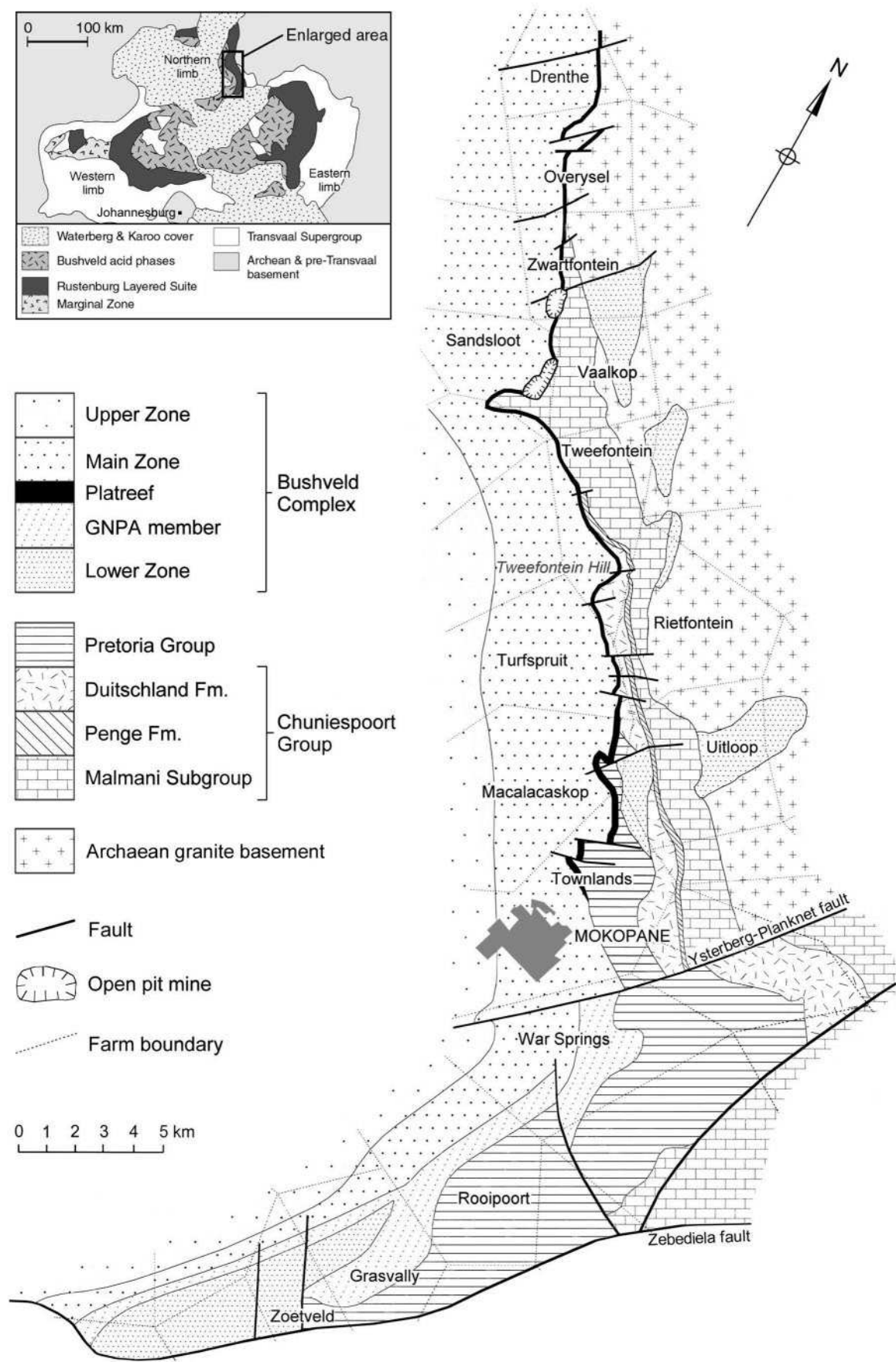
The Platreef of the northern limb of the Bushveld Complex, South Africa, is currently one of the most extensively explored deposits of platinum-group elements (PGEs) in the world. It is a pyroxenitic unit located between gabbonorites attributed to the Main Zone of the complex, and floor rocks comprising Palaeoproterozoic metasediments and Archaean granite-gneiss basement. PGE mineralisation is heterogeneously distributed through the pyroxenite unit, and is usually present in the immediate footwall and occasionally in the immediate hangingwall.^{1,9,16,22} The northern limb of the Bushveld Complex comprises a succession of ultramafic-mafic lithologies, that have been broadly correlated by some authors with the Rustenburg Layered Suite (RLS) present in the eastern and western limbs.^{20,24–26} The well-defined igneous stratigraphy of the RLS comprises the Lower Zone of harzburgites and pyroxenites, the Critical Zone of cyclic chromitites, pyroxenites and norites, the Main Zone norites and gabbonorites, and the Upper Zone of magnetites, gabbonorites and anorthosites. In the

northern limb, the stratigraphy differs in several important respects. The ultramafic Lower Zone is developed south of the town of Mokopane, and as satellite bodies within the floor rocks north of the town (Fig. 1). Recent work has also shown that the Lower Zone extends for a limited distance north of Mokopane, with a series of serpentinised peridotites and pyroxenites present on Macalakaskop being attributed to the Lower Zone.¹⁴ The Critical Zone is not fully developed, and there is debate as to whether it is present at all.¹⁸ The Main Zone of the northern limb lacks correlatory horizons with the Main Zone in the rest of the complex, and includes a sequence of troctolites unique to the northern limb.²⁰ The Upper Zone has not been linked extensively with the rest of the complex, though one magnetite layer has been correlated with the Main Magnetite Layer on the basis of V₂O₅ content.^{20,21} From south to north, the Platreef rests upon a succession of progressively older sedimentary units of the late Archaean to early Proterozoic Transvaal Supergroup, and Archaean granite/gneiss basement, in what has been termed an 'igneous transgression'.²⁵ The

footwall units are, north from Mokopane: quartzites and shales of the Timeball Hill Formation; sediments of the Duitschland Formation; the Penge banded iron formation; the Malmani dolomite and, north of

Zwartfontein, the Archaean basement granites and gneisses (Fig. 1).

The timing of intrusion of the Platreef with respect to the units above it, and the general stratigraphy of



1 Geological map of the Platreef showing localities referred to in the text. After Kinnaird and Nex,¹³ von Gruenewaldt et al.,²⁴ and Hammerbeck and Schürmann⁷

the northern limb of the Bushveld Complex remain contentious issues. Traditionally, the Platreef pyroxenites north of Mokopane have been correlated with the Merensky Reef,^{25,26} and a series of norite–pyroxenite–anorthosites with a chromitite layer (the GNPA member) south of Mokopane (Fig. 1), with the Critical Zone.^{10,20,24,26} Overlying gabbro-norites have traditionally been correlated with the Main Zone. Kruger¹⁵ suggested that the Platreef is the equivalent to the Merensky Reef and formed as a result of the first influx of Main Zone magma, therefore placing both reefs in the lower Main Zone. McDonald *et al.*¹⁸ suggested another alternative; that the Platreef and the GNPA member are the products of one or more mixing events between Lower Zone and Main Zone magma, and these represent a transitional zone before the intrusion of the major influx of Main Zone magma. All these models imply that the Platreef was intruded before the Main Zone gabbro-norites. Conversely, Friese,⁴ and Friese and Chunnatt⁵ suggested that a thrust zone developed along the intrusive margin between the Main Zone gabbro-norites and the footwall country rocks, and hypothesised that the Platreef represents a syn-tectonic, sheet-like intrusion intruded along this shear zone in post-lower Main Zone times. This paper aims to review these models using first-order field and petrological observations to constrain the relative timing of the Platreef and hangingwall gabbro-norites.

METHODS

Samples and observations presented in this paper are part of an on-going study into the Platreef between Sandsloot and Overysel. Field relationships have been mapped and samples collected from Anglo Platinum's open pit mines at Sandsloot and Zwartfontein South and from borehole cores drilled at Overysel (Fig. 1). The down-stepping benches in the two pits have subvertical faces 10–15 m high, and several faces from both pits were mapped in detail at 1:100 scale and sampled at regular intervals. Examples from the Sandsloot pit are given in Figure 2 and in Armitage *et al.*¹ and McDonald *et al.*¹⁸ Two cores from Overysel (boreholes OY335 and OY387) were also logged and sampled, and many others were logged and described. Detailed mineralogical analysis was performed at Cardiff University using a Cambridge Instruments LEO S360 scanning electron microscope, coupled to an Oxford Instruments INCA energy dispersive X-ray analysis system.

LITHOLOGICAL UNITS

The hangingwall is made up of medium-grained norites and gabbro-norites containing cumulus plagioclase, cumulus and intercumulus orthopyroxene (En_{64–70}) and generally oikocrystic clinopyroxene. The base of the hangingwall is often characterised by a thin, fine-grained, poikilitic leuconorite up to 30 cm thick, containing up to 90% cumulus plagioclase and oikocrystic pyroxenes. Occasional xenoliths of

calc–silicate derived from metamorphosed dolomite similar to that observed in the footwall are present in the hangingwall,^{6,14} and pyroxenites with petrographic and geochemical characteristics similar to the Platreef are present within the hangingwall.¹⁸

The Platreef is made up primarily of heterogeneously textured feldspathic pyroxenite, containing cumulus orthopyroxene (En_{74–78}), and intercumulus clinopyroxene and plagioclase. Base metal sulphide (BMS) and PGE mineralisation is present within the interstitial assemblage. There is, occasionally, a fine-grained, feldspathic pyroxenite, barren of BMS and PGE mineralisation at the top of the Platreef succession. The maximum thickness observed for this unit in any of the faces mapped is 7 m. In parts of the Sandsloot pit and at Zwartfontein, portions of the pyroxenites appear to have been affected by a late-stage, Fe-rich fluid¹⁸ which has removed plagioclase, and overprinted pyroxene with Fe-rich olivine (Fo_{60–70}) forming ultramafic lithologies that we have termed olivine-replaced reef (ORR). This has altered the normally telluride-dominant platinum-group mineral (PGM) assemblage to one dominated by alloys.⁹ Calc–silicate xenoliths are common within the reef and are often extensively serpentinised.¹

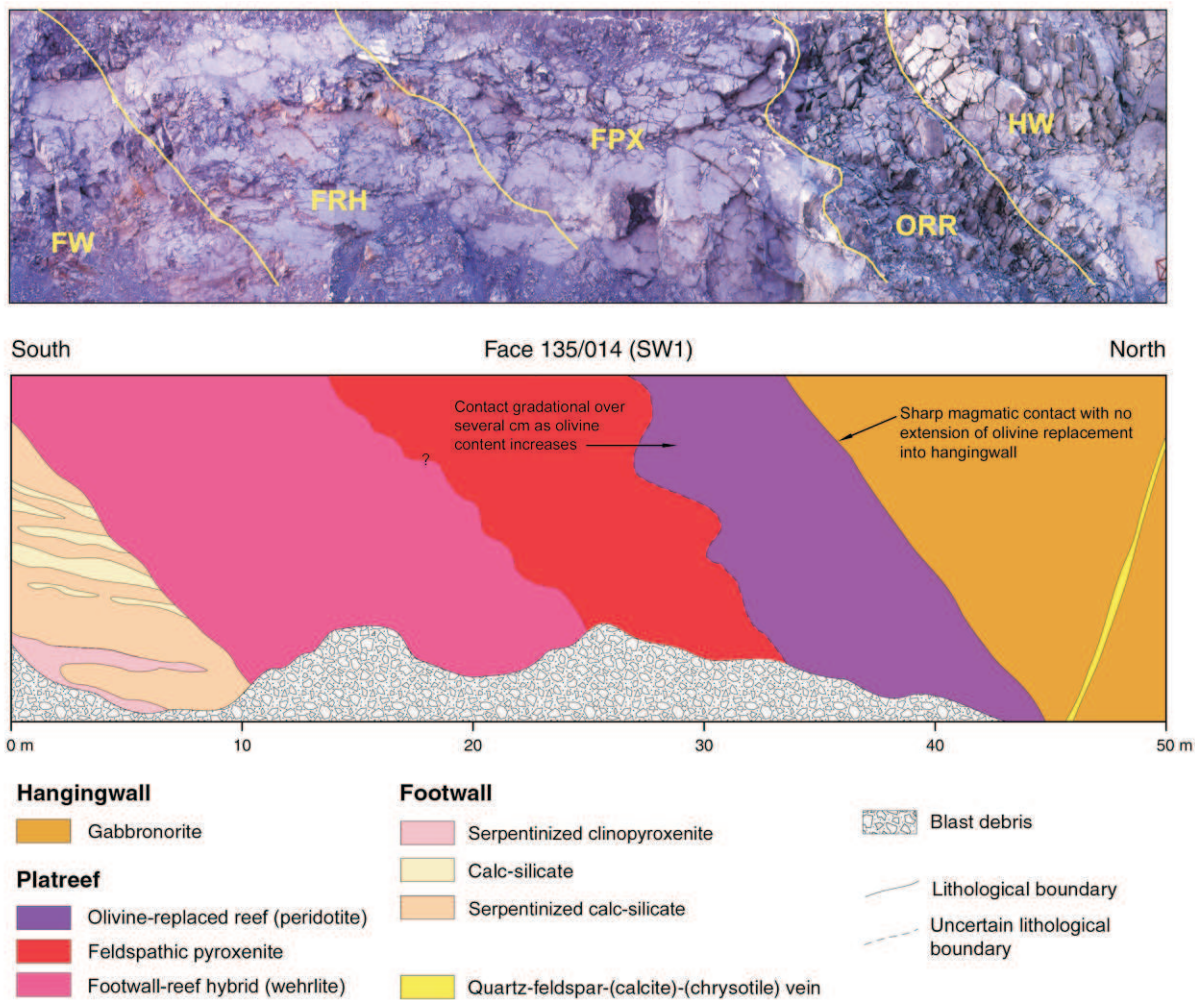
The nature of the footwall varies along strike (Fig. 1). At Sandsloot and Zwartfontein South, the Platreef rests on dolomite of the Malmani Formation, which is metamorphosed to calc–silicates, which are variably serpentinised. At the transition from Platreef pyroxenite into calc–silicate, a unit termed 'parapyroxenite' is usually present which contains granoblastic clinopyroxene and is considered metamorphic in origin on the basis of whole-rock Cr and CaO content.⁸ Below this transitional zone, parapyroxenite also occurs as smaller lensoidal bodies with gradational contact to the surrounding calc–silicate. In the northern part of Zwartfontein, and at Overysel, the Platreef pyroxenites overlie gneisses and granites of the Archaean basement.

OBSERVATIONS

Macroscopic relationships

In most of the faces studied, a planar magmatic contact is observed where poikilitic leuconorite or gabbro-norite directly overlie the reef pyroxenites. Only a few faces show evidence for a sheared contact; in these sections, the uppermost pyroxenites are sheared and subsequently altered by serpentine, sericite or carbonate. However, the overlying hangingwall rocks show no evidence of shearing or alteration.

In areas of the Sandsloot pit where the Platreef has undergone Fe-replacement, the rocks are visibly darker and the replaced zones display a greater degree of fragmentation in response to blasting than the rest of the reef and the hangingwall (Fig. 2). In all cases where these feldspar-poor, ultramafic zones have been recognised, they are truncated by hangingwall lithologies that contain fresh plagioclase. The replacement event appears to be restricted to the Platreef and is not present in the hangingwall.



2 Photograph and geological interpretation of a vertical face in the south-western part of the Sandsloot pit showing an exposed section of olivine-replaced reef, displaying a distinct darkening and different fracture pattern to the surrounding lithologies. The replaced reef is truncated at a magmatic contact with the hangingwall gabbronorite. FW, footwall; FRH, footwall–reef hybrid; FPX, feldspathic pyroxenite; ORR, olivine-replaced reef; HW, hangingwall

Petrography of the contact

Perhaps the most striking evidence for the nature of the contact is shown in Figure 3, which illustrates the contact between hangingwall poikilitic leuconorite and coarse-grained, mineralised Platreef pyroxenite in thin section of a sample taken from the northern part of the Sandsloot pit. The cumulus orthopyroxene crystals at the top of the Platreef are visibly eroded and resorbed against cumulus plagioclase of the fine-grained, poikilitic leuconorite. The leuconorite does not permeate the pyroxenite in any sense, and the embayments made by the small plagioclase crystals into the pyroxenes strongly suggest that the Platreef was completely, or nearly completely, solidified before intrusion of the overlying unit.

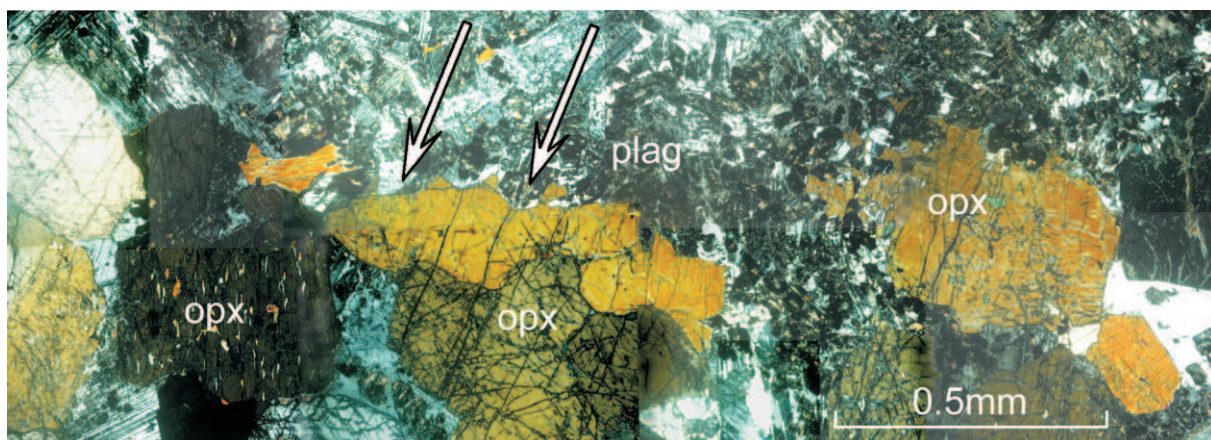
PGE mineralisation

In all of the sections mapped, in cases where the hangingwall overlies the fine-grained, barren pyroxenite, there is no PGE mineralisation in the immediate hangingwall. However, where the hangingwall is in contact with coarse-grained mineralised reef, the base of

the hangingwall consistently contains PGE mineralisation, with grades sometimes comparable to that in the main reef. This relationship also holds true for virtually all borehole cores that we have logged and described from the Sandsloot–Overysel section. Typically, this zone of mineralisation is in the lowermost metre of the hangingwall, and is rarely more than 3 m thick. One such occurrence of hangingwall mineralisation is described by Holwell *et al.*,⁹ where an assemblage of Pd-bearing pentlandite, Pt–Fe alloy–BMS intergrowths and laurite is observed, which is characteristic of an orthomagmatic PGM association.¹² Such assemblages have not been observed in the Platreef pyroxenites.^{1,9,11} The presence of mineralisation appears to be very localised and highly constrained by the nature of the reef on which the hangingwall rests.

Xenoliths

Xenoliths of calc–silicate are common throughout the Platreef and are also present in the hangingwall, up to 100 m above the Platreef contact, and are also present further north several kilometres north of the last



3 Composite photograph of a thin section showing the contact between fine-grained, hangingwall poikilitic leuconorite (upper half of photograph) and coarse-grained, mineralised Platreef feldspathic pyroxenite (lower half). Note the embayments made by hangingwall plagioclase in the cumulus Platreef orthopyroxenes (arrowed). Dark patches within the plagioclase are alteration

footwall outcrop of dolomite, *e.g.* at Drenthe (Fig. 1).⁶ At Sandsloot, we have mapped rare occurrences of pyroxenite xenoliths in gabbro-norites at the base of the hangingwall. These pyroxenites have whole-rock and cumulus orthopyroxene (En_{78}) compositions consistent with the Platreef. Intercumulus clinopyroxene showed evidence of partial recrystallisation.

DISCUSSION

In almost all current models for the formation of the Platreef and northern limb of the Bushveld Complex, the Platreef is taken to be the lowermost unit of the complex north of Mokopane, and the gabbro-norites attributed to the Main Zone conformably overlie the Platreef. Prior to this study, most authors, with the exception of Friese,⁴ have believed that the Platreef and the gabbro-norites formed together, without any significant break in time and that the magma above the Platreef contributed some (or all) of the PGEs to the reef.^{2,15} The field relationships and mineralogical evidence presented in this paper identify features of the Platreef–hangingwall contact that have not been previously recognised and require a fundamental re-assessment of these assumptions. Each line of additional evidence is considered in turn below.

Cross-cutting relationships

Some of the earliest work undertaken on the Platreef by Wagner²⁵ describes veins of hangingwall norite intruding down into the Platreef, which would clearly imply a post-Platreef intrusion of the hangingwall. Evidence of a time-break between the emplacement of the Platreef and the gabbro-norites that we have identified lies in the truncation of certain features of the Platreef. For example, where the reef has been partially replaced by Fe-rich olivine, the olivine replacement is present directly below the hangingwall contact, but does not extend into the hangingwall at all. The replacement is thought to be formed from the percolation of a late-stage, Fe-rich fluid through the

reef¹⁸ that post-dates formation of interstitial plagioclase and telluride-dominant PGMs. Late Fe-rich ultramafic replacement bodies preferentially replace plagioclase-rich units in the RLS in the eastern and western Bushveld,²³ producing a Christmas-tree pattern of replacement; there seems no obvious reason why they should stop and not continue into the plagioclase-rich hangingwall at Sandsloot, unless it was not there. The obvious and consistent truncation of the Fe-rich olivine-replaced reef by the gabbro-norites shows that the Platreef pyroxenites had both crystallised, and undergone alteration, before the intrusion of the hangingwall gabbro-norites.

Shear zones that are common in the Platreef pyroxenites, with associated alteration appear truncated by the hangingwall gabbro-norites, with the hangingwall occasionally resting on sheared pyroxenite, but with no evidence of deformation or extension of alteration into the gabbro-norites. This would imply that either the shearing took place before intrusion of the gabbro-norites, or that competency contrasts between the pyroxenites and gabbro-norites led to pyroxenites being sheared preferentially under conditions of deformation. In the first case, the gabbro-norites must have been intruded after the Platreef and the shearing events. In the second case, it is not possible to constrain any relative timing, but preferential shearing of the reef is considered unlikely for shear zones which exhibit a high angle to the hangingwall contact.

We have mapped occurrences of pyroxenite xenoliths at the base of the hangingwall that have orthopyroxene compositions consistent with the Platreef. The fact that these xenoliths show evidence of recrystallisation of clinopyroxene also suggests intrusion of hot Main Zone magma over relatively cool Platreef pyroxenite.

Chilling and erosion at the base of the hangingwall

Perhaps the most compelling piece of evidence for this is shown in Figure 3. The erosion of the Platreef orthopyroxene by fine-grained, hangingwall plagioclase can

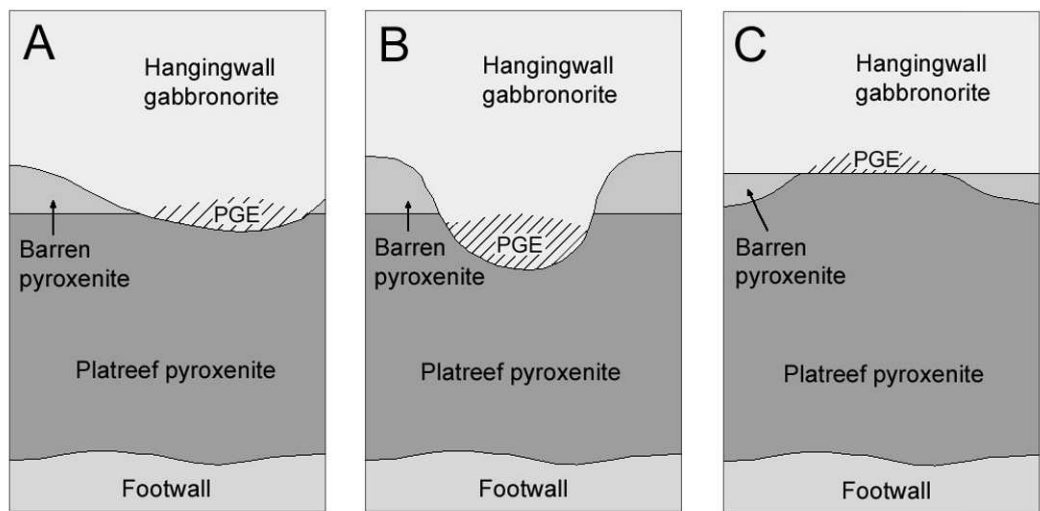
only be explained by the intrusion of a hot magma onto crystallised Platreef pyroxenite. The texture clearly demonstrates erosion of a solid pyroxenite with rigid properties, not a crystal mush. This inherently requires a significant time-break after the Platreef emplacement so as to cool the rock sufficiently for it to behave in this manner.

PGE mineralisation in the hangingwall

The observation of hangingwall mineralisation occurring exclusively in places where the gabbronorites directly overlie mineralised reef is intriguing, and one that has not been previously recognised. The question is: where do the PGEs in the mineralised zones of hangingwall come from? The Main Zone itself is a possible source of PGEs. In the Merensky Reef, the overlying Main Zone is depleted of PGEs;¹⁷ however, in the Platreef hangingwall, we have consistently found Pt and Pd concentrations to be around 5–15 ppb, which indicates that the Main Zone in the northern limb is PGE fertile and, by implication, did not have any of its PGEs extracted to form the Platreef. The localisation of hangingwall mineralisation in anorthosite and gabbronorite directly overlying mineralised Platreef pyroxenite and its corresponding absence above non-mineralised feldspathic pyroxenite strongly suggests incorporation of reef PGE into the basal zone of Main Zone magma by localised processes operating on a metre scale. The barren, fine-grained feldspathic pyroxenite is stratigraphically higher than the coarser-grained, mineralised feldspathic pyroxenite, and is quite thin (maximum 7 m in the sections mapped). It is possible that this barren, fine-grained unit was present continuously after the Platreef was intruded, and that the Platreef–hangingwall contact represents a magmatic unconformity surface, which has cut down through the uppermost barren pyroxenite and in places cut into

mineralised reef, assimilating some PGEs and enough sulphur to attain sulphur saturation, and producing very localised, basal zones of orthomagmatic PGE mineralisation.

The three-dimensional structure of the contact on a larger scale is uncertain due to the limited lateral distance exposed by the bench faces, but it is likely to: (i) be an irregular, undulatory surface (Fig. 4A); (ii) contain abrupt pothole-like structures (Fig. 4B); or (iii) be a planar surface, with the contact between fine-grained and coarse-grained pyroxenite undulatory (Fig. 4C). In either of the first two cases, PGEs are scavenged from the reef and recrystallised virtually *in situ* in depressions. The localisation of mineralisation within these depressions suggests that the overlying Main Zone magma was static, or had very low turbulence at the time of formation. Such a situation would support the pothole-like model, where the potholes may have formed after the hot Main Zone magma had been sitting on the cold Platreef for some time before melting the footwall thus creating a pothole-like structure. In such a model, one would expect occasionally to see the edges of such structures exposed in the bench faces, with the mottled anorthosite cutting down and truncating the fine-grained reef; however, as yet, none of the faces we have mapped have shown such a relationship, and further mapping is planned to attempt to confirm the true nature of the contact. It is important to emphasise that there is an important genetic distinction between this contact and the unconformable contacts associated with the potholes of the Merensky Reef and UG2 chromitite, which formed at magmatic or close to magmatic temperatures. There is no evidence of prior cooling of the footwall before their formation, such as chilling at the base. Here, we use the term pothole as a morphological, rather than genetic, analogue.



4 Schematic representation of the possible nature of the Platreef–hangingwall contact and the localisation of hangingwall PGE mineralisation in gabbronorite that directly overlies mineralised Platreef pyroxenite. (A) The contact is an irregular, magmatic unconformity; (B) the contact exhibits occasional pothole-like structures which cut down into the Platreef abruptly; (C) the contact between mineralised and non-mineralised Platreef pyroxenite is undulatory, and the gabbronorite forms a planar contact, occasionally cutting mineralised Platreef

Source of calc–silicate xenoliths

A prerequisite for any model which involves the Platreef being intruded before the hangingwall gabbro-norites are emplaced is to explain the occurrences of calc–silicate xenoliths within the gabbro-norites, which occur to heights up to 100 m above the Platreef contact at Sandsloot (A. Bye, personal communication) and at Drenthe.⁶ Frieze⁴ used this as evidence of the Main Zone being intruded prior to intrusion of the Platreef, assuming that, if the Platreef was formed first, it would have provided an impenetrable barrier between the footwall sediments and the Main Zone magma. This is not necessarily the case, and the occurrences of calc–silicate in the Main Zone can be explained in a number of ways, which still involve the Platreef being intruded first. An irregular floor topography is one explanation: if structures such as the domal dolomite tongue, immediately to the south of the Sandsloot pit (Fig. 1) are pre-Bushveld, then the relatively thin Platreef may have intruded around such structures, thus leaving areas of exposed dolomite topographically higher than the Platreef. Such areas would, therefore, have been exposed to the Main Zone magma as it was intruded, and the incorporation of xenoliths of calc–silicate within the Main Zone is entirely possible. Pre-existing fold structures do appear to be influential in controlling the thickness of the reef. The Sandsloot pit shows some large antiformal and synformal footwall structures⁴ and our mapping indicates that the Platreef is thicker (> 30 m true thickness) in synformal basins and thinner (< 10 m true thickness) close to the crests of the antiforms. This supports the possibility that the Platreef may not have completely covered larger antiforms.

Another possible explanation that produces an analogous situation is that of footwall diapirism initiated by the intrusion of the Platreef. Domal structures in the floor of the eastern Bushveld Complex have been interpreted to represent diapirism in the floor rock sediments of the Transvaal Supergroup during the early stages of magma emplacement.¹⁹ The process produces basins with finger-shaped intrusions separated by domes and ridges. If this were also the case in the northern limb, then structures such as the dolomite tongue (and presumably many unexposed structures) would represent syn-Bushveld structures, but would facilitate the exposure of footwall lithologies above the topographic level of the Platreef, as in the previous model.

A third possible explanation of calc–silicate xenoliths within the Main Zone is the possibility that they are xenoliths derived from country rocks that formed the roof of the Platreef. In the main part of the Bushveld Complex, the floor rocks are quartzites of the Magaliesburg Formation. These were unconformably capped by volcanic rocks of the 2061 Ma Rooiberg Group, and the intrusion of the mafic suite of the Complex is thought to have immediately followed the eruption of the Rooiberg Group, and was intruded along the unconformable contact, with the Magaliesburg quartzites forming the floor rocks and the Rooiberg acting as a low-density carapace. Thus, the roof rocks in the main part of the complex are thought to have been the Rooiberg Group. This is not

necessarily the case in the northern limb. It is clear from the transgressive nature of the Platreef–footwall contact that the Platreef was intruded obliquely to the country rock stratigraphy, as shown in the face maps in Figure 2 and in Armitage *et al.*¹ and it is entirely possible that the country rocks which formed the floor of the relatively thin Platreef also formed its roof.

Our observations outlined above are mutually supporting and strongly suggest that the Platreef was intruded first and that there was a sufficient break in time to allow almost total crystallisation, cooling and local alteration of the Platreef before intrusion of the hangingwall gabbro-norites. The time taken for the Platreef to solidify and undergo Fe-replacement is unknown, but cannot have been less than hundreds of years. If the fine-grained pyroxenite at the top of the Platreef represents the remnants of an upper chill zone, it implies that the Platreef may have originally been a very thin, possibly sill-like, package of pyroxenites without any significant column of magma above it. Intrusion of the magma that formed the hangingwall took place as a separate, later event, and the cool Platreef formed the floor of this larger intrusion.

With such evidence, the model of Platreef intrusion in post lower Main Zone times^{4,5} seems untenable. This model is based on several lines of evidence that can be interpreted in more than one way, or is directly contradicted by the new evidence that we present. Frieze⁴ considered a thrust zone at the contact between the footwall and the Main Zone, along which the Platreef has later intruded, and states that the Platreef is bounded by major thrust zones at the contacts with the footwall and hangingwall. Whilst there is occasionally sheared pyroxenite below the hangingwall contact, this is by no means wide-spread, and no evidence of shearing in the hangingwall is seen. We have also found no evidence of the footwall contact being sheared, and Frieze⁴ misinterprets the observation by Armitage *et al.*¹ of lenses of serpentinite following the layering as representing thrust duplexes. These bands are elongate bodies and layers of serpentinite, usually with transitional boundaries, which represent compositional variations in the original bedded sediments, where forsterite has preferentially formed during contact metamorphism and been subsequently serpentinised. Figure 2 shows that the bands/lenses of compositional variations in the footwall have a relatively high angle to the footwall contact, and are truncated at the contact, strongly suggesting that they are not tectonic lenses formed by shearing along the contact zone.

Source of PGEs in the Platreef

The discovery that there is a magmatic break associated with the base of the hangingwall has profound implications for the genesis of PGE mineralisation in the Platreef. Until now, most studies have assumed that there was an extensive column of magma above the Platreef (represented by the hangingwall units) that could have supplied PGEs via settling of immiscible sulphides to the reef. If the Platreef was intruded and crystallised before intrusion of the hangingwall magma, this cannot be the

source of PGEs for the Platreef. The mass balance question of how to account for the enormous mass of PGEs in the Platreef is unresolved.³ If the hangingwall magma is not responsible, another source of, and mechanism for, concentration of PGEs in the Platreef must be considered.

CONCLUSIONS

The evidence we present from mapping observations on a metre scale to mineralogical textures on a millimetre scale support the hypothesis that the Platreef formed prior to intrusion of the hangingwall gabbro-norites. Furthermore, the presence of: (i) PGE mineralisation located at the base of the hangingwall where it is in direct contact with mineralised reef; (ii) mineralogical textures at the contact that indicate chilling and erosion; (iii) the truncation of replaced reef and sheared pyroxenite by the hangingwall; and (iv) partially recrystallised reef xenoliths within the hangingwall, suggest that the Platreef pyroxenites were cooled and almost completely crystallised before the Main Zone was intruded. The intrusion of the Main Zone magma imparted an unconformable contact on the Platreef; where, the Main Zone magma cut down into mineralised portions of Platreef, PGEs and S from the reef were incorporated into the new magma, and localised zones of basal PGEs and BMS mineralisation were formed in topographic hollows. The incorporation of xenoliths of calc-silicate into the Main Zone magma show that if the Platreef was intruded first, it could not have formed a complete barrier between the footwall and the Main Zone magma. This can be explained by there being an irregular floor topography at the time of Platreef intrusion, possibly caused by syn-emplacement diapirism of the footwall; or by interpreting the xenoliths as derived from the roof of the cold, thin Platreef, rather than from the floor beneath.

ACKNOWLEDGEMENTS

The authors would like to thank the management of Anglo Platinum, and in particular Alfred Sarila, for allowing Paul Armitage and David Holwell to undertake fieldwork on the Potgietersrus Platinums Limited lease area. Alan Bye and Richard Montjoie are acknowledged for their useful discussions, and Jay Cockayne is thanked for proof-reading the manuscript. David Holwell's PhD research is funded by the Natural Environment Research Council and supported by Anglo Platinum through Industrial CASE project (NER/S/C/2003/11952). Rais Latypov and Julian Menuge are thanked for their positive reviews and suggestions on improving the manuscript.

REFERENCES

1. P. E. B. ARMITAGE, I. McDONALD, S. J. EDWARDS AND G. M. MANBY: 'Platinum-group element mineralization in the Platreef and calc-silicate footwall at Sandsloot, Potgietersrus District, South Africa', *Appl. Earth Sci. (Trans. Inst. Min. Metall. B)*, 2002, **111**, B36–B45.

2. D. L. BUCHANAN and J. E. ROUSE: 'Role of contamination in the precipitation of sulphides in the Platreef of the Bushveld Complex', (eds. D. L. Buchanan and M. J. Jones), *Sulphide deposits in mafic and ultramafic rocks*, 141–146, 1984, London, IMM.
3. R. G. CAWTHORN, R. K. W. MERKLE and M. J. VILJOEN: 'Platinum-group elements in the Bushveld Complex', (ed. L. J. Cabri), *The geology, geochemistry, mineralogy and mineral beneficiation of platinum-group elements*. Special Volume 54, 389–430, 2002, Canadian Institute of Mining, Metallurgy and Petroleum.
4. A. E. W. FRIESE: 'Geology and tectono-magmatic evolution of the PPL concession area, Villa Nora-Potgietersrus Limb, Bushveld Complex', *Geological Visitor Guide*, Potgietersrus Platinums Limited, 2004, 1–57.
5. A. E. W. FRIESE and G. K. CHUNNETT: 'Tectono-magmatic development of the northern limb of the Bushveld Igneous Complex, with special reference to the mining area of Potgietersrus Platinums Limited', *Geoscience Africa 2004*, Abstract Volume, July 2004, University of the Witwatersrand, Johannesburg, South Africa, 209–210.
6. S. B. GAIN and A. B. MOSTERT: 'The geological setting of the platinoid and base metal sulphide mineralization in the Platreef of the Bushveld Complex in Drenthe, north of Potgietersrus', *Econ. Geol.*, 1982, **77**, 1395–1404.
7. E. C. I. HAMMERBECK and L. W. SCHÜRMANN: 'Nickel', (eds. M. G. C. Wilson and C. R. Anhaeusser), *The mineral resources of Southern Africa*, 471–482, 1998, Council for Geoscience.
8. C. HARRIS and J. B. CHAUMBA: 'Crustal contamination and fluid-rock interaction during the formation of the Platreef, Northern Limb of the Bushveld Complex, South Africa', *J. Petrol.*, 2001, **42**, 1321–1347.
9. D. A. HOLWELL, I. McDONALD and P. E. B. ARMITAGE: 'Platinum-group mineral assemblages in the Platreef at Sandsloot mine, Limpopo Province, South Africa', *Geoscience Africa 2004*, Abstract Volume, July 2004, University of the Witwatersrand, Johannesburg, South Africa, 282–283.
10. L. J. HULBERT: 'A petrographical investigation of the Rustenburg Layered Suite and associated mineralization south of Potgietersrus', Unpublished DSc dissertation, University of Pretoria, 1983, 1–511.
11. D. HUTCHINSON, J. A. KINNAIRD and L. W. SCHÜRMANN: 'Complex, multi-stage mineralization history in the southern sector of the Platreef, Bushveld Complex, RSA', *Geoscience Africa 2004*, Abstract Volume, July 2004, University of the Witwatersrand, Johannesburg, South Africa, 293–294.
12. E. D. KINLOCH and W. PEYERL: 'Platinum-group minerals in various rock types of the Merensky Reef: genetic implications', *Econ. Geol.*, 1990, **85**, 537–555.
13. J. A. KINNAIRD and P. A. M. NEX: 'Mechanisms of marginal mineralization in the Bushveld Complex', *Appl. Earth Sci. (Trans. Inst. Min. Metall. B)*, 2003, **112**, B206–B208.
14. J. A. KINNAIRD, D. HUTCHINSON, L. W. SCHÜRMANN, P. A. M. NEX and R. DE LANGE: 'Petrology and mineralization of the southern Platreef: northern limb of the Bushveld Complex, South Africa', *Mineralium Deposita*, 2005, In press.
15. F. J. KRUGER: 'Filling the Bushveld Complex magma chamber: lateral expansion, floor interaction, magmatic unconformities and giant chromitite and PGE deposits', *Mineralium Deposita*, 2005, In press.
16. C. A. LEE: 'A review of mineralization in the Bushveld Complex and some other layered mafic intrusions', (ed. R.

- G. Cawthorn), Layered Intrusions, 103–146; 1996, Amsterdam, Elsevier Science.
17. W. D. MAIER and S. J. BARNES: 'Platinum-group elements in silicate rocks of the Lower, Critical and Main Zones at Union Section, western Bushveld Complex', *J. Petrol.*, 1999, **40**, 1647–1671.
18. I. McDONALD, D. A. HOLWELL and P. E. B. ARMITAGE: 'Geochemistry and mineralogy of the Platreef and 'Critical Zone' cumulates of the Northern limb of the Bushveld Complex, South Africa: implications for Bushveld stratigraphy and the development of PGE mineralization', *Mineralium Deposita*, 2005, In press.
19. R. UKEN and M. K. WATKEYS: 'Diapirism initiated by the Bushveld Complex, South Africa', *Geology* 1997, **25**, 723–726.
20. M. J. VAN DER MERWE: 'The layered sequence of the Potgietersrus Limb of the Bushveld Complex. *Econ. Geol.*, 1976, **71**, 1337–1351.
21. M. J. VAN DER MERWE: 'The geology of the basic and ultramafic rocks of the Potgietersrus Limb of the Bushveld Complex', Unpublished PhD thesis, University of the Witwatersrand, 1978, 1–176.
22. M. J. VILJOEN and L. W. SCHÜRMANN: 'Platinum group metals', (eds. M. G. C. Wilson and C. R. Anhaeusser), The mineral resources of Southern Africa, 532–568; 1998, Council for Geoscience.
23. M. J. VILJOEN and R. N. SCOON: 'The distribution and main geologic features of discordant bodies of iron-rich ultramafic pegmatite in the Bushveld Complex', *Econ. Geol.*, 1985, **80**, 1109–1128.
24. G. VON GRUENWALDT, L. J. HULBERT and A. J. NALDRETT: 'Contrasting platinum-group element concentration patterns in cumulates of the Bushveld Complex', *Mineralium Deposita*, 1989, **24**, 219–229.
25. P. A. WAGNER: 'The platinum deposits and mines of

South Africa', Edinburgh, Oliver and Boyd, 1929, 1–326.

26. J. A. WHITE: 'The Potgietersrus Prospect – Geology and exploration history', XVth CMMI Congress, Johannesburg, SAIMM, vol. 3, 1994, 173–181.

Authors

David Holwell graduated with a BSc (Hons) in Geology from the University of Durham, UK, in 2001, and subsequently gained an MSc in Mining Geology from the Camborne School of Mines, UK, where his research area was the Merensky Reef of the Bushveld Complex. He is now a PhD student at Cardiff University, UK, working on Platreef mineralisation and emplacement in collaboration with Anglo Platinum.

Paul Armitage graduated with a BA (Hons) in Scandinavian and Icelandic studies from University College London in 1993 and subsequently gained BSc and MSc degrees in Geology from the University of Tromsø, Norway. His main area of study was the structural development of Precambrian terrains in northern Norway, partly in collaboration with the Norwegian Geological Survey. He is now a PhD student in PGE mineralisation at the University of Greenwich and works as a geologist with London Bridge Associates, a tunnelling consultancy.

Iain McDonald obtained a BSc degree in Chemistry and Geology from Glasgow University, UK, in 1989 and a PhD from the University of Cape Town, South Africa, in 1993. Following postdoctoral work on sulphide-poor PGE mineralisation at Manchester University, UK, he became a lecturer in geochemistry at the University of Greenwich. He is currently manager of the ICP laboratories at the School of Earth, Ocean and Planetary Sciences, Cardiff University, Wales.

APPENDIX 3

Full reference:

MCDONALD I., HOLWELL D.A. & ARMITAGE P.E.B. (2005). Geochemistry and mineralogy of the Platreef and “Critical Zone” cumulates of the Northern limb of the Bushveld Complex, South Africa: implications for Bushveld stratigraphy and the development of PGE mineralization. *Miner. Deposita*, **40**, 526-549.

Iain McDonald · David A. Holwell
Paul E. B. Armitage

Geochemistry and mineralogy of the Platreef and “Critical Zone” of the northern lobe of the Bushveld Complex, South Africa: implications for Bushveld stratigraphy and the development of PGE mineralisation

Received: 14 February 2004 / Accepted: 27 July 2005
© Springer-Verlag 2005

Abstract The northern lobe of the Bushveld Complex is currently a highly active area for platinum-group element (PGE) exploration. This lobe hosts the Platreef, a 10–300-m thick package of PGE-rich pyroxenites and gabbros, that crops out along the base of the lobe to the north of Mokopane (formerly Potgietersrus) and is amenable to large-scale open pit mining along some portions of its strike. An early account of the geology of the deposit was produced by Percy Wagner where he suggested that the Platreef was an equivalent PGE-rich layer to the Merensky Reef that had already been traced throughout the eastern and western lobes of the Bushveld Complex. Wagner’s opinion remains widely held and is central to current orthodoxy on the stratigraphy of the northern lobe. This correlates the Platreef and an associated cumulate sequence that includes a chromitite layer—known as the Grasvalley norite-pyroxenite-anorthosite (GNPA) member—directly with the sequence between the UG2 chromitite and the Merensky Reef as it is developed in the Upper Critical Zone of the eastern and western Bushveld. Implicit in this view of the magmatic stratigraphy is that similar Critical Zone magma was present in all three lobes prior to the development of the Merensky Reef and the Platreef. However, when this assumed correlation is examined in detail, it is obvious that there are significant differences

in lithologies, mineral textures and chemistries (Mg# of orthopyroxene and olivine) and the geochemistry of both rare earth elements (REE) and PGE between the two sequences. This suggests that the prevailing interpretation of the stratigraphy of the northern lobe is not correct. The “Critical Zone” of the northern lobe cannot be correlated with the Critical Zone in the rest of the complex and the simplest explanation is that the GNPA-Platreef sequence formed from a separate magma, or mixture of magmas. Chilled margins of the GNPA member match the estimated initial composition of tholeiitic (Main Zone-type) magma rather than a Critical Zone magma composition. Where the GNPA member is developed over the ultramafic Lower Zone, hybrid rocks preserve evidence for mixing between new tholeiitic magma and existing ultramafic liquid. This style of interaction and the resulting rock sequences are unique to the northern lobe. The GNPA member contains at least seven sulphide-rich horizons with elevated PGE concentrations. Some of these are hosted by pyroxenites with similar mineralogy, crystallisation sequences and Pd-rich PGE signatures to the Platreef. Chill zones are preserved in the lowest Main Zone rocks above the GNPA member and the Platreef and this suggests that both units were terminated by a new influx of Main Zone magma. This opens the possibility that the Platreef and GNPA member merge laterally into one another and that both formed in a series of mixing/quenching events involving tholeiitic and ultramafic magmas, prior to the main influx of tholeiitic magma that formed the Main Zone.

Editorial handling: A. Boyce

I. McDonald (✉) · D. A. Holwell
Department of Earth, Ocean and Planetary Sciences,
Cardiff University, P.O. Box 914, Cardiff,
CF10 3YE, UK
E-mail: iain@earth.cf.ac.uk
E-mail: holwell@Cardiff.ac.uk

P. E. B. Armitage
Department of Earth and Environmental Sciences,
University of Greenwich, Chatham Maritime,
Kent, ME4 4TB, UK

Keywords Bushveld Complex · Platreef · Merensky Reef · Stratigraphy · Platinum-group elements

Introduction

The Bushveld Complex of South Africa is the largest repository of platinum-group elements (PGE) in the

world (Lee 1996; Cawthorn 1999a). All PGE mining activities in the eastern and western lobes of the Bushveld Complex currently take place from tabular horizons within the layered sequence associated with sulphides or chromitite where the PGE are concentrated. The most important of these are the Merensky Reef and the UG2 chromitite layer. The stratigraphy and the positions of the PGE horizons in the eastern and western lobes of the complex are broadly the same (Lee 1996; Cawthorn and Lee 1998; Barnes and Maier 2002a). This, as well as other geophysical evidence, led Cawthorn and Webb (2001) to infer that the eastern and western lobes were connected throughout much of the evolution of the Bushveld Complex, that similar magmas were present in both lobes and that mineralisation processes operated concurrently in both lobes to produce stratiform PGE deposits such as the Merensky Reef and the UG2 chromitite.

While PGE mining and exploration in the eastern and western lobes of the Bushveld Complex to date have produced sufficient data to bring genetic understanding of the Merensky Reef and UG2 chromitite mineralisation to a mature stage, the same cannot be said of the PGE mineralisation in the northern (Potgietersrus) lobe of the complex. In this sector, PGE are associated with a basal unit called the Platreef that rests directly on the early Proterozoic sediments and Archaean granite that form the floor of the complex (Fig. 1). The Platreef is a contaminated, frequently xenolith-rich, unit that is geologically more complex than any of the PGE reefs in the eastern and western lobes, but which is also thicker and carries sufficiently consistent grade to allow large-scale open pit mining along some areas of its strike (Viljoen and Schürmann 1998; Bye 2001; Kinnaird and Nex 2003). Anglo Platinum, currently operates one open pit mine on the farm Sandsloot 236KR, is developing a second on the farm Zwartfontein 818LR, and has plans for others at staged intervals over the next 30 years (Bye 2001). The potential for more high-tonnage and low-cost open pits in this sector have led other companies to explore on the Platreef adjacent to Anglo Platinum's licence area and the northern lobe is currently the most active exploration centre on the Bushveld Complex.

The Platreef was discovered not long after the discovery of the Merensky Reef in the eastern Bushveld in 1924 and was systematically explored and mined until 1930, when the platinum price collapsed during the Great Depression (Buchanan et al. 1981). The most comprehensive early account of the geology of the deposit is given by Wagner (1929) who recognised and documented key features of the Platreef, most notably: (a) the great thickness of the mineralised layer(s); (b) the position of the mineralised pyroxenite ("bronzitite") at the base of the igneous sequence in contact with the metamorphosed sediments and granite; (c) the ratio of Pt:Pd at unity or lower; and (d) the presence of PGE mineralisation in metamorphosed and metasomatised footwall, often at considerable distance from the igneous rocks.

Wagner (1929) observed a "feldspathic bronzitite" and a "pseudoporphyrific poikilitic diallage norite" at many sites along the Platreef and termed these as "Merensky Reef" because of a similar appearance to the rocks of Merensky Reef that were already known in the eastern and western lobes of the Bushveld Complex. Wagner (1929) took this further and evidently believed that not only were the Platreef and the Merensky Reef similar, but that they represented the same layer:

"The Main Potgietersrust or Merensky Platinum Horizon...is the main platinum horizon of the Potgietersrust fields. This is taken to be the equivalent of the Merensky Horizon of the Lydenburg and Rustenburg districts." (p.167).

In discussing the wider genetic aspects of the mineralisation, Wagner (1929)

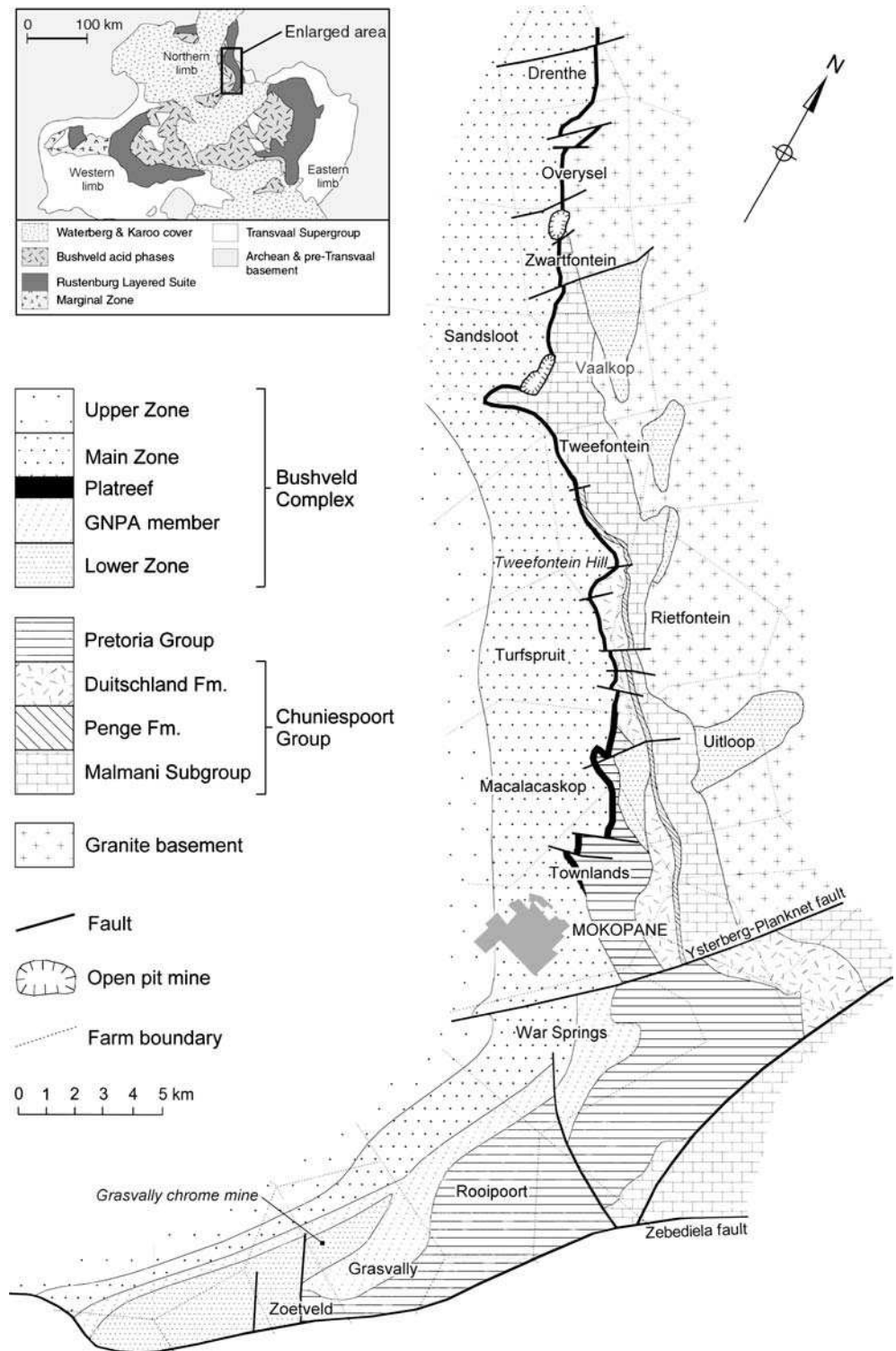
"...maintains that in endeavouring to arrive at the correct solution of the problem, the platinum deposits of the Potgietersrust district must be viewed in their entirety. In other words, the Zwartfontein deposits must be viewed in their relation to the Merensky Horizon as developed to the north and south of them and in the Rustenburg and Lydenburg districts." (p.182).

Wagner's suggestion that there was a direct correlation between the Platreef of the northern lobe and the Merensky Reef elsewhere in the Bushveld Complex is of great importance because it has been accepted uncritically in most subsequent work on the Platreef (e.g. Buchanan et al. 1981; Kinloch 1982; Buchanan and Rouse 1984; White 1994; Vermaak 1995; Viljoen and Schürmann 1998). More fundamentally, the assumed link between the two units is one of the foundations of the prevailing view of the stratigraphy of the northern lobe and its relationship with the rest of the complex.

The northern lobe

The stratigraphy of the northern lobe and the widely accepted view of its relationship with the rest of the Bushveld Complex are summarised in Figs. 2, 3. The northern lobe is divided into four principal zones but detailed elements of the stratigraphy are different from the eastern and western lobes. Lower Zone (LZ) rocks comprise > 1,600 m of pyroxenites and harzburgites with chromitite layers, consisting of at least 37 different cyclic units (Hulbert 1983; Hulbert and Von Gruenewaldt 1985). The LZ is best developed to the south of Mokopane on the farms Grasvalley 293KR and Zoetveld 294KR (Hulbert and Von Gruenewaldt 1986) but also occurs as small satellite bodies north of the town (Fig. 1). The mafic rocks

Fig. 1 Geological map of the lower portion of the northern limb of the Bushveld Complex showing the localities described in the text

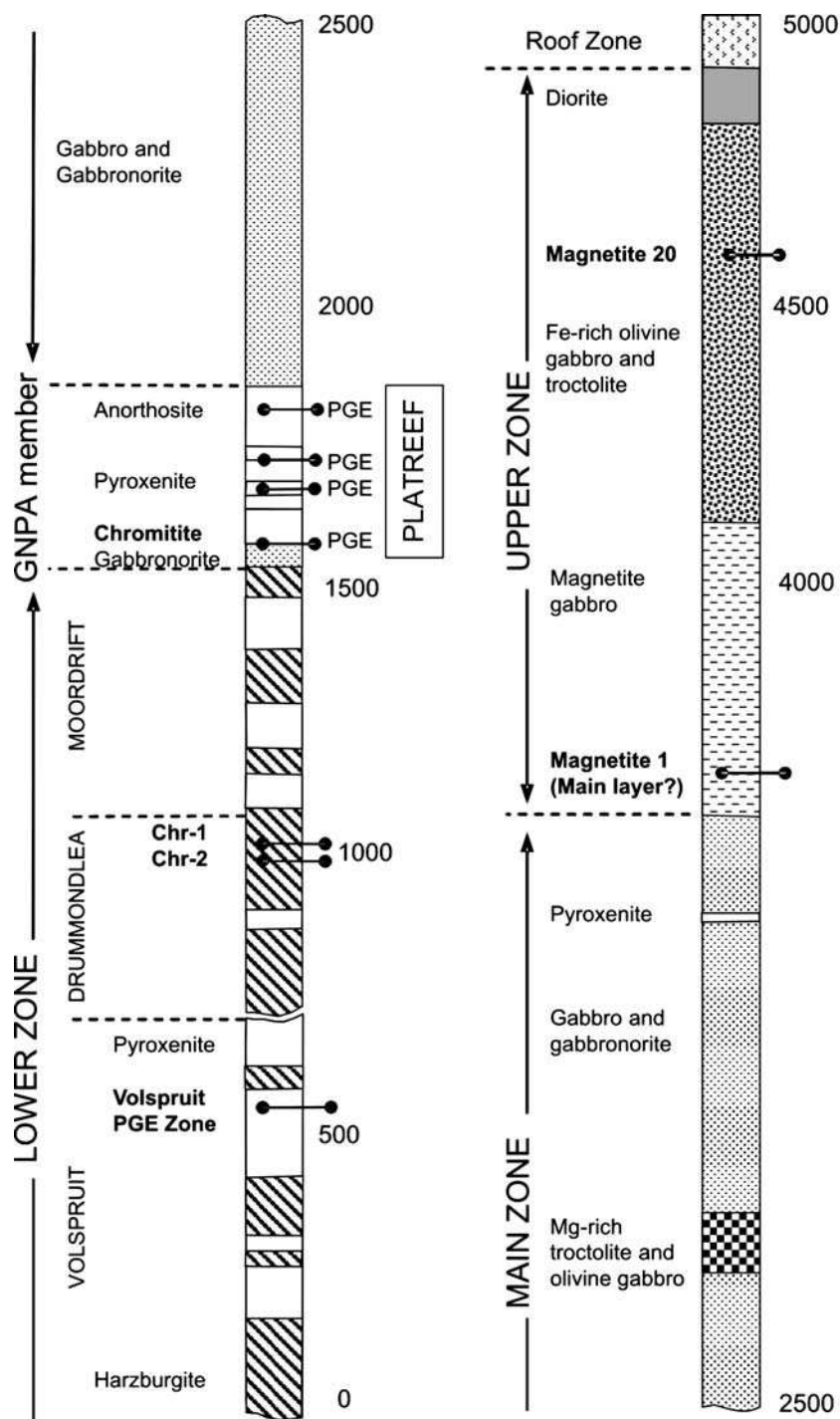


of the LZ here have higher Mg# ($(\text{Mg}/(\text{Mg} + \text{Fe}))$) values in olivine and orthopyroxene and contain chromitites with higher Cr_2O_3 than similar LZ-type rocks in the rest of the Bushveld Complex. In addition, a sulphide horizon with PGE occurs in the Volspruit Subzone (Fig. 2), whereas the LZ in the rest of the complex contains no

stratiform PGE mineralisation (Hulbert and Von Gruenewaldt 1982; Hulbert 1983). Van der Merwe (1976, 1998) considers these as unique features of the northern lobe, distinctive from the rest of the complex.

A thin sequence of rocks known as the Grasvally norite-pyroxenite-anorthosite (GNPA) member is

Fig. 2 Stratigraphy of the northern lobe showing the major chromitite, magnetite and Ni-Cu-PGE deposits (after Von Gruenewaldt et al. 1989)



developed over LZ rocks and sediments of the Pretoria Group south of Mokopane (Hulbert 1983; Hulbert and Von Gruenewaldt 1985, 1986; Fig. 1). This sequence contains layered norites, gabbro-norites and anorthosites along with a chromitite layer and is termed as the “Critical Zone” in all the current literature on the northern lobe. Hulbert (1983) termed the chromitite layer in the GNPA member the “UG2-like” chromitite and it has been correlated directly with the UG2

chromitite by some authors (e.g. Van der Merwe 1998). The top of the GNPA member is xenolith-rich and hosts PGE mineralisation. The occurrence of both xenoliths and PGE has led to suggestions that the upper part of the GNPA member may correlate with the Platreef north of Mokopane (Von Gruenewaldt et al. 1989).

Van der Merwe (1976) placed the Platreef (“Platinum Horizon” of Wagner 1929 and Willemse 1969) at the base of the Main Zone (MZ). This correlation is not

universally accepted and other authors (e.g. Von Gruenewaldt et al. 1989; White 1994) believe the Platreef to be a part of the Upper Critical Zone (UCZ). The Platreef can be traced for over 30 km along strike north of Mokopane and is generally developed between norites and gabbro-norites ascribed to the MZ and the floor of the complex. As the Platreef strikes north, it transgresses sedimentary rocks of the Transvaal Sequence, and eventually rests on Archaean granite (Fig. 1). The rest of the MZ comprises 2,200 m of gabbros and gabbro-norites. The only reliable markers in this part of the sequence are four prominent pyroxenites developed 300 m above the Platreef and a 100–200-m thick troctolite that is found 1,100 m above the Platreef. These layers have no equivalents in the rest of the Bushveld Complex. Van der Merwe (1976) suggested that a pyroxenite corresponding to the Pyroxenite Marker is developed 2,000 m above the Platreef, but Harris et al. (2004) have discounted this correlation. The pyroxenite unit also appears to be absent in the south of Mokopane and is missing from the stratigraphic compilations by Hulbert (1983) and Von Gruenewaldt et al. (1989).

The Upper Zone is approximately 1,400 m thick and comprises a sequence of magnetite gabbros, anorthosites and olivine diorites, along with a number of magnetite layers. As indicated in Fig. 3, one of these may be correlated on the basis of thickness and vanadium content with the Main Magnetite layer developed elsewhere in the Bushveld Complex (Van der Merwe 1976; Von Gruenewaldt et al. 1989).

The question of how the Platreef and other cumulates that have been ascribed to the “Critical Zone” in the northern lobe actually relate to the stratigraphy of the rest of the Bushveld Complex has important implications for the timing and genesis of the Platreef mineralisation. If it is not equivalent to the Merensky Reef and formed in a separate event, then genetic models constructed for the Platreef on the basis of what is known about the Merensky Reef or which link the two horizons in time may be inappropriate. The purpose of this paper is to critically review the geology of the Platreef and Merensky Reef, using existing knowledge and new geochemical and mineralogical data, with the aim of establishing the validity of the assumed link between the two units.

Samples

Samples of Platreef used in this study were collected from faces 135/014 and 138/014 in the southwest corner (SW1 and SW2 series) and faces 132/038 and 141/011 along the north wall (N1 and N3 series) of the southern central pit at Anglo Platinum’s Sandsloot open pit mine (Fig. 4). The footwall is composed primarily of siliceous dolomite and calc-silicate. Close to the contact, these rocks are transformed into a mixture of massive diopside clinopyroxenites, locally rich in metamorphic olivine (commonly referred to as “parapyroxenites”), that have

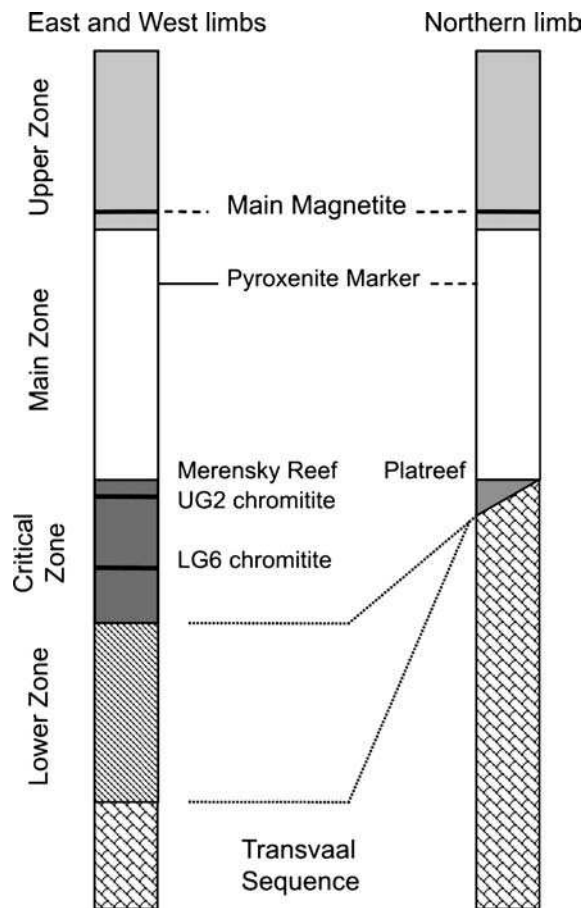


Fig. 3 Currently accepted stratigraphic relationships between the eastern and western limbs and the northern limb of the Bushveld Complex (after White 1994; and Cawthorn and Lee 1998)

suffered variable serpentinisation (Armitage et al. 2002). Additional samples of footwall were collected from faces that connect to the three reef sections along the south and east walls of the pit. These samples are labelled as the S series and the E series, respectively. Sample DH-G is a grab sample collected from the same area as Face 132/038 and is included with the N1 series for comparison.

Analytical methods

The initial preparation of samples was as described by Armitage et al. (2002). Detailed mineralogical examinations and the analysis of silicates were carried out at Cardiff University using a Cambridge Instruments LEO S360 scanning electron microscope coupled to an Oxford Instruments INCA energy dispersive X-ray analysis system. Additional analyses were also carried out at the Natural History Museum using a JEOL 5900LV (SEM) with attached Oxford instruments EDX INCA system. Typical analytical conditions and procedures are described in Hutchinson (2001). Bulk analysis for major

element and trace elements was carried out using a JY Horiba Ultima 2 inductively coupled plasma optical emission spectrometer (ICP-OES) and Thermo X7 series inductively coupled plasma mass spectrometer (ICP-MS). Samples were first ignited at 900°C to determine loss on ignition and then fused with Li metaborate on a Claisse Fluxy automated fusion system to produce a melt that could be dissolved in 2% HNO₃ for analysis. Full details of the ICP analysis procedures and the instrumental parameters are given in McDonald et al. (2005). Geochemical data for Platreef, hanging wall and footwall samples are given in Tables 1, 2, 3. A complete set of silicate mineral data, comprising over 200 analyses, is available from the first author on request.

Petrography of the Platreef at Sandsloot

White (1994) recognised three principal rock types within the Platreef that he termed as A reef, B reef and C reef. The A reef is a pegmatoidal feldspathic pyroxenite at the base of the sequence that carries sporadic base metal sulphide mineralisation. Above this is the B reef, the principal PGE carrier, which is a coarse grained pyroxenite with 50–90% orthopyroxene, common base metal sulphides and very sporadic chromitite. At the top of the sequence is the C reef, which is a fine-grained feldspathic pyroxenite that may contain up to 70% clinopyroxene. Despite the fact that they are essentially mining terms designed to categorise Platreef facies on a broad scale, these have become entrenched in the recent literature (Lee 1996; Viljoen and Schürmann 1998; Cawthorn and Lee 1998; Barnes and Maier 2002a; Cawthorn et al. 2002a) leading to the dangerous misconception that the A–B–C sequence represents “typical” Platreef.

Sections of the Platreef have been described in several papers prior to the A–B–C terminology being introduced, and reveal how, without any preconceived subdivisions, the terminology is simply not applicable in many parts of the Platreef. On the farm Drenthe 788LR, Gain and Mostert (1982) describe a basal feldspathic pyroxenite overlain by norites and melanorites, capped by a feldspathic pyroxenite. This sequence of pyroxenite–norite–pyroxenite is inconsistent with the A, B and C reefs, as the inferred ‘B-reef’ is noritic and contains cumulus plagioclase. In the adjacent farm to the south, Overysel 815LR, Cawthorn et al. (1985) describe the Platreef as often having a thin medium-grained norite at the base which grades upwards into a coarse pyroxenite with inhomogenous mineralogy, overlain by gabbro and norite.

More recent work has also revealed limitations with the “A–B–C” terminology (Armitage et al. 2002; Kinnaid et al. 2005). The definitions of the reef types do not conform to the recognised IUGS classifications, are not sufficient to allow unambiguous distinctions between different units, and encourage pigeonholing rather than proper description of potentially new rock types. For

example, in the faces mapped by Armitage et al. (2002) at Sandsloot, rocks corresponding to the A and C reef types were conspicuously absent. That study and new data presented here reveal other lithologies that form components of the Platreef at Sandsloot and do not fit into the previous terminology at all. For these reasons we avoid it and classify our samples according to the established IUGS guidelines.

Maps of face 132/038 (N1), and faces 138/014 (SW1) and 141/021 (SW2) are shown in Figs. 4, 5, 6. Sample points and numbers for all of the samples collected for petrography and/or geochemical analysis are indicated on each map. The upper portion of Platreef in face 132/038 has been described previously (as face 132/035) in Armitage et al. (2002); it has a true thickness of 12–15 m and is dominated by coarse grained pyroxene-rich gabbro-gabbro-norite that grades locally into pyroxenite and websterite. Cumulus orthopyroxene is ubiquitous and is accompanied by cumulus or intercumulus

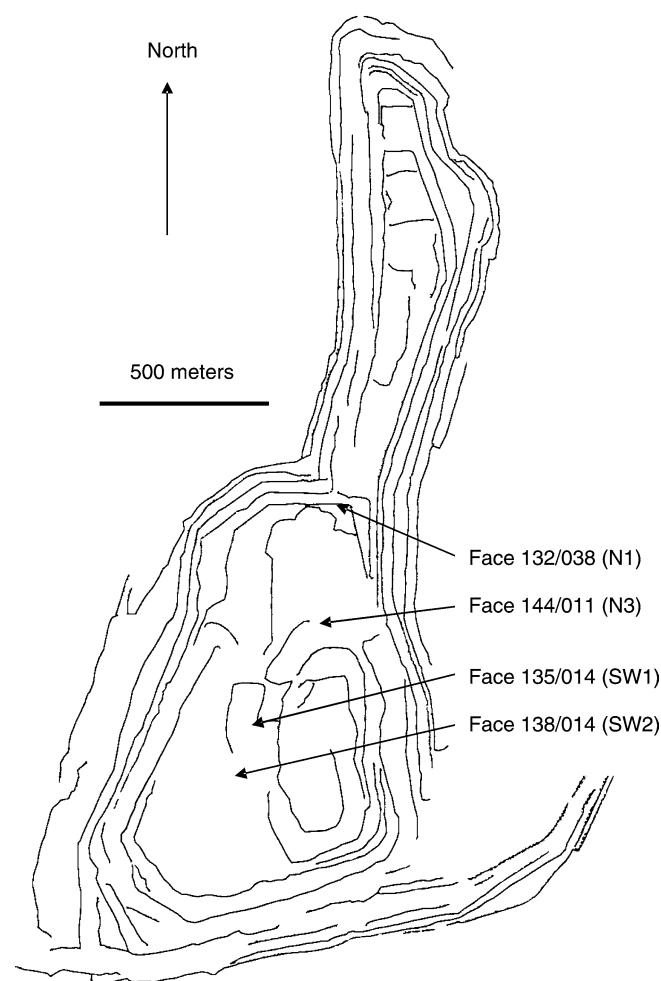


Fig. 4 Wireframe plan view of the Sandsloot open pit in July 2000 showing the locations of the faces mapped and sampled in this study. Solid lines represent the bench tops and the deepest area of the pit (south central area) is approximately 190 m below the level of the outer wall

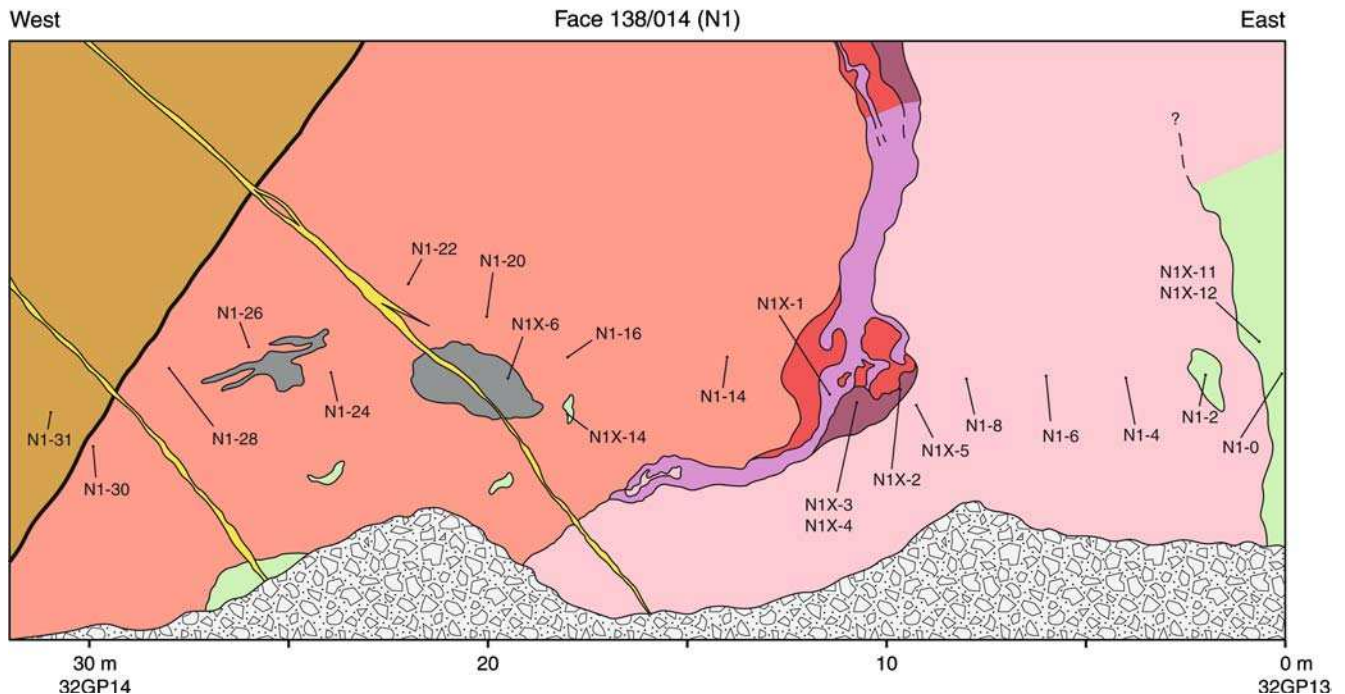
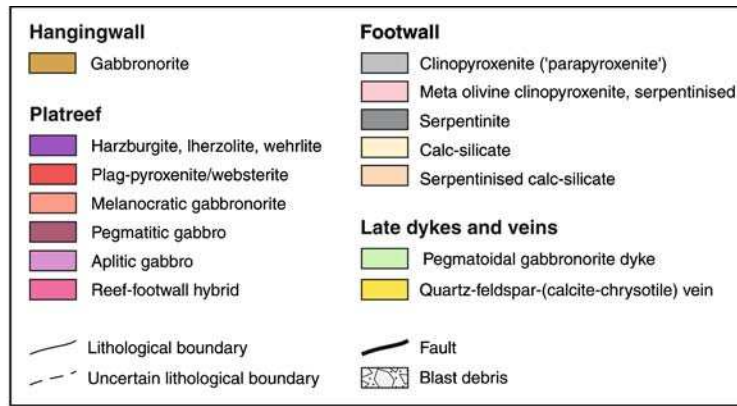


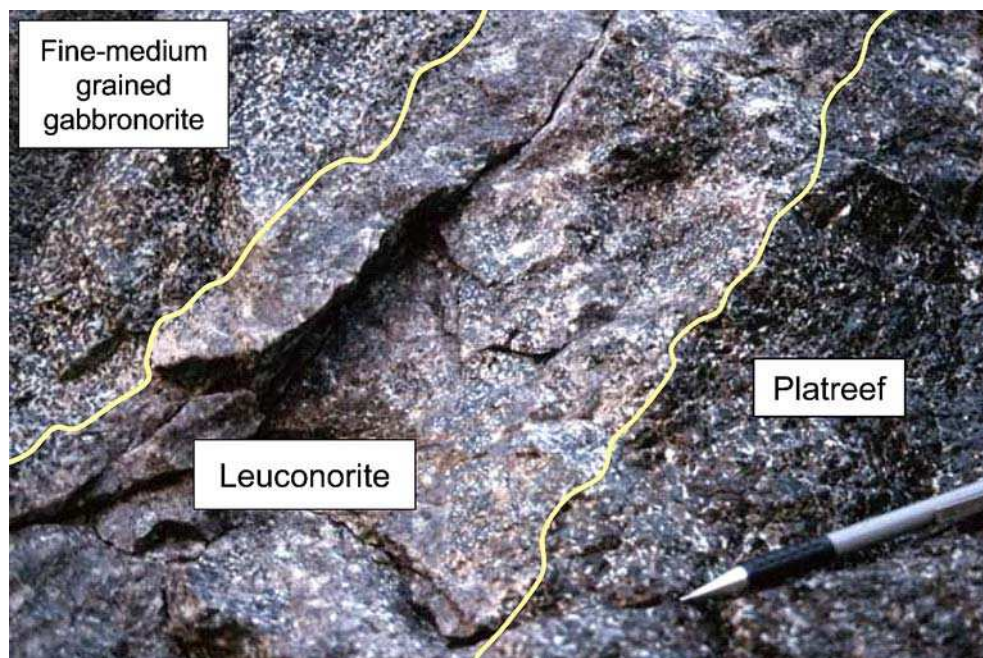
Fig. 5 Dip parallel section through the Platreef on face 132/035 (N1). This shows the major lithologies and the positions of samples taken for petrographic/geochemical analysis. 32GP13 and 32GP14 are the positions of mine survey geopoints

clinopyroxene, and intercumulus plagioclase that may occur as large oikocrysts. Sulphides and PGM are generally restricted to interstitial sites between the cumulate pyroxenes. Chromite, ilmenite, rutile, armalcolite, perovskite, phlogopite and zircon are present as accessories. A pegmatoidal zone of aplitic gabbro and fragmented pyroxenite occurs along the footwall contact where the reef thickens but is absent from thinner reef lower down the face. The contact with the hanging wall in this face is tectonised, and comprises a serpentinitised brittle-ductile shear zone up to 20 cm thick (Fig. 3). The hanging wall is a medium-coarse grained norite with cumulus plagioclase and intercumulus pyroxene (sample N1-31). The Platreef in face 144/011 (N3) appears similar to face N1 and the top contact of the reef was photographed and sampled. Here, instead of a tectonite, there is a planar magmatic contact between the top of

the Platreef and the hanging wall gabbros. The contact is marked by a 10–15 cm thick leuconorite with cumulus plagioclase and orthopyroxene oikocrysts, overlain by a 5 cm thick layer of fine-grained gabbro (Fig. 6). The leuconorite and gabbro are samples N3X4B and N3X4A in Table 1.

Platreef in the southwest corner of the pit shows important mineralogical and textural differences from the reef exposed to the north. Towards the top contact, Fe-rich olivine is widespread and occurs as a late-stage mineral. It replaces orthopyroxene through many metres of the reef. Plagioclase may also be replaced by Fe-rich clinopyroxene leading to the development of Fe-rich wehrlites, olivine lherzolites and harzburgites and an overall darkening of the rock. These rock types have been noted to the south where the Platreef rests on banded ironstone (Buchanan et al. 1981; Buchanan and

Fig. 6 Leuconorite and fine-grained gabbronorite at the hanging wall contact in face 141/011 (N3). The pen on the right is 12-cm long



Rouse 1984), but have not been described elsewhere. The Fe enrichment and reaction textures observed here are similar to those found in Fe-rich pipes and pegmatoids elsewhere in the complex (Schiffries 1982; Viljoen and Scoon 1985) and may result from reaction between Platreef pyroxenites and gabbros and a late-stage Fe-rich melt or fluid. For the ease of discussion, this type of Fe-rich (ultramafic) Platreef is hereafter referred to as “replaced reef”.

Face 135/014 (SW1) shows Platreef cutting the footwall lithologies at a high angle. A serpentinised mixed rock comprising relict metamorphic clinopyroxenite (with or without olivine) and pyroxenites and websterites with igneous textures, (termed as “footwall-reef hybrid”) forms the base of the Platreef. The primary Platreef is heavily replaced and mixtures of orthopyroxenites, websterites, gabbronorites and wehrlites are common. The rocks become more pegmatoidal and olivine-rich upwards, grading into Fe-rich olivine lherzolite close to the hanging wall contact (Fig. 7). The hanging wall for a few metres above the contact is fine-grained gabbronorite with cumulus plagioclase (sample SW1-47).

Face 138/014 (SW2) also shows Platreef cutting the footwall calc-silicates at a high angle to the remnant layering and is similar in some respects to Face 135/014. Olivine in the footwall is heavily serpentinised and these rocks contain an extensive fracture network filled with magnetite and ilmenite. A thick zone of serpentinised hybrid rocks is present at the base of the reef and wehrlite occurs close to the hybrid rocks. This merges upwards into gabbronorite and pyroxenite that become very Fe-rich, but without much development of olivine, close to the hanging wall. A 15-cm wide dark xenolith of websterite (sample SW2-83) that carries high levels of Cr

and some PGE grade is present a few metres above the contact in the hanging wall gabbronorite (Fig. 8; Table 3).

Geochemical trends associated with the Platreef at Sandsloot

Harris and Chaumba (2001) noted that the igneous Platreef was richer in Cr, Co and Fe than the footwall or the hanging wall lithologies, which is replicated here (Tables 1, 2, 3). The footwall clinopyroxenites and serpentinites contain less Si and Fe than the reef but more Ca and Mn. Similarly, the hanging wall norites and gabbronorites typically contain more Si, Al, Na, K, Rb, Sr and Ba than the reef or the footwall. Harris and Chaumba (2001) noted an upward trend of Fe enrichment in their reef samples and in the N1 face, where there is the least evidence of replacement; we find a similar gradual increase in Fe towards the top of the reef. In replaced reef (e.g. face SW1), the Fe enrichment is dramatic and these areas are also enriched in Ti, Mn, Hf and Nb (and sometimes U and Th) relative to primary reef. The plagioclase-rich hanging wall rocks and the cross-cutting pegmatoidal gabbronorite dyke in the N1 face are also characterised by a consistently positive Eu anomaly ($\text{Eu}/\text{Eu}^* > 1.0$), while the opposite is generally true of the reef and the footwall. As might be expected, footwall-reef hybrid rocks show concentrations of Si, Mg, Ca, Fe, Co and Cr that are intermediate between reef and footwall (Tables 2 and 3) but nevertheless the Cr concentration is a useful indicator for primary reef, hybrid zones and footwall where the lithological relations are ambiguous.

Table 1 Geochemical data for faces N1 and N3

	E195	E205	E227	N1-02	N1-2	N1-4	N1-6a	N1-6b	N1-14	N1-X6	N1-22	N1-24	N1-26	N1-30	N1-31	DH-G	N3X4A	N3X4B
Unit	FW	FW	DYKE	DYKE	DYKE	FW	FW	FW	PR	XN	PR	PR	PR	PR	HW	PR	HW	HW
Rock Type	SPT	PPX	GBNRT	GBNRT	GBNRT	CS-PPX	PPX	SPT vein	Fel PX	SPT	Fel PX	GBNRT	GBNRT	GBNRT	NRT	WBST	GBNRT	LCNRT
SiO ₂ (wt%)	39.55	46.26	49.40	50.44	48.77	39.61	43.22	37.08	52.55	33.92	49.18	51.86	50.59	51.25	51.87	50.39	51.81	50.85
TiO ₂	0.09	0.26	0.33	0.17	0.18	0.12	0.26	0.07	0.19	0.20	0.20	0.16	0.17	0.14	0.16	0.19	0.20	0.09
Al ₂ O ₃	2.77	3.22	16.52	14.81	16.85	12.87	11.31	8.46	6.42	10.88	4.28	5.19	5.70	4.17	22.63	5.79	17.48	26.64
Fe ₂ O ₃	6.34	9.12	8.00	7.17	8.43	10.52	7.21	14.44	11.52	8.36	15.07	13.96	13.26	13.93	5.56	12.82	9.75	1.95
MnO	0.22	0.57	0.15	0.13	0.14	0.35	0.52	0.42	0.21	0.73	0.26	0.23	0.26	0.23	0.10	0.22	0.14	0.04
MgO	34.39	21.25	8.05	10.58	9.61	17.59	14.09	28.04	22.14	34.18	22.88	23.23	21.19	22.53	5.38	19.74	6.48	1.61
CaO	2.36	15.51	10.73	9.60	10.00	11.76	18.95	1.78	5.20	0.32	4.57	4.18	5.41	4.03	11.52	8.83	11.17	13.08
Na ₂ O	0.01	0.21	2.79	3.76	1.91	0.22	0.05	0.02	0.50	0.02	0.58	0.46	0.91	0.66	2.77	0.26	1.79	3.35
K ₂ O	0.01	0.15	1.99	0.72	1.20	0.50	0.05	0.09	0.24	0.03	0.20	0.14	0.07	0.05	0.52	0.01	1.30	0.79
P ₂ O ₅	0.01	0.03	0.04	0.05	0.02	0.03	0.02	0.02	0.03	0.01	0.03	0.03	0.04	0.03	0.02	0.03	0.00	0.00
LOI	12.98	3.38	2.98	2.84	1.17	5.58	5.64	11.14	0.41	11.90	1.20	0.76	0.56	1.75	1.33	0.87	1.14	0.90
Total	98.73	99.95	100.99	100.26	98.27	99.14	101.30	101.55	99.42	100.55	98.46	100.21	98.16	98.76	101.85	99.13	101.25	99.30
Sc (ppm)	8.12	33.8	18.6	18.4	15.8	15.34	26.8	8.2	28.2	24.7	30.8	13.3	29.7	28.3	30.9	27.8	30.8	5.7
V	44.5	153.2	126.9	128.0	93.4	81.5	133.2	51.0	171.1	51.6	168.5	120.3	130.4	125.1	123.1	135.5	190.9	60.9
Cr	14.4	37.3	485.0	279.9	610.9	198.5	331.9	111.5	1817.4	144.1	1734	1916	1688	3021	462.9	1741	424.0	285.8
Co	42.0	20.4	68.3	44.8	43.9	41.1	55.9	83.1	88.0	35.8	158.1	112.8	110.0	121.4	53.3	98.1	40.9	14.7
Ni	389.8	62.6	289.5	165.1	716.0	253.6	408.1	152.1	1292	64.0	2818	4020	2597	3206	160.4	1736	346.2	56.9
Cu	115.2	69.3	148.7	11.6	310.6	139.3	133.1	227.3	210.1	93.6	1549	1577	885	834.7	74.5	610.1	120.6	79.0
Ga	5.2	5.8	13.5	12.26	14.4	10.7	10.99	15.14	6.71	18.62	5.9	6.3	6.76	4.86	22.9	6.72	18.2	24.64
Rb	0.0	16.2	107.2	36.32	59.7	34.0	1.79	6.24	3.50	1.02	7.2	8.2	1.08	2.74	28.9	2.10	49.9	20.70
Sr	7.7	14.1	280.3	236.0	238.6	164.7	66.3	16.3	101.9	9.5	37.8	54.4	55.4	35.0	332.6	16.9	332.8	385.5
Y	3.2	10.1	7.7	7.1	4.3	3.8	10.2	1.6	5.5	4.4	6.0	5.1	6.5	3.2	5.7	5.7	7.4	2.21
Zr	3.6	24.3	26.0	38.2	32.3	14.0	40.3	16.6	25.7	35.4	11.5	10.0	49.8	10.5	8.8	17.6	11.5	4.31
Nb	0.21	0.73	2.40	0.82	0.83	0.80	3.08	2.66	2.94	2.78	0.48	0.44	0.30	0.26	0.65	0.47	0.4	0.15
Ba	n.d.	8.4	186.3	211.7	217.7	108.9	26.1	16.1	80.0	8.5	23.1	28.3	40.6	35.2	111.2	19.1	149.6	151.1
La	1.50	4.02	6.51	4.16	2.47	3.59	4.21	1.33	2.89	1.28	2.51	1.84	2.17	1.74	4.96	2.97	2.59	4.75
Ce	1.89	9.06	9.45	7.21	5.58	5.86	9.67	2.29	5.73	2.89	5.63	4.88	4.76	2.57	8.33	5.15	5.14	8.33
Pr	0.24	1.32	1.22	0.83	0.68	0.73	1.31	0.26	0.72	0.41	0.73	0.63	0.53	0.27	0.99	0.62	0.66	0.90
Nd	0.92	5.39	4.67	3.74	2.43	2.70	5.56	0.95	2.90	1.84	2.81	2.40	2.41	1.31	3.47	2.96	2.54	3.06
Sm	0.17	1.26	1.06	0.92	0.49	0.55	1.34	0.19	0.61	0.47	0.59	0.51	0.54	0.28	0.62	0.70	0.60	0.46
Eu	0.06	0.27	0.51	0.40	0.49	0.33	0.54	0.11	0.21	0.10	0.16	0.19	0.15	0.09	0.62	0.20	0.34	0.71
Gd	0.24	1.35	1.07	0.94	0.54	0.56	1.50	0.18	0.67	0.51	0.66	0.59	0.59	0.34	0.64	0.86	0.68	0.43
Tb	0.04	0.23	0.18	0.16	0.09	0.09	0.26	0.04	0.13	0.10	0.12	0.10	0.10	0.06	0.11	0.14	0.12	0.06
Dy	0.37	1.51	1.15	1.05	0.61	0.58	1.61	0.23	0.83	0.65	0.81	0.71	0.71	0.47	0.71	1.09	0.87	0.39
Ho	0.09	0.28	0.22	0.21	0.13	0.11	0.33	0.05	0.18	0.14	0.17	0.15	0.14	0.09	0.14	0.24	0.18	0.07
Er	0.35	0.90	0.73	0.65	0.44	0.38	0.86	0.14	0.50	0.39	0.61	0.57	0.48	0.33	0.47	0.76	0.64	0.21
Tm	0.06	0.13	0.11	0.09	0.07	0.06	0.13	0.02	0.08	0.07	0.10	0.09	0.08	0.06	0.07	0.12	0.10	0.03
Yb	0.48	0.81	0.70	0.68	0.46	0.36	0.94	0.20	0.65	0.50	0.68	0.58	0.56	0.43	0.48	0.92	0.69	0.17
Lu	0.09	0.14	0.12	0.10	0.08	0.06	0.19	0.08	0.15	0.13	0.11	0.10	0.07	0.05	0.08	0.14	0.11	0.03
Hf	0.09	0.67	0.67	0.73	0.64	0.36	1.20	0.42	0.60	1.08	0.29	0.22	0.14	0.17	0.20	0.43	0.25	0.09
Ta	0.02	0.07	0.18	0.08	0.07	0.05	0.23	0.18	0.21	0.21	0.06	0.05	0.05	0.03	0.04	0.05	0.01	0.01
Th	0.45	1.08	1.52	0.64	0.57	0.67	1.19	0.37	1.11	0.86	0.95	0.54	0.49	0.34	0.51	0.62	0.39	0.26
U	0.85	0.20	0.37	0.18	0.09	0.11	0.30	0.12	0.29	0.26	0.11	0.13	0.11	0.06	0.06	0.12	0.01	0.02
Eu/Eu*	0.90	0.64	1.45	1.29	2.86	1.81	1.16	1.79	1.02	0.62	0.78	1.05	0.78	0.93	2.97	0.79	1.63	4.78
La/LuN	1.77	3.03	5.85	4.12	3.39	6.66	2.34	1.82	2.01	1.03	2.42	1.98	3.16	3.35	6.48	2.16	2.42	19.42
PGE grade	n/a	n/a	n/a	v. low	n/a	low	n/a	n/a	n/a	n/a	inter	inter	high	high	v. low	inter	inter	v low
Pt/Pd	n/a	n/a	n/a	0.75	n/a	0.90	n/a	n/a	n/a	n/a	1.04	0.98	1.94	0.93	1.36	1.03	0.91	0.87

Rare earth element values in chondrite used for normalisation come from Taylor and McLennan (1985)

PGE grade bands based on total Rh + Pt + Pd + Au: <0.1 ppm = very low; 0.1–2.0 ppm = low; 2.0–6.0 = intermediate; 6.0–10.0 = high; >10.0 = very high

Major units: *FW* footwall; *DYKE* cross-cutting pegmatoidal dykes; *PR* primary reef; *XN* xenoliths; *HW* hanging wall

Rock types: *SPN* serpentinite; *PPX* para(clino)pyroxenite; *CS* calc-silicate; *GBNRT* gabbornorite; *PX* pyroxenite; *NRT* norite; *WBST* websterite; *LCNRT* leuconorite

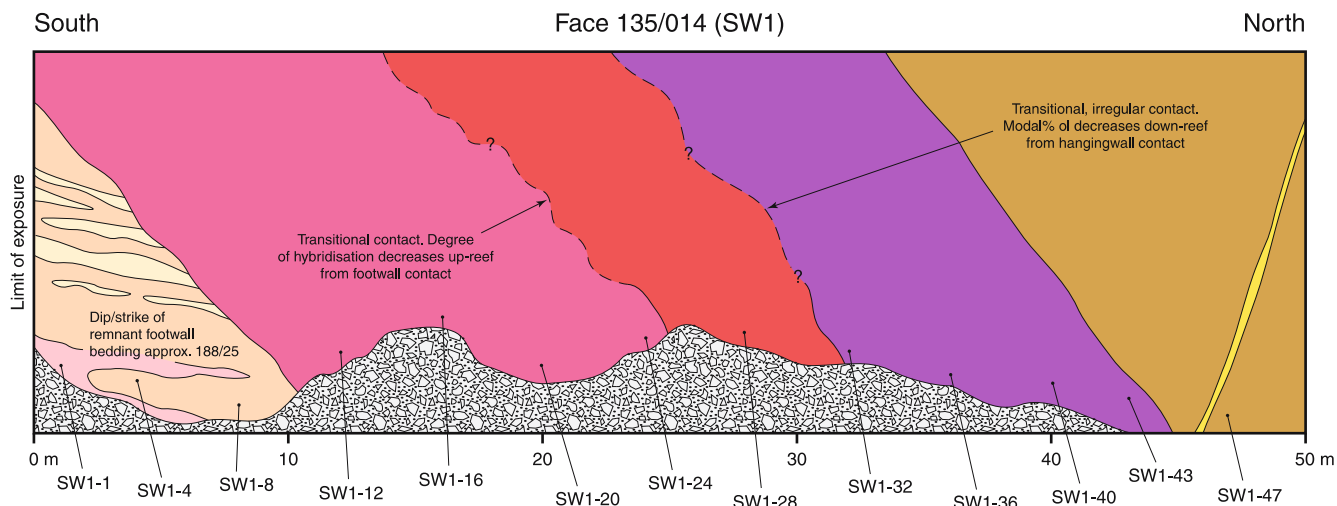


Fig. 7 Slightly oblique section through the Platreef on face 135/014 (SW1). This shows the major lithologies with contacts extrapolated/inferred at height and the positions of samples taken for petrographic/geochemical analysis. The key is as in Fig. 5

Links between the Platreef and the Merensky Reef

Stratigraphic context

The modern consensus stems from Willemse (1969) and van der Merwe (1976) who followed Wagner (1929) and correlated the Platreef with the Merensky Reef. This interpretation is primarily based on the nature of the rocks immediately above the Platreef. The hanging wall norites and gabbros are visually similar and have similar orthopyroxene compositions to MZ rocks elsewhere in the Bushveld Complex. Von Gruenewaldt et al. (1989) suggested that the Platreef might be correlated with the upper part of the GNPA member (shown in detail in Fig. 9). Evidence cited in support of this includes: the layering of some units and the presence of cumulus chromite and development of a chromitite layer. These are the characteristic features of the UCZ in the eastern and western Bushveld and the MZ is notable for the absence of both. The terms “Critical Zone” and “Main Zone” when applied to the northern lobe effectively refer

to whether the rocks are located above or below the Platreef. The veracity of this assumption will be tested below.

Petrographic similarities between the Platreef and the Merensky Reef

Both units are dominated by cumulus orthopyroxene, with subordinate amounts of plagioclase and clinopyroxene, and carry an assemblage of interstitial sulphides and elevated concentrations of PGE. Buchanan et al. (1981) suggested that pyroxene compositions in the Platreef were the same as in the Merensky Reef (see below for discussion). In places, both units develop pegmatoidal facies. Chromite in the form of one or two chromitite layers is a ubiquitous feature of the Merensky Reef and the highest PGE grades are generally associated with one or both chromitites (Lee 1996; Kinnaird et al. 2002). Chromite occurs as isolated crystals, or as rare pods/schlieren, in the Platreef (Viljoen and

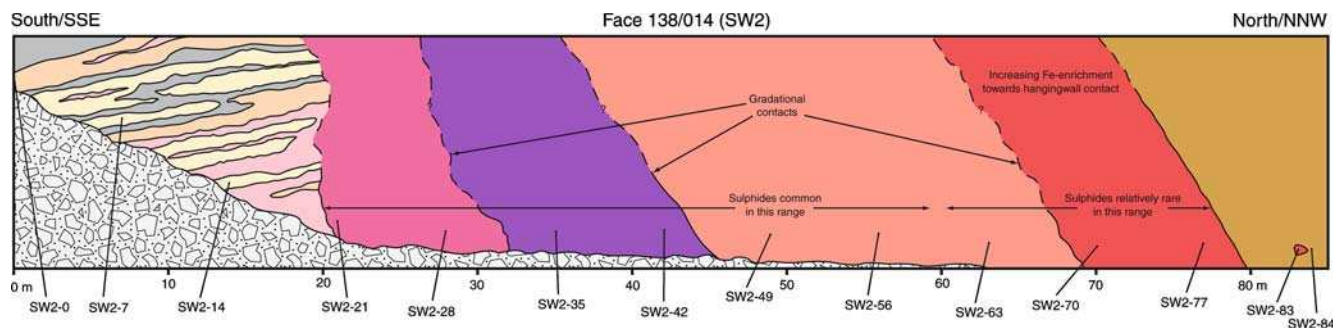


Fig. 8 Oblique section through the Platreef on face 138/014 (SW2). This shows the major lithologies with contacts extrapolated/inferred at height and the positions of samples taken for petrographic/geochemical analysis. The key is as in Fig. 5

Table 2 Geochemical data for face SW1

	SW1-1	SW1-4	SW1-8	SW1-20	SW1-24	SW1-28	SW1-32	SW1-36	SW1-40	SW1-43	SW1-47B	SW1-47A
Unit	FW	FW	FW	HYB	HYB	PR	RR	PR	RR	RR	HW	HW
Rock Type	PPX	CS	CS	n/a	n/a	WBST	LHRZ	PX	HZBG	LHRZ	GBNRT	GBNRT
SiO ₂ (wt%)	43.51	40.24	40.94	44.38	42.66	45.16	44.84	46.55	48.11	44.21	51.44	49.44
TiO ₂	0.42	0.29	0.09	0.62	0.15	0.14	0.18	0.14	0.21	0.23	0.19	0.16
Al ₂ O ₃	6.08	3.32	2.48	5.47	6.27	3.61	3.44	3.70	2.56	3.29	16.48	16.30
Fe ₂ O ₃	8.03	3.89	7.38	13.49	12.86	13.28	19.36	13.43	17.85	22.08	8.83	9.04
MnO	0.35	0.68	0.73	0.31	0.29	0.24	0.33	0.22	0.32	0.38	0.19	0.15
MgO	14.79	29.81	27.00	10.62	18.43	20.63	22.58	23.27	23.46	21.76	6.93	8.55
CaO	23.83	9.61	11.52	24.30	16.05	12.36	6.31	8.99	4.75	6.48	12.06	11.75
Na ₂ O	0.19	0.03	0.01	0.19	0.29	0.67	0.37	0.33	0.10	0.33	2.43	2.52
K ₂ O	0.02	0.00	0.01	0.02	0.46	0.13	0.15	0.13	0.19	0.23	0.41	0.43
P ₂ O ₅	0.03	0.00	0.01	0.03	0.02	0.03	0.05	0.02	0.03	0.04	0.01	0.02
LOI	0.83	10.85	8.28	0.27	4.00	3.09	1.06	1.57	0.52	0.57	1.34	2.27
Total	98.09	98.73	98.45	99.69	101.48	99.33	98.66	98.35	98.12	99.59	100.32	100.65
Sc (ppm)	28.0	5.57	4.90	46.12	26.9	34.8	24.3	30.0	25.8	31.0	37.8	28.1
V	159.2	46.1	47.4	333.4	117.7	129.2	126.5	126.3	145.4	187.9	200.0	152.2
Cr	41.5	27.7	48.3	835.0	601.8	3065	3042	3061	3104	2304	292.0	551.5
Co	37.8	11.3	56.4	71.0	92.9	123.3	116.4	134.9	131.3	136.9	48.3	59.1
Ni	1683	189.7	3732	928.3	2286	2156	2769	3921	2804	3390	406.9	376.1
Cu	1448	87.1	2097	675.5	839.0	828.7	764.5	1477	1156	1329	170.5	186.6
Ga	7.6	6.3	4.3	10.2	6.5	4.88	5.50	4.5	5.2	5.6	18.1	15.7
Rb	1.9	−0.1	0.1	3.7	26.3	6.32	5.72	7.3	15.4	11.9	7.3	11.9
Sr	25.5	7.6	7.2	25.6	31.3	47.1	85.5	60.9	34.4	66.1	282.2	233.9
Y	18.2	29.6	14.9	12.3	6.6	6.7	7.9	5.3	6.5	10.3	11.7	8.2
Zr	67.5	7.8	3.0	58.2	12.6	15.7	19.5	10.3	14.0	15.5	5.1	7.0
Nb	1.36	2.08	0.52	1.51	0.61	0.54	0.98	0.49	0.78	0.62	0.03	0.15
Ba	2.1	n.d.	n.d.	1.8	37.7	54.0	85.6	44.2	37.3	52.1	76.6	71.6
La	5.53	6.27	1.93	3.91	1.82	1.90	3.24	1.69	1.82	2.52	1.80	2.04
Ce	15.56	17.57	5.40	9.40	4.61	4.47	6.94	3.46	4.54	6.35	4.03	4.53
Pr	2.26	2.26	0.75	1.43	0.67	0.59	0.87	0.50	0.64	0.97	0.60	0.64
Nd	9.29	8.51	3.10	6.16	2.91	3.06	4.07	2.22	2.67	4.23	2.68	2.75
Sm	2.27	2.11	0.81	1.69	0.74	0.81	0.98	0.56	0.62	1.11	0.75	0.73
Eu	0.61	0.46	0.21	0.42	0.23	0.21	0.28	0.18	0.17	0.29	0.39	0.45
Gd	2.49	2.64	1.19	1.80	0.88	0.96	1.04	0.70	0.72	1.27	0.95	0.86
Tb	0.42	0.54	0.24	0.30	0.16	0.16	0.19	0.11	0.13	0.21	0.18	0.16
Dy	2.64	3.68	1.74	1.86	1.02	1.09	1.23	0.81	0.94	1.48	1.23	1.07
Ho	0.48	0.73	0.37	0.34	0.19	0.22	0.25	0.15	0.19	0.28	0.24	0.21
Er	1.60	2.68	1.44	1.11	0.65	0.64	0.73	0.54	0.68	0.99	0.86	0.72
Tm	0.24	0.43	0.25	0.17	0.09	0.09	0.13	0.08	0.11	0.15	0.14	0.11
Yb	1.45	2.80	1.70	1.11	0.59	0.65	0.80	0.51	0.74	0.99	0.91	0.73
Lu	0.22	0.44	0.27	0.19	0.09	0.08	0.13	0.08	0.13	0.16	0.15	0.11
Hf	1.93	0.27	0.09	1.70	0.32	0.35	0.38	0.26	0.35	0.37	0.21	0.20
Ta	0.12	0.64	0.06	0.09	0.04	0.04	0.09	0.04	0.07	0.05	0.01	0.01
Th	1.63	11.93	1.32	1.45	0.52	0.58	0.86	0.51	0.76	0.71	0.29	0.29
U	0.86	0.95	0.11	0.41	0.10	0.11	0.26	0.04	0.15	0.12	0.00	0.01
Eu/Eu*	0.78	0.60	0.65	0.73	0.85	0.72	0.84	0.86	0.76	0.75	1.40	1.74
La/LuN	2.57	1.48	0.74	2.11	2.08	2.40	2.57	2.13	1.44	1.66	1.28	1.87
PGE grade	v. high	low	v. high	inter	inter	high	inter	high	inter	v. high	low	low
Pt/Pd	0.86	0.65	0.99	0.88	0.67	1.28	0.81	0.74	0.55	0.70	0.95	0.97

Rare earth element values in chondrite used for normalisation come from Taylor and McLennan (1985)

PGE grade bands based on total Rh+Pt+Pd+Au: <0.1 ppm = very low; 0.1–2.0 ppm = low; 2.0–6.0 = intermediate; 6.0–10.0 = high; >10.0 = very high

Major units: *FW* footwall; *DYKE* cross-cutting pegmatoidal dykes; *HYB* footwall hybrid; *PR* primary reef; *RR* replaced reef; *HW* hanging wall

Rock types: *PPX* para(clino)pyroxenite; *CS* calc-silicate; *GBNRT* gabbonorite; *PX* orthopyroxenite; *LHRZ* lherzolite; *HZBG* harzburgite

Schürmann 1998; Armitage et al. 2002), but is most commonly an accessory component. A more widespread chromitite (inferred from the presence of chromite at the same level in many drillcores) is apparently developed in the Platreef to the south of Sandsloot on the farm Tweefontein 238KR. PGE grades are highest in the pyroxenite immediately beneath the chromitite and Viljoen and Schürmann (1998) suggest that at this locality

the Platreef bears the greatest similarity to normal Merensky Reef.

Strontium and osmium isotopes

Cawthorn et al. (1985) found a wide range of ⁸⁷Sr/⁸⁶Sr initial ratios in Platreef whole rock samples that they

Table 3 Geochemical data for face SW2

	S2-6	S2-12	S2-18	SW2-14	SW2-28	SW2-35	SW2-49	SW2-77	SW2-83
Unit	FW	FW	FW	FW	HYB	RR	PR	RR	XN
Rock Type	SPPX	SPPX	CS	SPPX	n/a	WHRL	GBNRT	PX	WBST
SiO ₂ (wt%)	40.71	31.57	26.73	34.12	46.60	46.40	48.49	50.03	52.78
TiO ₂	0.12	0.11	0.34	0.29	0.19	0.21	0.21	0.37	0.17
Al ₂ O ₃	3.69	11.32	8.27	17.65	5.37	5.26	5.44	4.35	3.42
Fe ₂ O ₃	11.02	8.79	11.85	7.66	8.83	15.53	16.48	16.95	10.23
MnO	0.54	0.26	0.31	0.26	0.40	0.33	0.29	0.34	0.23
MgO	27.08	20.30	21.95	13.22	23.53	20.27	18.63	16.33	22.59
CaO	7.50	15.98	18.17	20.09	13.09	11.07	8.73	9.65	8.64
Na ₂ O	0.06	0.02	0.10	0.14	0.13	0.44	0.84	0.69	0.37
K ₂ O	0.06	0.00	0.02	0.08	0.03	0.17	0.25	0.05	0.23
P ₂ O ₅	0.03	0.04	0.03	0.02	0.02	0.03	0.06	0.02	0.02
LOI	8.05	10.12	11.68	5.41	2.98	1.02	0.86	0.57	0.93
Total	98.85	98.52	99.45	98.93	101.17	100.73	100.28	99.34	99.61
Sc (ppm)	11.5	3.1	4.8	16.0	20.6	32.3	28.8	48.3	37.4
V	55.7	8.1	28.8	76.6	76.0	137.1	132.9	261.0	157.2
Cr	64.5	20.5	35.9	215.3	777.1	2467	2406	1568	3435
Co	47.2	34.9	8.4	35.0	52.8	122.3	112.9	84.6	80.6
Ni	860.0	764.5	113.2	408.4	1451	3231	2779	559.1	1034
Cu	130.4	201.4	330.3	18.8	372.5	867.8	1395	139.1	198.2
Ga	4.46	21.09	8.77	20.67	6.36	6.75	7.16	7.16	5.2
Rb	2.24	0.06	2.21	1.86	2.01	3.08	13.74	1.34	9.7
Sr	10.8	5.0	3.3	28.7	74.4	101.4	106.9	44.9	38.1
Y	4.8	12.8	10.4	8.0	7.6	9.3	7.7	18.2	6.6
Zr	18.3	15.3	13.2	49.0	31.7	28.0	23.1	46.2	9.9
Nb	0.31	0.23	0.00	3.18	2.75	2.87	1.01	3.61	0.39
Ba	33.3	15.1	15.1	39.7	75.4	84.1	105.2	23.4	33.7
La	2.71	3.64	0.18	3.29	2.17	2.69	3.84	4.27	1.43
Ce	5.76	9.00	0.29	8.17	5.12	6.33	7.82	10.92	3.71
Pr	0.76	1.32	0.04	1.18	0.76	0.94	0.87	1.67	0.55
Nd	3.82	6.80	0.52	4.98	3.41	4.15	4.03	7.66	2.33
Sm	1.00	1.63	0.30	1.15	0.90	1.10	0.93	2.06	0.55
Eu	0.23	0.37	0.08	0.31	0.29	0.35	0.26	0.60	0.18
Gd	1.07	1.69	0.71	1.21	1.02	1.29	1.05	2.36	0.68
Tb	0.17	0.29	0.16	0.21	0.19	0.24	0.18	0.44	0.12
Dy	1.17	1.78	1.24	1.30	1.18	1.47	1.25	2.79	0.86
Ho	0.23	0.36	0.28	0.27	0.26	0.31	0.25	0.60	0.17
Er	0.68	1.02	0.92	0.68	0.65	0.82	0.78	1.62	0.62
Tm	0.10	0.16	0.17	0.10	0.09	0.12	0.12	0.24	0.09
Yb	0.68	1.03	1.13	0.72	0.71	0.91	0.87	1.83	0.61
Lu	0.09	0.16	0.19	0.15	0.14	0.17	0.13	0.33	0.10
Hf	0.36	0.23	0.31	1.60	0.95	0.75	0.55	1.22	0.27
Ta	0.05	0.02	0.01	0.22	0.19	0.20	0.08	0.26	0.03
Th	0.53	0.37	0.19	0.83	0.58	0.75	1.27	1.39	0.49
U	0.19	0.04	0.02	0.22	0.17	0.21	0.39	0.50	0.05
Eu/Eu*	0.66	0.67	0.51	0.79	0.91	0.89	0.80	0.83	0.91
La/LuN	3.00	2.43	0.10	2.32	1.58	1.63	3.10	1.33	1.52
PGE grade	v. low	low	v. low	n/a	n/a	n/a	high	n/a	low
Pt/Pd	2.76	0.55	2.81	n/a	n/a	n/a	1.48	n/a	1.65

Rare earth element values in chondrite used for normalisation come from Taylor and McLennan (1985)

PGE grade bands based on total Rh + Pt + Pd + Au: <0.1 ppm = very low; 0.1–2.0 ppm = low; 2.0–6.0 = intermediate; 6.0–10.0 = high; >10.0 = very high.

Major units: *FW* footwall; *DYKE* cross-cutting pegmatoidal dykes; *HYB* footwall hybrid; *PR* primary reef; *RR* replaced reef; *HW* hanging wall

Rock types: *SPPX* serpentinised para(clino)pyroxenite; *CS* calc-silicate; *GBNRT* gabbornorite; *PX* pyroxenite; *WBST* websterite; *WHRL* wehrlite

ascribed to the effects of contamination by local granite footwall. In a follow-up study, Barton et al. (1986) determined ⁸⁷Sr/⁸⁶Sr initial ratios in orthopyroxene and plagioclase mineral separates and found that most of the radiogenic Sr was hosted by plagioclase and other intercumulus minerals. The lowest ⁸⁷Sr/⁸⁶Sr initial ratio found in orthopyroxene separated from the Platreef was

0.7079, outside the normal UCZ range of 0.7055–0.7065, but within the range of initial ratios determined for the Merensky Reef (e.g. Kruger 1994).

Chaumba et al. (1998) reported initial ¹⁸⁷Os/¹⁸⁸Os ratios for the Platreef that ranged from 0.10974 to 0.20292. The Platreef range encompasses the range of initial ratios found in the Merensky Reef (Os minerals

with $^{187}\text{Os}/^{188}\text{Os}_i \sim 0.94$, and laurite with $^{187}\text{Os}/^{188}\text{Os}_i$ 0.142–0.151; Hart and Kinloch 1989; McCandless and Ruiz 1991). Chaumba et al. (1998) interpret this as indicating that Os in the Merensky Reef and the Platreef came from the same source. On close inspection though, the comparison is less robust than it first appears. Chaumba et al. (1998) only presented the range of initial ratios they found. No information was given on what samples were analysed, their positions within or outside the igneous reef, or which initial ratios came from samples with the most Os. Until more information is available, these Os data are open to multiple interpretations and cannot be used to argue strongly for a link between the Merensky Reef and Platreef.

Differences between the Platreef and the Merensky Reef

There are other lines of evidence that would seem to contradict the stratigraphic link implied in Fig. 3. These are outlined below:

Mineralogy of the “Critical Zone” of the northern lobe

Hulbert (1983) divided the GNPA member into two sub-zones (Fig. 9). The lower sub-zone contains orthopyroxene-clinopyroxene, orthopyroxene-clinopyroxene-chromite and orthopyroxene cumulates with subordinate plagioclase-rich units. The upper sub-zone is dominated by plagioclase cumulates with minor norites. Clinopyroxene is ubiquitous at between 5 and 25 modal%, even where chromite is present, and clinopyroxene is sometimes a cumulus mineral with chromite (Hulbert and Von Gruenewaldt 1985). Clinopyroxene is less abundant in the UCZ elsewhere in the complex (typically <10 modal%; Cameron 1982; Maier and Barnes 1998) and is never present in a cumulus association with chromite. Unusual orthopyroxene-clinopyroxene-chromite cumulates (at –85 and +10 m; Fig. 9) are only developed where the GNPA member rests on LZ cumulates and are unknown from elsewhere in the complex (Hulbert and Von Gruenewaldt 1985). Chromite in the GNPA member has TiO_2 contents (1.77–3.08 wt%; Hulbert 1983) that are generally higher than UCZ stratiform chromites outside of Fe-rich replacement pegmatoids (e.g. Stumpfl and Rucklidge 1982) and the Ti enrichment increases with stratigraphic height in the GNPA sequence.

Rocks of the upper sub-zone of the GNPA member are also unusual because the basal layers of all of the cyclic units recognised by Hulbert (1983) are plagioclase-only cumulates. The crystallisation order for this part of the sequence appears to be governed by the liquidus order plagioclase-orthopyroxene-clinopyroxene (Hulbert 1983). A few cyclic units with basal plagioclase-rich units are known from the UCZ in the eastern and western Bushveld but even in these, plagioclase is

invariably joined by orthopyroxene or chromite as the cumulus phase (Cameron 1982).

Considering only those cumulates containing >50% orthopyroxene (in order to minimise the effects of reaction with trapped liquid; cf Cawthorn 1996, 2002), the compositions of cumulus orthopyroxene in the GNPA member range between $\text{Mg}\#_{75-78}$ (Hulbert 1983; Fig. 9). These pyroxenes are systematically more Fe-rich than those in similar UCZ cumulates elsewhere in the Bushveld Complex ($\text{Mg}\#_{78-84}$; Cameron 1982; Naldrett et al. 1986; Eales et al. 1993; Maier and Eales 1994; Cawthorn 2002). The available data show that the cumulus plagioclase compositions in the GNPA member are An_{68-78} (Hulbert 1983). This range overlaps with the lower part of the range of UCZ plagioclase compositions observed in the rest of the complex (An_{68-85} ; Cameron 1982; Naldrett et al. 1986; Kruger and Marsh 1985; Maier and Eales 1994), but not with the upper part of the range.

Mineralogy of the Platreef and the Merensky Reef

The primary Platreef records differences in mineral textures from those commonly found in the Merensky Reef. In the Merensky Reef, the liquidus order is orthopyroxene-plagioclase-clinopyroxene (e.g. Cawthorn 2002). In the mafic units of the Platreef, clinopyroxene either follows orthopyroxene or crystallises concurrently with it, and generally precedes plagioclase, which is usually intercumulus. Contamination of the Platreef with dolomite at Sandsloot may promote clinopyroxene crystallisation (e.g. Harris and Chaumba 2001) but it is important to note that the same crystallisation order also occurs where the footwall comprises rocks other than dolomite. For example, orthopyroxene-clinopyroxene-chromite cumulates occur in the Platreef on Overysel 815LR, where the footwall is granite (Hulbert 1983; D Holwell unpublished data). In this sense, the Platreef shows greater similarity with the orthopyroxene-clinopyroxene cumulates of the GNPA member (which are floored by harzburgites or quartzites) than the Merensky Reef. Chromite also shows important petrographic differences. Chromite is consistently the earliest phase in the Merensky Reef, forming layers and inclusions in pyroxenes, but it is most commonly post-cumulus in the Platreef.

Olivine is an important component of the Merensky Reef in some sectors of the Bushveld Complex. In the western lobe around the Union and Rustenburg sections, olivine (Fo_{79-80}) is common and the reef may be developed as a pegmatoidal harzburgite (Vermaak and Hendriks 1976; Kruger and Marsh 1985; Maier and Eales 1994) but in other areas of the complex, olivine is absent from the Merensky Reef. Primary olivine in the Platreef is more problematic. Van der Merwe (1976; Fig. 3 and p.1341) alludes to olivine (Fo_{84}) in a harzburgite or lherzolite at the base of the Platreef but the locality is not described. High-Mg metamorphic olivine

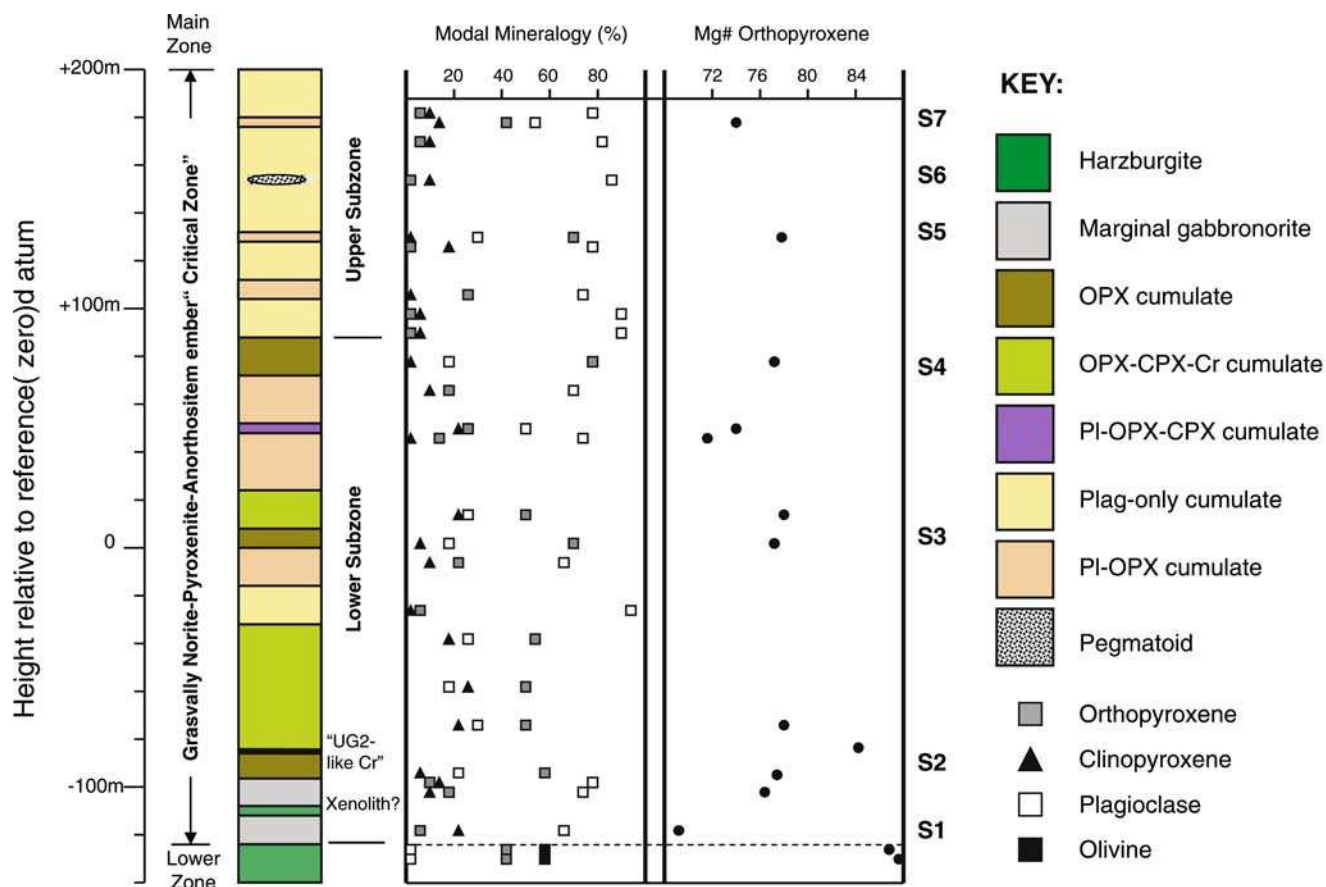


Fig. 9 Summary of the cumulate sequence in the Grasvally Norite-Pyroxenite-Anorthosite member (adapted from Hulbert 1983). Modal mineralogy comprises percentages of olivine (*black square*); orthopyroxene (*grey square*); clinopyroxene (*black triangle*); and plagioclase (*white square*). Layers indicated with S1–S7 contain

sulphide mineralisation with PGE. The high Mg# of orthopyroxene in association with chromite in the “UG2-like chromitite” is not primary, but the result of reaction (Fe loss) between the pyroxene and spinel (Hulbert 1983)

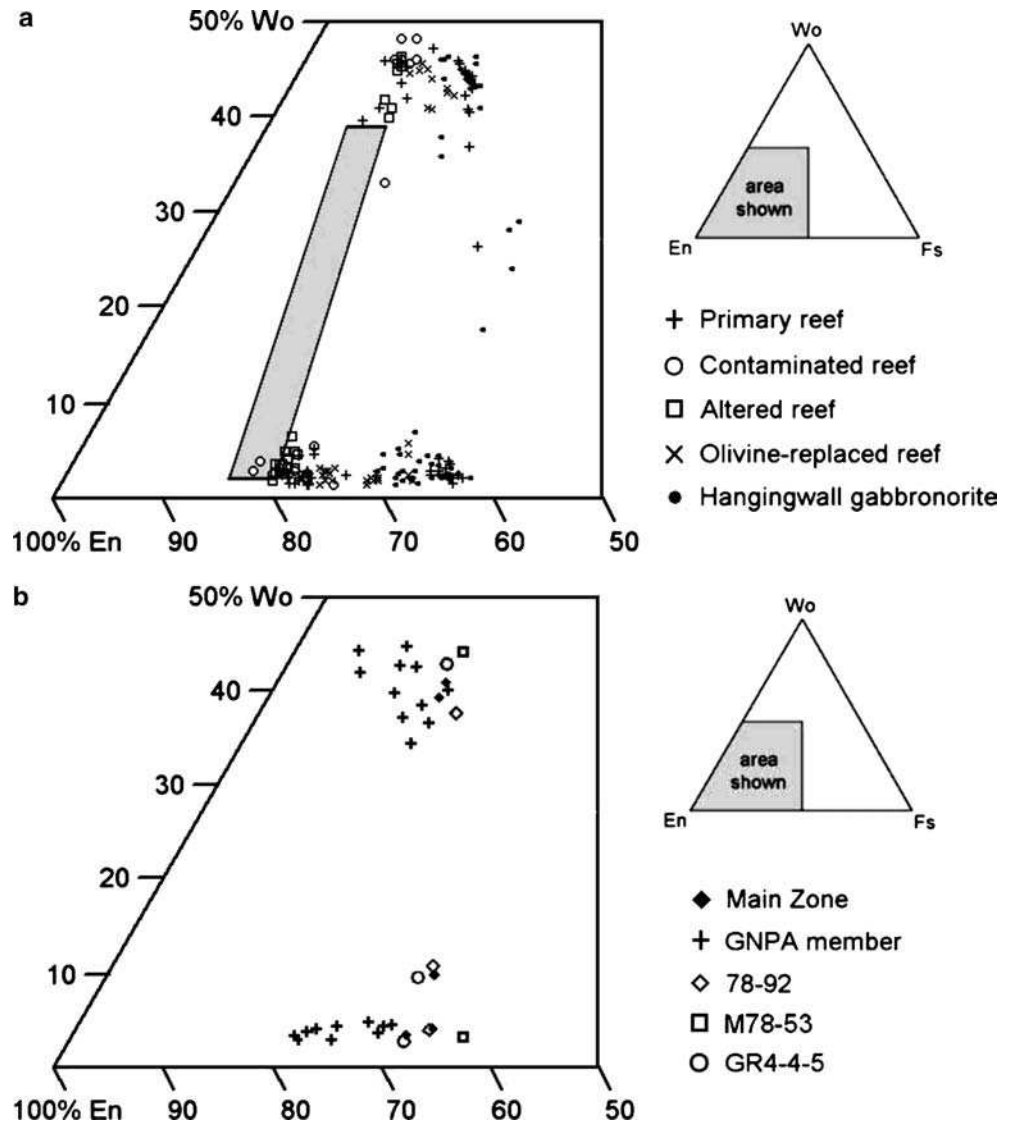
(Fo_{82-85}) occurs in the footwall at Sandsloot (Harris and Chaumba 2001; this work) but Kinnaird et al. (2005) also report the presence of igneous harzburgites with magnesian olivine at the base of the Platreef on the farm Macalacaskop 243KR. These rocks may belong to satellite intrusions of the LZ (see Discussion below). Buchanan and Rouse (1984) found Fe-rich olivine (Fo_{71}) in a basal “peridotitic” Platreef facies on the farm Turfspruit 241KR which they ascribed to the assimilation of banded ironstones into the reef. Similarly Fe-rich olivine (Fo_{64-72}) occurs in replaced reef at Sandsloot. Buchanan et al. (1981) analysed apparently igneous olivine (Fo_{75-76}) and this is currently the best (and only) estimate of the composition of primary Platreef olivine.

The most common mineral in the Platreef is orthopyroxene and this allows the most systematic comparison between different localities. Buchanan et al. (1981) studied orthopyroxenes on the farm Tweefontein 238KR where the reef is contaminated by banded ironstone and dolomite. They found pyroxenes with $\text{Mg}\#_{74-78}$ in primary reef but more Fe-rich pyroxenes ($\text{Mg}\#_{36-42}$) in contaminated units. Orthopyroxenes in the Platreef on Drenthe 788LR and Overysel 815LR, where the reef is

contaminated by granite, gneiss and dolomite (Fig. 1), show a range of compositions with a similar upper limit ($\text{Mg}\#_{65-77}$; Gain and Mostert 1982; Cawthorn et al. 1985).

Pyroxene compositions in the Platreef at Sandsloot are complicated by the presence of a reactive footwall that is rich in both Ca and Mg. Our data show a range of orthopyroxene compositions with a main population between $\text{Mg}\#_{76-80}$ (Fig. 10) in samples of primary reef. The main population is similar to results obtained by Harris and Chaumba (2001), but smaller sub-populations with $\text{Mg}\#_{81-83}$ and $\text{Mg}\#_{64-74}$ exist. The high $\text{Mg}\#$ population come from a gabbro (N1-26) associated with ragged serpentinite xenoliths (Fig. 4) and from a gabbro (SW2-49) in the southwest corner that has been partially altered to a mixture of tremolite, actinolite, chlorite and sericite. Analyses from N1-26 and SW2-49 are shown as “contaminated reef” and “altered reef”, respectively in Fig. 10. In both cases, the Ca contents of clinopyroxenes are higher than expected for igneous pyroxenes (Wo_{45-48} ; Fig. 10) and the pyroxene compositions in these samples appear to be affected by local enrichment in Ca and Mg.

Fig. 10 a Compositions of pyroxenes from different types of Platreef at Sandsloot Mine. Shaded area shows the range of typical Merensky Reef pyroxenes (Buchanan et al. 1981; Cawthorn et al. 1985). Note the high En and Wo contents of pyroxenes from contaminated reef where enrichment of Ca and Mg has taken place (see text for more information). **b** Compositions of pyroxenes from the GNPA member, GNPA member chilled magmas and chilled MZ at Grasvalley (data from Hulbert 1983)



The low Mg# population in our dataset comes from samples of replaced reef, located close to the top of the reef in southwest corner of the pit. Fe-rich olivine is common as a replacement for orthopyroxene in many of these rocks and this strongly suggests that the Fe-rich pyroxene composition is not primary. Orthopyroxene in a coarse-grained pyroxenite (SW2-77) at the top of the reef is as Fe-rich as the hanging wall gabbro (Mg#₆₄₋₆₆; Fig. 10), but the rock has cumulus orthopyroxene and lacks obvious textural evidence for replacement. It may represent differentiated Platreef that crystallised from a residual melt or which underwent some kind of reaction with the hangingwall liquid.

Based on all the data summarised above, if one accepts Mg#₈₀ and Mg#₇₆ as the upper compositional limits of orthopyroxene and olivine in primary Platreef, then the pyroxene composition is consistent with the GNPA member (Fig. 10). However, the Platreef silicates appear systematically more Fe-rich than their

equivalents in the Merensky Reef (Mg#₇₈₋₈₄ for orthopyroxene and Mg#₇₉₋₈₀ for olivine; Buchanan et al. 1981; Kruger and Marsh 1985; Naldrett et al. 1986; Holwell 2002; Scoon and Mitchell 2002).

Rare earth element geochemistry

Rare earth element data for reef, hanging wall and footwall lithologies at Sandsloot are given in Tables 1, 2, 3. The footwall rocks have a characteristic and sometimes quite pronounced negative Eu anomaly when normalised to chondrite ($\text{Eu}/\text{Eu}^* 0.48\text{--}0.80$) and show a range of LREE:HREE fractionation. La/Lu_N in the footwall varies between 0.09 and 5.89, but most samples fall within the range 1.2–4.0, which overlaps with the narrow range (1.3–3.3) observed in the reef rocks. Small negative Eu anomalies ($\text{Eu}/\text{Eu}^* 0.72\text{--}0.93$) are observed in most of the reef samples, with the exception of some

more plagioclase-rich reef gabbro-norites from the north wall (e.g. N1-14 and N1-24), where there are very small positive anomalies ($\text{Eu}/\text{Eu}^* = 1.02\text{--}1.05$).

These observations are in marked contrast to the melanorites in the Merensky Reef at Union Section studied by Barnes and Maier (2002b). These rocks show a much broader range of La/Lu_N ratios (2.8–5.7) and a more pronounced negative Eu anomaly ($\text{Eu}/\text{Eu}^* = 0.42\text{--}0.80$) when compared with the Platreef. Other pyroxenites in the UCZ between the MG4 chromitite and the Bastard Reef show La/Lu_N ratios (1.8–5.8), commonly above Platreef values. These pyroxenites also show more pronounced positive and negative Eu anomalies ($\text{Eu}/\text{Eu}^* = 0.6\text{--}1.4$; Maier and Barnes 1998). The Platreef would appear to have formed from a less LREE-enriched magma that had experienced less plagioclase fractionation than the magma that formed the Merensky Reef.

PGE mineralogy

The PGE in the Platreef and the Merensky Reef are carried by common groups of PGM. Kinloch (1982) recognised eight major categories of PGM and found all of these in the Platreef and in the different regional facies of Merensky Reef. Regional PGM variation in the Merensky Reef was ascribed to proximity to magmatic feeders and other local factors such as potholes and occurrence of replacement pegmatoids (Kinloch 1982; Kinloch and Peyerl 1990). The Platreef also shows local variation in PGM assemblages (Viljoen and Schürmann 1998) but these changes seem to correlate with changes in the footwall lithology that interacted with the Platreef magma. For example, Kinloch (1982) found a high proportion of Pt sulphides in boreholes that intersected the Platreef on the northern portion of the farm Zwartfontein 818LR and the farm Overysel 815LR, where the footwall is mostly granite. Boreholes on the southern portion of Zwartfontein and samples from the Sandsloot open pit, where the footwall is primarily dolomite, show almost no Pt or Pd sulphides and the assemblage is dominated by Pt and Pd tellurides and alloys (Kinloch 1982; Armitage et al. 2002).

PGE Geochemistry

One of the most striking differences between the PGE deposits of the northern lobe and the rest of the Bushveld Complex is to be found in their noble metal budgets; a feature first noted by Wagner (1929). Davies and Tredoux (1985) were the first to observe that the chondrite normalised PGE pattern of the Merensky Reef was almost parallel to the pattern of high-Mg basaltic sills thought to represent the parental (B1) magma of the Lower Zone and possibly the Critical Zone (Sharpe 1981; Harmer and Sharpe 1985). This similarity has led various authors to infer that the formation of the

Merensky Reef transposed the PGE signature of the magma largely unchanged into the sulphide-bearing reef (Davies and Tredoux 1985; Tredoux et al. 1995; Cawthorn 1999b; Ballhaus and Sylvester 2000). Similar normalised patterns are found from other sulphide-bearing reefs (Pseudoreef, Boulder Bed, Tarentaal and Bastard) in the UCZ of the eastern and western Bushveld (Maier and Barnes 1999) and, like the Merensky Reef, these layers provide a snapshot of the PGE chemistry of the magma that formed the reef. One might therefore expect that the PGE signatures of sulphide-bearing reefs in the UCZ of the eastern and western Bushveld and the GNPA member and the Platreef of the northern lobe should be broadly similar, if these layers formed from a common magma—as the currently accepted stratigraphy implies.

The Merensky Reef PGE data compiled by Kinnaird et al. (2002) and Cawthorn et al. (2002b) show variation in the Pt/Pd ratio between different mining areas, from 1.8 to 2.9. This highlights the fact that UCZ cumulates in general through the eastern and western Bushveld are systematically richer in Pt than in Pd, i.e. Pt/Pd is > 2.0 (with isolated values up to 24), for most of the sequence regardless of whether the rocks contain sulphide or not. The reasons for this striking Pt enrichment are not well understood and cannot be explained by silicate-sulphide or sulphide-sulphide liquid fractionation (Maier and Barnes 1999) and there are no matching Pd-rich cumulates in the MZ or UZ to satisfy the mass balance (Barnes and Maier 2002c). The excess platinum seems to

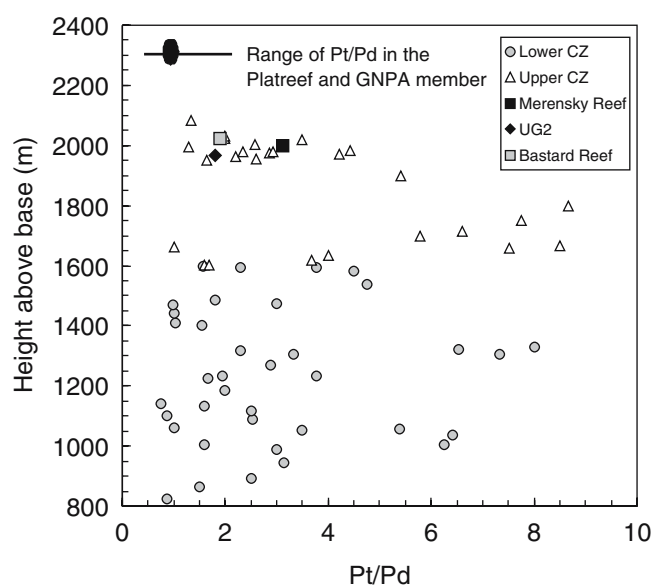


Fig. 11 Variation in Pt/Pd ratios through the Critical Zone in the western lobe (Maier and Barnes 1999) compared with the range (represented by the *bar*) and the mean (represented by the *ellipse*) for the “Critical Zone” and Platreef of the northern lobe (Von Greunewaldt et al. 1989; this work). Very high Pt/Pd ratios in some Critical Zone rocks that are off scale are not shown in the diagram. Note the generally lower Pt/Pd ratios in the northern lobe compared with the Critical Zone elsewhere in the complex

be a fundamental compositional feature of the magma(s) that fed the UCZ.

Platinum group element ratios for the Platreef and the sulphide-rich reef of the GNPA member are compared with those in sulphide reefs of the UCZ in Table 4. These comparisons indicate that all the sulphide-bearing reefs in the northern lobe are different from those found in the UCZ. The Platreef and all of the sulphide reefs in the GNPA member show greater fractionation of low-temperature PGE (Pt and Pd) from high-temperature PGE (Ir and Ru) and all of them are Pd-rich compared with reefs between the UG2 and the Merensky Reef in the eastern and western lobes. It is important to note that this comparison does not take account of PGE in the footwall. High-grade zones in the footwall at Sandsloot often show even lower Pt/Pd ratios than the main reef (Tables 1, 2, 2), suggesting that there may have been preferential mobilisation of Pd over Pt into the footwall from the proto-reef. The outcome of this would be to raise the apparent Pt/Pd ratio of the Platreef, i.e. the original Pt/Pd ratio of the Platreef before it preferentially lost Pd to the footwall could have been even lower and further removed from UCZ values than it appears currently.

An important primary observation from the northern lobe is that the GNPA member and the Platreef (and silicate rocks with total PGE contents as low as 10ppb; Tables 1, 2, 3) show lower and more restricted Pt/Pd ratios than the UCZ, where Pt/Pd ratios may exceed those in the northern lobe until well above the level of the Bastard Reef (Fig. 11). Whatever the reason for the striking Pt enrichment in the eastern and western lobes during formation of the UCZ, it is not repeated in any of

the sulphide-bearing reefs of the GNPA member, or in the Platreef!

Discussion

Implicit in current models for the evolution of the northern lobe is the idea that UCZ magma entered the northern lobe and formed a sequence of layered cumulates represented by the GNPA member prior to the development of the Platreef (e.g. Van der Merwe 1976, 1998; Von Gruenewaldt et al. 1989). The GNPA member was subsequently covered by mixed UCZ-MZ magma that spread out to the north, interacted with the footwall rocks, and formed the Platreef. If the Platreef is correlated with the Merensky Reef, then introduction of this magma into the northern lobe may be assumed to be coincident with the massive injection of MZ magma that led to the formation of the Merensky Reef and the MZ sequence elsewhere in the complex (e.g. Kruger 2003).

In most tholeiitic magmas, chromite crystallisation terminates before clinopyroxene attains cumulus status due to a reaction relationship between spinel and pyroxene but this reaction is sensitive to oxygen fugacity. The lack of reaction between chromite and clinopyroxene in the orthopyroxene-clinopyroxene-chromite cumulates of the GNPA member led Hulbert (1983) to conclude that the GNPA member magma had an unusually high fO_2 that provided enough ferric iron to stabilise chromite. If this is correct, it follows that the Fe-rich nature of the pyroxenes in the GNPA member cannot be ascribed to fO_2 as, if the GNPA member started with the same composition as the UCZ, a higher

Table 4 Platinum group elements ratios of Upper Critical Zone sulphide-rich reefs and parental magmas (see text for further details)

	Pt/Pd	Pt/Ir	Pd/Ir	Pd/Rh	Source
Eastern and western lobes					
Bastard Reef	3.03	41.8	13.8	3.45	1
Merensky Reef (eastern lobe)	1.57	41.1	26.2	12.9	1
Merensky Reef (western lobe)	1.94	41.9	21.6	8.46	1
Boulder Bed	3.04	32.6	10.7	4.97	2
Tarentaal	4.43	105.6	23.8	5.41	2
Pseudoreef	2.35	37.2	15.9	3.52	1
Northern lobe					
Lower Platreef (Drenthe)	0.81	76	93	18	3, 8
Upper Platreef (Drenthe)	0.65	89	139	58	3, 8
Platreef (Sandsloot)	0.95	96	63	15	4
S7 Norite (top of GNPA member)	0.29	65	230	31	3
S6 Pegmatitic gabbro-norite	0.99	41	41	19	3
S4 Ni-rich leuconorite	0.41	30	73	20	3
S2 Footwall (UG2-like chromitite)	0.43	63	130	19	3
S1 Basal gabbro-norite	0.39	54	140	21	3
Pyroxenite (Unit 36 Lower Zone)	0.34	n/a	n/a	n/a	5, 6
UpperVolspruit (Unit 11 Lower Zone)	0.72	34	47	6.8	3, 7
Parental magmas					
B1 (Lower/Critical Zone)	1.64	56.2	34.3	10	1
B3 (Main Zone)	1.55	77.8	50	15	1

Data sources: (1) Barnes and Maier 2002a; (2) Naldrett et al. 1986; (3) recalculated from Von Gruenewaldt et al. 1989; (4) this work; (5) Hulbert 1983; (6) van der Merwe 1998; (7) R.M. Harmer (personal communication); (8) A.J. Naldrett (personal communication). S1 to S7 refer to sulphide reefs in Fig. 8

fO_2 would be expected to generate more Mg-rich silicates. The lower Mg/Fe ratios observed in the GNPA member are therefore most probably a consequence of a starting magma composition that was more Fe-rich than the UCZ magma.

We have shown above that, apart from the visually similar appearance and the presence of high PGE concentrations, evidence linking the Platreef with the Merensky Reef is not strong. Significant mineralogical and geochemical differences exist between the Platreef and the GNPA member of the northern lobe and the Merensky Reef and the UCZ in the rest of the Bushveld Complex. In contrast, the greater similarities in terms of pyroxene compositions (Fig. 10), crystallisation sequences and PGE signatures between the Platreef and the GNPA member are more consistent with a model whereby these units formed from the similar or related magmas.

The simplest explanation for this apparent paradox is that the Merensky Reef and the Platreef (along with any related pre-reef cumulates) formed from separate magmas with different Mg/Fe ratios and PGE budgets. On the basis of a higher modal clinopyroxene content, the lower Mg# of orthopyroxene and the PGE ratios, the northern lobe rocks formed from a magma that was poorer in Mg, richer in Ca and Fe, was more highly PGE fractionated (greater Pt/Ir and Pd/Ir ratios) and was Pd rather than Pt-dominant relative to the magma(s) that formed the UCZ and Merensky Reef in the eastern and western lobes.

The obvious question is what was this northern lobe magma? The B1 magma of Sharpe (1981), believed to be parental to the Lower and Critical Zones in the eastern and western lobes, is a high Mg basaltic andesite that produces a crystallisation sequence olivine; olivine-orthopyroxene, orthopyroxene, orthopyroxene-plagioclase that is observed in the Lower and Critical Zones (Barnes and Maier 2002a). In contrast, the B3 (tholeiitic) magma believed to be parental to the MZ crystallises plagioclase-orthopyroxene, and then plagioclase plus both pyroxenes (Harmer and Sharpe 1985; Barnes and Maier 2002a). Neither of these magmas on their own can generate the observed crystallisation sequences for the GNPA member or the Platreef.

In order to account for the different PGE ratios, Cawthorn et al. (2002a) proposed that UCZ-type magma similar to that formed the UG2 chromitite in the eastern lobe (which has a Pt/Pd ratio close to unity) could have either flowed northwards or been present in the northern lobe prior to the formation of the Platreef. Cawthorn et al. (2002a) suggest that this magma did not form any chromitite layers and retained its PGE signature until the event that formed the Platreef. This is not supported by the available evidence as the GNPA member contains a chromitite layer as well as thick pyroxenite cumulates with disseminated chromite. The model also fails to explain the Fe-rich nature of the orthopyroxenes, the abundance of clinopyroxene in the GNPA member and why and all the reefs actually have

Pt/Pd ratios lower than unity. In any case, the magma in the eastern lobe became Pt-dominant again at the level of the Merensky Reef. No evidence for this is found in the northern lobe.

Development of the GNPA member

The answer to the question may lie with a marginal member defined by Hulbert (1983) that is developed at the base of the GNPA member where it rests on LZ ultramafic cumulates and Pretoria Group sediments. He suggested that these unusual pigeonite gabbro-norites were chilled "Critical Zone" magma or hybrids of chilled magma with LZ or sedimentary footwall melts. Hulbert (1983) suggested that a sample (M78-53) found in the marginal zone above the Pretoria Group might represent the closest match to the initial "Critical Zone" magma composition. Another fine-grained pigeonite gabbro-norite (GR4-4-5) developed above LZ cumulates has similar characteristics. The bulk chemistries of these two rocks are compared with estimated compositions of the parental magmas for the Critical and Main Zones in Table 5 and their pyroxene compositions are compared with GNPA member and MZ compositions in Fig. 10. It is clear that both M78-53 and GR4-4-5 lie closer to the model MZ magma than CZ magma.

If this is correct and these rocks represent chilled tholeiitic (MZ) magma, then it offers a possible explanation for the unique orthopyroxene-clinopyroxene-chromite cumulates and the lack of mineralogical or geochemical similarity between the GNPA member and the UCZ in the rest of the complex. Where the marginal member rests on the LZ, Hulbert (1983) cited the fine grain size, the abundance of pigeonite and rapid reversal in orthopyroxene compositions—from Mg#₈₄ in the last LZ harzburgite to Mg#₆₇₋₇₁ just above the contact (Fig. 9)—as evidence for undercooling and crystallisation of new liquid to form the marginal gabbro-norites.

Hulbert (1983) observed at least five cyclic sub-units within the marginal member, each with a fine-grained basal gabbro-norite. Skeletal plagioclase crystals with trapped melt and orthopyroxenes with Mg#s close to the bulk Mg# of the rock (e.g. M78-53) suggest rapid supercooling, which becomes less effective upwards. Each sub-unit shows upward increases in the Mg# of orthopyroxene and in the absolute concentrations of Ni, Cu and PGE, which are most enriched in coarser (sometimes pegmatitic) zones above the fine-grained base of each sub-unit. Hulbert (1983) suggested that the marginal member was emplaced as a series of thin pulses of colder, denser liquid at the base of the magma chamber. Model crystallisation of liquids with M78-53 or GR4-4-5 compositions at 1,500 bars in the PELE programme (Boudreau 1999) produces liquidus temperatures of 1210–1230°C and crystallisation sequences of plagioclase, plagioclase-orthopyroxene, then plagioclase as well as both pyroxenes, which mirror the observed textures. The idealised section given by Hulbert

Table 5 Comparison of fine-grained gabbronorite chills with estimated Critical and Main Zone magma compositions.

Sample Position	GR4-4-5 LZ-GNPA	78-53 Pret-GNPA	B1 (LZ/CZ)	B3 (MZ)	Crit Zone	Main Zone	78-92 GNPA-MZ	N3X4A Plat-MZ	SW1-47B Plat-MZ	SW1-47A Plat-MZ
SiO ₂ (wt%)	52.11	49.97	53.17	50.70	55.87	50.48	53.61	51.81	51.44	49.44
TiO ₂	0.10	0.62	0.36	0.41	0.37	0.71	0.34	0.20	0.19	0.16
Al ₂ O ₃	17.31	15.67	11.36	16.03	12.55	15.79	17.36	17.48	16.48	16.30
FeO	5.34	8.82	10.72*	9.14*	9.15*	11.61*	5.13	n/a	n/a	n/a
Fe ₂ O ₃	1.60	2.12	n/a	n/a	n/a	n/a	1.84	9.75*	8.83*	9.04*
MnO	0.15	0.19	0.20	0.17	0.21	0.18	0.13	0.14	0.19	0.15
MgO	8.86	7.77	14.93	9.21	12.65	7.26	7.42	6.48	6.93	8.55
CaO	11.66	10.91	7.47	11.14	7.29	10.86	11.58	11.17	12.06	11.75
Na ₂ O	2.15	2.15	1.57	2.52	1.53	2.20	2.38	1.79	2.43	2.52
K ₂ O	0.67	0.58	0.17	0.23	0.77	0.16	0.58	1.30	0.41	0.43
P ₂ O ₅	0.02	0.10	0.07	0.08	0.10	0.16	0.04	0.01	0.01	0.02
Sc (ppm)	n/a	n/a	n/a	n/a	41	35	n/a	31	38	28
V	90	232	n/a	n/a	179	182	119	191	200	152
Cr	390	396	1240	205	939	335	317	424	292	551
Co	80	88	n/a	n/a	73	53	66	41	48	59
Ni	184	184	337	162	329	128	128	346	407	376
Cu	75	120	n/a	n/a	58	62	23	121	170	187
Rb	30	20	4	7	27	3	13	50	7	12
Sr	385	353	183	324	170	340	275	333	282	234
Y	7	19	15	n/a	n/a	n/a	13	7	12	8
Zr	6	30	47	20	80	60	39	12	5	7
Source	1	1	2	2	3	3	1	4	4	4

Position key: LZ Lower Zone; MZ Main Zone; Plat Platreef; Pret Pretoria Group; GNPA GNPA member

Sources: (1) Hulbert 1983; (2) Sharpe 1981; (3) Barnes and Maier 2002b; (4) this work

* indicates total Fe as FeO or Fe₂O₃ as appropriate

and Von Gruenewaldt (1986) shows the marginal member developed across the LZ cumulates and over the adjacent Pretoria Group quartzites. In this situation, heat loss would have taken place primarily against the quartzites and a thermal gradient extended laterally from this zone into the liquid overlying the LZ cumulates. General coarsening of units upwards from the contact suggests more effective thermal insulation as the member thickened (Hulbert 1983).

Hulbert (1983) noted that pyroxenes in the marginal member overlying the LZ cumulates were more Mg-rich than those developed in the gabbronorites against the Pretoria Group and that abundant sulphides, high PGE and Cr concentrations were also restricted to the marginal member above the LZ. He argued that these features could only be accounted for by adding some residual LZ melt to the new liquid as the marginal member developed. This may also provide a mechanism to generate the unusual orthopyroxene-clinopyroxene-chromite cumulates associated with the “UG2-like” chromitite (Fig. 9). In addition to the unusual crystallisation order, these units are very rich in Cr (2,500–28,500 ppm) and it is hard to see how to generate them from liquids similar to M78-53 (with <400 ppm Cr) alone. We suggest that mixing the new tholeiitic liquid with an existing volume of overlying resident LZ-type magma crystallising olivine, orthopyroxene (Mg_{#84–88}) and chromite could produce a hybrid magma that crystallises orthopyroxene and chromite, followed by orthopyroxene, chromite and clinopyroxene, which mirrors the observed sequence in the lower part of the GNPA member (Fig. 9). Densities calculated in PELE for melts of M78-53 and GR4-4-5 at 1,500 bars are 2.71

and 2.65 g.cm⁻³, respectively, and may be sufficiently high to displace a hotter (>1,270°C) LZ-type liquid upwards in the manner suggested by Tegner et al. (1993). Undercooling of the resident LZ-type liquid by repeated injections of colder liquid at the base, coupled with gradual heating of the new liquid as thermal insulation of the thickening marginal member becomes more efficient would lower the temperature gradient and the density contrast to the point where the mafic and tholeiitic liquids might mix.

A second cycle with basal orthopyroxenite and orthopyroxene-clinopyroxene-chromite cumulates occurs higher in the sequence at the zero reference, and a third one at +75 metres is overlain by anorthosite (Fig. 9). These orthopyroxene-rich cumulates are additionally important because they carry sulphides and associated Pd-rich PGE mineralisation. Decreasing volumes of orthopyroxene-clinopyroxene-chromite cumulates and the trend of Ti enrichment in chromite developed with height probably reflect diminishing volumes of mafic magma available for mixing as the chamber becomes swamped with tholeiitic magma. Peck and Keays (1990) have independently proposed a similar process, involving injection of small volumes of gabbroic liquid into a larger volume of ultramafic magma, to explain the development of thin layers of chromite gabbronorite in harzburgites of the Heazlewood River Complex.

We suggest that the explanation for why the orthopyroxene-clinopyroxene-chromite cumulates are unique to the northern lobe is because these two magma types do not mix together in this manner elsewhere in the Bushveld Complex. The process outlined here is similar in some respects to the mixing of ultramafic (U-type) and

tholeiitic (T-type) magmas proposed by Irvine and Sharpe (1986) for the origin of stratiform chromitite and PGE reefs, including the Merensky Reef. The principal difference lies in the nature of the U-type magma and the degree of interaction. The Critical Zone in the eastern and western lobes preserves chemical and isotopic signatures inherited from the LZ and the new, distinctively Pt-rich, magma(s) which hybridised with it during the formation of the UCZ. The base of the UCZ marks the change from olivine-orthopyroxene cumulates to a chromite-orthopyroxene-plagioclase liquidus order, which persists throughout the UCZ, until the introduction of MZ magma coincident with the formation of the Merensky Reef (Kruger 1994), where the last cumulus chromite appears. Mass balance modelling by Barnes and Maier (2002b) suggests that the Merensky event involved ~40% tholeiitic magma mixed with ~60% UCZ-type magma crystallising orthopyroxene and plagioclase.

In the northern lobe, we suggest that there was no distinctive Pt-rich magma and no intermediate stage where the liquidus order shifted from olivine-orthopyroxene to chromite-orthopyroxene-plagioclase. The GNPA member formed by a series of rapid and dramatic interactions between progressively larger volumes of new tholeiitic liquid and a resident LZ-type liquid. In addition, we suggest that the tholeiitic and mafic liquids are derived from different sources with different isotopic signatures (see below) and within a few mixing/quenching interactions following the first introduction of the tholeiitic liquid, the reservoir of mafic liquid was exhausted or it ceased to be supplied to the chamber. Magmatic evolution beyond that point is controlled by the chemistry of the dominant tholeiitic liquid which later formed the MZ of the northern lobe.

Further support for the involvement of tholeiitic magma comes from the rocks at the top contact of the GNPA member. Above a prominent mottled anorthosite which caps the member, Hulbert (1983) found a 1–2-m thick layer of medium-grained gabbro-norite (sample 78–92) with distinctive radiating clusters of acicular plagioclase and inverted pigeonite. He interpreted this as an influx of new MZ magma which supercooled and chilled against the GNPA cumulates. The composition of 78–92 is close to the chilled rocks at the base of the GNPA member (Table 5). This can only be explained if MZ-type magma was involved prior to, during, and after the formation of the GNPA member.

This interpretation apparently contradicts the view that there was major hiatus between the emplacement of the magmas of the LZ and the MZ (Van der Merwe 1978). Field evidence cited to support this is based on apparently transgressive relationships established between LZ intrusives and the Platreef north of Mokopane that are not in dispute, plus the assignment of the GNPA member to a pre-Platreef UCZ, which is disputed. Fundamentally, van der Merwe's model rests on two assumptions; first, that the LZ was fully crystallised (not just the satellite intrusions where the transgressive relationships occur) and second, that the

Platreef and the GNPA member are unrelated to the LZ. The evidence presented above suggests that mafic liquid remained in the Grasvally magma chamber up to the development of the GNPA member and it is possible that supply of magma into the northern satellite chambers ceased while mafic magma continued to enter the Grasvally chamber. The role of LZ magma in the formation of the Platreef is discussed in the next section.

Links between the GNPA member and the Platreef

The exact relationship between the Platreef and the LZ and the GNPA member to the north of the Grasvally area is poorly known and will only be revealed as further exploration takes place on farms between Grasvally and Mokopane. Hammerbeck and Schürmann (1998) indicate that the "Critical Zone" wedges out to the south of Mokopane but Von Gruenewaldt et al. (1989) equated xenolith-rich portions of the GNPA member with the Platreef and implied that one might merge laterally into the other; a proposal supported by the data presented here. Kinnaird et al. (2005) report that north of Mokopane, LZ rocks may occur below the Platreef but the LZ appears to wedge out on the farm Macalacaskop 243KR and the Platreef rests directly on metasedimentary footwall from Macalacaskop northwards to Zwartfontein. Indeed it seems more than a coincidence that the modal mineralogy of the GNPA member orthopyroxene and orthopyroxene-clinopyroxene cumulates (55–60% opx, 15–25% plag, 20–25% cpx), the crystallisation order, orthopyroxene compositions (Mg_{70-78} ; Fig. 10) and Pd-dominant PGE mineralisation are similar to the Platreef at Sandsloot at many of the localities described above. Orthopyroxene-clinopyroxene-chromite cumulates, apparently similar to those that occur in the GNPA member, occur in the Platreef on the farm Overysel 815LR (Hulbert 1983).

It is also possible that the contacts between the GNPA member and the Platreef with the base of the MZ may correlate along strike. At Sandsloot, the unshered contact with the hanging wall MZ gabbros is marked by leuconorite ("mottled anorthosite") and a fine to medium-grained gabbro-norite (Fig. 6). This unit contains traces of inverted pigeonite, PGE grade up to 2.0 g/t, and a PGM assemblage containing laurite (RuS_2) and Pd-bearing pentlandite that is very different from that in the Platreef (Holwell et al. 2004). On Turfspruit 241KR, Kinnaird et al. (2005) observed that the upper contact of the Platreef with the MZ is marked by a prominent mottled anorthosite and on Drenthe 788LR, inverted pigeonite is also found in the MZ immediately above the Platreef (Gain and Mostert 1982). These associations are remarkably similar to the rocks at the contact between the MZ and GNPA member at Grasvally (Hulbert 1983). The chemistry of fine-grained gabbro-norites from just above the Platreef are compared with a MZ chill against the GNPA cumulates (78–92) in Table 5. These

rocks are separated by ~40 km (Fig. 1) but the match between their major and trace element signatures is striking and suggests that chilled MZ magma may terminate both the GNPA member and the Platreef. The presence of PGE in the MZ basal chill zone further suggests that the quenching of MZ magma may be an important trigger for the development of PGE-rich zones around rafts of disaggregated country rock in the MZ (e.g. on Drenthe 788LR and other farms).

In the light of the above, the finding by Barton et al. (1986) that orthopyroxene separated from the Platreef has an $^{87}\text{Sr}/^{86}\text{Sr}$ initial ratio of 0.7079 may be highly significant. Barton et al. (1986) suggested that even this should be considered an upper limit because of the possibility that the pyroxene separates contained traces of plagioclase with elevated $^{87}\text{Sr}/^{86}\text{Sr}$ initial ratios influenced by late-stage melts or fluids derived from the footwall. The MZ magma in the northern lobe shows $^{87}\text{Sr}/^{86}\text{Sr}$ initial ratios in the range 0.708–0.710 (Barton et al. 1986). Data for the Lower LZ in the northern lobe is lacking but if one assumes that this magma had a similar initial ratio to LZ rocks in the western Bushveld (0.705–0.707; Kruger 1994), then the lowest initial ratio of 0.7079 found by Barton et al. (1986) in the Platreef is consistent with a mixture of MZ-type and LZ-type magmas. In the absence of further geochemical data, particularly REE and isotopes from the GNPA member and elsewhere on the Platreef, the proposed link between the two must be considered possible, but unproven, at this stage. Nevertheless, the similarity is intriguing and underlines the need for further research into these rocks.

Implications for connectivity between the northern lobe and the rest of the Bushveld Complex

Cawthorn and Webb (2001) concluded that the eastern and western lobes were linked throughout the development of the Critical, Main and Upper Zones but that links with other lobes, including the northern lobe, were less certain and had to remain speculative. Kruger (1999, 2003), following the conventional stratigraphy, considered the northern lobe to have been linked with the eastern and western lobes during UCZ and MZ times. In his model, a mixed MZ and UCZ magma flows north across the chamber, overtops the Thabazimbi-Murchison Lineament (locally manifested as the Zebediela and Ysterberg-Planknek Faults; Fig. 1) and flows into the northern lobe, generating the Platreef along the base. LZ-type magma plays no role in forming the Platreef.

This work has shown that the conventional stratigraphic interpretation shown in Fig. 3 is untenable. The “Critical Zone” of the northern lobe, incorporating the “UG2-like” chromitite and Platreef cannot be correlated with the UG2-Merensky Reef package in the rest of the complex. The UCZ-type magma with its high Mg/Fe ratios, chromite-orthopyroxene-plagioclase-clinopyroxene crystallisation sequence and distinctive Pt enrichment did not play a role in the development of the

GNPA member or the Platreef. The orthopyroxene-clinopyroxene-chromite cumulates of the GNPA member and the Pd-dominant PGE mineralisation contained in it and the Platreef are unique to the northern lobe of the complex. Their origin requires different magmatic components.

We interpret the available evidence to suggest that the GNPA member and the Platreef may represent a transitional period where the earliest tholeiitic MZ-type magmas interacted with pre-existing mafic LZ-type magmas. It should perhaps be renamed the Transitional Zone of the northern lobe. The questions of when these two major magma types were introduced into the northern lobe, how their introduction relates to emplacement of magmas in the eastern and western lobes, and how their interaction might have generated the mass of PGE present in the GNPA member and the Platreef all remain unclear at this time and need further research.

In our view, the Merensky Reef and the Platreef formed from compositionally different magmas with different lineages and there is no genetic link between them. The possibility remains that introduction of tholeiitic magma into the northern lobe took place at the same time as into the eastern and western lobes but this cannot be proved unequivocally and a reliable time line cannot be drawn between the Merensky Reef and the Platreef. The “Critical Zone” of the northern lobe is not the Critical Zone as known from the rest of the Bushveld Complex. The former term is confusing and should be discontinued. There may be a reliable link between lobes in the Upper Zone at the level of the Main Magnetite (Fig. 3), but it remains to be established how closely the stratigraphy of the MZ of the northern lobe matches that seen in the rest of the complex. The northern lobe may have been completely separated from the rest of the complex until intrusion of the Upper Zone. The stratigraphy of the northern lobe must be evaluated on its own merits, without premature attempts to fit it into that established elsewhere.

Conclusions

This work has shown that the Platreef and the GNPA member, long thought to correlate with the Merensky Reef and the UCZ elsewhere in the complex, formed from a different magma than that which generated the UCZ in the eastern and western lobes of the complex. The Platreef and the GNPA member show pyroxene compositions that are systematically more Fe-rich and PGE signatures that are more fractionated and more Pd-rich than the Merensky Reef and other reefs of the UCZ. This work demonstrates that UCZ magma, with its characteristic and economically significant Pt enrichment, was not involved in the generation of the Platreef and that there is no compelling evidence linking the formation of the Platreef either genetically or temporally with the Merensky Reef.

Chilled MZ-type magma is preserved at the base and the top of the GNPA member and this unit is suggested to have formed from the mixing of existing LZ-type magma and new tholeiitic MZ-type magma that first intruded along the floor of the Grasvally chamber. Mixing/quenching events produced a series of orthopyroxenites that grade upwards into orthopyroxene-clinopyroxene-chromite cumulates that are unique to this area of the complex. The basal orthopyroxenites are invariably associated with the presence of sulphide and elevated base metal and PGE values. The GNPA member rocks show similarities in terms of mineral chemistries, modal mineralogy, crystallisation sequences, and PGE ratios with Platreef rocks and a compositionally similar MZ liquid is chilled against the top of both the GNPA member and the Platreef. These similarities open up the possibility that the Platreef and GNPA member merge laterally into one another and that both result from interactions between MZ and LZ-type magmas.

On a final note, although we have demonstrated that Wagner's original link between the Platreef and the Merensky Reef may be incorrect, it would be unjust to be overly critical of him. The visual similarity between the two reefs is striking and this, coupled with the apparently unlikely possibility that there could be another fantastically rich platinum horizon in addition to the Merensky Reef, must have played a part in forming his opinion. The fact that the assumed link has remained unchallenged for so long is surely a measure of the immense respect that Wagner's pioneering work still commands 75 years after his death.

Acknowledgements The authors would like to thank the staff at Anglo Platinum's Sandsloot Mine, particularly Alan Bye and Alfred Sarila, for logistical support during the mapping and sampling. Eveline de Vos and Peter Fisher are thanked for their assistance with the ICP and SEM analyses at Cardiff and Terry Williams, John Spratt and Anton Kearsley are thanked for their assistance with analytical work by Paul Armitage at the Natural History Museum. Wes Gibbons and Jock Harmer are thanked for their advice and input. The paper benefited from constructive reviews by Chris Lee and Tony Naldrett. Tony Naldrett also kindly made available his unpublished PGE assays from Drenthe for use in Table 4 and this is greatly appreciated. This research makes new use of Larry Hulbert's remarkable 1983 DSc thesis and re-interprets his work into the GNPA member in the light of new data. The authors would like to thank Wolf Maier for helping us to obtain a copy of this thesis. Key elements of this paper could not have been assembled without Dr Hulbert's original work and we are extremely grateful to have had access to it. We accept full responsibility for our conclusions (and any errors in interpretation), particularly where they differ from the original. Paul Armitage's PhD research was funded by the University of Greenwich. David Holwell's PhD research is funded by the NERC and supported by Anglo Platinum through Industrial CASE project (NER/S/C/2003/11952). PGE analytical work at Cardiff is supported by the Leverhulme Trust (grant F/00407/K to IMcD) and the ICP laboratory is supported by the NERC, through Joint Infrastructure Fund award NER/H/S/2000/00862. Finally, the first author would like to thank Steph and Robbie for their patience and support throughout the completion of this work.

References

- Armitage PEB, McDonald I, Edwards SJ, Manby GM (2002) Platinum-group element mineralisation in the Platreef and calc-silicate footwall at Sandsloot, Potgietersrus district, South Africa. *Appl Earth Science (Trans Inst Min Metall B)* 111:B36–B45
- Ballhaus C, Sylvester P (2000) Noble metal enrichment processes in the Merensky Reef, Bushveld Complex. *J Petrol* 41:545–561
- Barnes SJ, Maier WD (2002a) Platinum-group element distributions in the Rustenburg Layered Suite of the Bushveld Complex, South Africa. In: Cabri L (ed) *The geology, geochemistry, mineralogy and mineral beneficiation of the platinum-group elements*. Can Inst Min Metall Special Volume 54:431–458
- Barnes SJ, Maier WD (2002b) Platinum-group elements and microstructures of normal Merensky Reef from Impala Platinum Mine, Bushveld Complex. *J Petrol* 43:103–128
- Barnes SJ, Maier WD (2002c) Platinum-group elements in the Upper Zone of the Rustenburg Layered Suite of the Bushveld Complex: preliminary results from the Bellevue Borehole. In: 9th international platinum symposium, Billings, Montana, (abstract)
- Barton JM, Cawthorn RG, White J (1986) The role of contamination in the evolution of the Platreef of the Bushveld Complex. *Econ Geol* 81: 1096–1104
- Boudreau AE (1999) PELE—A version of the MELTS software program for the PC platform. *Comput Geosci* 25:21–203
- Buchanan DL, Rouse JE (1984) Role of contamination in the precipitation of sulphides in the Platreef of the Bushveld Complex. In: Buchanan DL, Jones MJ (eds) *Sulphide deposits in mafic and ultramafic rocks*. Inst Min Metall, Lond, pp 141–146
- Buchanan DL, Nolan J, Suddaby P, Rouse JE, Viljoen MJ, Davenport JWJ (1981) The genesis of sulfide mineralisation in a portion of the Potgietersrus lobe of the Bushveld Complex. *Econ Geol* 76:568–579
- Bye AR (2001) Mining the Platreef. *Appl Earth Science (Trans Inst Min Metall B)* 110:B209–B210
- Cameron EN (1982) The upper critical zone of the Eastern Bushveld Complex – precursor of the Merensky Reef. *Econ Geol* 77:1307–1327
- Cawthorn RG (1996) Re-evaluation of magma compositions and processes in the uppermost Critical Zone of the Bushveld Complex. *Min Mag* 60: 131–148
- Cawthorn RG (1999a) The platinum and palladium resources of the Bushveld Complex. *S Afr J Sci* 95:481–489
- Cawthorn RG (1999b) Platinum-group element mineralisation in the Bushveld Complex – a critical reassessment of geochemical models. *S Afr J Geol* 102:268–281
- Cawthorn RG (2002) Delayed accumulation of plagioclase in the Bushveld Complex. *Min Mag* 66:881–893
- Cawthorn RG, Lee CA (1998) Field excursion guide to the Bushveld Complex. In: 8th international platinum symposium. Geol Soc South Africa and S African Inst Min Metall, p 113
- Cawthorn RG, Webb SJ (2001) Connectivity between the western and eastern lobes of the Bushveld Complex. *Tectonophysics* 330:195–209
- Cawthorn RG, Barton JM Jr, Viljoen MJ (1985) Interaction of floor rocks with the Platreef on Overysel, Potgietersrus, northern Transvaal. *Econ Geol* 80:988–1006
- Cawthorn RG, Merkle RK, Viljoen M (2002a) Platinum-group element deposits in the Bushveld Complex, South Africa. In: Cabri L (ed) *The geology, geochemistry, mineralogy and mineral beneficiation of the platinum-group elements*. Can Inst Min Metall 54:389–429
- Cawthorn RG, Lee CA, Schouwstra RP, Mellowship P (2002b) Relationship between PGE and PGM in the Bushveld Complex. *Can Mineral* 40:311–328

- Chaumba JB, Harris C, Tredoux M, Reisberg L, Arndt NT (1998) Oxygen, strontium and osmium isotope geochemistry of the Platreef of the northern lobe of the Bushveld Complex, South Africa. In: 8th international platinum symposium, S African Inst Min Metall Symposium Series S18:71–72
- Davies G, Tredoux M (1985) The platinum-group element and gold contents of marginal rocks and sills of the Bushveld Complex. *Econ Geol* 80: 838–848
- Eales HV, Botha WJ, Hattingh PJ, de Klerk WJ, Maier WD, Odgers ART (1993) The mafic rocks of the Bushveld Complex. *J Afr Earth Sci* 16: 121–142
- Gain SB, Mostert AB (1982) The geological setting of the platinoid and base metal sulphide mineralisation in the Platreef of the Bushveld Complex on Drenthe, north of Potgietersrus. *Econ Geol* 77:1395–1404
- Hammerbeck ECI, Schürmann LW (1998) Nickel. In: Wilson MGC, Anhaeusser CR (eds) *The Mineral Resources of South Africa*. Coun Geosci Handbook 16:471–482
- Harmer RE, Sharpe MR (1985) Field relations and strontium isotope systematics of the marginal rocks of the Eastern Bushveld Complex. *Econ Geol* 80:813–837
- Harris C, Chaumba JB (2001) Crustal contamination and fluid-rock interaction during the formation of the Platreef, northern lobe of the Bushveld Complex, South Africa. *J Petrol* 42:1321–1347
- Harris C, Pronost JM, Ashwal LD, Cawthorn RG (2004) Oxygen and hydrogen isotope stratigraphy of the Rustenburg Layered Suite, Bushveld Complex: constraints on crustal contamination. *J Petrol* 46:579–601
- Hart SR, Kinloch ED (1989) Osmium isotope systematics in Witwatersrand and Bushveld ore deposits. *Econ Geol* 84:1651–1655
- Holwell DA (2002) Base-metal sulphide geochemistry of the Merensky Reef, Bushveld Complex. MSc dissertation, Cambridge School of Mines, (unpublished)
- Holwell DA, McDonald I, Armitage PEB (2004) Platinum-group mineral assemblages in the Platreef at Sandsloot Mine, Limpopo Province, South Africa. *Geoscience Africa*, University of the Witwatersrand, 12–16 July 2004 (abstract)
- Hulbert LJ (1983) A petrographical investigation of the Rustenburg Layered Suite and associated mineralisation south of Potgietersrus. DSc dissertation, University of Pretoria, (unpublished)
- Hulbert LJ, Von Gruenewaldt G (1982) Nickel, copper and platinum mineralisation in the Lower Zone of the Bushveld Complex, south of Potgietersrus. *Econ Geol* 77:1296–1306
- Hulbert LJ, Von Gruenewaldt G (1985) Textural and compositional features of chromite in the lower and critical zones of the Bushveld Complex south of Potgietersrus. *Econ Geol* 80:872–895
- Hulbert LJ, Von Gruenewaldt G (1986) The structure and petrology of the upper and lower chromitite layers on the farms Grasvalley and Zoetveld, south of Potgietersrus. In: Anhaeusser CR, Maske S (eds) *Mineral Deposits of Southern Africa*. Geol Soc South Africa, Johannesburg, 2:1237–1249
- Hutchinson D (2001) The origin and distribution of platinum-group mineralisation in the oceanic upper mantle: a comparison of samples from the Lizard and Troodos ophiolite complexes and dredge samples from the Tonga trench. PhD thesis, Cardiff University, (unpublished)
- Irvine TN, Sharpe MR (1986) Magma mixing and the origin of stratiform oxide ore zones in the Bushveld and Stillwater complexes. In: Gallagher MJ, Ixer RA, Neary CR, Prichard HM (eds) *Metallogeny of Basic and Ultrabasic rocks*. Inst Min Metall, Lond, pp 183–198
- Kinloch ED (1982) Regional trends in the platinum-group mineralogy of the critical zone of the Bushveld Complex, South Africa. *Econ Geol* 77: 1328–1347
- Kinloch ED, Peyerl W (1990) Platinum-group minerals in various rock types of the Merensky Reef, genetic implications. *Econ Geol* 85:537–555
- Kinnaird JA, Nex PAM (2003) Mechanisms of marginal mineralisation in the Bushveld Complex. *Appl Earth Science (Trans Inst Min Metall B)* 112: B206–B208
- Kinnaird JA, Kruger FJ, Nex PAM, Cawthorn RG (2002) Chromitite formation – a key to understanding processes of platinum enrichment. *Appl Earth Science (Trans Inst Min Metall B)* 111:B23–B35
- Kinnaird JA, Hutchinson D, Schürmann L, Nex PAM, de Lange R (2005) Petrology and mineralisation of the southern Platreef: northern limb of the Bushveld Complex, South Africa. *Mineral Deposita* (this volume)
- Kruger FJ (1994) The Sr-isotopic stratigraphy of the western Bushveld Complex. *S Afr J Geol* 97:393–398
- Kruger FJ (1999) The Bushveld Complex unconformity related ore deposits: an isotopic perspective. In: Stanley CJ et al (eds) *Mineral deposits: processes to processing*. Balkema, Rotterdam, pp 737–738
- Kruger FJ (2003) Filling the Bushveld Complex magma chamber: intra-chamber magma dynamics and the generation of giant chromite and PGE deposits. *Appl Earth Science (Trans Inst Min Metall B)* 112: B208–B209
- Kruger FJ, Marsh JS (1985) The mineralogy, petrology and origin of the Merensky Cyclic Unit in the Western Bushveld Complex. *Econ Geol* 80: 958–974
- Lee CA (1996) A review of mineralisation in the Bushveld Complex and some other layered intrusions. In: Cawthorn RG (ed) *Layered intrusions*. Elsevier, Amsterdam, pp 103–146
- Maier WD, Barnes SJ (1998) Concentrations of rare earth elements in silicate rocks of the Lower, Critical and Main Zones of the Bushveld Complex. *Chem Geol* 150:85–103
- Maier WD, Barnes SJ (1999) Platinum-group elements in silicate rocks of the Lower, Critical and Main Zones at Union Section, Western Bushveld Complex. *J Petrol* 40:1647–1671
- Maier WD, Eales HV (1994) A facies model for the interval between the UG2 chromitite and Merensky Reef, western Bushveld Complex. *Appl Earth Science (Trans Inst Min Metall B)* 103:B22–B30
- McCandless TE, Ruiz J (1991) Osmium isotopes and crustal sources for platinum-group mineralisation in the Bushveld Complex, South Africa. *Geology* 19:1225–1228
- McDonald I, Irvine GJ, de Vos E, Gale AS, Reimold WU (2005) Geochemical search for impact signatures in possible impact-generated units associated with the Jurassic-Cretaceous boundary in southern England and northern France. In: Cockell C, Gilmour I, Koeberl C (eds) *Biological Processes Associated with Impacts*. Springer, Berlin, Heidelberg, New York pp 101–131
- van der Merwe MJ (1976) The layered sequence of the Potgietersrus lobe of the Bushveld Complex. *Econ Geol* 71:1337–1351
- van der Merwe MJ (1998) Platiniferous horizons of the Potgietersrus lobe of the Bushveld Complex. In: 8th international platinum symposium. S Afr Inst Min Metall Symposium Series S18:407–409
- Naldrett AJ, Gasparrini EC, Barnes SJ, von Gruenewaldt G, Sharpe MR (1986) The Upper Critical Zone of the Bushveld Complex and a model for the origin of Merensky-type ores. *Econ Geol* 81:1105–1118
- Peck DC, and Keays RR (1990) Geology, geochemistry and origin of platinum-group element-chromite occurrences in the Heazlewood River Complex, Tasmania. *Econ Geol* 85:765–793
- Schiffries CM (1982) The petrogenesis of a platiniferous dunite pipe in the Bushveld Complex: infiltration metasomatism by a chloride solution. *Econ Geol* 77:1439–1453
- Scoon R, Mitchell AA (2002) The Merensky Reef at Winnaarshoek, Eastern Bushveld Complex: insights from a wide reef facies. In: Boudreau A (ed) 9th international platinum symposium, extd abstracts, Billings, Montana, pp 401–404
- Sharpe MR (1981) The chronology of magma influxes to the eastern compartment of the Bushveld Complex as exemplified by its marginal border groups. *J Geol Soc Lond* 138:307–326
- Stumpfl EF, Rucklidge JC (1982) The platiniferous pipes of the Eastern Bushveld. *Econ Geol* 77:1419–1431
- Taylor SR, McLennan SM (1985) *The continental crust: its composition and evolution*. Blackwell, Oxford

- Tegner C, Wilson JR, Brooks CK (1993) Intraplutonic quench zones in the Kap Edvard Holm layered gabbro complex, East Greenland. *J Petrol* 34: 681–710
- Tredoux M, Lindsay NM, Davies G, McDonald I (1995) The fractionation of the platinum-group elements in magmatic systems with the suggestion of a novel causal mechanism. *S Afr J Geol* 98:157–167
- Vermaak CF (1995) The Platinum-Group Metals—A Global Perspective. Mintek, Randburg
- Vermaak CF, Hendriks LP (1976) A review of the mineralogy of the Merensky Reef, with specific reference to new data on the precious metal mineralogy. *Econ Geol* 71:1244–1268
- Viljoen MJ, Schürmann LW (1998) Platinum-group metals. In: Wilson MGC, Anhaeusser CR (eds) *The mineral resources of South Africa. Coun Geosci Handbook* 16:532–568
- Viljoen MJ, Scoon RN (1985) The distribution and main geologic features of discordant bodies of iron-rich ultramafic pegmatite in the Bushveld Complex. *Econ Geol* 80:1109–1128
- Von Gruenewaldt G, Hulbert LJ, Naldrett AJ (1989) Contrasting platinum-group element concentrations in cumulates of the Bushveld Complex. *Mineral Deposita* 24:219–229
- Wagner PA (1929) *The platinum deposits and mines of South Africa*. Oliver and Boyd, Edinburgh
- White JA (1994) The Potgietersrus prospect – geology and exploration history. In: Anhaeusser CR (ed) *Proceedings XVth CMMI Congress*. S Afr Inst Min Metall, Johannesburg, vol. 3, pp 173–181
- Willemse J (1969) The geology of the Bushveld Complex: the largest repository of magmatic ore deposits in the world. *Econ Geol Monograph* 4: 1–22

APPENDIX 4

Full reference:

HOLWELL D.A., McDONALD I. & ARMITAGE, P.E.B. (2006). Platinum-group mineral assemblages in the Platreef at the South Central Pit, Sandsloot Mine, northern Bushveld Complex, South Africa. *Miner. Mag.*, **70**, 83-101.

Platinum-group mineral assemblages in the Platreef at the Sandsloot Mine, northern Bushveld Complex, South Africa

D. A. HOLWELL¹, I. McDONALD¹ AND P. E. B. ARMITAGE²

¹ School of Earth, Ocean and Planetary Sciences, Cardiff University, Main Building, Park Place, Cardiff CF10 3YE, UK

² Department of Earth and Environmental Sciences, University of Greenwich, Chatham Maritime ME4 4TB, UK

ABSTRACT

Platinum group mineral (PGM) assemblages in the Platreef at Sandsloot, northern Bushveld Complex, in a variety of lithologies reveal a complex multi-stage mineralization history. During crystallization of the Platreef pyroxenites, platinum group elements (PGE) and base-metal sulphides (BMS) were distributed throughout the interstitial liquid forming a telluride-dominant assemblage devoid of PGE sulphides. Redistribution of PGE into the metamorphic footwall by hydrothermal fluids has formed arsenide-, alloy- and antimonide-dominant assemblages, indicating a significant volatile influence during crystallization. Serpentinization of the footwall has produced an antimonide-dominant PGM assemblage. Parts of the igneous reef were subjected to alteration by a late-stage, Fe-rich fluid, producing ultramafic zones where the telluride-dominant assemblage has been recrystallized to an alloy-dominant one, particularly rich in Pt-Fe and Pd-Pb alloys. A thin, small-volume zone of PGE-BMS mineralization along the base of the hangingwall contains a primary PGM assemblage that is locally altered to one dominated by Pt/Pd germanides. This is thought to have formed when the new pulse of Main Zone magma entered the chamber, and scavenged PGE from the underlying Platreef pyroxenites. That each major rock type at Sandsloot contains a distinctive PGM assemblage reflects the importance of syn- and post-emplacement fluid and magmatic processes on the development of Platreef mineralization.

KEYWORDS: PGM, Bushveld Complex, South Africa, Sandsloot mine, Platreef, Pt, Pd, base-metal sulphides.

Introduction

THE Bushveld Complex of South Africa is the largest layered igneous intrusion in the world and is the largest single host of platinum-group elements (PGE) yet discovered. The major PGE deposits of the Bushveld Complex are the stratiform Merensky Reef and UG2 chromitite layer, and the stratabound, but not stratiform, Platreef. The complex can be divided into an eastern and western limb of similar size; a southern limb, identified beneath cover rocks by gravity studies; and a smaller northern limb (Cawthorn *et al.*, 2002). The Platreef, located in

the northern limb, has an estimated Pt+Pd reserve of 16.3 million ounces (Cawthorn, 1999), and is currently being mined by open-pit methods by Potgietersrus Platinums Ltd., a subsidiary of Anglo Platinum, at the Sandsloot and Zwartfontein South pits ~30 km northwest of the town of Mokopane (formerly Potgietersrus; Fig. 1).

The northern limb of the Bushveld Complex strikes approximately north–south and is slightly sinuous in shape (Fig. 1). Mafic igneous lithologies of the Rustenburg Layered Suite (RLS) of the complex dip west-southwest with the pyroxenitic Platreef located at the base of the igneous package north of Mokopane, in direct contact with metamorphosed sedimentary and igneous country rocks. A thick sequence of fairly homogenous gabbro-norites and norites attributed

* E-mail: HolwellDA@cf.ac.uk
DOI: 10.1180/0026461067010315

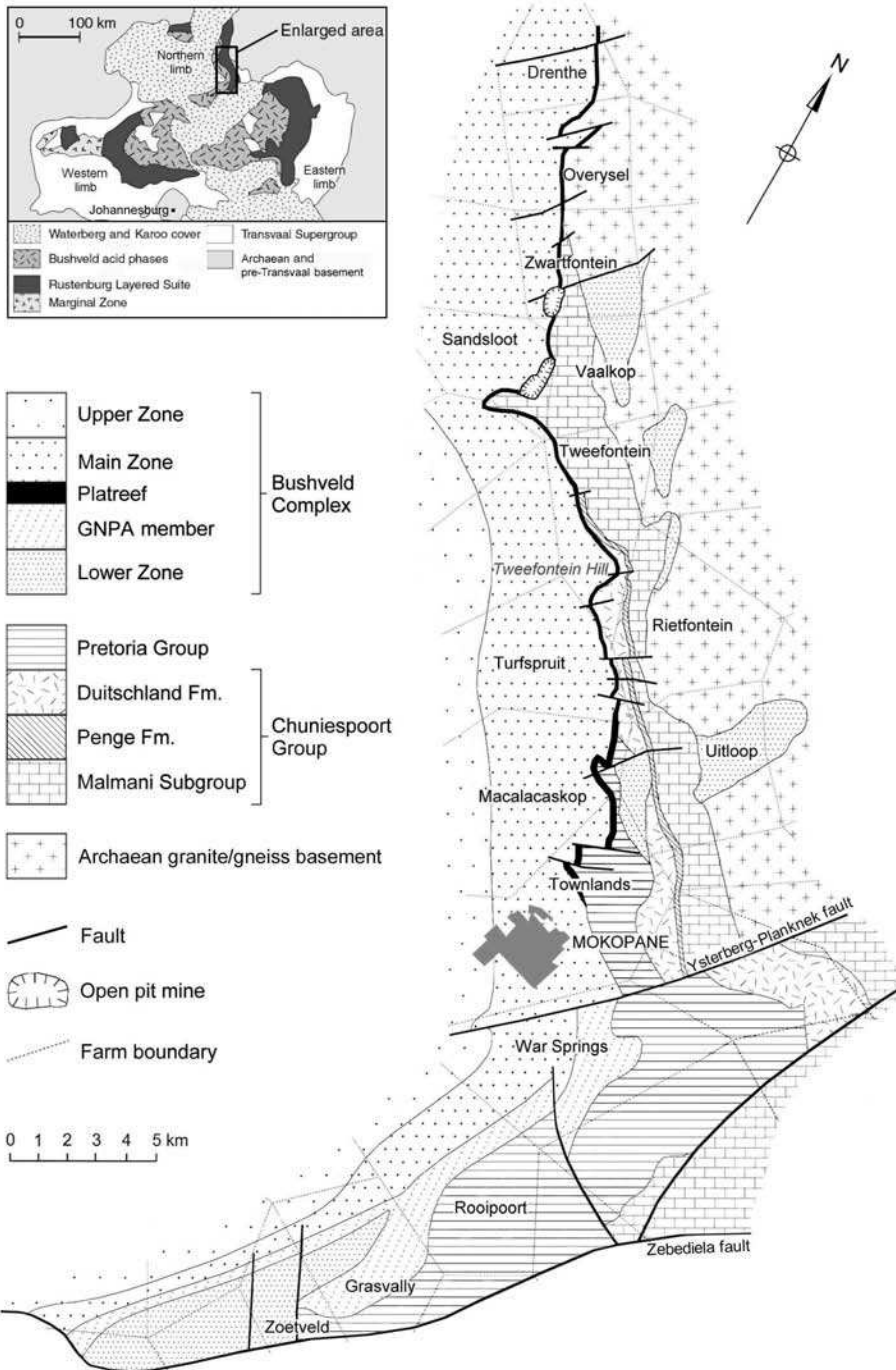


FIG. 1. Geological map of the central and southern sections of the northern limb of the Bushveld Complex, showing the Platreef and localities and lithologies referred to in the text (after Kinnaird and Nex (2003), von Gruenewaldt *et al.* (1989) and Hammerbeck and Schürmann (1998)).

to the Main Zone of the RLS overly the Platreef pyroxenites.

Other than brief references to the most common platinum-group minerals (PGM) by Schneiderhöhn (1929) and Gain and Mostert (1982), very few data on the PGM assemblages within the Platreef have been published. Kinloch (1982) summarized data from exploration boreholes on Zwartfontein and Overysel, north of the current Sandsloot mine and suggested that regional variations could be related to the amount of assimilation and contamination from the differing floor-rock lithologies. This was discussed further by Viljoen and Schürmann (1998), who summarized the overall abundances of PGM types in the Platreef as 30% Pt/Pd tellurides, 26% alloys, 21% PGE arsenides, and 19% sulphides, and highlighted the variations observed on different farms along strike. According to Viljoen and Schürmann (1998), from north to south, the most important PGM groups are: tellurides on the farm Drenthe; sulphides and tellurides on Overysel; alloys and tellurides on Zwartfontein and Sandsloot; sulphides on Tweefontein north; and tellurides at Tweefontein Hill. Recent work by Hutchinson *et al.* (2004) has shown the Platreef on Macalacaskop and Turfspruit to be rich in Pd bismuthides, tellurides and antimonides. Armitage *et al.* (2002) presented the results from a preliminary study of the PGE mineralization at Sandsloot, which found the PGM assemblage to be rich in alloys and tellurides and devoid of sulphides. This study builds on these findings and aims to provide further evidence of the processes governing the distribution of PGE in the Platreef.

Geology

From south to north, the northern limb of the Bushveld Complex rests upon a succession of progressively older sedimentary units of the late Archaean–early Proterozoic Transvaal Supergroup and Archaean granite/gneiss basement, in what has been termed an ‘igneous transgression’ (Wagner, 1929). The footwall units are, north from Mokopane: quartzites and shales of the Timeball Hill Formation; shales of the Deutschland Formation; the Penge Banded Iron Formation; dolomite of the Malmani Formation and, north of Zwartfontein, Archaean granite/gneiss basement (Fig. 1). Samples used in this study were taken from the Sandsloot mine, where the footwall is Malmani Dolomite. The hangingwall along the entire strike of the reef is

composed of gabbro-norites and norites ascribed to the Main Zone of the RLS.

The geology of the Platreef at Sandsloot Mine has been described by Harris and Chaumba (2001), Armitage *et al.* (2002), McDonald *et al.* (2005b), and Holwell *et al.* (2005) and is summarized below, together with the authors’ own observations on previously undescribed lithologies. The majority of the Platreef ‘package’ can be divided into hangingwall lithologies, igneous Platreef lithologies, and a variety of metamorphic footwall lithologies. There are variations in lithology on a metre scale along the length of the Platreef in the Sandsloot pit, and the variations are summarized in Fig. 2.

Footwall lithologies

The lowermost footwall lithology exposed in the Sandsloot pit is a series of highly altered and variably serpentinized, metamorphosed calc-silicate rocks, derived from the Malmani Dolomite. These generally retain some semblance of the original bedding and are often interbanded with more massive clinopyroxenites and thin serpentinites. In many places, the immediate footwall to the Platreef pyroxenites, separating the igneous reef and the calc-silicates, and are a series of clinopyroxenites, which are either green, granoblastic diopsidites, often recrystallized with 120° grain boundary triple junctions, or more amorphous purple-grey clinopyroxenites. Olivine is present in variable amounts, and is usually serpentinized, occasionally to a stage where no relict olivine remains. The rocks are of metamorphic origin, as shown by a higher Ca content in the clinopyroxenes compared to those in the igneous pyroxenites, and a whole-rock Cr content much lower than the igneous reef (Harris and Chaumba, 2001). These rocks were termed ‘parapyroxenites’ by Wagner (1929). Xenoliths of clinopyroxenite and calc-silicate where all original features have been overprinted occur regularly throughout the igneous reef at Sandsloot and are usually serpentinized.

Igneous Platreef lithologies

The igneous reef pyroxenites are typically coarse-grained, occasionally pegmatitic, and made up of cumulus orthopyroxene, with intercumulus plagioclase and clinopyroxene. In many cases plagioclase makes up >10% of the modal

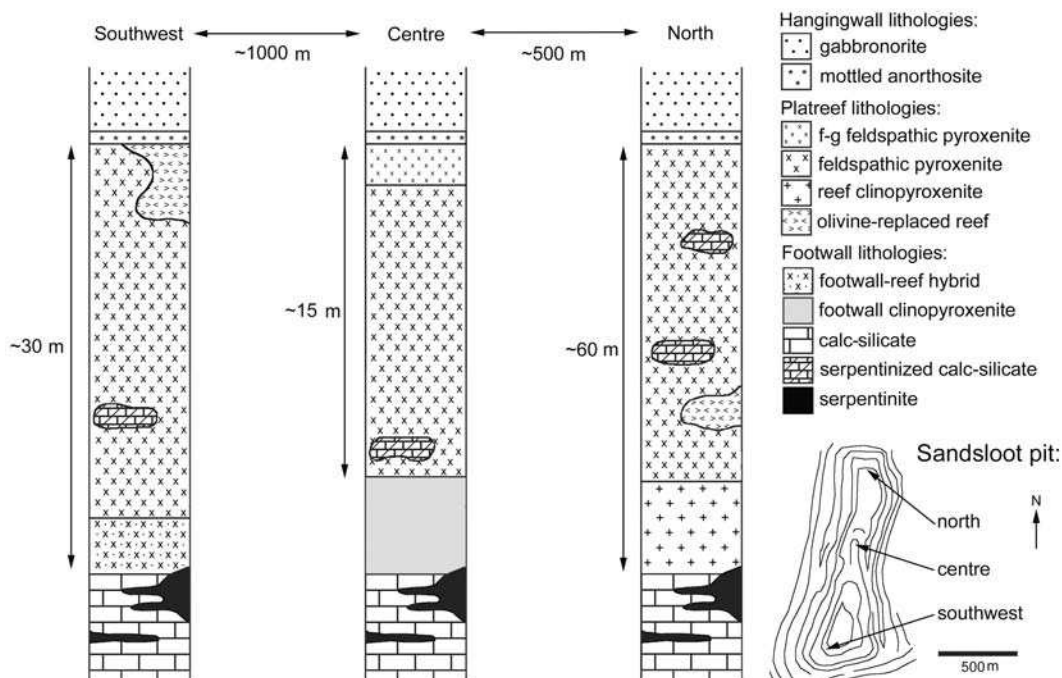


FIG. 2. Simplified stratigraphic representation showing all major rock units in the southwestern, central and northern parts of the Sandsloot pit.

mineralogy, and therefore the rock should be classified as gabbronorite under IUGS classification. However, in keeping with general Bushveld nomenclature in which names generally reflect the cumulus mineralogy, we refer to these rocks as feldspathic pyroxenites, and gabbronorites are rocks with both pyroxenes, and cumulus plagioclase. A fine-grained feldspathic pyroxenite barren of mineralization, located below the hangingwall contact, is present in the central part of the Sandsloot pit. Plagioclase is commonly altered to fine-grained white mica and epidote minerals. Base-metal sulphides (BMS) occur within the interstitial assemblage and are discussed below. Chromitites were not encountered, though chromite, ilmenite and rare armalcolite are present as minor phases, with ilmenite particularly common in the pegmatitic lithologies and most commonly found as inclusions along cleavage planes in interstitial clinopyroxene. Some areas of the igneous reef in the southwestern and northern parts of the pit contain a considerable amount of replacement olivine, which is Fe-rich (Fo_{62-67}) and overprints orthopyroxene, producing peridotitic zones with up to

60% olivine (Fig. 3a). This is thought to have formed from the reaction of a late-stage, Fe-rich, SiO_2 -poor fluid with the primary Platereef pyroxenites (McDonald *et al.*, 2005b), causing desilicification of orthopyroxene to form olivine. Parts of the igneous reef are also overprinted with a secondary, low-grade metamorphic assemblage that includes chlorite, sericite, actinolite and sphene highly suggestive of abundant fluid alteration. The basal part of the igneous reef in some sections in the southwest part of the pit is marked by a wehrlitic rock, with igneous, though not cumulus, textures, which is often partially serpentinized. This has been interpreted as a footwall-reef hybrid lithology by McDonald *et al.* (2005b), on the basis that geochemically, the rocks are intermediate between reef pyroxenite and footwall clinopyroxenite in terms of Ca and Cr content. In the northern part of the pit, the lower part of the igneous Platereef comprises clinopyroxenite, with cumulus clinopyroxene, and ~5% highly altered interstitial plagioclase. These rocks contain 1000–2000 ppm Cr and the clinopyroxenes have a composition of Wo_{45} which are consistent with the Platereef pyroxenites.

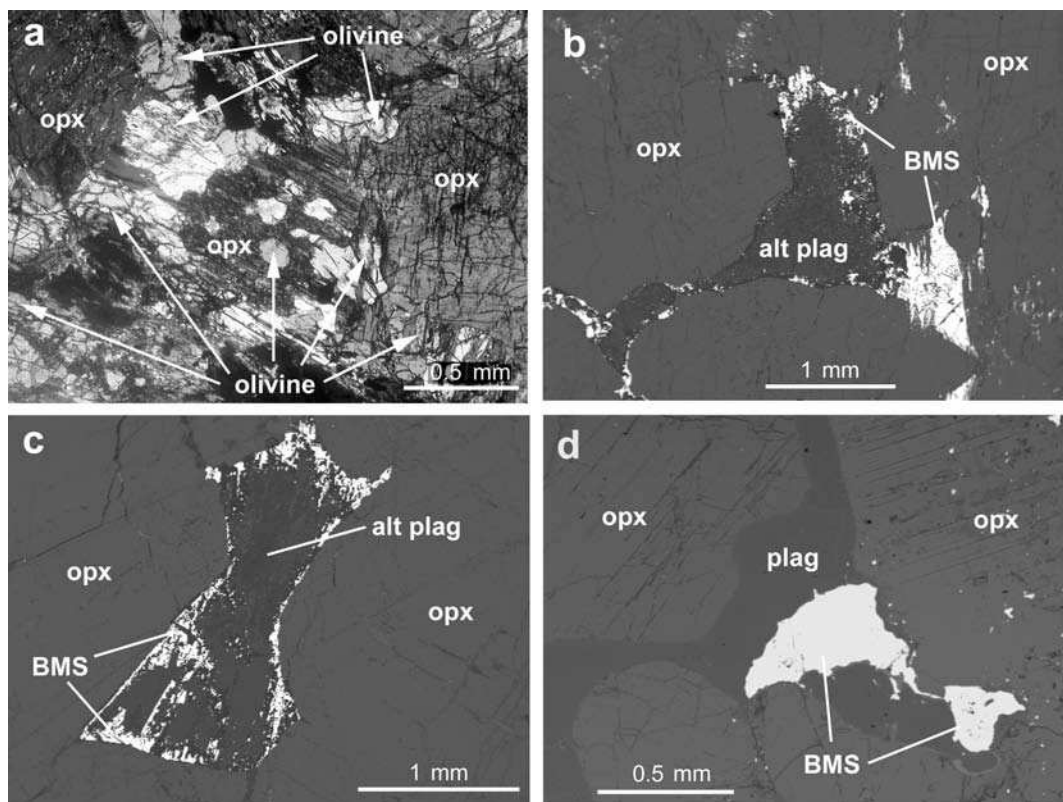


FIG. 3. (a) Thin section of olivine-replaced reef showing olivine overprinting orthopyroxene (opx); in cross-polarized transmitted light. (b–d) Backscattered electron photomicrographs of (b and c) typical associations of base-metal sulphides (BMS) intergrown with altered plagioclase (alt plag) at the edge of the interstitial region enclosing cumulus, sulphide-free orthopyroxene in Platreef pyroxenites at Sandsloot, and (d) typical association of discrete BMS grains with unaltered plagioclase (plag) from the Merensky Reef in the eastern Bushveld, for comparison.

In contrast, footwall clinopyroxenites contain <100 ppm Cr and have clinopyroxene compositions of Wo_{50} .

Hangingwall lithologies

The hangingwall to the Platreef pyroxenites is made up of norites and gabbronorites, resembling those of the Main Zone elsewhere in the Bushveld Complex. Plagioclase is the cumulus phase and makes up ~50–70% of the modal assemblage, with oikocrystic orthopyroxene and clinopyroxene making up the remainder in a crystallization sequence plagioclase-orthopyroxene-clinopyroxene. Base-metal sulphides (pentlandite, pyrrhotite and chalcopyrite) and oxides (almost exclusively ilmenite) are rare. A thin (<1 m) mottled anorthosite layer is often present at the

base of the hangingwall. The contact with the underlying pyroxenites is sharp and undulatory and is described in detail by Holwell *et al.* (2005).

Mineralization

Base-metal sulphides (primary pyrrhotite, pentlandite, chalcopyrite and minor secondary pyrite and bornite) are common throughout the reef pyroxenites, though heterogeneously distributed, and occur within the interstitial assemblage. However, the sulphides do not occur as well defined euhedral crystal aggregates with sharp linear contacts with surrounding silicates as, for example, they do in the Merensky Reef. They are invariably 'ragged' in morphology due to the common intergrowth with plagioclase and secondary amphiboles, particularly actinolite,

epidote and micas (Fig. 3*b,c,d*). In samples where plagioclase has been replaced by white mica, small blebs of sulphide commonly rim the outer edge of the interstitial region (Fig. 3*b,c*), and rarely encroach into orthopyroxene, though interstitial clinopyroxene often contains blebs of sulphide along cleavage planes. In the footwall, the assemblage is more diverse and contains the above assemblage along with minor amounts of sphalerite (ZnS), millerite (NiS), galena (PbS), chalcocite (Cu₂S) and alabandite (MnS).

Platinum group mineralization occurs throughout the igneous reef, its xenoliths, into the footwall and occasionally at the base of the hangingwall. Grades are variable within the igneous reef, and are more erratic through the footwall, though it is generally lower than in the igneous reef, however some serpentinized units carry very high grades. Table 1 shows Pt/Pd ratios for a range of reef, footwall and hangingwall samples together with an indication of grade. The Pt/Pd ratios in the igneous reef and hangingwall are around unity, which decrease slightly into the footwall, as would be expected if PGE were transported into the footwall via fluid activity, due

to the greater relative mobility of Pd compared to Pt and the other PGE (e.g. Wood, 2002). Conversely, Pt/Pd ratios >1 in some reef samples may indicate removal of greater amounts of Pd during remobilization of PGE into the footwall and therefore it is likely that the original Pt/Pd ratio of the igneous Platreef was probably unity or lower.

Platinum group minerals

Fifty-eight polished thin sections and blocks from the hangingwall, igneous reef and metamorphic footwall from the Sandsloot pit were analysed at Cardiff University using a Cambridge Instruments LEO S360 scanning electron microscope, coupled to an Oxford Instruments INCA energy dispersive X-ray analysis system. More than 1000 individual PGM grains were identified and are listed in Table 2. Each individual grain was classified by type and association. The vast majority of PGM were Pt and Pd minerals, while the only major carriers of Ir, Ru and Rh identified were members of the hollingworthite/platarsite/irarsite series. No carriers of Os were found, which may suggest that

TABLE 1. Pt/Pd ratios and relative grade for selected hangingwall (HW), reef and footwall (FW) samples. PGE grade based on Rh+Pt+Pd+Au. low: <2.0 ppm; intermediate: 2.0–6.0 ppm; high: >6.0 ppm.

Sample	Lithology	PGE grade	Pt/Pd
PA-N1-31	HW norite	low	1.36
PA-N3X4A	HW gabbro-norite	low	0.87
PA-SW1-47B	HW gabbro-norite chill	low	0.95
PA-SW1-32	Reef feldspathic pyroxenite	intermediate	0.81
PA-SW1-28	Reef feldspathic pyroxenite	high	1.28
PA-SW1-20	Reef feldspathic pyroxenite	intermediate	0.88
PA-N1-30	Reef feldspathic pyroxenite	high	0.93
PA-N1-22	Reef feldspathic pyroxenite	intermediate	1.04
PA-N1-24	Reef feldspathic pyroxenite	intermediate	0.98
PA-N1-26	Reef feldspathic pyroxenite	high	1.94
PA-SW2-49	Reef feldspathic pyroxenite	high	1.48
DH-G	Reef feldspathic pyroxenite	high	1.03
DH-P	Reef pegmatoidal pyroxenite	intermediate	0.79
PA-SW1-40	Olivine-replaced reef	intermediate	0.55
PA-SW1-43	Olivine-replaced reef	high	0.70
SNN1-68	Reef clinopyroxenite	low	0.81
PA-SW1-8	Serpentinized calc-silicate xenolith	high	0.99
PA-SW1-1	FW clinopyroxenite	high	0.86
PA-E55	FW clinopyroxenite	intermediate	0.98
PA-EX6	FW calc-silicate	intermediate	0.84
PA-SW1-4	FW serpentinized calc-silicate	low	0.65
PA-S2-12	FW serpentinized calc-silicate	low	0.55
PA-S0	FW serpentinite	low	0.54

Os may not be present in discrete minerals, but as a trace component in BMS, for example. The PGM identified were grouped as: (1) Pt/Pd tellurides; (2) Pt/Pd bismuthides; (3) Pt/Pd arsenides; (4) Pt/Pd antimonides; (5) Pt/Pd germanides; (6) PGE sulphides; (7) PGE sulpharsenides; (8) PGE alloys with Fe, Cu, Sn, Pb and Tl; and (9) Au and Ag bearing phases. Each occurrence was also classified by its association: enclosed in sulphide, at sulphide-silicate boundary, or enclosed by silicates, in keeping with other studies of the PGE deposits of the Bushveld Complex.

Grain size and morphology

Each PGM grain's long and short axes were measured in micrometres. Grains $<1\ \mu\text{m}$ were ignored due to their relative volumetric insignificance, and the difficulties in accurately determining their composition. Relative proportions of the various mineral phases and PGM species type are based on an estimation of area (and by inference, volume) of each grain. Using the long- and short-axes dimensions, the area of each grain was approximated to the area of an ellipse around the two axes. This therefore produces data which accurately reflect the relative proportions of each PGM type within an assemblage. This method of data presentation is preferable to proportions of PGM type by number of grains, which can be biased by a relatively large amount of very small grains, for example. This approach is particularly pertinent when comparing PGM data with Pt/Pd ratios. If, say, the Pt/Pd ratio of the whole-rock

sample is around unity, when using the proportion by number of grains method, there may appear to be a deficit of one particular PGE represented by discrete PGM phases, which may be wrongly attributed to its presence in BMS phases or silicates. Therefore we present all the assemblage data in percentage of total area of all PGM.

Grain-size data for all PGM grains $>1\ \mu\text{m}$ in their longest dimension are shown in Fig. 4. From Fig. 4, it can be seen that in most rock types, ~80% of grains were $<10\ \mu\text{m}$ in length, with the exception of pegmatitic reef rocks, which had a higher average grain size with 50% of grains $>5\ \mu\text{m}$. The units with the lowest average PGM grain sizes ($>70\%$ of grains $<5\ \mu\text{m}$) were the footwall calc-silicates, the reef clinopyroxenites and the hangingwall gabbro-norite. No grains of $>100\ \mu\text{m}$ were found.

The PGM morphology varies with individual phases and also with association. Where surrounded by sulphides, PGM, and particularly electrum, are commonly present as rounded blebs. Where surrounded by silicates, grains vary from anhedral to euhedral. Moncheite (PtTe_2) is commonly found as laths, Pt_2Fe as cubic crystals, and sperrylite as tetrahedra. Most PGM identified occur as single-phase grains, though they may occasionally occur as compositionally zoned (Fig. 5a) or polyphase grains (Fig. 5b).

Assemblages

The PGM mineralogy in the variety of host-rock lithologies studied are summarized in Table 3. The most notable characteristic of the Sandsloot

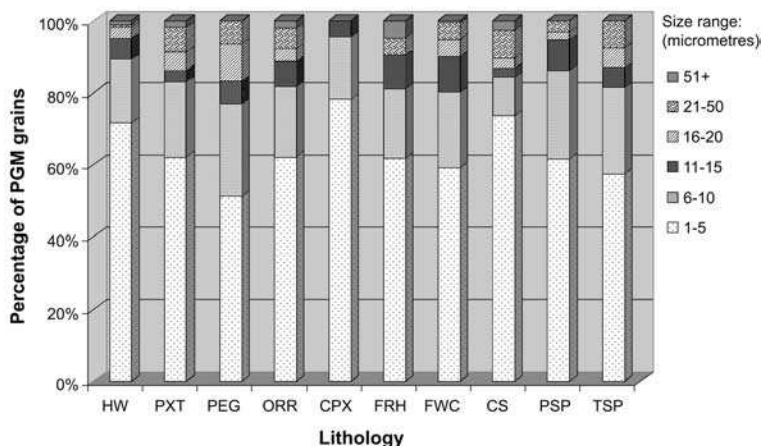


FIG. 4. Range of PGM grain size (longest axis) in the various host-rock lithologies at Sandsloot. See Table 2 for lithology abbreviations.

TABLE 2. Name and ideal formulae of all occurrences of PGM and Au-Ag minerals in the variety of host-rock types.

Name	Formula	HW	PXT	PEG	ORR	CPX	FRH	FWC	CS	PSP	TSP	Total
Kotulskite	PdTe	7	53	24	45	1	2	7	8	44	1	192
Sperrylite	PtAs ₂		30	6	6		2	52	18	13	4	131
Moncheite	PtTe ₂	1	50	36	18	6	1	5	1	9	1	128
unnamed	(Pd,Pt) ₂ Ge	65		3								68
Electrum	Au,Ag	1	15	4	9		1	5	1	20	2	58
Hessite	Ag ₂ Te		36					5	1	2		44
Sudburyite	PdSb							5	5		29	39
Zvyagintsevite	Pd ₃ Pb	4		2	21					1		28
Palladoarsenide	Pd ₂ As		2	1	1		18	4		1		27
Paolovite	Pd ₂ Sn	1						20		3		24
Geversite	PtSb ₂			4						5	14	23
unnamed	Pd ₃ Bi ₃ (Te,Sb) ₂							23				23
Pt-Fe alloy	Pt ₂ Fe	10			8					4		22
Froodite	PdBi ₂		1		2				1	16		20
Michenerite	PdBiTe	1	6			3		6				16
Sobolevskite	PdBi		2		3	3		3		5		16
unnamed	Pd ₂ (Sn,Sb)							15				15
Stibiopalladinite	Pd ₅ Sb ₂		2		3	1		4	1	3		14
Mertieite II	Pd ₈ (Sb,As) ₃		7						6			13
Atokite	Pd ₃ Sn				5		1	1	1			8
Native silver	Ag		5		1					2		8
Hollingworthite	RhAsS				1			2			4	7
unnamed	Pd ₃ Tl	7										7
Irarsite	IrAsS		2	1	2							5
Isoferroplatinum	Pt ₃ Fe		2	1				1				4
Merenskyite	PdTe ₂		2		2							4
Tulameenite	Pt ₂ FeCu			4								4
Platarsite	PtAsS		3									3
Rustenburgite	Pt ₃ Sn			3								3
Tetraferroplatinum	PtFe	1		2								3
Stillwaterite	Pd ₈ As ₃	1	1									2
unnamed	Pd ₅ Sb ₃									2		2
Auricupride	Au,Cu			1								1
Insizawite	PtBi ₂			1								1
Laurite	RuS ₂	1										1
Majakite	PdNiAs							1				1
Menshikovite	Pd ₃ Ni ₂ As ₃		1									1
Niggliite	PtSn										1	1
Palarstenide	Pd ₅ SnAs										1	1
Palladian gold	Au,Ag,Pd			1								1
Palladobismutharsenide	Pd ₂ (Bi,As)	1										1
Plumbopalladinite	Pd ₃ Pb ₂							1				1
Stannopalladinite	Pd ₅ Sn ₂ Cu			1								1
unnamed	PtAg ₂		1									1
unnamed	Pt ₂ SbSb										1	1
unnamed	PdTe ₃ Pb ₃							1				1
unnamed	Pd ₂ Bi							1				1
unnamed	Pd ₃ Bi ₂							1				1
unnamed	Pd ₂ (Sb,Bi,Te)							1				1

PGM assemblages identified here is the complete lack of PGE sulphides (also noted by Armitage *et al.*, 2002), with the exception of a single grain of laurite (RuS₂) in the hangingwall gabbronorite. This is unusual in that throughout the Merensky Reef, the UG2 chromitite and elsewhere in the

Platreef, namely Zwartfontein north, Overysel (Kinloch, 1982) and Drenthe (Gain and Mostert, 1982), PGE sulphides are ubiquitous in the form of cooperite (PtS), braggite [(Pt,Pd)S], laurite and other rarer minerals. The only other PGM found at Sandsloot containing any sulphur are a few

PGM ASSEMBLAGES FROM THE PLATREEF, BUSHVELD COMPLEX

Table 2 (contd.)

Name	Formula	HW	PXT	PEG	ORR	CPX	FRH	FWC	CS	PSP	TSP	Total
Unconstrained phases:												
	Pd-As-Sb			2								2
	Pd-Te-Bi				2							2
	Pt-Cu-Fe-Ag							2				2
	Pt-Pd-Sb-As								1		1	2
	Pt-Pb-Ag		1									1
	Pt-Fe-Te	1										1
	Pt-Au-Cu-Fe				1							1
	Pt-Pd-Pb-Te				1							1
	Pd-Pb-Te				1							1
	Pd-Pb-Pt				1							1
	Pd-Bi-Pb-Pt				1							1
	Pt-Pd-Te-Sb										1	1
	Pt-As-Sn-Sb										1	1
	Pt-Fe-Te-Pb										1	1
Composite polyphase grains, unconstrained compositions:												
	Pd-Sn-As-Te-Pb				1							1
	Au-Cu-Pt-Pd-Ag				1							1
	Pd-Pt-Fe-Cu-Sn-Te				1							1
	Pd-Pb-Te-Pt-Ir				1							1
	Pd-Pt-Te-Bi-Cu-Fe				1							1
	Pd-Bi-Sb-Sn-Te							1				1
	Ni-Bi-Pd-Ag-Au								1			1
	Pt-Sb-Te-Bi-Pb-As										1	1
	Pt-Sb-As-Au-Pb										1	1
	Pd-Sn-Sb-Pt-As										1	1
	Pt-Sb-Te-Bi-As										1	1
Total PGM grains:		102	222	79	156	23	23	163	44	132	64	1008

HW: hangingwall gabbro-norite; PXT: reef pyroxenite; PEG: reef pegmatite; ORR: olivine-replaced reef; CPX: reef clinopyroxenite; FRH: footwall-reef hybrid; FWC: footwall clinopyroxenite; CS: calc-silicate; PSP: partially serpentinized footwall; TSP: totally serpentinized footwall. Unconstrained phases were too small to determine formulae.

occurrences of the sulpharsenide hollingworthite/platarsite/irarsite series. As a whole, the Platreef at Sandsloot can be said to be dominated by Pt/Pd tellurides, alloys, and to a lesser extent, PGE arsenides and antimonides. In detail though, there is a great variation from one host rock type to another, particularly in terms of igneous reef versus metamorphic footwall, and several major trends in the PGM assemblage can be identified.

Reef pyroxenites and pegmatites

The igneous reef pyroxenites and pegmatites are dominated by Pt and Pd tellurides, particularly moncheite and kotulskite (PdTe). Hessite (Ag₂Te) and electrum (Au,Ag) are common in the pyroxenites. Arsenides, particularly sperrylite, as throughout the deposit as a whole, are common, particularly in the pegmatites. The immediate

associations of the PGM are shown in Table 4. Most PGM in the pyroxenites and pegmatites are surrounded by silicates or located at the BMS-silicate boundary. However, even where surrounded by silicates, the PGM retain a strong spatial relationship with the BMS and many are in association with secondary amphiboles which replace BMS, and very few are found completely isolated from any BMS. The secondary assemblages of tremolite and actinolite around BMS grains in the primary Platreef pyroxenites are similar to those found in the Merensky Reef and UG2 chromitite, described by Li *et al.* (2004). The appearance of PGM as satellite grains around BMS grains may be due to the regression of the BMS boundary, with the PGM (originally at the edge of the sulphide blebs) remaining in their original positions. This association has also been noted in the Platreef at Macalacaskop and

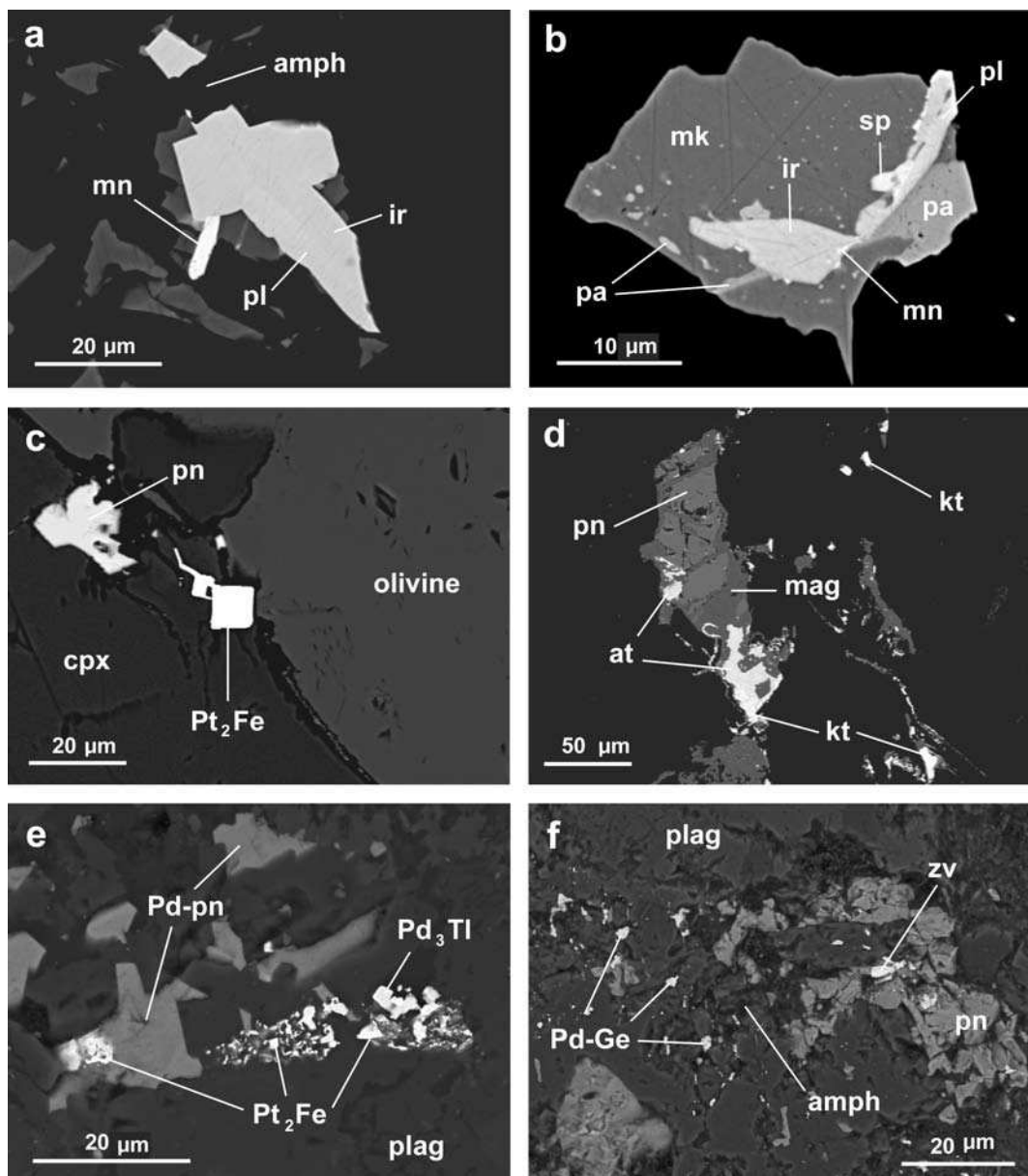


FIG. 5. Backscattered electron photomicrographs of PGM found in Sandsloot Platreef samples. (a) Zoned grain of irarsite (ir) and platarsite (pl) with moncheite (mn) from pegmatoidal pyroxenite reef. Note how the grain is cut by a secondary amphibole. (b) Polyphase PGM from pyroxenite reef consisting of menshikovite (mk), irarsite (ir), platarsite (pl), palladoarsenide (pa), sperrylite (sp) and moncheite (mn). (c) Typically cubic crystal of Pt_2Fe from olivine-replaced reef. (d) Association of atokite (at) and kotulskite (kt) with pentlandite (pn), oxidized to magnetite (mag) in a partially serpentinized sample of footwall. (e) Typical association of Pt_2Fe intergrown with palladian pentlandite (Pd-pn) and Pd_3Ti from hangingwall gabbronorite. (f) Cluster of Pd germanides surrounded by secondary amphiboles replacing non-Pd-bearing pentlandite with zvaigintsevite (zv) in the same hangingwall gabbronorite as in e.

TABLE 3. Proportions of PGM type within each lithology in percentage of the total area of PGM. See Table 2 for the lithology abbreviations.

PGM type:	HW	PXT	PEG	ORR	Lithology:		FWP	CS	PSP	TSP
					CPX	FRH				
Pt tellurides	0.6	40.1	38.8	4.9	11.6	0.3	10.3	0.2	6.8	0.2
Pd tellurides	6.0	19.2	18.2	31.1	26.6	3.6	1.6	6.1	26.4	
Pt bismuthides				0.1						
Pd bismuthides	0.4	0.8		3.5	4.0		22.3	0.1	21.8	
Pt arsenides		10.8	23.4	20.1	8.5	1.1	18.6	79.5	21.6	9.1
Pd arsenides	0.5	0.5	0.5			89.2	0.2		0.1	
Pt antimonides									2.6	46.3
Pd antimonides		0.9		2.7	39.4		4.9	2.8	0.6	35.0
Pd germanides	55.3		0.5							
PGE sulphides	0.4									
PGE sulpharsenides		0.8	14.5	0.1			0.3			4.4
Pt-dominant alloys	28.2	0.1		25.3			0.3		0.2	3.0
Pd-dominant alloys	8.6	3.8	0.3	9.1		5.8	40.1	11.3	0.6	0.2
Au/Ag-bearing phases		23.0	3.8	3.1	9.9		1.4		19.3	1.6
Total no. of grains	102	222	79	156	23	23	163	44	132	64

Turfspruit (Hutchinson and Kinnaird, 2005). The replacement by amphiboles and epidote appears to be paragenetically late as there is evidence of secondary minerals cross-cutting the PGM, such as in Fig 5a. Most electrum is found as rounded blebs within BMS grains. PGE antimonides were found to be extremely rare in the Platreef pyroxenites.

Olivine-replaced reef

Samples of reef pyroxenite which have undergone replacement by Fe-rich olivine have their own distinctive Pd-rich and alloy-dominant PGM assemblage, with abundant Pd tellurides, and Pt-Fe alloys. Table 3 indicates that Pt arsenides are also very abundant; however, Table 2 shows that only six sperrylites, in a total of 156 grains, were identified, though all were large relative to the other grains, which has caused the high percentage by area in Table 3. Table 1 shows that the Pt/Pd ratio in these rocks is ~0.6, therefore in this case, the proportion by area data in Table 3 appears to have been skewed by a small number of particularly large grains. We therefore consider that the true dominant species in this assemblage are Pd tellurides and alloys. The most common telluride, kotulskite, commonly contains much higher concentrations of Pb (up to 12 wt.%) than kotulskite in the unaltered pyroxenites, with a representative

composition in these rocks of $\text{Pd}_1\text{Te}_{0.74}\text{Bi}_{0.14}\text{Pb}_{0.12}$. The most common Pd alloy is zvyagintsevite (Pd_3Pb), which is particularly characteristic of this lithology. The Pt-Fe alloys have a typical composition of Pt_2Fe , which is intermediate between isoferroplatinum (Pt_3Fe) and tetraferroplatinum (PtFe), and is therefore referred to under the nomenclature of Cabri and Feather (1975) as Pt-Fe alloy. In these rocks, Pt-Fe alloys occur as discrete cubic crystals (Fig. 5c) rather than as intergrowths with BMS or magnetite, which is the more common mode of occurrence in the Merensky Reef (Kinloch, 1982; Kinloch and Peyerl, 1990). The other common Pt-dominant alloy in the olivine-replaced rocks is tulameenite (Pt_2FeCu), which was not found in any of the other lithologies. A few examples of PGE bismuthides and antimonides were also found in the replaced reef, which are absent or extremely rare in the unaltered pyroxenite reef. Arsenides and electrum are also present. Only 8% of PGM are included in BMS (Table 4) and many of the 43% which are surrounded by silicates do not show the close spatial relationship to BMS that those in the unaltered reef show, with some often isolated along veins.

Reef clinopyroxenites

The reef clinopyroxenites at the base of the Platreef in the northern part of the pit were found

TABLE 4. Textural associations of PGM (excluding Au/Ag alloy) in the variety of host-rock types and the percentage of grains. See Table 2 for lithology abbreviations.

All PGM, Au, Ag phases Association:	HW	PXT	PEG	ORR	CPX	FRH	FWP	CS	PSP	TSP
Enclosed in BMS (%)	10.3	12.6	9.1	8.2		77.8	10.4	6.4	21.2	
BMS-silicate contact (%)	29.9	38.1	16.9	49.0	30.4	11.1	27.6	14.9	60.6	11.5
Enclosed in silicate (%)	59.8	49.3	74.0	42.8	69.6	11.1	62.0	78.7	18.2	88.5
Pt-dominant phases Association:	HW	PXT	PEG	ORR	CPX	FRH	FWP	CS	PSP	TSP
Enclosed in BMS (%)	23.1	8.4	11.9	6.5			9.8	4.3		
BMS-silicate contact (%)	53.8	37.3	26.2	41.3			14.8	8.7	67.6	7.4
Enclosed in silicate (%)	23.1	54.2	61.9	52.2	100.0	100.0	75.4	87.0	32.4	92.6
Pd-dominant phases Association:	HW	PXT	PEG	ORR	CPX	FRH	FWP	CS	PSP	TSP
Enclosed in BMS (%)	8.0	8.5	3.1	6.1		72.2	10.5	8.7	29.2	
BMS-silicate contact (%)	22.7	34.1	3.1	51.0	40.0	16.7	34.7	21.7	55.6	16.1
Enclosed in silicate (%)	69.3	57.3	98.8	42.9	60.0	11.1	54.8	69.6	15.3	83.9

to be low grade (Table 1). The grade is also known to decrease with depth away from the contact with overlying feldspathic pyroxenites, such that the calc-silicate footwall is not exposed in the northern part of the pit. From Table 3 it appears that the 23 PGM grains found differed from the reef pyroxenites in that they contained a large proportion of antimonides. Table 2, however, reveals that this figure comes from a single, relatively large grain of stibiopalladinite, and other than this, the assemblage is similar to the reef pyroxenites, containing mainly tellurides. The small number of grains located requires any trends identified to be taken with caution, though it appears that the assemblage is similar to that of the reef pyroxenites, with a slight increase in the number of PGM containing Bi and Sb. None of the PGM is included in BMS, and all of the Pt phases and 60% of the Pd phases are located in silicates, which is much higher than in the reef pyroxenites (Table 4). Overall grain size was very small (Fig. 4), with most grains <5 µm long, and the largest being only 15 µm in its longest dimension.

Footwall clinopyroxenites

The footwall clinopyroxenites are dominated by Pd-dominant alloys, particularly paolovite

(Pd₂Sn) and the similar, but unnamed phase Pd₂(Sn,Sb), which contain Sn and Sb in equal proportions. Bismuthides, and in particular an unnamed phase with composition close to Pd₃Bi₃(Te,Sb)₂, are also common. Almost a third of all grains were sperrylite, making it the most abundant phase by occurrence, although sperrylite only made up 19% of the assemblage by area (Tables 2, 3). Other than sperrylite, very few of the PGM grains were Pt phases. A few tellurides and antimonides make up the remainder of the assemblage. Almost two-thirds of PGM in the footwall clinopyroxenites are surrounded by silicates (Table 4). This figure increases to three-quarters when only the Pt-dominant phases are considered, which reflects the preference of sperrylite to be isolated in silicate grains away from BMS grains.

Footwall calc-silicates

The calc-silicates, like the clinopyroxenites, are telluride-poor, and are rich in arsenides, particularly sperrylite, which makes up nearly 80% of the assemblage (Table 3). There are fewer alloys than in the clinopyroxenites, although Pd-dominant alloys are still the second most common PGM type. However, in contrast to the clinopyroxenites, bismuthides are very rare.

Table 4 shows 79% of all PGM grains being enclosed within silicate minerals, a figure probably enlarged partially by the relative paucity of BMS in the calc-silicates compared to the igneous reef. As in the clinopyroxenites, the Pt phases (largely sperrylite) show a strong preference to be associated with silicates.

Footwall-reef hybrid

A sample of footwall-reef hybrid rock contained a large number of palladoarsenide (Pd_2As) grains, concentrated in and along fractures in BMS grains. Comparatively few PGM were found elsewhere in the sample, which include a few tellurides. The small number of PGM grains in the sample means any trends must be viewed cautiously, though it does show a marked increase in arsenides and Pd minerals compared to the primary reef pyroxenites, possibly indicating a more volatile influenced environment more akin to the footwall assemblages than the igneous pyroxenites.

Footwall serpentinites

Two types of serpentinite were studied: partially and completely serpentinitized footwall. In the partially serpentinitized samples, where up to 60% fresh metamorphic olivine (Fo_{88}) is still present, the PGM assemblage is dominated by Pd tellurides and lesser amounts of Pd bismuthides and Pt arsenides. As in the olivine-replaced reef, kotulskite contains relatively high concentrations of Pb (often higher than Bi) which substitutes for Te in the ideal formula PdTe . Significantly, the PGM in this rock type are very much associated with BMS (Table 4) which are variably oxidized to Fe-oxide phases (Fig. 5d), an association also noted in serpentinitized parts of the Platreef on Drenthe by Gain and Mostert (1982). Li *et al.* (2004) describe BMS being replaced by magnetite in areas of serpentinitization in the Merensky Reef and UG2 in the western Bushveld. Nearly all of the kotulskite and electrum is found in association with these partially oxidized blebs of BMS. The PGM in the completely serpentinitized rocks, however, are almost completely silicate-associated (Table 4), with completely serpentinitized footwall containing very few BMS, with most altered to magnetite. This PGM assemblage has the most predominant enrichment in antimony in any of the assemblages and is characterized by the presence of gersverseite (PtSb_2) and sudburyite

(PdSb). A few arsenides, tellurides and sulpharsenides make up most of the remainder of the assemblage.

Hangingwall gabbroonorite

Samples from the base of the hangingwall were surprisingly found to contain appreciable occurrences of PGM. Sporadic BMS occur in both the mottled anorthosite and the basal part of the overlying gabbroonorite in places where the hangingwall sits on coarse-grained mineralized reef (Holwell *et al.*, 2005). One sample of gabbroonorite, taken from just above the basal contact with the thin mottled anorthosite that forms the base of the hangingwall in places, was considerably rich in PGM. Patches of Pt_2Fe intergrown with chalcopyrite and pentlandite are common (Fig. 5e), an association which differs from the discreet cubic crystals of Pt_2Fe found in the replaced reef. The only grain of PGE sulphide (laurite) found in the entire suite of samples studied was located in the centre of one of these Pt_2Fe alloy-BMS intergrowths. Also associated with the intergrowths were several grains of the unknown Pd-Tl alloy, Pd_3Tl (Fig. 5e). The only other published occurrences of any Pd-Tl minerals is a very rare, unconstrained Pd-Tl phase from the Platreef on Zwartfontein and the Merensky Reef in the eastern Bushveld (Kinloch, 1982) and a mineral close to the formula Pd_3Tl , with some substitution of Tl by Re, in the Wetlegs deposit of the Duluth Complex, Minnesota (Severson and Hauck, 2003). Significantly, the pentlandite which is intergrown with Pt-Fe and Pd-Tl alloys in Fig. 5e also contains up to 6 wt.% Pd, which is the highest recorded natural concentration of Pd in pentlandite (L. J. Cabri, pers. comm.). Overall, however, the sample was particularly rich in the unnamed Pd germanide phase with composition close to Pd_2Ge . Sixty four individual grains, plus many $<1\ \mu\text{m}$, were found, of which 11 contained some Pt in place of Pd, and most contained some As in place of Ge. Typical analyses of this phase are shown in Table 5, together with the ideal compositions for Pd_2Ge and $\text{Pd}_{11}\text{Ge}_5$, the latter of which the analyses match more closely. Armitage *et al.* (2002) noted a single grain of $(\text{Pd,Pt})_2\text{Ge}$ in the Platreef, and the only other recorded occurrences of PGE-germanides anywhere in the world are an unconstrained Pd-Ge phase from the UG-2 chromitite (McLaren and de Villiers, 1982), Pd_2Ge recorded from the Noril'sk Ni-Cu-PGE

TABLE 5. Compositions of unnamed Pd-germanide phase from the base of the hangingwall gabbro-norite, together with the ideal compositions of Pd₂Ge and Pd₁₁Ge₅.

Grain no:	1	2	3	4	Pd ₂ Ge	Pd ₁₁ Ge ₅
Wt.% Pd	75.84	76.52	60.00	59.51	74.56	76.32
Pt			18.33	17.23		
Ge	21.80	20.42	21.96	21.44	25.43	23.67
As	2.54	3.53	0.77			
Total	100.18	100.47	100.28	98.95	100.00	100.00

orebody (Komarova *et al.*, 2002) and (Pd,Pb)₂Ge (Grokhovskaya *et al.*, 2005). The Pd₂Ge grains, and some rarer kotulskite and Pd arsenides are found as satellite grains around larger BMS minerals which are intergrown with secondary amphiboles (Fig. 5f). The association of Pd-bearing pentlandite, PGE alloy intergrowths and PGE sulphides with unaltered BMS does not hold any PGE germanides, whereas germanides are present in association with non-PGE-bearing, partially replaced BMS. The remainder of the hangingwall assemblage is made up of zvyagin-tsevit, kotulskite and a few arsenides.

Discussion

The results from this study show the Platreef to be a very complex PGE orebody both lithologically and mineralogically. The PGM mineralogy at Sandsloot is distinctive within the Platreef compared to other areas. In detail, we have shown that the variety of host rock types in the Platreef contain their own, characteristic PGM assemblages which reflect the processes involved in redistributing the PGE through the reef and into the footwall during the evolution of the Platreef, though the mechanism which led to the initial introduction of PGE into the Platreef has yet to be resolved.

The most characteristic feature of the Sandsloot PGM assemblage, in comparison to most other tabular Bushveld PGE orebodies, is the complete lack of PGE sulphides. Throughout the Merensky Reef, PGE sulphides make up a substantial proportion of the overall PGM assemblage (e.g. Kinloch, 1982; Mostert *et al.*, 1982; Mossom, 1986; Prichard *et al.*, 2004). In the Platreef, on the farms Drenthe and Overysel, to the north of Sandsloot, these minerals make up greater than or nearly half the volume percentage of the assemblage (Gain and Mostert, 1982; Kinloch,

1982). Kinloch (1982, Table 6) lists PGM from eight borehole cores on Zwartfontein, the first five of which are sulphide-poor, alloy- and telluride-dominant, the remaining three are sulphide-dominant and similar to the Overysel data in the same table. The footwall changes from dolomite in the southern and central part of Zwartfontein (Fig. 1) to Archaean basement in the northern part of the farm. The cores listed in Table 6 of Kinloch (1982) are shown in south to north order (P. Hey, pers. comm.) with the change from a dolomite footwall to one composed of granite and gneiss directly corresponding to the change in the PGM assemblage with respect to the presence of PGE sulphides. South of Sandsloot, on Tweefontein where BIF and shales of the Duitchland Formation form the footwall, sulphides are again reported (Viljoen and Schürmann, 1998). Immediately to the south though, on Turfspruit and Macalacaskop where the footwall is Duitchland Formation and Pretoria Group shales and sandstones, Hutchinson *et al.* (2004) describe a number of PGM assemblages with very few PGE sulphides. The lack of sulphides is probably due to low f_{S_2} which would have prevented any free S being available to combine with PGE. This appears to be directly related to footwall lithology, with low f_{S_2} conditions characteristic of areas where the Platreef magma has interacted with dolomitic footwall. Elsewhere in the Bushveld Complex, potholed Merensky Reef (Kinloch, 1982) and the platiniferous dunite pipes (Tarkian and Stumpfl, 1975) contain relatively few PGE sulphides and are dominated by alloys, tellurides and sperrylite. Volatile activity is thought to be important in both these mineralizing environments, which therefore suggests a link between volatile activity and sulphide-poor, alloy-dominated PGM assemblages. The Platreef at Sandsloot is certainly more alloy-rich and sulphide-poor than at Overysel and Drenthe (Gain and Mostert, 1982;

Viljoen and Schürmann, 1998) where the footwall is Archaean granite/gneiss basement. This would suggest that greater volatile activity affected the Platreef where it intruded the dolomites than where it intruded the granites and gneisses, which is manifested in distinctively different PGM assemblages.

The pyroxenites and pegmatites of the igneous reef contain a typical PGM assemblage dominated by Pt and Pd tellurides, electrum and some arsenides. Their presence in the interstitial regions, in a proximal association with BMS, indicates a spatial relationship with the sulphides. Typically, magmatic PGE associations are of Os, Ir and Ru with chromite (Lee, 1996), and Pt, Pd and Rh concentrated with sulphides (Naldrett and Duke, 1980). In a typical immiscible sulphide separating from a silicate magma and collecting base metals and PGE (e.g. Naldrett *et al.*, 1986), the sulphide liquid collects the PGE, and PGM are commonly found included in, or more commonly, at the margins of BMS grains. In our samples, most PGM are found either at the sulphide-silicate boundary, or are silicate-hosted as satellite grains around altered BMS. The intergrowth of BMS with plagioclase and the frequent distribution of small blebs of sulphide and PGM around the edge of interstitial areas suggests that if PGE were originally held in the sulphide liquid, redistribution of the PGE occurred during fluid fluxing after orthopyroxene crystallization, but before the interstitial fluid crystallized, unless the PGM crystallized directly from the melt. The fact that the pegmatitic rocks show a considerably larger average PGM grain size also suggests that the PGM crystallized at a similar, early stage, though their relative enrichment in Pd tellurides and sperrylite would suggest greater degrees of fluid activity, which would be expected if the pegmatoidal nature of the lithology is due to fluid interaction. The reef clinopyroxenites have a similar PGM assemblage, although do contain a few antimonides and bismuthides, more commonly found in the footwall. Texturally, the PGM in these rocks have less of an association with BMS, which is more characteristic of the footwall lithologies. This evidence, together with the fact that the PGE grade decreases away from the contact with the reef pyroxenites, may suggest that the PGE have been transported from the feldspathic pyroxenites by hydrothermal activity.

Base-metal sulphides in the igneous reef have been variably altered around their margins and replaced by actinolite, tremolite and epidote. The

appearance of PGM as satellite grains around BMS may be the result of PGM, originally at the edge of the sulphide grains, remaining *in situ*, as the BMS boundary regressed. A similar association was found in the Merensky Reef and UG2 chromitite by Li *et al.* (2004), who suggested possible reactions for the replacement of BMS by amphiboles and epidote. All of the reactions proposed by Li *et al.* (2004) involve the addition of aqueous Ca, Mg and Si, all of which are readily available from the assimilation of the siliceous Malmani dolomite. However, rather than the BMS being replaced directly by silicates, it is more likely that the hydrous fluids reacted with the BMS to form sulphuric acid, dissolving the BMS around its margins and hydrous silicates were able to grow into the voids around the regressed margins. The PGM appear to be paragenetically earlier than the episode of alteration that formed the hydrous silicates, as seen by the cross-cutting of PGM by the secondary minerals (Fig. 5a). This observation for the Platreef would appear to contrast with the conclusions of Li *et al.* (2004) who suggested that secondary hydrothermal alteration may have been important in redistributing PGE in the Merensky Reef. In the case of the Platreef at Sandsloot, it seems that fluid fluxing at or close to the time of crystallization, and not later hydrothermal alteration, was the most important factor in redistributing PGE through the primary reef.

The presence of Pt-Fe alloy in crystal form (rather than as intergrowths), Pd alloys and Pd tellurides in olivine-replaced portions of reef is analogous to the volatile-influenced ultramafic platiniferous pipes of the eastern Bushveld and pegmatoid-replaced Merensky Reef potholes (Kinloch and Peyerl, 1990). The olivine-replaced lithologies are thought to have formed from a late-stage Fe-rich, Si-poor fluid (McDonald *et al.*, 2005b) which percolated through parts of the pyroxenite, replacing orthopyroxene with olivine (Fig. 3a). At present, the origin of this fluid remains unclear, although it may have been derived from serpentinization of the olivine-bearing footwall lithologies. The fluid also appears to have been Pb-rich as seen by the formation of abundant zvyagintsevite (Pd₃Pb), and the replacement of some Te by Pb in kotulskite. If PGM were present in the protolith (probably reef pyroxenite), the Fe-rich fluid seems likely to have recrystallized Pt into Pt-Fe alloys, and the assemblage therefore post-dates the main episode of mineralization.

The difference in the nature of the PGM between the igneous reef and metamorphic footwall units that contain PGE mineralization is striking. The dominance of tellurides, alloys and electrum with a complete lack of antimony observed in the igneous reef, is reversed in the footwall, with arsenides, bismuthides and antimonides dominating. The dominance of PGM containing elements such as As and Sb in the footwall lithologies suggests a significant amount of volatile activity involved in the redistribution of PGE into the footwall. However, the role of elements such as As, Sb, Se and Te is believed to be to immobilize the PGE, rather than be transported with them, as reduced forms of these elements cannot be transported with Pt and Pd (Wood, 2002). The almost total absence of antimonides in the igneous reef is analogous to normal Merensky Reef, where PGE antimonides are very rare (Kinloch, 1982), whereas in areas where fluid activity has been prevalent, antimonides are common. For example, the type localities for the PGE antimonides genkinite, geversite, stibiopalladinite, stumpflite, sudburyite and naldrettite and ungavaite are, respectively: the Onvervacht pipe (Bushveld Complex, RSA); the Driekop pipe (Bushveld Complex, RSA); Tweefontein Hill (Bushveld Complex, RSA); the Driekop pipe; Copper Cliff (Sudbury, Canada), and the Mesamax Northwest deposit (Québec, Canada) (Cabri, 2002; Cabri *et al.*, 2005; McDonald *et al.*, 2005a), all of which have been fluid affected. This would imply that PGE antimonides are indicative of fluid transport of PGE, and are present in secondary assemblages. The fluid activity that redistributed the PGE would be expected to have preferentially transported the more mobile Pd into the footwall over Pt, therefore producing low Pt/Pd ratios in the footwall, and raising the Pt/Pd slightly in the igneous reef. Table 1 shows Pt/Pd ratios for reef samples in the range 0.79–1.94, whereas in footwall samples the ratio is 0.54–0.98, and in the replaced reef it is ~0.6, showing a relative enrichment in Pd over Pt in the areas where the greatest fluid activity appears to have taken place, indicating that the PGE were introduced by fluid activity.

Partial serpentinization of footwall olivine desulphurizes BMS to form magnetite, a feature also seen in the Merensky Reef and UG2 (Li *et al.*, 2004) and in its early stages appears to form a telluride-dominant PGM assemblage (often Pb-

bearing) which is not dissimilar to that found in the olivine-replaced reef. If there is a link between the two assemblages, it may be that the Fe-rich fluids that altered the reef originated from serpentinization of the footwall. Further degrees of serpentinization are associated with a generally fine-grained, disseminated, low-temperature PGM assemblage rich in volatile elements such as Sb and As. The antimonide-dominant assemblage formed is likely to represent recrystallization of the telluride dominant-assemblage.

The PGM assemblage at the base of the hangingwall is of particular interest, as until very recently (Holwell *et al.*, 2005) the hangingwall was not thought to contain any PGE mineralization, except around calc-silicate rafts (Kinnaird *et al.*, 2005). Holwell *et al.* (2005) concluded that the Platreef was almost completely crystallized when the hangingwall gabbro-norites were intruded. Localized assimilation of mineralized reef into the new magma incorporated PGE-rich sulphide into the hangingwall magma. The observed high Pd content in pentlandite requires rapid cooling, which would be likely if the hangingwall magma chilled against a crystallized and relatively cooled Platreef. The PGE-rich sulphide liquid cooled rapidly to form, first monosulphide solid solution (mss), then the 'primary' assemblage of Pd-pentlandite, Pt-Fe alloy-BMS intergrowths and laurite. In particular, the presence of Pt-Fe alloy-BMS intergrowths is a characteristic texture associated with primary BMS, present in Merensky Reef that has not undergone significant volatile interaction (Kinloch, 1982) and in other layered intrusions (Cabri, 2002). Here we refer to 'primary' magmatic sulphides as pyrrhotite and pentlandite derived from the recrystallization of mss on cooling from magmatic temperatures. The PGE mineralization seems to exhibit a two-stage crystallization history. The primary assemblage appears to have been locally altered on a centimetre-scale, with Pd apparently exsolved from pentlandite, BMS surrounded by secondary amphiboles, and the PGM assemblage altered to one rich in germanides.

Holwell *et al.* (2005) suggested that the PGE in the basal portion of the hangingwall originated in the Platreef, and was assimilated into the magma that formed the hangingwall gabbro-norites, forming an unusual, primary assemblage of PGM at the base of the hangingwall which is distinct from, and post-dates, the main episode of mineralization in the Platreef.

Conclusions

The variety of characteristic PGM assemblages in the host of rock types of the Platreef at Sandsloot reflects the fluid and magmatic processes which affected the Platreef during and after emplacement. The method of initial introduction of PGE is still to be resolved; however, from the data presented here, it is possible to describe a sequence of events which redistributed PGE and/or recrystallized PGM through the reef and its footwall and hangingwall, each of which producing a characteristic assemblage in distinct lithologies.

(1) During crystallization of the igneous reef, PGM crystallized around the margins of BMS within the interstitial liquid forming a telluride-dominant assemblage, in close spatial association with BMS. Fluids, originating from assimilation and metamorphism of the dolomitic floor, are likely to have circulated within the interstitial liquid during crystallization. The lack of PGE-sulphides suggests conditions during this time were characterized by low f_{S_2} .

(2) During emplacement of the reef, fluid activity was very significant in redistributing PGE into the footwall. The footwall contains characteristic arsenide-, alloy- and antimonide-dominant PGM assemblages, showing a significant volatile influence during crystallization of this secondary assemblage.

(3) Serpentinization of footwall olivine also appears to convert earlier BMS to oxides, with PGE-tellurides remaining in association with the remnant sulphides. Further degrees of serpentinization, where all olivine is replaced, produces a more volatile-enriched antimonide-dominant PGM assemblage, without the association with BMS.

(4) Late-stage, Fe-rich fluids percolating through certain parts of the igneous reef desilicified orthopyroxene to form olivine, producing peridotitic zones. PGM were also recrystallized by this fluid, to form an alloy-dominant PGM assemblage of Pt-Fe and Pd-Pb alloys, together with possibly pre-formed tellurides.

(5) After a period of cooling and almost total crystallization of the pyroxenitic reef, the hangingwall magma was intruded, locally assimilating PGE-rich pyroxenite reef and cooling quickly to form a separate, primary PGM-BMS assemblage of Pd-bearing pentlandite, Pt-Fe alloy-BMS intergrowths and laurite. Later, localized alteration has recrystallized PGM, producing a germanide-dominant PGM assem-

blage of satellite grains around altered BMS.

This paper summarizes the assemblages present in various rock types at Sandsloot. Elsewhere along the Platreef the rock types and PGM assemblages are known to be different (e.g. Kinloch, 1982; Viljoen and Schürmann, 1998; Hutchinson and Kinnaird, 2005) and the Platreef is obviously a highly complex orebody with a varied and complex magmatic and fluid history determined by several factors, most importantly, the interaction of the Platreef magma with the varying floor rocks. The results of this study reveal the importance of syn- and post-emplacement fluid activity on the mineralogy and distribution of PGE in the Platreef on a metre scale at this locality, with the presence of dolomite as the footwall rock producing a distinctively PGE sulphide-poor PGM assemblage. Further work is planned to attempt to constrain this footwall control by investigation into the PGM mineralogy in other sections along strike where the footwall is different.

Acknowledgements

The authors would like to thank the management of Anglo Platinum for allowing access to Sandsloot mine for Paul Armitage and David Holwell to collect samples and their permission for publication of this work. David Holwell's PhD research is funded by the Natural Environment Research Council and supported by Anglo Platinum through Industrial CASE project (NER/S/C/2003/11952). Pete Fisher is thanked for his assistance in the SEM analytical work at Cardiff University. Louis Cabri, Chris Ballhaus and Grant Cawthorn are thanked for their reviews and suggestions which have helped to improve the quality of the manuscript.

References

- Armitage, P.E.B., McDonald, I., Edwards, S.J. and Manby, G.M. (2002) Platinum-group element mineralization in the Platreef and calc-silicate footwall at Sandsloot, Potgietersrus District, South Africa. *Applied Earth Science (Transactions of the Institute of Mining and Metallurgy B)*, **111**, B36–45.
- Cabri, L.J. (2002) The platinum-group minerals. Pp. 13–129 in: *The Geology, Geochemistry, Mineralogy and Mineral Beneficiation of Platinum-Group Elements* (L.J. Cabri, editor). Canadian Institute of Mining, Metallurgy and Petroleum, Special Volume **54**.

- Cabri, L.J. and Feather, C.E. (1975) Platinum-iron alloys: a nomenclature based on a study of natural and synthetic alloys. *The Canadian Mineralogist*, **13**, 117–126.
- Cabri, L.J., McDonald, A.M., Stanley, C.J., Rudashevsky, N.S., Poirier, G., Durham, B.R., Mungall, J.E. and Rudashevsky, V.N. (2005) Naldrettite, Pd₂Sb, a new intermetallic mineral from the Mesamax Northwest deposit, Ungava region, Quebec, Canada. *Mineralogical Magazine*, **69**, 89–97.
- Cawthorn, R.G. (1999) The platinum and palladium resources of the Bushveld Complex. *South African Journal of Science*, **95**, 481–489.
- Cawthorn, R.G., Merkle, R.K.W. and Viljoen, M.J. (2002) Platinum-group elements in the Bushveld Complex. Pp. 389–430 in: *The Geology, Geochemistry, Mineralogy and Mineral Beneficiation of Platinum-Group Elements* (L.J. Cabri, editor). Canadian Institute of Mining, Metallurgy and Petroleum, Special Volume **54**.
- Gain, S.B. and Mostert, A.B. (1982) The geological setting of the platinoid and base metal sulphide mineralization in the Platreef of the Bushveld Complex in Drenthe, north of Potgietersrus. *Economic Geology*, **77**, 1395–1404.
- Grokhovskaya, T.L., Lapina, M.I., Ganin, V.A. and Grinevich, N.G. (2005) PGE mineralization in the Burakovsk Layered Complex, Southern Karelia, Russia. *Geology of Ore Deposits*, **47**, 283–308.
- Hammerbeck, E.C.I. and Schürmann, L.W. (1998) Nickel. Pp. 471–482 in: *The Mineral Resources of Southern Africa* (M.G.C. Wilson and C.R. Anhaeusser, editors). Council for Geoscience.
- Harris, C. and Chaumba, J.B. (2001) Crustal contamination and fluid-rock interaction during the formation of the Platreef, Northern Limb of the Bushveld Complex, South Africa. *Journal of Petrology*, **42**, 1321–1347.
- Holwell, D.A., Armitage, P.E.B. and McDonald, I. (2005) Observations on the relationship between the Platreef and its hangingwall. *Applied Earth Science (Transactions of the Institute of Mining and Metallurgy B)*, **114**, B199–207.
- Hutchinson, D. and Kinnaird, J.A. (2005) Complex, multi-stage mineralization history in the southern sector of the Platreef, Bushveld Complex, RSA. *Applied Earth Science (Transactions of the Institute of Mining and Metallurgy B)*, **114**, B208–224.
- Hutchinson, D., Kinnaird, J.A. and Schürmann, L.W. (2004) Complex, multi-stage mineralization history in the southern sector of the Platreef, Bushveld Complex, RSA. *Geoscience Africa 2004, Abstract Volume*, University of the Witwatersrand, Johannesburg, South Africa, pp. 293–294.
- Kinloch, E.D. (1982) Regional trends in the platinum-group mineralogy of the Critical Zone of the Bushveld Complex, South Africa. *Economic Geology*, **77**, 1328–1347.
- Kinloch, E.D. and Peyerl, W. (1990) Platinum-group minerals in various rock types of the Merensky Reef: genetic implications. *Economic Geology*, **85**, 537–555.
- Kinnaird, J.A. and Nex P.A.M. (2003) Mechanisms of marginal mineralization in the Bushveld Complex. *Applied Earth Science (Transactions of the Institute of Mining and Metallurgy B)*, **112**, B206–208.
- Kinnaird, J.A., Hutchinson, D., Schürmann, L., Nex, P.A.M. and de Lange, R. (2005) Petrology and mineralization of the southern Platreef: northern limb of the Bushveld Complex, South Africa. *Mineralium Deposita*, **40**, 576–597.
- Komarova, M.Z., Kozyrev, S.M., Simonov, O.N. and Lulko, V.A. (2002) The PGE mineralization of disseminated sulphide ores of the Noril'sk-Taimyr region. Pp. 547–567 in: *The Geology, Geochemistry, Mineralogy and Mineral Beneficiation of Platinum-Group Elements* (L.J. Cabri, editor). Canadian Institute of Mining, Metallurgy and Petroleum, Special Volume **54**.
- Lee, C.A. (1996) A review of mineralization in the Bushveld Complex and some other layered mafic intrusions. Pp. 103–146 in: *Layered Intrusions* (R.G. Cawthorn editor). Elsevier Science, Amsterdam.
- Li, C., Ripley, E.M., Merino, E. and Maier, W.D. (2004) Replacement of base metal sulphides by actinolite, epidote, calcite and magnetite in the UG2 and Merensky Reef of the Bushveld Complex, South Africa. *Economic Geology*, **99**, 173–184.
- McDonald, A.M., Cabri, L.J., Stanley, C.J., Rudashevsky, N.S., Poirier, G., Mungall, J.E., Rossa, K.C. and Rudashevsky, V.N. (2005a) Ungavaite, Pd₄Sb₃, a new intermetallic mineral from the Mesamax Northwest deposit, Ungava region, Quebec, Canada: Description and genetic implications. *The Canadian Mineralogist*, **43**, 1735–1744.
- McDonald, I., Holwell, D.A. and Armitage, P.E.B. (2005b) Geochemistry and mineralogy of the Platreef and 'Critical Zone' cumulates of the Northern lobe of the Bushveld Complex, South Africa: implications for Bushveld stratigraphy and the development of PGE mineralization. *Mineralium Deposita*, **40**, 526–549.
- McLaren, C.H. and de Villiers, J.P.R. (1982) The platinum-group chemistry and mineralogy of the UG-2 chromitite layer of the Bushveld Complex. *Economic Geology*, **77**, 1348–1366.
- Mossom, R.J. (1986) The Atok Platinum Mine. Pp. 1143–1154 in: *Mineral Deposits of Southern Africa* (C.R. Anhaeusser and S. Maske, editors), vols I and II. Geological Society of South Africa, Johannesburg.

- Mostert, A.B., Hofmeyr, P.K. and Potgieter, G.A. (1982) The platinum-group mineralogy of the Merensky Reef at the Impala Platinum Mines, Bophuthatswana. *Economic Geology*, **77**, 1385–1394.
- Naldrett, A.J. and Duke, J.M. (1980) Platinum metals in magmatic sulphide ores. *Science*, **208**, 1417–1424.
- Naldrett, A.J., Gasparini, E.C., Barnes, S.J., von Gruenewaldt, G. and Sharpe, M.R. (1986) The Upper Critical Zone of the Bushveld Complex and the origin of Merensky-type ores. *Economic Geology*, **81**, 1105–1117.
- Prichard, H.M., Barnes, S.-J., Maier, W.D. and Fisher, P.C. (2004) Variations in the nature of the platinum-group minerals in a cross-section through the Merensky Reef at Impala Platinum: implications for the mode of formation of the reef. *The Canadian Mineralogist*, **42**, 423–437.
- Schneiderhöhn, H. (1929) The mineragraphy, spectrography and genesis of the platinum-bearing nickel-pyrrhotite ores of the Bushveld Complex. Pp. 206–246 in: *The Platinum Deposits and Mines of South Africa* (P.A. Wagner, editor). Oliver and Boyd, Edinburgh, UK.
- Seversen, M.J. and Hauck, S.A. (2003) *Platinum group elements (PGEs) and platinum group minerals (PGMs) in the Duluth Complex*. Technical Report NRRI/TR-2003/37. Natural Resources Research Unit, University of Minnesota, Duluth, USA, 296 pp.
- Tarkian, M. and Stumpfl, E.F. (1975) Platinum mineralogy of the Driekop Mine, South Africa. *Mineralium Deposita*, **10**, 71–85.
- Viljoen, M.J. and Schürmann, L.W. (1998) Platinum group metals. Pp. 532–568 in: *The Mineral Resources of Southern Africa* (M.G.C. Wilson and C.R. Anhaeusser, editors). Council for Geoscience.
- von Gruenewaldt, G., Hulbert, L.J. and Naldrett, A.J. (1989) Contrasting platinum-group element concentration patterns in cumulates of the Bushveld Complex. *Mineralium Deposita*, **24**, 219–229.
- Wagner, P.A. (1929) *The Platinum Deposits and Mines of South Africa*. Oliver and Boyd, Edinburgh, UK, 326 pp.
- Wood, S.A. (2002) The aqueous geochemistry of the platinum-group elements with applications to ore deposits. Pp. 211–249 in: *The Geology, Geochemistry, Mineralogy and Mineral Beneficiation of Platinum-Group Elements* (L.J. Cabri, editor). Canadian Institute of Mining, Metallurgy and Petroleum, Special Volume **54**.

[Manuscript received 16 May 2005;
revised 12 October 2005]

APPENDIX 5

Full reference:

ARMITAGE P.E.B., McDONALD I. & TREDoux M. (2007). A geological investigation of the Waterberg hydrothermal platinum deposit, Mookgophong, Limpopo Province, South Africa. *Appl. Earth Sci. (Trans. Inst. Min. Metall. B)*, **116**, 113-129.

A geological investigation of the Waterberg hydrothermal platinum deposit, Mookgophong, Limpopo Province, South Africa

P. Armitage^{*1}, I. McDonald² and M. Tredoux³

The geology around the unusual quartz-vein hosted Waterberg platinum deposit was mapped using aerial photographs at a scale of 1 : 1000 to establish possible controls on this unique style of mineralisation. The study area is located in the Mookgophong (Naboomspruit) District of the Limpopo Province in South Africa and is dominated by a gently to moderately, NNW-dipping irregular sequence of bimodal (rhyolite–basalt) volcanics, interbedded with many sedimentary rocks, that form part of the extensive 2.06 Ga Rooiberg Group, that are cut by variably striking, steep to subvertical quartz veins. The regional geology of the area was mapped at various scales in the 1920s and 1940s, but much of this work remains inaccessible and mapping during this study has uncovered more detail. The major platiniferous quartz vein (known as the 'Main Lode') juxtaposes volcanic rocks of Rooiberg age against Triassic sandstones and therefore occupies a fault. There is no textural evidence that quartz veining was syntectonic and may be much younger. The well-exposed vein fabrics show many features typical of low pressure epithermal quartz veins and probably formed near the present-day surface beneath a highly eroded Karoo cover, suggesting a recent age for veining and Pt mineralisation. The Main Lode can be followed for at least 3 km along strike, but Pt mineralisation is concentrated in a short section of the vein around 500 m in length. A major regional fault (the Welgevonden Fault) occurs about 2 km to the northwest of, and parallel to, the Main Lode. The Welgevonden Fault zone is suggested to extend to the northeast and merge with the Planknek–Ysterberg Fault system, south of Mokopane (Potgietersrus). The Welgevonden Fault is presently geothermally active, but this fluid system does not carry significant concentrations of Pt and may represent a younger Pt-depleted stage of hydrothermal activity related to the event that formed the Main Lode. It is unlikely that the Rooiberg volcanics and younger rocks supplied the platinum-group elements in the deposit and the source for these metals must lie elsewhere. It is suggested that shearing along the Welgevonden–Planknek Fault system transposed PGE-bearing mafic rocks of the northern Bushveld Complex to a position at unknown depth beneath the Waterberg deposit, or provided a network of shear zones which could be exploited by a recent hydrothermal event that transported platinum and other metals westwards along the fault system and redeposited them near the surface.

Keywords: Platinum, Quartz veins, Hydrothermal, Rooiberg, Welgevonden Fault, Waterberg

Introduction

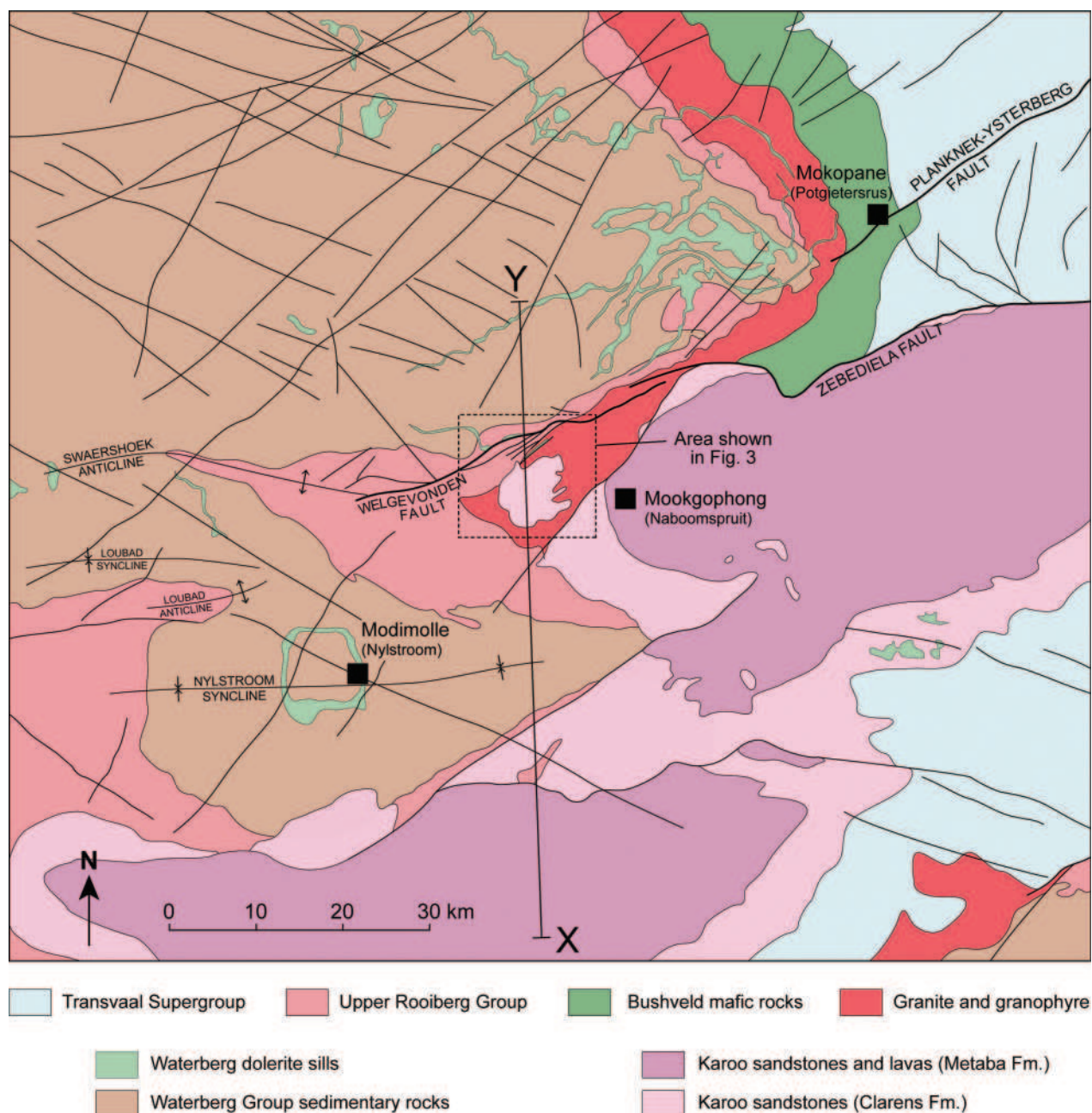
The 'Waterberg platinum deposit', first formally described by Wagner,³⁹ is located on the farms Welgevonden 353KR and Rietfontein 513KR, some 15 km west of the town of Mookgophong (formerly Naboomspruit) in the Limpopo Province of South Africa (*see* Fig. 1). The deposit occurs on the northern

¹Department of Mineralogy, Natural History Museum, Cromwell Road, London SW7 5BD, UK

²School of Earth, Ocean & Planetary Sciences, Cardiff University, Park Place, Cardiff CF10 3YE, UK

³Department of Geology, University of the Free State, PO Box 3440, Bloemfontein 9300, South Africa

*Corresponding author, email peba@totalise.co.uk



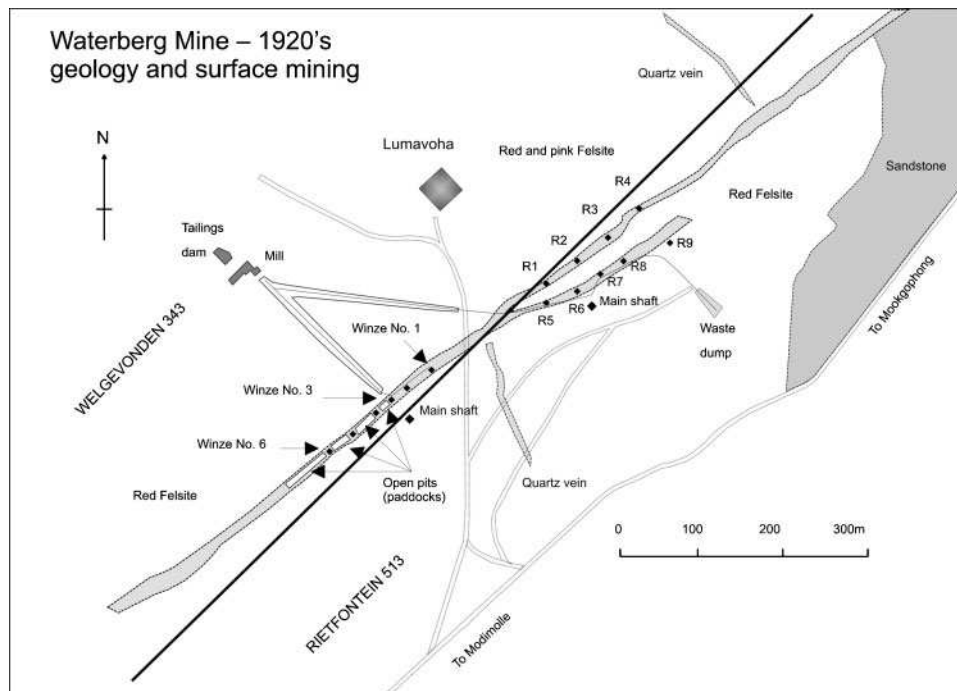
1 Simplified geological map of the Modimolle (Nylstroom) region after the Nylstroom 1:250 000 geological map published by the Council for Geoscience.⁵ X–Y is the line of a profile across the structural grain (see Fig. 13)

limb of the Swaershoek Anticline, one of a set of large, gently plunging folds that affect all pre-Karoo age lithologies in the region. The area is transgressed by steep, subparallel faults related to the Welgevonden Fault; part of the regional Thabazimbi-Murchison Lineament (TML) relay fault system^{6,18} that formed in the mid-Archaeon and has been periodically reactivated since that time.⁸ Linear to curvilinear, WNW-ESE striking pre-Karoo faults and NE-SW striking post-Karoo faults cross the region.

Some potentially confusing terms should be explained at this point. The name 'Waterberg platinum deposit' does not allude to the age of the deposit or the Waterberg Group (Fig. 1), but rather to the geographical proximity of the deposit to the Waterberg area. Likewise, the term 'Bushveld sandstone'³⁹ is used in compatibility with early mapping studies. This refers to the occurrence of the sandstone within the Bushveld region and not to the age of the sandstone, which is early

Mesozoic and therefore significantly younger than the 2.06 Ga Bushveld Complex.

The Waterberg deposit is perhaps the most unusual example in the class of epigenetic Au-PGE (platinum-group element) deposits, because it is dominated by Pt while Pd and Au are subordinate: in other notable deposits in the class, e.g. Serra Pelada and Minas Gerais (Brazil), and Gold Ridge and Alligator River (Australia), the concentrations of the metals follow the sequence $Pt < Pd \ll Au$.^{2,25,31} The Waterberg deposit comprises two quartz veins that occupy a fault between northwest dipping Rooiberg volcano-sedimentary rocks and horizontally bedded Mesozoic sandstones. The deposit has enormous historical as well as genetic significance, as its discovery by the prospector Adolph Erasmus in June 1923 marked the first find of platinum as a primary metal in South Africa.^{38,39} The deposit was mined between 1923 and 1926 by Transvaal Platinum Ltd and an account of the short and somewhat



2 Plan of the platinum lodes and the mining infrastructure when the mine was operational in 1926 (modified from Refs. 23 and 38)

disastrous mining history is given by McDonald and Tredoux.²³ Brief accounts of the geology and setting of the deposit are given by Wagner and Trevor,³⁸ Wagner³⁹ and McDonald and Tredoux.²⁰ Details of the mineralogy and geochemistry of the Waterberg platinum mineralisation have also been published.^{19,21}

In 1999, the authors began a programme of mapping around the Waterberg mine and research into the history of mining and geological studies in the area. The aim of this paper is to present a new 1 : 10 000 scale geological map of the deposit and surrounding area, with implications for local stratigraphy and controls on the development of mineralisation.

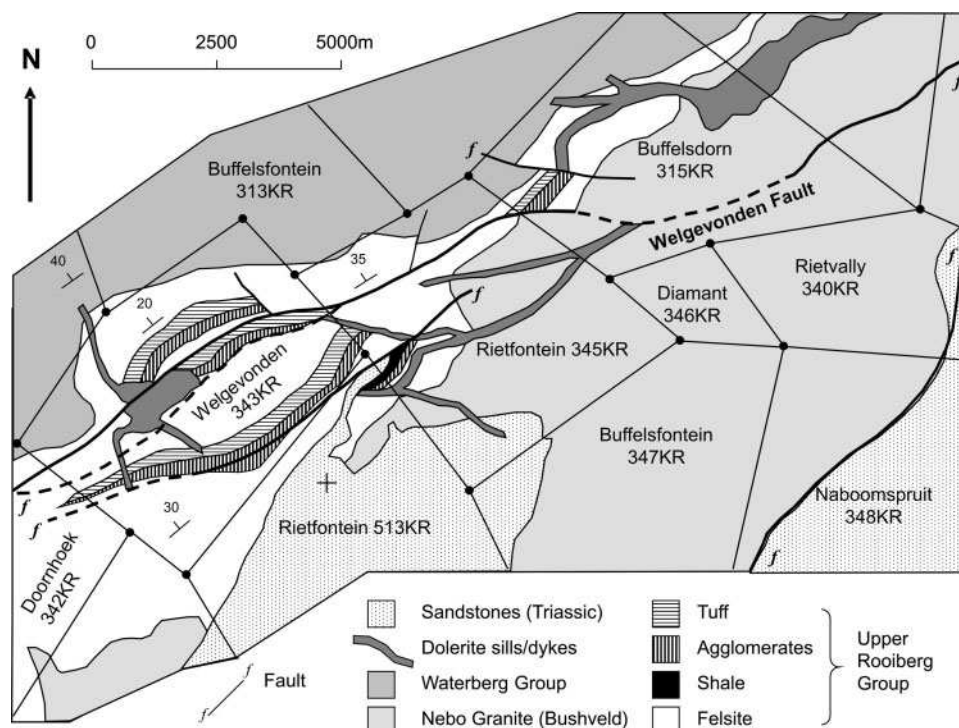
Since the original mine closed in 1926, the potential of the deposit has been periodically re-evaluated (generally during periods of high Pt prices), but up to 2005 no firm plans to resume mining had been developed. In 2005, Centurion Gold Holdings Incorporated ('Centurion') announced that they had signed an agreement to acquire prospecting rights for the area encompassing the Waterberg mine and for areas of the adjacent farms Rietfontein 345KR and Diamant 356KR. Centurion's own estimate of the contained metal content of the Naboom Project was close to 2.4 million ounces of PGE, with a headline value in excess of \$(US) 2 billion.⁴ In 2006, Centurion commissioned an independent 'competent persons' report by the consultants SRK Ltd which rated the project more conservatively as an exploration plays with an unknown resource (and a correspondingly lower value) but with significant potential.³² At the time of writing, Centurion have been awarded a new order prospecting permit for the Naboom property by the South African Department for Minerals and Energy and are attempting to raise finance for new exploration.

Previous mapping

The geology of the Mookgophong district was first mapped by Mellor and Kynaston between 1905 and

1909^{16,24} following the discovery of several important tin deposits at Zaaipplaats and Doornhoek²⁹ but the presence of PGE and Au remained unknown. The most detailed contemporary account of the discovery of the Waterberg deposit and the local geology that had been outlined during the initial phase of exploration was published by Wagner and Trevor.³⁸ This paper also contains the only widely available geological map of the deposit which focuses on a short section of the main platinum-bearing vein (called the 'Main Lode'), close to where a branching vein/fault (termed the 'Branch Lode') also contains high concentrations of platinum. Despite its simple appearance, Wagner and Trevor's map³⁸ summarises the key structural setting of the deposit: the Main Lode is hosted within a fault that juxtaposes dipping felsites of the Rooiberg Group (now known to have an age of 2.06 Ga)⁴⁰ against younger horizontally bedded pink sandstones that were assigned to the early Jurassic Stormberg Group of the Karoo Supergroup on the basis of Mellor's earlier mapping. The vein dips to the southeast at angles of 60–80°, with the hangingwall downthrown to the south. Apart from the immediate vicinity of the vein, no further information on the local geology was provided in Wagner and Trevor's account. The key elements of Wagner and Trevor's map, combined with a plan of the mine workings in 1926 by McDonald and Tredoux²³ are shown in Fig. 2.

Welgevonden 353 KR, Rietfontein 513 KR and several surrounding farms were remapped in 1944 by D.P. van Rooyen on behalf of the Geological Survey of South Africa.³⁵ Van Rooyen's hand drawn field sheet was incorporated into a report³⁷ and subsequently into the Nylstroom 1 : 250 000 regional geological map⁵ that is summarised in Fig. 1. Note that, although Nylstroom has recently been renamed Modimolle, the map retains its original name. A portion of van Rooyen's map of the area northwest of Naboomspruit is redrafted in Fig. 3. The map shows a simplified sequence of Nebo Granite



3 Redrafted map of the Naboomspruit area, originally hand drawn by van Rooyen³⁵

of the Bushveld Complex intruded into felsite, agglomerates, shale and tuff of the Upper Rooiberg Group, conformably overlain by clastic sedimentary rocks of the Waterberg Group and unconformably overlain by horizontally bedded Triassic sandstones. Post-Waterberg dolerite sills and dykes intrude all pre-Karoo lithologies. Northeast-Southwest to ENE-WSW striking, anastomosing faults traverse the area and apparently recognisable sequences are tectonically repeated in a pattern that implies downthrow to the southeast.

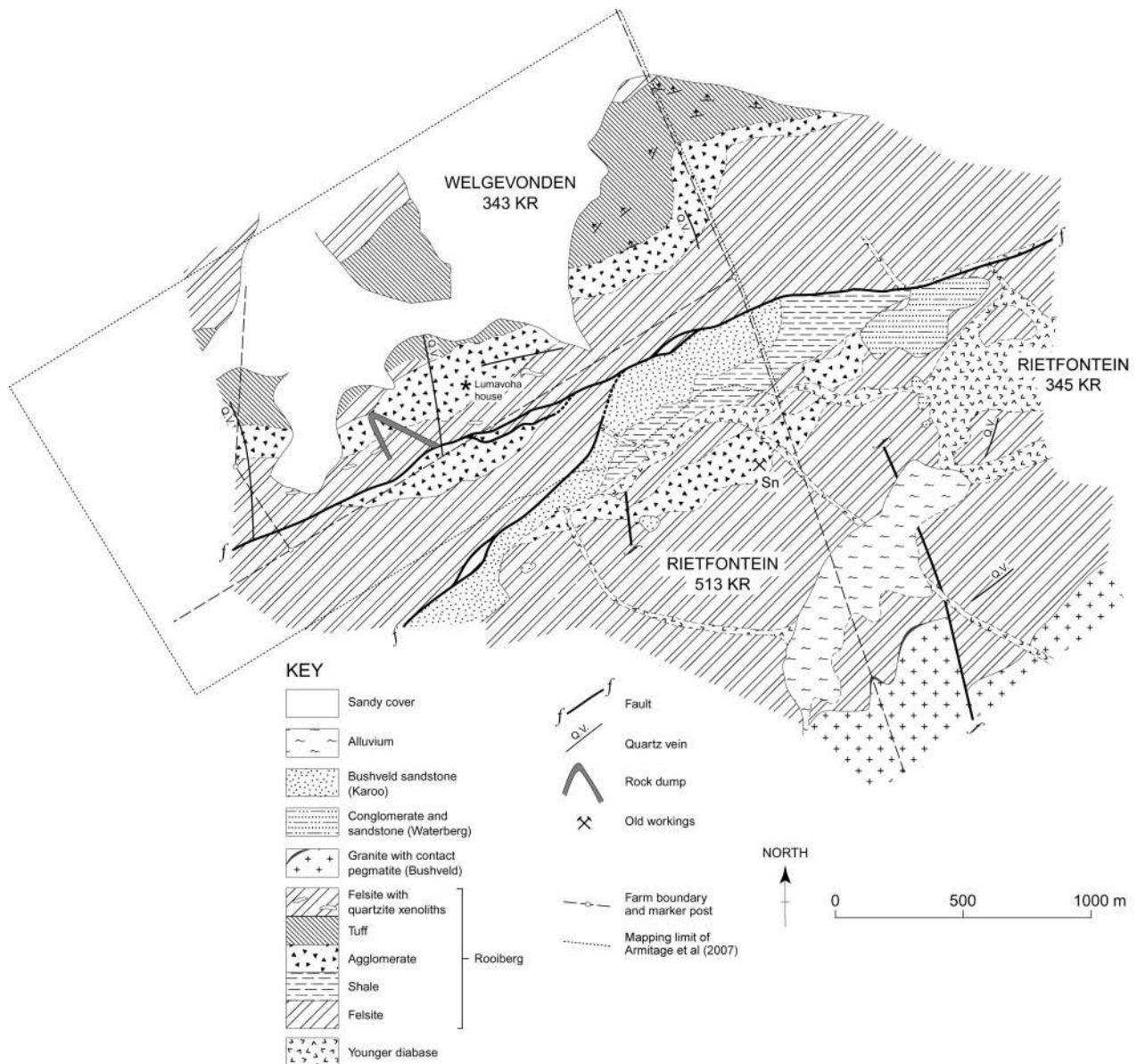
In mid-1945, van Rooyen produced a hand drawn map of the local geology around the Waterberg deposit, embracing parts of the farms Welgevonden 353 KR and Rietfontein 513 KR.³⁶ This map is redrafted in Fig. 4 with an English translation of van Rooyen's Afrikaans legend. In essence it shows the same sequence of units as Fig. 3 but in greater lithological and structural detail, and also shows some of the mining related features. A peculiarity of the map is the occurrence of a 'younger diabase' dyke in 'Bushveld sandstone' of Karoo age, while in the same location in Fig. 3 the dyke is covered by the sandstone. The discrepancy is assumed to be a drafting error in the later of the two maps. Furthermore, in Fig. 3 the 'younger diabase' is placed below the oldest Rooiberg lithology at the base of van Rooyen's map legend, so the time reference of its 'younger' age is uncertain. It is assumed that the diabase was interpreted to be post-Waterberg, which is the relative age the diabase has in Fig. 3 and in the Nylstroom 1:250 000 map,⁵ and that the stippled boundary of the diabase dyke in Fig. 3 merely infers intrusion into older Rooiberg lithologies beneath the sandstone. The other possible interpretation is that van Rooyen mapped the diabase as a post-Karoo hypabyssal system, which the authors consider unlikely. Further interesting features of van Rooyen's original map are two corrections made to the legend. He initially ascribed the shale and 'Bushveld

sandstone' units to Karoo age, then made an alteration in which in the shale unit and 'conglomerate and sandstone' unit were ascribed to Waterberg age. He subsequently made a final alteration in which the Bushveld sandstone was ascribed to Karoo age, the shale to Rooiberg age and the conglomerate and sandstone unit to Waterberg age. The redrafted map in Fig. 4 reflects the final, corrected legend. As far as the authors can determine, these maps, at this level of detail, have remained unpublished.

While the 1945 map substantially improves knowledge of the geology surrounding the Waterberg platinum mine, it lacks detail in the immediate vicinity of the deposit itself. The present study began with the aim of producing a new geological map of the Waterberg deposit and providing more detailed structural data and geological information on various lithologies surrounding the vein, from sections of the vein sampled by the authors and from historical vein samples that form part of the Wagner collection at the University of Cape Town.

Methods

As a prelude to detailed mapping, an initial interpretation of structures in the area using aerial photographs at a scale of 1:30 000 was carried out. The results of this analysis (Fig. 5) highlighted the potential extent of the Main Lode and the fact that it follows a similar strike to the larger Welgevonden Fault. Mapping was carried out on a digitally enhanced air photograph at a scale of approximately 1:1000. The positions of all localities were determined using a hand held GPS system and recorded on a UTM grid. A number of samples were collected for geochemical analysis. These were cut with a diamond saw to remove any weathering rinds before being crushed to chips in a manganese steel jaw crusher and reduced to fine powder in agate ring and ball mills. Some samples of mixed units (e.g. PA-99-21) contained more than one rock type and sub-samples (~1 cm³



4 Redrafted geological map of the area immediately around the Waterberg mine digitally traced from van Rooyen's hand drawn original³⁶

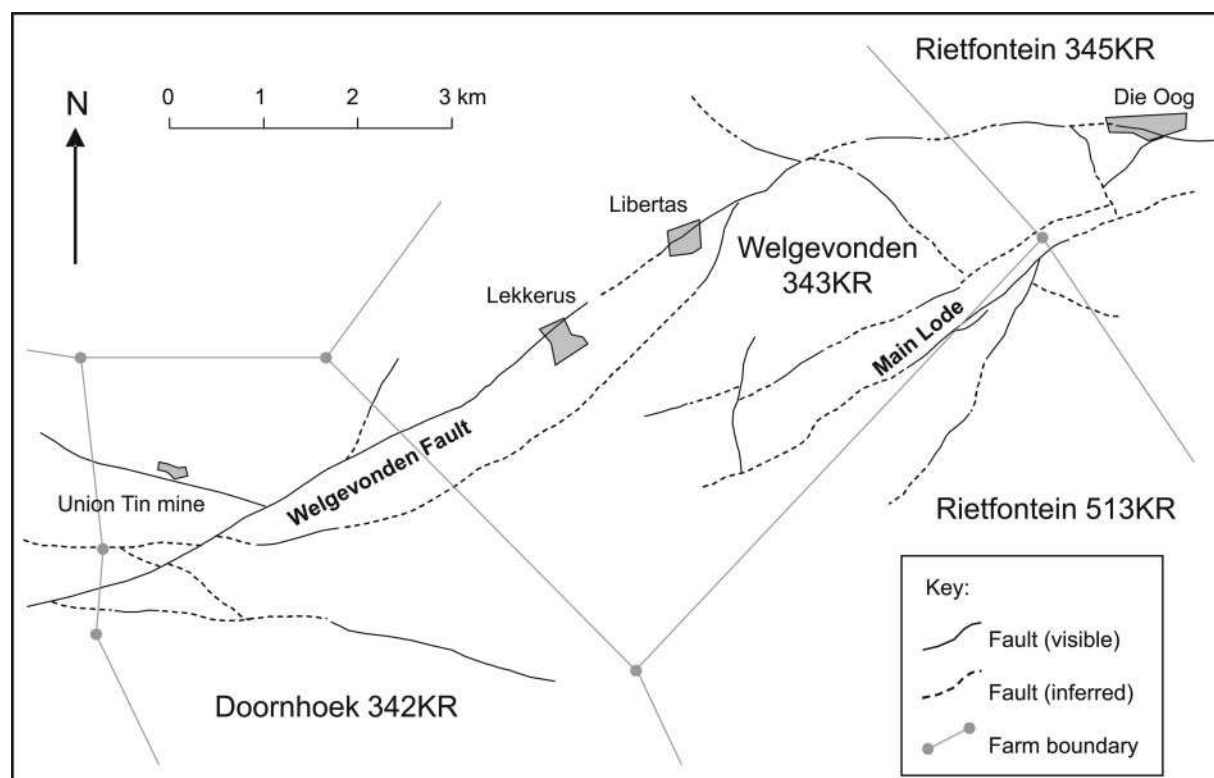
cubes) of (visually) pure felsic and mafic lithologies were prepared using a small diamond saw. These small cubes were broken into chips using a hammer and then hand ground in an agate mortar and pestle.

Solutions for analysis were prepared by fusing the samples with Li metaborate flux and dissolving the resulting melt in 2% HNO₃. Concentrations of major and trace elements were determined using a combination of ICP-OES and ICP-MS. A more complete description of all the analytical procedures for rock samples is given in McDonald and Viljoen.²² Water samples were collected from hot springs in plastic bottles, filtered on site under vacuum through 0.45 µm filters using a hand pump and later acidified to an effective acidity of 10% HCl using ultrapure concentrated HCl, before analysis by ICP-MS.

Results

The results of the mapping carried out in this study are presented in Fig. 6. This new map confirms many of the

findings of van Rooyen³⁶ (Fig. 3) but resolves some of his broad lithological units into individual rock types and adds considerably more structural detail. Both the Rooiberg volcanics and sediments and the younger Mesozoic rocks are cut by high-angle quartz veins that occupy faults, such as the 'Main Lode', which strike approximately NE-SW with a component of down-to-southeast normal movement evidenced by the juxtaposition of Mesozoic sandstones against Palaeoproterozoic felsites. The bedrock geology of the map area is largely concealed by recent ferricrete and by savannah-type cover and vegetation. Lithological contacts are rarely exposed and correlation along strike between isolated exposures is made tentative by the extensive cover and by the paucity of continuous marker horizons and distinctive stratigraphic sequences. Correlation is also complicated by the obliteration of kinematic indicators by quartz veining in the faults, which precludes even a simple estimation of separation or sense of displacement across the veins. For these reasons a detailed stratigraphic column is not attempted.



5 Structural interpretation of the study area based on aerial photographs 998 and 1005 (modified from Ref. 20)

Lithologies

The oldest lithologies are volcanic effusives and associated sedimentary rocks belonging to the 2.06 Ga Rooiberg Group⁴⁰ with a divide across the Main Lode between dominantly red and grey massive felsites to the southeast with relatively little evidence of sedimentary interbeds, and a bimodal volcanic sequence to the northwest with more mafic lavas and perceptibly greater volumes of interbedded sedimentary rocks. Cherts and shales occur within the lowermost mapped part of the south block, and cherts and sandstones occur within the north block. A body of dolerite intrudes the far western part of the study area and is probably part of the extensive dolerite sill system of post-Waterberg age shown on the regional geological map (Fig. 1). More detailed descriptions of individual lithologies are given below. Geochemical data for various samples of acid and basic volcanics, sandstones and portions of the mineralised veins are compiled in Table 1.

Felsites

Grey and red felsites dominate the eastern and southern parts of the map area. The felsites are consistently microcrystalline to fine-grained, and three main types are recognised in the map area:

- (i) massive, fine grained, grey and red felsite
- (ii) massive red felsite with small (<2 mm) green pinitoid grains after feldspar phenocrysts
- (iii) layered felsite with local flow structures, with layers and bands defined by differences in crystallinity, vesicularity and lithophysae.

Pebble to cobble sized xenoliths also occur sporadically. Some of these are volcanic blocks and bombs that have formed compactive dimples and sags in the underlying strata and were subsequently overdraped (Fig. 7a).

The present study has revealed two types of irregular quartzite bodies in the felsite:

- (i) vitreous, medium-grained quartz in a partly porous, sugary texture with a dusty, pale pink, interstitial cement that is possibly a clay derived from altered feldspar. These bodies have thicknesses of a few metres on the surface. The clarity of the quartz grains suggests that the rock is not sedimentary, and one possibility for its genesis is alteration of felsite in hydrothermal pipes, where feldspar was broken down to fine mica and the chemically resistant quartz left largely unaffected
- (ii) amorphous, totally recrystallised red quartzite that probably represents fragments of a pre-eruptive metasedimentary sequence.

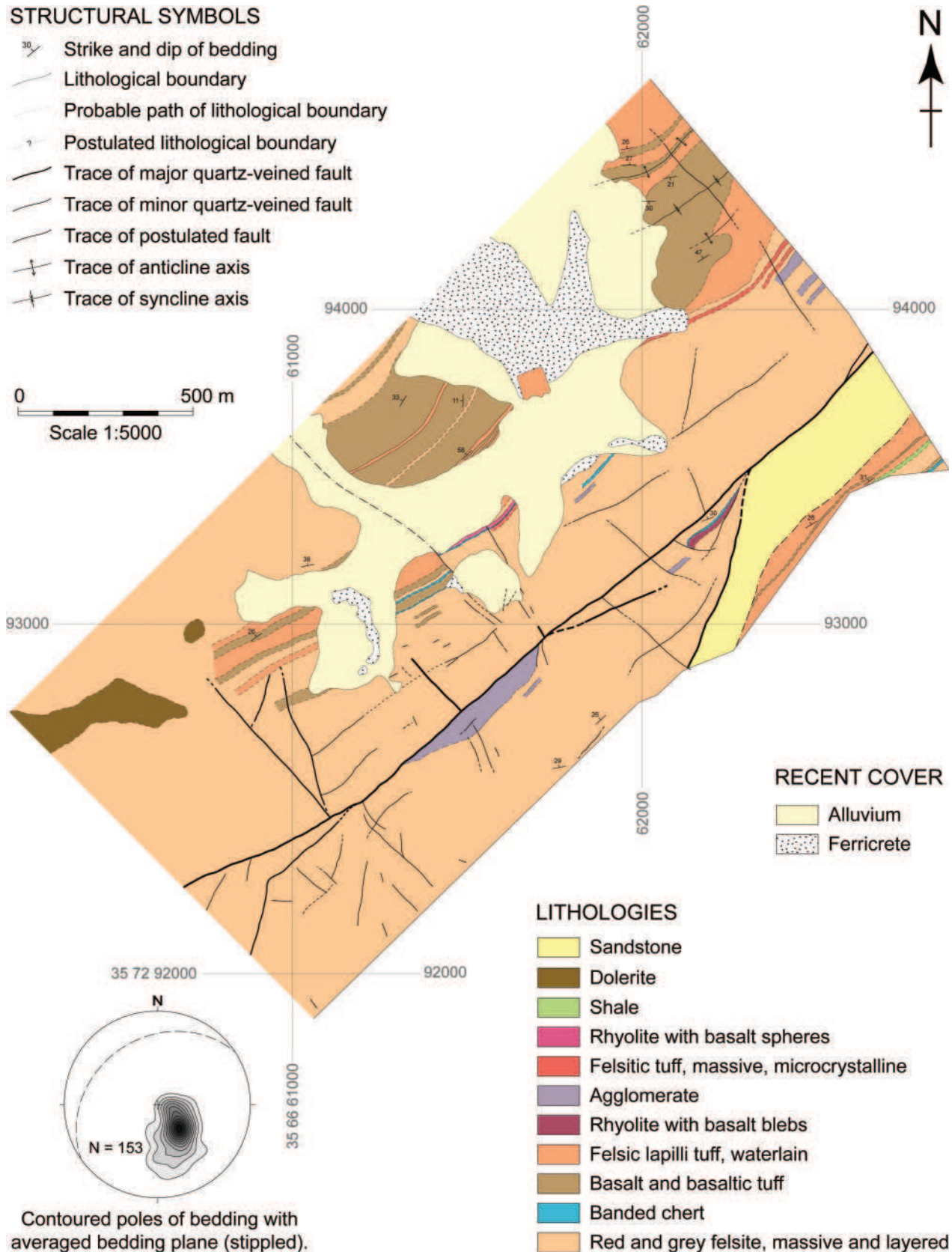
Agglomerate

The term 'agglomerate' is used for a rock of porphyritic appearance containing 5–40 mm, dark brown angular clasts in a paler, fine-grained groundmass (Fig. 7b). There is no oriented fabric and the surfaces of clasts are slightly indented relative to the groundmass as a result of differential weathering. The general appearance of the clasts is similar to the altered felsite fragments of the Main Lode, so they may be early formed felsite that underwent a degree of alteration before being fragmented by an erupting magma to form a volcanic mush. Units of agglomerate several metres thick occur at various levels in the stratigraphy, and continuously for more than 400 m in a thick bed or lens adjacent to the hangingwall contact of the Main Lode. It is interesting to note that this prominent band of agglomerate coincides with the area between Number 3 and Number 6 winzes on the Welgevonden section of the original mine, where high PGE grades were proven during mining.^{23,39}

STRUCTURAL SYMBOLS

- Strike and dip of bedding
- Lithological boundary
- Probable path of lithological boundary
- Postulated lithological boundary
- Trace of major quartz-veined fault
- Trace of minor quartz-veined fault
- Trace of postulated fault
- Trace of anticline axis
- Trace of syncline axis

0 500 m
Scale 1:5000



6 Detailed map of the geology surrounding the Waterberg hydrothermal platinum deposit. The map area comprises the eastern part of Welgevonden 343 KR and northern part of Rietfontein 513 KR (cf. Figs. 2–5)

Basalts and basaltic tuffs

Microcrystalline to fine-grained plagiophyric basalt occurs in 20–50 cm thick, internally massive layers representing individual flows northwest of the Main Lode. The outer 2–3 cm of exposed layering surfaces is a

red weathering rind that superficially resembles felsite, but a darker rock is revealed on fresh surfaces. The relatively resistant basalt layers are conspicuous by their protrusion above the eroded felsites and felsic tuffs and by their smoother layering and fracture surfaces

(Fig. 7c). Cavities after plagioclase phenocrysts are seen in this massive basalt. Basaltic tuffs also occur in thinner, upward-fining, graded beds up to a few centimetres in thickness (Fig. 7d), some of which have a basal zone of tiny (~1 mm) lapilli. Geochemical analysis of samples 99-22 and 99-25, collected from different flow units located close to and far from the Main Load, shows that although the basalts have been extensively affected by alteration and silicification, concentrations of Mg, Fe, Cr and Ni remain significantly higher than the felsites (Table 1).

Silicified basalt spheres in rhyolite

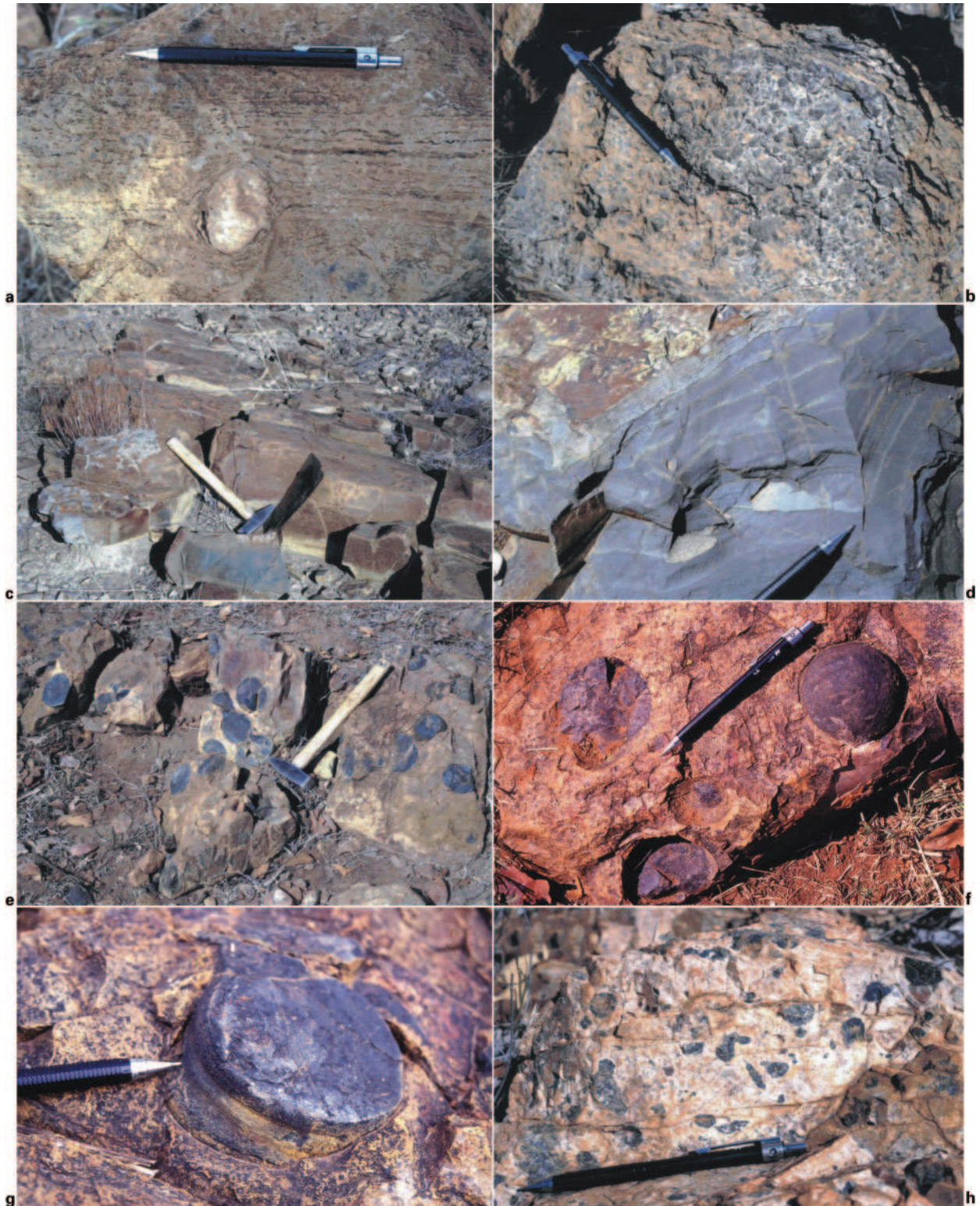
This highly distinctive lithology occurs northwest of the Main Lode and consists of a very fine-grained, massive, yellow-brown rhyolite containing randomly distributed, fine grained, apparently mafic bodies in the form of spheres that are 5–8 cm across (Fig. 7e and f). The boundaries between the dark spheres and surrounding pale rhyolite are consistently sharp. The rock was found at one locality only (see Fig. 6) where it has a

stratigraphic thickness of a few metres with concealed upper and lower contacts. It overlies a 1.5–2 m thick unit of banded chert and underlies an extremely fine-grained, hard, massive lithology of uncertain thickness, texturally resembling silt- or claystone. Weathered-out dark spheres and large chert blocks were found 200 m further west, indicating that the unit continues at least that far. Sample IM-B/SP (Table 1) is a ~8 cm³ cube cut from the centre of one of the largest mafic spheroids in this unit.

In three dimensions, some of these mafic bodies are not spherical but exhibit tubular or crude caterpillar-like forms (e.g. Fig. 7g), which is interpreted as an expression of pinching of a single mafic globule in plastic state, in an igneous analogy to tectonic boudinage. Other mafic bodies display a peanut-shell shape, interpreted as either an advanced stage of pinching where a single large globule in a plastic state was in the process of splitting when it solidified; or two globules collided gently, began to fuse, and solidified. There is other evidence of collision and/or fusing of more than two globules of different sizes in a molten or near-plastic state.

Table 1 Geochemical data for Waterberg vein samples and country rocks

Sample	IM-B/SP	99-25	99-22	99-21B	99-21A	99-21F	95-6	99-STN	99-4a	99-2	W317	W347	W350
Lithology	Basalt	Basalt	Basalt	Basalt	Felsite	Felsite	Felsite	Stone	Stone	Vein	Vein	Vein	Vein
Major elements													
SiO ₂ Wt-%	63.97	72.03	69.29	64.15	77.32	78.77	80.35	91.84	98.74	69.65	93.97	74.05	92.81
TiO ₂	0.68	0.25	0.48	0.77	0.26	0.30	0.23	0.13	0.01	0.23	0.08	0.24	0.05
Al ₂ O ₃	16.60	10.78	13.44	15.36	12.07	10.88	11.66	3.82	0.71	4.95	2.98	4.83	1.53
Fe ₂ O ₃	9.35	6.94	7.84	12.91	3.12	1.99	2.62	0.63	0.45	21.71	2.24	18.94	4.13
MnO	0.02	0.07	0.02	0.03	0.01	0.01	0.02	0.01	0.01	0.03	0.01	0.02	0.01
MgO	4.74	3.82	2.80	2.74	0.31	0.28	0.31	0.01	0.1	0.27	0.17	0.36	0.15
CaO	0.89	0.26	0.52	0.82	0.01	0.16	0.07	0.01	0.01	0.03	0.01	0.03	0.02
Na ₂ O	1.09	0.30	0.87	1.43	0.14	0.18	0.17	0.08	0.02	0.02	0.02	0.01	0.01
K ₂ O	1.19	3.19	2.45	0.38	4.03	4.14	3.89	0.61	0.12	1.2	0.52	1.38	0.28
P ₂ O ₅	0.13	0.03	0.02	0.05	0.02	0.02	0.03	0.01	0.01	0.04	0.01	0.05	0
LOI	0.83	2.27	1.56	1.04	2.52	2.16	1.32	3.13	0.53	1.46	0.67	0.79	1.17
Total	99.49	99.95	99.30	99.68	99.82	98.89	100.68	100.29	100.71	99.59	100.68	100.70	100.16
Trace elements													
Sc ppm	33.7	4.2	14.5	51.6	3.4	3.2	4.4	1.8	0.3	10.5	1.6	6.4	1
V	62.3	34.7	20.2	84.5	2.2	22.9	8.1	45.6	2.5	45.3	7.4	15.5	6.1
Cr	78.8	203	95.3	110	2.9	17.9	8.0	7.1	21	20.3	281	229	25.8
Co	15.7	11.9	9.9	20.9	2.0	4.8	3.2	6.3	0.4	11	1.4	2.5	1.1
Ni	324	178	23.2	82.4	3.7	6.2	8.3	12.4	29.5	28.5	30.9	29.9	38.4
Cu	85.7	34.4	145	131	31.4	132	39.4	0.7	2.2	205	22.7	177	34.7
Zn	88.9	72.3	147	111	15.8	54.8	29.1	7.5	6	89.5	12.8	93.5	10.4
Ga	35.4	14.8	36.4	37.0	19.7	18.6	16.2	6.1	1.9	10.2	5.7	11.6	3.2
Sr	117	24.0	81.8	133	6.1	31.5	19.8	13.5	5.9	13.9	9.5	14.8	6.8
Y	107	47.9	45.3	26.1	64.6	51.9	52.4	12.1	0.5	48.3	20.9	48.9	7
Zr	313	391	410	315	459	372	402	379	4	140	79.1	130	48.2
Nb	4.8	19.0	11.5	5.9	19.2	24.0	20.1	12.9	0.3	71.3	9.1	18.9	3.4
Ba	409	316	305	226	741	719	641	162	71.5	214	157	131	45.9
La	130	48.1	22.1	47.6	98.3	50.2	79.5	16.1	0.9	55.1	27.3	191	25.7
Ce	175	50.4	52.3	59.4	123	103	102	17.8	1.2	23.2	36.6	228	20.7
Pr	25.7	9.9	6.1	9.2	21.3	11.4	17.0	3.0	0.3	9.4	5.2	29.6	3.4
Nd	79.9	32.8	23.5	28.4	70.8	39.9	56.1	9.8	0.9	27	15	81.8	9.4
Sm	15.2	5.6	6.7	5.3	13.6	7.9	10.4	1.9	0.2	4.3	2.4	10.5	1.2
Eu	3.7	1.0	1.4	1.4	2.5	1.4	1.8	0.4	0	0.5	0.3	0.9	0.1
Gd	15.0	5.2	6.3	4.6	11.6	7.2	9.4	1.4	0.2	4.3	2.2	8.1	1
Tb	2.6	0.9	0.9	0.7	1.7	1.1	1.6	0.2	0	0.8	0.4	1.1	0.2
Dy	17.1	6.2	5.5	3.9	10.2	6.9	8.2	1.6	0.2	6.3	2.5	7.2	1.2
Ho	3.1	1.4	1.1	0.8	1.8	1.4	1.6	0.4	0	1.3	0.6	1.4	0.2
Er	9.0	4.8	3.9	2.5	5.5	4.7	4.3	1.3	0.1	4.6	2	4.9	0.8
Tm	1.3	0.8	0.7	0.4	0.9	0.8	0.7	0.3	0	0.8	0.3	0.8	0.1
Yb	7.9	5.6	5.0	3.2	6.0	5.4	4.8	1.9	0.1	5.2	2.3	5.2	0.9
Lu	1.1	0.9	0.8	0.6	0.9	0.9	0.8	0.3	0	0.8	0.4	0.8	0.1
Hf	7.6	9.5	9.3	8.3	10.3	9.4	9.6	8.6	0.2	3.3	1.7	3.2	1.2
Ta	0.9	1.2	1.6	0.9	1.3	1.3	1.9	0.2	0	0.6	0.3	0.7	0.2
Th	14.8	18.4	13.5	16.2	20.3	16.7	28.0	7.5	0.1	28.7	8.7	27.7	4.2
U	4.1	4.2	4.9	4.6	5.4	5.0	8.9	2.0	0.3	10.6	1.9	5.5	2.8



a volcanic bomb in layered felsite (UTM coordinates 62539 94116): note depression beneath and draping above the bomb; *b* agglomerate adjacent to the Main Lode; *c* thick-layered basalt north of the Main Lode (UTM 61310 93740); *d* layered and graded basaltic tuffs north of the Main Lode (UTM 61486 93720); *e* rhyolite with basaltic spheres north of the Main Lode (UTM 61628 93537); *f* close view showing spherical nature of basalt; *g* example of elongate tubular basalt in rhyolite; *h* rhyolite with basalt blebs south of the Main Lode (UTM 62227 934386): hammer is 40 cm long; pencil is 12 cm long

7 Felsic and basic volcanics

The segregation into mafic bodies and felsic groundmass probably occurred before eruption of the mixed magma, as the contacts are sharp, indicating that mafic bodies may have been in the solid state at time of extrusion. Furthermore, it is unlikely that the mafic

bodies were deposited as bombs, as there is no evidence of other ejecta in the rhyolitic groundmass, no evidence of impact disturbance of the groundmass, and no evidence of impact fracturing in the mafic bodies. It is suggested that the rock formed by injection of a hot



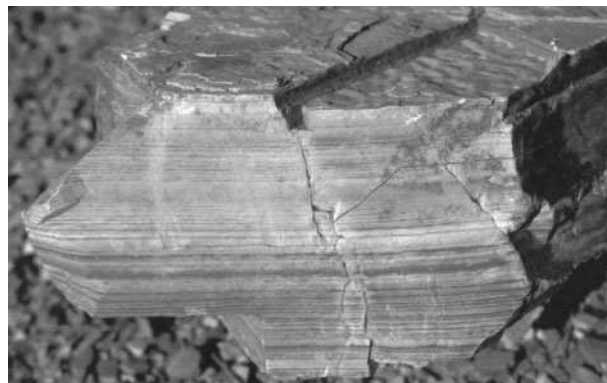
8 Layered lapilli tuff with basal zones rich in spherical lapilli (UTM 61958 94570)

mafic melt into cooler felsic magma chamber, with consequent segregation of the mafic melt into globules due to thermal and density contrast with the felsic magma. The hotter mafic globules were cooled below their solidus temperature, crystallised, and were carried as solid bodies in the felsic magma during effusion or relatively gentle eruption. It is possible that the injection of mafic melt superheated the felsic magma above its liquidus temperature and induced eruption.

An equally peculiar variant occurs in a 15–20 m thick unit southeast of the Main Lode. Here, the mafic component is present as very irregular rounded blebs up to 4 cm in the longest axis, in a groundmass that is paler and finer (Fig. 7h) than the variant northwest of the Main Lode. These distinctions, in addition to the fact that the lithologies under- and overlying the two variants are entirely different, makes it unlikely that they are part of a single unit tectonically repeated across the Main Lode. Rather, they probably represent related but temporally separate episodes of igneous activity in a cyclic igneous process. The finer grain size, more irregular bleb shapes and smaller bleb size of the southeastern variant probably attests to a shorter time between magma mixing and eruption. In this interpretation, the mafic component has either been injected more suddenly and dispersed, or been disrupted to a greater degree after its injection into the felsic melt, relative to its counterpart northeast of the Main Lode. There was neither the time nor sufficiently calm thermal and fluid conditions in the host melt to allow development of the mafic component into larger globules or spheres. Sample PA-99-21 is an example of this rock and analyses of separated mafic and felsic components (99-21B and 99-21A and 99-21F respectively) are shown in Table 1. The mafic portion is enriched in Ti, Al, Cr, Co, Ni (and somewhat surprisingly, Na) compared with the felsic portion. Elevated concentrations of immobile Al and Ga in the mafic portion probably reflect significant plagioclase in the primary rock although only traces were found in thin section. This feldspar has been altered by later fluids, with considerable removal of Ca and to a lesser extent, Na.

Layered felsic lapilli tuffs

Units of layered tuff occur north and south of the Main Lode, interbedded with felsites or, more commonly in the north, with basalts and basaltic tuffs. These felsic tuffs are characterised by 1–3 cm thick rhyolitic (*sensu lato*) beds, most of which exhibit a basal zone of up to



9 Rippled marked shale in a cutting on the north side of unpaved road in far southeast corner of map area (UTM 62669 93616)

70 vol.-% grey or red, 1–2 mm microgranitic lapilli. The lapilli appear spherical in hand specimen but have slightly irregular, ragged edges under a microscope. The groundmass is very fine-grained throughout with a tan/beige, sometimes pale grey colour (Fig. 8). Wave ripples and scour marks are well developed on some bedding surfaces, indicating subaqueous deposition or reworking of pyroclastic materials. A finer-grained, harder variant, common in the northern part of the map area, exhibits a regular lamination (layers <1 cm). This variant has smoother fracture surfaces and is darker, with no observed evidence of water action.

Shale

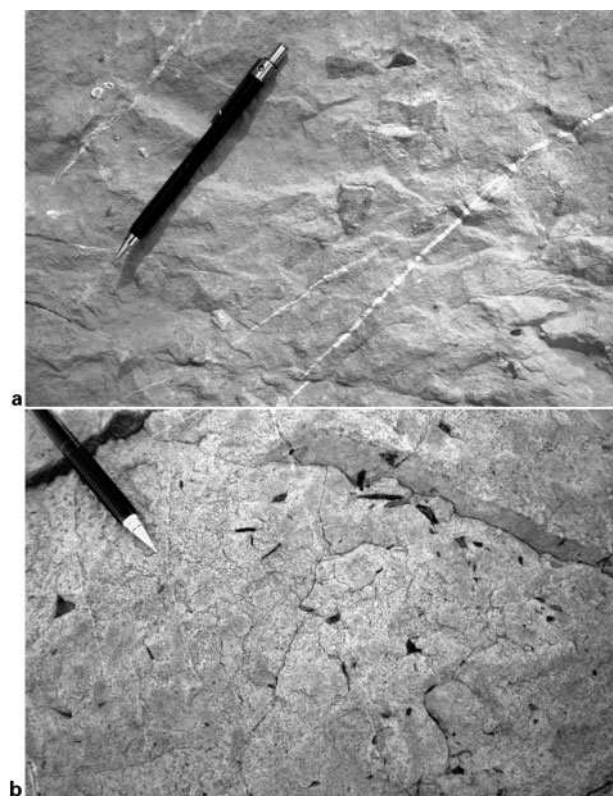
A highly fissile, brown shale with a purple hue is well exposed at the roadside below the farm perimeter fence close to the southeast corner of the map area (Fig. 6). The shale exhibits a very planar and well-defined lamination, a characteristic green colour on fracture/joint surfaces, and small ripples on some bedding surfaces (Fig. 9). The orientations of bedding in both the shale and the Rooiberg lithologies north of the Main Lode are similar, and the lithologies overlying the shale are similar to others elsewhere in the map area, suggesting the shale is of Rooiberg age. The shale is meso- and microscopically devoid of fossils, and there is no other evidence that it belongs to a younger sequence.

Banded chert

Cryptocrystalline chert with characteristic conchoidal fracture occurs as numerous 0.5–2 m thick beds throughout the sequence to the northwest of, and distant from, the Main Lode, but is rare within the red and grey felsite to the southeast and immediately northwest of the Main Lode. The chert bands are characterised by slightly undulating bands up to a few millimetres thick with white, grey, black and red colouring, and may have formed through alteration of felsites.

Massive microcrystalline lithologies

A number of minor, microcrystalline lithological units of uncertain genesis also occur within the stratigraphy. Most cannot be traced for more than a few meters along strike beneath the cover and are therefore not mapped as discrete units. Texturally, most of these lithologies resemble clay- or siltstone but do not display the typical fracture or jointing pattern of pelites, and their colours



10 *a* friable Bushveld sandstone with accidental lithic fragments south of and abutting the Main Lode (UTM 62399 93679) and *b* Bushveld sandstone south of the Main Lode with dark, angular fragments: origin of these features remains to be resolved (UTM 62317 93601)

vary from cream through pale grey to deep red-brown. They are interpreted as very fine-grained volcanics that may represent the lightest, latter stages of felsic pyroclastic deposits.

Dolerite

An undeformed, medium- to coarse-grained dolerite with very minor sulphide (pyrite-chalcopyrite) mineralisation crops out as scattered small, rounded, resistant knolls protruding from the cover in the west corner of the map area (Fig. 6). The margin of the dolerite is not exposed and is inferred to occur between the observed exposures of dolerite and surrounding felsite. The inferred trace of the margin appears gives the dolerite body an irregular shape that is discordant to bedding in the country rocks. The relative chronology of intrusion, faulting and quartz veining is unknown, as no definitive cross-cutting relationships were found. However, the dolerite could belong to a hypabyssal system of post-Waterberg age that crops out at many locations in the Nylstroom region, particularly in the Waterberg Group north of the map area (Fig. 1), or may be even younger; a Karoo age intrusion.

Sandstone

The southeastern part of the study area is dominated by a friable, cream to pink, fine-grained sandstone containing accidental lithic fragments of various lithologies up to pebble size and spheres of hard sandstone up to 8 mm in diameter (Fig. 10). Another distinct minor component is small, dark, elongate, sharp-ended clasts that

appear to be concentrated in local clusters. Although the sandstone matrix looks homogeneous in outcrop, microscopic inspection shows it to be quite poorly sorted at the fine end of the grain size scale.

The unit is bounded to the north by the Main Lode and to the west by an older NNE-SSW trending fault that has been filled by a quartz vein. Throughout the exposure, the angular clasts comprise a very small proportion of the rock volume and their distribution is highly variable. A number of spoon-shaped and spoon-size brown stains were observed, possibly representing microslumps in the unconsolidated sand. The discontinuities created by the slumps were later preferentially stained by Fe oxides during burial and consolidation.

Adjacent to the hydrothermal quartz veins, the sandstone has been chemically indurated to a hard quartzite. A very fine lamination was observed at a couple of localities, but unfortunately only in loose blocks. Therefore the orientation of the bedding/lamination, and thus the relationship of this unit to the Rooiberg lithologies, could not be confirmed. The friability of the rock, however, attests to a relatively young age and it has been previously mapped as sandstone of Karoo age by workers familiar with this sequence in the region.^{16,35,37} In fact, the sandstone belongs to the horizontal Mesozoic sedimentary sequence deposited in pull-apart basins and half grabens of the Sprinkbok Flats and it has been assigned to the (Triassic) Clarens formation on the 1:250 000 scale Nylstroom geological map.⁵ Large angular clasts and the pea-size spheres are frequently encountered, and represent silicified CaCO_3 concretions of an inorganic nature (H. Praekelt, pers. comm., 2007), although the small spheres may have been organically induced. The origin of the smaller, dark, angular fragments also observed remain uncertain: one interpretation is that they represent petrified wood, which would point to a post-Silurian age, compatible with the interpreted Mesozoic age for the sandstone, and another is that they are Fe-oxides which were accumulated during the original aeolian formation of the Clarens sandstones (ibid.).

Structural geology

Bedding

A stereonet showing contoured poles of bedding in Rooiberg volcanic and sedimentary lithologies is given in Fig. 6. The strike of bedding is generally NE-SW but varies between N-S and E-W, with gentle to moderate dips but approaching steep angles at a few localities. Layering was not observed *in situ* in the younger sandstone in the southeastern part of the map area.

The spread of dip angles between 7 and 65° has an uncertain cause. Possible explanations are:

- (i) draping of volcanic rocks over an irregular substrate
- (ii) fault-block rotation and drag folding adjacent to faults
- (iii) doming of bedding over volcanic vents in Rooiberg time and by emplacement of post-Rooiberg igneous bodies such as the post-Waterberg hypabyssals or the Nebo Granite, which crops out on the adjacent farms Rietfontein 513KR and Rietfontein 345KR (Fig. 3)

- (iv) folding, which is addressed in more detail below.

Any combination of these mechanisms is also possible.

Faults

Since the Main Lode is a quartz vein that is known to occupy a fault and the stratigraphy of the area is largely covered, it was decided the best way build a structural image of the area was to locate and trace the resistant quartz veins that protrude above the cover. Three sets of veins were identified:

- (i) NE-SW to ENE-WSW striking quartz veins representing faults and fractures subordinate to the similarly oriented Main Lode (Fig. 6)
- (ii) NW-SE quartz veins of unknown tectonic character. The largest of these veins may represent faults, as the dolerite in the west seems to be disrupted or truncated in the vicinity of an extrapolated major NW-SE vein. This particular vein was extensively trenched for exploration and despite the very different strike direction to the Main Lode, and the intensive trenching indicates the high significance attached to the lode-like fabric of the vein
- (iii) NNE-SSW and NNW-SSE striking, minor quartz veins. Only a minority of these exhibit the brecciated altered felsite seen in the Main Lode and other major veins, and even in these cases the felsite clast content is minor. Many of these veins are characterised by coarse 'dog tooth' quartz rather than massive hydrothermal quartz or generations of comb quartz that characterise the major veins. One exception is a NNW-SSW striking, trenched vein close to the southwest boundary of the map that meets the Main Lode at the same point as a major NW-SE vein (Fig. 6).

There are other significant quartz veins that have unique or uncommon orientations. One of these is the Branch Lode, interpreted as a splay fault that narrows north-eastwards and either rejoins the Main Lode further northeast (as inferred in Fig. 6) or is cut by an equally large vein striking NNE-SSW. This large vein is certainly a fault because it juxtaposes Rooiberg lithologies against Mesozoic sandstone. It was not recognised by Wagner and Trevor³⁸ but does appear on van Rooyen's local map (Fig. 4). Unlike the main and Branch Lodes, however, it contains little other than massive hydrothermal quartz, which probably explains why no exploration trenches are found along it. Another intensively trenched vein branches SW from the Main Lode at its western end and exhibits a peculiar 'knee' where its strike changes abruptly to SSW.

Three veins with an approximately NE-SW strike and slightly arcuate trace occur northwest of the Main Lode (Fig. 5). Together they define an *en echelon* pattern and, assuming that their proximity and approximate parallelism to the Main Lode indicates they are coeval, the pattern indicates a dextral shear component. Trenches were excavated in two of these three *en echelon* veins and the trenching immediately northeast of the Lumavoha farmhouse was probably carried out by Doornhoek Platinum Ltd, who explored this area adjacent to Transvaal Platinum's property in 1925–1926 without success.²³

Cross-cutting relationships are rarely exposed and are inconsistent. For example, some NW-SE striking veins can be traced across the Main Lode without offset and would appear to have formed later than the Main Lode. However, a greater number of NW-SE veins appear to be truncated by the Main Lode and are therefore older. This suggests two generations of NW-SE veins.

Quartz veining has completely obliterated kinematic indicators in the main fault zones. A few small-scale, brittle fault planes some distance from the quartz veins display sets of slickenlines and slickensteps overprinting each other, expressing movement in 2–3 very different directions. In road cuts a short distance east of the map area, several well developed brittle planes with a steep to subvertical orientation show unambiguous evidence of movement. Here, slickenlines and slickensteps on NW-SE to NNW-SSE striking planes express subhorizontal dextral movement, while similar indicators on N-S striking planes express oblique down-to-southeast movement. Geometrically and kinematically these appear to have no relationship to the Main Lode.

Folds

Folds are rare and poorly exposed. In the northeast part of the map area, adjacent to the perimeter fence, opposing dip directions to the northwest and southeast over distances of a few metres to several tens of metres makes compelling evidence for folding. The interpreted axial traces are parallel to those of the map-scale folds on the Nylstroom 1:250 000 scale geological map⁵ and a parasitic relationship is therefore suggested. Weak, subhorizontal to gently plunging parasitic folds may contribute to the variation in angle of dip throughout the map area.

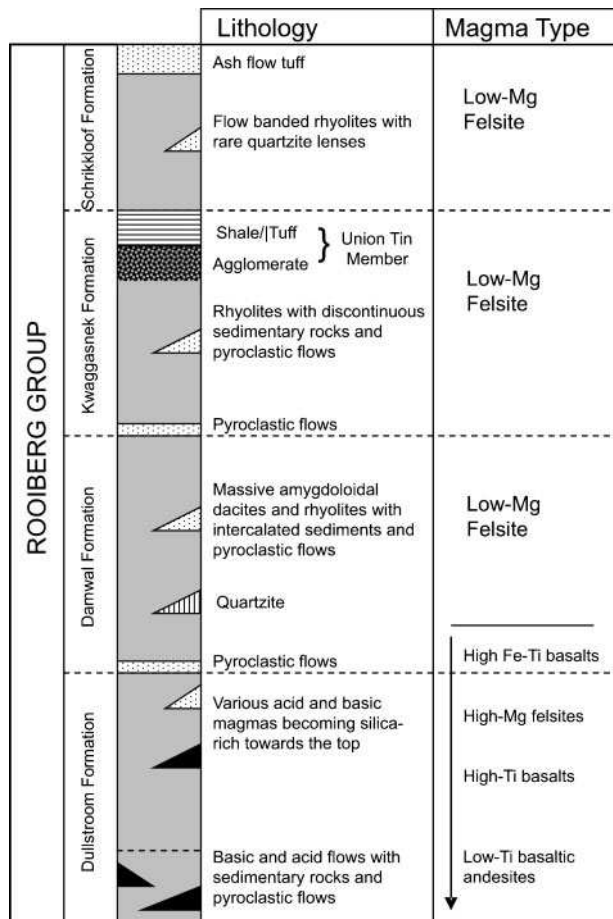
In the northeastern area where mesoscale folds were observed, van Rooyen³⁶ also recognised changes in dip direction. His map extends into the neighbouring farm Rietfontein 345 KR (Fig. 4) and shows the dip of bedding to vary between west and northeast, implying either part of a local dome or a north to northwest trending, moderately plunging fold axis.

Weakly developed, decimetre- to metre-scale, north-east-verging monoclines occur sporadically and have a well-developed axial-planar cleavage. These structures are scarce and their tectonic significance is not clear. In best estimation, they suggest a minor top-to-east movement relative to bedding. Again, this is compatible with a dextral component of shearing along the fault zones.

Discussion

Implications for Rooiberg Group stratigraphy and the main Bushveld magma chamber

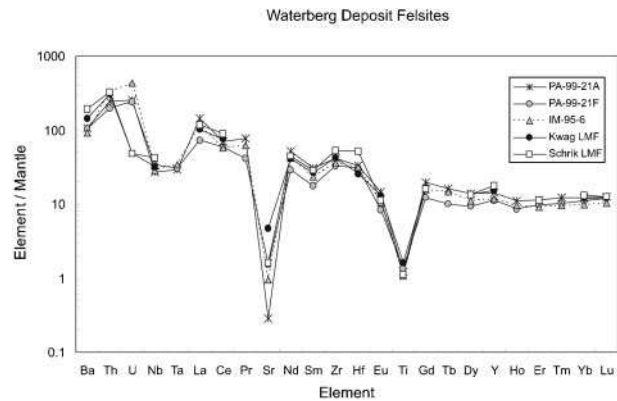
A surprising variety of lithologies, including intriguing expressions of bimodal volcanism and especially magma mixing, are developed in the Rooiberg Group rocks around the Waterberg deposit. This variety is unexpected if these units forms part of the upper Rooiberg Group (Kwaggasnek and Schrikkloof Formations) as is currently assumed on the regional geological map.⁵ The regional Rooiberg stratigraphy, compiled by Hatton and Schweitzer,¹¹ Schweitzer *et al.*³⁰ and Twist,³⁴ indicates a significant component of mafic lavas in the lower Rooiberg (Dullstroom formation) but only acid lavas and volcanoclastics in the upper Rooiberg group



11 Stratigraphy of the Rooiberg Group showing the expected predominance of felsic volcanics in the Kwaggasnek and Schrikkloof formations (modified from Refs. 11 and 31)

(Fig. 11). This leads to the conclusion that either the units observed here are not upper Rooiberg, or that mafic lavas were involved at different times and in different places across the Rooiberg volcanic province, and that the 'classic' stratigraphy, compiled from other Rooiberg sequences distant from Mookgophong, may oversimplify important volcanic facies variations. Apart from higher concentrations of U, which may have been introduced by later fluid activity, the felsites found around the Waterberg deposit are geochemically identical to the mean compositions of conventional Kwaggasnek and Schrikkloof low Mg felsites (Fig. 12), suggesting that the acid volcanics are probably also part of the upper Rooiberg and the presence of basic volcanics is anomalous.

Geochemical analysis shows that all units are heavily silicified and overprinted by Fe, U and REE. However, 'basaltic' units retain elevated levels of Cr, Ni and Co, compared with the felsites (Table 1) and suggest that they do indeed belong to a more primitive magma that was spatially associated with the more voluminous acid magma. It should also be noted that vein samples from the Main and Branch Lodes contain high concentrations of Cr (Table 1). Given the high degree of alteration it is conceivable that the Rooiberg basalts could have supplied some of this Cr to the veins, so the measured Cr concentrations in some basic units may underestimate the original Cr concentration, particularly for



12 Mantle normalised spidergrams of Waterberg felsites compared with mean compositions of Kwaggasnek and Schrikkloof low Mg felsites (LMF)¹¹

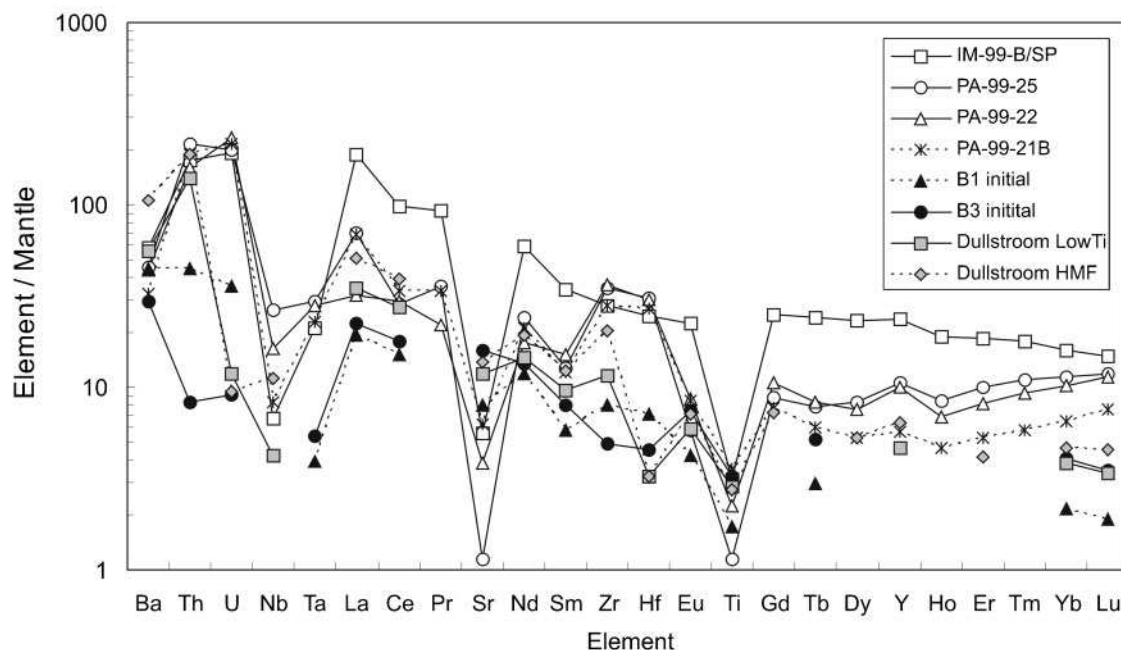
samples close to the lodes. Mantle normalised patterns from some of the basalts (the exception being IMP-99-B/SP, which is highly enriched in REE) show similarities with high Mg felsites and Low Ti andesites from the Lower Rooiberg Dullstroom Formation (Fig. 13), but also the B1 and B3 magma types believed to be parental to the Rustenburg Layered Suite (e.g. Barnes and Maier).¹ Concentrations of Cr, in excess of 200 ppm in the sample furthest from the most intense hydrothermal alteration (PA-99-25), exceed those in any of the Lower Rooiberg mafic lavas, and suggest (at least occasional) eruptions of very basic liquid. Based on the mapping carried out in this study, 10–20% of the volcanic sequence around the deposit may be basaltic. Van Rooyen³⁶ previously mapped these rocks as undifferentiated tuffs and traced similar units across the region (Fig. 3) suggesting that a larger volume of basic rocks may be present outside of the immediate study area.

These findings of high Cr volcanics are significant in the context of the wider Bushveld Complex as some workers (e.g. Cawthorn and Walraven³) have suggested that, in order to account for the enormous quantities of olivine and chromite in the Lower and Critical Zones of the Rustenburg Layered Suite (RLS) of the Bushveld complex, large volumes of magma (partially depleted in Cr and Mg) may have periodically escaped the main Bushveld magma chamber, either as lateral hypabyssal intrusions or as lavas, presumably after the RLS chamber was developed underneath the low density Rooiberg carapace. To date there has been no field evidence to support Cawthorn and Walraven's suggestion and it has remained controversial.^{7,15} This may be the first evidence to support occasional eruption of relatively Cr-rich mafic magma in Upper Rooiberg times and it merits further research.

Structural setting

In terms of structural geology, an obvious point to emphasise is that the Main Lode occupies a relatively recent fault that provided a ready pathway for fluids. This seems to be the case for most of the quartz veins in the study area, and while the local structural pattern is inconclusive when considered in isolation, it becomes more significant in the context of known regional structures. The northwesterly dip of bedding reflects the location of the map area on the northern limb of the approximately east-west trending Swaershoek Anticline

Waterberg Basic Volcanics



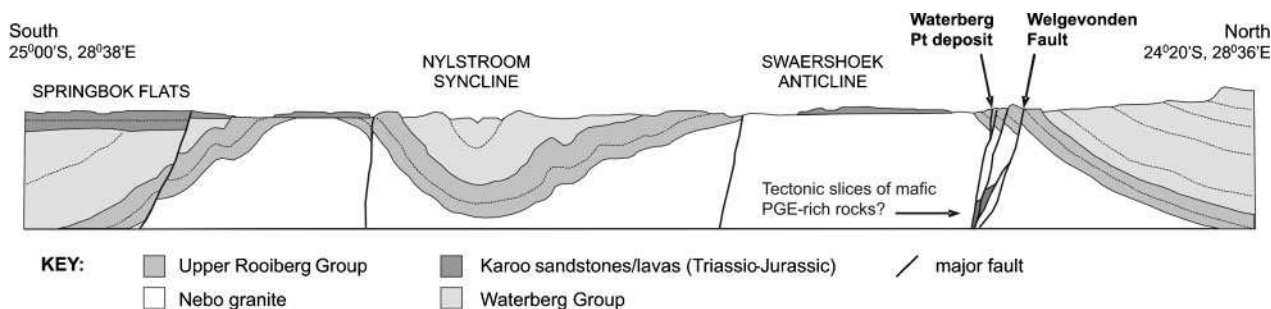
13 Mantle normalised spidergrams of Waterberg felsites compared with mean compositions of Lower Rooiberg Group Low Ti andesites (Low Ti) and high Mg felsites (HMF):¹¹ mantle normalisation values from Taylor and McLennan³³

(Figs. 1 and 14), which is cogenetic with the Nylstroom Syncline, Zwartkloof Anticline and related folds to the south. As the anticlines have west-pointing closures and the synclines have east-pointing closures, the fold axes are interpreted to have an approximately westward gentle plunge. The axial traces of these folds, however, are slightly bowed and indicate a degree of refolding which is more pronounced near the closures (Fig. 1). The question is whether the refolding was a temporally separate event or a progressive episode in, for example, a transpressional event involving initial folding normal to the shear boundary followed by refolding and axis rotation due to continued shearing. An answer may be sought in larger lineaments to the north and northeast of the study area such as the Welgevonden Fault and the larger Zebediela and Planknek-Ysterberg Faults.

On the Nylstroom 1:250 000 scale geological map, the eastern end of the Welgevonden Fault is suggested to merge with or abut against an unnamed NNE-SSW striking fault and the generally ENE-WSW striking Zebediela Fault (Fig. 1) and the Welgevonden Fault is commonly assumed to be an extension of the Zebediela fault system along the TML relay system.^{6,8} However

there may be an alternative explanation involving the Planknek-Ysterberg Fault which extends ENE from Mokopane for 40 km towards Polokwane (Pietersburg). While the current map indicates a 20 km gap between the eastern end of the Welgevonden Fault and the western end of the Planknek-Ysterberg Fault, both faults possess a near identical strike and there is some evidence to suggest they may merge into a common structure.

Aeromagnetic surveys conducted for exploration of Platereef-type mineralisation south of Mokopane^{27,29} indicate that the Planknek-Ysterberg Fault extends further southwest than shown on the Nylstroom map; across the farms Baviaanskloof 290KR and Waterval 297KR to the edge of the survey area at close to 24°19'S and 28°55'E. There are no publicly available geophysical data with which to trace the fault further southwest but an extrapolation of the strike encompasses the prominent granite scarp that runs across the farms Cyferfontein 298KR and Naboomfontein 320KR as well as an obvious line of waterpumps, disappearing streams and offset drainage that occur at the foot of the scarp and extend WSW on to the farm Rietfontein



14 Cross-section along line X-Y (Fig. 1) perpendicular to the structural grain showing the Welgevonden Fault and the Pt-bearing Main Lode, interpreted by the authors

318KR. The western end of the scarp and its associated hydrogeological features are developed close to the inferred eastern extension of the Welgevonden Fault on Rietfontein 318KR at 24°24'S and 28°46'E, and it is suggested that the Welgevonden Fault and the Planknek-Ysterberg Fault could form part of a larger, linked structure that crosscuts the Zebediela Fault and the unnamed NNE-SSW striking fault.

Some support for movements induced by stresses oblique to the ENE-WSW trend of the inferred Welgevonden-Planknek structure is found in the sigmoidal, strike-slip duplex, flower and transfer fault pattern of the region and in the area around the Waterberg deposit. In Fig. 5, a sigmoid outline is incompletely defined by the Main Lode and Welgevonden Fault. Whatever tectonic regime was in operation when the faults formed, it is clear that the latest movement in the study area involved a significant component of down-to-southeast movement. This indicates a relatively young, extensional event.

Age of faulting and mineralisation

Since the tectonically isolated sandstone in the south-eastern part of the map area is assumed to be of Karoo (Triassic) age,⁵ faulting along the Main Lode and related faults must be syn- or post-Triassic. The major post-Karoo event of interest is the crustal extension and rifting that progressed to the break-up of Gondwana at ~180 Ma. Extension occurred across a roughly NNE-SSW boundary reflected by the present N-S to NNE-SSW trending coastline of the southeastern African continent. The tensional stresses induced by this extension on pre-existing major ENE-WSW striking structures would be expected to cause sinistral transtension along a lineament like the TML, but the studies of Good and de Wit⁸ have revealed little or no response at this time. Furthermore, the admittedly minor indicators of shear sense in the present study are dextral. Thus the age of faulting in the study area, very likely related to an episode or episodes of fault (re)activation, is unknown, but probably younger than 180 Ma. The quartz veining and mineralisation associated with the Main Lode are the youngest features on the deposit-scale geological map (Fig. 6) and could have occurred after development of the initial fault. The concept of 'golden aftershocks' advanced by Mickelthwaite and Cox²⁶ where initial movement on a major structure triggers a period of aftershocks that lead to repeated ruptures and enhanced fluid flow through minor structures, could be important in the development of the Waterberg deposit.

Source of the platinum

The high purity of the native platinum and the greater lateral extent of the mineralisation relative to its vertical depth have led to suggestions that the mineralised veins might represent supergene enrichment of Pt from an earlier deposit or some other host rock (see discussion in Ref. 21). This seems unlikely, given the geometry of the deposit and the lack of any obvious source for supergene enrichment in the felsite. A supergene mechanism, moreover, is at odds with the breccia-hosted nature of the platinum, the vuggy nature of the quartz, and fluid inclusion studies which indicate that inclusions trapped in the platinum-associated quartz homogenised at temperatures around 200°C.²¹ It therefore seems certain that the metals were introduced via a fluid phase. It is

interesting to note that Cabral and Kwito-Ribeiro² came to the same conclusion about the Pd enrichment they observed in the Gongo Soco Fe-ore deposit in Brazil.

There is no obvious source for the PGE and Au in the Main and Branch lodes among the granites, felsites and minor basalts of the area. While these rocks could have supplied LREE, U, and also perhaps some Cr to the mineralising fluid, they lack significant concentrations of PGE and it seems more likely that the Pt comes from a source not outcropping in the immediate vicinity of the mineralisation. It is important to remember that although the Waterberg deposit is enriched in Pt over the other PGE and Au, McDonald *et al.*²¹ have shown that this, coupled with the high purity of the platinum, is likely to be a consequence of highly oxidising fluids and changes in pH which favour deposition of Pd and Au before Pt. This means that the source rocks need not be unusually Pt-rich, and that sources with Pt/Pd ratios significantly lower than those found in the mineralised veins (typically Pt/Pd ranges between 3 and 20) could be sources of the metals.

In this context, the proximity of the Waterberg deposit to larger structures such as the proposed Welgevonden-Planknek Fault system may be highly significant. The Planknek-Ysterberg Fault cuts the mafic rocks of the northern Bushveld Complex immediately south of Mokopane. One possibility is that slivers of PGE-rich mafic bodies such as the Platreef^{12,14,17} or the Volspruit Sulphide Layer^{9,13} might have been displaced from the area where they currently crop out south of Mokopane and be present as disrupted tectonic lenses along the steep fault zone (Fig. 14). This mechanism could provide a metal source by translating fault-bounded slivers of PGE reefs westwards to a position beneath the Waterberg deposit. Indeed, Hattingh and Pauls¹⁰ suggest that gravity signatures northwest of Mookgophong are caused by concealed mafic rocks. Alternatively, the fault system could simply generate an array of shear and fracture zones that became primed for fluids that subsequently liberated and redistributed PGE along the fault network.

A pertinent feature of the Welgevonden Fault is that it hosts leisure resorts (Die Oog, Libertas and Lekkerus – see Fig. 5) based around natural hot springs that exploit a presumably young and near-surface geothermal source. This fault zone is located barely 2 km northeast of the Waterberg deposit. The source of this heat is unclear but ICP-MS analysis of spring waters sampled at the nearby hot springs of Die Oog, Lekkerus and Libertas show only very low concentrations of PGE and Au, close to or below the limits of detection (Table 2) and not significantly different from control hot springs at Warmbaths where there is no known PGE mineralisation. However, considered together with (i) the

Table 2 Concentrations of Pd, Pt and Au in hot spring waters from the Welgevonden Fault (Die Oog, Lekkerus, Libertas) and PGE-poor springs at Warmbaths*

	Warmbaths A	Warmbaths B	Die Oog	Lekkerus	Libertas
Pd 0-033	0-057	0-047	0-052	0-039	
Pt <0-015	<0-015	<0-015	<0-015	<0-015	
Au 0-012	<0-009	0-011	0-021	0-016	

*All concentrations expressed in parts per billion (ng per mL).

likely tectonic relationship between the Welgevonden Fault and the Main Lode, and (ii) the fabrics of the Main Lode which indicate recent quartz veining and mineralisation, the present hot springs may represent a waning, mineral-depleted stage of hydrothermal activity, unrelated to that which generated the Waterberg deposit (cf. Ref. 26).

Another, more exciting possibility is that the PGE source was not tapped and redeposited in only one small area, but that other parts of the fault system with favourable country rocks may also host significant concentrations of Pt. During the early phases of exploration immediately following the discovery of the Waterberg deposit, Wagner and Trevor³⁸ noted other reported discoveries of platinum on several farms (Doornhoek 352KR, Kromkloof 203KR, Geelhoutkloof 202KR and Zuikerboschfontein 198KR) to the west of the Waterberg deposit where the Welgevonden Fault and related veins are also developed. While it is likely that many of these claims were made purely to drive the share prices of the companies owning the land (see discussion in McDonald and Tredoux),²³ most have never been re-evaluated using modern exploration methods and it would be premature to rule out the possibility that another deposit like the Waterberg might exist elsewhere along the structure.

Conclusions

This study has significantly improved geological knowledge of the Waterberg platinum deposit and the surrounding lithologies. Mapping has shown that in the Rooiberg sequence north of the deposit, there is a surprising amount of basic volcanic rocks (basalts and basaltic tuffs) associated with the more voluminous felsites, agglomerates and felsic tuffs. Two volcanic units contain immiscible felsic and basaltic liquids, implying that Rooiberg volcanism in this area was bimodal, with both magmas occasionally erupted together. This episode of bimodal volcanism in the upper Rooiberg sequence has not been recognised before and may have implications for models that invoke occasional loss of mafic magma from the underlying Bushveld Complex magma chamber.

The fault that hosts the mineralised Main Lode is one of the youngest geological features in the area. The strike of the Main Lode parallels the larger, and geothermally active, Welgevonden Fault immediately to the north and it is highly likely that the Main Lode forms a companion structure to the Welgevonden Fault. Furthermore, evidence from aeromagnetic surveys and analysis of topography and drainage patterns to the northeast of the study area suggests that the Welgevonden Fault may be an extension of the Planknek-Ysterberg Fault system that cuts mafic rocks (including PGE reefs) of the Bushveld Complex south of Mokopane. If these faults are linked, it would provide a link to a potential source of PGE for the Waterberg deposit. The PGE could be derived from slivers of PGE-rich reefs that were displaced along the fault zone to a position below the Main Lode, or via fluids that leached PGE from source rocks close to Mokopane and then travelled along the fault zone to deposit platinum and other metals in the Main Lode.

Authors

Paul Armitage graduated with a BA (Hons) in Scandinavian and Icelandic studies from University

College London in 1993 and subsequently gained BSc and MSc degrees in geology from the University of Tromsø, Norway. His main area of study was the structural development of Precambrian terrains in northern Norway, partly in collaboration with the Norwegian Geological Survey. He is completing a PhD at the University of Greenwich, is an academic visitor at the Natural History Museum and currently works as a geologist with London Bridge Associates, a tunnelling consultancy.

Iain McDonald graduated with a BSc degree in Chemistry and Geology from Glasgow University, Scotland, in 1989 and a PhD from the University of Cape Town, South Africa, in 1993. Following post-doctoral work at Manchester University on the genesis of sulphide-poor PGE mineralisation in Madagascar, he became a lecturer in geochemistry at the University of Greenwich. He is currently manager of the ICP laboratories at the School of Earth, Ocean and Planetary Sciences at Cardiff University where he leads an active research group working on the northern limb of the Bushveld Complex.

Marian Tredoux graduated with a BSc degree in Geology, Geochemistry and Chemistry from Stellenbosch University, South Africa, and a BSc (Hons) in Geochemistry from the University of Cape Town. After a spell as a research chemist at JCI Group laboratories, she completed her PhD on the analysis and geochemistry of the PGE at the Schonland Research Centre for Nuclear Sciences, University of the Witwatersrand. Between 1989 and 2005, she was Senior Lecturer at the Department of Geological Sciences, University of Cape Town and is currently Associate Professor at the University of the Free State.

Acknowledgements

Numerous friends and colleagues have helped with advice and gathering material for this study. These include: Ian Pringle, Gerry Levin, Chris Lee, Maarten de Wit, Grant Cawthorn, Herman Praekelt and Simon Dominy. Eveline de Vos is thanked for help with some of the ICP analyses and Nicola Dakin painstakingly separated and crushed basalt and felsite from sample PA-99-21. The paper was improved by an anonymous reviewer. Finally the authors would like to express their thanks to the Bodemer family, the current owners of Lumavoha, for being such warm and hospitable hosts on all the occasions when the authors visited their farm to study these fascinating rocks. The University of the Free State is thanked for financial support.

References

1. S.-J. Barnes and W. D. Maier: 'Platinum-group element distributions in the Rustenburg Layered Suite of the Bushveld Complex, South Africa', in 'The geology, geochemistry, mineralogy and mineral beneficiation of platinum-group elements', (ed. L. J. Cabri), Special Volume 54, 553–580; 2002, Calgary, Alberta, Canadian Institute of Mining, Metallurgy and Petroleum.
2. A. R. Cabral and R. Kwitko-Ribeiro: 'On the rosettes of 'native palladium' from Minas Gerais, Brazil: evidence from Gongo Soco', *Canadian Mineralog.*, 2004, **42**, 683–687.
3. R. G. Cawthorn and F. Walraven: 'Emplacement and crystallization time for the Bushveld Complex', *J. Petrol.*, 1998, **40**, 1669–1687.
4. Centurion Gold Holdings Incorporated: 'Centurion gold holdings doubles its assets with the acquisition of Naboom platinum', Press Release, 28th April, 2005, available at: www.centuriongold.com

5. M. D. Du Plessis (compiler): '1:250,000 Geological Series. 2428, Nylstroom', Council for Geoscience, Pretoria, South Africa, 1978.
6. C. P. Du Plessis and F. Walraven: 'The tectonic setting of the Bushveld Complex in Southern Africa part 1: structural deformation and distribution', *Tectonophysics*, 1990, **179**, 305–319.
7. H. V. Eales: 'Caveats in defining the magmas parental to the mafic rocks of the Bushveld Complex and the manner of their emplacement: review and commentary', *Mineralog. Magazine*, 2002, **66**, 815–832.
8. N. Good and M. J. de Wit: 'The Thabazimbi-Murchison Lineament of the Kaapvaal Craton, South Africa: 2700 Ma of episodic deformation', *J. Geol. Soc., London*, 1997, **154**, 93–97.
9. R. E. Harmer: 'The Volspruit PGE-Ni reef: platinum mineralization in the Lower Zone south of Mokopane', *Goescience Africa 2004, Abstract Volume*, University of the Witwatersrand, Johannesburg, South Africa, 256–257.
10. P. J. Hattingh and N. D. Pauls: 'New palaeomagnetic results from the northern Bushveld Complex of South Africa', *Precambrian Res.*, 1994, **69**, 229–240.
11. C. K. Hatton and J. K. Schweitzer: 'Evidence for synchronous extrusive and intrusive Bushveld magmatism', *J. African Earth Sci.*, 1995, **21**, 579–594.
12. D. A. Holwell and I. McDonald: 'Petrology, geochemistry and mechanisms determining the distribution of platinum-group element and base metal sulphide mineralization in the Platreef at Overysel, northern Bushveld Complex, South Africa', *Mineral. Depos.*, 2006, **41**, 575–598.
13. L. J. Hulbert and G. von Gruenewaldt: 'Nickel, copper and platinum mineralization in the Lower Zone of the Bushveld Complex, south of Potgietersrus', *Econom. Geol.*, 1982, **77**, 1296–1306.
14. J. A. Kinnaird and I. McDonald: 'Preface: an introduction to mineralization in the northern limb of the Bushveld Complex', *Appl. Earth Sci. (Trans. Inst. Min. Metall. Sect. B)*, 2005, **114B**, 194–198.
15. F. J. Kruger: 'Filling the Bushveld complex magma chamber: lateral expansion, roof and floor interaction, magmatic unconformities and the formation of giant chromitite, PGE and Ti-V-magnetite deposits', *Mineral. Depos.*, 2005, **40**, 451–472.
16. H. Kynaston and E. T. Mellor: 'The geology of the Waterberg tin-fields', *Memoir number 4, Geol. Surv. Union of South Africa*, Pretoria, South African, 1909.
17. T. D. Manyeruke, W. D. Maier and S.-J. Barnes: 'Major and trace element geochemistry of the Platreef on the farm Townlands, northern Bushveld Complex', *South African J. Geol.*, 2005, **108**, 391–406.
18. S. McCourt: 'The crustal architecture of the Kaapvaal crustal block South Africa, between 3·5 and 2·0 Ga', *Mineral. Depos.*, 1995, **30**, 89–97.
19. I. McDonald, M. Tredoux and D. J. Vaughan: 'Platinum mineralization in quartz veins near Naboomspruit, central Transvaal', *South African J. Geol.*, 1995, **98**, 168–175.
20. I. McDonald and M. Tredoux: 'Locality 2·3 – Waterberg Platinum Lodes', in *Proc. 8th Platinum Symp. on 'Field excursion to the Bushveld Complex'*, Johannesburg, South Africa, 1998, Geological Society of South Africa, 53–55.
21. I. McDonald, D. Ohnenstetter, J. P. Rowe, M. Tredoux, R. A. D. Patrick and D. J. Vaughan: 'Platinum precipitation in the Waterberg deposit, Naboomspruit, South Africa', *South African J. Geol.*, 1999, **102**, 184–191.
22. I. McDonald and K. S. Viljoen: 'Platinum-group element geochemistry of mantle eclogites: a reconnaissance study of xenoliths from the Orapa kimberlite, Botswana', *Appl. Earth Sci. (Trans. Inst. Min. Metall. Sect. B)*, 2006, **115B**, 81–93.
23. I. McDonald and M. Tredoux: 'The history of the Waterberg deposit: why South Africa's first platinum mine failed', *Appl. Earth Sci. (Trans. Inst. Min. Metall. Sect. B)*, 2005, **114B**, 264–272.
24. E. T. Mellor and A. L. Hall: 'Explanation of sheet no. 7 (Potgietersrust)', *Geol. Surv. Union of South Africa*, South Africa, 1910.
25. T. P. Mernagh, C. A. Heinrich, J. F. Leckie, D. P. Carville, D. P. Gilbert, R. K. Valenta and L. A. I. Wyborn: 'Chemistry of low-temperature hydrothermal gold, platinum and palladium (+/- uranium mineralization) at Coronation Hill, Northern Territory, Australia', *Econ. Geol.*, 1994, **89**, 1053–1073.
26. S. Micklethwaite and S. F. Cox: 'Fault segment rupture, after-shock-zone fluid flow, and mineralization', *Geology*, 2004, **32**, 813–816.
27. C. Muller: 'Inferred resource declaration, War Springs (Oorlogsfontein 45KS), Northern Limb Platinum Property, Limpopo Province, Republic of South Africa', Technical Report submitted in compliance with National Instrument 43–101 for Platinum Group Metals Ltd, 10 November 2005, available at: www.sedar.com
28. I. C. Pringle: 'The Union Tin mine, Naboomspruit district', in 'Mineral Deposits of Southern Africa', (ed. C. R. Anhaeuser and S. Maske), 1301–1306; 1986, Johannesburg, Geol. Soc. South Africa.
29. K. Roberts: 'Technical report on the Platreef project, Northern Limb, Bushveld Complex, Limpopo Province Republic of South Africa', Technical Report for Anooraq Resources Corporation, March 19, 2004, available at: www.sedar.com
30. J. K. Schweitzer, C. J. Hatton and S. A. de Waal: 'Economic potential of the Rooiberg group: volcanic rocks in the floor and roof of the Bushveld Complex', *Mineral. Depos.*, 1995, **30**, 168–177.
31. A. K. Şener, C. J. Grainger and D. J. Groves: 'Epigenetic gold-platinum-group element deposits: examples from Brazil and Australia', *Appl. Earth Sci. (Trans. Inst. Min. Metall. Sect. B)*, 2002, **101B**, B65–72.
32. SRK Consulting: 'Competent person's report on the Naboom Platinum project – prepared for Centurion Gold Holdings Ltd' Johannesburg, May 2006, 77, available at: www.centuriongold.com
33. S. R. Taylor and S. M. McLennan: 'The continental crust: its composition and evolution', 312; 1985, Oxford, Blackwell Scientific.
34. D. Twist: 'Geochemical evolution of the Rooiberg silicic lavas in the Loskop Dam area, Southeastern Bushveld', *Econom. Geol.*, 1985, **80**, 1153–1165.
35. D. P. van Rooyen: 'Naboomspruit Gebied (10 myl W en NW van Naboomspruit)', Unpublished map, 1944.
36. D. P. van Rooyen: 'Die geologie van die ou platinum myn', Unpublished map, 1945.
37. D. P. van Rooyen: 'Die geologie van'n gedeelte van gebied 7 (Potgietersrust)', Unpublished report of the Geological Survey of South Africa, 1954, 116.
38. P. A. Wagner and T. G. Trevor: 'Platinum in the Waterberg district – a description of the recently discovered Transvaal deposits', *South Afr. J. Industr.*, 1932, **6**, 577–597.
39. P. A. Wagner: 'The platinum deposits and Mines of South Africa'; 257–263; 1929, Edinburgh, Oliver & Boyd.
40. F. Walraven, R. A. Armstrong and F. J. Kruger: 'A chronostratigraphic framework for the north central Kaapvaal craton, the Bushveld Complex and the Vredefort structure', *Tectonophysics*, 1990, **17**, 23–48.